[redacted]

UNCLASSIFIED

CLASSIFICATION CHANGE

GDS EO11652 dtd 6/30/7

Date 12/31/75

[redacted]

FACILITY FORM

(ACCESSION NUMBER)	(THRU)
432	20
(PAGES)	(CODE)
CR 85314	28
(NASA CR OR TMX OR AD NUMBER)	(CATEGORY)

[redacted]

A STUDY OF COMPOSITE PROPULSION SYSTEMS FOR ADVANCED LAUNCH VEHICLE APPLICATIONS

MAIN TECHNICAL REPORT

VOLUME 3 (PART 2 OF 2)

SEPTEMBER 1966 REPORT NO. 25,194

PREPARED UNDER NATIONAL AERONAUTICS AND SPACE ADMINISTRATION CONTRACT NAS7-377

THE MARQUARDT CORPORATION

ROCKETDYNE

LOCKHEED-CALIFORNIA COMPANY

[redacted]

[redacted]

DATE 16 September, 1966

REPORT 25, 194
Volume 3

This docu[redacted]contains information [redacted]e national defense of [redacted] the meaning of the Espionage Laws, [redacted] 18, U. S. C., Sections 793 and 794, the transmission [redacted]lation of which in any manner to an unauthorized pe[redacted]is prohibited by law.

[redacted]

A STUDY OF COMPOSITE PROPULSION SYSTEMS FOR ADVANCED LAUNCH VEHICLE APPLICATIONS

VOLUME 3 (Part 2 of 2): MAIN TECHNICAL REPORT, COMPOSITE ENGINE STUDY

Contract: NAS 7-377

Project: 5402

PREPARED BY

William J. D. Escher
William J. D. Escher
Project Engineer

Bruce J. Flornes
Bruce J. Flornes
Supervisor, Propulsion
Systems Analysis

APPROVED BY

Robert E. Fisher
Robert E. Fisher
Vice President, Research

GROUP [redacted]
D[redacted]GRADED AT 3 [redacted]AR INTERVALS;
DECLA[redacted]TER 12 YEARS

[redacted]

THE Marquardt CORPORATION
VAN NUYS, CALIFORNIA

U. S. [redacted]nment Agencies and

MAC A1190

FOREWORD

This volume 3 is a portion of the final report documentation under National Aeronautics and Space Administration Contract NAS 7-377. The main Technical Report is presented in two parts. The placement of this volume in the seven volumes of this report series is indicated below.

Volume 1 -- Summary Report

Volume 2 -- Main Technical Report, Part 1

Volume 3 -- Main Technical Report, Part 2

Volume 4 -- Class 0 Engine Fact Sheets, Part 1

Volume 5 -- Class 0 Engine Fact Sheets, Part 2

Volume 6 -- Class 1 Engine Information

Volume 7 -- Class 2 Engine Information

ACKNOWLEDGEMENT

The Rocketdyne Division, North American Aviation, Inc., contributed the following sections of the Main Technical Report Documentation presented herein:

Section	Subject Material
5.2	Comparison rocket engine specification and vehicle/mission analysis
5.4	Identification of candidate concepts (Joint effort)
6.2	Propulsion system analysis (Joint effort)
7.3	Primary rocket subsystem analysis and design, Class 1
8.3	Primary rocket subsystem analysis and design, Class 2
Appendix A	Rocket oriented composite propulsion systems

The Lockheed-California Company contributed the following sections of the Main Technical Report documentation presented herein:

Section	Subject Material
3.3	Vehicle/mission model description
6.5	Vehicle characteristics (Consultation)
7.6	Vehicle system analysis and design, Class 1
8.6	Vehicle system analysis and design, Class 2
Appendix F	A method of augmenting payload in certain air liquefaction based composite propulsion systems

Both Rocketdyne and Lockheed participated in the technology assessment effort (Section 9.2) and assisted in arriving at the specific (Sections 5.5, 6.7, 7.8, 8.7 and 9.3) and general conclusions (Section 11.0) which are presented.

The Rocketdyne and Lockheed contributions have been separately published in reports to the Marquardt Corporation in fulfillment of the respective subcontract purchase orders. Although these reports have been given strictly limited distribution in view of their assimilation into the present main technical report (Report 25,194) they are cited below for completeness:

"A Study of Composite Propulsion Systems for Advanced Launch Vehicle Applications", Rocketdyne Division Report R-6465, 11 March 1966. CONFIDENTIAL.

"A Study of Composite Propulsion Systems for Advanced Launch Vehicle Applications", Lockheed California Company Report LR 19611-LAC/608177, 31 March 1966. CONFIDENTIAL.

THE MARQUARDT CORPORATION CONTRIBUTION

In addition to overall project coordination and administration of National Aeronautics and Space Administration Contract NAS 7-377, Marquardt contributed to the technical effort recorded here.

The efforts of H. Frank in mission analysis and vehicle coordination, W. R. Hammill in engine design and weight analysis, C. R. Orr in performance computation, A. F. Truitt and J. J. Kuhlmeier in project documentation, M. Fraser and L. J. Skubic in report illustration, and T. E. Blake in technical editing and final preparation of this document are gratefully acknowledged. Finally, the contribution of Mr. H.W. Welsh, who managed the program effort reported here, is noted with appreciation.

ROCKETDYNE DIVISION CONTRIBUTION

The contribution of the Rocketdyne Division, North American Aviation, Inc., to the study program was conducted via Marquardt Purchase Order 500307 (Rocketdyne General Order No. 8712) under National Aeronautics and Space Administration Contract NAS 7-377. The Rocketdyne section of the program documentation was prepared and approved as follows:

Prepared By:

H. A. Singer
Project Engineer

Approved By:

S. F. Iacobellis
S. F. Iacobellis
Director, Advanced Projects Department
Large Engines

The efforts of Messrs. J. Steinkamp and W. Moser in the baseline rocket and systems analysis, Messrs. H. Hoche and W. Barber in the primary rocket subsystem design, Messrs. J. Gerstley and J. Slaminski in the heat transfer analysis, Messrs. J. Hyde and K. Hill in the nozzle and plume analysis, Messrs. G. Wong, J. Blake, and F. Catterfield in the turbomachinery analysis and design, and Mr. M. Pucker in the initial coordination of this program are gratefully acknowledged.

LOCKHEED-CALIFORNIA COMPANY CONTRIBUTION

The contribution of the Lockheed-California Company to this study program was conducted via Marquardt Purchase Order 500309 under National Aeronautics and Space Administration Contract NAS 7-377. The Lockheed section of the program documentation was prepared and approved as follows:

Prepared By:

N. B. Williams

N. B. Williams
Project Engineer

Approved By:

D. L. Kelly

D. L. Kelly
Program Manager

The efforts of R. E. Morris in the vehicle/engine integration effort, A. J. Erjavac in vehicle design, R. D. Mijares in weight analysis, R. Peyton in aerodynamics, and H. Harper and D. Sherwood in system performance analysis are gratefully acknowledged. The contributions of G. Horie (inlet design and performance), M. Verheagh (structure), and F. Bevan (design) are also acknowledged.

THE NATIONAL AERONAUTICS AND SPACE ADMINISTRATION

Contract NAS 7-377 was sponsored by the Liquid Rocket Propulsion Technology group of the NASA Office of Advanced Research and Technology (OART).

The Project Manager was Mr. Jack Suddreth, NASA - Headquarters.

The NASA Technical Managers were as follows:

Mr. D. D. Thompson	Marshall Space Flight Center
Mr. P. K. Pierpont	Langley Research Center
Mr. T. J. Gregory	Mission Analysis Division, OART (at Ames Research Center)

The following NASA personnel provided technical consultation for the program:

Mr. G. R. Woodcock	Marshall Space Flight Center
Mr. J. von Puttkamer	Marshall Space Flight Center
Mr. J. Nugent	Flight Research Center

TABLE OF CONTENTS*

---

* See outline at end of report for a detailed listing of contents.

TABLE OF CONTENTS (Continued)

TABLE OF CONTENTS (Continued)

LIST OF ILLUSTRATIONS

LIST OF ILLUSTRATIONS (Continued)

LIST OF ILLUSTRATIONS (Continued)

LIST OF ILLUSTRATIONS (Continued)

LIST OF ILLUSTRATIONS (Continued)

LIST OF ILLUSTRATIONS (Continued)

LIST OF ILLUSTRATIONS (Continued)

LIST OF ILLUSTRATIONS (Continued)

LIST OF ILLUSTRATIONS (Continued)

LIST OF ILLUSTRATIONS (Continued)

LIST OF ILLUSTRATIONS (Continued)

LIST OF ILLUSTRATIONS (Continued)

TABLES

TABLES (Continued)

This page intentionally left blank

8.0 CLASS 2 SYSTEMS PHASE

8.1 General Considerations

The Class 2 systems phase of the study was the final phase of the three engine concept-associated efforts. The phase centered about the two selected composite engines (see Section 7.7) and it included the combined efforts of Marquardt, Rocketdyne, and Lockheed.

Prior to describing the technical results achieved and the methodologies applied, the objective, scope, and approach used for the Class 2 phase will be briefly reviewed.

8.1.1 Objectives

The primary purpose of the Class 2 phase was to perform a final, higher conference level orbital payload performance evaluation, per the original guidelines (Section 3.1), for the two selected composite engine systems. The two non-composite reference systems, the "Very Advanced" Rocket (Engine No. 0) and the Advanced Turbomachine-Based Airbreather (Engine No. X), were also to be fully carried along in this evaluation. Previous assessment (Classes 0 and 1) of these two comparison systems were at a significantly lower level of scope as will be noted in Section 8.1.2 below.

This primary Class 2 objective was directed toward satisfaction of the first of the two overall program objectives, namely, determination of the (payload) significance of composite engines for advanced launch missions (Section 2.0).

In addition, the Class 2 work had as another major goal significant further penetration (with reference to Class 1 accomplishments) into the detailed engine technical areas. For instance, assessment of subsystem drive penalties to overall engine performance was to be appraised. This goal was established primarily to assist in the program's technology assessment task (Overall Objective No. 2, Section 2.0). Obviously, this penetration was also quite consistent with the basic performance evaluation requirement for more realistic engine data, as previously described.

8.1.2 Scope

The Class 2 phase comprised the following three major effort areas:

1. Detailed conceptual design of the primary rocket subsystem (Rocketdyne)

2. Conceptual design and performance analysis of the composite engine (Marquardt)

3. Vehicle/engine integration and mission performance evaluation (Lockheed)

These efforts were carried out approximately in parallel by the three companies which, clearly, required a significant interface coordination effort.

The technical scope of the task was essentially defined by the objectives and the engine and vehicle configurations under study: two composite engines, two reference engines, and a two-stage, reusable orbital vehicle mission profile - for all engines.*

Also emphasized in the study phase was composite engine performance and weight component sensitivity analyses. Alternate (cruise) missions for composite engine powered first stage vehicles were also briefly examined (Appendix D).

A note or two relative to the results achieved for the reference non-composite propulsion systems (Engines Nos. 0 and X) is in order at this point.

It will be recalled that the "Very Advanced" Rocket comparison system Engine No. 0) was defined by Rocketdyne early in the study (Section 5.2). Nevertheless, the rocket was not fully exercised to show its maximum potential until the Class 2 Phase. Previously, for the general two-stage reusable vehicle model emphasized in the study, the rocket system was placed in an "HTO-gear" mode. That is, the vehicle took off horizontally by means of unaided first stage rocket engine thrust. The fact that both vertical takeoff (VTO) and sled launch horizontal takeoff techniques are significantly superior to this unaided horizontal mode became strikingly clear in the Class 2 activity, where all three modes were co-evaluated for the first time.

On the other hand, the inclusion of the second reference engine, namely, the turbomachine-based airbreathing system (Engine No. X), was not a formal program feature until the Class 2 Phase. The Turboramjet, selected as a typical system, was informally included by Lockheed in the Class 1 Phase. Its general showing was, as a matter of fact, generally substantiated by a more definitive Class 2 examination of the capability of the engine.

It should be pointed out that the propulsion system details for the turbomachine are considered outside the scope of this study. Hence, uninstalled turboramjet propulsion information is not documented in this report. For this type of information see Reference 26.

- - - - - - - - - - -

* Single stage systems were not included in the Class 2 Phase. Choice of the two-stage model provided concentration of phase resources in a significantly less problematical mission context (See Appendix E).

In summary, the Class 2 results, alone, are considered definitive (to the extent of the study) with regard to the payload potentials of Engines Nos. 0 and X, although the previous results are nevertheless documented.

8.1.3 Approach

As indicated above, a coordinated Marquardt/Rocketdyne/Lockheed effort was required to effect the Class 2 Phase work. Briefly, the phasing of the activity was approached as follows.

The initial Class 2 engine performance was essentially refined - and, for SERJ, resized - Class 1 data rederived by Marquardt. This was used initially by Lockheed, while Marquardt and Rocketdyne pursued various Class 2 engine design topics. Following a selection of the major design point variables, including initial thrust size estimates (from the parallel Lockheed studies), final on-design engine performance was calculated by Marquardt. The performance sensitivity (off-design) task was then pursued while final Marquardt/Lockheed activity in engine/vehicle integration was completed.

The results which were achieved are described in the following sections and in Volume 7, "Class 2 Engine Information."

8.2 Engine Performance

This section describes the performance aspects of the two Class 2 Composite Engines -- the Supercharged Ejector Ramjet (Engine No. 11) and the ScramLACE (Engine No. 22). Continuing the Methodology/Results orientation used heretofore, parametric analysis results for each of the two engine concepts are given followed by a comparative evaluation of the two systems. The results of the engine sensitivity studies (first order off-design analysis), unique to the Class 2 effort, conclude this section. As for the Class 0 and 1 detailed engine results, the Class 2 information is separately contained (See Volume 7).

8.2.1 Methodology

The basic methodology for the Class 2 engine performance analysis was that used for the earlier work. Certain refinements were added, generally as either a reflection of the increased technical penetration characteristic of the Class 2 activity, or as a ramification of the more closely coordinated vehicle integration aspect. Illustrative of these two refinement areas in the methodology are, respectively, (1) inclusion of turbopump drive penalties (i.e., secondary gas generator flow requirements), and (2) establishment of engine thrust levels consistent with Lockheed's choice of number of engines for the vehicles and payload optimization or initial vehicle thrust loading (T/W).

With the above as a preface, the methodology considerations are given below and they will be found to center about the subject of (internal) engine sizing and parametric analysis.

Engine performance data for both Class 2 engines in all operating modes were computed as for the Class 1 engines. All data except those for the Scramjet mode were obtained using the previously described IBM 7040 fixed geometry program. Scramjet data were obtained from Reference 20. Consistent component efficiencies were used and the performance effects of varying the efficiencies and other cycle variables are presented in the Class 2 Engine Information Book (Volume 7). A comparison of the two Class 2 engines and a number of the sensitivity analysis results are discussed in the following section.

One difference in performance computations between the Class 1 and Class 2 engines was the inclusion of turbopump gas generator drive propellant penalties for all Class 2 engine performance data. The propellant assessment does not affect engine thrust, only the specific impulse (i.e., inclusion of drive propellant penalty) computations. The effect on specific impulse ranges from 1 to 4 percent, depending on the engine and operation mode. Typically, this provides a minimum effect for the ejector mode. The Class 2 engine data with turbopump drive propellant assessment were used subsequently to update all published Class 1 engine performance with the exception of those for the ejector mode.

8.2.1.1 Supercharged Ejector Ramjet (Engine No. 11)

The Class 2 Supercharged Ejector Ramjet (Engine No. 11) differs from the Class 1 version in two design parameters, namely, primary chamber pressure and secondary-to-primary mass flow ratio.

A 2000 psia chamber pressure was used for the Class 1 studies while 1500 psia was selected for the Class 2 studies. The reduction in pressure was made on the basis of several factors: desirability of some design margin (reusable connotation); possible chamber tube oxidation problems at a stoichiometric mixture ratio; and the association of a nearer term, lower technical risk with the Supercharged Ejector Ramjet. Further discussion is given in Section 8.3.

The change in secondary-to-primary mass flow ratio (W_s/W_p) from Class 1 to Class 2 also stems from several factors. As discussed in Section 7.2, the composite engines obtain their best ejector mode augmentation with a relatively high W_s/W_p (toward 3.0) and are typically constrained to the lower side of the W_s/W_p band by practical limitations, mainly the usual engine volume vehicle packaging requirements. Lockheed vehicle system studies in Class 1 evaluated both a 3.0 and a 1.5 W_s/W_p Ejector Ramjet (Engines 9-1 and 9-2, respectively). A potential payload improvement of 15 percent was indicated for the 3.0 W_s/W_p engine. This suggested that an intermediate W_s/W_p at about 2.0 might maximize payload performance while satisfying practical installation constraints.

Consultation with Lockheed on the sizing of the Class 2 Supercharged Ejector Ramjet indicated that the engine should be tailored to fit within a cylindrical envelope with a diameter equal to the outside diameter of the exit bell of the 1.5 W_s/W_p engine. The high and low W_s/W_p engines evaluated by Lockheed were Class 0 designs with a primary chamber pressure at 1000 psia. The 1500 psia selected for Class 2 increases the W_s/W_p for a given combination of mixer area and design thrust. Supercharging of the cycle also increases the W_s/W_p as discussed in Section 7.4

Supercharged Ejector Ramjet sizing data were computed with the parametric IBM 7040 program. Primary chamber pressures of 1000, 1500, and 2000 psia were run to obtain data on the effect of this variable even though 1500 psia had been nominally selected as the design pressure. Afterburner/mixer diffusion ratios (A_4/A_3) of 1.50, 1.75, and 2.00 were also investigated. A W_s/W_p range of 1.5 to 4.0 was selected. However, program difficulties eliminated any data above a W_s/W_p of 3.0 on the initial run. As mentioned earlier in Section 7.2, the parametric program has a convergence technique problem in holding a high specified mixer exit Mach number (M_3)(0.95 in this case) at high W_s/W_p ratios. It should be noted that this is not an engine cycle problem, but an IBM program peculiarity. The desired Supercharged Ejector Ramjet design was, however, within the initial run sizing and no further sizing calculations were made.

Figure 213 presents the sea level static thrust per unit mixer area (A_3) as a function of primary chamber pressure and W_s/W_p. A small but significant sizing gain is indicated with increasing chamber pressure and a strong effect (even with supercharging) of W_s/W_p on the engine size for a selected thrust level is shown. The specific impulse performance corresponding to Figure 213 is presented in Figure 214. Primary chamber pressure has a relatively significant effect on the sea level static specific impulse even with supercharging of the cycle. Figures 213 and 214 both show that the jet compression (second of a two-stage compression process) through mixing provides the major portion of the overall compression in the supercharged ejector mode cycle.

Figure 215 presents the mixer flow area (A_3) required for 250,000 pounds of design sea level static thrust. As shown earlier in Section 7.2 for both the Ejector Ramjet and RamLACE cycles, the diffusion ratio (A_4/A_3) has a small effect on engine thrust sizing. Figure 215 is plotted for the selected design primary chamber pressure of 1500 psia.

The corresponding effect of diffusion ratio on specific impulse is presented in Figure 216. Diffusion ratio has a more significant effect on specific impulse than on thrust sizing as is shown in the figure. Clearly, increasing the diffusion ratio (A_4/A_3) from 1.50 to 1.75 shows a relatively greater gain in specific impulse than the increase from 1.75 to 2.00. The 1.50 A_4/A_3 point at $W_s/W_p = 3.0$ thermally choked the afterburner, reflecting insufficient jet compression at the high W_s/W_p setting coupled with a low static pressure rise through diffusion prior to the afterburner heat addition.

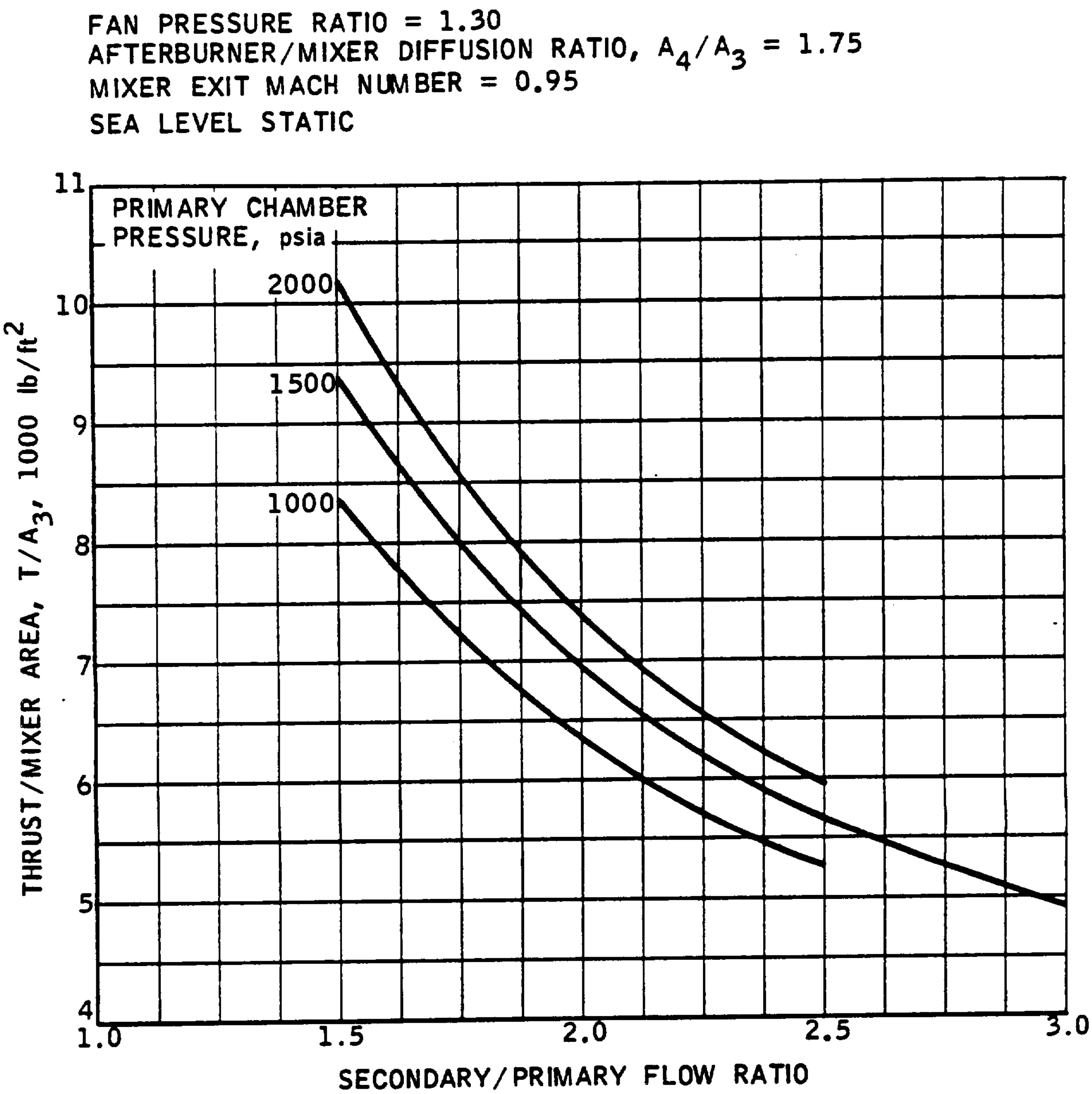

FIGURE 213. Effect of Primary Chamber Pressure on the Thrust/Mixer Area of the Supercharged Ejector Ramjet

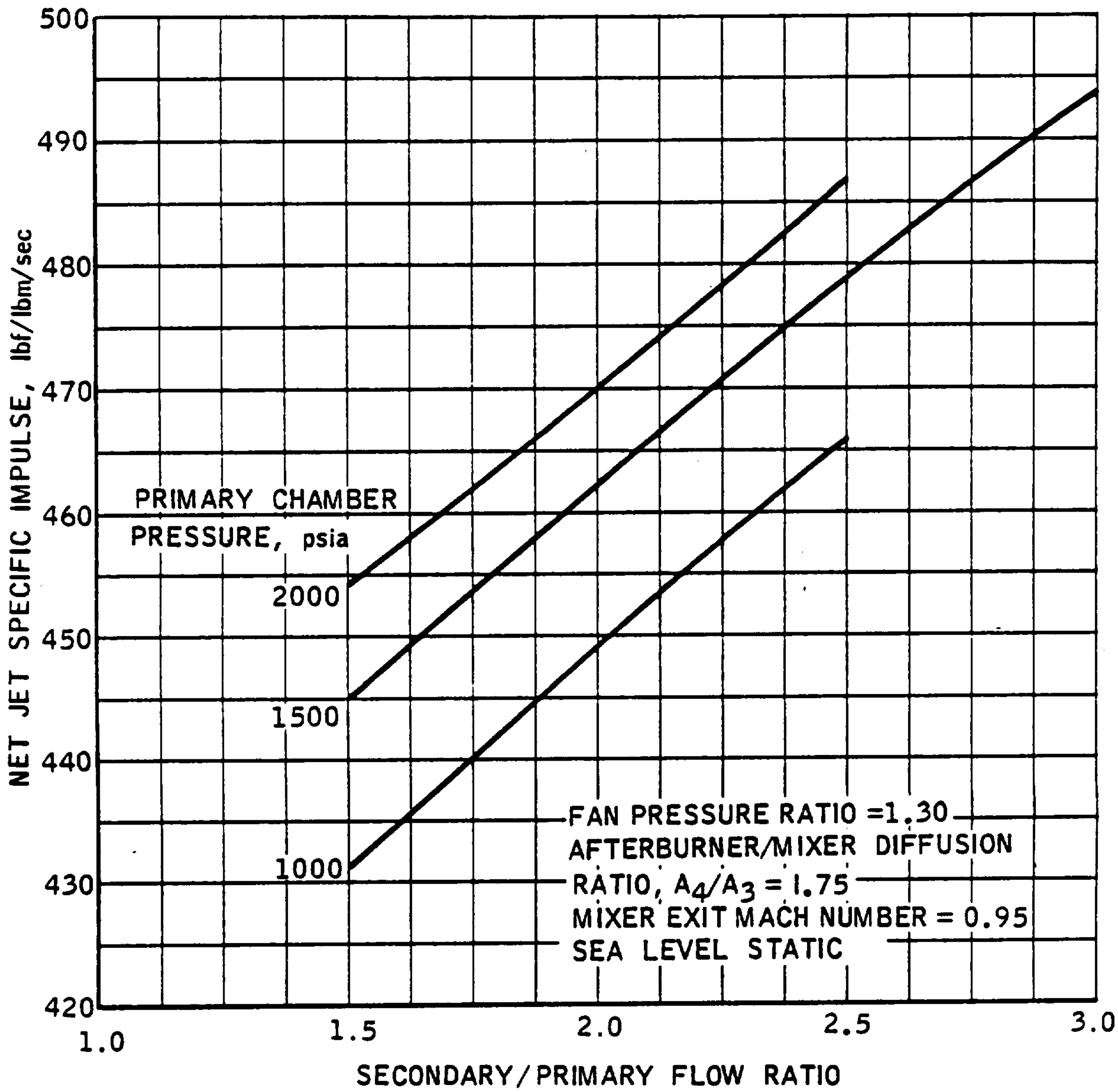

FIGURE 214. Effect of Primary Chamber Pressure on the Specific Impulse of the Supercharged Ejector Ramjet

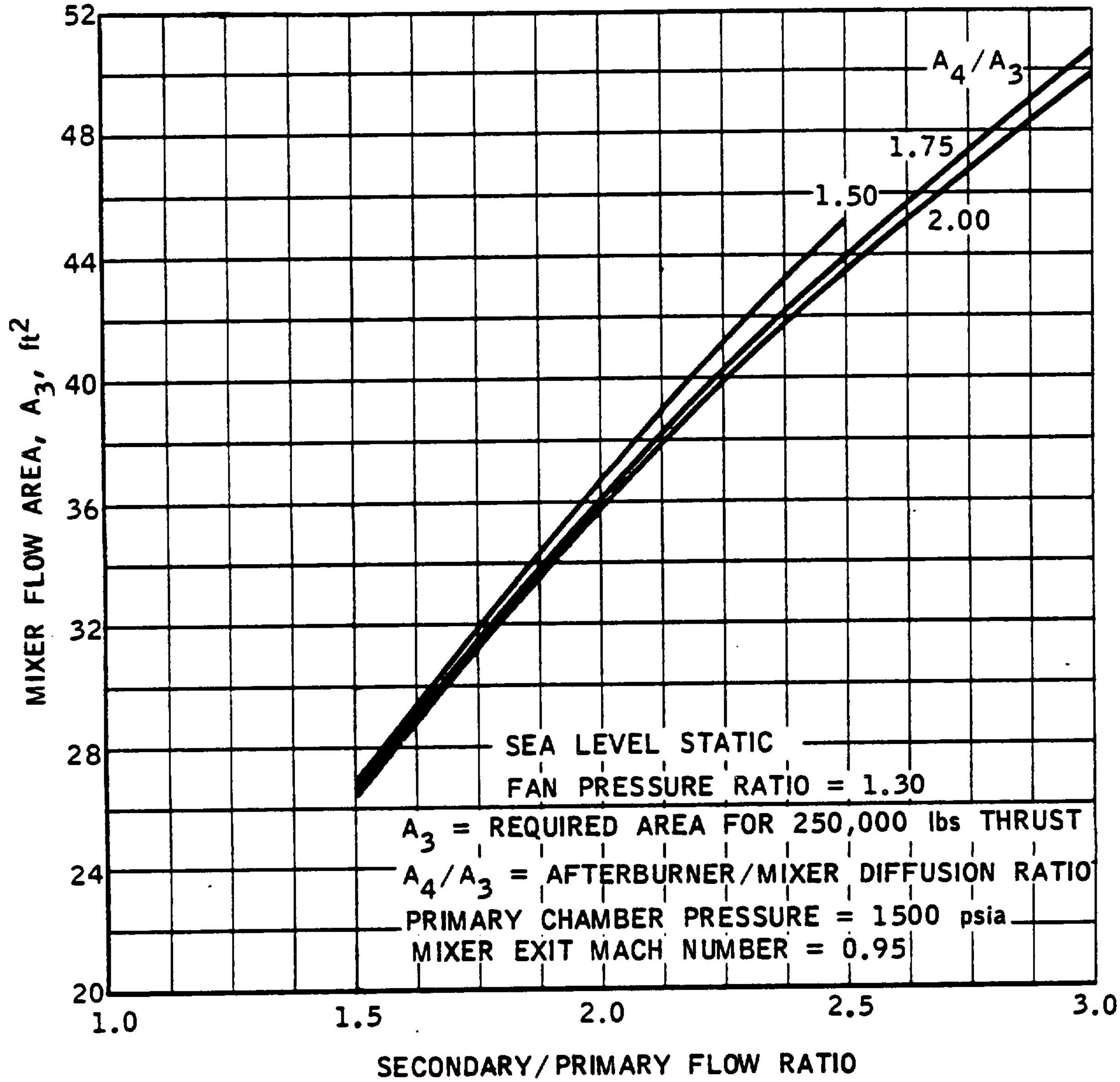

FIGURE 215. Effect of Diffusion Ratio on the Mixer Area of the Supercharged Ejector Ramjet

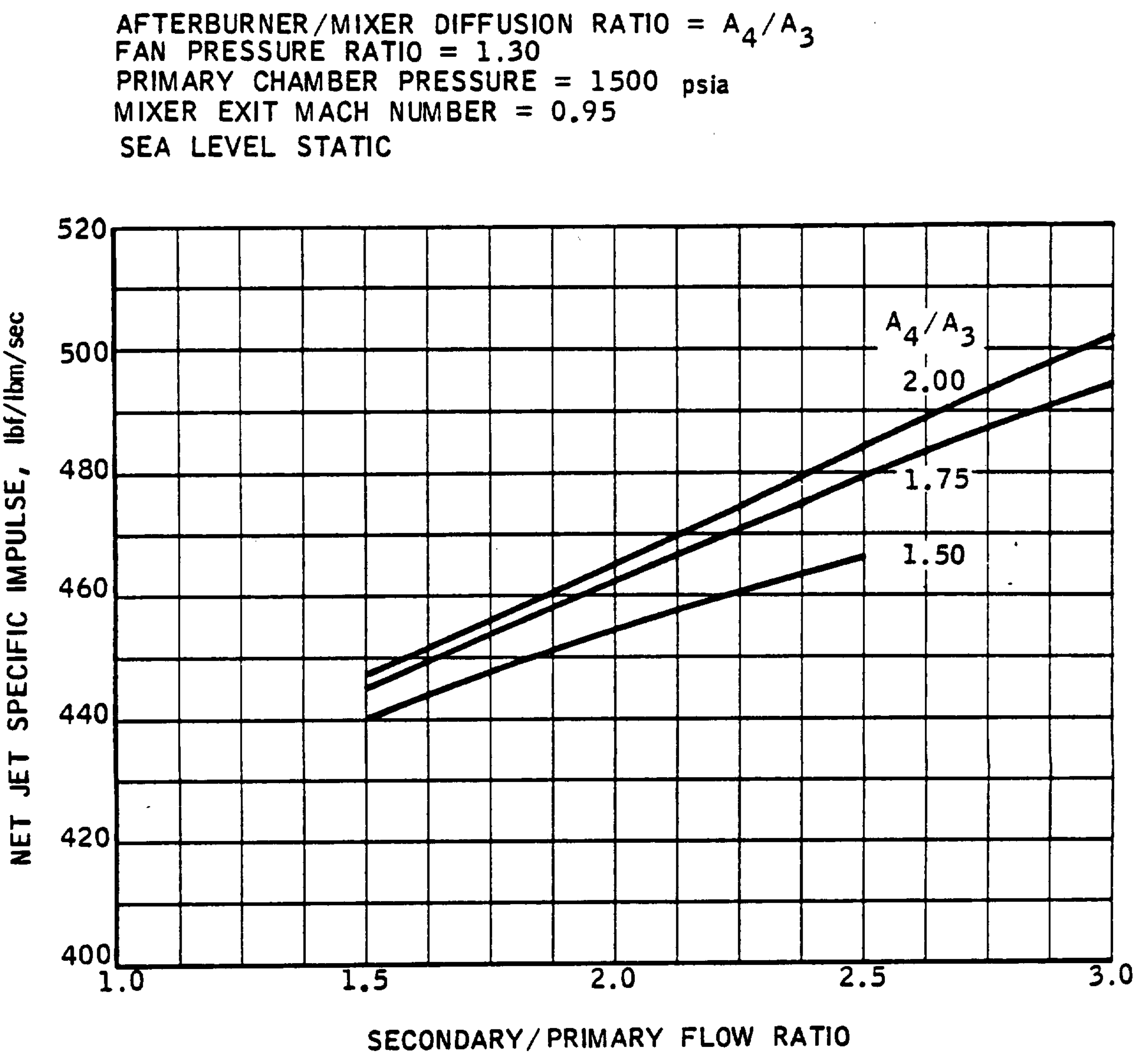

FIGURE 216. Effect of Diffusion Ratio on the Specific Impulse of the Supercharged Ejector Ramjet

The final sizing iterations for the Class 2 Supercharged Ejector Ramjet engine began with a maximum exit nozzle area of about 125 sq ft for a design sea level static thrust of 250,000 pounds. Preliminary engine layouts and consideration of the variable exit nozzle area variation and packaging requirements lead to the selection of a design W_s/W_p of 3.0 with a diffusion ratio (A_4/A_3) of 1.75. This, in turn, yielded a mixer flow area of 50.7 sq ft per Figure 215 and an afterburner flow area of 89 sq ft. This combination yielded almost maximum sea level static performance within the volume constraints, and provided a high W_s/W_p associated with good augmentation with increasing flight speed during the supercharged ejector mode.

The basic Ejector Ramjet (non-supercharged) parametric sizing data presented earlier in Section 7.2 indicate a W_s/W_p of about 2.0 (trading off minor condition differences). Hence, as demonstrated, supercharging provided about a 50 percent increase in design W_s/W_p for the engine.

Initial Class 2 vehicle system evaluation of the $W_s/W_p = 3.0$ Supercharged Ejector Ramjet engine using preliminary data indicated a maximum payload vehicle thrust loading of 1.08 and an apparent best installation arrangement of five engines. The final design selection and performance computations for Engine No. 11 were made on this basis. Hence, the design sea level static thrust was adjusted to 215,000 pounds. All engine flow areas were directly scaled with this design point thrust level.

8.2.1.2 ScramLACE (Engine No. 22)

As noted, the Class 1 and Class 2 ScramLACE ejector mode performance differs from that of the Class 1 phase due to a more complete appraisal of off-design heat exchanger data for Class 2. For the eight Class 1 RamLACE based engines, the ejector mode performance maps were computed on the basis of constant sea level static design primary liquefied air flow rate with a constant net heat exchanger equivalence ratio of 8 for non-recycle engines. For Class 1, the only inclusion of off-design heat exchanger data was if the heat exchanger could not deliver the design liquefied air flow due to low inlet pressure. This occurs only at low flight speeds and/or high altitude conditions.

However, for certain combinations of high flight speed at low altitude, the heat exchanger can either process more air at the design equivalence ratio or the design air flow at slightly reduced equivalence ratio. The latter type of off-design heat exchanger is favorable to performance and it was included in the Class 2 ScramLACE ejector mode performance maps. In addition to the first effect (air flow limiting at low speed/high altitude), the engine effect of variation of heat exchanger equivalence ratio was evaluated in the sensitivity analysis (See Volume 7), and is briefly discussed later in this section.

The Class 2 ScramLACE, however, is basically the same engine design as that for Class 1 in terms of design primary chamber pressure, mass flow ratio, and flow areas. Scramjet mode requirements for inlet/mixer contraction ratio as discussed in Section 7.4 do not allow an increase in the Class 1 W_s/W_p of 1.5 without a corresponding increase in inlet cowl area. As already noted, increasing primary chamber pressure to decrease the mixer flow area provides minimal gain in terms of area reduction due to the relatively low energy hydrogen-air propellants (compared with hydrogen/oxygen) and would result in an increased heat exchanger equivalence ratio for an already fuel rich cycle as discussed in Section 7.2. Hence, the only significant change from Class 1 to Class 2 was a reduction in sea level static design thrust level from 250,000 pounds to 173,000 pounds to match a six-engine installation with an indicated vehicle thrust loading of 1.04.

8.2.2 Results

It is initially noted that a considerable portion of the results of Class 2 systems performance analysis are harbored in the preceding discussion of the methodological approach for this study phase (Section 8.2.1). Specifically, for reference to basic engine sizing with its accompanying parametric analysis aspects, that section should be consulted.

More specific outputs of the Class 2 engine analysis, including a comparison of the two engines and the sensitivity study general results, are given below. Volume 7, "Class 2 Engine Information" should be consulted for all detailed results.

8.2.2.1 Fan Ramjet Mode and Fan Drive Considerations (SERJ, Engine No. 11)

A new intermediate operating mode for supercharged engines was injected into the Class 2 studies of the Supercharged Ejector Ramjet. This has been labeled the fan ramjet mode. The low pressure ratio (1.30) fan is used to supercharge the ramjet mode of operation (primary rockets off) in the Mach 0.5 to 2.5 flight speed regime. The subsonic Mach 0 to 1.0 version of this mode with varying degrees of afterburning or plenum burning has been labeled "fan operation" and is oriented toward the end of mission loiter phase.

A comparison of the fan ramjet performance with pure ramjet and ejector mode performance is presented in Figures 217 and 218. The acceleration trajectory in the Mach 0 to 3.0 range used for this comparison is the same as the reference trajectory for the Class 2 sensitivity analysis. The trajectory is presented in Figure 219. As shown in Figure 217, the fan ramjet mode provides a significant thrust advantage over the ramjet in the acceleration flight speed regime commensurate with its intermediate position between the ejector and ramjet modes.

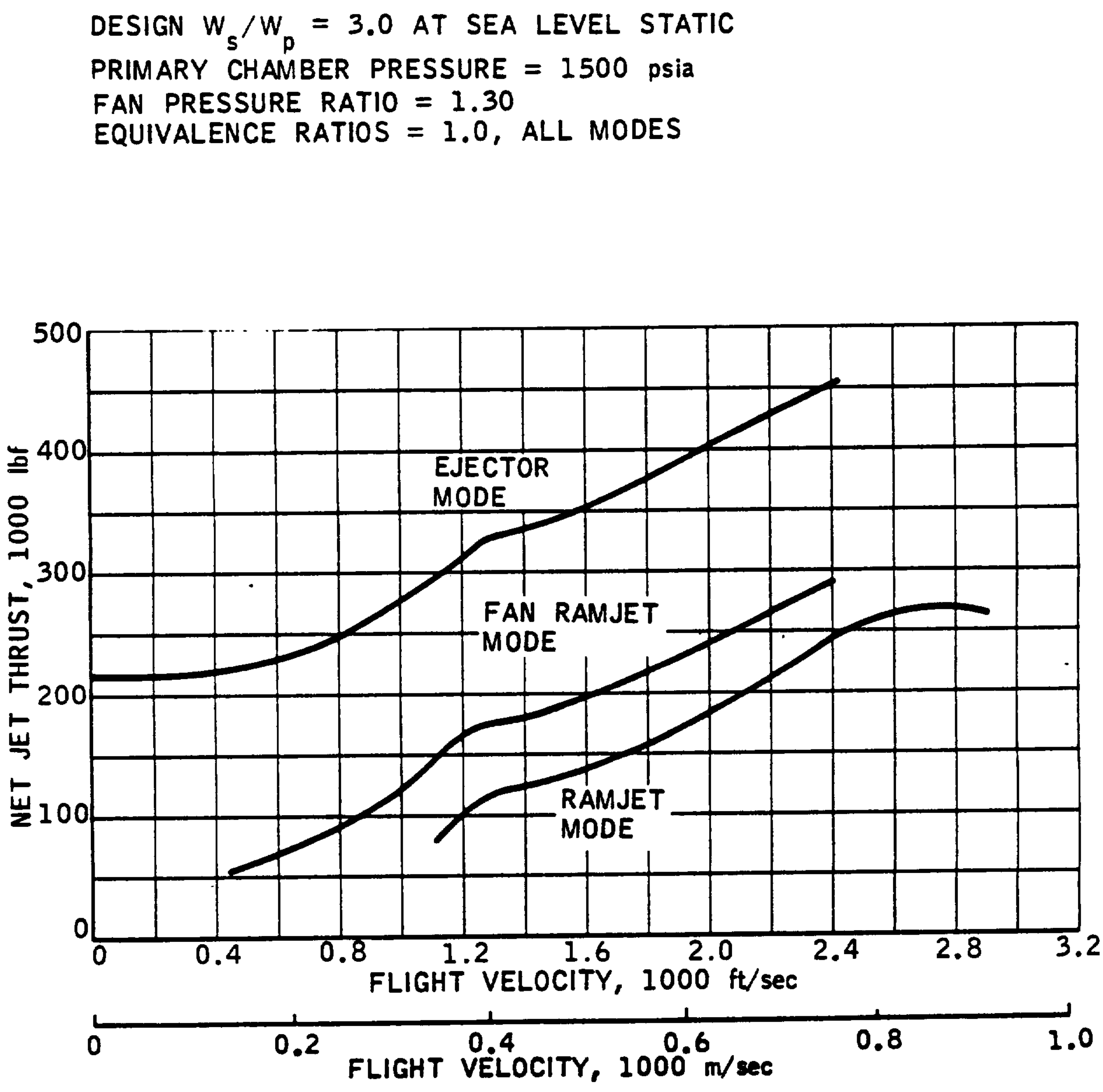

FIGURE 217. Acceleration Thrust of the Supercharged Ejector Ramjet

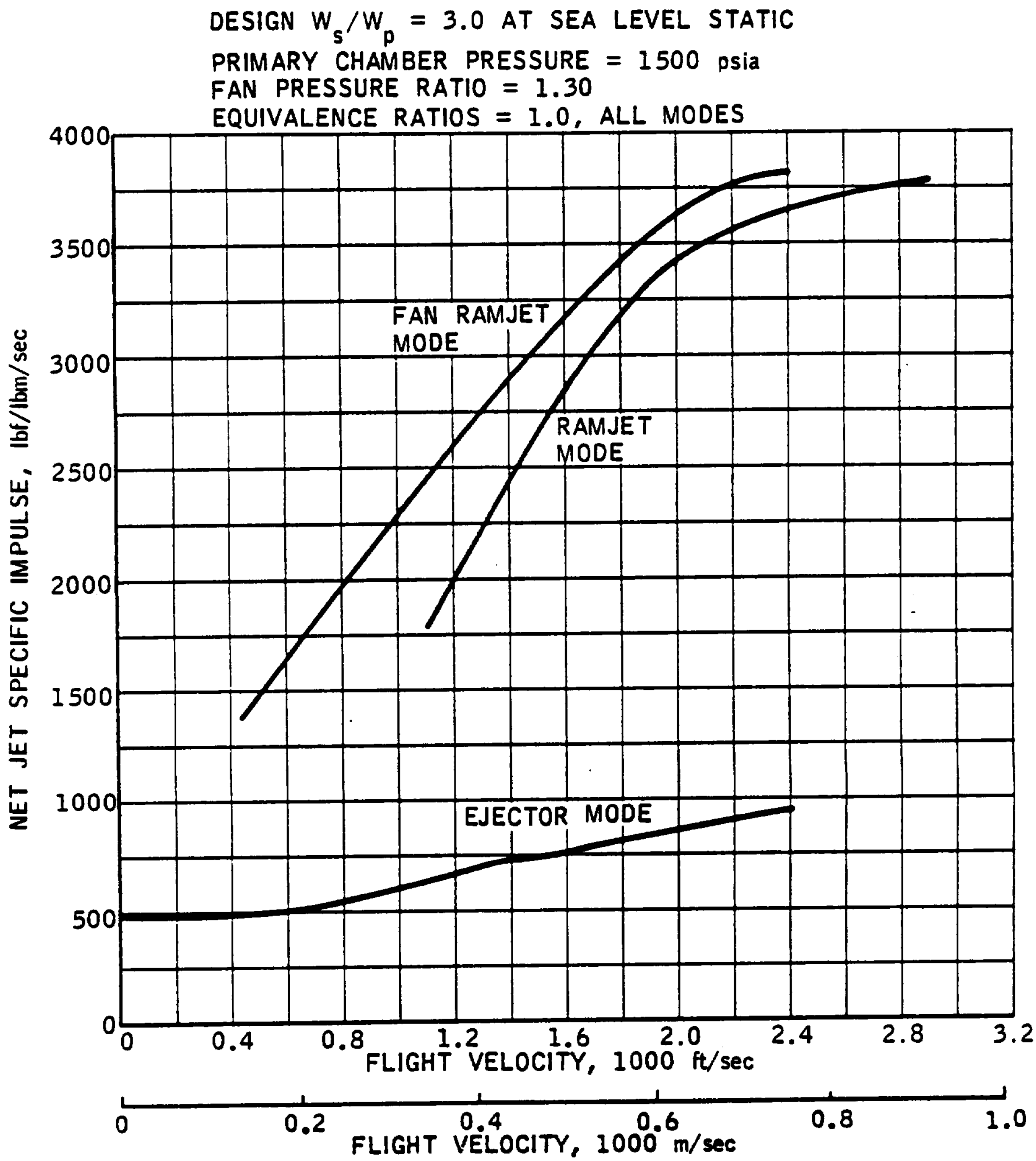

FIGURE 218. Acceleration Specific Impulse of the Supercharged Ejector Ramjet

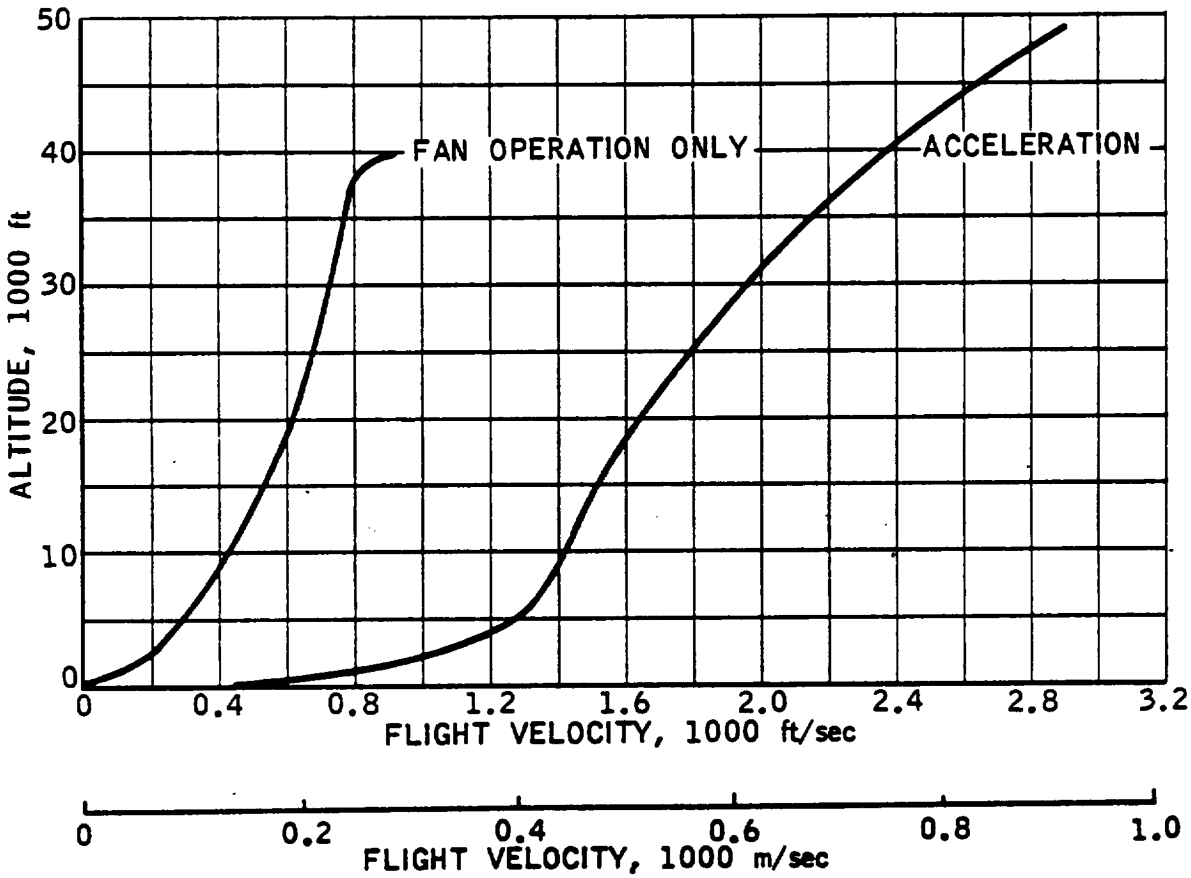

FIGURE 219. Reference Trajectories for Class 2 Analyses

Very significantly, this thrust increment allows a considerably earlier (flight speed) transition from the low specific impulse ejector operation (primary rocket shutdown). The specific impulse gains from the fan ramjet mode are shown in Figure 218. The fan ramjet performance data have been included for all supercharged Class 1 engines (See Volume 6). Note that fan ramjet operation reflects both superior thrust and specific impulse with respect to ramjet operation in this speed range.

All of the supercharged engine performance data for both Class 1 and Class 2 have been based on a hydrogen-fueled airbreathing gas generator fan drive (turbojet cycles). The propellant penalties for using a fuel-rich, hydrogen-oxygen, bipropellant gas generator as the drive power source for the fan have also been assessed. Rocketdyne turbopump bipropellant gas generator data were used for the fan drive gas generator base. The generator conditions were 1500 psia at an O/F of 1.25 providing 1500°F gas. The fuel-rich exhaust was used as part (or all depending on the mode) of the fuel for the secondary air. A comparison of specific impulse performance of the Class 2, Engine No. 11, was made for airbreathing and bipropellant gas generator fan drives for both the ejector mode and fan ramjet mode along the acceleration trajectory of Figure 219. The trajectory denoted "fan operation only" in Figure 219 was used for a similar subsonic loiter-oriented comparison.

Figure 220 presents the ejector mode fan drive comparison. The percentage plot at the bottom shows the percent specific impulse decrease for the bipropellant gas generator (BPGG) drive relative to that of the airbreathing gas generator drive (ABGG). The fuel-rich BPGG exhaust was injected into the afterburner. If the BPGG exhaust were dumped overboard, the percentage penalty would roughly double. The corresponding thrust trend (see the reference trajectory) for the ejector mode is presented in Figure 221. Thrust is not affected by the fan drive assumption and is included here for reference only.

The fan ramjet comparison is presented in Figure 222 and the reference thrust in Figure 223. The specific impulse increment for the fan ramjet mode in Figure 223 is considerably larger than for the ejector mode, but may be no more significant in terms of overall vehicle system performance. The choice of an airbreathing or bipropellant gas generator as a fan drive would probably not be dictated by the ejector or fan ramjet modes, but rather by the subsonic fan operation or loiter mode performance. The mechanical design and drive system integration may also be a factor. For example the tip-turbine fan drive scheme is by nature adapted to the low pressure ratio gas generator. This low pressure is associated with airbreathing gas generator units, not with bipropellant gas generators of the turbopump drive variety.

The fan operation specific impulse comparison for the ABGG and BPGG is presented in Figure 224. Specific impulse differences range from 20,000

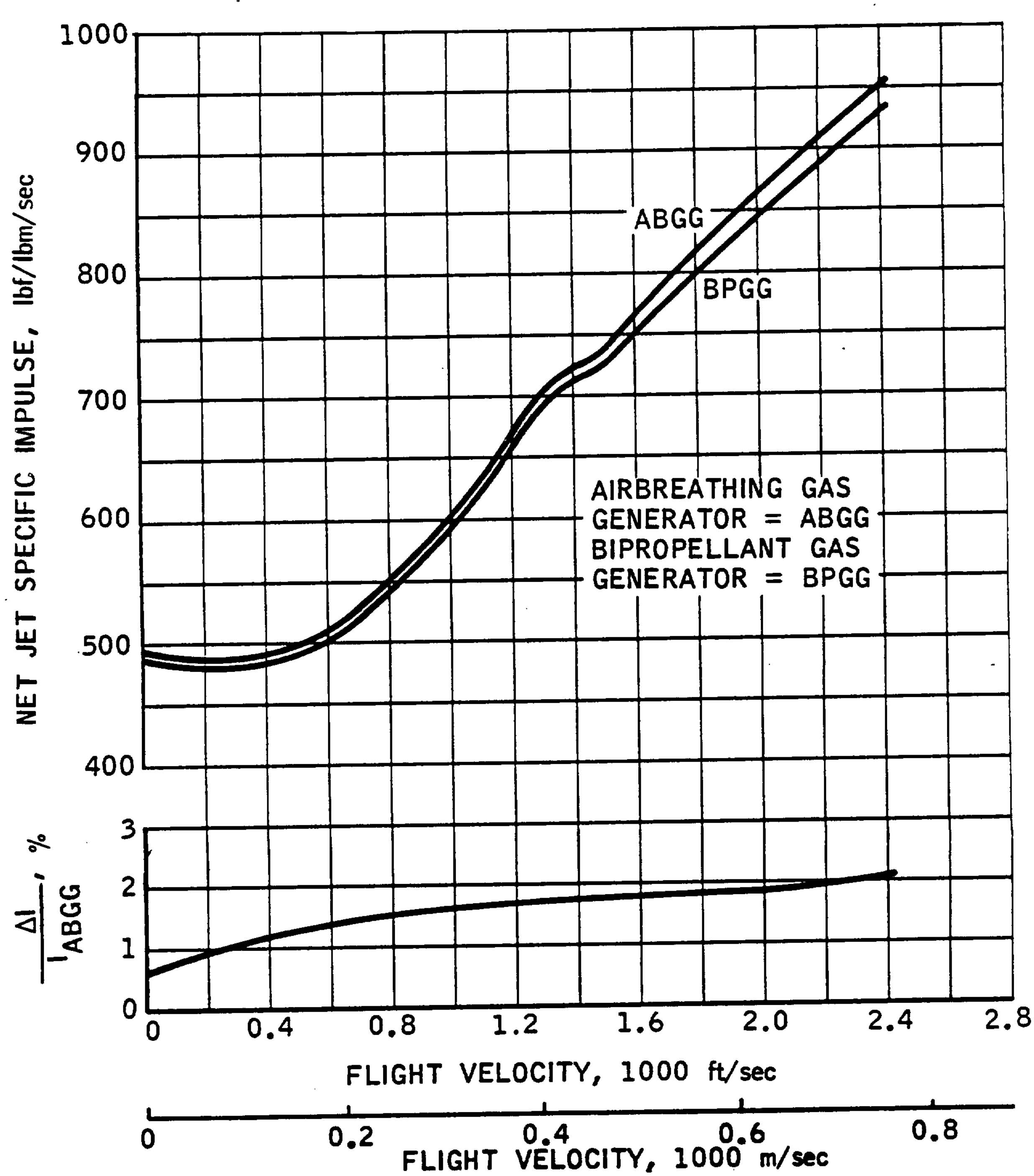

FIGURE 220. Fan Drive Comparison for the Supercharged Ejector Ramjet, Ejector Mode

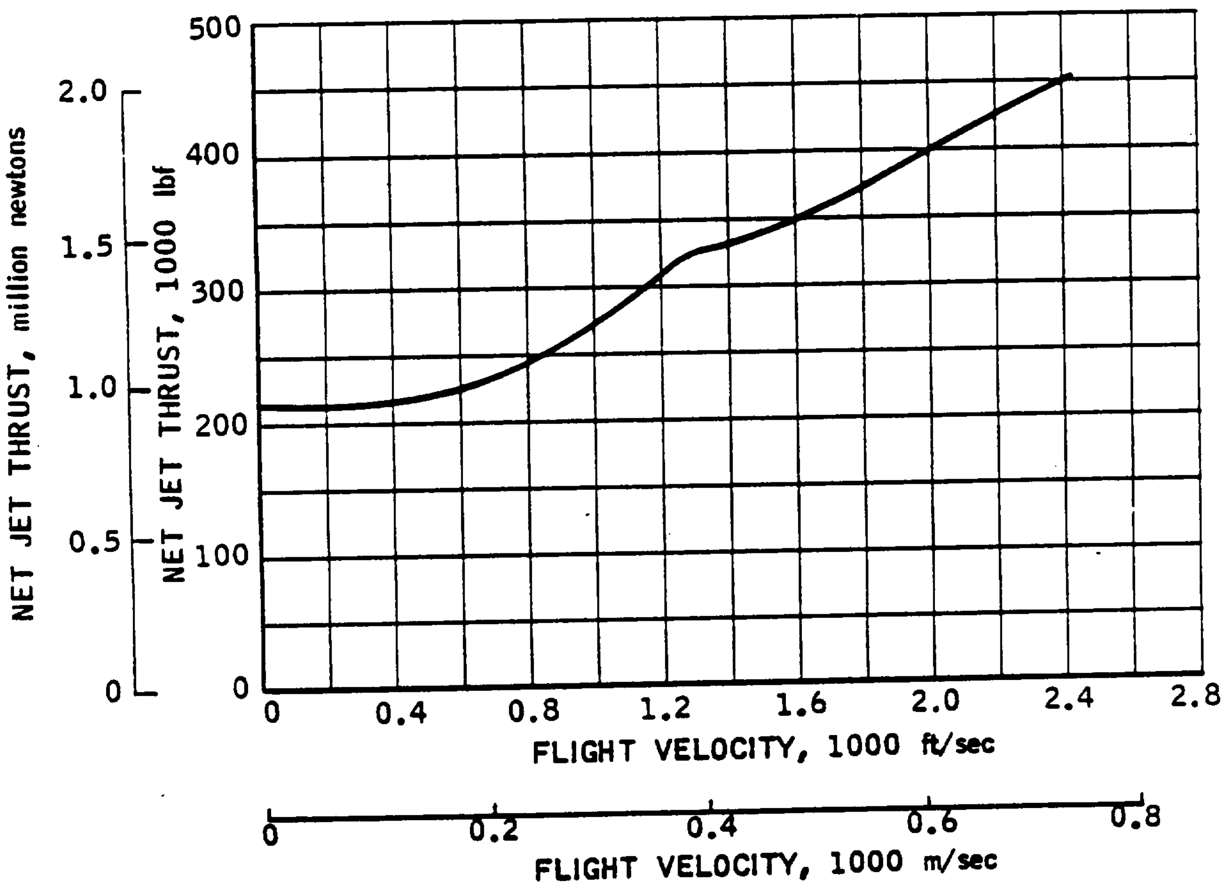

FIGURE 221. Thrust of the Supercharged Ejector Ramjet in the Ejector Mode

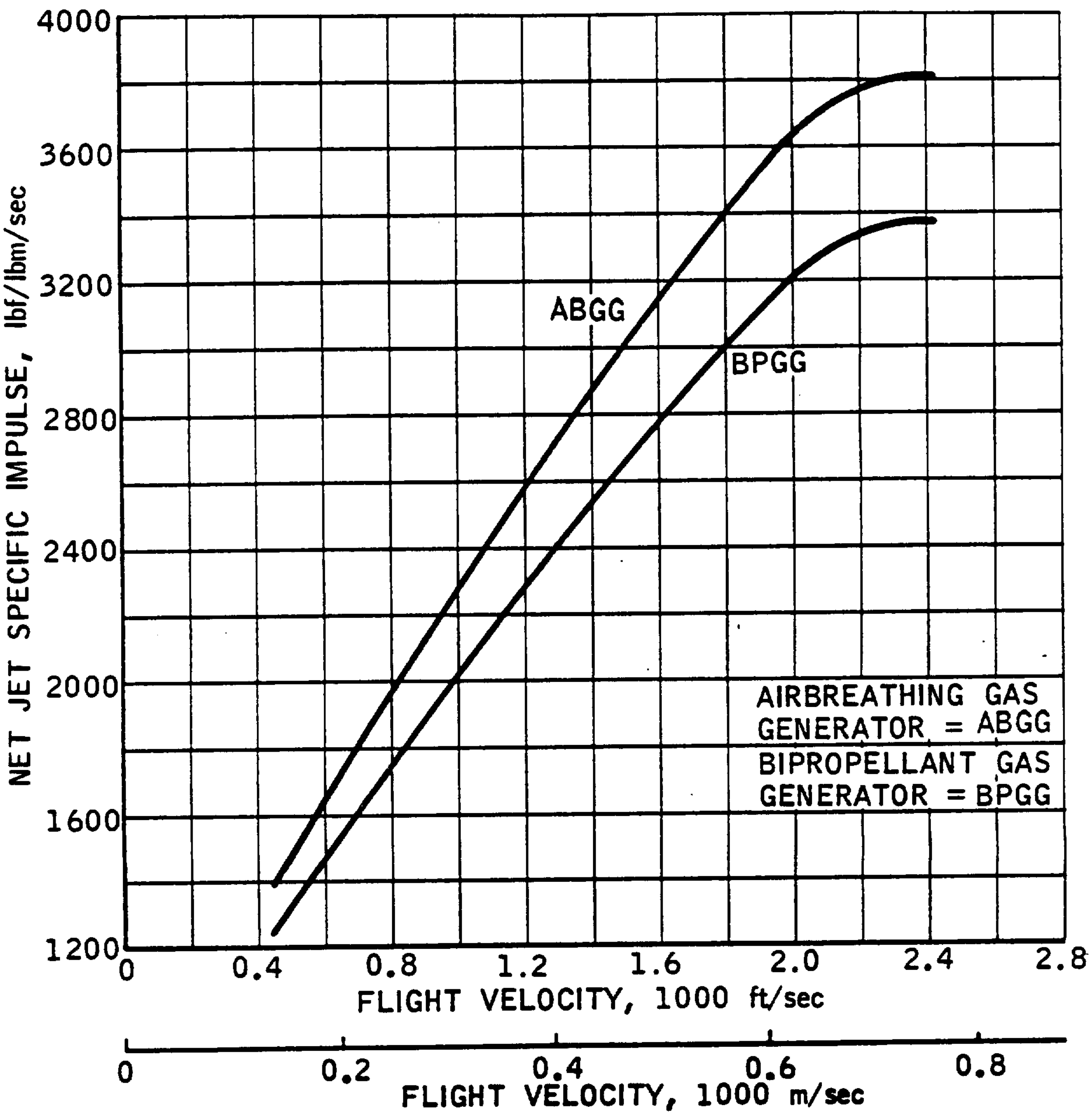

FIGURE 222. Fan Drive Comparison for the Supercharged Ejector Ramjet, Fan Ramjet Mode

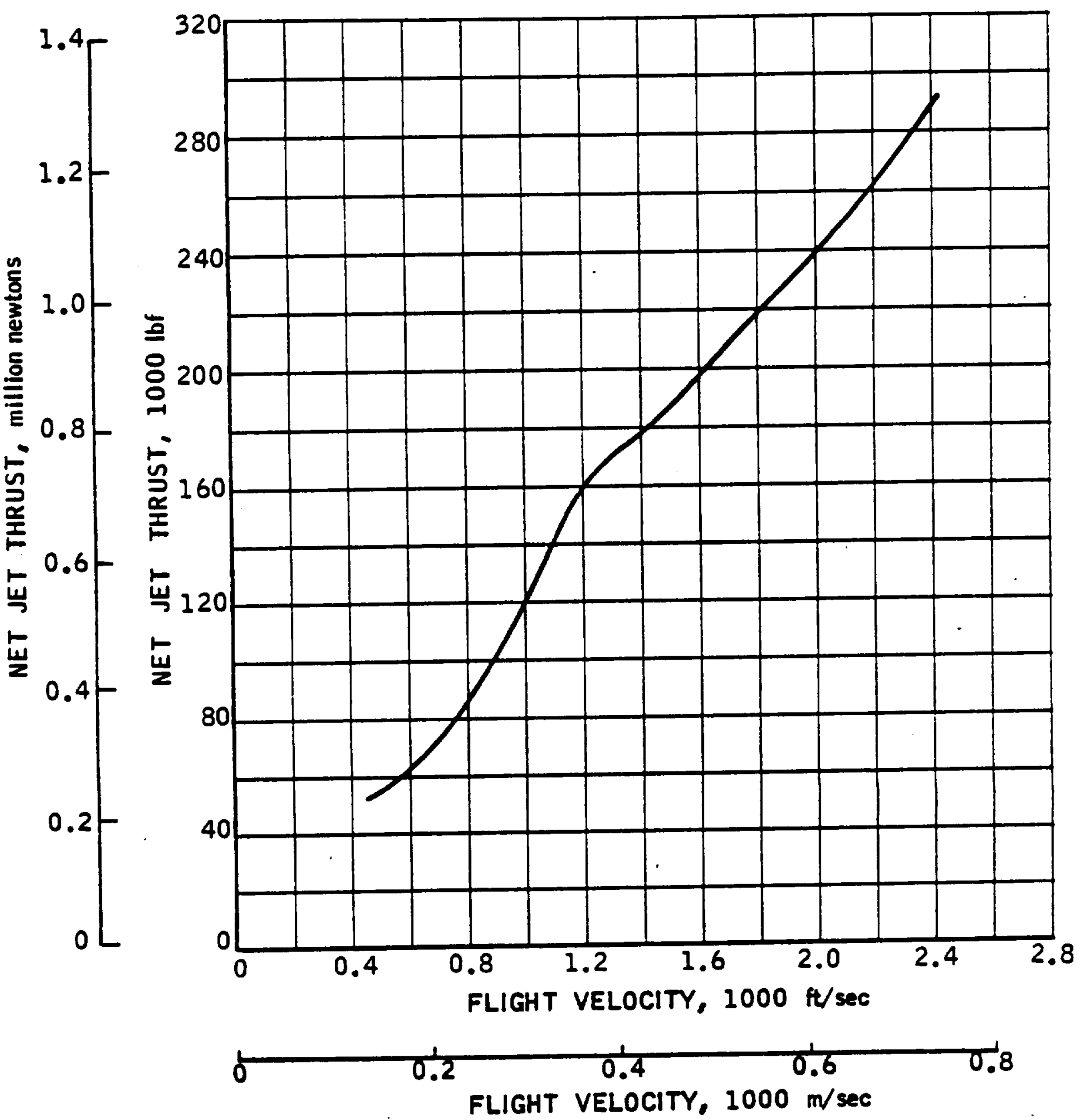

FIGURE 223. Thrust of the Supercharged Ejector Ramjet in the Fan Ramjet Mode

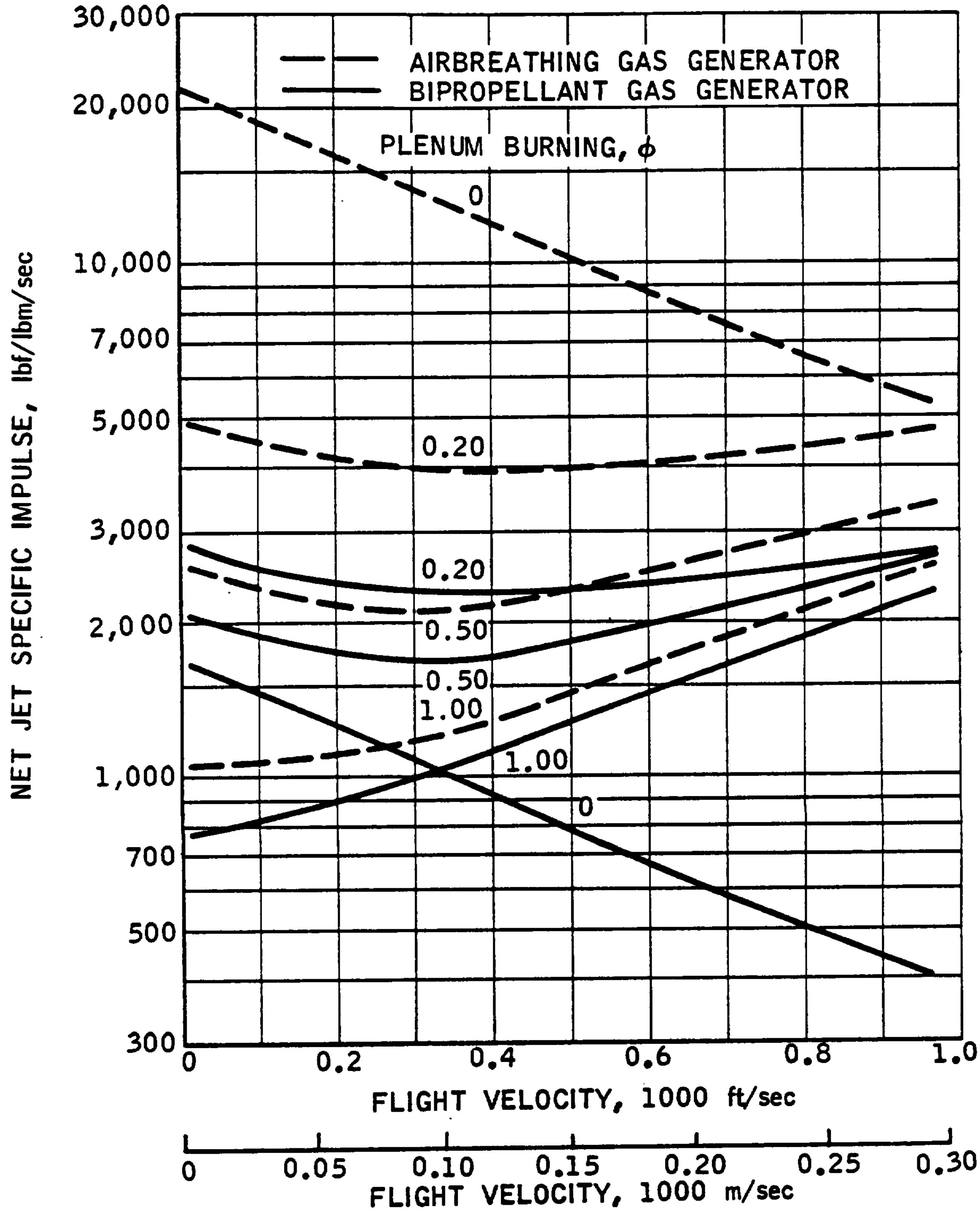

FIGURE 224. Fan Drive Comparison for the Supercharged Ejector Ramjet, Fan Operation

seconds for zero plenum burning at sea level static to several hundred for stoichiometric burning at Mach 1.0. The fuel-rich BPGG exhaust is sufficient to provide a plenum burning ϕ of about 0.23. Hence, at $\phi = 0$, the BPGG is assumed to be completely dumped overboard and at $\phi = 0.20$, the excess drive gas fuel is about 90 percent utilized. The propellant flow expense represented by the noncombustible portion of the BPGG exhaust, however, yields about a 50 percent impulse decrease at $\phi = 0.20$.

Figure 225 presents the corresponding thrust for fan operation. The design sea level static thrust of the Class 2 Supercharged Ejector Ramjet is 215,000 pounds. As shown in Figure 225, fan operation can provide about 10 percent of the engine design thrust at low subsonic flight speeds with a minimum of plenum burning. If this is sufficient for loiter (as demonstrated in the Class 2 vehicles studies), the ABGG provides a significant specific impulse advantage for extended loiter.

If the required level of loiter thrust dictates a large amount of plenum burning, the choice of an airbreathing or bipropellant gas generator drive will strongly depend on loiter time. This statement is made again, without consideration of fan drive mechanization.

8.2.2.2 Comparative Performance Evaluation and Sensitivity Study Results

The results of the Class 2 engine sensitivity analysis are presented in full detail in Volume 7. The significant component operating point variables and process efficiencies were varied over selected off-design ranges for all operating modes of both engines. Up to ten items (ejector mode operation) were evaluated for off-design performance effects.

For each selected efficiency or parameter level, all other items were held at the baseline value. Occasionally, specifically in the ScramLACE engine ejector mode, the parameter being investigated in turn affected other engine computational parameters, particularly engine air flow. For the supercharged Ejector Ramjet, anything affecting the mixing process (inlet pressure recovery, primary chamber equivalence ratio and efficiences, and the mixing efficiency itself) can cause the mixer exit to choke ($M_3 = 1.0$), thereby reducing the secondary air flow below that of the reference performance. The effect of this phenomenon was included in the analysis.

During operation in the ScramLACE ejector mode, the instantaneous hydrogen flow (sole vehicle stored propellant) is dictated by the air liquefaction requirements of the heat exchanger, not by the desired primary chamber and secondary air equivalence ratios. Hence, if the secondary air flow is reduced due to mixer choking, the afterburner equivalence ratio simultaneously increases, thus introducing the effect of another variable. Since the ScramLACE ejector mode typically chokes in the afterburning, any efficiency or variable except those concerning the exit nozzle may cause a secondary effect which is reflected in engine performance. This "internal compensation" effect

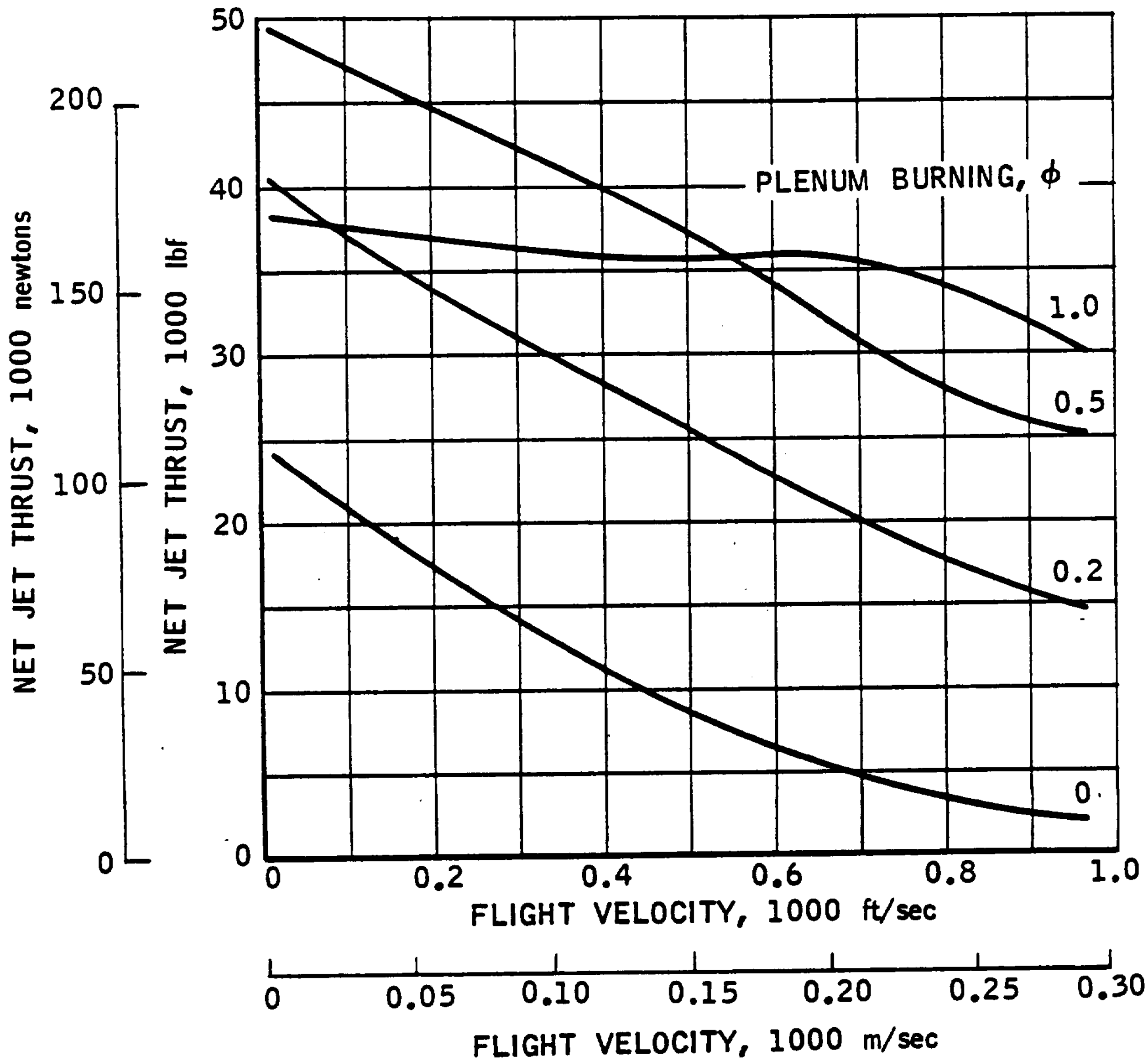

FIGURE 225. Thrust of the Supercharged Ejector Ramjet, Fan Operation

within the computational process is akin to an actual engine situation and should not be interpreted as invalidating the sensitivity analysis results.

Generally, in the sensitivity analysis results, the parameters that materially affected performance were not the typical component efficiencies, combustion efficiency, nozzle efficiency, etc., but parameters such as inlet pressure recovery, afterburner equivalence ratio, exit nozzle area ratio, and, for the SERJ (Engine No. 11), the fan pressure ratio. The selected ranges for these parameters were fairly broad and caused significant performance variations at certain flight conditions. A comparison of the effects of these more significant parameters for the ejector mode of both Class 2 engines follows.

8.2.2.2.1 Baseline Performance

For reference, the baseline specific impulse and thrust trends of the Class 2 engines are presented in Figures 226 and 227, respectively. The acceleration trajectory is that of Figure 219. Increasing specific impulse and thrust are shown for both engines with increasing flight speed reflecting typical increased augmentation with speed. Note that the design point sea level static thrust as shown in Figure 227 is 215,000 pounds for Engine No. 11 and 173,000 pounds for Engine No. 22. This, it will be recalled, is based on a five and six engine vehicle complement for the 1.0 million lbf gross weight vehicle, with payload - maximum thrust/weight ratios.

8.2.2.2.2 Effect of Inlet Recovery

The sensitivity analysis range of inlet pressure recovery is presented in Figure 228. The baseline recovery shown applies specifically to Engine No. 22 in the Mach 3.0 to 6.0 range. Figure 228 is used here to show the Mach 0 to 3.0 inlet recovery which was the same for both engines. Also note that the reduced subsonic flight speed regime recovery is not indicative of a normal shock inlet in this speed regime. The reduced recovery of 0.90 was selected to illustrate the performance effects and it has been integrated with the normal shock inlet characteristic (which is supersonic only) in the following figures for convenience and continuity.

Since the ScramLACE ejector mode has both a secondary air flow and a primary (liquefied) air flow, processed by the air liquefying heat exchanger, the assessment of inlet pressure recovery effects must include both the main engine throughout (mixer) and the heat exchanger. Figure 229 presents the variation in heat exchanger equivalence ratio along the reference trajectory to liquefy a constant amount of primary chamber air flow. The baseline schedule reflects the off-design heat exchanger characteristics utilized in Class 2 Engine No. 22 performance maps discussed earlier. The ϕ_{HX} = 8.0 for the initial portion of the normal shock inlet line

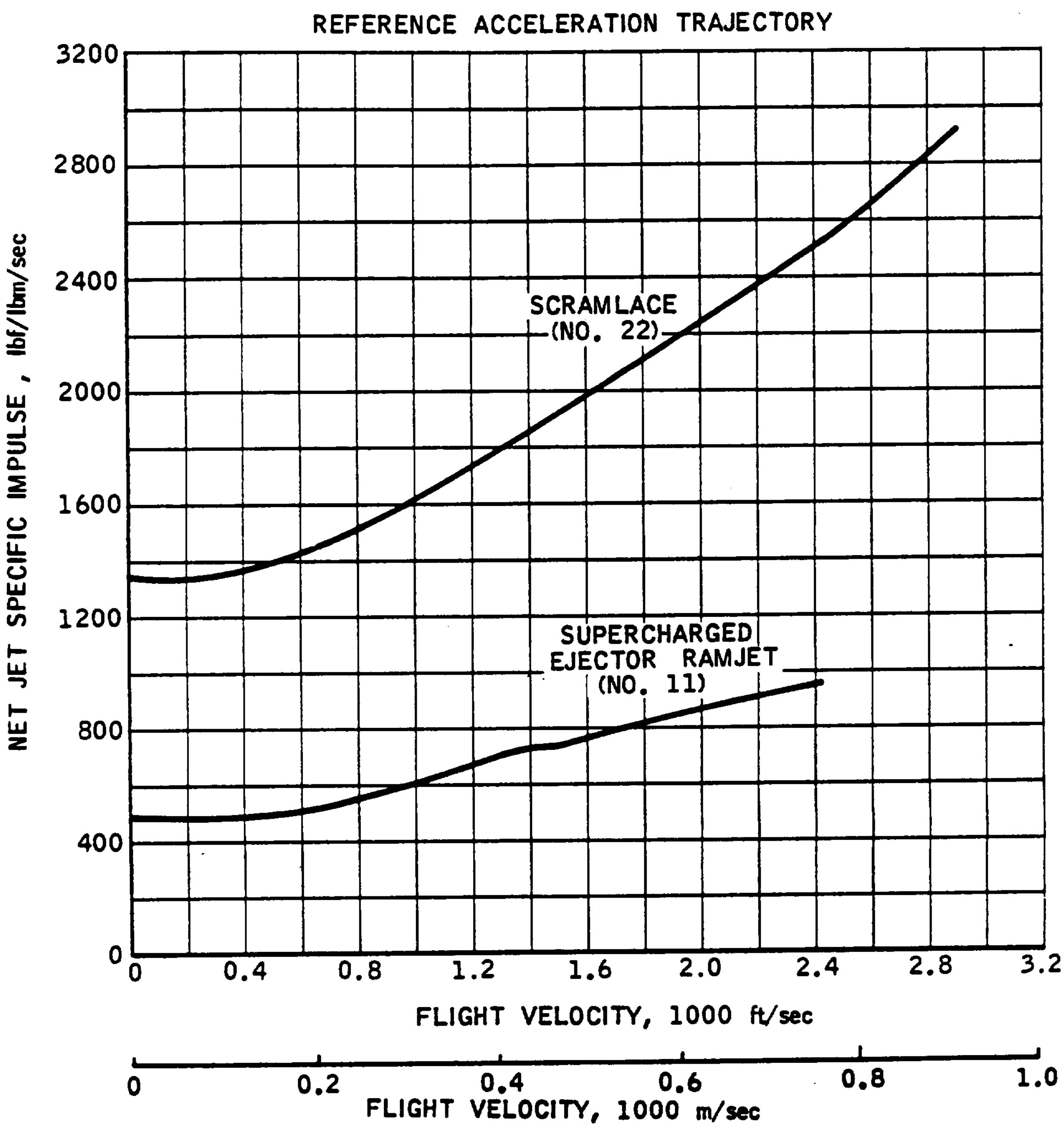

FIGURE 226. Specific Impulse Comparison for Class 2 Engines, Ejector Mode

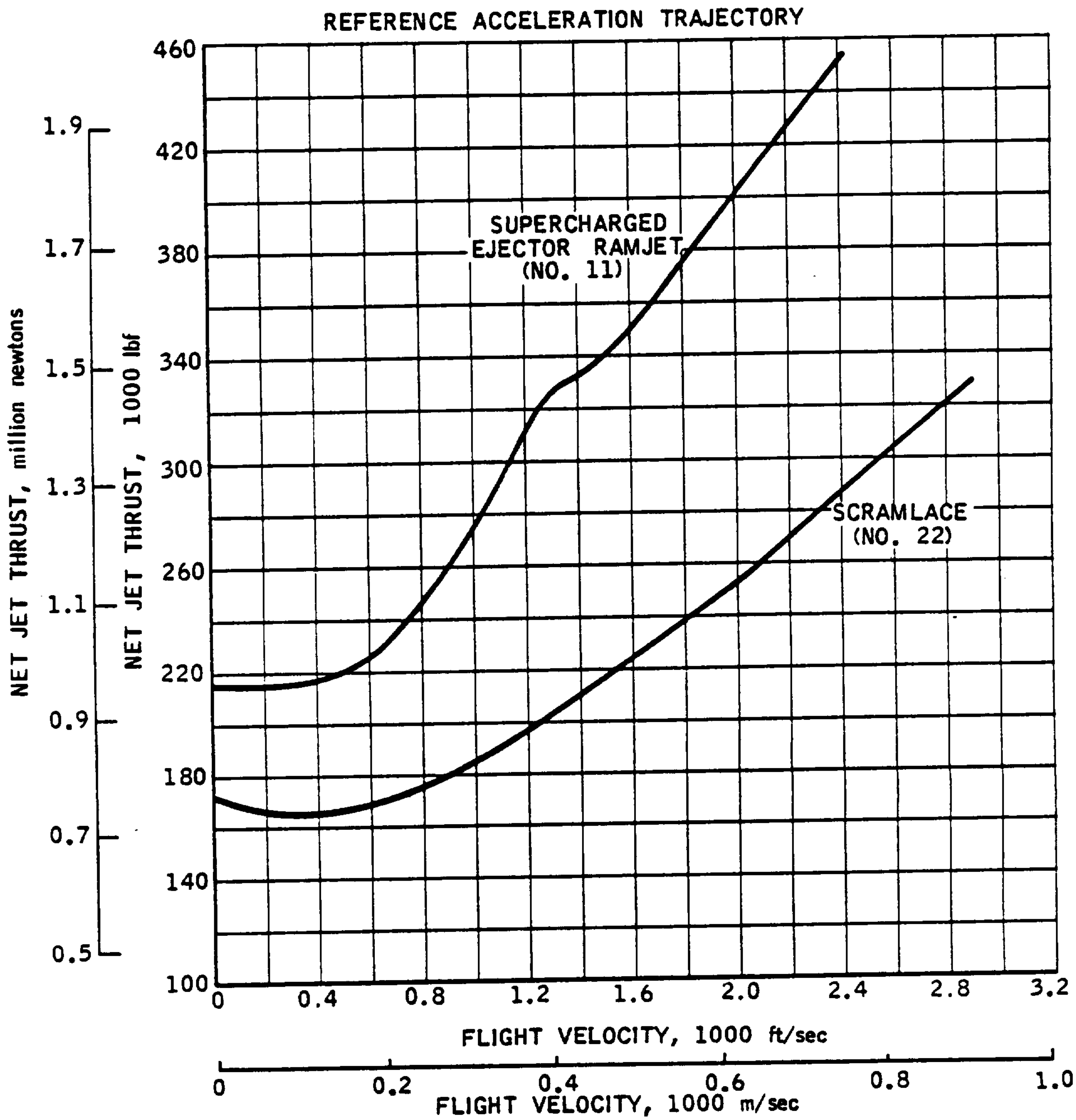

FIGURE 227. Thrust Comparison for Class 2 Engines, Ejector Mode

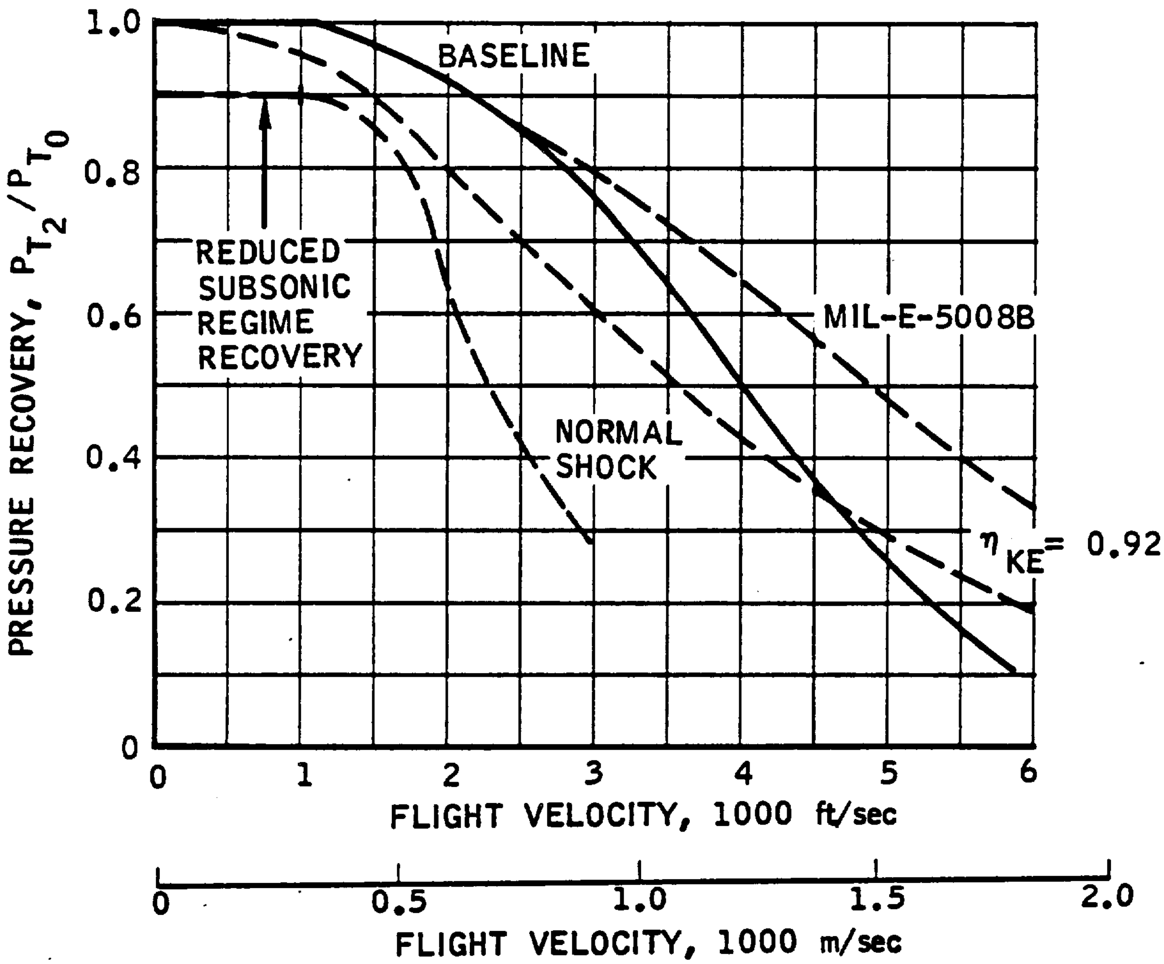

FIGURE 228. Inlet Pressure Recovery Sensitivity Analysis for the ScramLACE

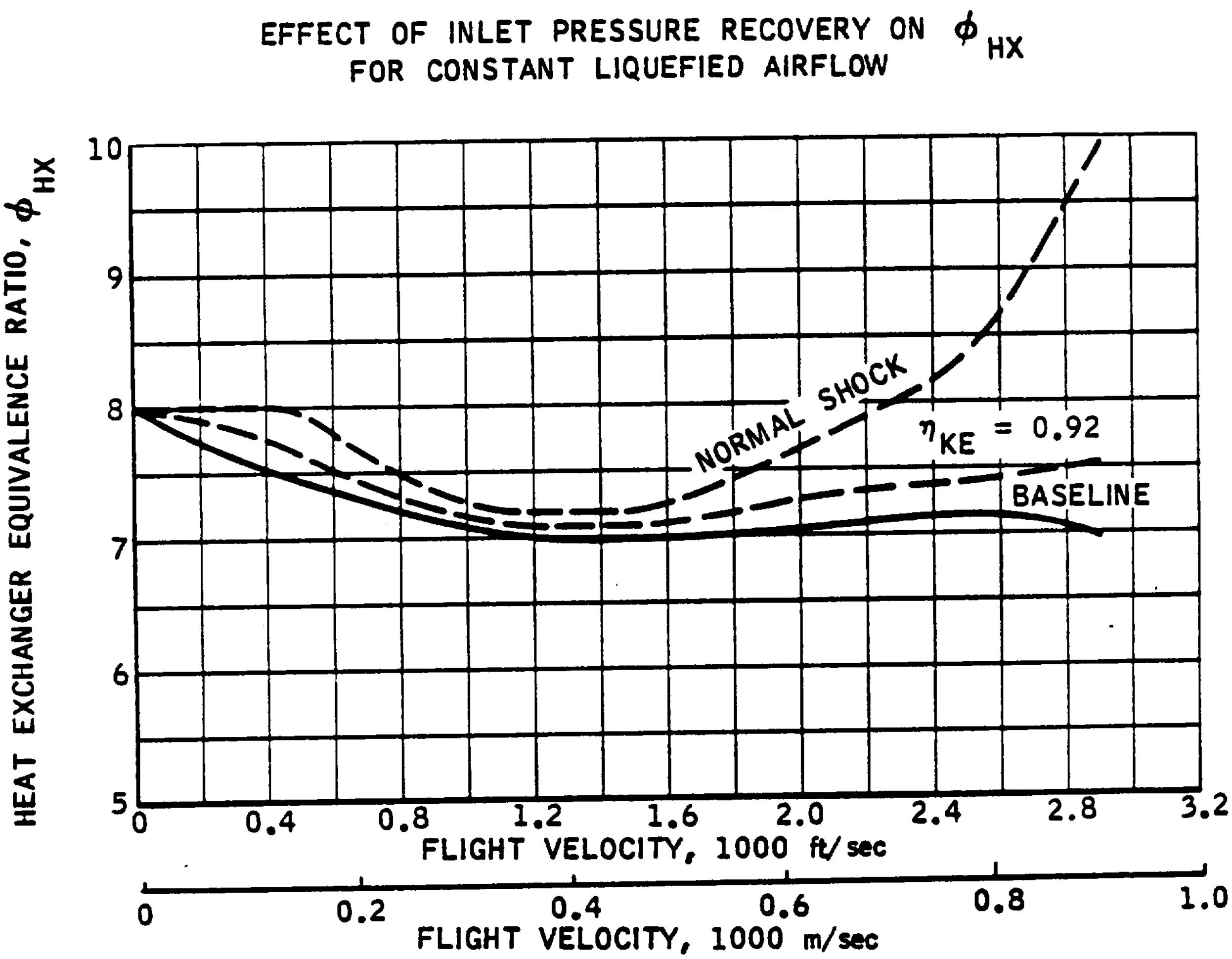

FIGURE 229. Heat Exchanger Equivalence Ratio Sensitivity Analyses Ratio, Ejector Mode

in Figure 229 was assumed and the 0.90 reduced inlet recovery in the 0 to 500 ft/sec flight speed regime was reflected in a reduced liquefied air flow. This instance is the only exception to the constant air flow specified. Figure 230 presents the resulting afterburner equivalence ratio for the ϕ_{HX} schedules of Figure 229. Note that the reduced liquefied air flow at very low flight speeds for the normal shock inlet line is directly reflected in the reduced ϕ_{AB} in Figure 230. A reduction in liquefied air flow means less total fuel relative to the other reference inlet recovery lines at sea level static (all ϕ_{HX} values = 8.0). Also, the low recovery was noted to reduce the heat exchanger air to a greater degree than the secondary air flow.

The effect of inlet pressure recovery on the ejector mode performance of both engines is presented in Figures 231 and 232. Figure 231 shows the specific impulse variation. The higher flight speed normal shock inlet effect for Engine No. 22 is amplified by the adversely high ϕ_{HX} and ϕ_{AB} for this inlet at these conditions. Thrust variations are shown in Figure 232. The reduced subsonic flight speed regime recovery has a greater effect on Engine No. 22 than on Engine No. 11 due to the compound effect of reduced liquefied air flow. Quite similar effects are shown for both engines for most of the flight speed regime. It should be noted in both Figures 231 and 232 that a normal shock inlet (decoupled from the low subsonic regime recovery) is a fairly adequate inlet up to about Mach 1.5.

8.2.2.2.3 Effect of Afterburner Equivalence Ratio

Another significant variable in off-design performance was the afterburner equivalence ratio. For the Supercharged Ejector Ramjet, ϕ_{AB} was varied from the design point (1.00) up to 1.50 and down to 0.50. The afterburner equivalence ratio for the ScramLACE engine is intrinsically tied to the heat exchanger equivalence ratio as seen in the previous discussion and figures.

For a comparison of the two Class 2 engines on the basis of ϕ_{AB}, a nominal heat exchanger equivalence ratio variation was selected as shown in Figure 233. The baseline schedule was perturbed by a nominal plus and minus one ϕ_{HX} unit. The resulting ϕ_{AB} variation is shown in Figure 234.

Specific impulse and thrust variations for this ϕ_{AB} schedule for Engine No. 22 and the preselected variation quoted above for Engine No. 11 are presented in Figures 235 and 236, respectively. Engine No. 22 shows a moderate effect on specific impulse in Figure 235 and Engine No. 11 is only slightly affected by the ϕ_{AB} variation. The thrust effects, as shown in Figure 236, are reversed. A low ϕ_{AB} has a significant effect on the thrust of Engine No. 11 and a high ϕ_{AB} provides only a slight thrust increase. The fuel-rich ScramLACE is essentially unaffected by the ϕ_{AB} variation which, it will be recalled, only varies the degree of richness in an inherent fuel-rich cycle.

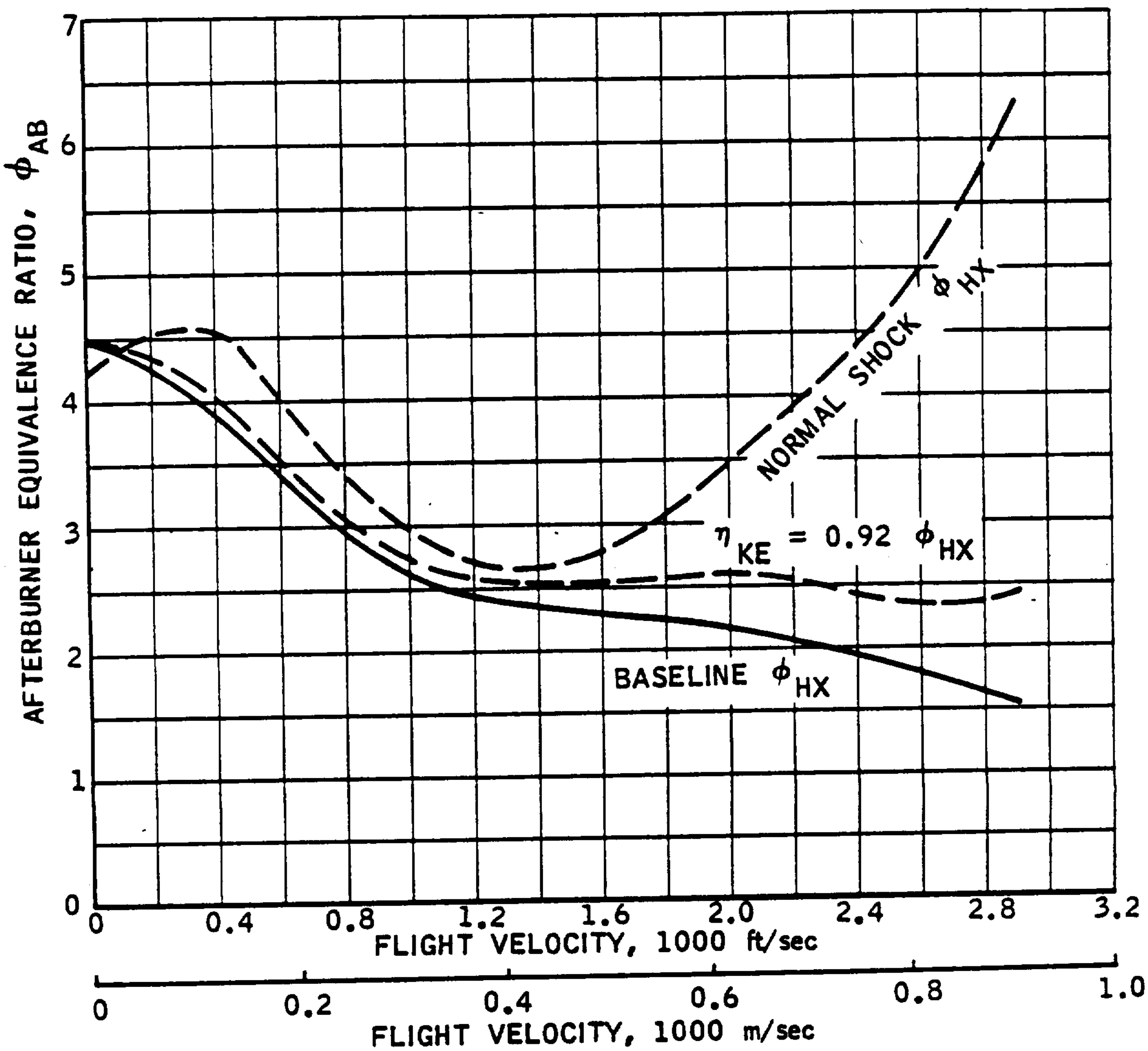

FIGURE 230. Afterburner Equivalence Ratio Sensitivity Analysis Range for the ScramLACE Engine, Ejector Mode

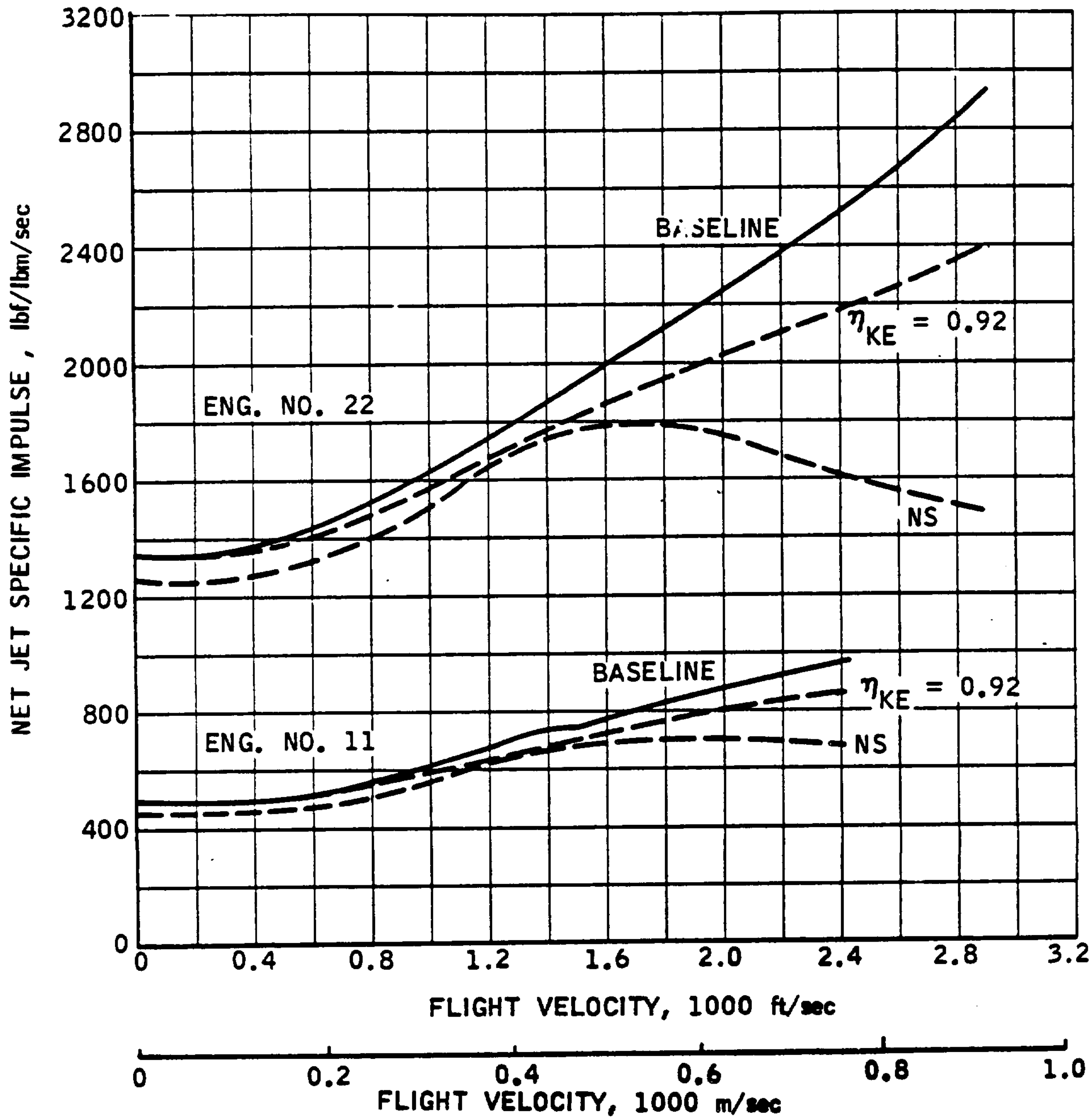

FIGURE 231. Specific Impulse Comparison for Class 2 Engines, Effect of Inlet Pressure Recovery, Ejector Mode

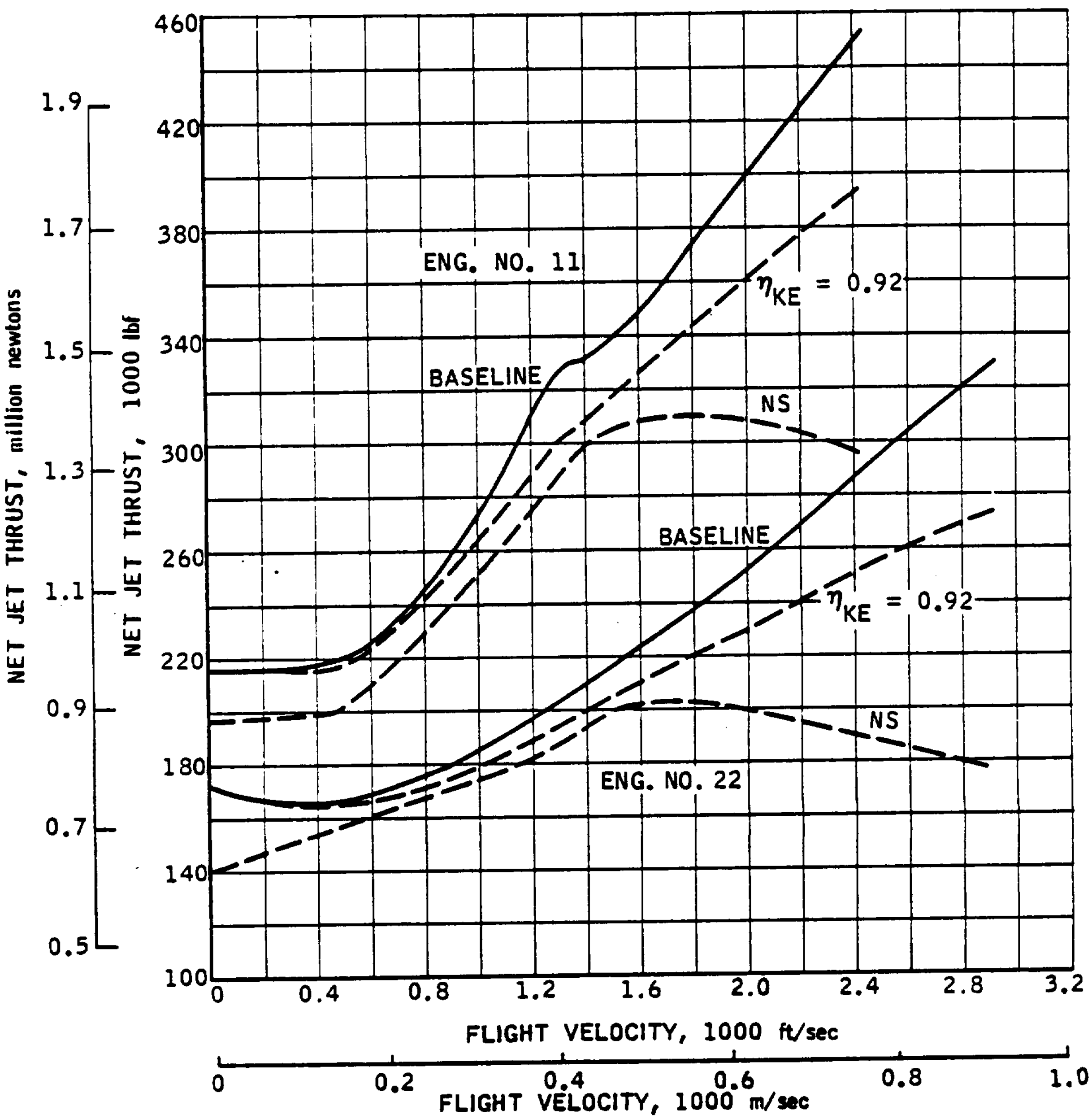

FIGURE 232. Thrust Comparison for Class 2 Engines, Effect of Inlet Pressure Recovery, Ejector Mode

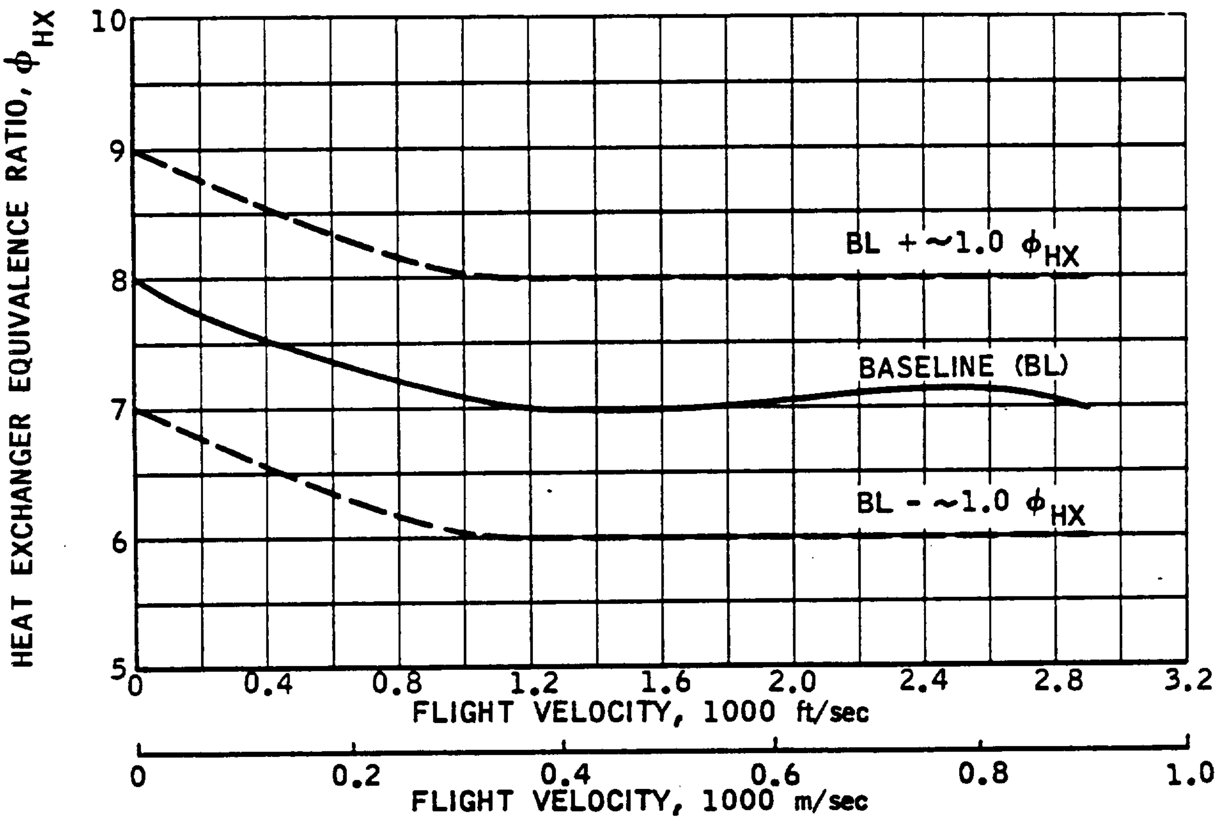

FIGURE 233. Heat Exchanger Equivalence Ratio Sensitivity Analysis Range for the ScramLACE, Ejector Mode

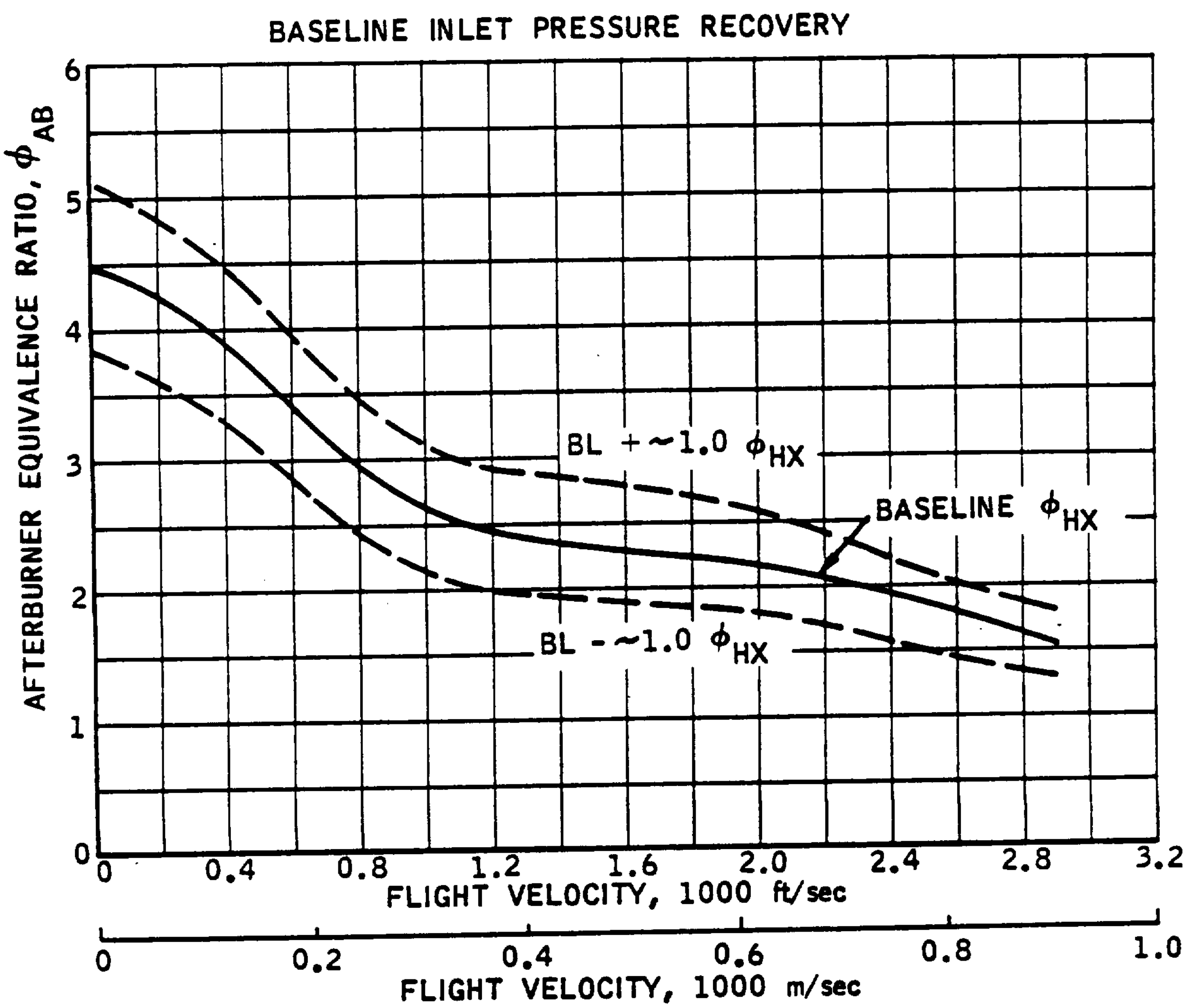

FIGURE 234. Afterburner Equivalence Ratio Sensitivity Analysis Range for the ScramLACE, Ejector Mode

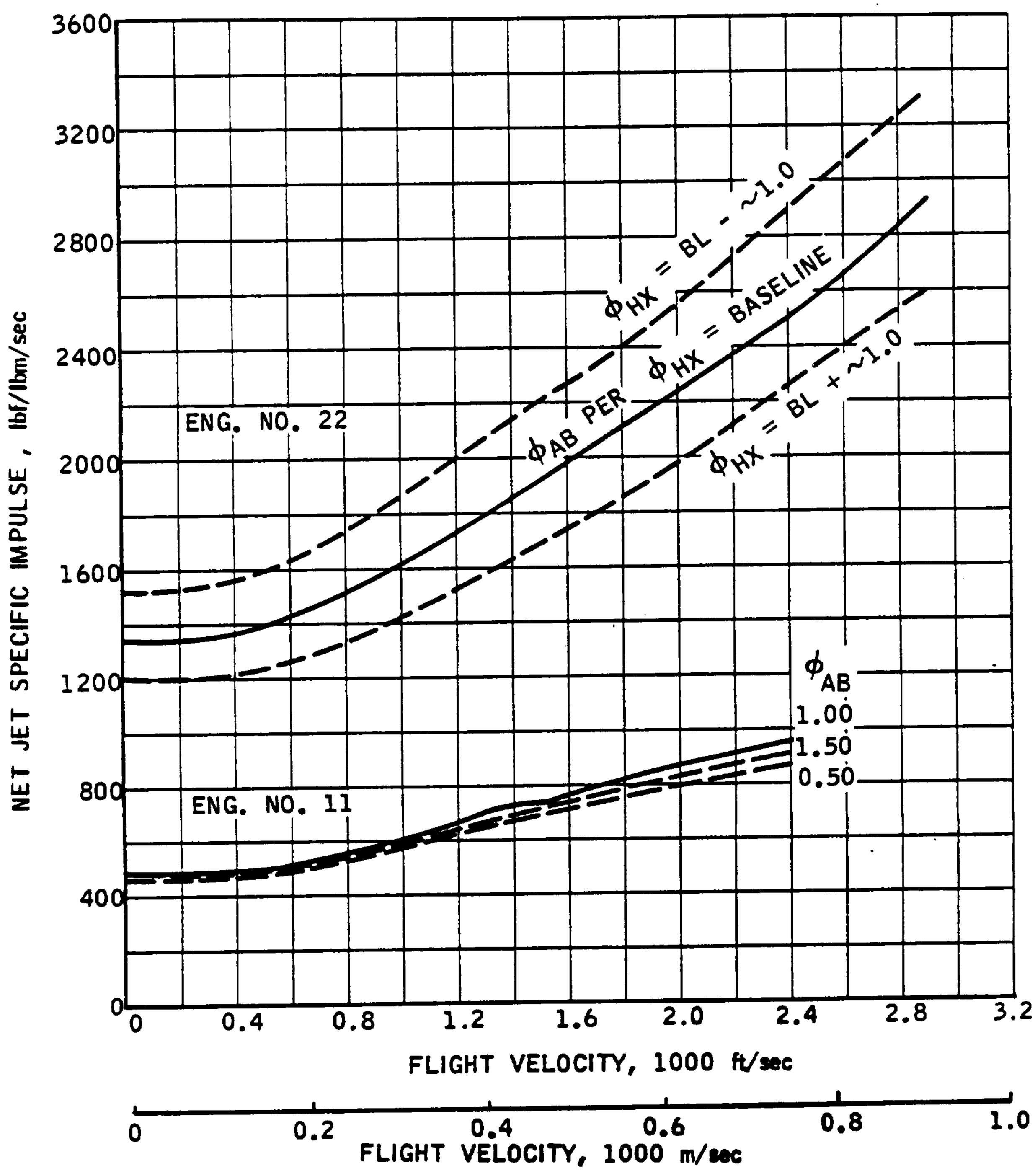

FIGURE 235. Specific Impulse Comparison for Class 2 Engines, Effect of Afterburner Equivalence Ratio, Ejector Mode

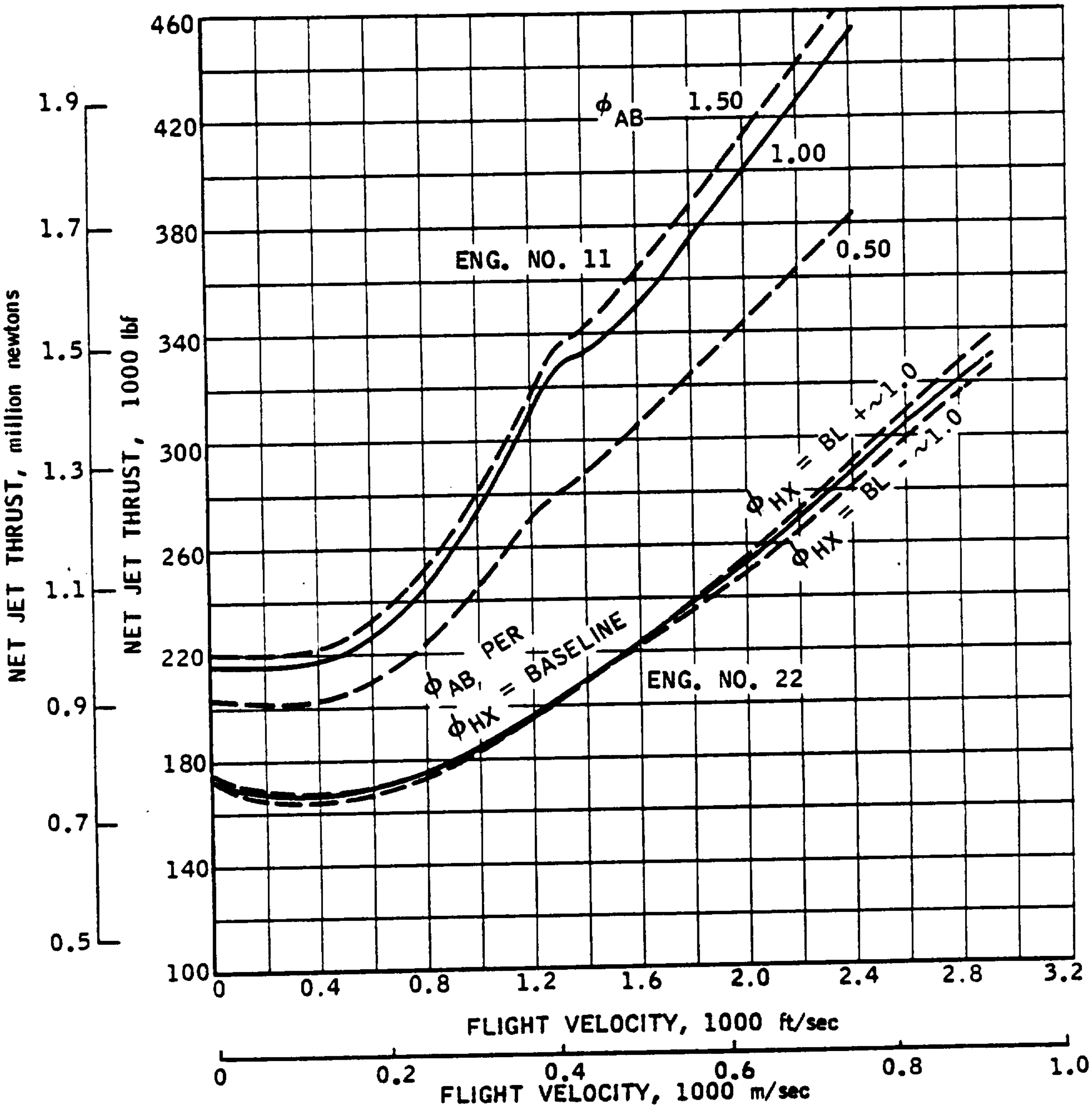

FIGURE 236. Thrust Comparison for Class 2 Engines, Effect of Afterburner Equivalence Ratio, Ejector Mode

8.2.2.2.4 Effect of Exit Nozzle Area Ratio

For the sensitivity analysis study of the exit nozzle area or expansion ratio (A_6/A_5), the baseline ratio from the reference case was varied plus and minus 25 percent. The variation of the baseline (BL) expansion ratio with flight speed and the perturbation values are presented in Figures 237 and 238 for Engines Nos.11 and 22, respectively. As shown in both figures, the reduced expansion ratio (0.75 BL) was evaluated only in the flight speed range where the resulting absolute A_6/A_5 value was greater than 1.0.

In Figure 237, the change in the slope of the baseline A_6/A_5 curve at 1500 ft/sec flight velocity and the moderate increase in A_6/A_5 thereafter is due to an A_6 limit for Engine No. 11. In the flight velocity range from 1500 to 2400 ft/sec, A_6 is constant at the limit and the increase in A_6/A_5 is due to a decreasing A_5 (exit throat area) with flight speed. Hence, the increased expansion ratio (1.25 BL) in this velocity regime provides Engine No. 11 with semioptimum expansion as can be seen in the following performance figures. The ScramLACE Engine No. 22 utilizes the vehicle aft surface for expansion and the baseline A_6/A_5 line in Figure 238 represents optimum expansion.

The effects of the expansion ratio variations on the specific impulse trends of both Engines Nos. 11 and 22 are presented in Figure 239. For engine No. 22 with a baseline optimum expansion, both variations cause a slight performance decrease. The effect diminishes with increasing flight speed and is better in performance with underexpansion than with overexpansion.

Engine No. 11 shows about the same percentage performance loss in specific impulse for overexpansion at low flight speeds and indicates a greater loss for underexpansion at the higher flight speeds. The overexpansion case for Engine No. 11 at higher flight speeds is actually nearer optimum as discussed above and provides a slight performance increase.

The expansion ratio effects on thrust are presented in Figure 240. Identical trends to the specific impulse variations are shown. The percentage losses or gains are the same for both thrust and specific impulse with the expansion ratio variable as can be seen in the sensitivity result plots of the Class 2 Engine Information Book (Volume 7).

8.3 Primary Rocket Subsystem Design

For the Class 2 Composite Engine selected, Rocketdyne performed the task of carrying out detailed conceptual designs of the primary rocket subsystem. This comprised the thrust chamber and primary and afterburner turbopump elements. Also considered was the entire subsystem packaging aspect, including external cooling provisions for those sections exposed to the high temperature recovery air reached at high vehicle flight speeds. Two oxidizers (liquid oxygen and liquid air) were evaluated, with liquid hydrogen being the fuel.

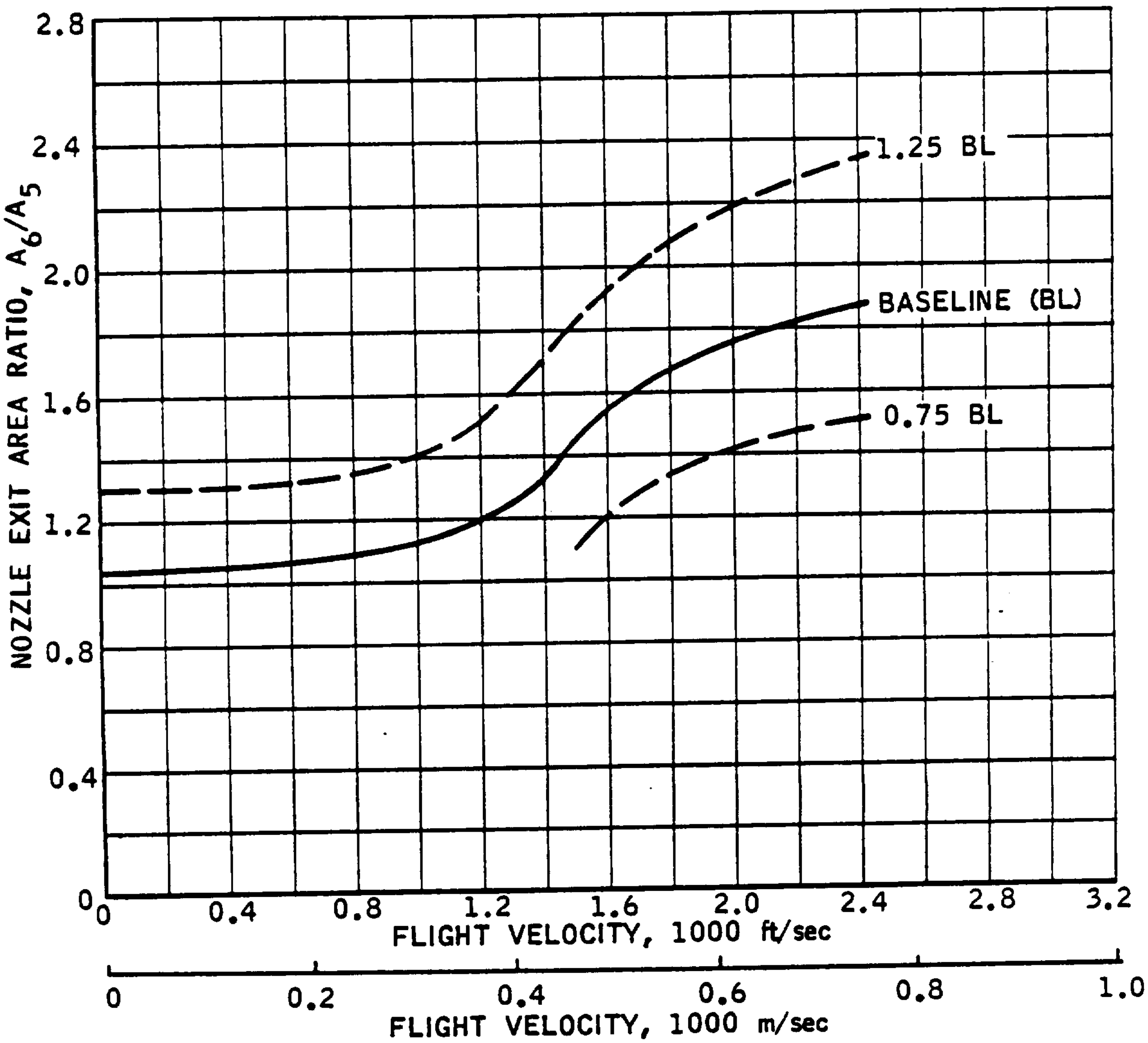

FIGURE 237. Exit Nozzle Area Ratio Sensitivity Analysis Range for the Supercharged Ejector Ramjet, Ejector Mode

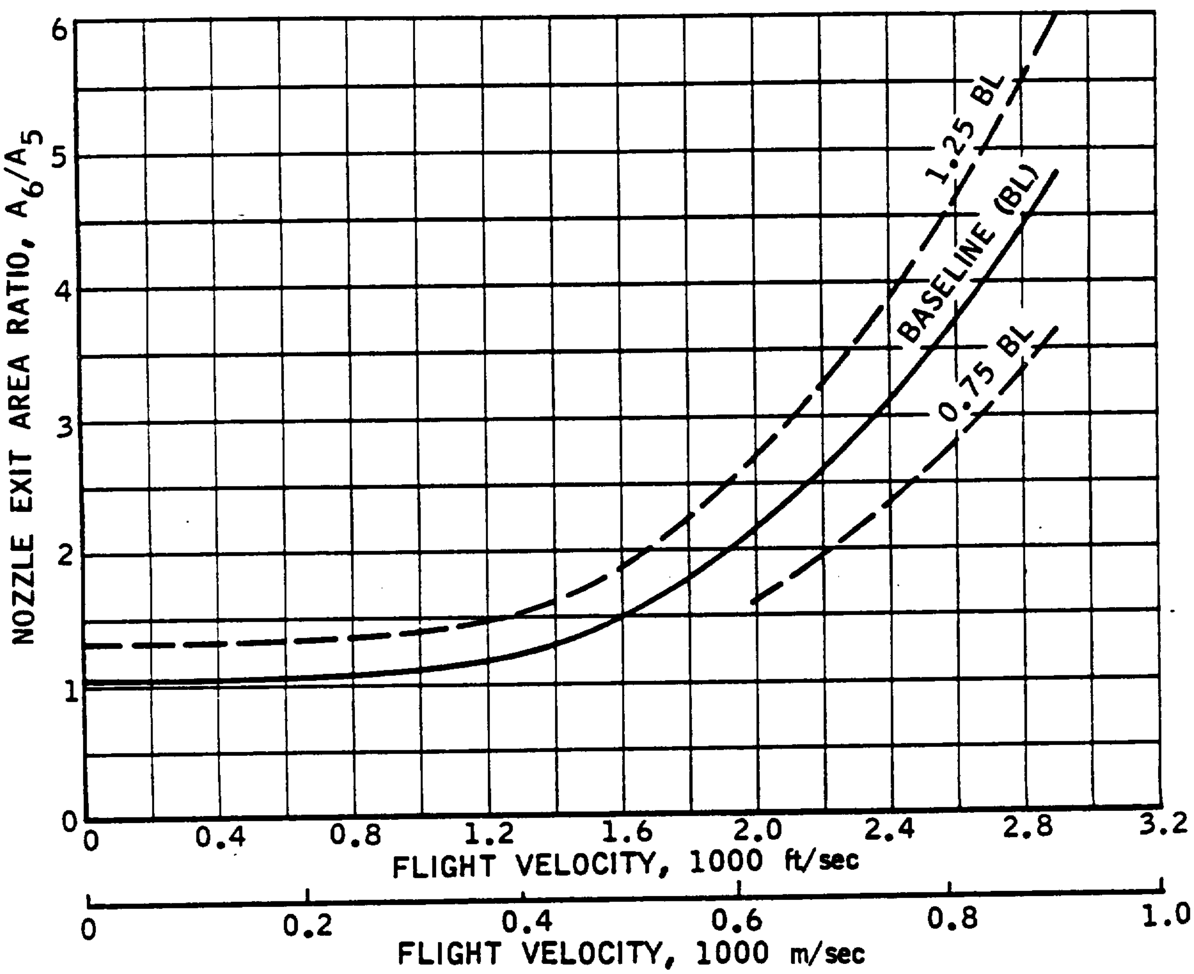

FIGURE 238. Exit Nozzle Area Ratio Sensitivity Analysis Range for the ScramLACE, Ejector Mode

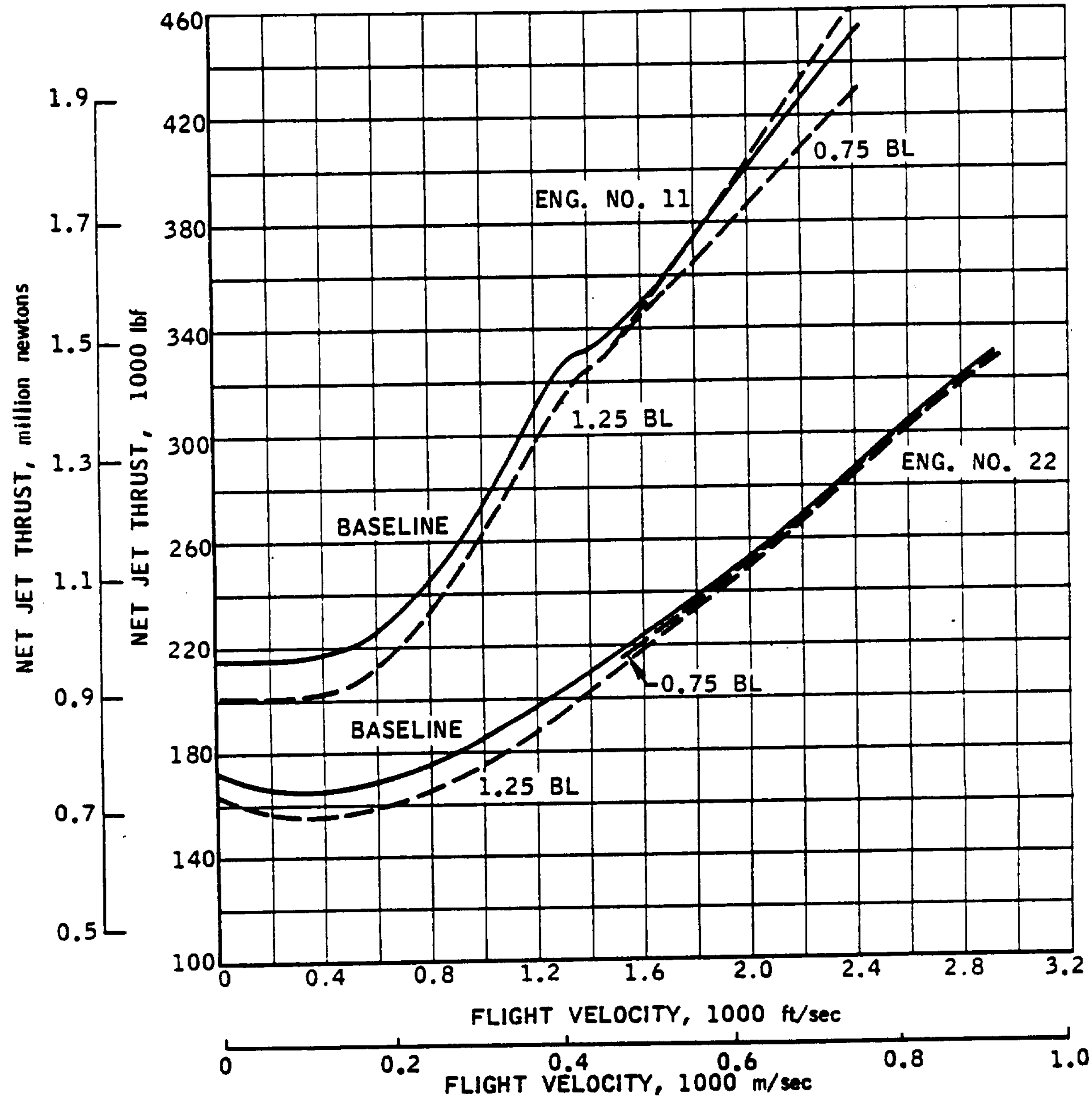

FIGURE 239. Thrust Comparison for Class 2 Engines, Effect of Exit Nozzle Area Ratio, Ejector Mode

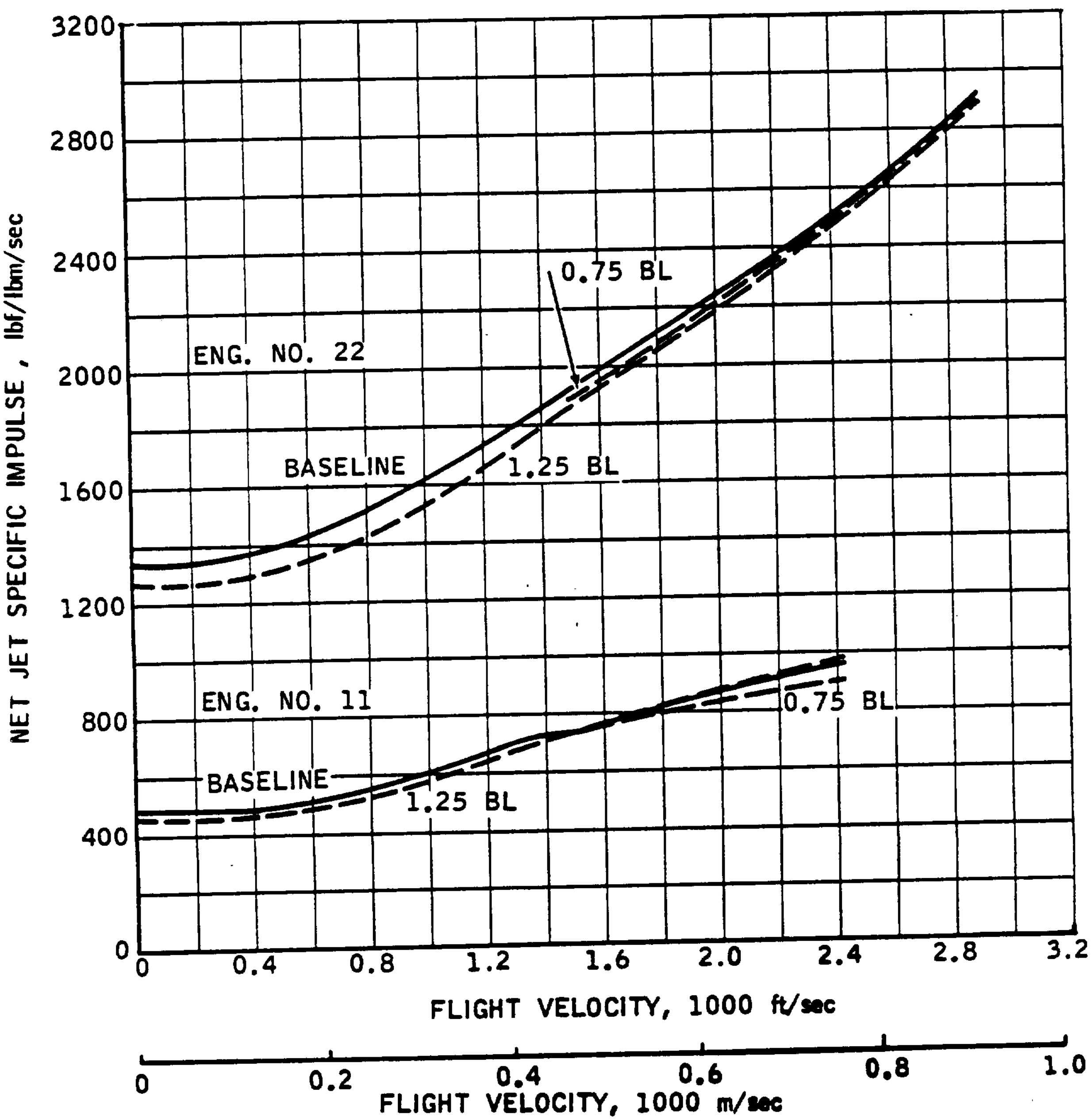

FIGURE 240. Specific Impulse Comparison for Class 2 Engines, Effect of Exit Nozzle Area Ratio, Ejector Mode

For the two point-design engines, the primary rocket performance was defined and specific configurations were established to permit overall subsystem envelopes and weight estimates to be achieved. This established a basis for the overall composite engine designs to be subsequently described (Section 8.4.2).

8.3.1 Methodology

A description of the basic specifying constraints on the Class 2 primary subsystem designs is provided in this section. The techniques used for the heat transfer and cooling, nozzle aerodynamics, turbomachinery, and hardware weight analyses are briefly covered. The results are summarized below.

8.3.1.1 Configuration Selection

The nominal design parameters of the rocket primaries for the Class 2 composite engines (Supercharged Ejector Ramjet (Engine No. 11) and ScramLACE (Engine No. 22)) are listed below:

Composite Engine	No. 11	No. 22
Propellants	LO_2/H_2	$LAIR/H_2$
Design thrust (sea level), lbf	162,200	102,600
(Final thrust value, lbf)*	(139,500)	(106,500)
Specific impulse, lbf-sec/lbm	354.2	205.1
Chamber pressure, psia	1500	1000
Mixture ratio (O/F)	8:1	34.3:1
Exit pressure, psia	18.0	10.6
Nozzle area ratio	12.45	9.66

A specific impulse efficiency of 96 percent was used to calculate the above data.

- - - - - - - - - -

*In the final Class 2 vehicle/engine integration effort, the thrust values changed somewhat. For both Engines Nos. 11 and 22, the primary rocket design thrust corresponding to these "final" values are those given in parentheses. Since there is no fundamental design implication in this change, no attempt has been made to "update" the primary rocket design given here.

The chamber pressure of the rocket primary to be used in the Class 2 Ejector Ramjet engine is 1500 psia. This is lower than the 2000 psia used previously for the Class 1 engine evaluation. The reduction in the rocket operating pressure for the Class 2 work was due to the following factors:

1. The reusable connotation inherent in this study of composite engines for advanced launch vehicles makes some design margin desirable.

2. The possibly severe regenerative coolant tube oxidation problem at the specified rocket mixture ratio of 8:1 has not been fully appraised.

3. The Supercharged Ejector Ramjet engine has, relative to the ScramLACE engine, a nearer term, lower technical risk association. Hence, it is not desirable to push the technological limits involved with chamber cooling.

8.3.1.2 Primary Rocket Heat Transfer Analysis

A parametric thermal analysis of the rocket primaries for the Class 2 engines was conducted. The LO_2/H_2 and $LAIR/H_2$ primaries were examined at stoichiometric mixture ratios and 1500 and 1000 psia chamber pressures, respectively. Thrust variations of plus and minus 50 percent from the nominal were investigated. Regenerative tube materials of stainless steel, copper, and molybdenum alloy were considered for the LO_2/H_2 engine whereas only the first two materials were considered for the $LAIR/H_2$ engine.

The tube size is of interest, since fewer tubes generally result in a lower cost engine. For a given engine size, coolant flow rate ($\dot{W}_c$), mass velocity requirement (G), and wall thickness (t), the following equation can be obtained for a round tube of outside diameter d_o:

$$\frac{(d_o - 2t)^2}{d_o} = \frac{4}{\pi^2} \frac{\dot{W}_c}{G D \eta}$$

where η is the fraction of the engine circumference cooled on a given pass and D is the overall diameter of the annular rocket primary. The important items determining the tube size are thus seen to be the coolant flow rate avaliable per unit of engine circumference, the mass velocity requirements, and the coolant pass arrangement.

Another consideration in determining the feasibility of a hydrogen coolant design is the coolant pressures required to prevent a choking condition (Mach 1.0) in the tubes. Although this is not a problem with the LAIR/H_2 engine nor with the molybdenum alloy tubes in the LO_2/H_2 engine, because of the low coolant velocities required, it is a limitation with copper and stainless steel for the LO_2/H_2 case. Since the mass velocity is a function of both density and velocity, which in turn are a function of temperature and pressure, a minimum coolant pressure can be determined for a given mass velocity and coolant temperature, as well as a coolant Mach number. A Mach number of 0.5 was chosen as being a nominal design condition.

8.3.1.3 Nozzle Contour Analysis

The Class 2 rocket primaries were analyzed to determine the nozzle wall contours for maximum performance. The nozzle configuration used in all cases was an annular bell design. A summary of the design parameters is given in Table XLIII. The specific heat ratio (γ) was assumed to be constant and equal to a mean representative value for the products of combustion for each case. A value of $\gamma = 1.13$ was used for the LO_2/H_2 engine and $\gamma = 1.28$ for the LAIR/H_2 engine. The nozzles were designed to give exit pressures of 18.0 psia and 10.6 psia for the LO_2/H_2 and LAIR/H_2 engines, respectively.

The nozzle analysis and design procedure has been discussed previously (Section 7.3.1.3) and it will not be repeated here.

8.3.1.4 Turbopump Studies

The turbomachinery requirements of the selected Class 2 composite engines were studied to (1) establish the preliminary advanced turbopump designs for these engines and (2) indicate the technological implications of these designs. Generally, the basic design criteria for flight type turbopumps are reliability, efficiency, weight, and size. High reliability is achieved by having design simplicity and through proven component usage. High efficiency, light weight, and compact size are achieved by a high rotational speed design. The highest speed that can be used, however, will depend on the technological limits in the areas of suction performance, rolling contact bearing DN, dynamic seal rubbing velocity, and the structural integrity of the rotating components.

For convenience in notation, the primary rocket fuel turbopump, primary rocket oxidizer turbopump, and ramjet afterburner fuel turbopump will be called turbopumps A, B, and C, respectively. All of the turbopumps for the Supercharged Ejector Ramjet engine will bear the number 11 as a subscript while those for the ScramLACE engine will have the number 22 as a subscript.

TABLE XLIII

SUMMARY OF NOZZLE GEOMETRY FOR CLASS 2 ROCKET PRIMARIES*

Propellants	LO_2/H_2	$LAIR/H_2$	
Chamber Designation	--	Inner	Outer
Mixture ratio (O/F)	8:1	34.3:1	34.3:1
Chamber pressure, psia	1500	1000	1000
Thrust (sea level), lbf	162,200	41,800	60,800
γ	1.13	1.28	1.28
R_t, in.	4.68	2.99	3.61
Area ratio	12.45	9.66	9.66
C_F	1.8087	1.6769	1.6769
$C_F/C_{F_{ideal}}$	0.9936	0.9890	0.9890
X/R_t	1.230	0.916	0.7525
Y_{o_1}/R_t	7.428	7.496	9.008
Y_{o_2}/R_t	7.154	7.223	8.783
ρ/R_t	0.1029	0.10184	0.08435
R/R_t	0.103	0.102	0.084
Y_{e_1}/R_t	7.716	7.688	9.171
Y_{e_2}/R_t	6.861	7.029	8.621

* See Figure 98 (in Volume 2) for nozzle nomenclature

A LO_2/H_2 gas generator system was used to power all the turbopumps considered. The gas generator operated at the primary rocket chamber pressure and its mixture ratio of 1.25:1 produced 1500°F combustion products for the turbines. The possibility of using a liquid air/hydrogen gas generator system for operation with Engine 22 was not investigated. It is believed that the power requirements and resulting flow rates would, perhaps, rule out such a system.

The turbopump performance requirements for both composite engines are shown in Table XLIV. Liquid hydrogen is used as the fuel for both the rocket and ramjet engines; however, liquid oxygen is used as the oxidizer for Engine No. 11 and liquid air for Engine No. 22. The ramjet turbopumps have a flow excursion of over a factor of 2 for a constant pump discharge pressure of 1000 psia. The inlet pressure or NPSH (Net positive suction head) available to the oxidizer pumps is seen to be quite low. The turbine exhaust gases are ducted into the ramjet combustion section to best utilize the very fuel-rich exhaust. In order to prevent any back pressure effects on the turbines, the turbine exit pressure must be sufficiently high to choke the exhaust gases at the injection point into the afterburner chamber. This is indicated in Table XLIV.

8.3.1.5 Weight Analysis

Primary rocket subsystem weight estimates derived from the detailed conceptual design layouts are described. Estimation techniques associated with conventional rocket system preliminary weight studies were used. Cooling tube weights derived directly from the heat transfer analysis results (Section 8.3.2.3) and turbopump weights were found to be a strong function of operating speed assumptions (Section 8.3.2.5.1).

The bases for the overall Class 2 composite systems, in the primary rocket as a major subsystem, are given in Section 8.4.1.2. The detailed weight breakdowns are listed in Section 8.3.2.7 for the primary rocket subsystems and in Volume 7 for the overall engines.

8.3.2 Results

This section represents the degree of penetration arrived at for the rocket primary subsystem investigation in this study. Following a presentation of the two primary chamber layouts, the cooling analysis and nozzle design efforts required for the layouts are presented. The turbomachinery designs are presented in considerable detail, and the section is terminated with brief summaries of the rocket control approach and weight estimations.

8.3.2.1 Primary Chamber Design -- (ScramLACE Liquid Air/Hydrogen)

The ScramLACE system features a supersonic combustion ramjet mode for flight Mach numbers above approximately Mach 6. Supersonic combustion

TABLE XLIV

TURBOPUMP PERFORMANCE REQUIREMENTS FOR ENGINES NOS. 11 AND 22

	Rocket Engine Fuel Pump	Rocket Engine Oxidizer Pump	Ramjet Afterburner Fuel Pump
Engine No. 11			
Turbopump Designation	A_{11}	B_{11}	C_{11}
Propellant	LH_2	LO_2	LH_2
Weight flow, lbf/sec	51	407	40 to 100
Volume flow, gpm	5,200	2,560	4,080 to 10,170
Discharge pressure, psia	3,500	1,950	1,000
Inlet pressure, psia	20	20	20
NPSH, ft	173	10.8	173
Pressure rise, psia	3,480	1,930	980
Turbine exhaust pressure, psia	> 93	> 93	> 280
Operational life, hrs	10	10	100
Engine No. 22			
Turbopump Designation	A_{22}	B_{22}	C_{22}
Propellant	LH_2	Liquid Air	LH_2
Weight flow, lbf/sec	14.2	486.8	60 to 155
Volume flow, gpm	1,448	4,000	6,130 to 15,770
Discharge pressure, psia	2,000	1,320	1,000
Inlet pressure, psia	20	8	20
NPSH, ft	173	10	173
Pressure rise, psia	1,980	1,312	980
Turbine exhaust pressure, psia	> 93	> 93	> 185
Operational life, hrs	10	10	100

NPSH = Net positive suction head

is most efficient, thermodynamically speaking, when it occurs at the highest available pressure and lowest local Mach number. This is at the minimum flow area condition for a supersonic stream. The minimum cross-sectional area of the composite engine is at the station of the rocket primary, since the rocket chamber assembly represents a local geometric contraction (blockage) of the otherwise constant area mixer. It would be, therefore, desirable to locate the Scramjet fuel injectors at, or upstream from this region. Thus, it is appropriate to have the rocket primary structure serve a dual role: (1) provide primary flow during initial acceleration, and (2) act as a fuel injector array during Scramjet operation.

A rocket primary configuration that attempts to satisfy this dual requirement is shown in Figure 241. The rocket primary itself is composed of two concentric, toroidal combustion chambers having annular bell nozzles. The selection of the two concentric chamber geometry was motiviated by the desire to achieve a uniform distribution of injected fuel during the Scramjet mode. This geometry also provides a high interfacial shear surface for air-augmented rocket operation. The exterior surface of the rocket primary requires cooling during the high Mach number regime and it is this coolant which is used for fuel injection purposes. A detailed view is provided in Figure 242.

Further, the moderate heat transfer situation met with in the LAIR-H_2 rocket (as contrasted to O_2-H_2 at higher pressure, see Section 8.3.3.3) permits a multiple annular configuration. This avenue is not necessarily available with the oxygen-hydrogen primary as will be seen.

A cross section of one of the rocket primary chambers is shown in Figure 243. The injector is a fixed orifice, coaxial injection design. The liquid oxidizer is injected through the center post and it is surrounded by an annular gaseous fuel stream. The injector is a flat face type with a Rigimesh transpiration cooled face fabricated from 347 CRES. The injector is designed for maximum combustion efficiency.

Figure 244 is a perspective view of a cross section of the two concentric chambers, radial strut, and support ring. The toroidal thrust chambers are supported with six radial struts that cantilever off the outer support ring. The structural components of the engine were evaluated on the basis of utilizing Inconel 718 working at a 100,000 psi stress level. The outer support ring is designed for the combined effects of torsional bending and the resulting out-of-plane ring bending.

The thrust chambers use the Rocketdyne subsonic baffle structure. The combustion chamber basically consists of two rings arranged to resist the internal pressure. With the subsonic baffle approach, the rings are tied radially at equal angular increments to the backup structure. Thus, the chamber acts essentially as a "fixed-fixed" beam whose length is the arc length between the baffles. This type of design yields a structure that is rigid and light weight. A more detailed sketch of the subsonic baffle is given in Figure 245.

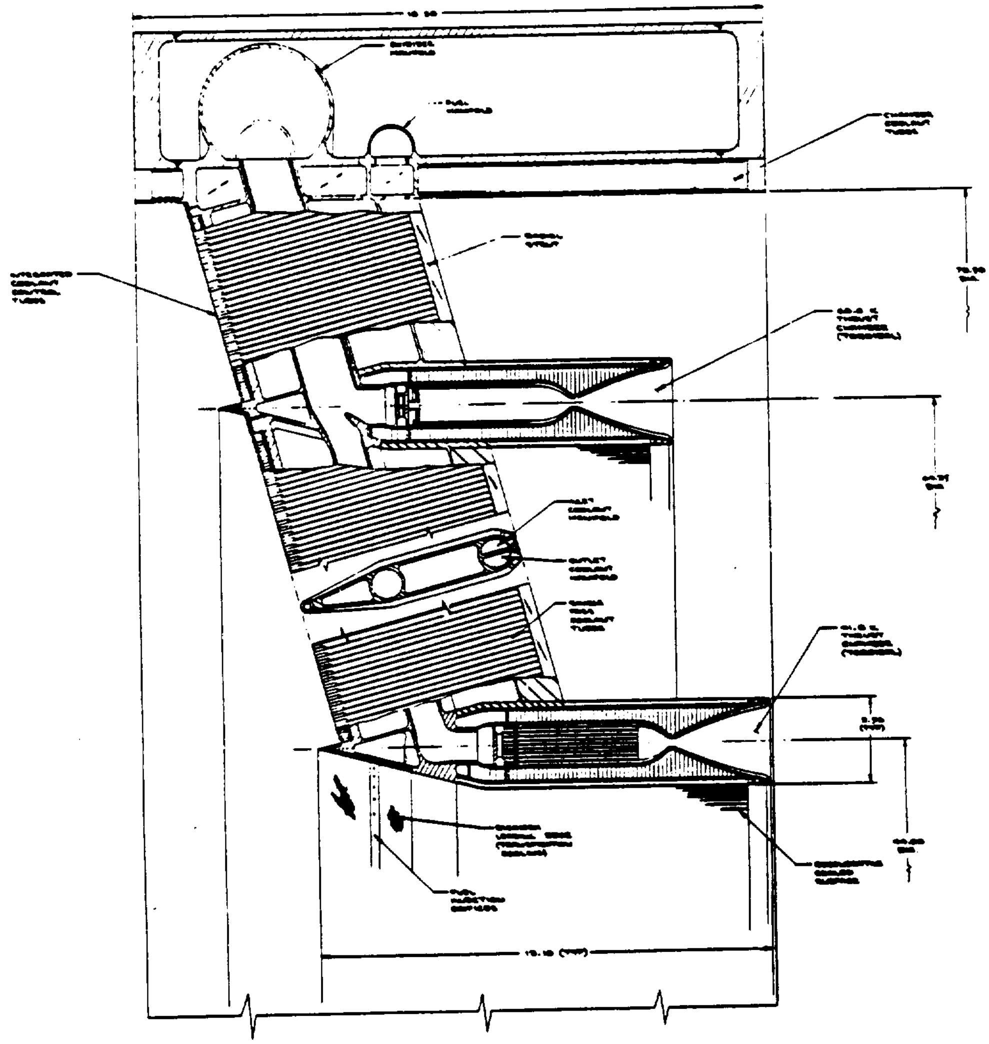

FIGURE 241. Layout of LAIR/H_2 Rocket Primary

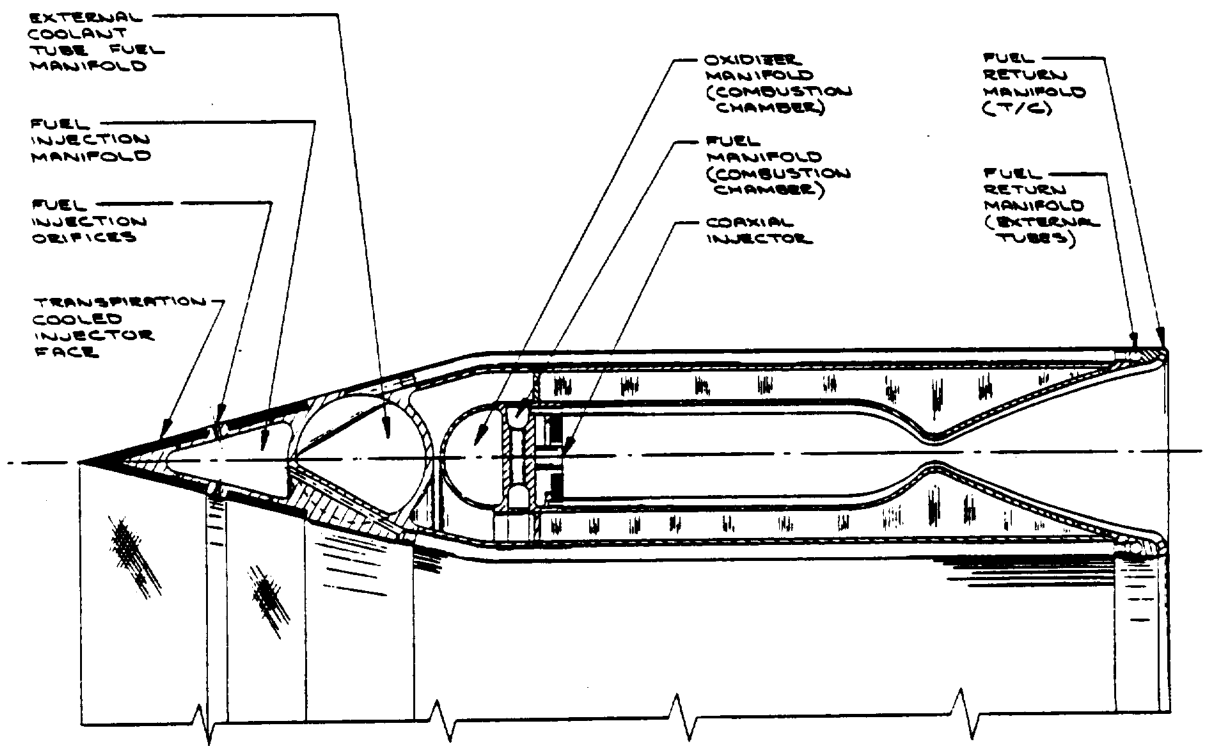

FIGURE 242. Cross Section of Class 2 LAIR/H_2 Rocket Primary Chamber

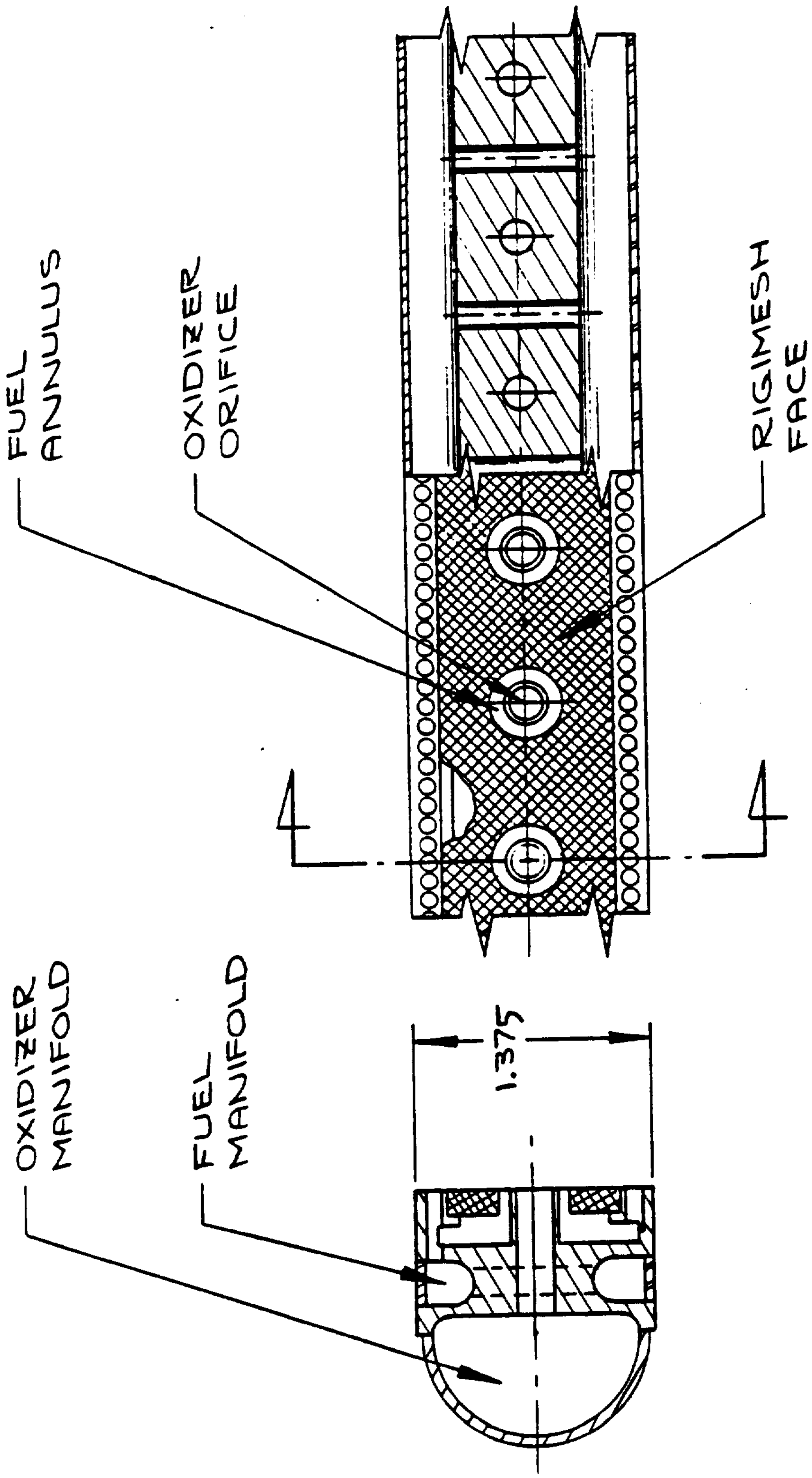

FIGURE 243. Coaxial Injector Assembly for the LAIR/H_2 Rocket Primary

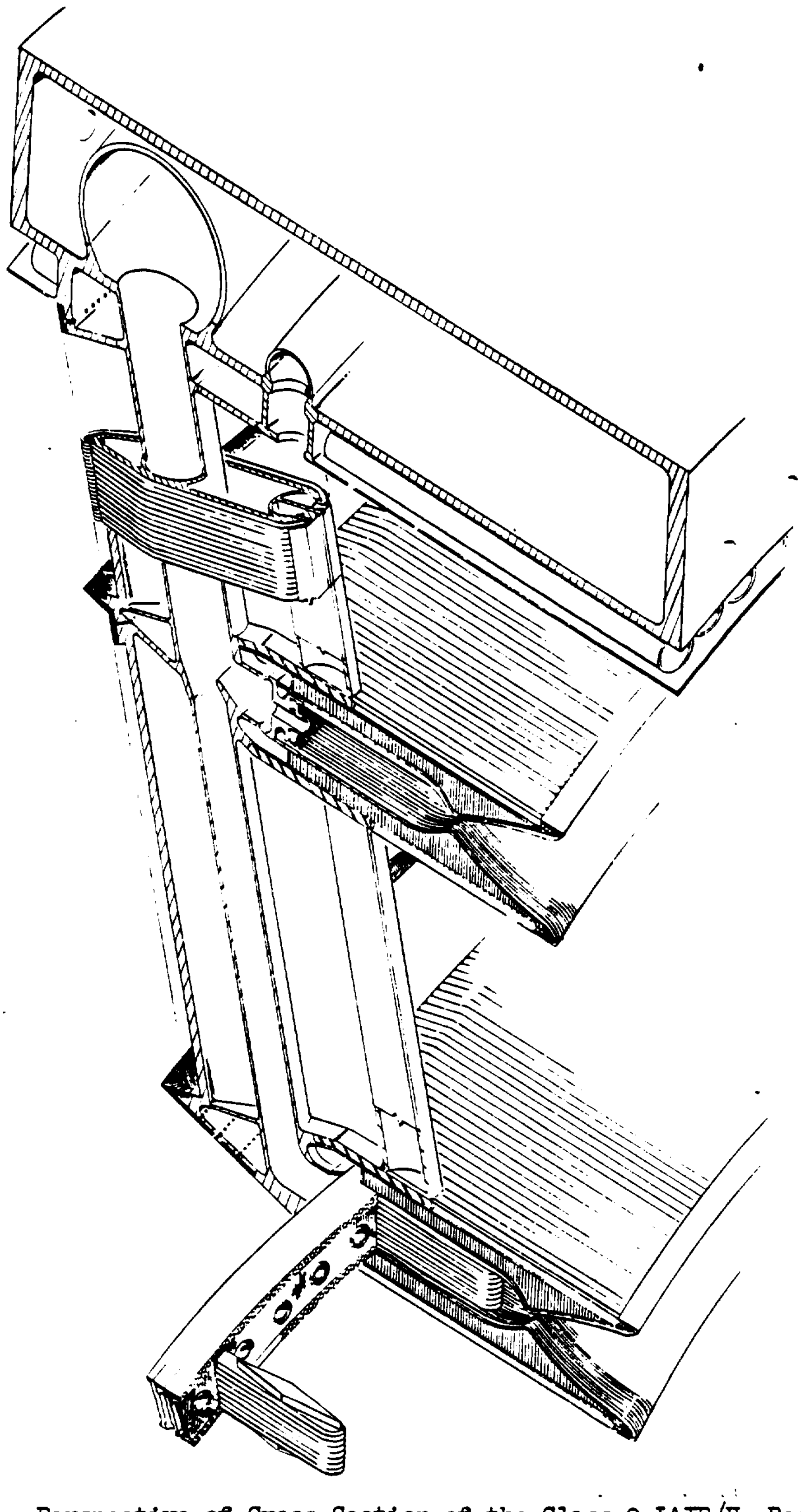

FIGURE 244. Perspective of Cross Section of the Class 2 LAIR/H_2 Rocket Primary

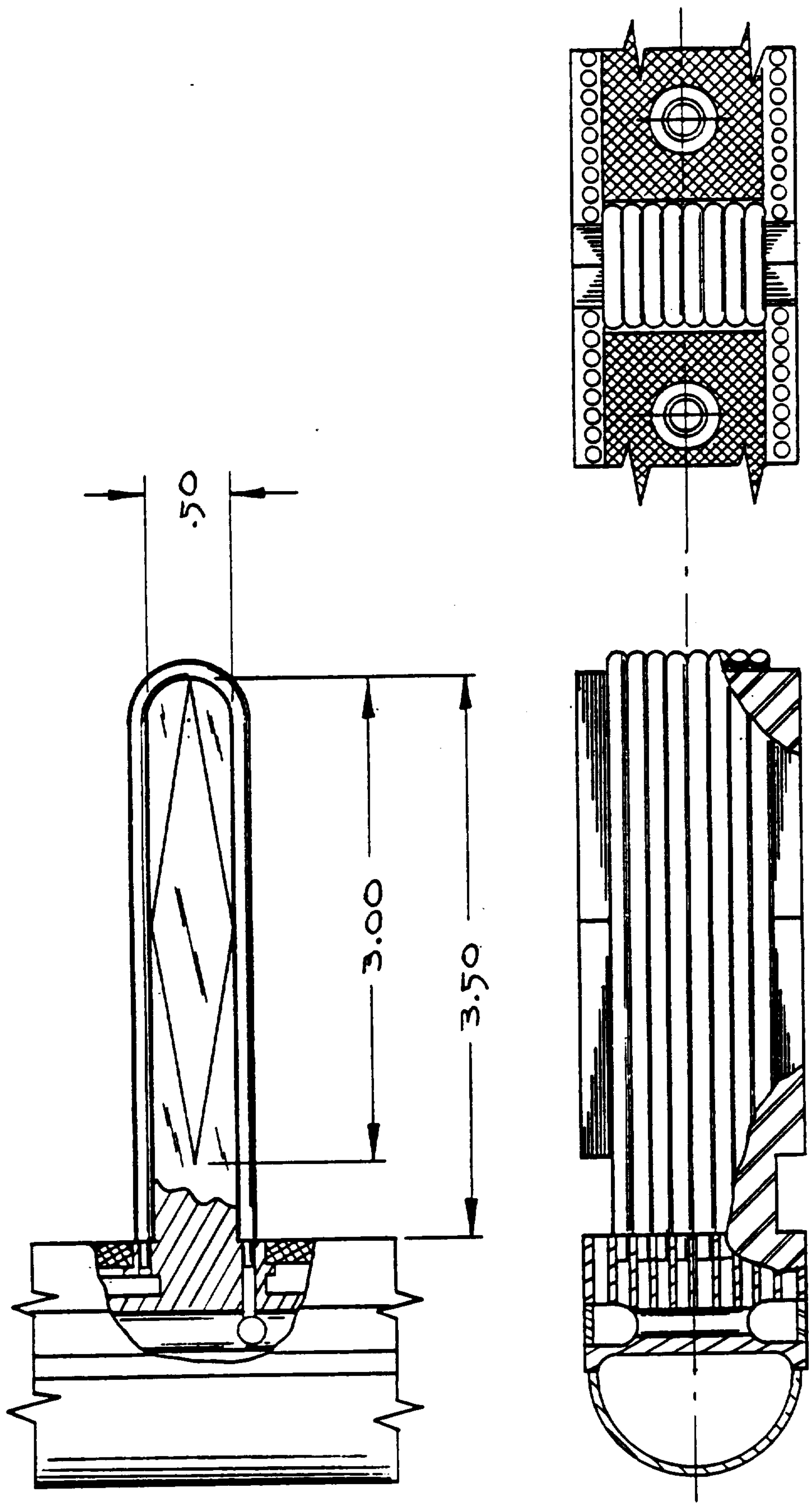

FIGURE 245. Detail of Subsonic Baffle for the LAIR/LH_2 Rocket Primary

The baffle is regeneratively cooled by a single pass coolant circuit. Fuel is bled from the two fuel inlet manifolds and discharged into the fuel injector manifold.

Figure 246 is an assembly drawing of the rocket primary chambers and mounting structure showing the positioning of the fuel and oxidizer turbopumps and feed lines. A perspective view of the assembly is shown in Figure 247. The staggered placement of the two toroidal chambers is a function of the radial strut slope which is fixed by aerodynamic considerations. The radial strut is identically affixed to each chamber and provides for identical coolant tubes, manifolding techniques, and other fabricational similarities for the two concentric chambers.

8.3.2.2 Primary Chamber Design - Supercharged Ejector Ramjet (Liquid Oxygen/Hydrogen)

The rocket primary for the Supercharged Ejector Ramjet is a single toroidal combustion chamber with an annular bell engine. The toroidal geometry was selected for its high interfacial shear surface provided for mixing during air-augmented rocket operation. The choice of a single toroidal chamber rather than the two concentric chamber configuration used for the LAIR/H_2 rocket primary results from the fact that splitting the LO_2/H_2 rocket primary into more than one chamber would mean lower thrust operation for the individual chambers and thereby would significantly aggravate the regenerative cooling problem.

Figure 248 is a cross section through the rocket primary, strut, and support ring. The combustion chamber of the rocket primary is canted 20° from the nozzle centerline. This provides for a simplified regenerative coolant circuit for the radial mounting strut while still retaining a compact packaging arrangement for the rocket primary itself. The entire exterior surface of the engine system is regeneratively cooled during the high Mach number subsonic combustion ramjet mode (to Mach 8). The regenerative coolant (hydrogen) is eventually injected into the ramjet combustion chamber by conventional fuel injection struts. The leading edges of the rocket primary and radial support struts are cooled using the "integrated coolant control tube" approach mentioned previously. A perspective view of the rocket primary structure is shown in Figure 249.

The design details of the LO_2/H_2 rocket primary are similar to those of the LAIR/H_2 engine. Figure 250 shows the complete assembly of the rocket primary system. The major distinguishing feature between the two rocket primaries from an overall design standpoint is in the number of toroidal combustion chambers used.

8.3.2.3 Primary Chamber Cooling

The first step in the analysis was to determine the throat heat fluxes. Experimental data obtained under a J-2 related program were used for

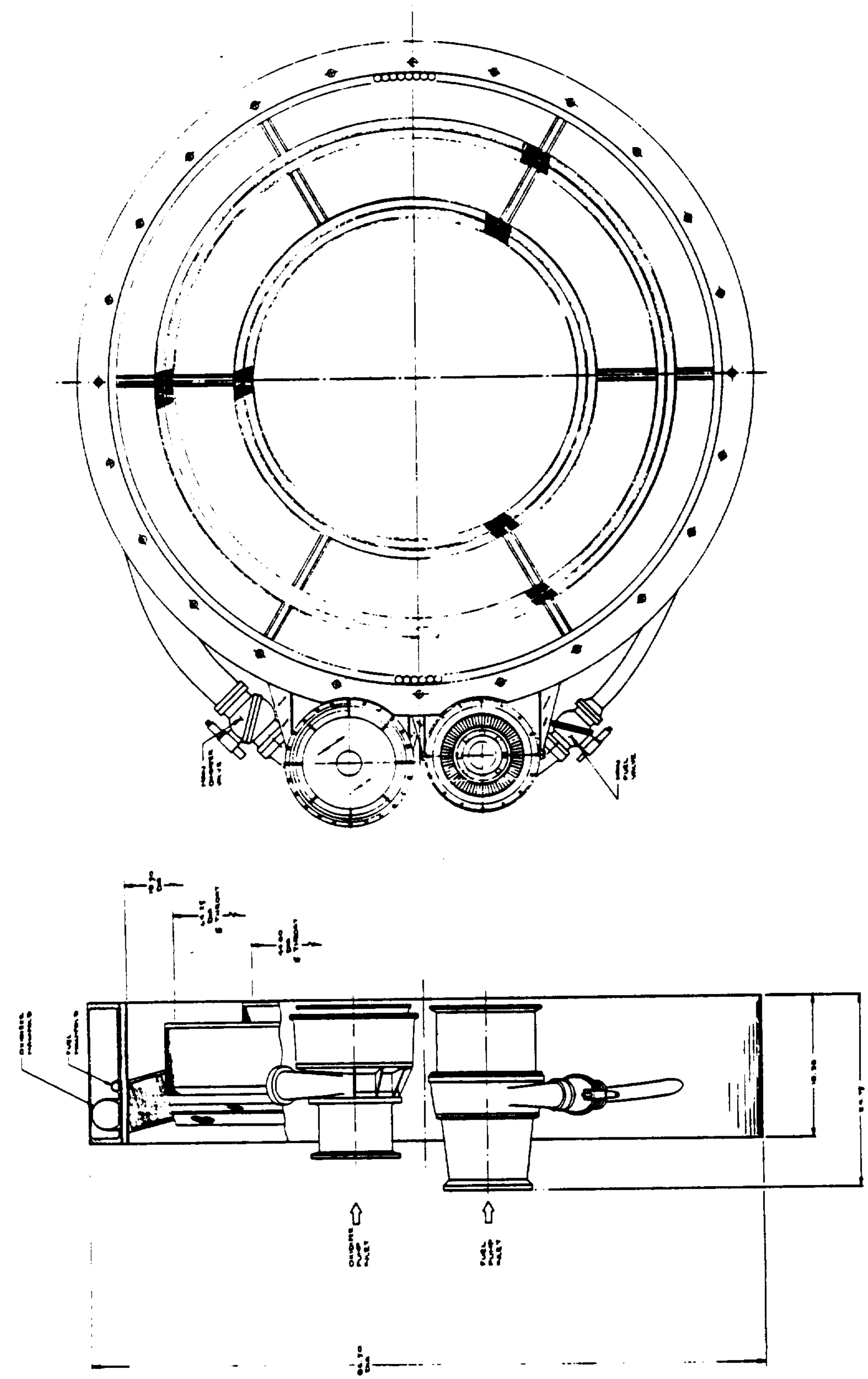

FIGURE 246. Assembly of the Primary Rocket Subsystem for the Class 2 ScramLACE

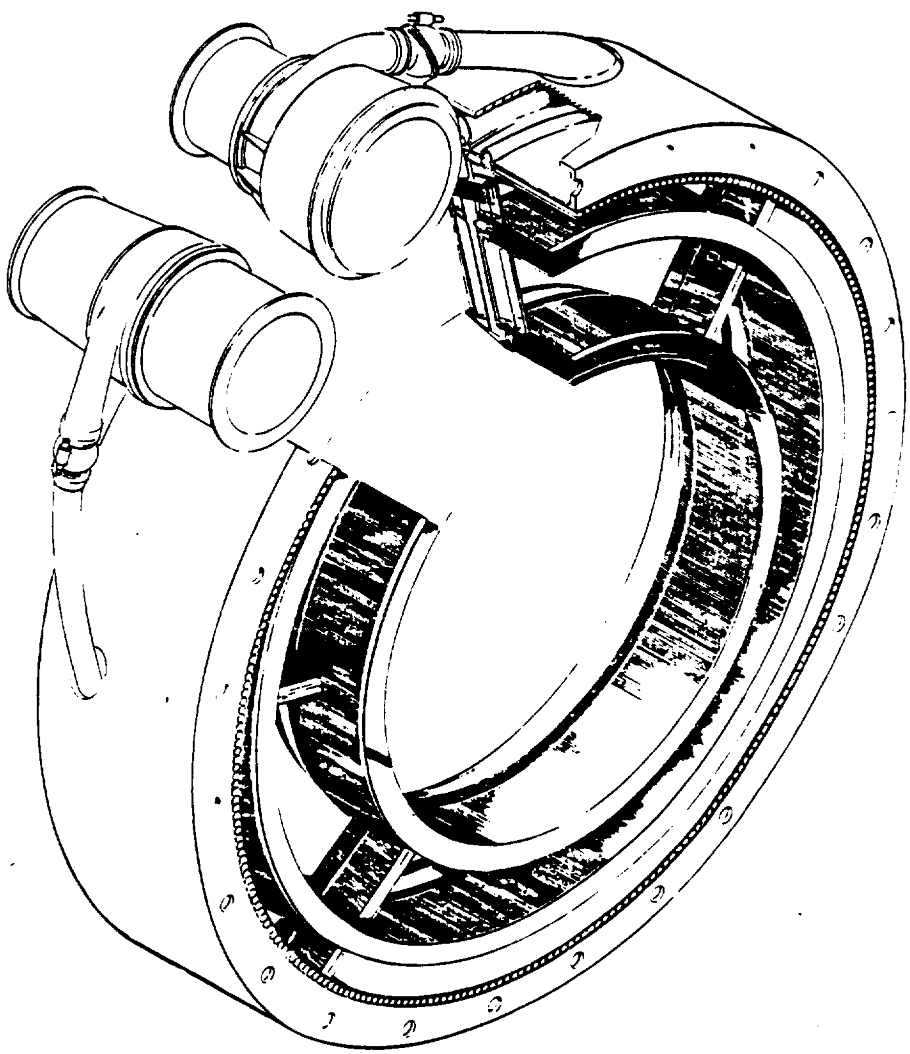

FIGURE 247. Perspective of the Class 2 LAIR/LH_2 Rocket Primary Assembly

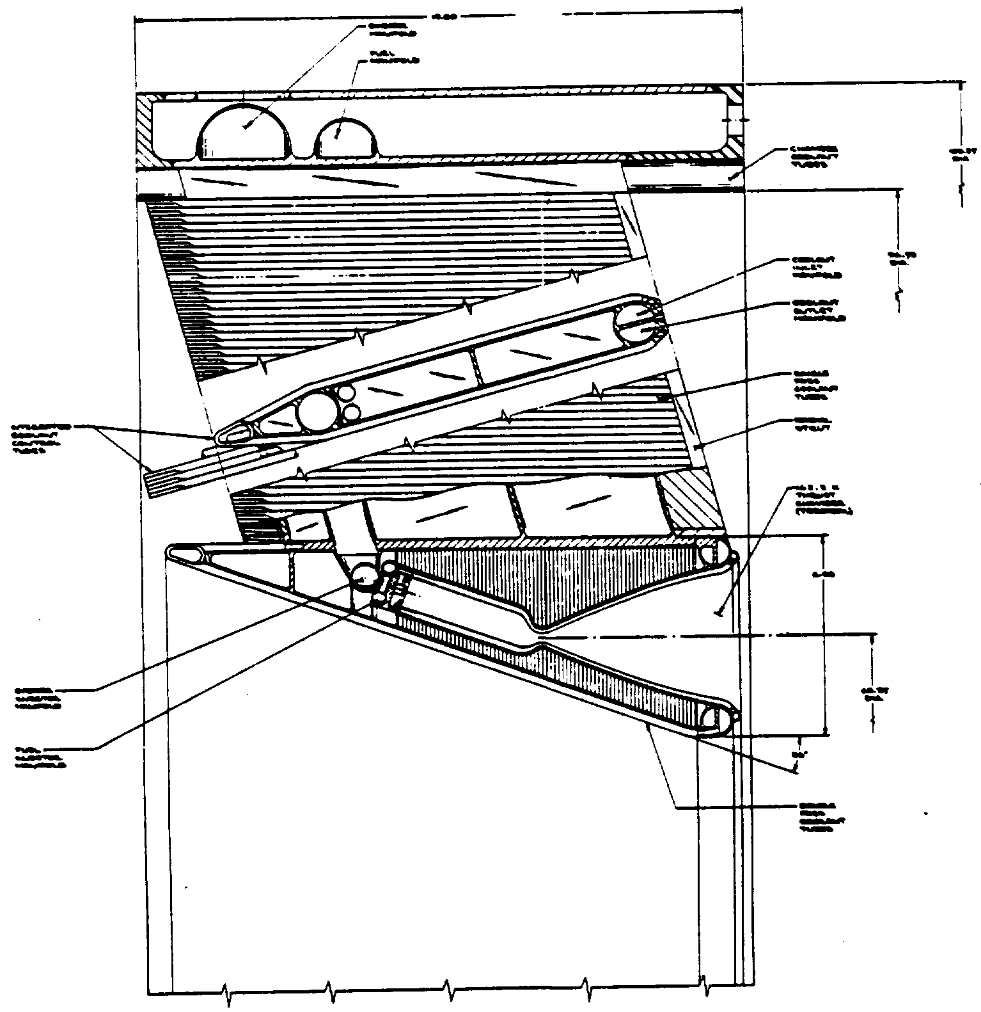

FIGURE 248. Layout of LO_2/H_2 Rocket Primary

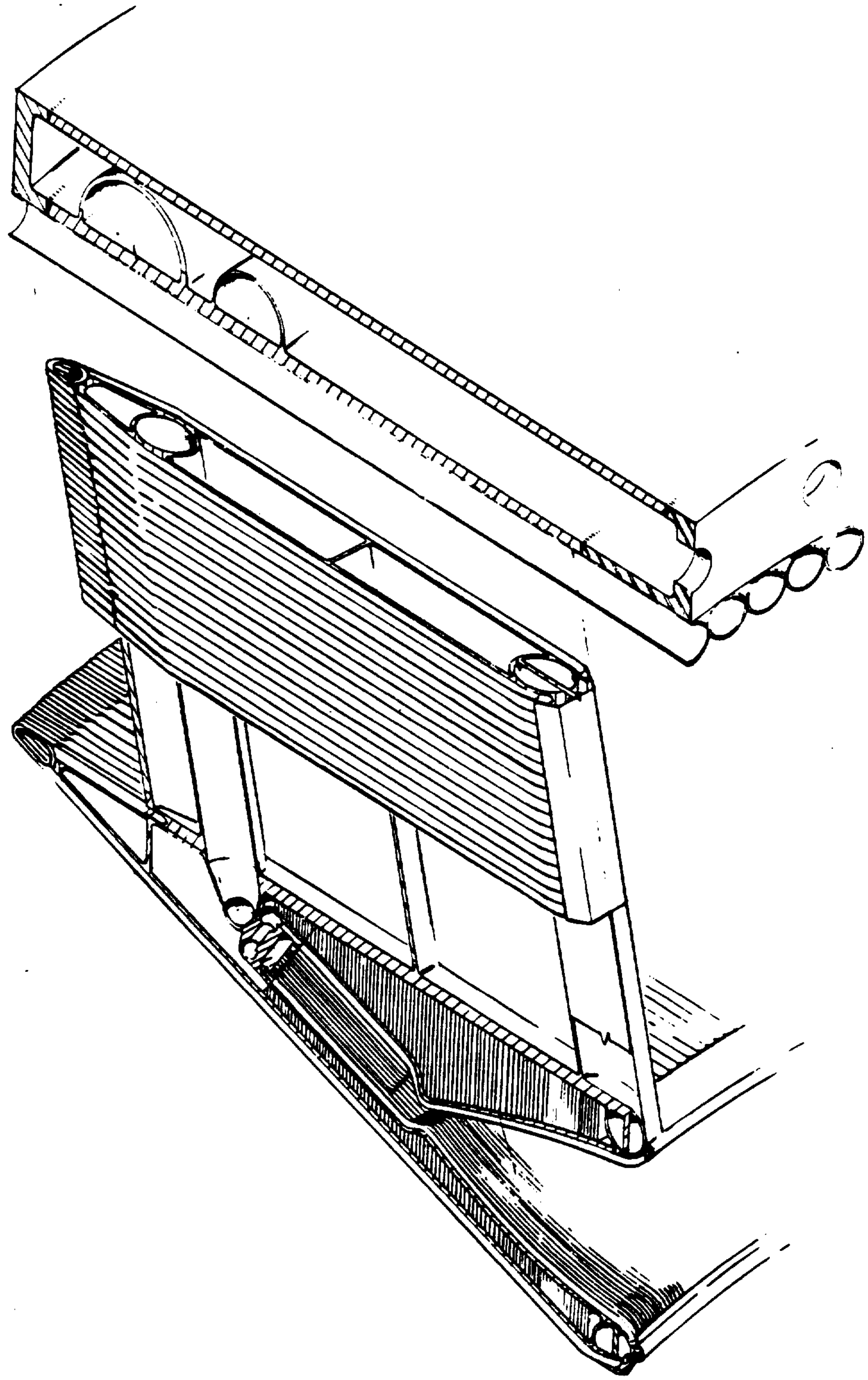

FIGURE 249. Perspective of Cross Section of the Class 2 LO_2/H_2 Rocket Primary

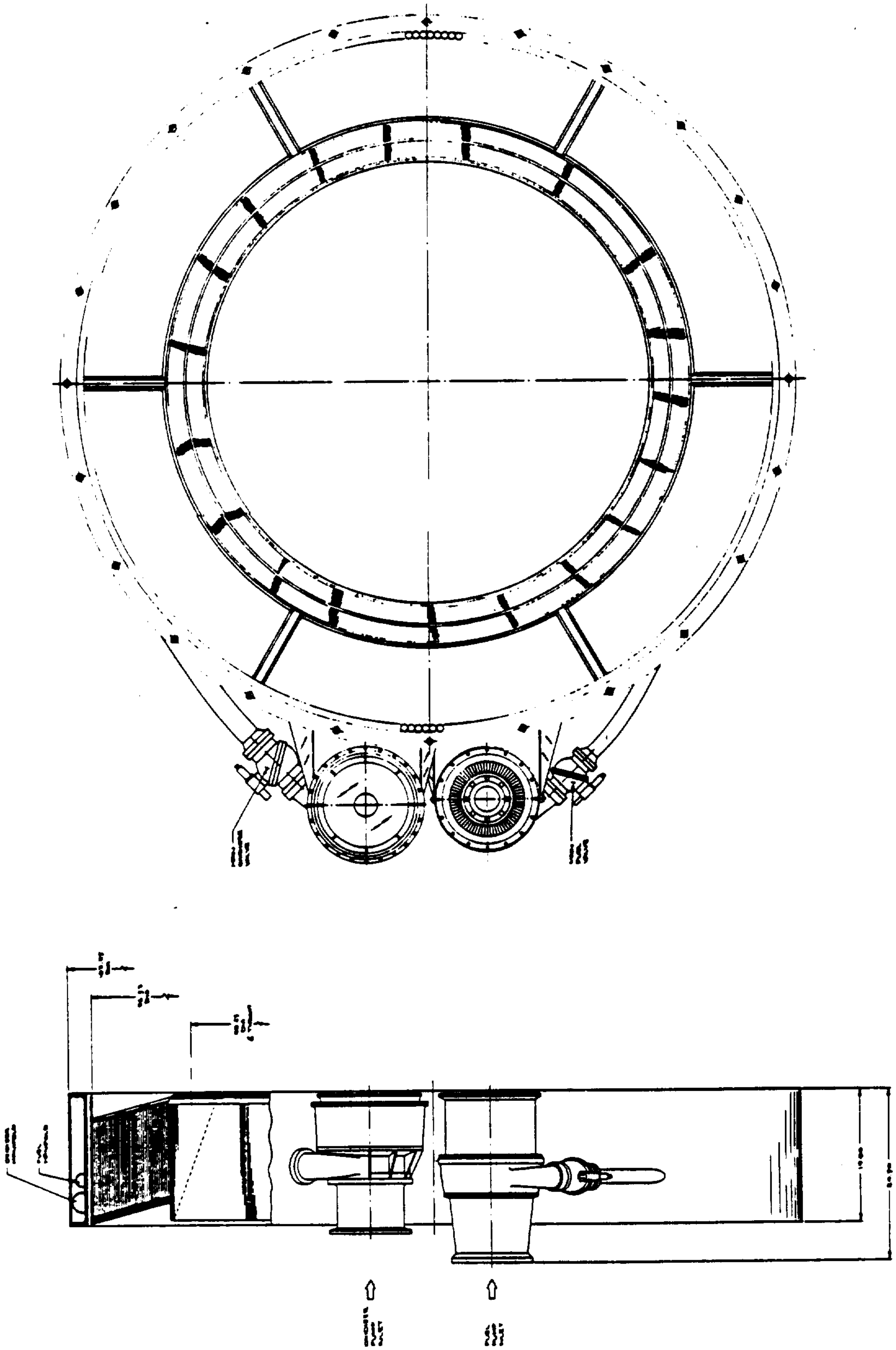

FIGURE 250. Assembly of the Primary Rocket Subsystem for the Class 2 Supercharged Ejector Ramjet

the LO_2/H_2 heat flux, adjusting the experimental values for chamber pressure and mixture ratio. The $LAIR/H_2$ values were then obtained by adjusting the appropriate thermal properties (principally specific heat and combustion temperature). Figure 251 shows the effect of gas wall temperature on the heat flux. Using these heat fluxes, the temperature drop across the wall was determined using the conduction equation

$$T_{WG} - T_{WC} = (Q/A)\ t/k$$

Typical gas side wall temperatures of 750°F, 1600°F, and 1800°F were considered for copper, stainless steel, and molybdenum, respectively.

The hydrogen regenerative coolant velocity requirements were determined using a modified form of the Dipprey and Sabersky equation which includes the effect of tube wall roughness. This equation was given in the previous discussion on the Class I rocket primary heat transfer analysis. For the Class 2 analysis, a curvature enhancement factor of 1.5 and a tube roughness of 50 micro inches were used.

The hydrogen bulk temperature was determined by integrating the heat flux along the nozzle and chamber separately. The individual heat inputs were then divided by the hydrogen flow rate and specific heat (3.5 Btu/lb-F for LO_2/H_2, 4.0 Btu/lb-F for $LAIR/H_2$ due to higher coolant temperature) to determine the temperature rise in the nozzle and chamber regions. From this, the hydrogen temperature was determined for each gas wall temperature and coolant pass arrangement. Hydrogen inlet temperatures of 60°R and 250°R were used for the LO_2/H_2 and $LAIR/H_2$ engines, respectively. The higher hydrogen inlet temperature for the $LAIR/H_2$ engine is due to the hydrogen first passing through the air liquefaction heat exchanger. The coolant temperatures at the throat region for the LO_2/H_2 engine are shown in Figure 252.

The hydrogen coolant mass velocity requirements at the throat of the LO_2/H_2 engine are given in Figure 253. This figure shows that copper at 750°F, and stainless steel at 1600°F require the same coolant velocities, with the copper being better only at higher bulk temperatures. The molybdenum is seen to be considerably better than either copper or stainless steel in terms of mass velocity requirements. It is also seen that the lowest mass velocity requirements occur at coolant bulk temperatures near 300°R for copper and stainless. As a result, the lowest coolant pressure drop and largest tube diameters will occur for the coolant pass arrangement which results in obtaining this hydrogen temperature requirement in the throat region. A second examination of Figure 252 indicates that this condition is best met using a single pass arrangement. Multiple pass configurations, while providing large tubes, will operate at more undesirable coolant temperatures.

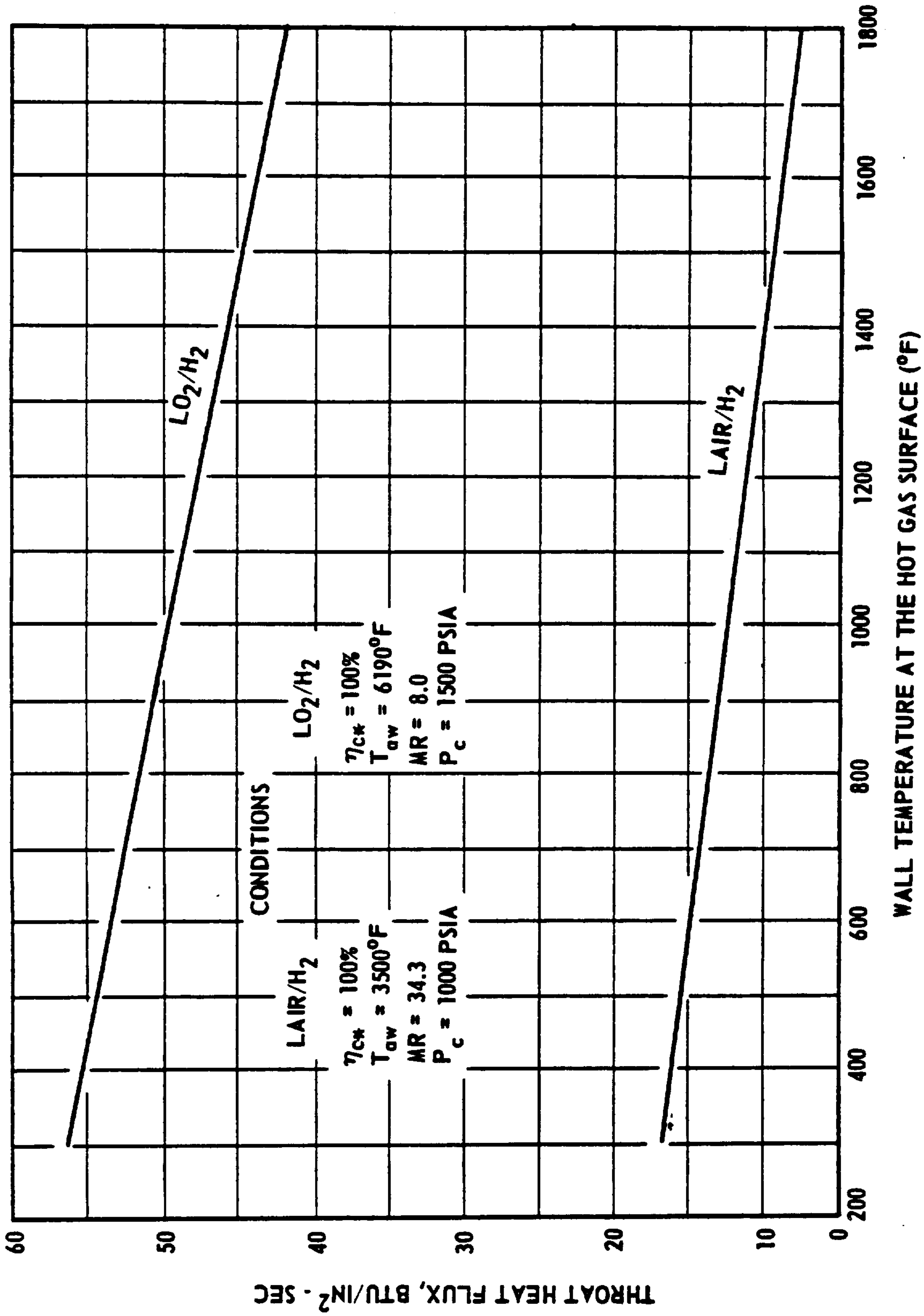

FIGURE 251. Throat Heat Flux Variation with Wall Temperature for the Class 2 Rocket Primaries

P_c = 1500 PSIA, MR = 8, D_{av} = 68.25 IN.

COOLANT TEMPERATURE AT THROAT (SERIES COOLED)

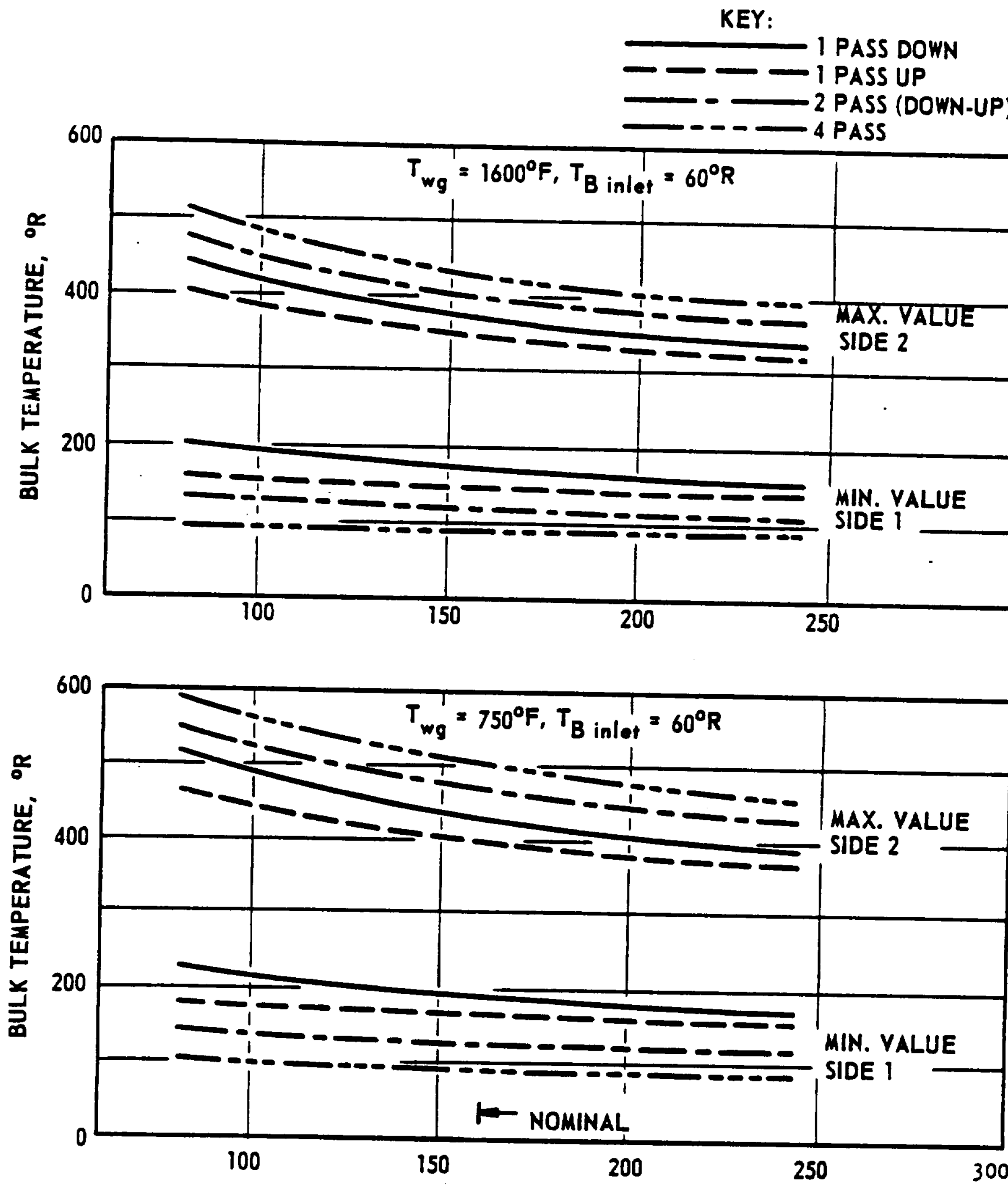

FIGURE 252. Coolant Temperature at Throat (Series Cooled) for the Class 2 LO_2/H_2 Rocket Primary

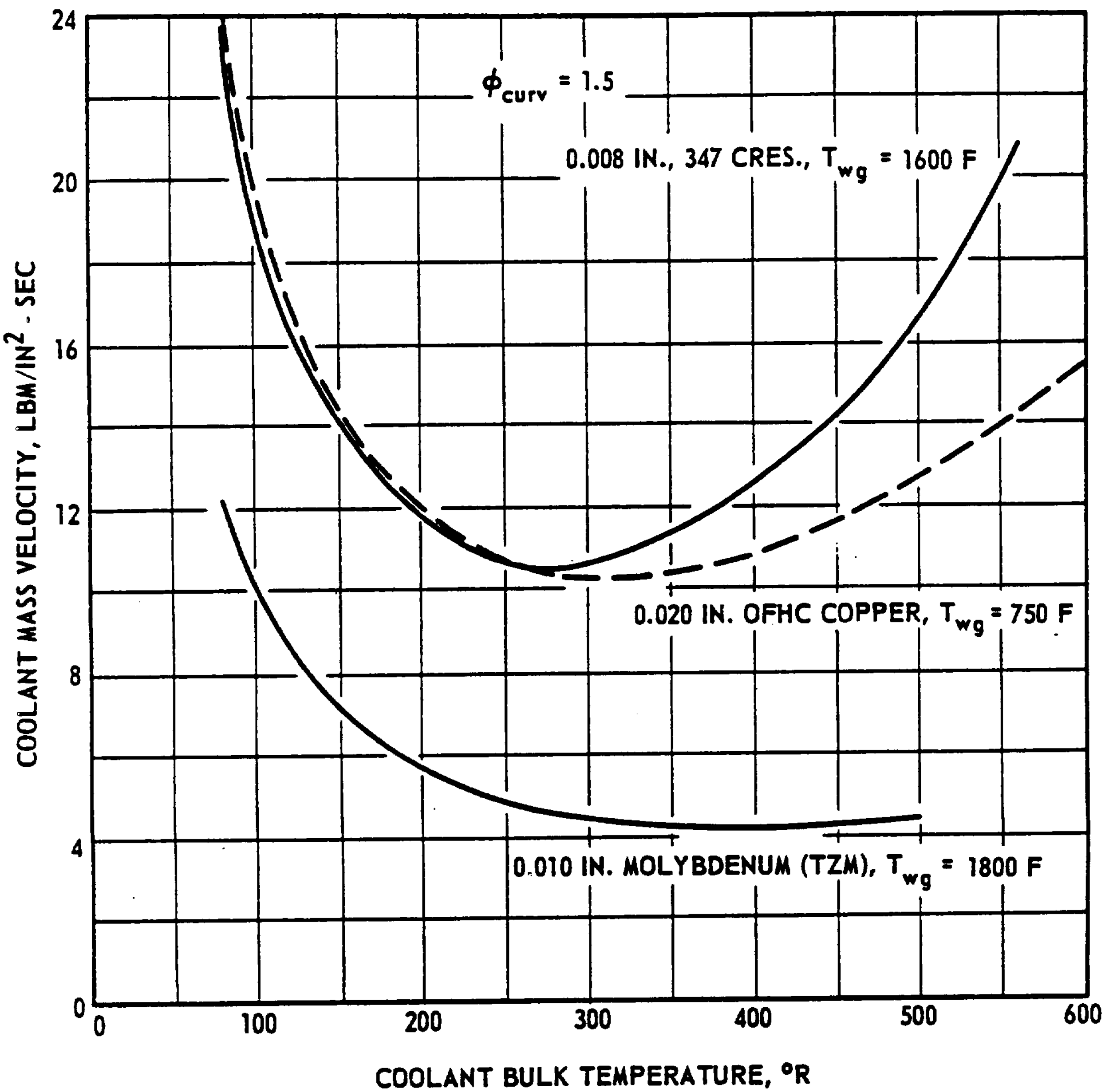

FIGURE 253. Required Coolant Mass Velocity as a Function of Bulk Temperature at the Engine Throat for the Class 2 LO_2/H_2 Rocket Primary

8.3.2.3.1 Liquid Oxygen/Hydrogen Primary Rocket Evaluation

The results of the heat transfer analysis of the LO_2/H_2 rocket primary are shown in Figure 254. This is for 0.008-inch thick 347 stainless steel tubes. A series flow system where the coolant cools one side of the chamber and then the other was used. A series cooling arrangement rather than a parellel arrangement (half the coolant per side) was chosen to maximize the tube size. At the nominal operating conditions, it is seen that a four-pass cooling system comes closest to a 0.10-inch tube, but because of its non-optimum operating conditions it also has the highest coolant velocity and total pressure requirements (2800 psi required for a Mach number of 0.5 in the throat region for the last coolant pass). Thus, the use of a four-pass system will result in high coolant pressures at the tube bundle exit, in relation to the chamber pressure of 1500 psia. From the standpoint of coolant pressure requirements, a four-pass configuration could be used for the first side and a single uppass for the second side, requiring only 2000 psia coolant pressure in the throat, but a tube diameter for the second side of only 0.055 inch. As would be expected, the higher thrust conditions are more attractive in terms of coolant choking pressure requirements and tube size, while for the low thrust applications high coolant pressures are required in the throat of Side 2 to prevent choking. This results in pump discharge pressure requirements considerably in excess of those dictated by injector and tube bundle pressure drops.

At nominal thrust conditions, copper appears more attractive than stainless steel to achieve larger tube sizes (Figure 255). A two-pass configuration for Side I has an 0.10-inch tube diameter and a single uppass for Side 2 has an 0.090-inch diameter and a 2100 psia coolant pressure requirement. Having fewer cooling passes, the coolant pressure drop will also be reduced.

Use of a refractory metal tube such as molybdenum will result in the largest tubes (Figure 256) and the lowest pressure drops. Because of the low velocity requirements, coolant choking is not a consideration with this material. A four-pass cooling circuit on Side I results in a 0.14-inch diameter tube, whereas a 0.17-inch diameter tube can be used for a two-pass circuit on Side 2. A four-pass circuit was not considered for Side 2 due to the large tubes resulting from the two-pass arrangement.

A summary of the regenerative coolant circuit characteristics for the LO_2/H_2 rocket primary at the nominal thrust condition is given below:

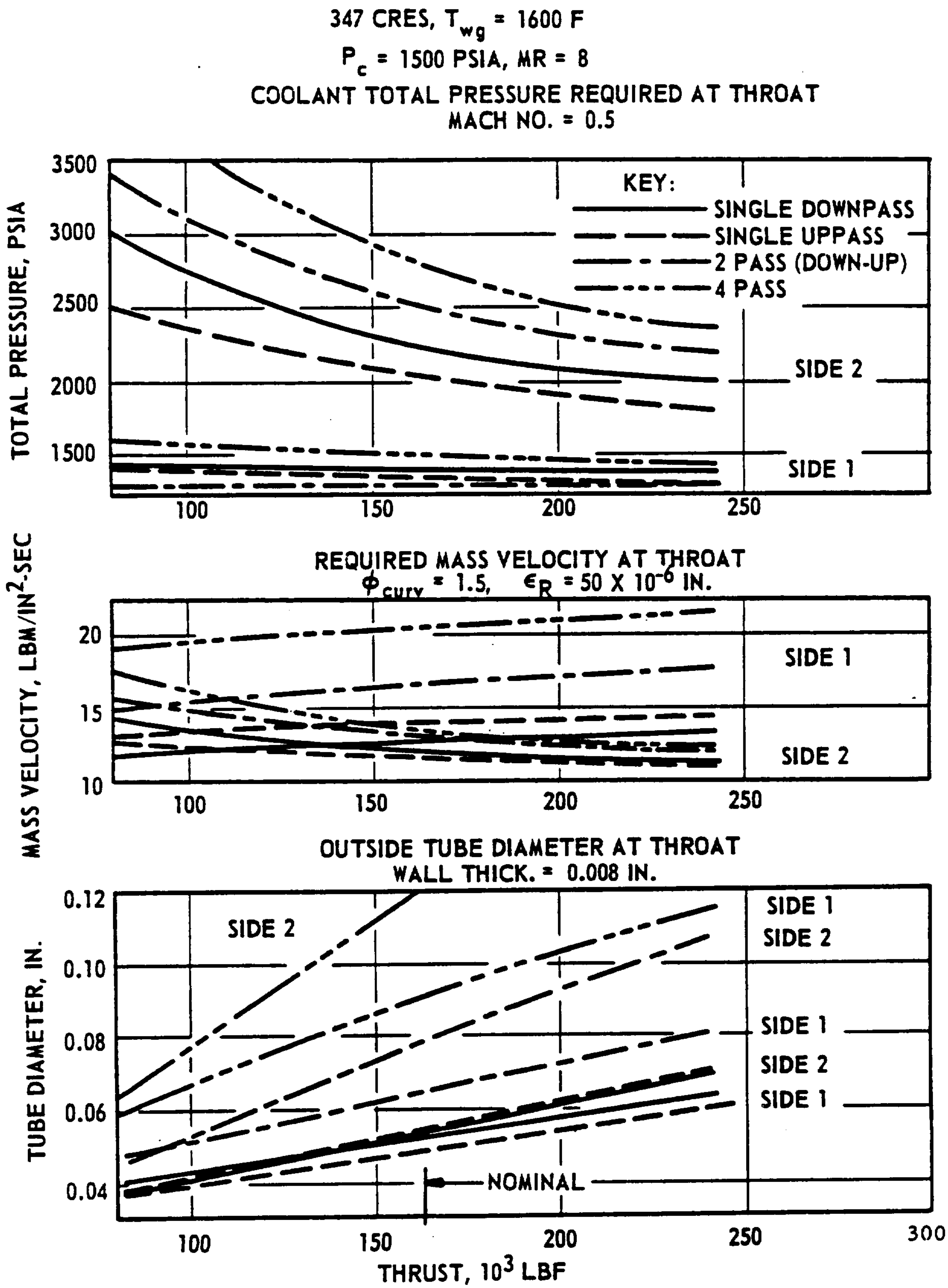

FIGURE 254. Heat Transfer Analysis for the Class 2 LO_2/H_2 Rocket Primary

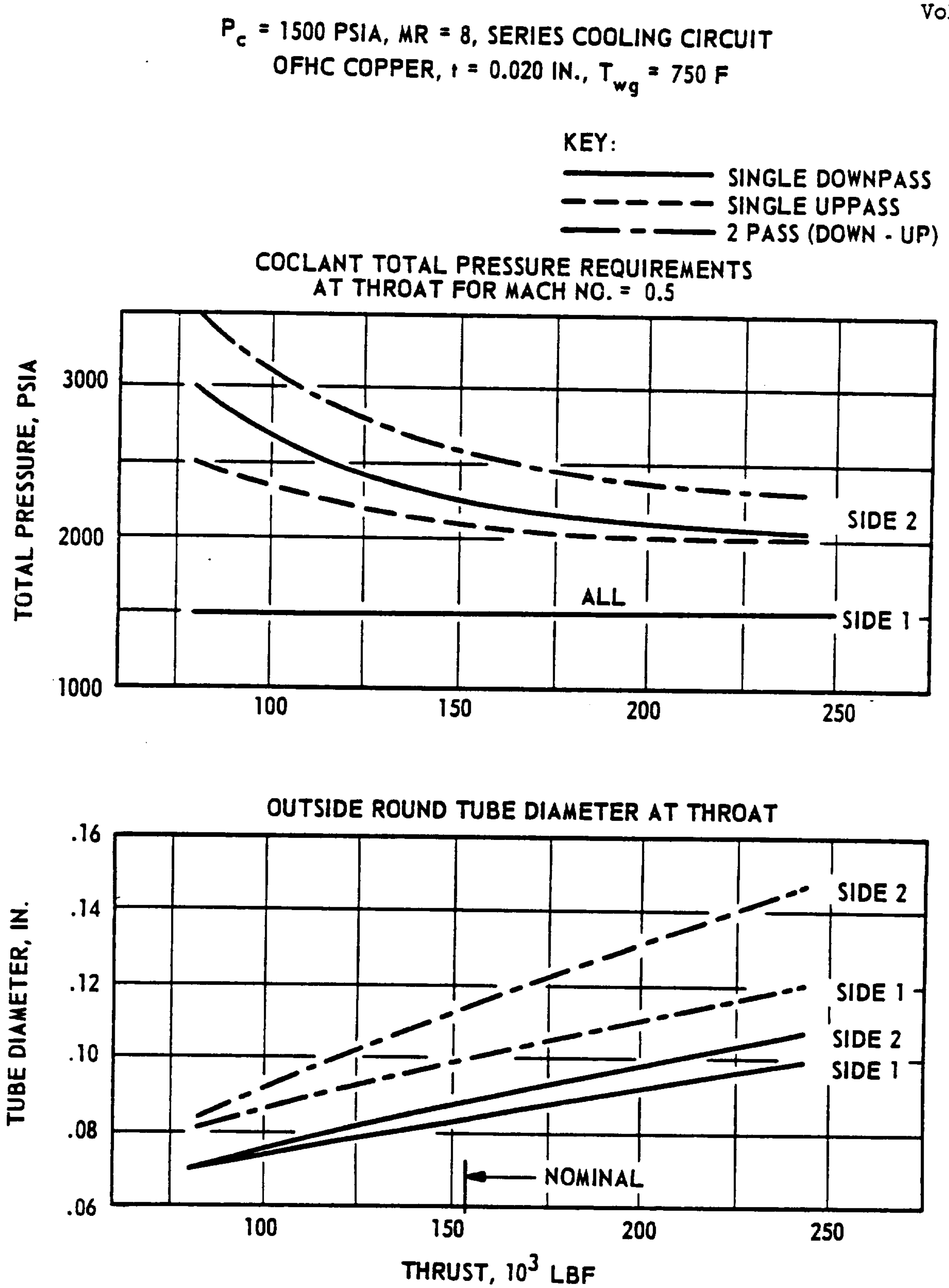

FIGURE 255. Coolant Pressure and Copper Tube Diameters for the Class 2 LO_2/H_2 Rocket Primary

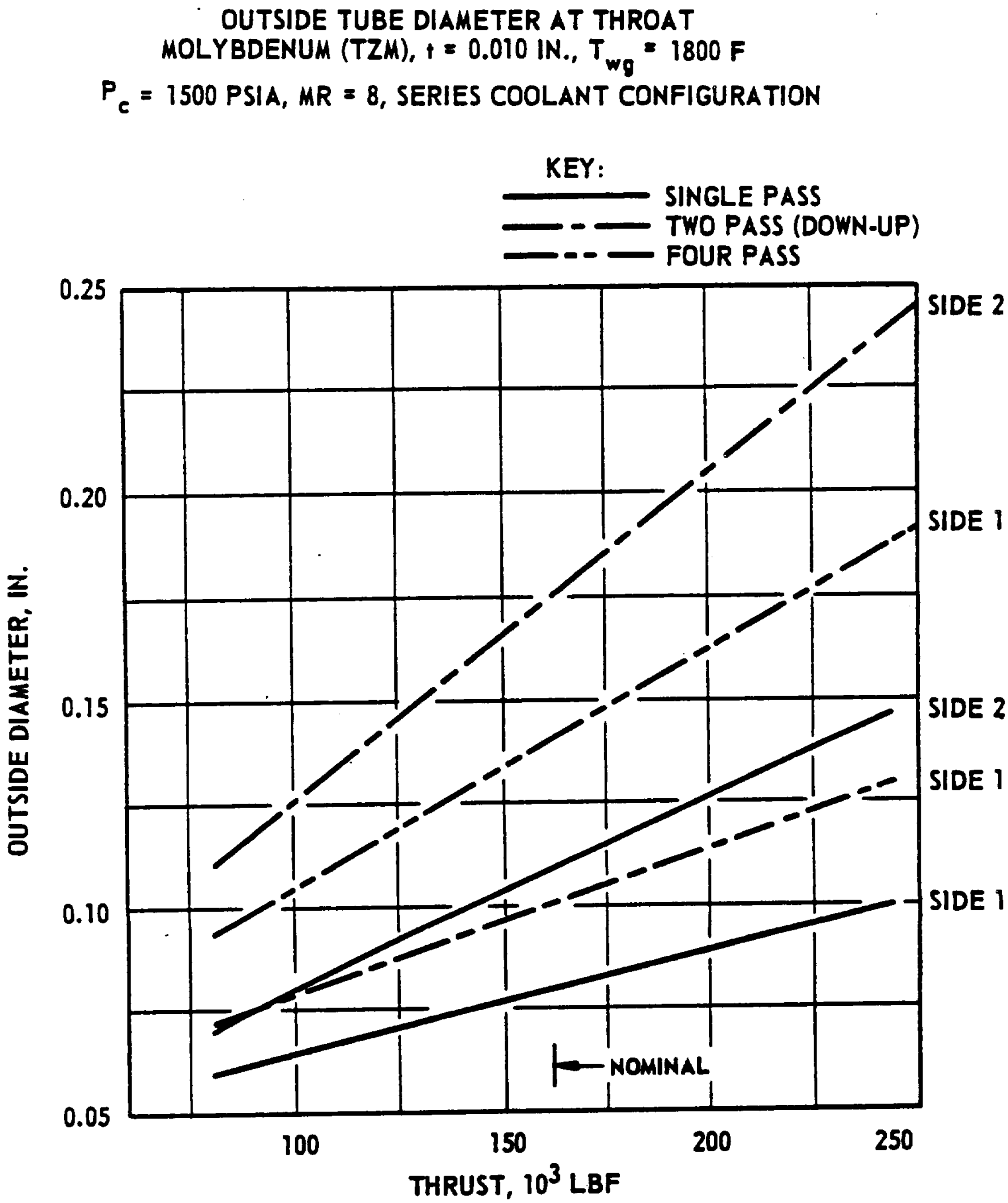

FIGURE 256. Molybdenum Tube Diameters for the Class 2 LO_2/H_2 Rocket Primary

Wall Material	T_{WG}, (°F)	No. of Passes	d_o, in.		P_{total}, throat, psia (Mach No. = 0.5), Side 2
			Side 1	Side 2	
347 CRES (t = 0.008 in.)	1600	1 down	0.052	0.054	2250
		1 up	0.048	0.054	2050
		2	0.064	0.078	2500
		4	0.090	0.120	2800
OFHC Copper (t = 0.020 in.)	750	1	0.085	0.090	2050
		2	0.102	0.117	2500
TZM (t = 0.010 in.)	1800	1	0.080	0.110	< 1500
		2	0.102	0.175	< 1500
		4	0.140	--	< 1500

The results of the LO_2/H_2 study indicate that the engine can be cooled with a conventional wall material such as stainless steel, but due to the low flow rates and large surface area to be cooled, either very small tubes or high coolant pressures will be required. Copper, although heavier, has the advantage of larger tubes for the same coolant total pressures required, whereas a refractory metal such as molybdenum would result in large tubes and a low coolant pressure requirement. Further work with the refractory metals is necessary to provide means of protection (coatings) against oxidation and hydrogen embrittlement, while being sufficiently ductile over the operating temperature range.

The Supercharged Ejector Ramjet engine has the implication of being a near term, low technical risk engine. Thus, it is desirable to use "almost" present state of the art technology and materials in the rocket primary structure. Consequently, the 347 stainless steel material was chosen for the regenerative cooling tubes. The four-pass cooling circuit arrangement was also chosen for use in this engine, since it results in tube sizes that are reasonable in the light of present standards and does not require a coolant total pressure much in excess of that required for the two-pass circuit. This does not mean that the tube sizes required for the two-pass arrangement are unreasonable but merely that the sizes for the four-pass arrangement are more easily achievable. The required hydrogen pump discharge pressure for the chosen regenerative circuit is 3500 psia.

8.3.2.3.2 <u>Liquid Air/Hydrogen Primary Rocket Evaluation</u>

The regenerative coolant requirements of the $LAIR/H_2$ engine are considerably less severe than those of the LO_2/H_2 engine. The $LAIR/H_2$

heat flux at the throat is 8.8 Btu/in.^{2}-sec as opposed to 44 Btu/in.^{2}-sec for the LO_2/H_2 engine. The maximum heat fluxes for these engines were comparatively shown in Figure 251 over the range of hot gas wall temperatures of interest. These values were predicted by adjusting experimental data to the appropriate operating conditions. The reasons for a low LAIR/H_2 heat flux are (1) a low hot gas specific heat (C_p) and viscosity, and (2) a low combustion temperature. However, the low characteristic velocity (C*) of LAIR/H_2 propellants somewhat counteracts the effect of the thermal properties and combustion temperature on heat transfer by raising the hot gas mass flux at any particular chamber pressure.

The geometry of the two toroidal chambers used for the LAIR/H_2 rocket primary is such that the outer and inner thrust chamber cross sections are identical. Since the throat gaps of both chambers are the same, the outer chamber has the larger total throat area and thrust. The chambers were examined parametrically over a thrust level variation of plus and minus 50 percent from the nominal value by varying the throat gap only, holding the engine diameters constant. The equivalence of the throat gaps gives a thrust/diameter ratio which is the same for both chambers. Thus the fuel flow rate available for cooling per unit circumference is the same for both chambers. This implies that the regenerative coolant tubes are the same size at the throat of each chamber.

Two tube materials were examined for the LAIR/H_2 engine: copper and 347 stainless steel. The coolant mass velocity requirements for these materials were determined with the modified Dipprey and Sabersky equation and heat flux values described previously. A wall temperature at the hot gas surface of 750°F was used for the copper, and 1600°F was used for the stainless. These result in throat heat fluxes of 14.2 and 8.8 Btu/in.^{2}-sec, respectively. The cooling requirements are presented in Figure 257 as a function of coolant bulk temperature. Copper has the higher mass fluxes because of the higher heat flux and a lower coolant side wall temperature. Since the inlet bulk temperature is 250°R, the coolant mass flow required is near the minimum, and the last pass of the multipass cooling system would fix the tube diameter. Coolant bulk temperature rises in the nozzle and combustion zone were calculated as discussed previously. Knowledge of the required coolant mass flux, throat bulk temperature, total coolant flow rate available, and the engine geometry leads to the calculation of the necessary tube diameter at the throat.

The tube diameters required for 1-, 2-, and 4-pass regenerative cooling circuits are given in Figure 258 for copper tube material. Multiple pass cooling actually means the number of passes per side of a given LAIR/H_2 thrust chamber, since the available coolant flow is split in half to cool the inner and outer circumferences. The largest bulk temperature rise occurs in the combustion zone, so that the highest throat bulk temperature is obtained with a downpass circuit for a single pass system, whereas the highest bulk temperature at the throat of the last pass of a multipass system occurs when the first pass is an uppass.

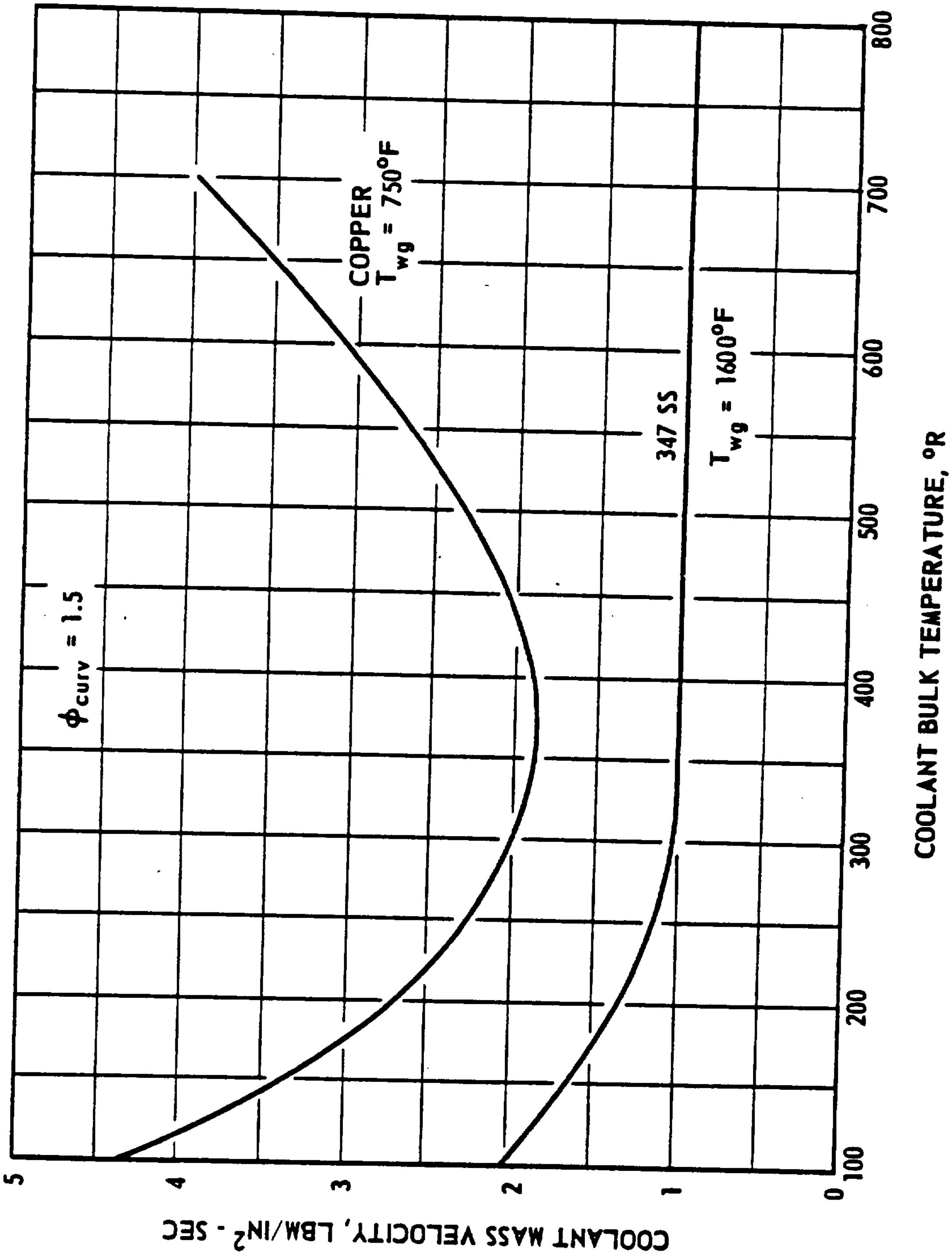

FIGURE 257. Required Coolant Mass Velocity as a Function of Bulk Temperature at the Engine Throat for the Class 2 LAIR/H_2 Rocket Primary

CONFIDENTIAL

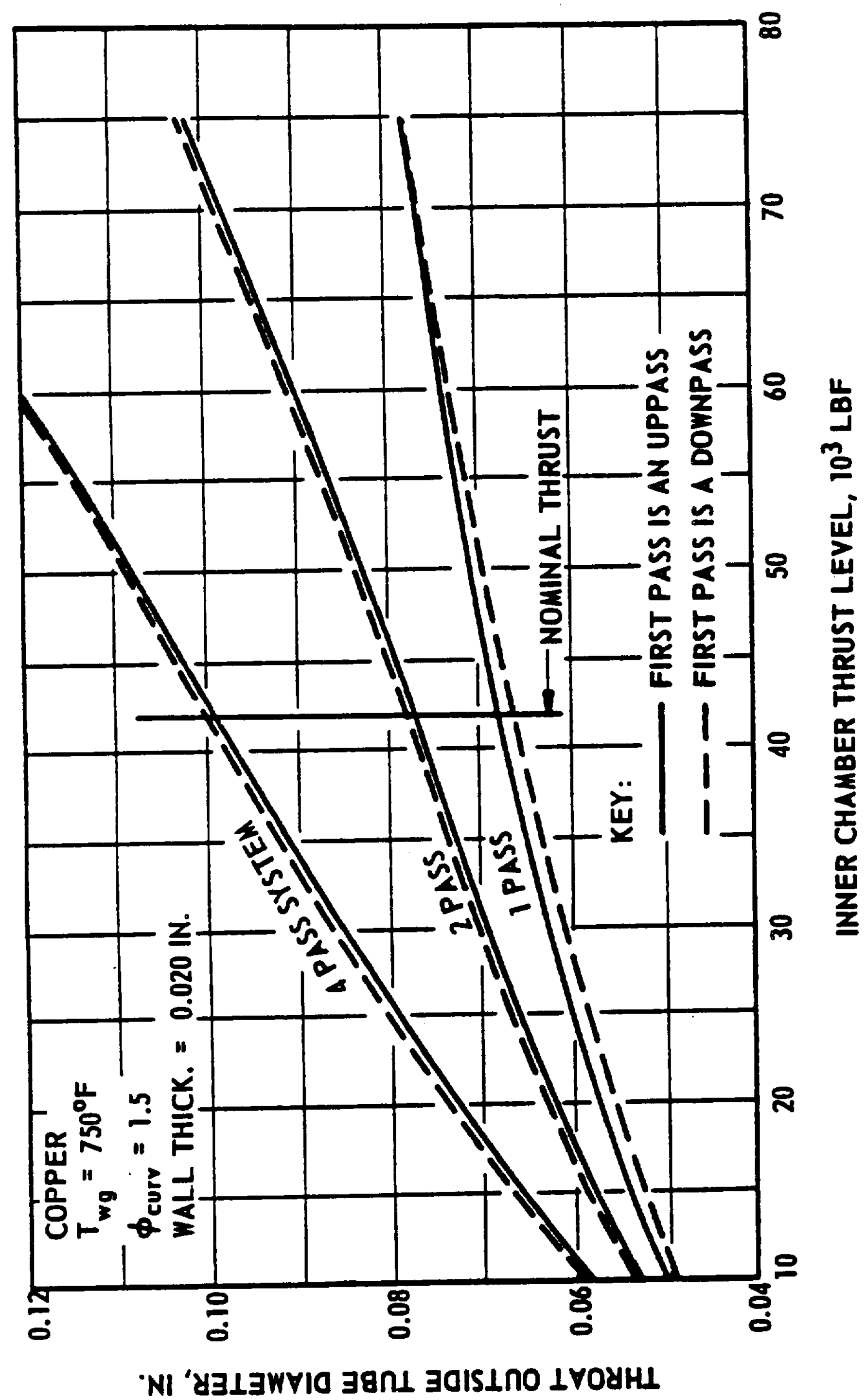

FIGURE 258. Copper Tube Size as a Function of Inner Chamber Thrust Level for the Class 2 TAIR/H_2 Rocket Primary

CONFIDENTIAL

This explains the dependence of tube diameter on the cooling circuit exhibited in Figure 259, since a higher bulk temperature requires a larger coolant mass flux and smaller tube diameter, as shown in Figure 257. Using a multipass system naturally results in a larger tube diameter because the flow rate per tube is increased. The tube diameters for a four-pass system are the maximum values computed for copper and these are fairly small (~0.1 in.) at the design point. Since the wall thickness accounts for 0.04 inch, or nearly half the nominal tube diameter, the chamber weight will be relatively high. At the one-half nominal thrust level (20.9K), the tube diameters are even smaller (~0.075 in.).

The 347 stainless steel tube material, on the other hand, exhibits larger diameters than the copper (greater than 0.1 in.) at the nominal condition with both 2- and 4-pass systems, as seen in Figure 259. The diameters are not a function of selecting an uppass or a downpass for the first pass, because the required coolant mass flux curve is insensitive to bulk temperature above 250°R.

A summary of the regenerative coolant circuit characteristics for the LAIR/H_2 rocket primary at the nominal thrust condition is given below.

Wall Material	T_{WG} (°F)	No. of Passes	d_o (in.)
OFHC Copper (t = 0.020 in.)	750	1*	0.066
		2*	0.078
		4*	0.010
347 CRES (t = 0.015 in.)	1600	1	0.076
		2	0.106
		4	0.160

* First pass is a downpass

The selected regenerative cooling circuit for the LAIR/H_2 rocket primary was the two-pass arrangement using 347 stainless steel tubes. Stainless steel was determined to be the better choice since it allows larger tube diameters and smaller chamber weight. The two-pass cooling circuit yielded a tube diameter greater than 0.10 inch over the entire thrust range examined.

8.3.2.4 Nozzle Design

A typical (Class 2) nozzle design map is shown in Figure 260. Lines of constant C_F are shown on the map. Figure 261 was plotted from the

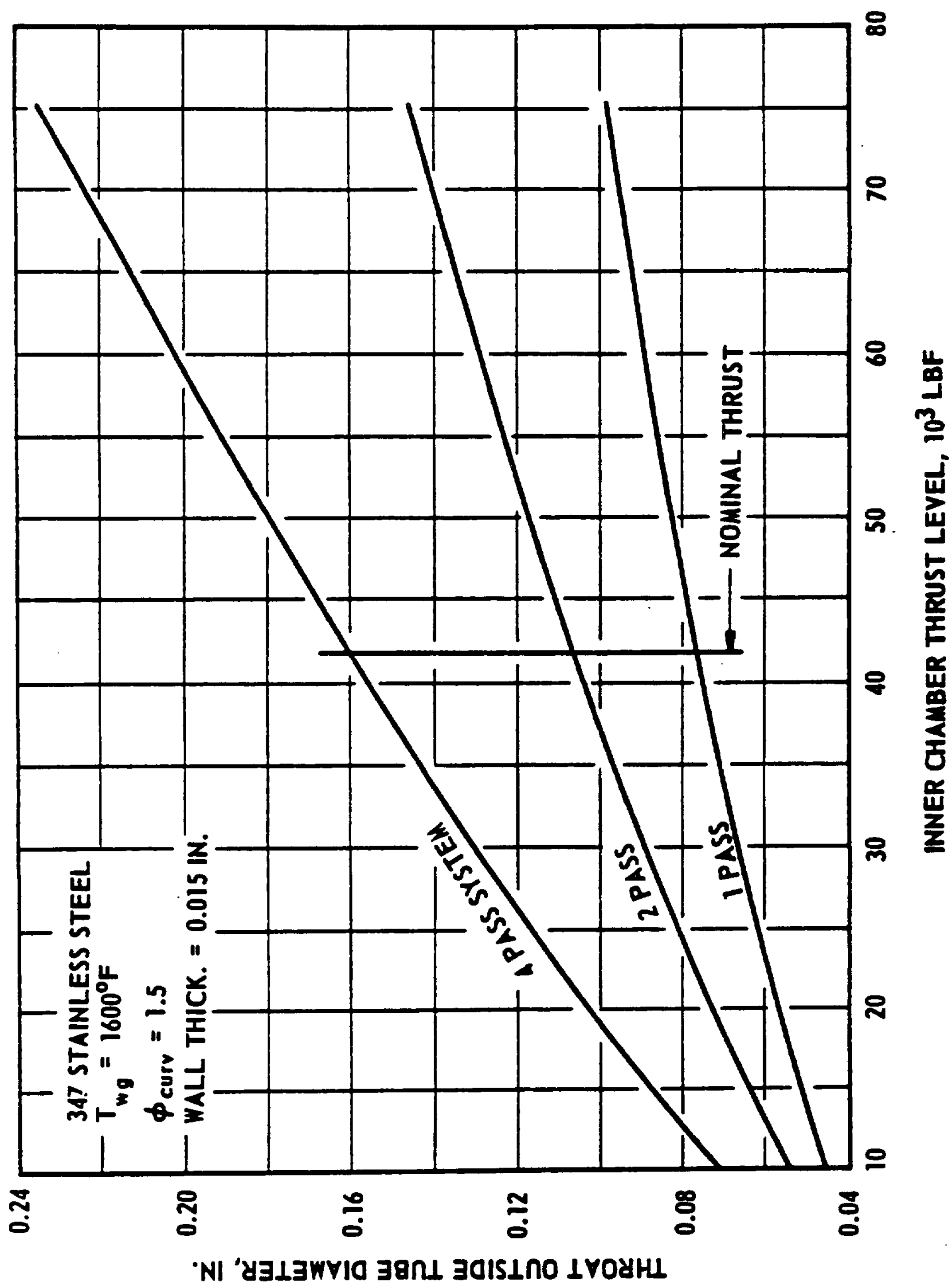

FIGURE 259. Tube Size as a Function of Inner Chamber Thrust Level for the Class 2 LAIR/H_2 Rocket Primary

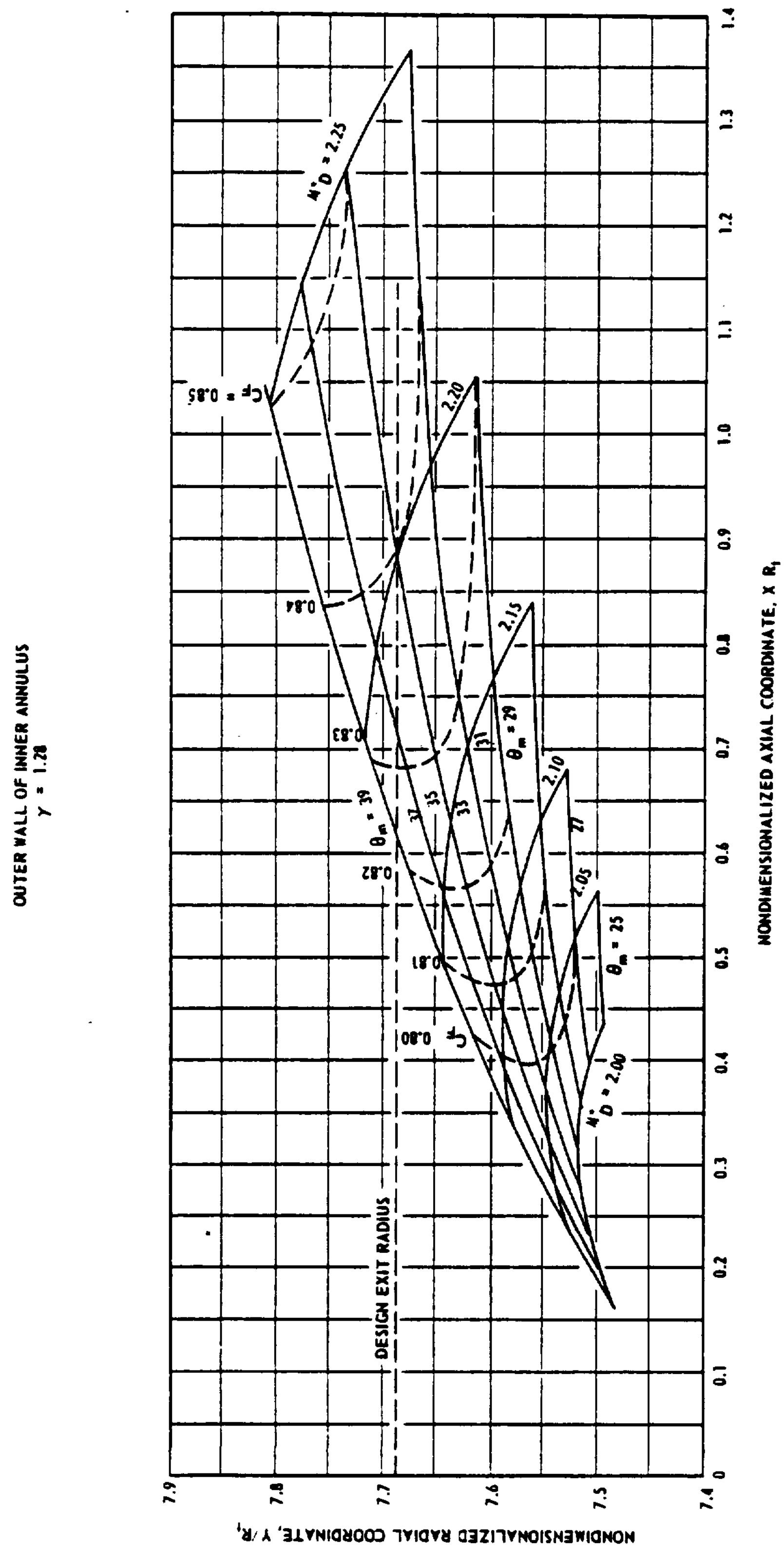

FIGURE 260. Typical Nozzle Design Map for Class 2 LAIR/H_2 Rocket Primary

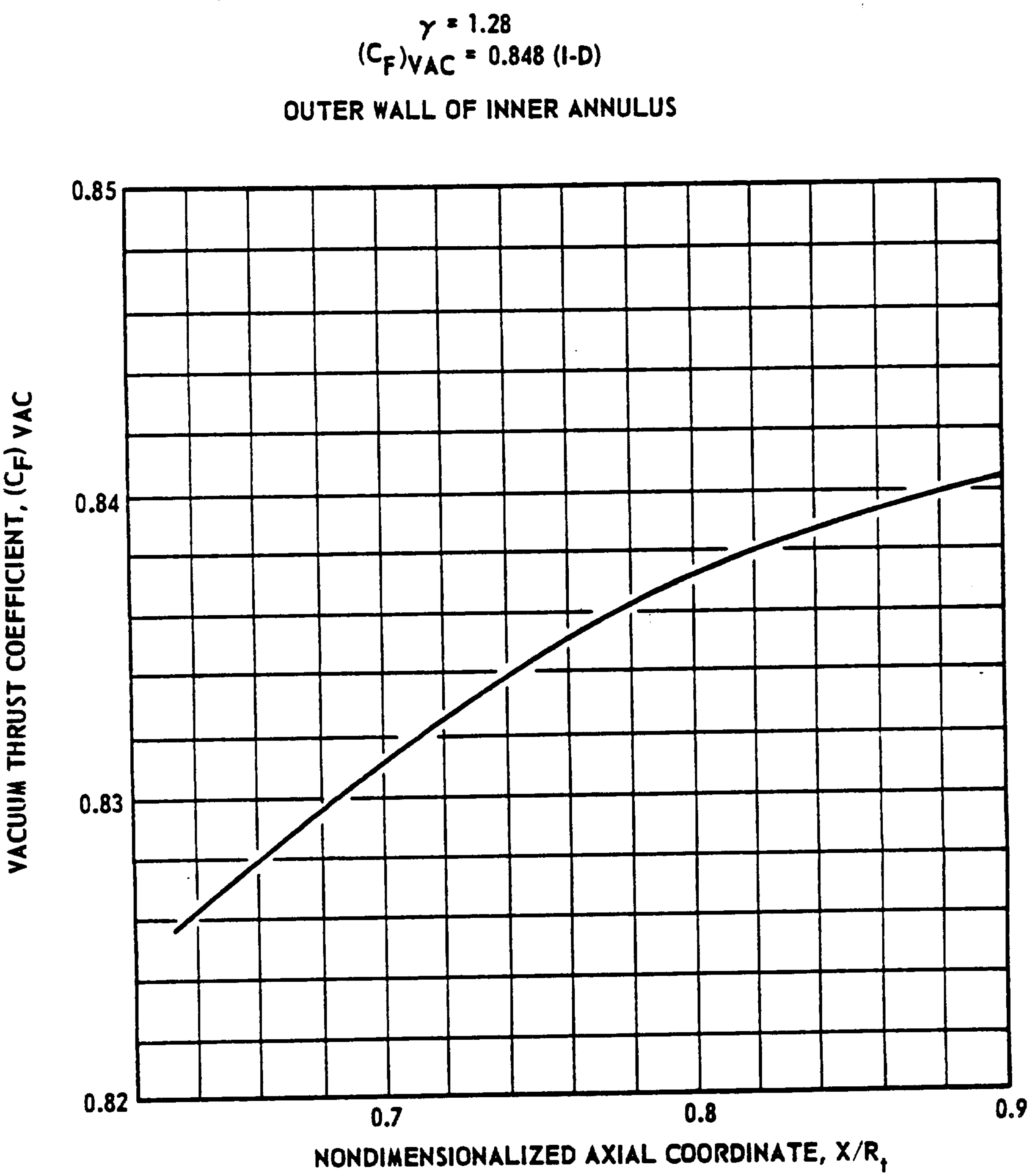

FIGURE 261. Effect of Nozzle Length on Vacuum Thrust Coefficient, Class 2 LAIR/H_2 Rocket Primary

map data and more clearly shows the variation of C_F with nozzle length for the given exit radius. The C_F values in Figures 260 and 261 are for the outer wall of the nozzle only. The inner wall is handled separately and the two are added to obtain total nozzle performance. Nozzle length is determined by trading off nozzle weight against performance. In this case X/R_t = 0.915 was selected for the nozzle length. The design nozzle lengths for all cases considered has been given in Table XLIII.

The nozzle contours for the LO_2/H_2 and $LAIR/H_2$ rocket primaries are presented in Figure 262.

8.3.2.5 Turbopump Design

Pump and associated drive turbines were evaluated for supplying primary fuel and oxidizer (liquid oxygen, liquid air) and secondary (afterburner) fuel and oxidizer. Advanced state of the art considerations, which are documented herein, were employed in selecting the turbopump configurations which are presented.

It will be noted from these results that turbopump considerations for composite propulsion systems differ in a number of significant ways (e.g., turbine backpressure requirements) from conventional or advanced all-rocket systems.

8.3.2.5.1 Effect of Speed on Turbopump Design

The significant effect of rotational speed on the turbopump weight is shown in Figure 263. Weight reductions of 30 to 50 percent can be obtained by doubling the operating speed. For liquid hydrogen turbopumps, Figure 264 indicates how pump efficiency increases with rotational speed. This increase occurs because of the improvement in pump specific speed obtained at the higher speed. However, the available NPSH, bearing and seal operating speeds, and life will place a limit to the maximum operating speed which can be used. Turbine stresses will also impose a speed limit. Thus, all design factors must be evaluated to determine which turbopump component first becomes speed-limited.

The cavitation-limited speed based on available NPSH, for all the turbopumps is given in Figure 265. Based on an advanced state of the art in rolling contact bearings, and on a 10 or 100 hour life requirement, bearing DN* limits for propellant lubricated bearings are estimated in Figure 266. The corresponding turbopump operating speed limits are indicated in Figures 267 and 268 for parametric values of pump discharge pressure. In these figures, the turbopump shaft size has been estimated from critical speed considerations. A correlation of operating seal speed with bearing DN values is shown in Figure 269. A summary of the turbopump speed limits imposed independently by each component is given below:

- - - - - - -

* DN = Bearing diameter (mm) x Shaft rotational speed

ANNULAR BELL NOZZLES

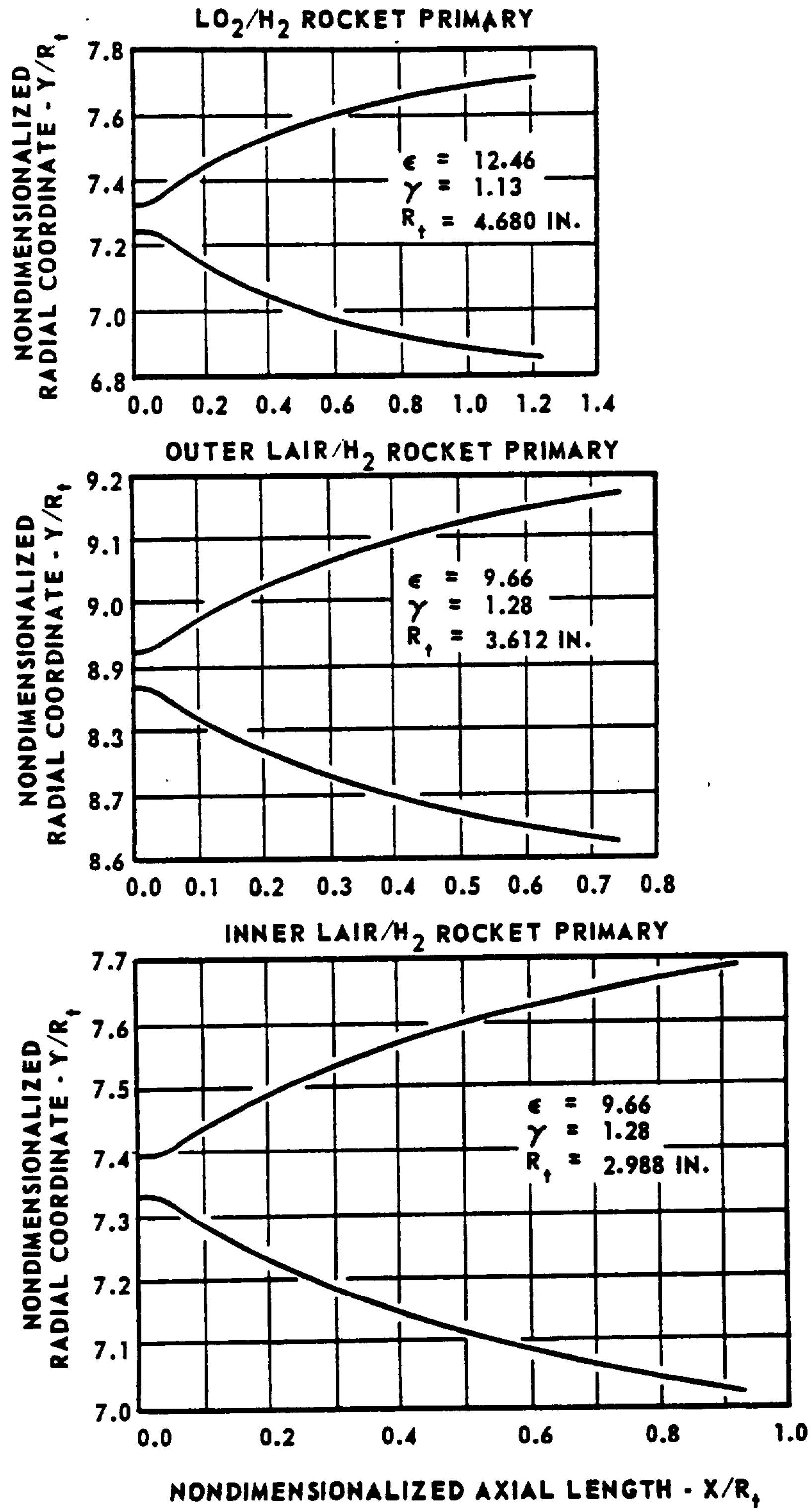

FIGURE 262. Nozzle Contours for Class 2 Rocket Primaries

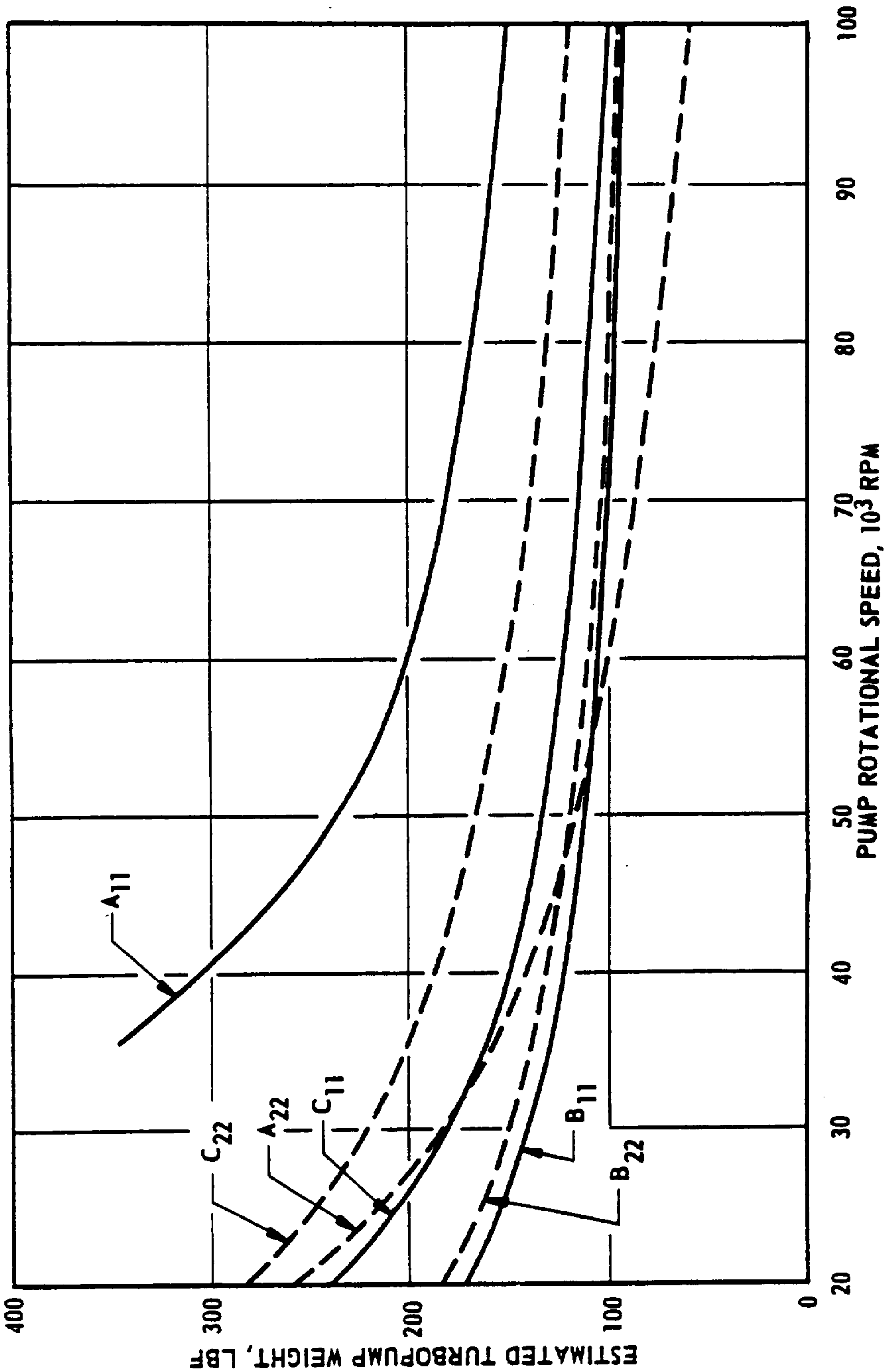

FIGURE 263. Effect of Rotational Speed on Estimated Turbopump Weight

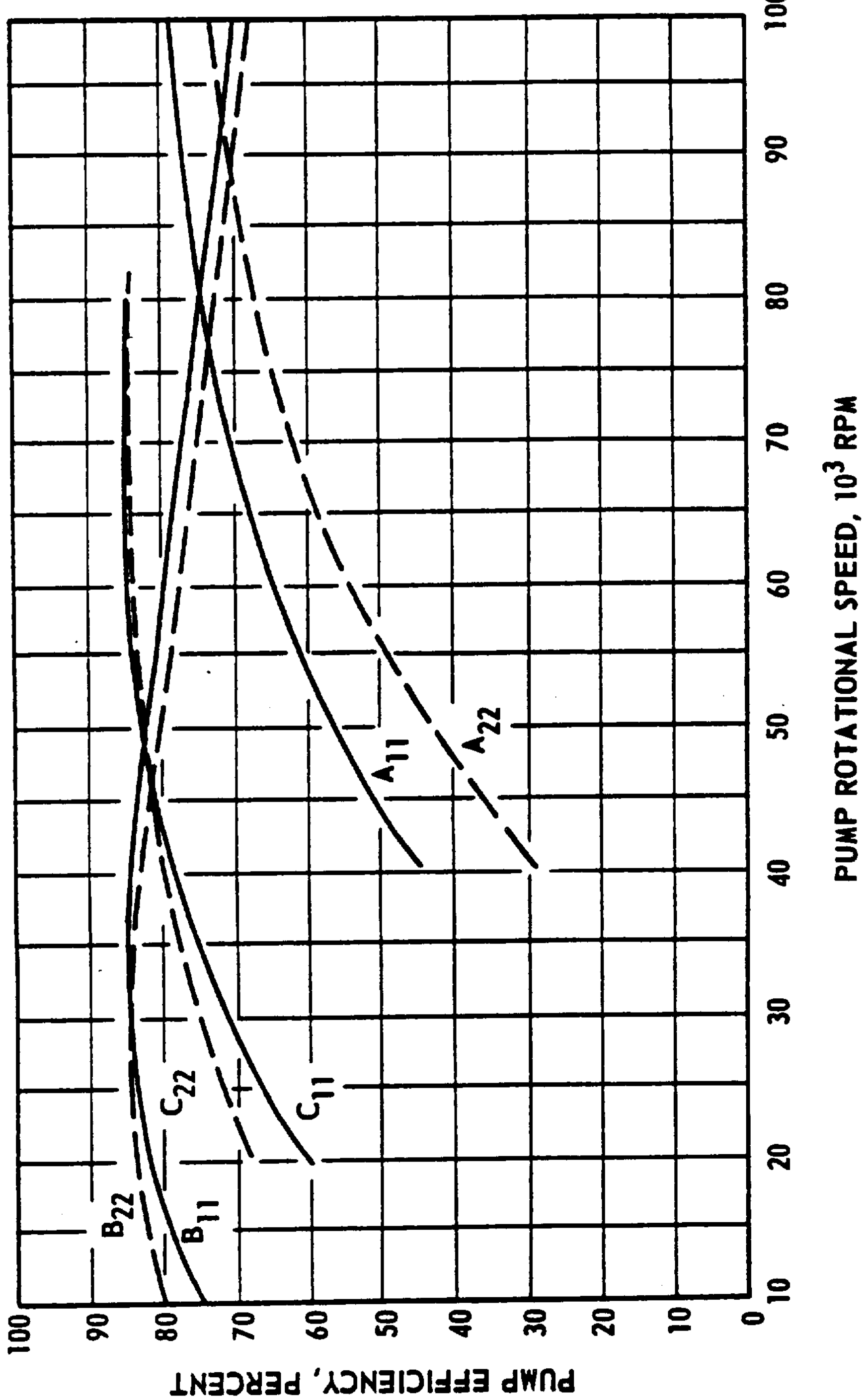

FIGURE 264. Effect of Turbopump Speed on Pump Efficiency

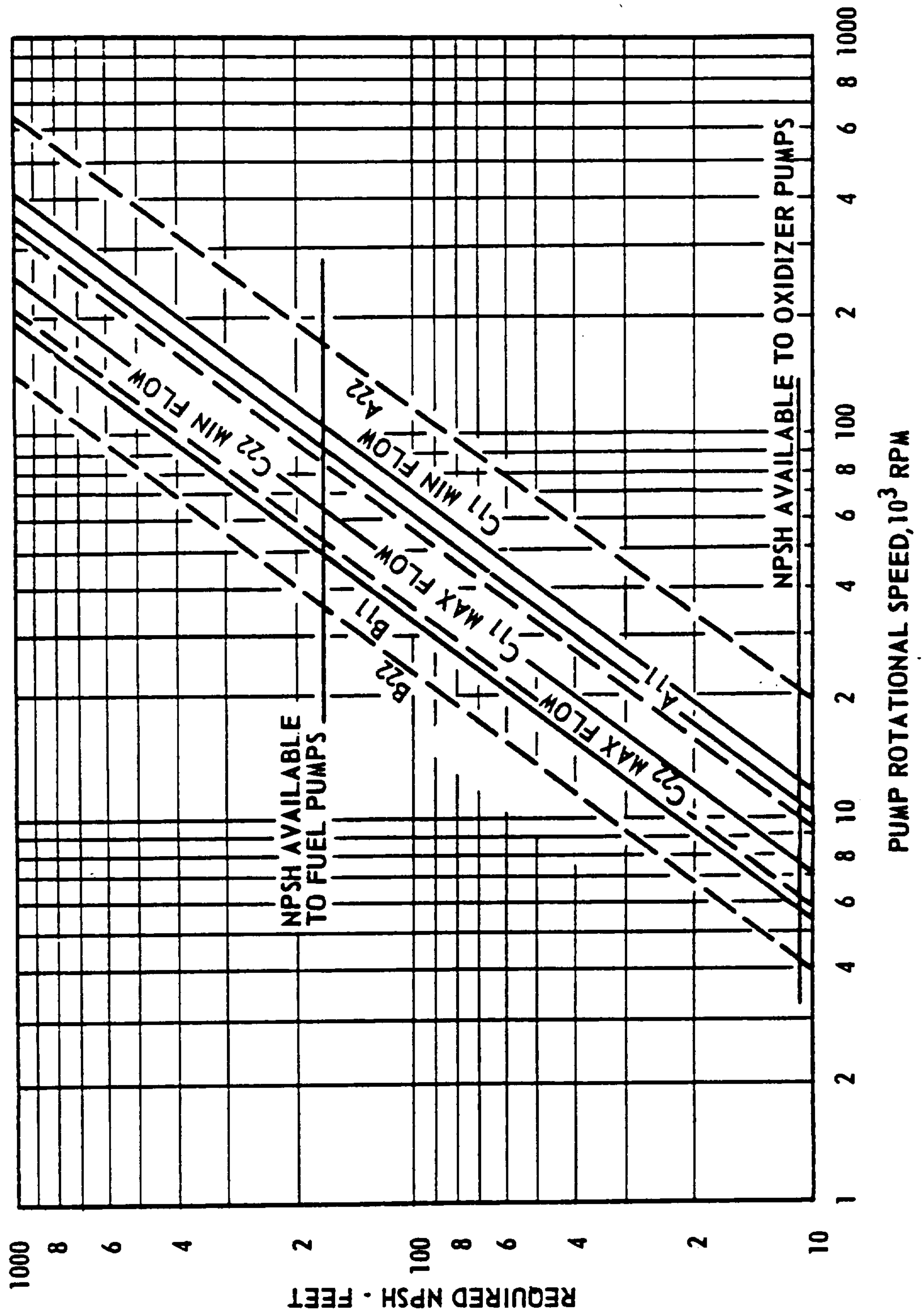

FIGURE 265. Effect of Pump Rotational Speed on Required Pump Net Positive Suction Head (To Avoid Cavitation)

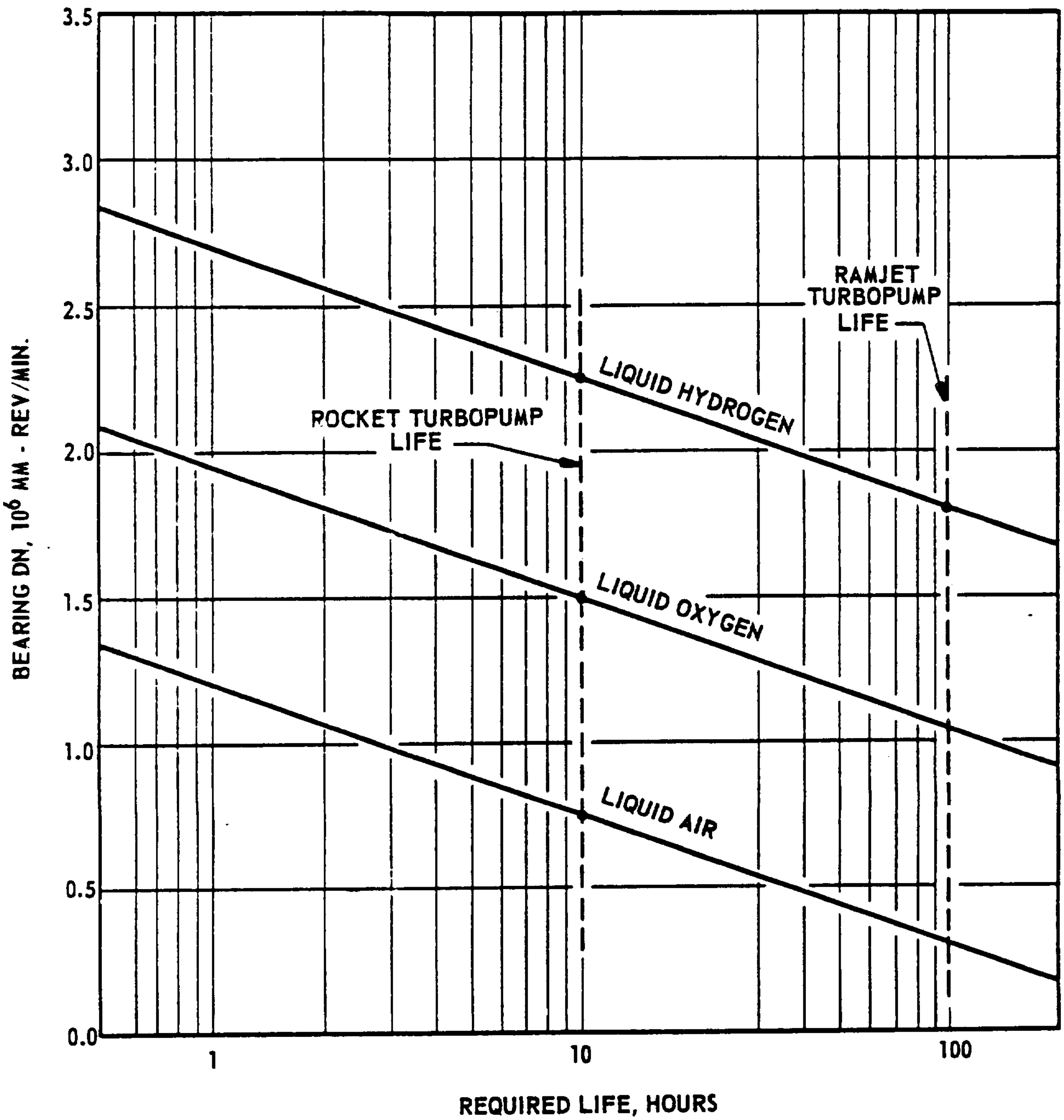

FIGURE 266. Allowable Design Bearing DN in Cryogenic Fluid vs. Operational Life, Rolling Contact Bearings

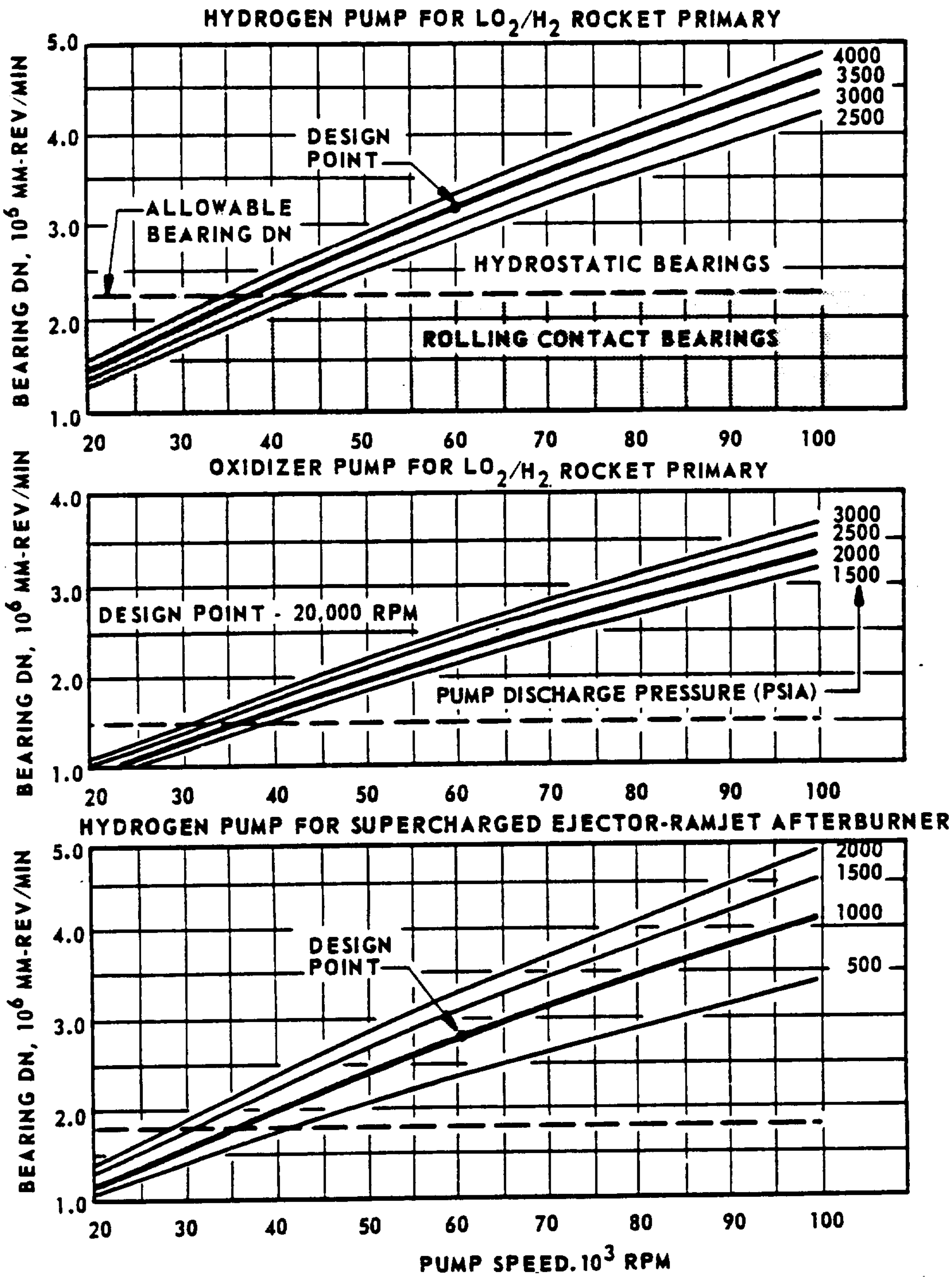

FIGURE 267. Required Bearing DN Values vs. Pump Rotational Speed, Shaft Sized by Critical Speed

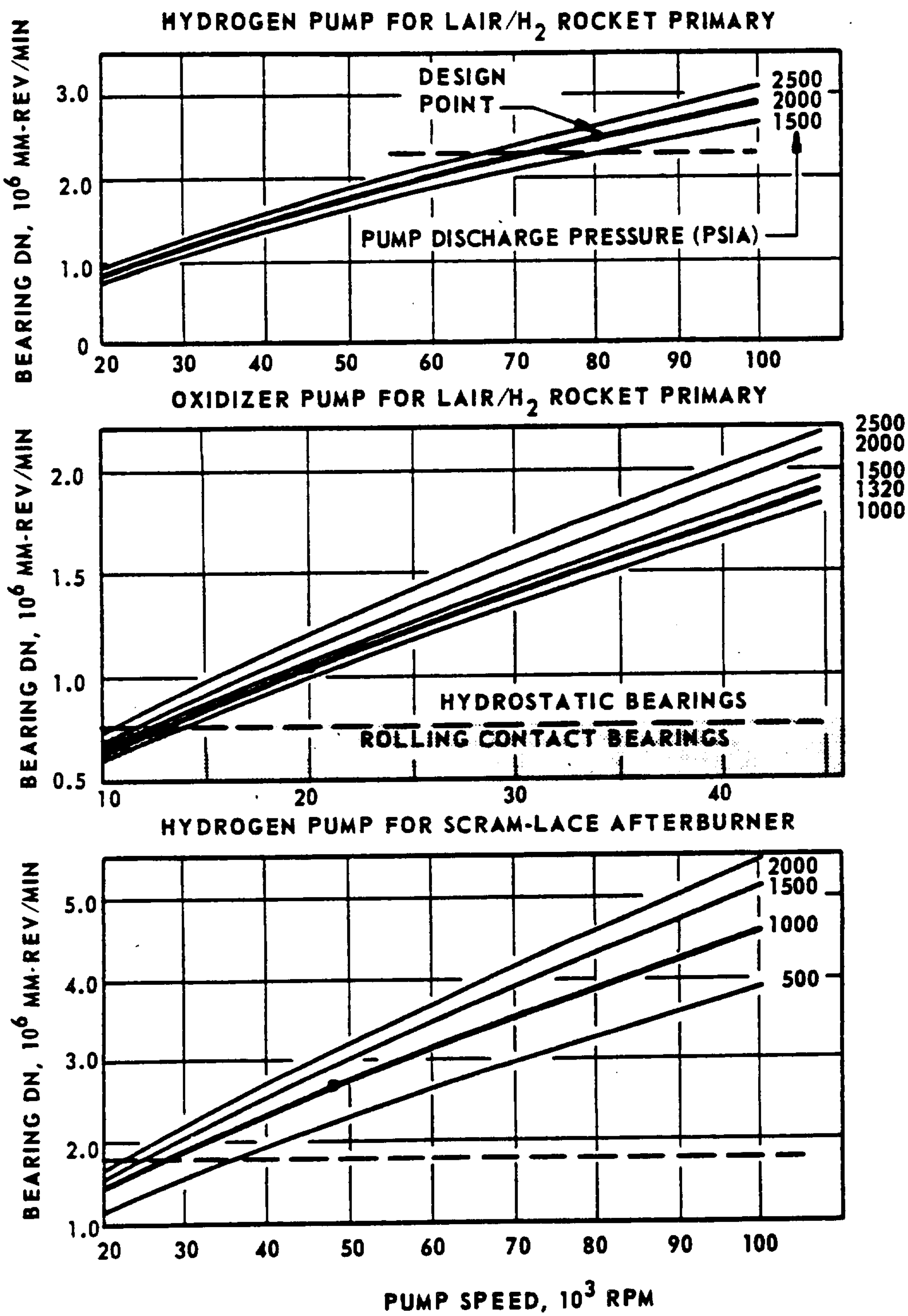

FIGURE 268. Required Bearing DN Values vs. Pump Rotational Speed, Shaft Sized by Critical Speed

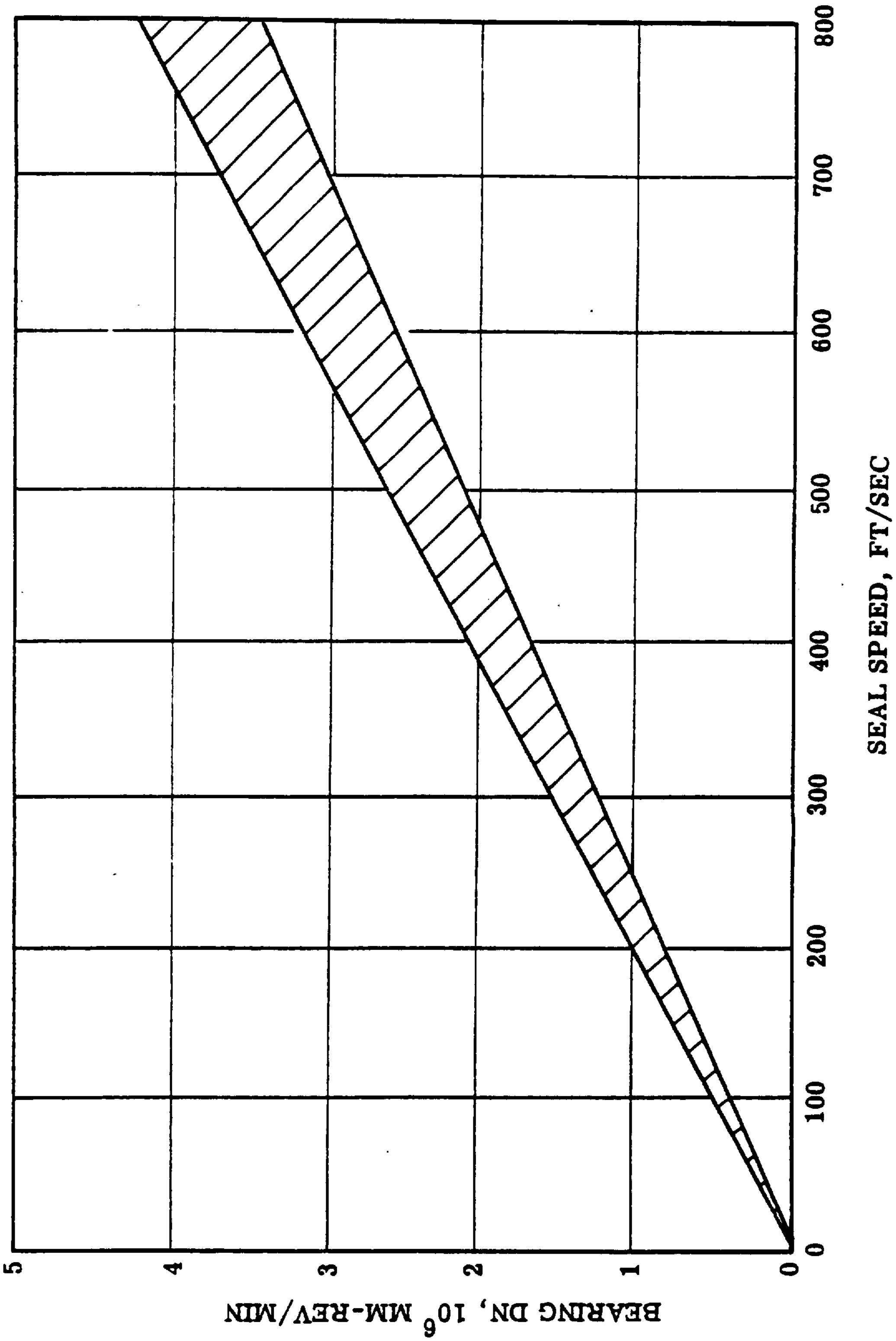

FIGURE 269. Correlation Between Bearing and Seal Speeds

Turbopump	NPSH (Cavitation) (rpm)	Bearing DN (Critical speed) (rpm)	Seal Speed (Based on bearing DN) (rpm)
A_{11}	85,000	37,500	31,000
B_{11}	5,800	36,000	36,000
C_{11}	60,000	34,000	37,000
A_{22}	160,000	70,000	57,000
B_{22}	4,000	12,800	19,000
C_{22}	48,500	29,000	33,000

In the liquid hydrogen turbopumps, the bearing and seal are seen to limit the turbopump speed to low rpm. If hydrostatic bearings and seals are used, it would be possible to attain the higher cavitation limited rpm. In the case of the oxidizer pumps, however, the NPSH is seen to limit the turbopump speed. By using a low speed pre-inducer (or boost pump) to obtain high suction performance, the higher bearing DN-limited speeds can be approached.

8.3.2.5.2 Primary Rocket Liquid Hydrogen Pumps

The relationship between head, flow, and the speed required of the pump generally determines the type of pump to use (in terms of specific speed). Because of the low density of hydrogen, the pump must develop a high head to deliver pressures of 1000 to 4000 psia. This condition will dictate a centrifugal pump of low specific speed operating at high impeller tip speed. An unshrouded, titanium impeller can attain a state of the art tip speed of 2400 ft/sec which would allow the above pressures to be obtained in a single stage pump. However, by using lower impeller tip speeds and a two-stage pump, the efficiency will be improved but the design will be more complex. A combination inducer-centrifugal stage is another approach to obtain high pressures in a single stage pump with good efficiency. All of these configurations have been studied for the rocket LH_2 turbopump. The pump design parameters are given in Table XLV as A_{11} and in Table XLVI as A_{22} for Engines Nos. 11 and 22, respectively.

A typical advanced design of the A_{11} turbopump is illustrated in Figure 270. It is a single stage, low specific speed (N_s = 740) centrifugal pump using hydrostatic bearings and seals and operating at 60,000 rpm. The rolling contact bearing, at the large shaft diameter, operates only at low speeds and will retract at high speeds as the hydrostatic bearing, located at the

TABLE XLV

TURBOPUMP DESIGN PARAMETERS FOR SUPERCHARGED EJECTOR RAMJET ENGINE NO. 11

	Rocket Engine Fuel Pump	Rocket Engine Oxidizer Pump	Ramjet Afterburner Fuel Pump
Turbopump designation	A_{11}	B_{11}	C_{11}
Propellant	LH_2	LO_2	LH_2
Pump type	Single stage centrifugal	Single stage centrifugal (With pre-inducer)	Single stage centrifugal
Speed, rpm	60,000	20,000	60,000
Efficiency, %	66	82	85
Horsepower, hp	14,700	3,430	4,880
Weight, lbf	205	165	122
Specific speed (per stage)	740	2,100	2,040
Impeller tip speed, ft/sec	2,220	461	1,550
Bearings	Hydrostatic	Rolling contact	Hydrostatic
Seals	Hydrostatic	Rubbing	Hydrostatic

Other Designs

	Inducer - Centrifugal Pump	Two-Stage Centrifugal	Inducer Pump (With Pre-inducer)	Inducer Pump (With Pre-inducer)
Speed, rpm	60,000	60,000	30,000	73,000
Efficiency, %	75	78	85	85
Horsepower, hp	13,000	12,470	3,310	4,880
Weight, lbf	195	190	150	113
Specific speed (per stage)	1,002	1,245	3,160	2,480
Impeller tip speed, ft/sec	1,812	1,562	640	1,600
Bearings	Hydrostatic	Hydrostatic	Rolling contact	Hydrostatic
Seals	Hydrostatic	Hydrostatic	Rubbing	Hydrostatic

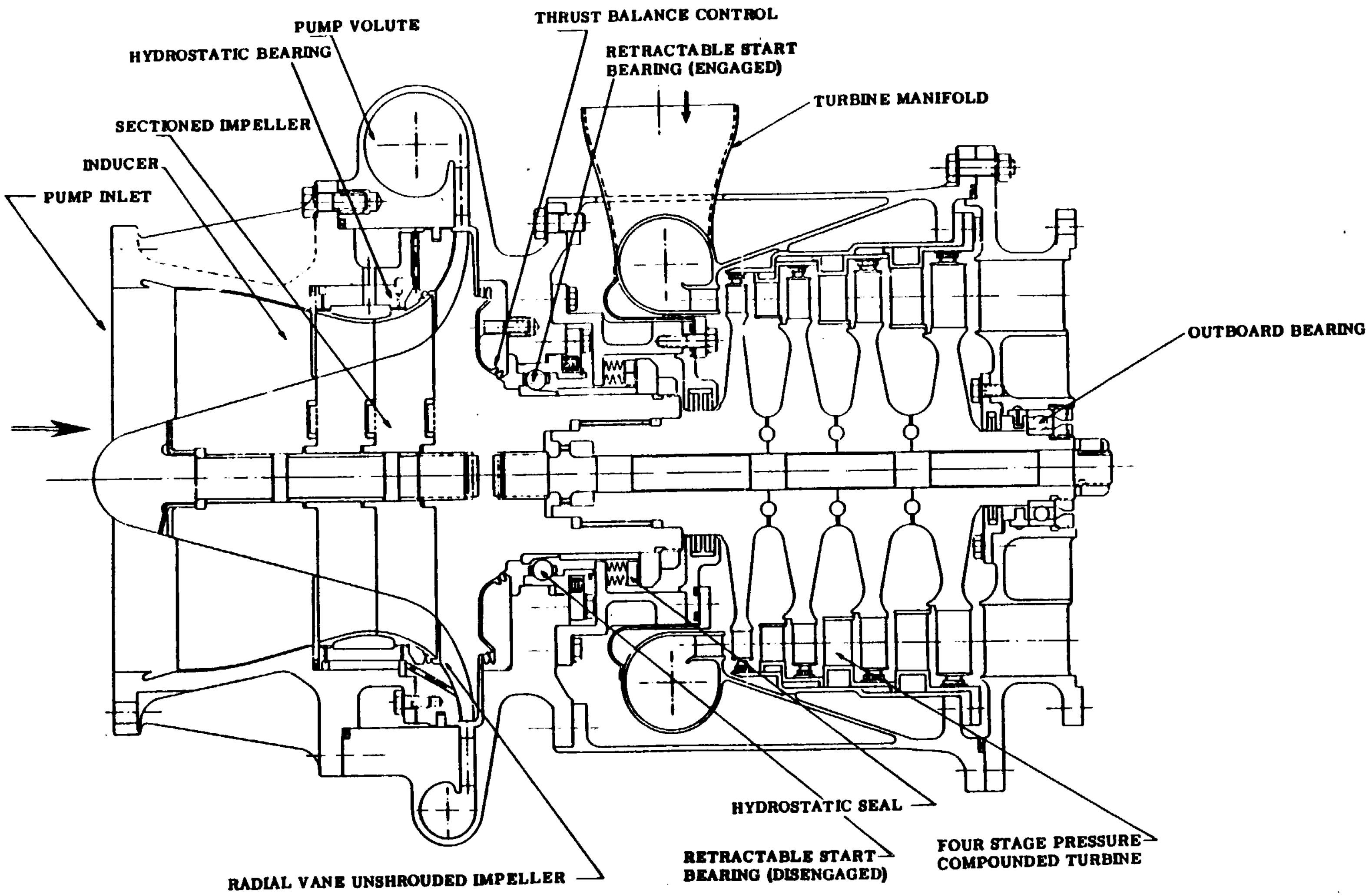

FIGURE 270. Assembly of the Hydrogen Turbopump for the Primary Rocket Subsystem of the Class 2 Supercharged Ejector Ramjet

impeller shroud, assumes the load. The pump uses an unshrouded, radial vaned, titanium impeller which operates at 2220 ft/sec tip speed and delivers a pressure of 3500 psia. The volute has a vaned diffuser which partially diffuses the flow and also acts as an integral structure to resist both volute and case opening forces.

8.3.2.5.3 Primary Rocket Liquid Oxygen Pump (Engine No. 11)

Because of the higher density of liquid oxygen, a single stage, high specific speed (N_s = 2100) centrifugal pump operating at 20,000 rpm will deliver the required discharge pressure of 1950 psia with high efficiency. As a result of the low available NPSH, a low speed pre-inducer will be required. A high speed, 35,000 rpm inducer pump was also studied. The design parameters for these pumps are given in Table XLV as B_{11}.

A typical advanced design of the B_{11} turbopump is illustrated in Figure 271. It is a single stage pump using high speed, rolling contact bearings and high speed, rubbing seals. The impeller uses backward curved blades. To meet the NPSH of 10.8 feet, a low speed pre-inducer must be used. This allows the main pump to operate at high speed. This pre-inducer is powered by hydraulic or mechanical means. Since the power required by the pre-inducer is small, the overall performance of the pump is not significantly affected. The configuration reflects a simple and compact design of a high speed, high suction performance pump.

8.3.2.5.4 Primary Rocket Liquid Air Pump (Engine No. 22)

The liquid air pump will be similar to the liquid oxygen pump but because of its higher flow and lower head it will have a higher specific speed (N_s = 2790) design. Since the inlet pressure to the pump is below atmospheric pressure, the available NPSH will be very low. Thus, to obtain a reasonable pump design, the heat exchanger was assumed to produce liquid air at sufficiently low temperatures to provide at least 10 ft of available NPSH. Bearings and seals operating in liquid air have not reached the same state of the art as those for liquid oxygen operation and, therefore, hydrostatic bearings and seals must be used at the pump design speed of 20,000 rpm. The design parameter for this pump, and for a higher speed inducer pump, are given in Table XLVI as B_{22}.

8.3.2.5.5 Afterburner Liquid Hydrogen Pumps (Ramjet)

The afterburner LH_2 pump design will have a higher specific speed (N_s = 2040) than the rocket LH_2 pumps because of its higher flow and lower head requirements (Table XLVI). However, the afterburner pump has a large flow excursion, while maintaining a discharge pressure of 1000 psia. A pump can be designed between these two extreme flow conditions to meet this

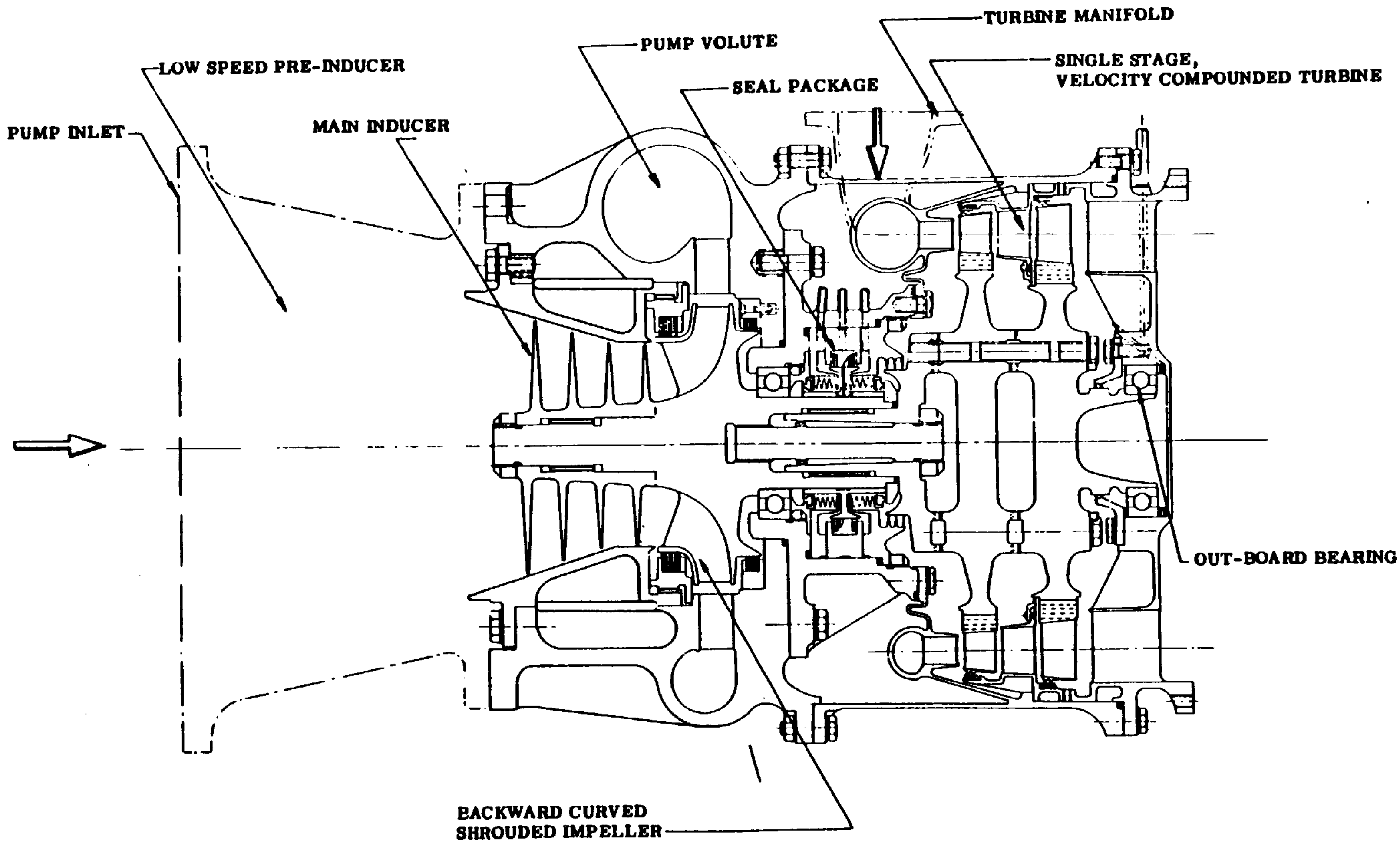

FIGURE 271. Assembly of the Liquid Oxygen Turbopump for the Primary Rocket Subsystem of the Class 2 Supercharged Ejector Scramjet

TABLE XLVI

TURBOPUMP DESIGN PARAMETERS FOR SCRAMLACE ENGINE NO. 22

	Rocket Engine Fuel Pump	Rocket Engine Oxidizer Pump	Ramjet Afterburner Fuel Pump
Turbopump designation	A_{22}	B_{22}	C_{22}
Propellant	LH_2	Liquid air	LH_2
Pump type	Single stage centrifugal	Single stage centrifugal (With Pre-inducer)	Single stage centrifugal
Speed, rpm	75,000	20,000	48,000
Efficiency, %	66	84	83
Horsepower, hp	2,410	3,660	7,640
Weight, lbf	82	184	170
Specific speed (per stage)	730	2,790	2,100
Impeller tip speed, ft/sec	1,775	450	1,558
Bearings	Hydrostatic	Hydrostatic	Hydrostatic
Seals	Hydrostatic	Hydrostatic	Hydrostatic

Other Designs

	Inducer - Centrifugal	Two-Stage Centrifugal	Inducer Pump (With Pre-inducer)	Inducer Pump (With Pre-inducer)
Speed, rpm	75,000	75,000	35,000	70,000
Efficiency, %	72	78	85	85
Horsepower, hp	2,210	2,040	3,620	7,470
Weight, lbf	78	74	140	140
Specific speed (per stage)	990	1,228	4,860	2,940
Impeller tip speed, ft/sec	1,462	1,280	750	1,870
Bearings	Hydrostatic	Hydrostatic	Hydrostatic	Hydrostatic
Seals	Hydrostatic	Hydrostatic	Hydrostatic	Hydrostatic

broad flow requirement. The performance map for these pumps is shown in Figure 272. By proper control of pump speed and the discharge valve, the high flow can be met by increasing the speed of the pump to approximately 115 percent of the nominal speed. The low flow can be obtained by reducing the speed of the pump to approximately 90 percent of nominal speed. A shrouded impeller with a 25° backward curve blade will meet this throttling requirement and will also have a good design point efficiency. A higher speed inducer pump, which will require a low speed pre-inducer, was also studied. The design parameters for both pumps are given in Table XLV as C_{11} and in Table XLVI as C_{22} for composite Engines Nos. 11 and 22, respectively.

8.3.2.5.6 Turbine Design

The engine cycle requirements were used to establish the turbine inlet and exhaust pressure and temperature conditions. Both single stage, velocity-compounded, turbine designs and multistage, pressure-compounded, turbine designs were studied where applicable. Because of the low pressure ratio available, the turbines for the rocket engine turbopumps were designed to operate in parallel instead of in series (where the high pressure turbine exhausts into the inlet of the low pressure turbine). An objective in the turbine design was to obtain the highest possible efficiency in order to keep the mass flow to approximately 3 percent of the engine flow. Although a pressure-compounded turbine (which is shown for the turbopump in Figure 270) would have an efficiency from 3 to 5 percent higher than a velocity-compounded turbine (shown for the turbopump B_{11} in Figure 271), a well designed velocity-compounded turbine can attain an efficiency as high as 65 to 70 percent and will have advantages in size and weight. A summary of velocity-compounded turbine designs for Engines Nos. 11 and 22 is given in Table XLVII. In all cases, except for Turbopump A_{22}, the turbopump rotational speed was dictated by the pump design rather than by the turbine design. For Turbopump A_{22}, the turbine blade stresses are high (75,000 rpm).

In order to meet the flow excursion requirement of the ramjet afterburner turbopumps (Figure 272), the turbines for Turbopumps C_{11} and C_{22} were designed with a variable area nozzle. These turbines will maintain relatively constant efficiency over a horsepower range ± 40 percent of the nominal design condition. The turbine mass flows at the off-design conditions are summarized below.

Turbopump	C_{11} (Mass flow, lbs/sec)	C_{22}
Reduced load (60 percent)	2.46	3.83
Nominal Load (100 percent)	4.25	6.65
Overload (140 percent)	6.10	9.47

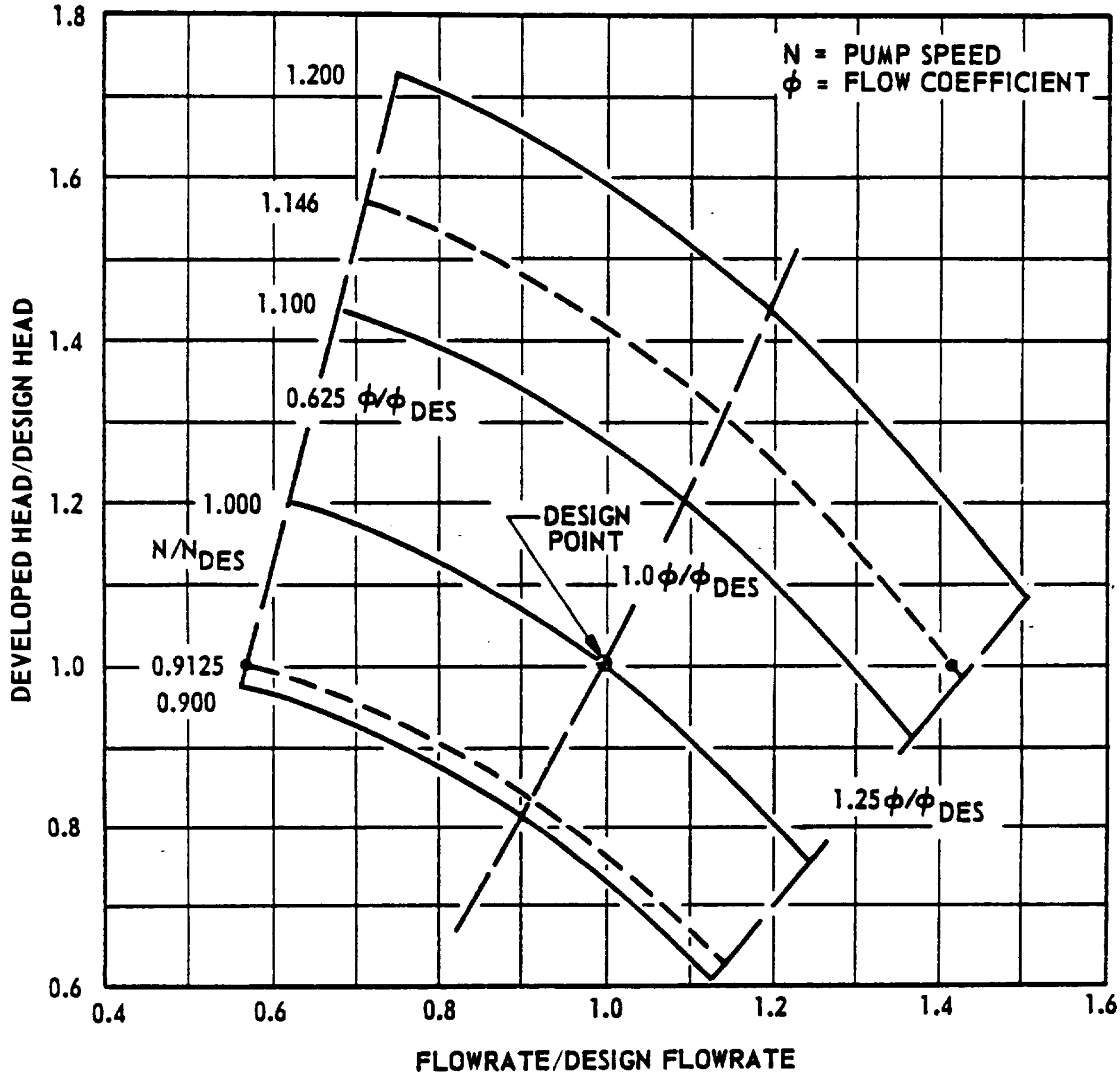

FIGURE 272. Performance Map for the Ejector Ramjet Afterburner Liquid Hydrogen Pump

TABLE XLVII

SUMMARY OF TURBINE DESIGN PARAMETERS FOR ENGINES NOS. 11 AND 22

Turbopump Designation	A_{11}	B_{11}	C_{11}
Speed, rpm	60,000	20,000	60,000
Horsepower	14,700	3,430	4,880
Inlet temperature, °F	1,500	1,500	1,500
Inlet pressure, psia	1,500	1,500	1,500
Pressure ratio	15	15	5
Pitch line velocity, ft/sec	1,600	700	1,600
Pitch diameter, ins.	6.0	8.0	6.0
Efficiency, %	70	40	67
Mass flow, lbs/sec	8.40	3.30	4.25
Turbopump Designation	A_{22}	B_{22}	C_{22}
Speed, rpm	75,000	20,000	48,000
Horsepower	2,410	3,660	7,640
Inlet temperature, °F	1,500	1,500	1,500
Inlet pressure, psia	1,000	1,000	1,000
Pressure ratio	10	10	5
Pitch line velocity, ft/sec	1,470	875	1,435
Pitch diameter, ins.	4.25	9.75	6.85
Efficiency, %	64	48	68
Mass flow, lbs/sec	1.50	3.40	6.65

8.3.2.6 Primary Subsystem Control

A schematic of the feed and control system for the rocket primaries is shown in Figure 273. A gaseous hydrogen energy source is used for starting the engine. An electro-pneumatic control system is used for engine valve operation. The control system derives its power from a regulated helium system supplied by a tank mounted within the gaseous hydrogen start tank.

The spark plugs are excited to initiate engine start. The main fuel valve is opened, followed by the start tank spin valve. Gaseous hydrogen flows through the turbine drive system to accelerate both turbopumps. When rated turbopump speed is obtained, the start tank spin valve is closed and simultaneously the main oxidizer valve and gas generator valve are opened. As soon as mainstaging has been recognized, the spark plugs are de-energized and rated thrust has been achieved.

Steady state operation is maintained until a cutoff signal is initiated. At this signal, the main oxidizer and gas generator valves are closed, followed by the closing of the main fuel valve. During steady state operation, gaseous hydrogen is bled from the fuel jacket to recharge the start tank.

8.3.2.7 Primary Subsystem Weights

A detailed breakdown of the weight estimates for the Class 2 rocket primaries is given below:

Rocket Primary	LO_2/H_2	$LAIR/H_2$
Outer combustion chamber and nozzle	518 lbm	324 lbm
Inner combustion chamber and nozzle	--	227
Chamber support structure	1138	1020
Turbopumps (Primary only)	370	266
Gas generator system	149	149
Propellant ducting and valves	67	71
Start system	148	148
Total weight	2390 lbm	2205 lbm
("Final" total weight)*	(2028 lbm)	(2334 lbm)

*Estimated for resized primaries (See Footnote at the beginning of Section 8.3.6.1) based on constant subsystem thrust/weight ratio over a -14 + 4% range.

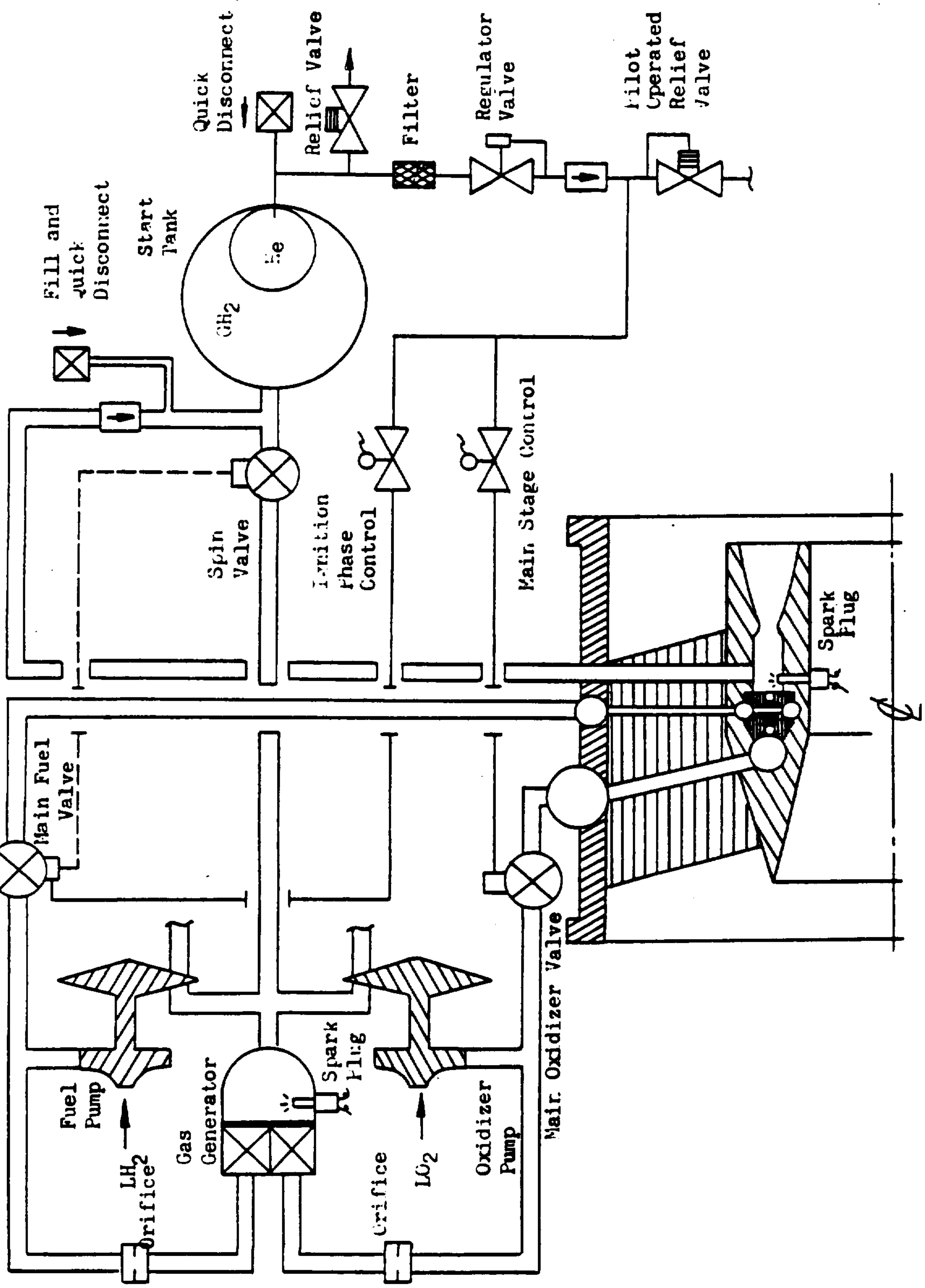

FIGURE 273. Schematic of Feed and Control System for the Rocket Primaries

8.4 Engine Design

The conceptual designs of the Class 2 Supercharged Ejector Ramjet and ScramLACE engines are presented in this section. Associated engine performance was previously presented in Section 8.2. Both performance and design aspects are presented in full detail in Volume 7. The design methodology and results are presented below.

8.4.1 Methodology

8.4.1.1 Engine Flow Area Specification

8.4.1.1.1 Supercharged Ejector Ramjet (Engine No. 11)

The results of the parametric performance analysis and the engine sizing studies presented in Section 8.2.1 defined the Class 2 Supercharged Ejector Ramjet (SERJ) engine design. The engine parameters and flow areas for the specified 215,000 pound sea level static thrust are as follows:

Secondary/Primary flow ratio, W_s/W_p	= 3.0
Primary rocket chamber pressure	= 1500 psia
Fan pressure ratio	= 1.30
Fan/Airbreathing gas generator bypass ratio	= 10.0
Mixer flow area, A_3	= 43.49 sq ft
Afterburner flow area, A_4	= 76.24 sq ft
Afterburner/Mixer diffusion ratio, A_4/A_3	= 1.75
Exit nozzle throat area, A_5	
Maximum	= 68.5 sq ft
Minimum	= 7.0 sq ft
Nozzle exit area, A_6	= 107.0 sq ft

The basic approach for the design study of the Class 2 Supercharged Ejector Ramjet was oriented toward a general design configuration suitable for installation with either an axisymmetric or a two-dimensional inlet. The high Mach number range (6 to 8) of the subsonic combustion ramjet operating mode for the Supercharged Ejector Ramjet also tends to require a higher maximum internal pressure than for engines that convert to the supersonic combustion mode at Mach 6. In view of these points, and with consideration of the Mission/Vehicle implications attending an engine configuration choice, an axisymmetric configuration with a maximum internal pressure of 150 psia was selected for the Supercharged Ejector Ramjet design.

8.4.1.1.2 <u>ScramLACE (Engine No. 22)</u>

As discussed in Section 8.2.1, the Class 2 ScramLACE engine is identical to the Class 1 ScramLACE with respect to the general design parameters of primary chamber pressure, secondary-to-primary flow ratio, and heat exchanger equivalence ratio. Engine performance differs slightly due to more refined off-design heat exchanger performance in Class 2, and due to the different design thrust levels, viz., 250,000 pounds for Class 1 and 173,000 pounds for Class 2. The general engine design point characteristics for the Class 2 ScramLACE design are as follows:

Secondary/primary flow ratio, W_s/W_p	= 1.5
Primary rocket chamber pressure	= 1000 psia
Mixer flow area, A_3	= 22.89 sq ft
Afterburner flow area, A_4	= 47.87 sq ft
Afterburner/Mixer diffusion ratio, A_4/A_3	= 2.1
Exit nozzle throat area, A_5	
Maximum = A_4	= 47.87 sq ft
Minimum	= 15 sq ft
Nozzle exit area maximum (Vehicle aft surface)	= 274 sq ft
Heat exchanger equivalence ratio	= 8.0

As discussed previously, the selection of design parameters for a composite engine utilizing a supersonic combustion ramjet mode is strongly affected by this mode. Selection of engine flow areas must consider the effects on ejector mode augmentation at the low flight speeds and the effects on Scramjet performance at the high flight speeds. Generally, Scramjet engines must be thoroughly aerodynamically integrated with the vehicle in order to fully utilize the vehicle forebody as an inlet compression surface and the vehicle afterbody as an exhaust expansion surface. The overall installation and packaging requirements almost invariably specify a two-dimensional inlet design. The moving panels of such an inlet require a constant inlet width. For minimum installation length and installed engine weight, the transition sections between the exit of the inlet diffuser and the mixer entrance should be minimized or eliminated. This leads to a rectangular mixer configuration with a length-to-height ratio roughly equal to the inlet capture area/mixer area contraction ratio, assuming a square cross section for the inlet at the lip station.

8.4.1.2 <u>Heat Transfer and Control Considerations</u>

Two aspects of overall engine design which were initially considered in the Class 2 phase were engine heat transfer and cooling, and engine

control. Although only cursorily evaluated here, this effort yielded several significant indicators for possible future engine work. An example is the identification of a "control by operating mode" approach as a favorable tack for effecting engine operation.

The limitations applied to these efforts are described below. Cooling and control topics for the primary rocket subsystem have been previously described (Section 8.3).

8.4.1.2.1 Heat Transfer

No specific heat transfer analysis of the Class 2 composite engines was made except for the primary rocket chambers. The subsonic and supersonic combustion ramjet operating modes of the composite engines obviously are similar in heat transfer to "pure" ramjet and Scramjet engines. Some general comparisons were made relating the heat transfer and cooling requirements of composite engines to general ramjet and Scramjet design data. A limited survey of pertinent reports (References 44 and 45) was made and technical personnel in the heat transfer area were consulted.

8.4.1.2.2 Control System Approaches

Engine control approaches were briefly investigated and block diagram level synthesis was performed. Engine multimode operation suggested that a control-by-mode tack be taken with either manual or automatic mode selection as appropriate for each engine. For the following listings, reference should be made to Volume 7. The control loops are represented in block diagram form on pages 26 to 29 and 113 to 115 of Volume 7.

Four operating mode control loops were determined for the Supercharged Ejector Ramjet (Engine No. 11) as follows:

1. Combustor/Afterburner fuel control systems

2. Rocket feed control system

3. Exit nozzle control system

4. Airbreathing gas generator control system

Five control loops were defined for the ScramLACE (Engine No. 22) as follows:

1. Liquid air level control system

2. Normal shock position control system (Exit modification)

3. Rocket feed control system

4. Exit nozzle control system

5. Fuel control system

8.4.1.3 Basis for Weight Estimates

The general content of previous Section 7.4.1.3, regarding the Class 1 engine weight studies is applicable to the Class 2 work. This section will outline the differences involved in the Class 2 weight estimation techniques with reference to the earlier work.

The two Class 2 concepts are characterized as point designs whose sizing was specified mainly by vehicle integration considerations. It will be recalled that the Class 1 systems were somewhat arbitrarily specified as 250,000-pound thrust systems. From this, an estimated engine thrust/weight variation covering a thrust range of 50,000 to 500,000 pounds was documented (See Volume 6). For the Class 2 engines, the effort was concentrated on design point analysis as opposed to broader objectives. Illustrative of this engine thrust/weight sensitivity to individual subsystem weight, variations of as much as 150 percent reflected an overall thrust/weight ratio variation of only a few points about the derived design point value.

As evidenced in the Class 2 weight statements presented in Section 8.4.2.3, the component breakdown of Class 1 was significantly extended. For example, the rocket subsystem weight which formerly was lumped, now considered individually, the weights of the chamber assembly, turbopumps, support structure, etc. The finer breakdown is significant in achieving a somewhat higher confidence level in the engine weight and thrust/weight values.

Finally, the Class 2 subsystem weight estimates are considered somewhat more realistic than those associated with earlier Class 0 and 1 analysis. From a comparison, for example, the primary rocket design analysis effort under the Class 1 and Class 2 phases (Sections 7.3.2 and 8.3.2, respectively) the reader can sense a considerable further degree of technical penetration, hence a resulting higher confidence level in weight estimates.

8.4.2 Results

8.4.2.1 Detailed Conceptual Design Layouts

8.4.2.1.1 Supercharged Ejector Ramjet

A detailed conceptual design layout of the Class 2 Supercharged Ejector Ramjet engine is presented in Figure 274. This layout is further reflected in the accompanying perspective (Figure 275). The locations of all of

[redacted]

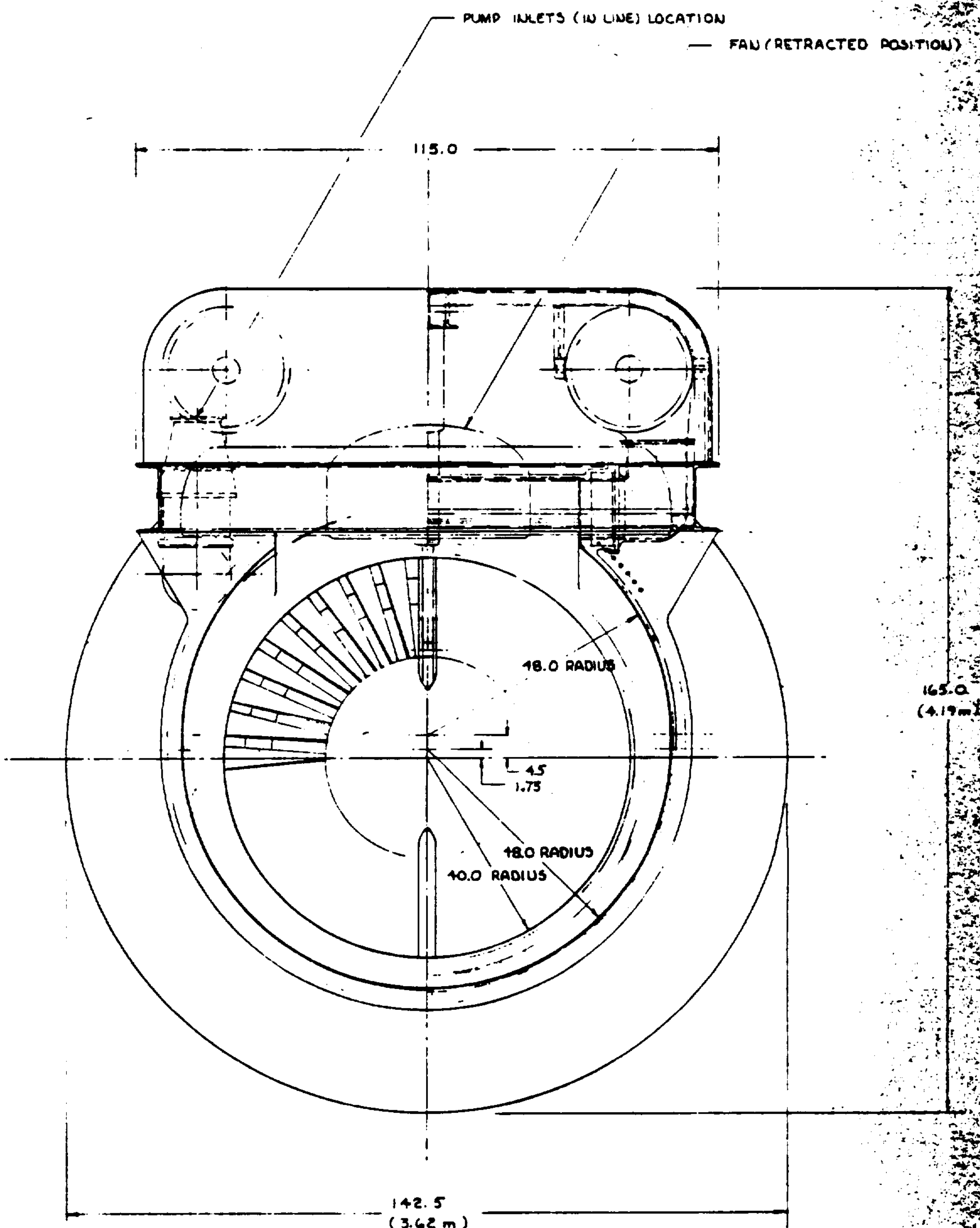

[redacted]

[redacted] 571-1

CONFIDENTIAL

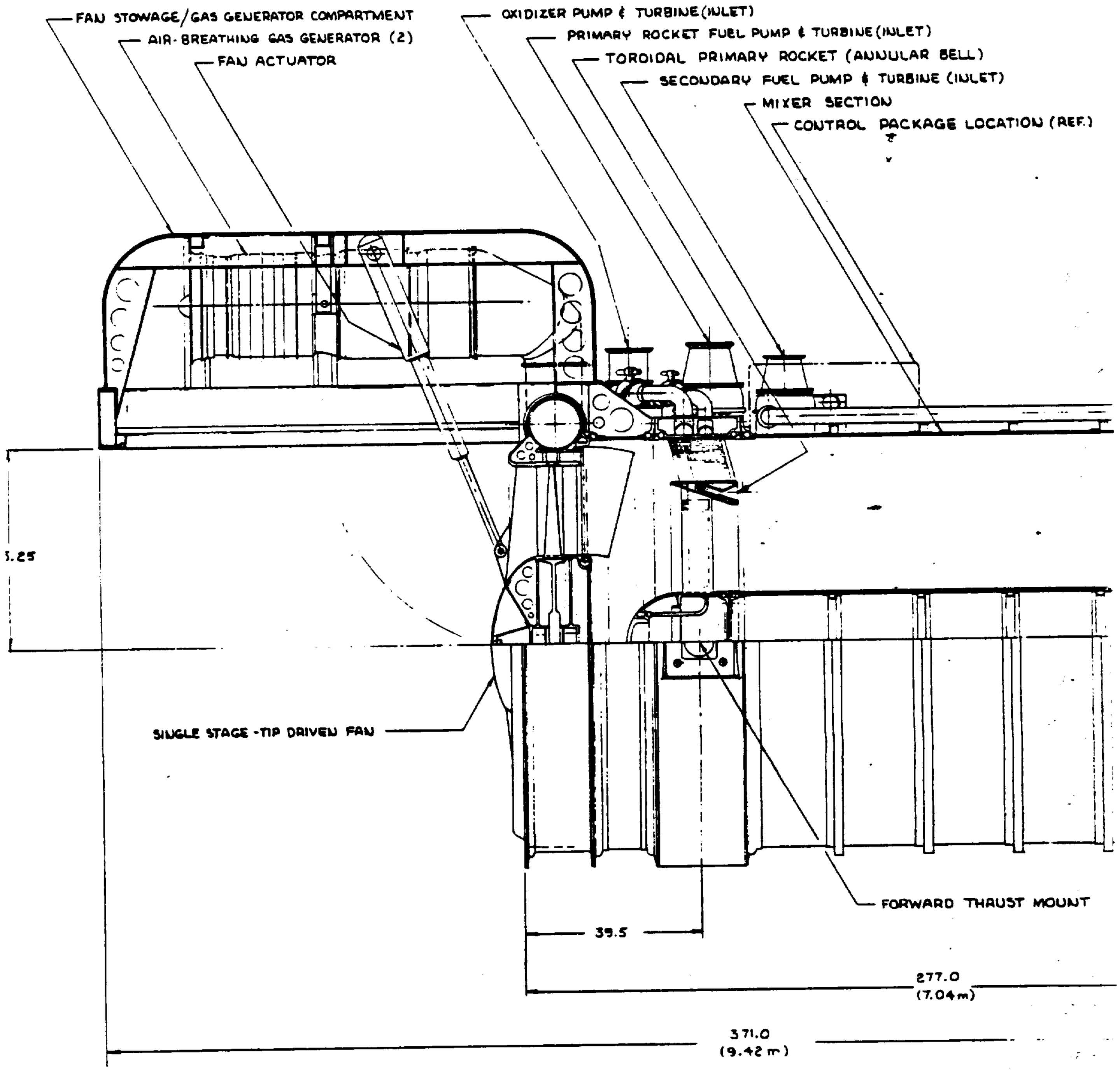

CONFIDENTIAL

5-71-2

[redacted]

~~CONFIDENTIAL~~

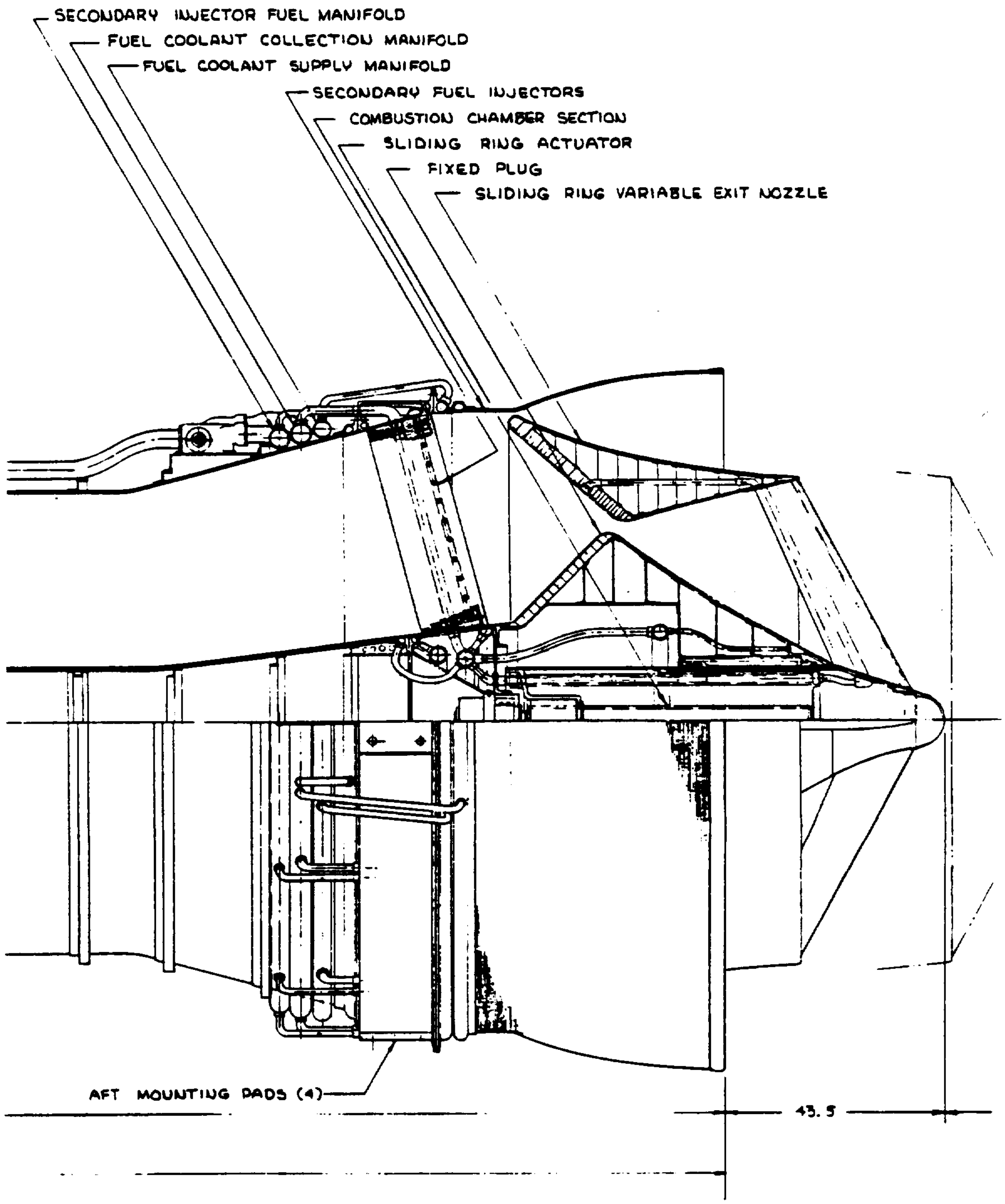

~~CONFIDENTIAL~~

572-[redacted]

[redacted]L

~~CONFIDENTIAL~~

2. THRUST, SEA ... 215,000 LBS
3. PROPELLANTS: HYDROGEN-OXYGEN

DESIGN PARAMETERS

1. SECONDARY/PRIMARY MASS FLOW RATIO (SLS): 5.0
2. PRIMARY ROCKET CHAMBER PRESSURE: 1500 PSIA
3. PRIMARY ROCKET O/F RATIO: (Φ=1.0) 7.94:1
4. MAXIMUM INTERNAL PRESSURE, DESIGN: 150 PSIA
5. FAN PRESSURE RATIO, DESIGN: 1.3:1
6. FAN/AIR-BREATHING GAS GENERATOR BY-PASS RATIO: 10:1
7. SECONDARY AIR EQUIVALENCE RATIO, NOMINAL: 1.0

ENGINE FLOW AREAS

1. MIXER, A_3 = 43.49 SQ. FT.
2. COMBUSTOR/AFTERBURNER, A_4 = 76.24 SQ. FT.
3. NOZZLE THROAT, A_5
   MAX. = 68.5 SQ. FT.
   MIN. = 7.0 SQ. FT.
4. NOZZLE EXIT, A_6 = 107.0 SQ. FT.
5. AFTERBURNER/MIXER DIFFUSION RATIO, A_4/A_3 = 1.75:1

OPERATION MODES

1. SUPERCHARGED EJECTOR, MACH 0-2.5
2. FAN RAMJET, MACH 0.5-2.5
3. RAMJET, MACH 1-8
4. FAN OPERATION, MACH 0-0.9

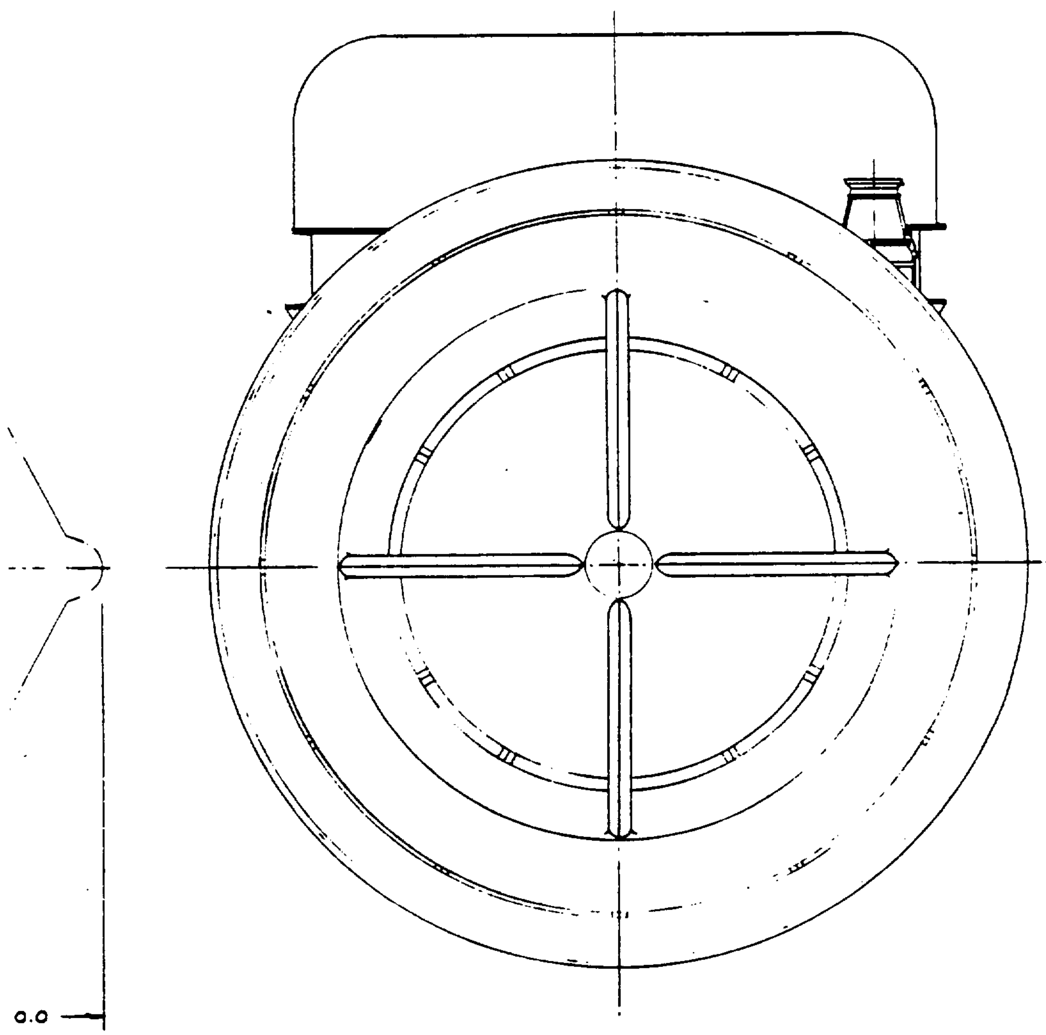

FIGURE 274. Conceptual Design Layout of the Class 2 Supercharged Ejector Ramjet

Note:
1. ALL DIMENSIONS IN INCHES UNLESS OTHERWISE STATED

CONFIDENTIAL

DRAWN HARDHILL 3/11/66	Marquardt
CHECKED FLORNES 3/20/66	SUPERCHARGED EJECTOR RAMJET ENGINE NO. 11 NAS 7-377 CLASS 2 STUDY PHASE
APPROVED ESCHER 3-25-66	
APPROVED	86845 R X 9056
	SCALE 1/40 SHEET 1 OF 1

[redacted]

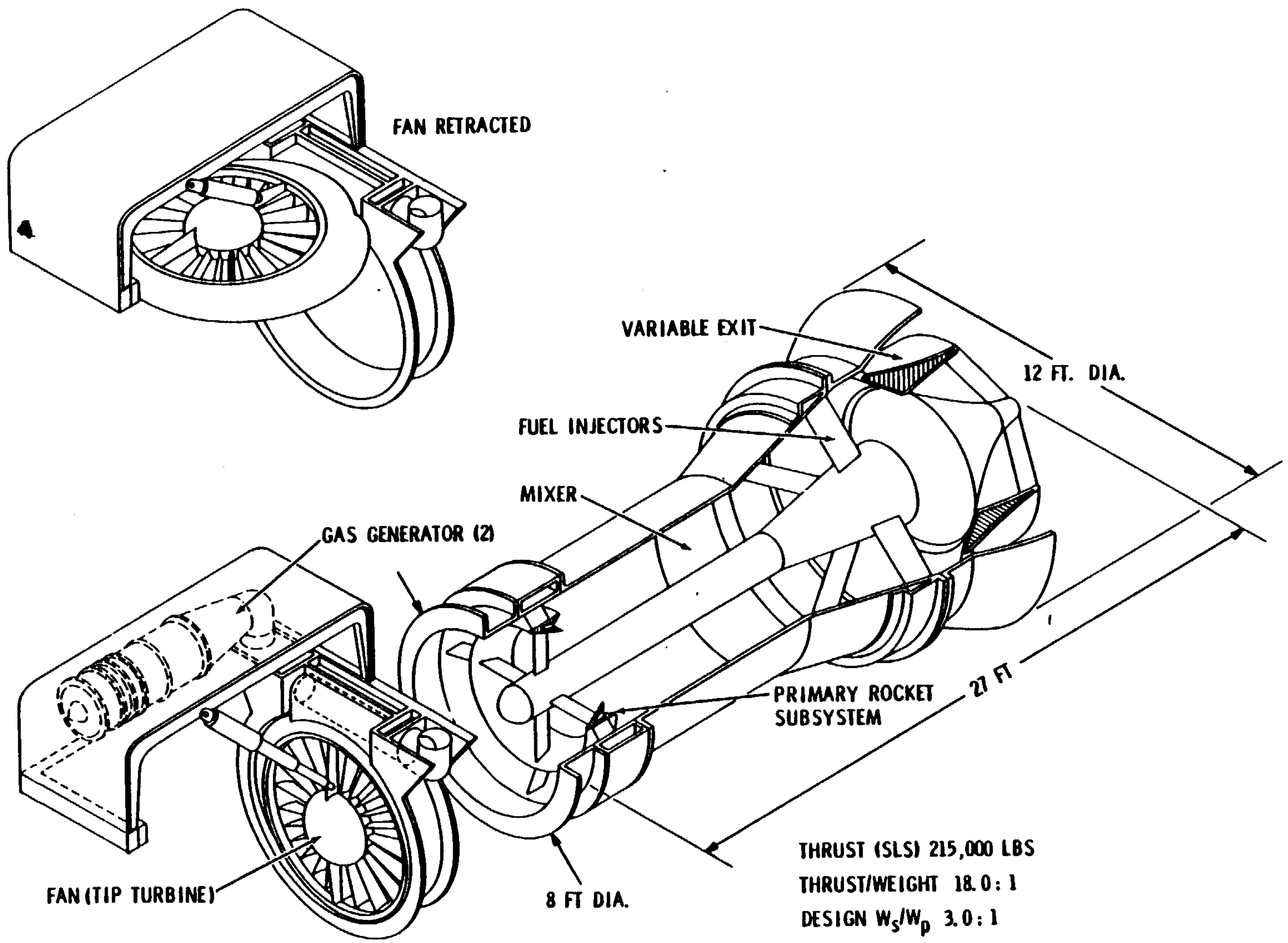

A279-38
6/30/66

FIGURE 275. Perspective of Conceptual Design of the Class 2 Supercharged Ejector Ramjet

the major engine components and subsystems are shown. The single stage, low pressure ratio fan is driven by a pair of airbreathing gas generators. Two gas generators were selected primarily to achieve minimum volume packaging although there is an additional redundancy aspect for the fan operation mode (reliability enhancement). The fan and gas generators are not regeneratively cooled. For stowage, the fan is retracted into the opening of the gas generator compartment as indicated. Cooled panels on the downstream side of the fan unit are closed on fan retraction to protect both the fan and the gas generator from the high Mach number flight speed environment.

The primary rocket chamber assembly and the turbopump units shown in Figure 274 are from the design studies by Rocketdyne presented in Section 8.3.2. The sizes of the components have been scaled from the 250,000 pound thrust base of the design study to the 215,000 pound thrust level of the final design Supercharged Ejector Ramjet. All of the turbopump gas generators operate fuel-rich (O/F = 1.25) to limit the turbine inlet temperature to approximately 1500°F. The generator exhaust is injected into the relatively low pressure afterburner where it provides part of the afterburner fuel.

The variable geometry exit nozzle design used for the Supercharged Ejector Ramjet design is a translating ring, fixed plug concept. The design has two concentric throats and dual expansion surfaces in conjunction with the fixed plug and the outer bell. High nozzle efficiencies, full area variability, and altitude compensation during low speed operation are provided by this design approach. The exit throat variation can be accomplished by the translating ring nozzle in a shorter length and small bell diameter as compared to an alternative expansion-deflection movable plug design. Since the exit bell diameter of composite engines appears to be one of the vehicle installation-engine packaging critical areas, the compact exit achieved with the translating ring plug is significant. This exit design concept was conceived under the Air Force sponsored Ejector Ramjet studies (Reference 12). It has been analytically evaluated, and it is presently scheduled for aerodynamic model tests.

The Supercharged Ejector Ramjet design of Figure 274 is completely regeneratively cooled except for the retractable fan unit as mentioned above. The necessity for regenerative cooling is primarily dictated by the high Mach number subsonic combustion ramjet operation. Low flight speed ejector mode operation with the high temperature rocket exhaust air mixture also requires partial cooling of the engine but the Mach 8 ramjet point determines the cooling circuit design.

8.4.2.1.2 <u>ScramLACE</u>

The ScramLACE rocket primary design previously shown (Section 8.3.2.1) is a double ring annular configuration for a round mixer. The design was "sectioned" to make eleven vertical strip primaries as shown in Figure 276.

[redacted]

~~CONFIDENTIAL~~

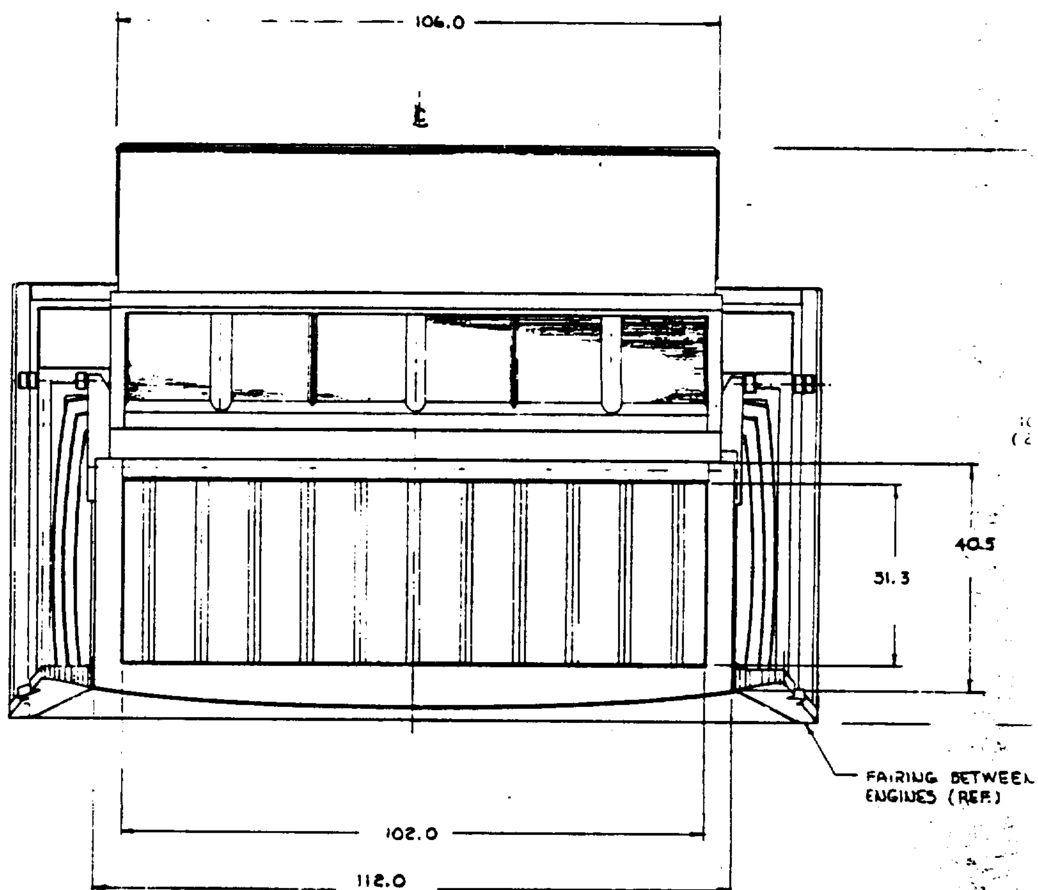

~~CONFIDENTIAL~~

[redacted]

575-1

[redacted]

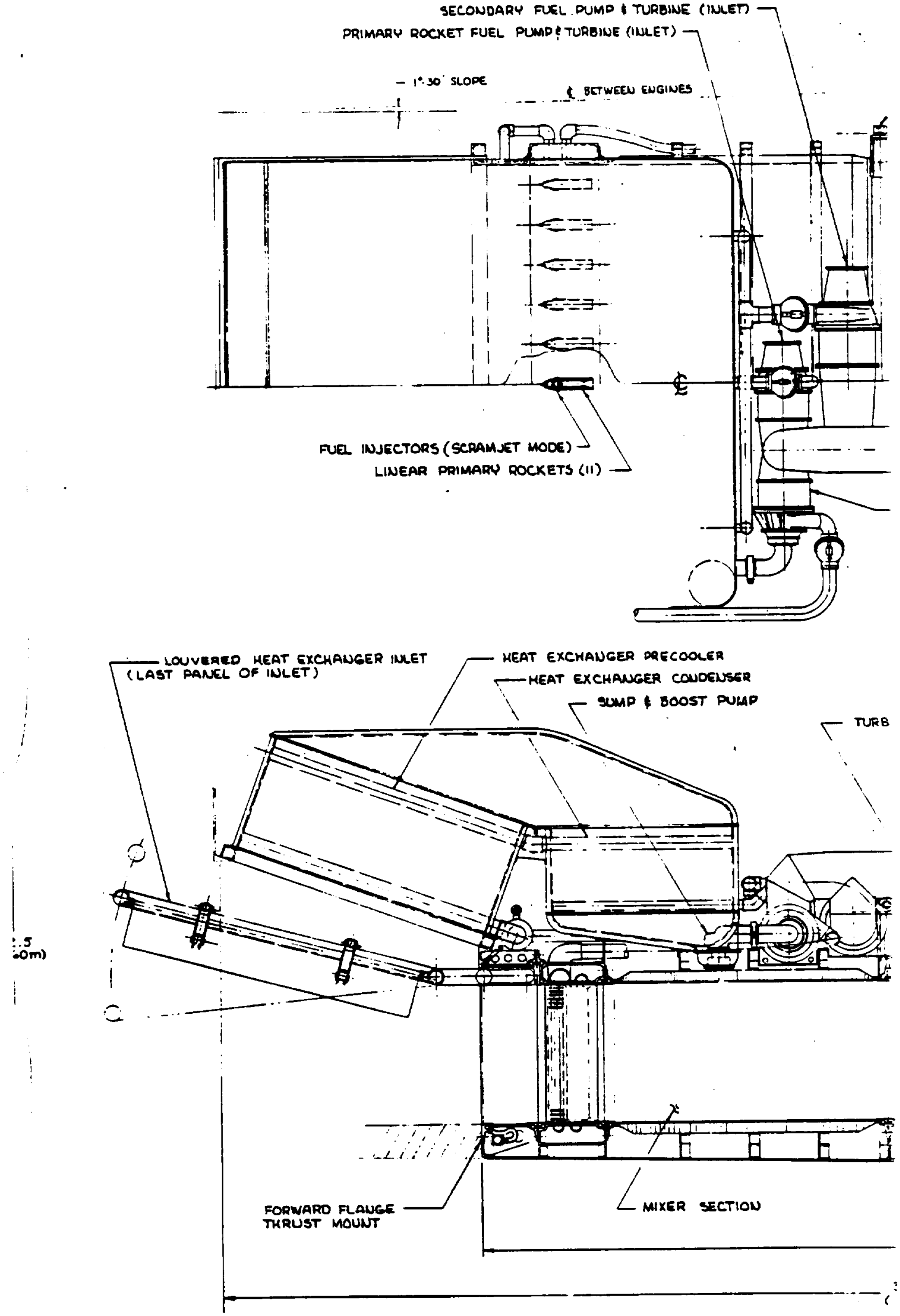

~~CONFIDENTIAL~~

[redacted]

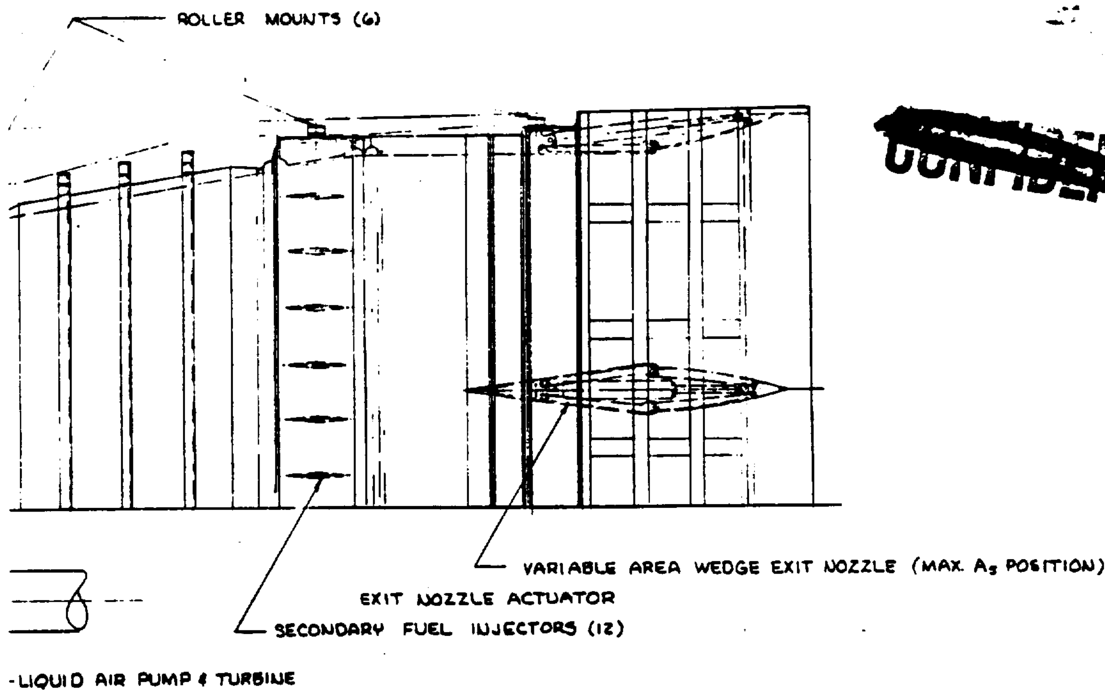

~~CONFIDENTIAL~~

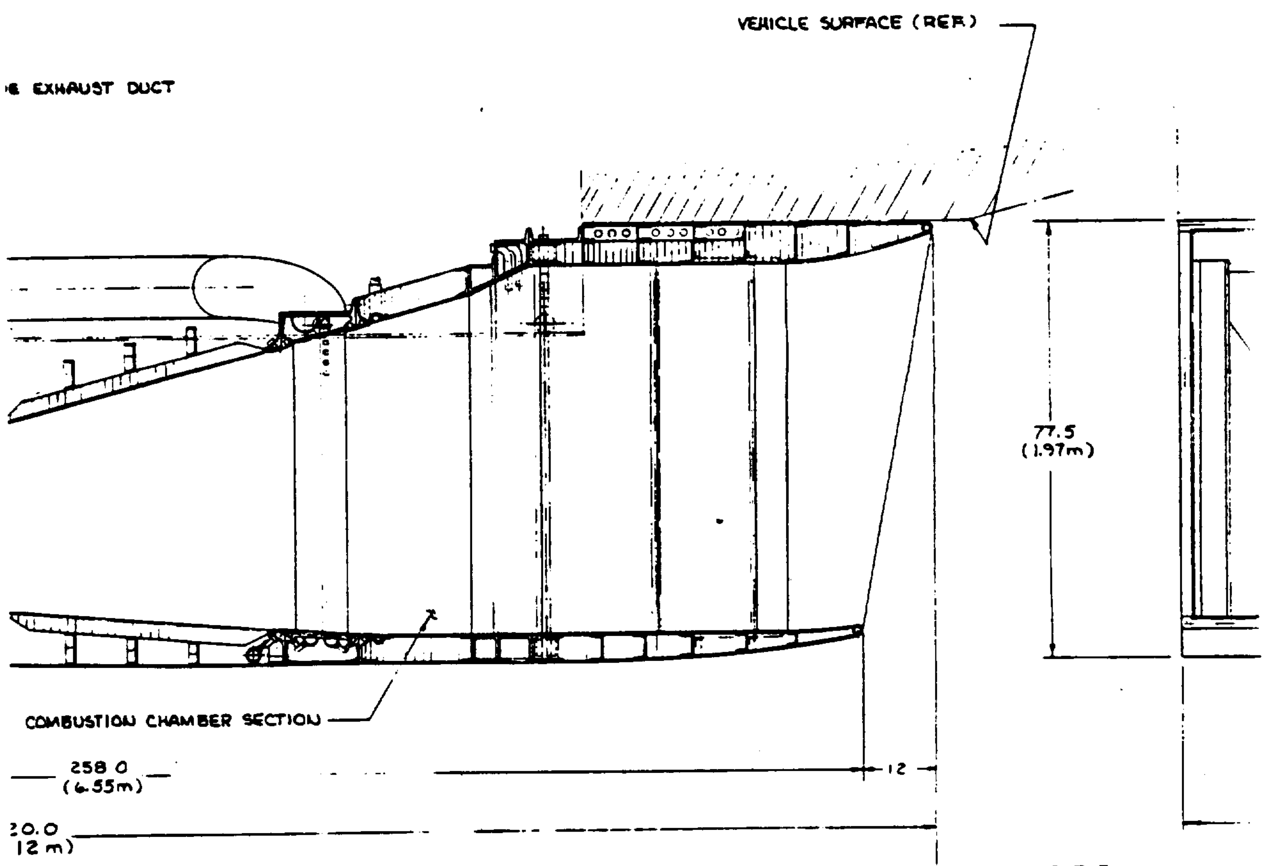

~~CONFIDENTIAL~~

[redacted]

DESIGN CHARACTERISTICS
1. MACH 12 FLIGHT SPEED CAPABILITY
2. THRUST, SEA-LEVEL STATIC: 173,000 LBF.
3. PROPELLANTS: HYDROGEN (AUXILIARY OXYGEN)

DESIGN PARAMETERS
1. SECONDARY / PRIMARY MASS FLOW RATIO (S.L.S.): 1.5
2. PRIMARY ROCKET CHAMBER PRESSURE: 1000 PSIA
3. PRIMARY ROCKET O/F RATIO: (ϕ=1.0) 34.3 : 1
4. MAXIMUM INTERNAL PRESSURE, DESIGN: 100 PSIA
5. SECONDARY AIR EQUIVALENCE RATIO, RAMJET: 1.0
6. HEAT EXCHANGER EQUIVALENCE RATIO: 8.0

ENGINE FLOW AREAS
1. MIXER / COMBUSTOR (SUPERSONIC) A_3 = 22.89 SQ. FT.
2. COMBUSTOR / AFTERBURNER (SUBSONIC) A_4 = 47.87 SQ. FT.
3. NOZZLE THROAT, A_5
   MAXIMUM = A_4 = 47.87 SQ. FT.
   MINIMUM = 15 SQ. FT.
4. NOZZLE EXIT (MAX. VEHICLE SURFACE) A_6 = 274 SQ. FT.
5. AFTERBURNER / MIXER DIFFUSION RATIO: A_4/A_3 = 2.1 : 1

OPERATION MODES
1. LIQUID AIR CYCLE EJECTOR MODE, MACH 0-3
2. SUBSONIC COMBUSTION RAMJET, MACH 1-6
3. SUPERSONIC COMBUSTION RAMJET, MACH 6-12

[redacted]

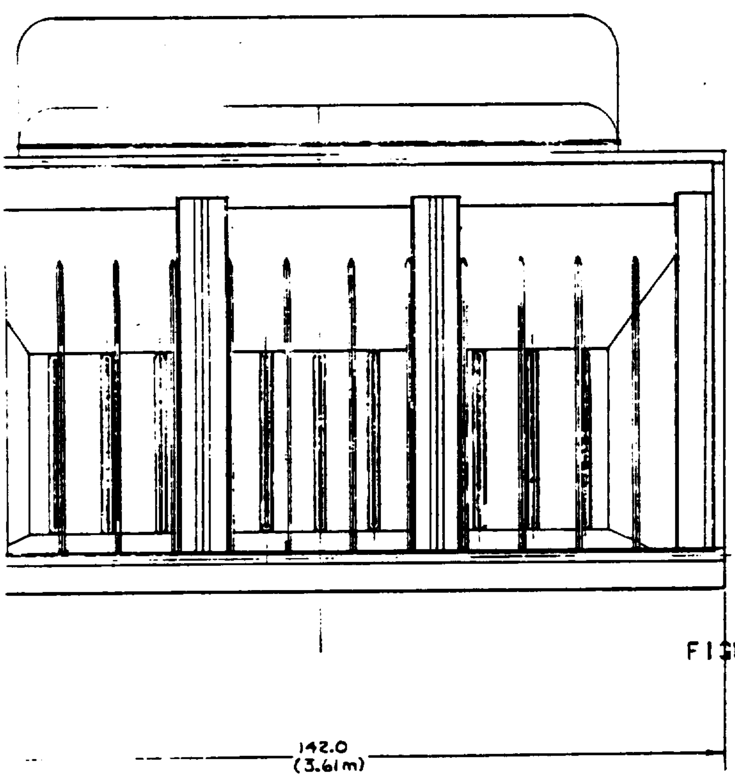

FIGURE 276. Conceptual Design Layout of the Class 2 ScramLACE

1. ALL DIMENSION IN INCHES UNLESS OTHERWISE STATED
Note:

CONFIDENTIAL

HAMMILL	
FLARNES	SCRAM LACE ENGINE NO. 22 NAS 7-377 CLASS 2 STUDY PHASE
ESCHER	
	86845 | R | X 9057
	SCALE 1/10 | SHEET 1 OF 1

[redacted]

The external primary rocket surfaces are regeneratively cooled as are all internal flow surfaces of the engine. Scramjet mode fuel is injected from both sides of each primary strip. The cross section of the ScramLACE primary presented in previous Figure 242 shows fuel injection orifices near the front of the primary chamber wedge. The orifices are for insertion of the actual fuel injection tubes which will inject the hydrogen at the beginning of the straight section and parallel to the surface (axial downstream injection).

The heat exchanger precooler and condenser core sections shown in Figure 276 are both rectangular in design. The precooler core matrix is a finned tube design and the condenser is a bare tube design. Fins are used in the precooler to improve the air side heat transfer and they provide maximum performance with minimum weight (See Section 7.2.2.3). The liquid air, primary fuel, and afterburner fuel turbopumps shown in Figure 276 are taken from the Rocketdyne design studies of Section 8.3.2.5. A minor adjustment in size was necessary due to a slight shift of design engine thrust for the ScramLACE. Again, the fuel-rich exhaust from the turbopump gas generators is utilized as part of the afterburner fuel.

The Class 2 ScramLACE engine design presented in Figures 276 and 277 reflects the above considerations. A rectangular mixer was selected to attach directly to the inlet diffuser. The last panel of the inlet diffuser ramp has been louvered to admit air to the heat exchanger for low flight speed operation. Cooled plates are used to close off the heat exchanger during high flight speed, high inlet temperature conditions.

The afterburner/mixer diffusion was accomplished primarily by physically diverging the flow passage to the sides and top as shown in Figure 276. This provides a better heat exchanger installation (less intrusion into the vehicle) with the low mixer and also directs the exhaust flow upward along the vehicle aft surface for expansion. The variable exit design concept shown in the figure was selected after consideration of the exit throat area requirements and possible variable geometry schemes. Throat area reduction was dictated by the subsonic combustion ramjet mode in the Mach 3.5 to 6.0 range. The exit throat is changed to full open for Scramjet operation and the variable geometry feature is not used for this mode.

8.4.2.2 Cooling Techniques

For composite engines employing a subsonic combustion ramjet mode operating up to Mach 6 and 8, the critical heat transfer condition is the high flight speed point. Under these conditions, the exit throat area of the ramjet is at a minimum and the cooling circuit design and requirements are concerned with a local peak heat flux at the throat, similar to the cooling situation in a rocket. The total heat sink capacity of hydrogen is typically only partially used in cooling a ramjet exit nozzle and combustor at Mach 8 conditions. The hydrogen has literally passed through this critical portion

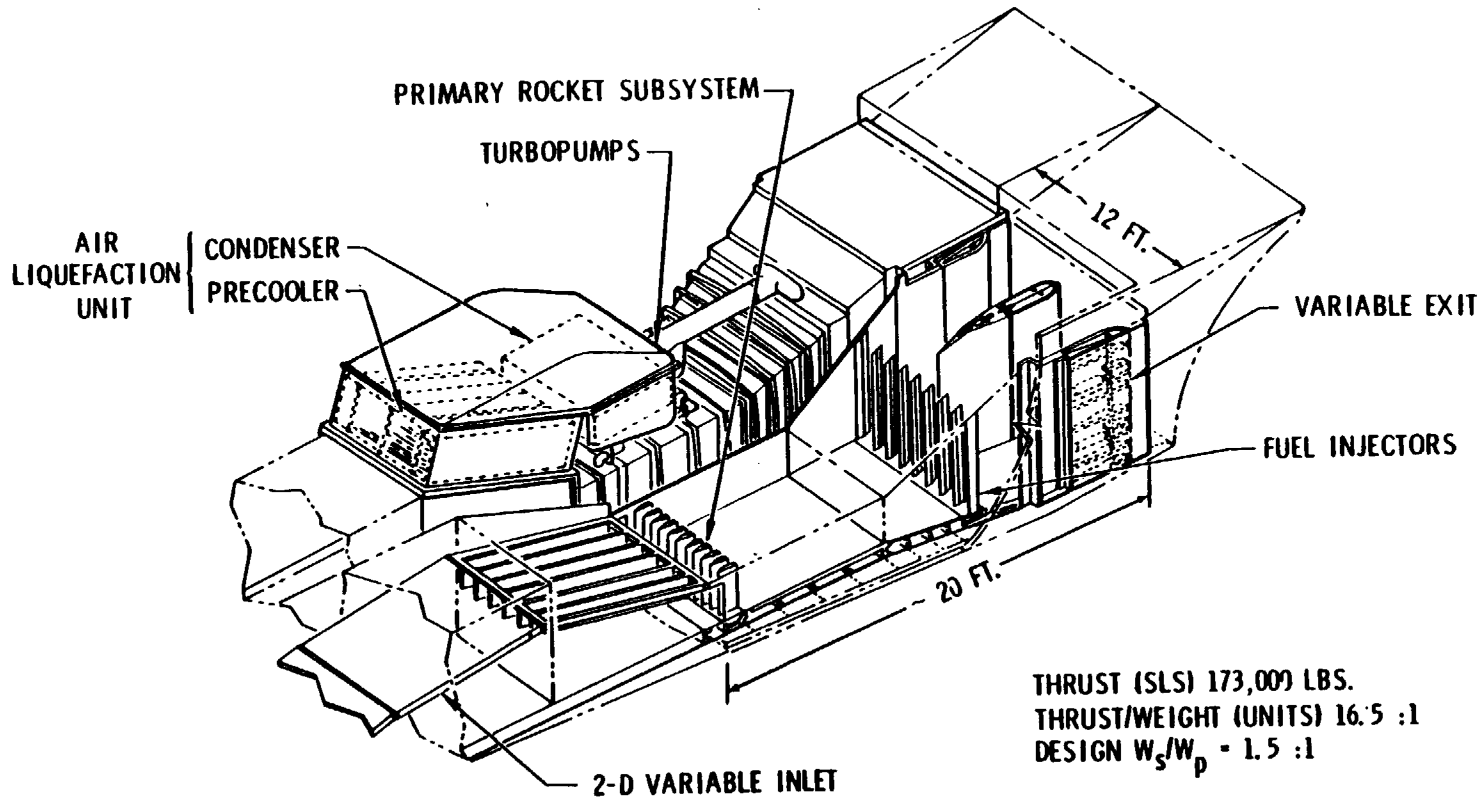

A279-36
6/30/66

FIGURE 277. Perspective of Conceptual Design of the Class 2 ScramLACE

of the engine too fast (to match the hot gas peak heat flux) to get hot (bulk temperature). Hence, there is still an adequate heat sink to cool the lower heat flux portions of the engine, such as the diffuser and mixer of either Class 2 engine, as well as sections of the inlet, etc.

The end-of-mixer and afterburner hot gas side conditions for the ejector mode of the Supercharged Ejector Ramjet, with a high energy, hydrogen-oxygen primary, are considerably less severe than the Mach 8 ramjet conditions. Although the gas temperatures are comparable, the ejector mode has a significantly lower internal pressure. Also, during the ejector mode, the exit nozzle throat or nozzle plug position is essentially full open and the peak heat flux from the hot gas is thereby further reduced.

Hence, it can be surmised with fair confidence that the critical heat transfer and cooling design point for the Supercharged Ejector Ramjet should be the Mach 8 ramjet mode condition and the ejector mode operation should pose no untenable problems. The ScramLACE engine not only has a significantly lower energy, hydrogen-air primary and lower temperature mixed flow during the ejector mode, but it has a fuel-rich, relatively cool afterburner flow and an abundance of hydrogen for cooling.

For supersonic combustion ramjet mode, operation (ScramLACE) heat transfer and cooling analysis would be concerned both with the possible local peak heat flux and the total heat sink capacity of the hydrogen coolant. Hot gas side heat flux problem areas appear to be related to the amount of inlet/combustor contraction ratio for Scramjets. High contraction ratio designs have combustion in a relatively low supersonic Mach number, high pressure portion of the engines. Combustors are typically constant area and the localized region of fuel heat release produces a peak heat flux. For engines with a relatively low inlet contraction ratio during Scramjet operation, such as the Class 2 ScramLACE design, the much higher local Mach numbers and low static pressures during combustion should significantly reduce heat flux problems. The main problem area should be satisfactory cooling of the internal engine surfaces with the heat sink capacity of a stoichiometric amount of hydrogen. The ScramLACE design has somewhat more internal surface (longer length) than a straight Scramjet but, as indicated above, this is accompanied by lower heat flux levels.

A significant point to be made relative to the cooling of engines with a supersonic combustion mode is the difference between the end of acceleration or boost conditions at Mach 12 and a typical cruise condition at this speed. The ultimate cruise condition altitude can be 20,000 feet higher than the end-of-boost altitude based on recent studies and the engine air flow is reduced by a factor of two or more. The engine internal geometry and surfaces to be cooled are constant and the stoichiometric fuel is reduced directly with air flow. The hot gas side temperature is also constant for all practical purposes. The heat flux on the hot gas side is directly related to the convection heat transfer

coefficient which in turn is proportional to the mass velocity (ρV or W/A) to the 0.8 power. The net effect is a nonlinear reduction of the hot gas heat flux with reduced air flow. For example, for a 50 percent reduction in air flow, the fuel or engine coolant is also reduced 50 percent but the hot gas convection coefficient is reduced only 42.5 percent. Hence, the heat transfer or cooling problems become more severe in the transition from end-of-boost to cruise conditions. Conversely, acceleration-mode-only Scramjet operation, as for the Class 2 ScramLACE design, may ease the heat transfer and cooling requirements.

8.4.2.3 Weight Study Results

Detailed weight statements for the Class 2 Supercharged Ejector Ramjet (Engine No. 11) and the ScramLACE (Engine No. 22) are presented in Tables XLVIII and XLIX, respectively. In general, the weight estimates have been made on the basis of conventional materials, structural design concepts, and regenerative cooling techniques. Conventional superalloy materials have been used for all high wall temperature areas and titanium and/or aluminum have been utilized wherever possible for minimum weight. The weight statements were based on the design maximum internal pressures of 150 psia for the Supercharged Ejector Ramjet and 100 psia for the ScramLACE.

Primary rocket subsystem weights were taken from the design studies of Section 8.3. In the fan subsystem area of the Supercharged Ejector Ramjet (Table XLVIII), the fan assembly and gas generator weights were assessed on a possibly conservative basis as discussed in Section 7.6.2.4.

The effects of variations in subsystem weight on the sea level static uninstalled thrust/weight ratio for the Supercharged Ejector Ramjet are presented in Figures 278 and 279. Figure 278 is for a ± 10 percent range in individual subsystem weight and Figure 279 is for a ± 50 percent range. As indicated in both figures, the total fan subsystem is the largest group in terms of engine weight percentage and hence, it causes the greatest effect on thrust/weight ratio for the subsystem weight perturbation. Updating the conservative weight estimate for the fan and gas generator assembly mentioned above, would improve the weight of this subsystem group by about 19 percent. Using Figure 279, this would increase the uninstalled thrust/weight ratio for the Supercharged Ejector Ramjet from 18.0 to about 19.3.

The effects of variation in subsystem weight for the ScramLACE engine are presented in Figures 280 and 281. The ± 10 percent range is shown in Figure 280 and the ± 50 percent range in Figure 281. For ScramLACE, the largest subsystem group in terms of engine weight percentage is the air liquefaction or heat exchanger unit. Referring to the weight breakdown for this subsystem in Table XLIX, the largest single weight item is the para/ortho catalyst. The catalyst weight is almost equal to the combined weight of the precooler and condenser cores. Further progress in catalyst development could effectively eliminate the catalyst as a significant weight item (See the discussion on

TABLE XLVIII

DETAILED WEIGHT STATEMENT FOR THE CLASS 2 SUPERCHARGED EJECTOR RAMJET

Component Group	Estimated Weight (lbm)		Proportion (%)
Fan Subsystem		4169	34.9
Fan assembly	1258		
Gas generators	1120		
Frame and trunnion unit	730		
Compartment structure	360		
Cover	210		
Actuator	115		
Transition section	306		
Miscellaneous (5%)	70		
Primary Rocket Subsystem		2028	17.0
Rocket chamber assembly	444		
Support structure	927		
Turbopumps	316		
Gas generator	127		
Ducting and valves	88		
Starting system	126		
Mixer/Diffuser Afterburner		2992	25.1
Mixer	1057		
Diffuser	540		
Fuel injection unit	635		
Combustor	315		
Forward centerbody	300		
Turbopump and miscellaneous	145		
Exit Nozzle Subsystem		2446	20.5
Exit bell	523		
Translating ring assembly	973		
Fixed plug	734		
Actuator unit	100		
Miscellaneous	116		
Controls, Lines		305	2.5
Control assemblies	80		
Valves and lines	225		
Total Weight, Dry (Thrust = 215,000 lbf)	11,940 lbm (5416 kg)		
Thrust/Weight Ratio, Uninstalled	18.0		

TABLE XLIX

DETAILED WEIGHT STATEMENT FOR THE CLASS 2 SCRAMLACE

Component Group	Estimated Weight (lbm)		Proportion (%)
Air Liquefaction Subsystem		3561	34.1
Precooler core	526		
Condenser core	465		
Forward shell	250		
Center shell	284		
Aft shell	130		
Sump	100		
Boost pump, ducting	307		
Catalyst (para/ortho)	969		
Closure and transition	530		
Primary Rocket Subsystem		2334	22.3
Rocket chamber assembly	588		
Support structure	1089		
Turbopumps	284		
Gas generator unit	149		
Ducting and valves	76		
Starting system	148		
Mixer/Diffuser/Afterburner Subsystem		2252	21.5
Mixer	605		
Diffuser	585		
Fuel injection unit	460		
Combustion chamber	495		
Miscellaneous	107		
Exit Nozzle Subsystem		2045	19.6
Rotating vane exit nozzle	1185		
Actuation assembly	240		
Exit nozzle	540		
Miscellaneous (5%)	80		
Controls, Lines		265	2.5
Control assemblies	80		
Valves and lines	185		
Total Weight, Dry (Thrust = 173,000 lbf)	10,457 lbm (4743 kg)		
Thrust/Weight Ratio, Uninstalled	16.5		

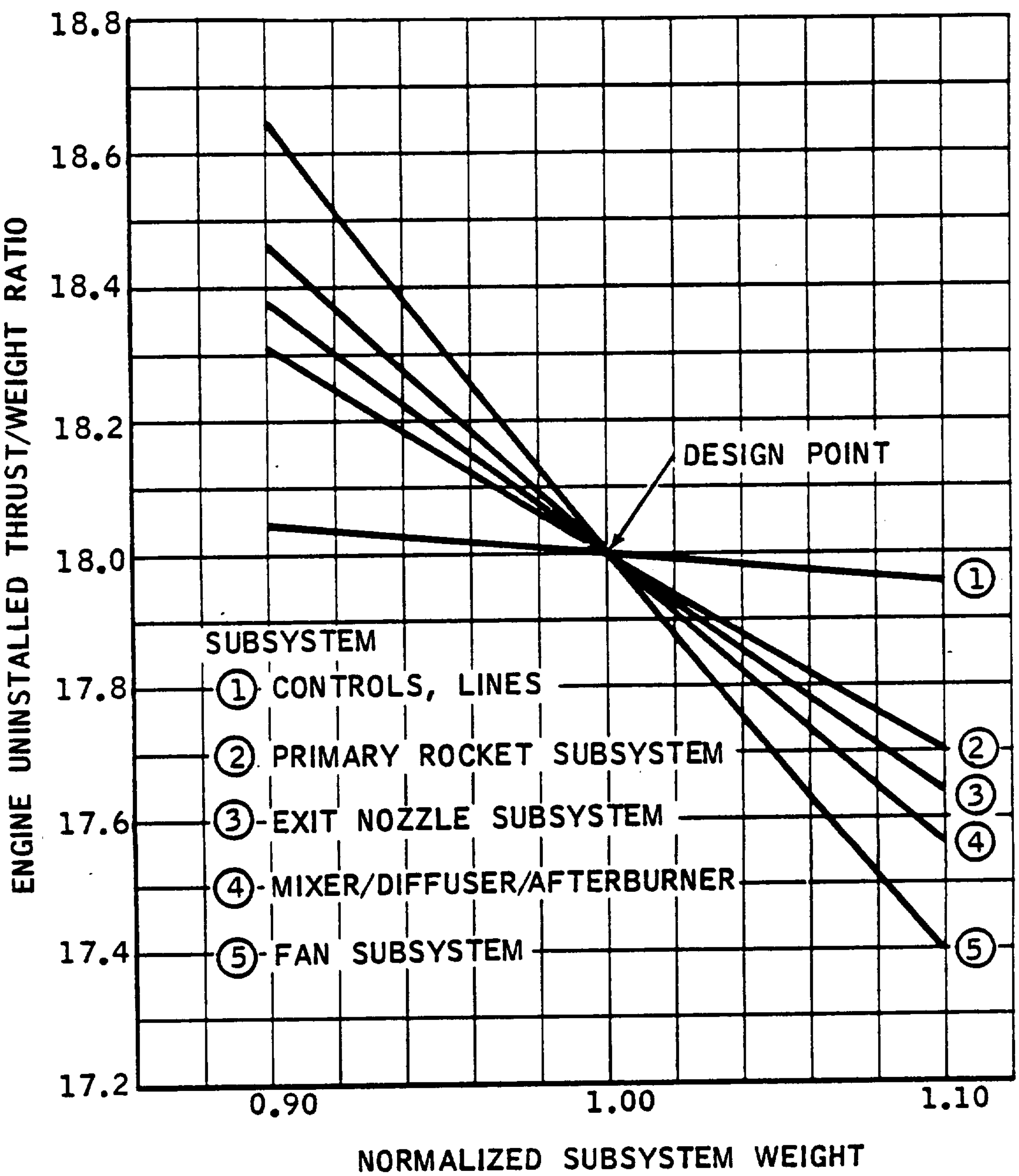

FIGURE 278. Effect of 10 percent Variation in Subsystem Weight on Engine Thrust/Weight Ratio for the Supercharged Ejector Ramjet

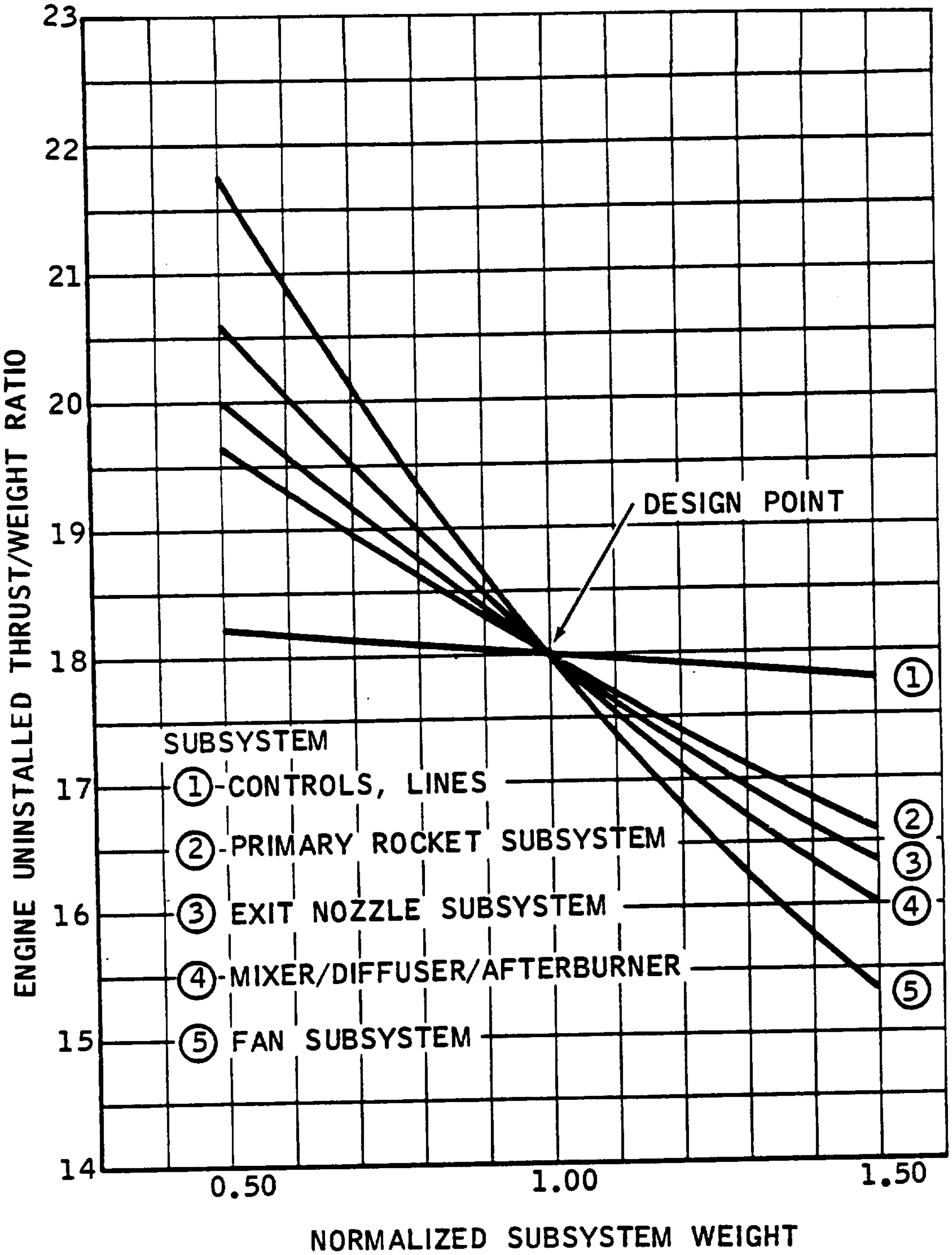

FIGURE 279. Effect of 50 percent Variation in Subsystem Weight on Engine Thrust/Weight Ratio for the Supercharged Ejector Ramjet

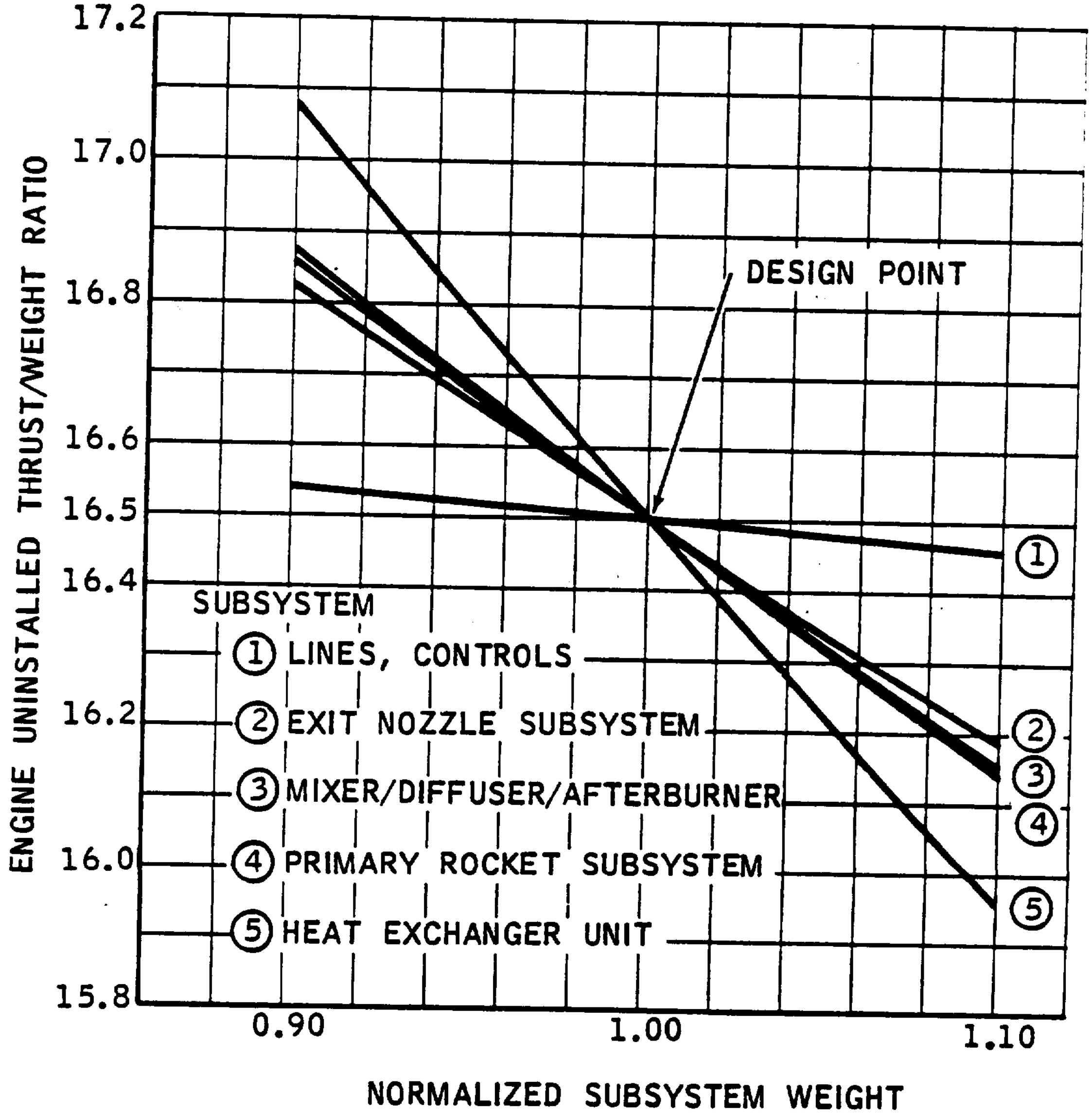

FIGURE 280. Effect of 10 percent Variation in Subsystem Weight on Engine Thrust/Weight Ratio for the ScramLACE

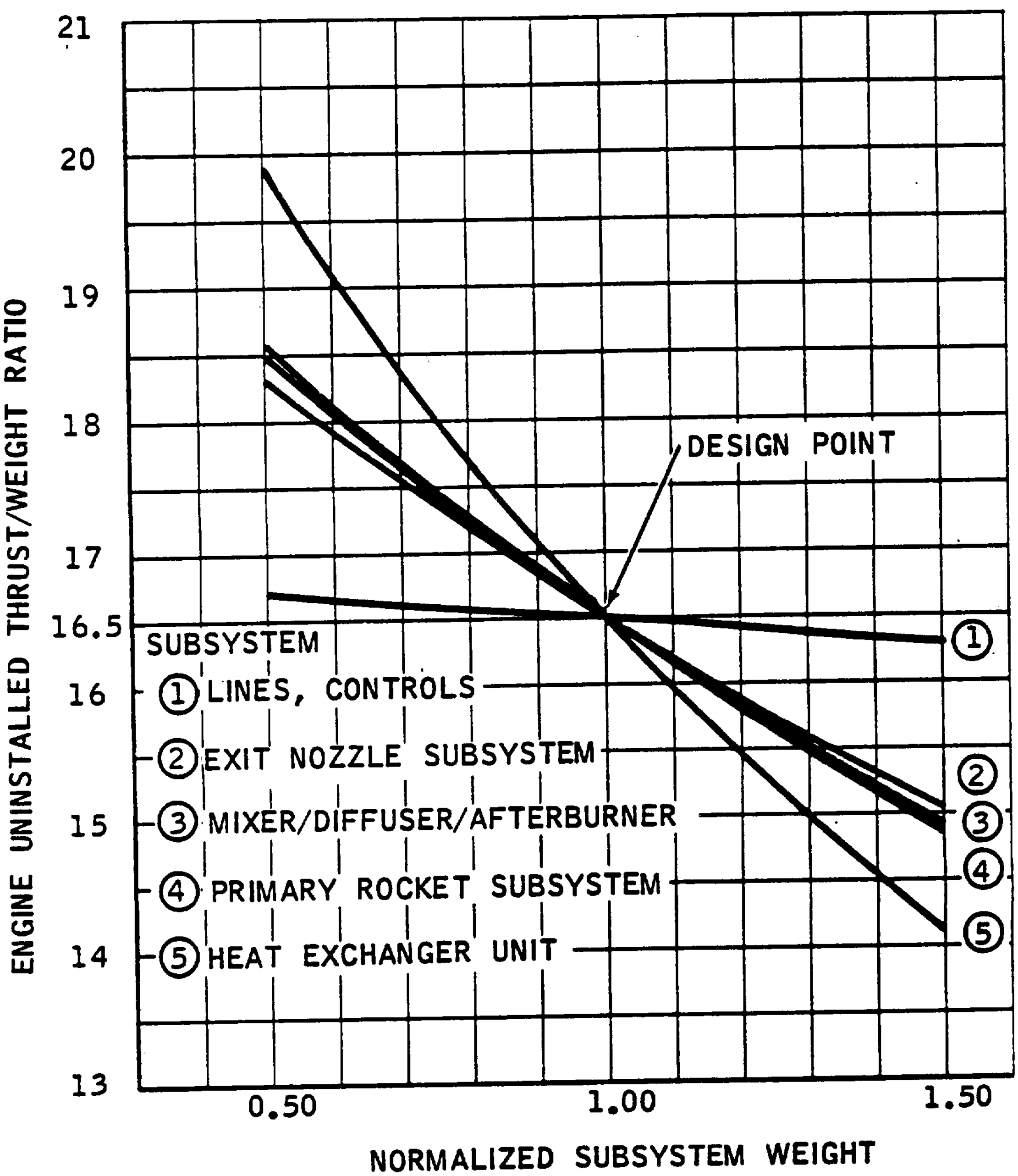

FIGURE 281. Effect of 50 percent Variation in Subsystem Weight on Engine Thrust/Weight Ratio for the ScramLACE

catalyst technology, Section 9.2.4). Deletion of the catalyst weight for the Class 2 ScramLACE would improve the weight of the air liquefaction subsystem by about 27 percent. From Figure 281, this would improve the uninstalled sea level static thrust for ScramLACE from 16.5 percent to about 18.2 percent. The improvements in uninstalled thrust/weight ratio posed for the ScramLACE and above for the Supercharged Ejector Ramjet would be of reduced magnitude on an installed basis because the inlet weights tend to at least equal the uninstalled engine weights.

8.5 Class 2 Engine Information Report (Volume 7)

Volume 7 includes a separate section for each of the two Class 2 engine concepts described in Section 7.7. The original numerical coding assigned to these engines as candidates (Class 0 Phase, Figure 27) is retained for continuity. The engine sections appear in numerical order.

The engine data presented in Volume 7 are oriented toward direct user processing for broad and diversified study activities. Performance, weight, physical envelope characteristics, operating mode availability, and other information of this genre are arranged here in a manner intended to promote effective assimilation of composite engine data by the reader. For this reason, the documentation of interpretative results of the engine data (e.g., mission application studies) is left to the main body of the report. Similarly, discussions bearing on the trade-off studies leading to selection of engine design parameters, such as primary rocket chamber pressure, also remain this main report, since - per se - these may not be of immediate utility to a systems analyst striving to assess the applicability of composite engines to his particular mission requirement.

Each of the two engine sections which follow is divided into two parts, namely,

1. Engine description, physical characteristics, and performance

2. Engine sensitivity analysis -- bases and results (Figures 282 to 289 are illustrative).

In further detail, the topics included are listed below in the order presented. The items are keyed to the sample pages by a lower case letter coding.

Engine Description, Physical Characteristics, and Performance

1. Descriptive text, schematic, operating mode block diagrams (a, b)

2. Detailed conceptual drawing (c, not shown)

3. Weight statement (d)

[redacted]

Marquardt — Page 18

SUPERCHARGED EJECTOR RAMJET. NO. 11

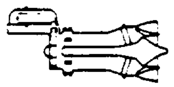

The Supercharged Ejector Ramjet (Engine No. 11, Class 2 Study Phase) is a 215,000 lbf thrust (sea level, static) engine with Mach 8 flight speed capability. The propellants are liquid hydrogen and liquid oxygen and the engine normally operates in four progressive modes: (1) supercharged ejector mode, (2) fan ramjet mode, (3) subsonic combustion ramjet mode and (4) fan operation mode.

As displayed in this section, the engine has an overall length of 371 in. (9.4 meters), an overall diameter of 142.5 in. (3.62 meters) and a height maximum of 165 in. (4.19 meters). The uninstalled engine weight is   lbm, yielding a sea level thrust-to-weight ratio of

The basic design specifiers for the engine are as follows: Design mass flow ratio 3.0 to 1, primary chamber pressure 1500 psia, fan pressure ratio 1.3, maximum internal pressure 150 psia.

The engine features a single stage retractable tip-turbine fan powered by a twin airbreathing gas generator installation. The fan bypass ratio is 10 to 1. The primary rocket is a regeneratively cooled annular belll configuration featuring a single toroidal combustion chamber fed by separate hydrogen and oxygen pumps. The turbopump drive operates on the gas generator cycle using self-pumped propellants. A third hydrogen pump provides fuel to the afterburner, during the supercharged ejector mode, and thereafter feeds the ramjet combustor during high speed operations. The afterburner fuel pump is also powered by a bi-propellant gas generator utilizing self-pumped fuel and pressurized liquid oxygen provided from the vehicle.

The basic engine structural components (mixer, diffuser, afterburner and exit nozzle) consist of regeneratively cooled assemblies employing a ring-stiffened Rene' 41 wire-wrapped, brazed regenerative Hastelloy X tube bundle construction. Within the mixer is an elongated centerbody which structurally connects a fixed aft plug with the forward thrust ring. The center body and plug assembly is supported by a multiplicity of radial low drag fuel injector struts commencing at the afterburner station. Variable exit geometry is accomplished by means of a translating ring operating continuously to provide two coaxial flow expansion compartments between the outer exit bell and the fixed plug. This dual throat design provides a minimum weight, single moving part design and provides high nozzle performance.

The engine was sized for a 1 million lbm gross weight, horizontal take off two-stage launch vehicle. The engine was located in a complement of five (5) along the bottom side of a high fineness ratio, low drag, lifting body boost stage. Air induction considerations for this installation consisted of a moving ramp, two-dimensional variable inlet with mixed external and internal compression. The inlet capture plane was located to make full use of body flow-field affects at speeds in excess of Mach 3. Exit gas expansion is considered to take place solely within the exit bell of the engine.

(a)

[redacted]

Marquardt — Page 19

Eng. No. 11

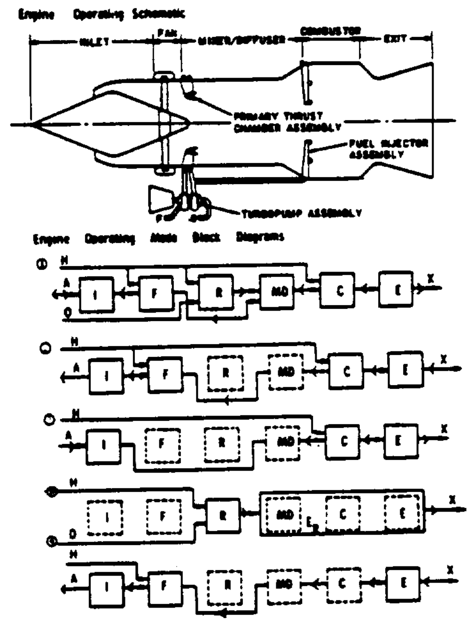

(b)

CONFIDENTIAL

ENGINE LAYOUT

DRAWING

(FOLD-OUT)

(c)

[redacted]

Marquardt — Page 21

Eng. No. 11

WEIGHT STATEMENT - ENGINE NO. 11

Fan Subsystem		4169 lbm
Fan Assembly	1258	(34.9%)
Gas Generators	1120	
Frame and Transion Unit	730	
Compartment Structure	360	
Cover	210	
Actuator	115	
Transition Section	306	
Miscellaneous (5%)	70	
Primary Rocket Subsystem		2028
Rocket Chamber Assembly	444	(17.0%)
Support Structure	987	
Turbopumps	316	
Gas Generator	127	
Ducting and Valves	88	
Starting System	126	
Mixer/Diffuser/Afterburner		2992
Mixer	1057	(25.1%)
Diffuser	540	
Fuel Injection Unit	635	
Combustor	315	
Forward Centerbody	300	
Turbopump and Miscellaneous	145	
Exit Nozzle Subsystem		2446
Exit Bell	583	(20.5%)
Translating Ring Assembly	973	
Fixed Plug	734	
Actuator Unit	100	
Miscellaneous	116	
Controls, Lines		305
Control Assemblies	80	(2.5%)
Valves and Lines	225	
Total Weight, Dry (Thrust = 215,000 lbf)		11,940 lbm (5416 kg)
Thrust/Weight, Uninstalled		18.0

(d)

[redacted]

FIGURE 282. Sample Engine Fact Sheets (Class 2 Engine No. 11)

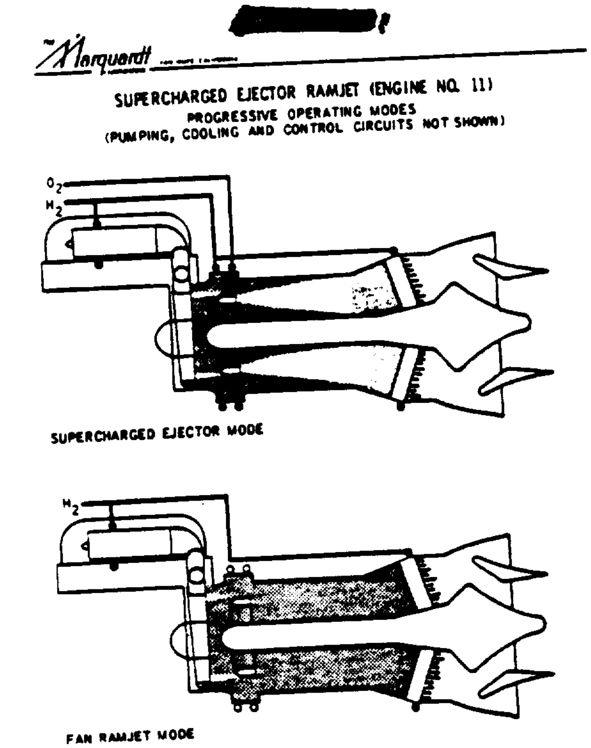

(e)

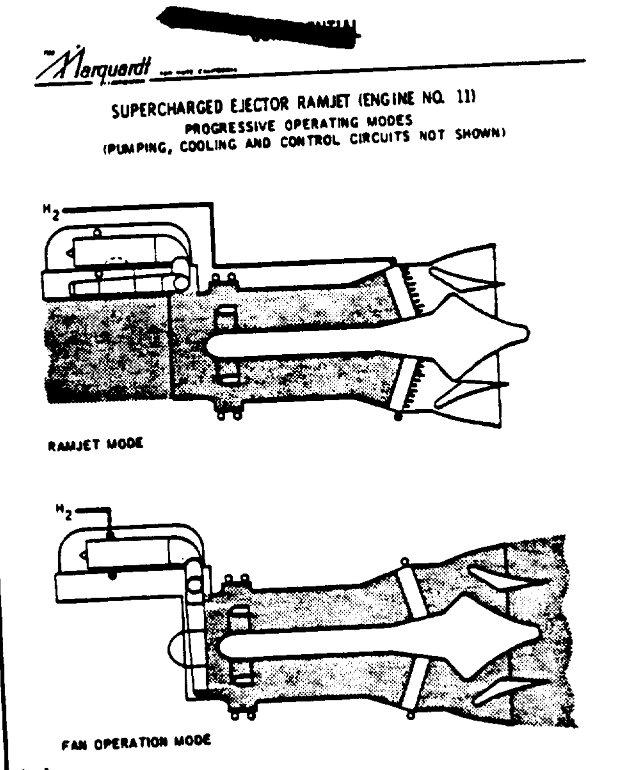

(f)

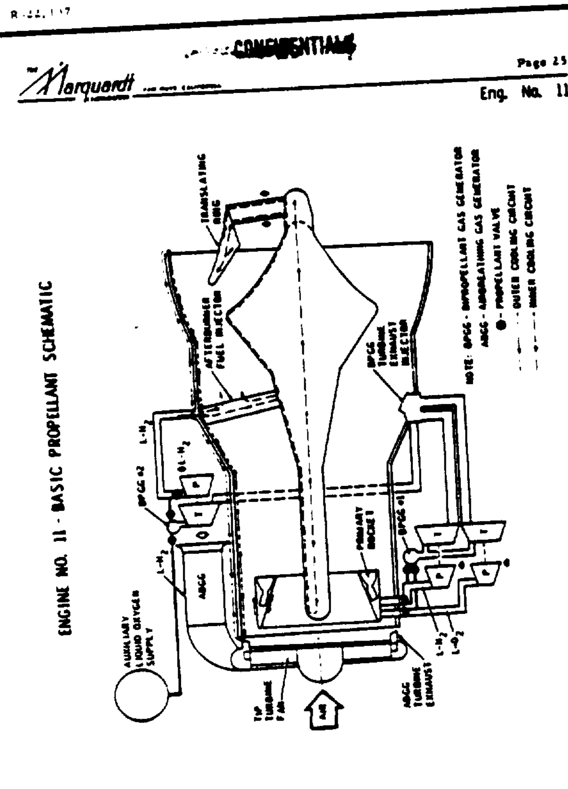

(g)

OPERATING MODE CONTROL SYSTEM
(BLOCK DIAGRAM)

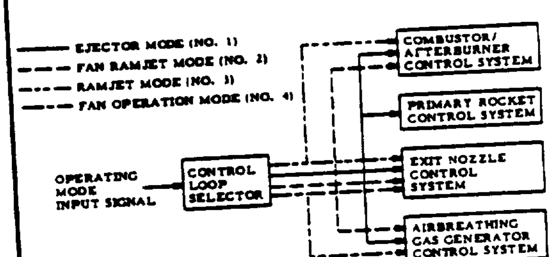

Engine control is based on manual and/or actual selection of operating modes via four active control loops as will be described. The fan subsystem is controlled to operate at design rpm with protection of both the fan tip-turbine and the basic gas generator from turbine over-temperature. Retraction of the fan is effected at mode shift from the fan ramjet to subsonic combustion ramjet mode. The primary rocket is scheduled (pre-orificed) to operate at design chamber pressure and design oxidizer-to-fuel ratio (8.0 to 1). The afterburner/combustor controller is designed for operation at an equivalence ratio of 1, providing maximum thrust consistent with good performance. The variable exit nozzle is controlled initially to provide a maximization of the product of fan pressure ratio and air mass flow (approximately). Once supersonic flight is reached the variable exit is translated to locate the inlet nozzle shock at the throat of the inlet. The exit also operates in an override loop to limit combustor pressure or inlet diffuser pressure to the maximum design condition of 150 psia.

(h)

[redacted]

FIGURE 283. Sample Engine Fact Sheets (Class 2 Engine No. 11)

CONFIDENTIAL

THE Marquardt CORPORATION VAN NUYS, CALIFORNIA

Report 25,194
Volume 3

VEHICLE LAYOUT

DRAWING

(FOLD-OUT)

(i)

[redacted]

Marquardt

Page 31
Eng. No. 11

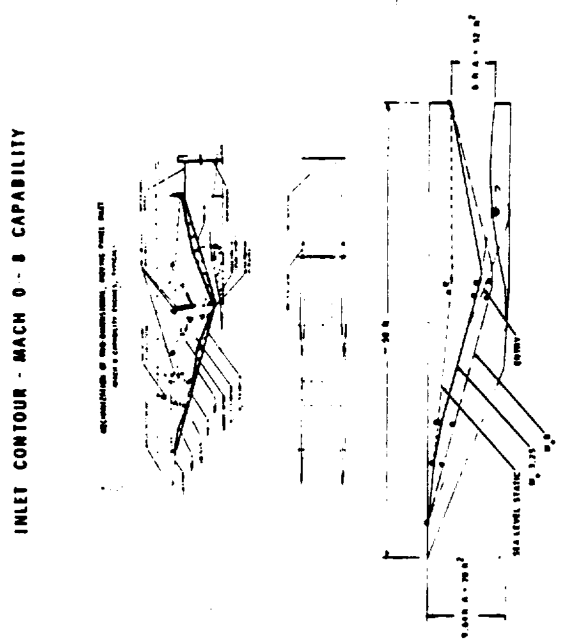

(j)

[redacted]

Marquardt

Page 32
Eng. No. 11

INLET PRESSURE RECOVERY

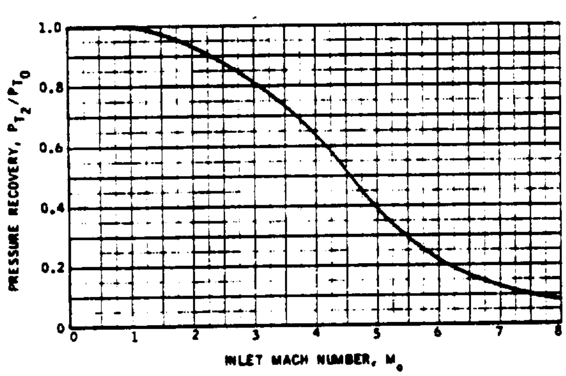

(k)

CONFIDENTIAL

[redacted]

Marquardt

Page 33
Eng. No. 11

INLET CAPTURE AREA

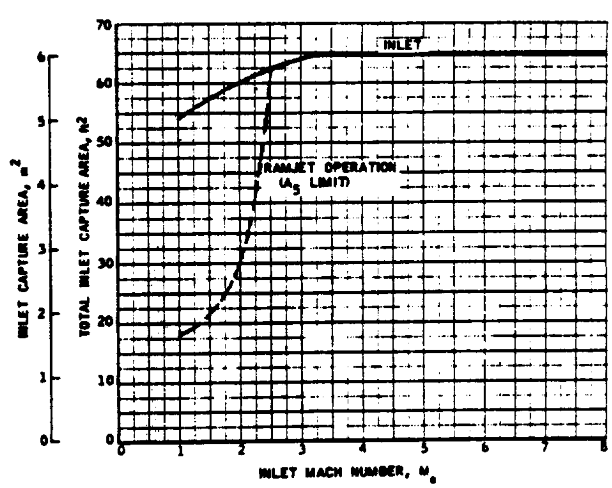

(l)

CONFIDENTIAL

FIGURE 284. Sample Engine Fact Sheets (Class 2 Engine No. 11)

CONFIDENTIAL

~~CONFIDENTIAL~~

Marquardt [redacted] Page 34
Eng. No. 11

EJECTOR MODE SPECIFIC IMPULSE

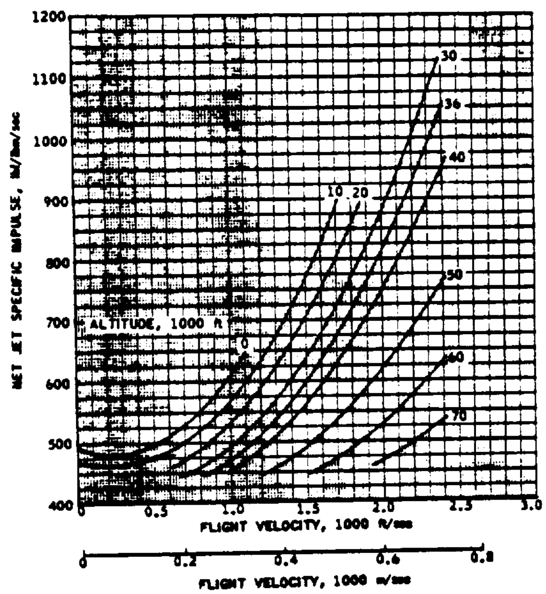

(m)

Marquardt [redacted] Page 35
Eng. No. 11

EJECTOR MODE THRUST

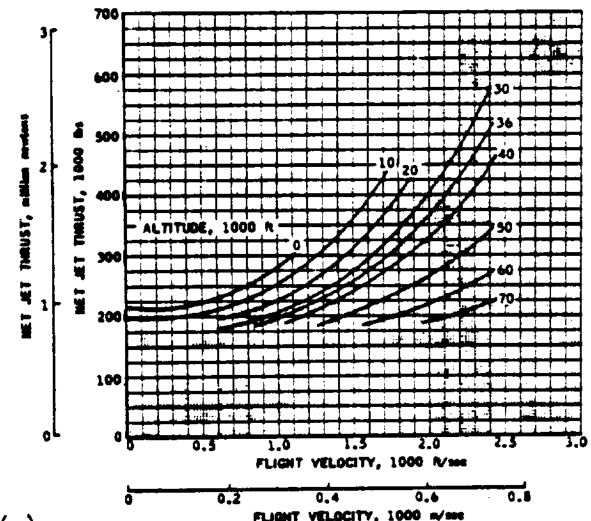

(n)

Marquardt [redacted] Page 36
Eng. No. 11

EJECTOR MODE AIRFLOW

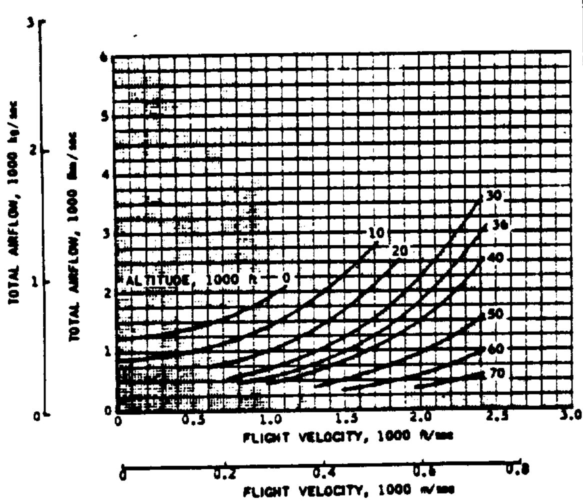

(o)

Marquardt [redacted] Page 37
Eng. No. 11

EJECTOR MODE CAPTURE AREA

NOTE: CURVE = UPPER LIMIT

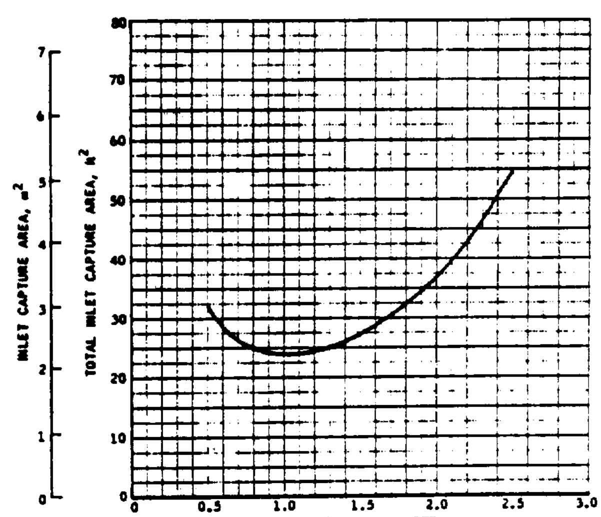

(p)

[redacted]

FIGURE 285. Sample Engine Fact Sheets (Class 2 Engine No. 11)

~~CONFIDENTIAL~~

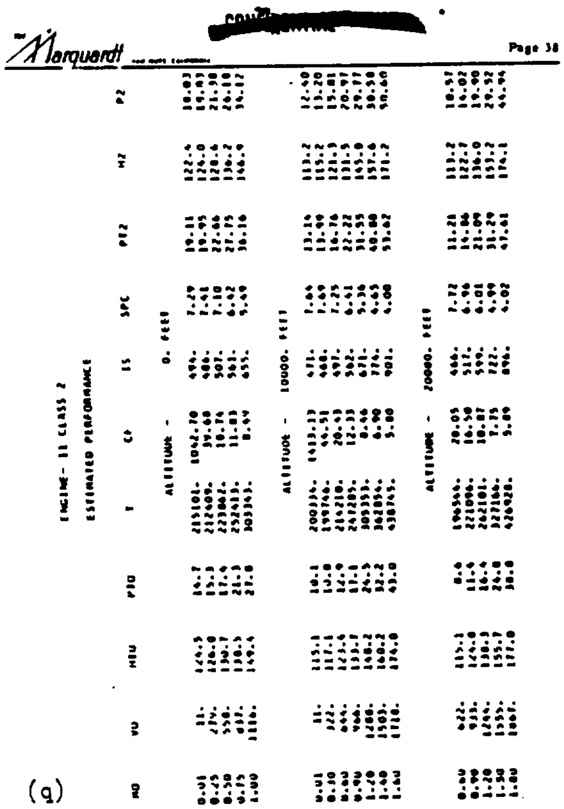

(q)

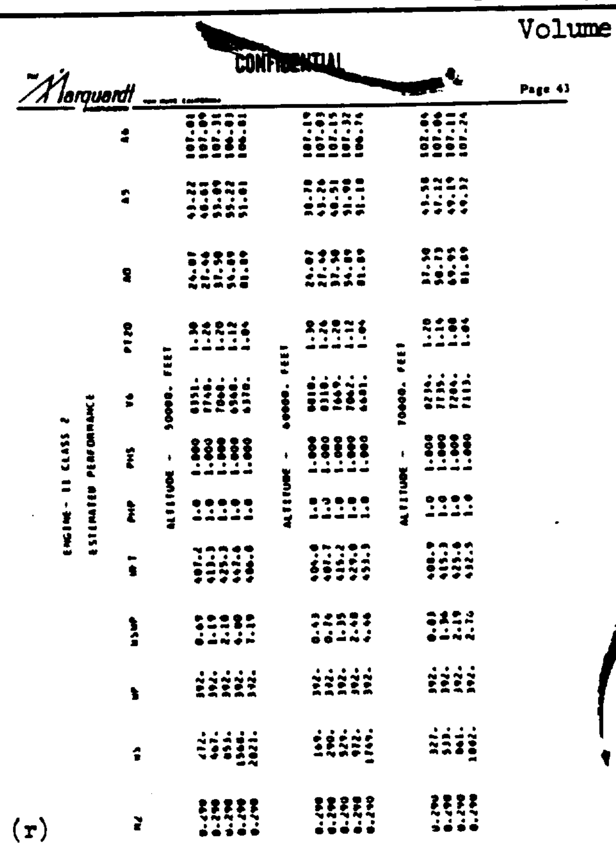

(r)

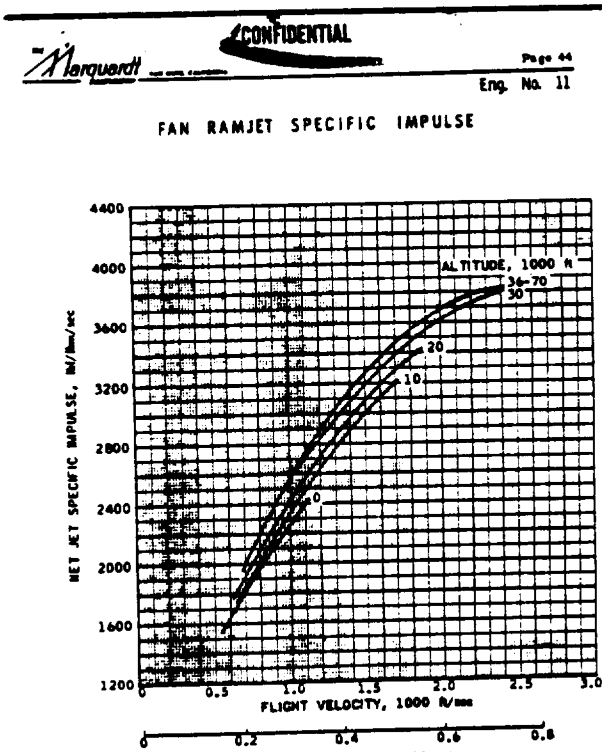

(s)

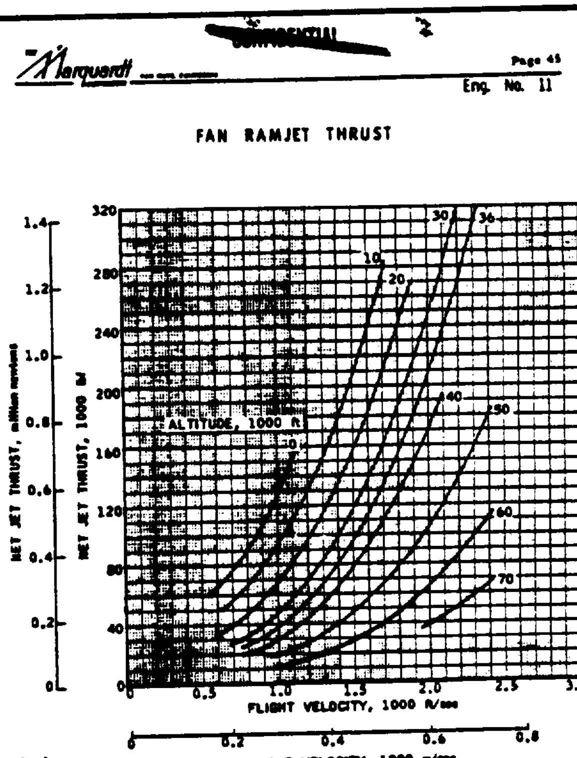

(t)

~~CONFIDENTIAL~~ ~~CONFIDENTIAL~~

FIGURE 286. Sample Engine Fact Sheets (Class 2 Engine No. 11)

Marquardt [redacted] Page 46

Eng. No. 11

FAN RAMJET CAPTURE AREA

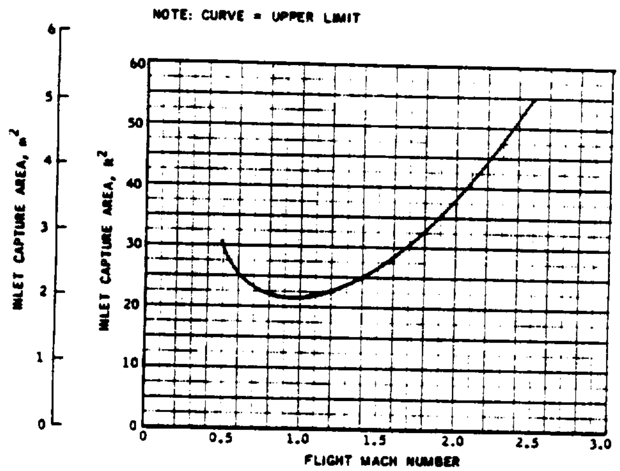

(u)

Marquardt [redacted] Page 47

Eng. No. 11

RAMJET SPECIFIC IMPULSE

SUBSONIC COMBUSTION

NO PRESSURE FIELD

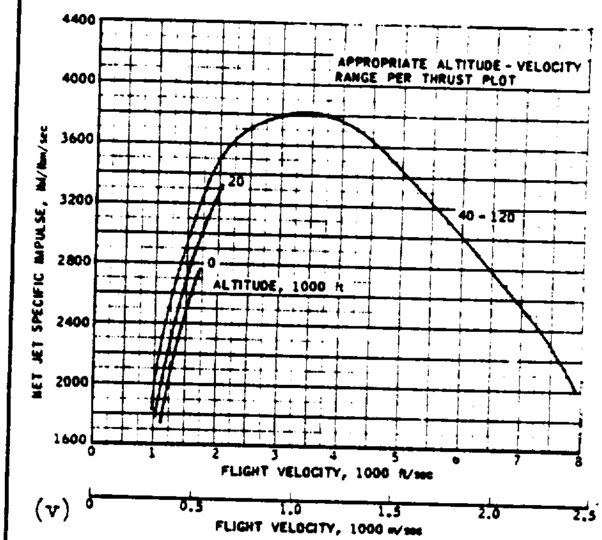

(v)

Marquardt [redacted] Page 48

Eng. No. 11

RAMJET THRUST

SUBSONIC COMBUSTION

NO PRESSURE FIELD

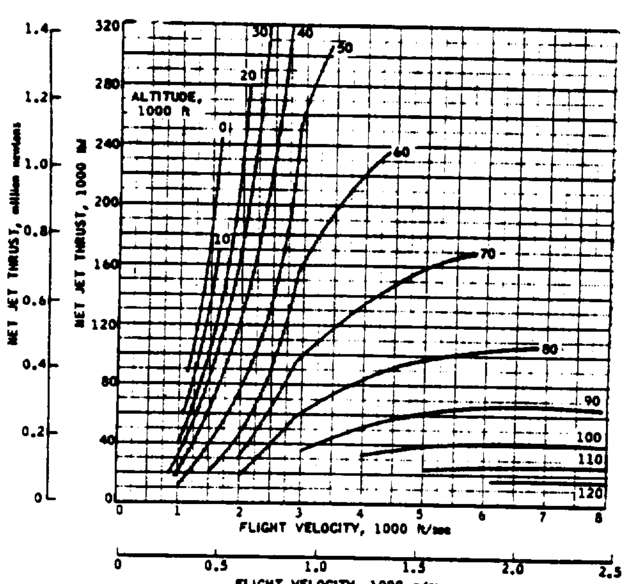

(w)

CONFIDENTIAL

Marquardt [redacted] Page 49

RAMJET SPECIFIC IMPULSE Eng. No. 11

SUBSONIC COMBUSTION

EFFECT OF PRESSURE FIELD

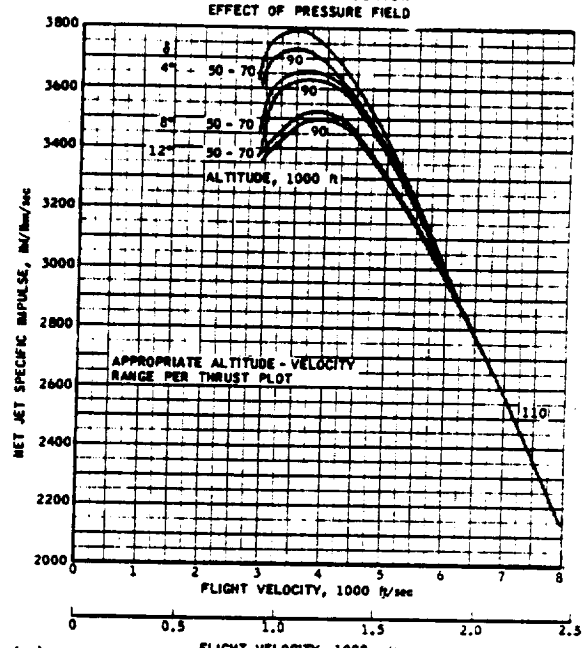

(x)

[redacted]

FIGURE 287. Sample Engine Fact Sheets (Class 2 Engine No. 11)

RAMJET THRUST

SUBSONIC COMBUSTION

EFFECT OF PRESSURE FIELD

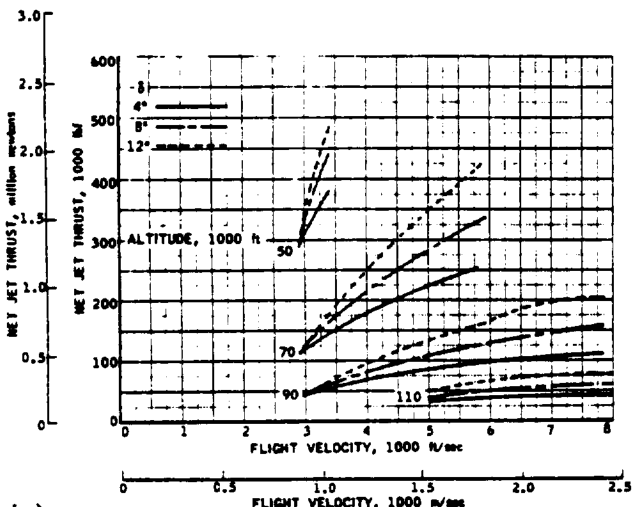

(y)

FAN OPERATION SPECIFIC IMPULSE

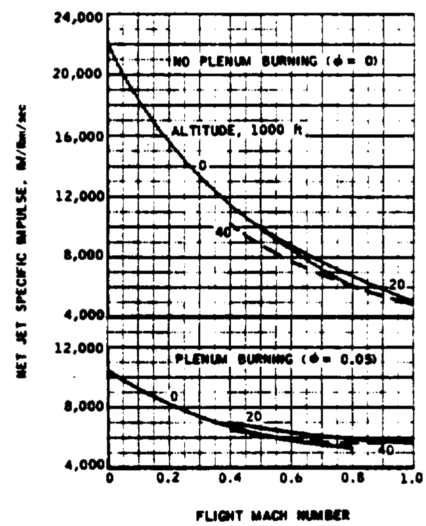

(z)

FAN OPERATION THRUST

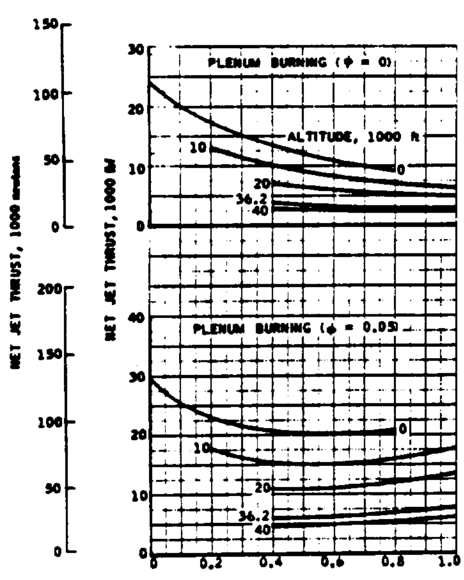

(aa)

CONFIDENTIAL

SUMMARY: SENSITIVITY ANALYSIS - BASES

The performance data shown in the present report, as well as in the Class 0 and 1 engine documentation (References 1 and 2), was computed on the basis of a singular set of internal component efficiencies, as well as stated operating points (e.g., design mass flow ratio, W_s/W_p). Compliment sensitivity studies were conducted as a major effort within the Class 2 study phase. The bases for the analysis are given here, followed immediately by the results.

The approach used was to define baseline performance, specific impulse and thrust (both net jet), for a reference trajectory. This was accomplished for each of the engine's operating modes over the normal range of flight velocities for that mode. It is appropriate here, to comment to the point that sensitivity studies of trajectory effects, per se, are already intrinsic in the previously displayed performance maps.

Proceeding from this basis of specific impulse and thrust discrete trends, each of the important engine variables was perturbed from the baseline value, e.g., afterburner combustion efficiency: Baseline value - 0.95, sensitivity excursions - 0.85 and 1.00. All of the remaining variables were essentially held at the baseline, or nominal value. Any exception to this resulted from the engine performance computer program's automatic compensation characteristics which, in some instances "retunes" some of the engine internal variables. The extent and implications of this situation are covered in the main technical report (Reference 3).

This section presents the following bases for the sensitivity analysis results to be given subsequently:

1. Reference trajectories
2. Baseline specific impulse (on reference trajectory)
3. Baseline thrust (on reference trajectory)
4. Ranges of sensitivity variables, with reference to the baseline values (both curve and tabular presentation)

(bb)

CONFIDENTIAL

FIGURE 288. Sample Engine Fact Sheets (Class 2 Engine No. 11)

[redacted]

Marquardt

Page 66

Eng. No. 11

SENSITIVITY ANALYSIS RANGES

	Base-Line	Range	
Ejector Mode:			
Inlet - Pressure recovery, P_{t_2}/P_{t_0}	Figure A		
Fan - Pressure ratio, PR_f	1.30	1.50	1.10
Primary			
Equivalence ratio, ϕ	1.00	1.10	0.90
Combustion efficiency, η_{c*}	0.975	1.00	0.92
Nozzle efficiency, η_N	0.98	1.00	0.95
Mixer - Mixing efficiency, η_M	0.80	1.00	0.50
Afterburner			
Equivalence ratio, ϕ_{AB}	1.00	1.50	0.50
Exit			
Nozzle efficiency, η_N	0.98	1.00	0.95
Exit area ratio, A_6/A_5	Figure B		
Fan Ramjet Mode:			
Inlet - Pressure recovery, P_{t_2}/P_{t_0}	Figure A		
Fan - Pressure ratio, PR_f	1.30	1.50	1.10
Afterburner			
Equivalence ratio, ϕ_{AB}	1.00	1.50	0.50
Combustion efficiency, η_c	0.95	1.00	0.85
Exit			
Nozzle efficiency, η_N	0.98	1.00	0.95
Exit area ratio, A_6/A_5	Figure C		
Subsonic Combustion Ramjet:			
Inlet - Pressure recovery, P_{t_2}/P_{t_0}	Figure A		
Combustor			
Equivalence ratio, ϕ	1.00	1.50	0.50
Combustion efficiency, η_c	0.95	1.00	0.85
Exit			
Nozzle efficiency, η_N	0.98	1.00	0.95
Exit area ratio, A_6/A_5	Figure D		
Fan Operation:			
Inlet - Pressure recovery, P_{t_2}/P_{t_0}	1.00	0.95	0.90
Fan - Pressure ratio, PR_f	1.30	1.50	1.10
Afterburner - Combustion efficiency, η_{AB}	0.95	1.00	0.85
Exit - Nozzle Efficiency, η_N	0.98	1.00	0.95

(cc)

[redacted]

Marquardt

Page 69

Eng. No. 11

Figure A INLET PRESSURE RECOVERY SENSITIVITY ANALYSIS RANGE

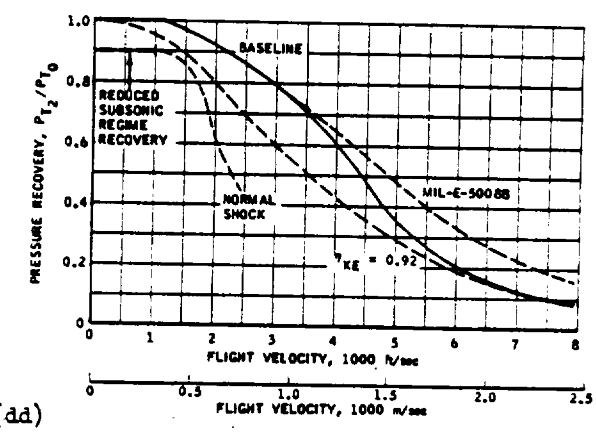

(dd)

[redacted]

Marquardt

Page 82

EXIT NOZZLE AREA RATIO EFFECT

EJECTOR MODE

Eng. No. 11

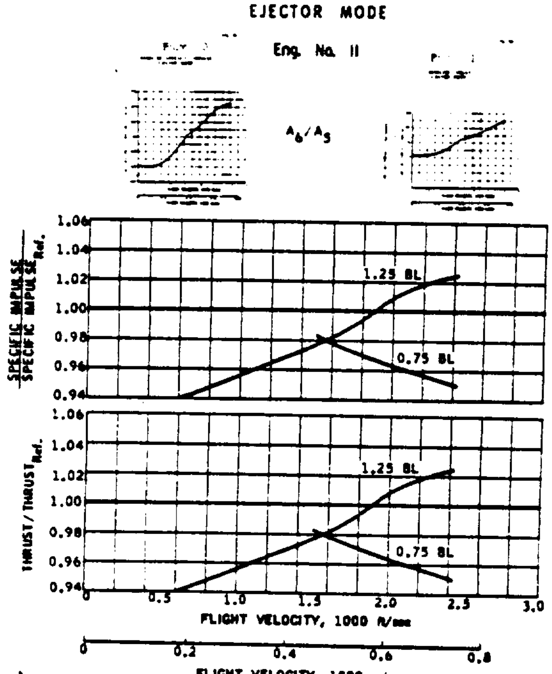

(ee)

[redacted]

Marquardt

Page 101b

Eng. No. 11

EFFECT OF SUBSYSTEM WEIGHT VARIATION ON ENGINE THRUST/WEIGHT

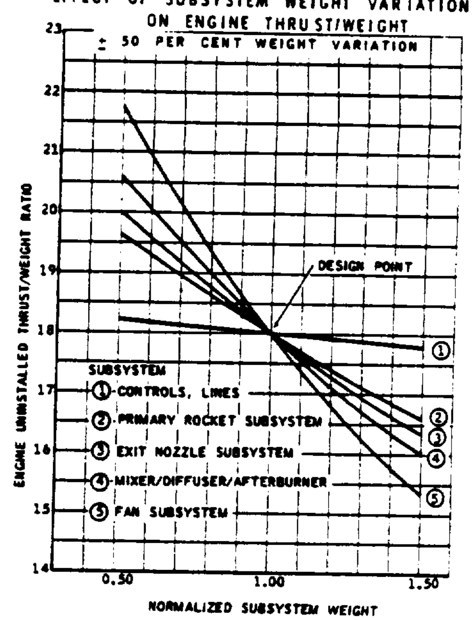

(ff)

[redacted]

FIGURE 289. Sample Engine Fact Sheets (Class 2 Engine No. 11)

4. Operating mode schematic diagrams (e, f)

5. Propellant flow circuit description (g)

6. Control system considerations (h)

7. Vehicle installation drawing (i, not shown)

8. Assumed inlet physical characteristics and pressure recovery schedule (j, k, l)

9. Ejector mode (or supercharged ejector mode) specific impulse, thrust, air flow maps, plus capture area, reflecting the effect of vehicle flight speed and altitude. These maps are backed up by computer-generated tabular data. (m -r)

10.* Fan ramjet mode specific impulse and thrust maps and capture area schedule (s, t, u)

11. Ramjet (subsonic combustion) specific impulse and thrust maps, including the effect of inlet air precompression (flow field) (v-y)

12.** Scramjet (supersonic combustion) specific impulse and thrust data, including the effect of inlet air precompression (flow field). This information is presented for three reference trajectories which follow the performance curves. (Not shown)

13.* Fan operation specific impulse and thrust maps, reflecting the effect of varying degrees of plenum burning (z, aa)

<u>Sensitivity Analysis - Bases and Results</u> (bb)

1. Range and limiting values of sensitivity parameters (cc)

2. Reference trajectories, inlet recoveries (dd)

3. Perturbed specific impulse and thrust -- results for each sensitivity parameter (ee)

4. Baseline specific impulse and thrust (both net jet) performance values derived on the reference trajectories (repeated in miniature on ee)

5. Effect of subsystem weight variations on engine thrust weight ratio (ff)

- - - - - - - - - - - - - - -

* Engine No. 11 only
** Engine No. 22 only

Preceding the individual engine sections of Volume 7, a general reference section appears which includes

1. Mach number/velocity conversion chart
2. Engine station nomenclature diagram
3. General nomenclature and legends
4. List of references

8.6 Vehicle System and Mission Analysis

Lockheed conducted the Class 2 vehicle/mission studies using essentially the same approaches and guidelines as for the Class 1 effort (Section 7.6). The four engines evaluated (two composite, two comparison) were as follows:

Engine No.	Name
0	Very Advanced Rocket
11	Supercharged Ejector Ramjet
22	ScramLACE
X	Turboramjet

The Class 2 phase of the vehicle/mission study featured increased technical depth and included, for example, airbreathing propulsion phase terminal velocity optimization (payload maximization) and delineation of payload sensitivity trends with respect to engine specific impulse and thrust/weight ratios and total vehicle drag. Single stage systems studies were not continued in the Class 2 phase, emphasis being on the two-stage lifting body configuration synthesized in the Class 1 effort.

8.6.1 Methodology

8.6.1.1 Vehicle Configurations

Layouts of the installations of the Class 2 Supercharged Ejector Ramjet (Engine No. 11), ScramLACE (Engine No. 22), and the Turboramjet (Engine No. X) integrated systems, utilizing the lifting body configuration are shown in Figures 290, 291, and 292, respectively.

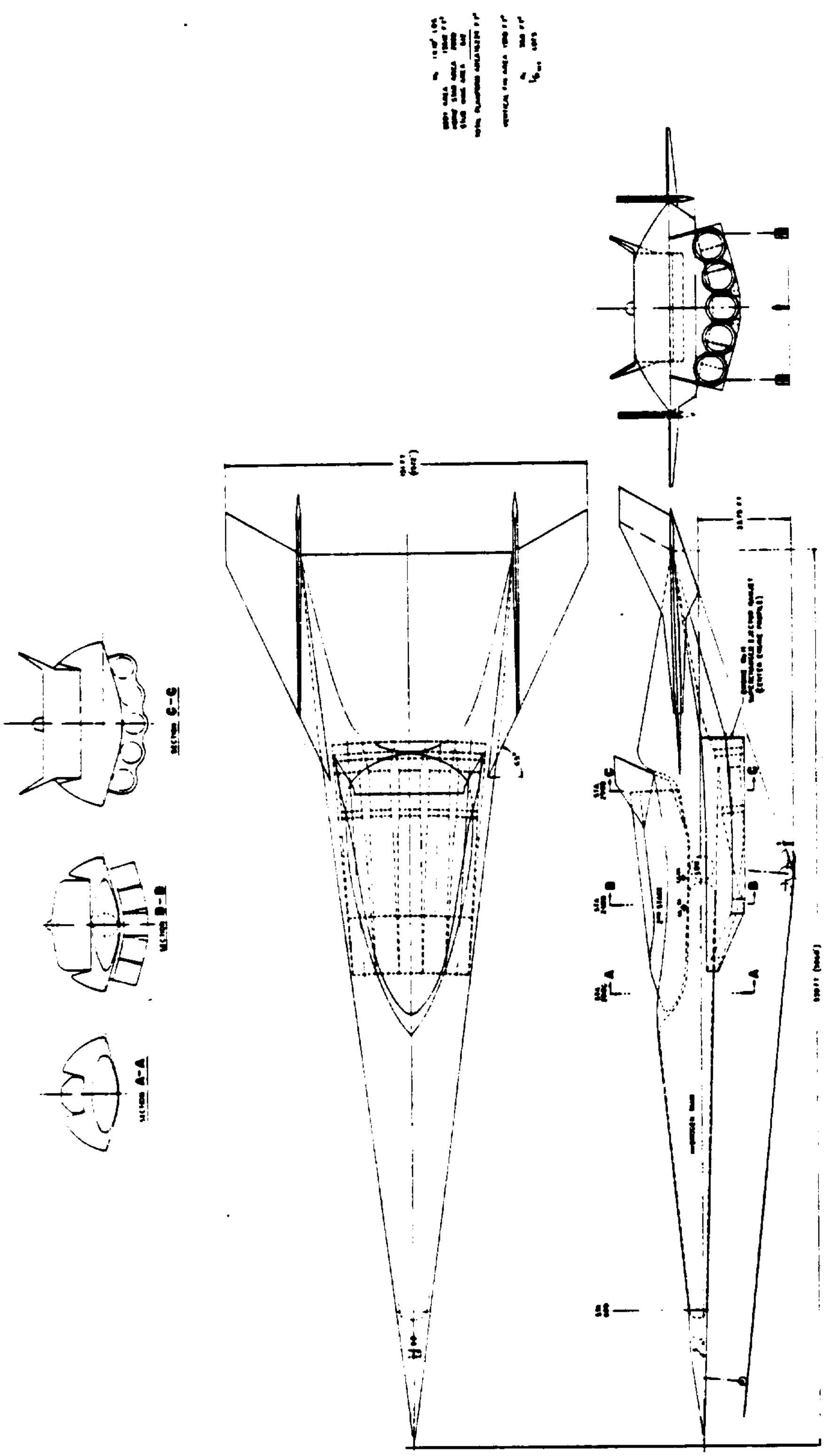

FIGURE 290. Layout of Lifting Body Vehicle Installation for the Class 2 Supercharged Ejector Ramjet (Engine No. 11)

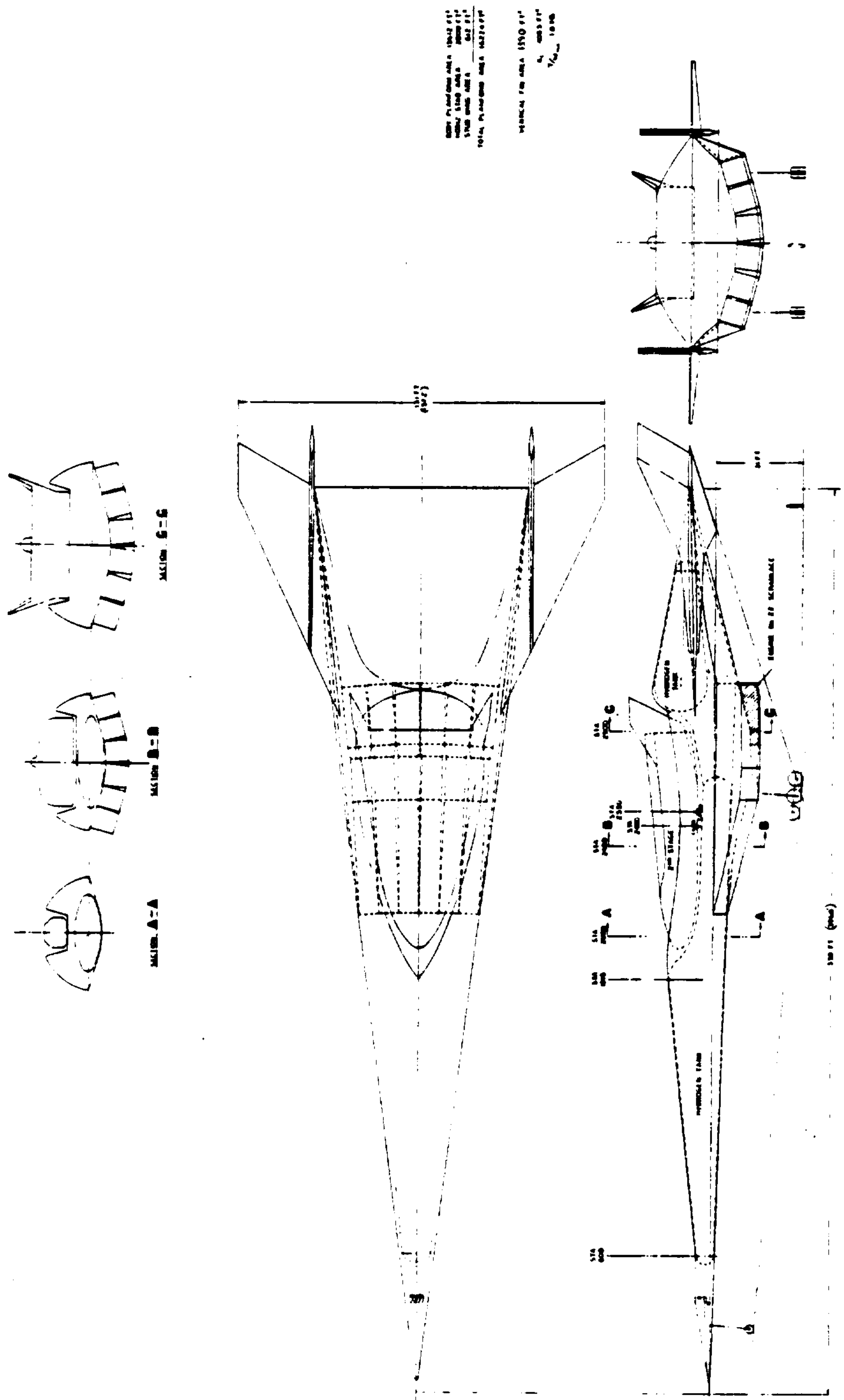

FIGURE 291. Layout of Lifting Body Vehicle Installation for the Class 2 ScramLACE (Engine No. 22)

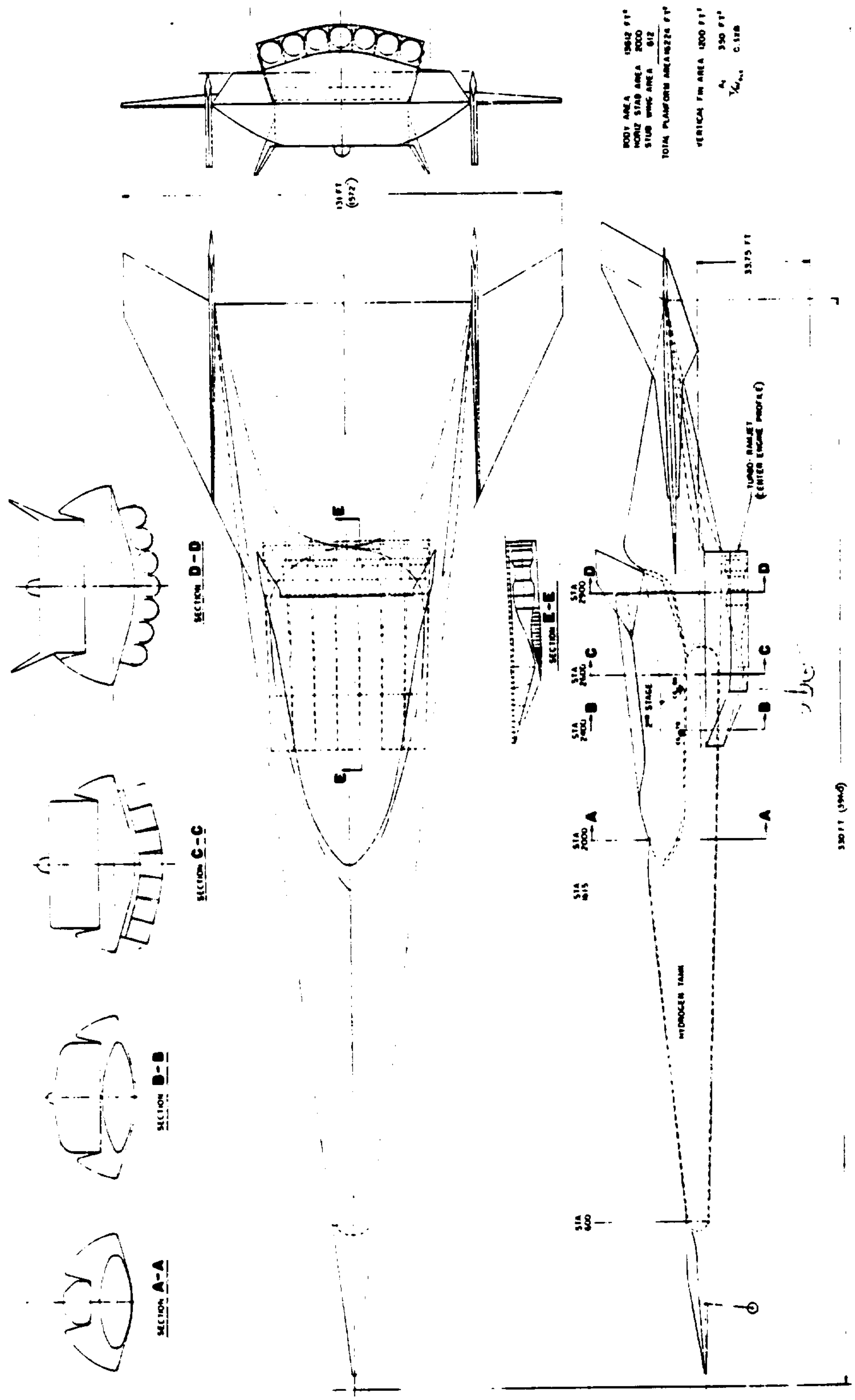

FIGURE 292. Layout of Lifting Body Vehicle Installation for the Class 2 Turboramjet (Engine No. X)

8.6.1.1.1 First Stage Vehicle

The design of the Class 1 systems established the configurations of the primary system elements (propellants, propulsion, and second stage) for minimum drag and inert weight. Stabilizing surface area located the Newtonian aerodynamic center (centroid of planform area) coincident with the most aft system center of gravity (experienced during the hypersonic air-breathing pull-up prior to stage separation). This provided for neutral stability and a valid relative comparison of the twelve basic Class 1 systems. Equivalent vehicle control for the hypersonic condition was maintained by providing equal control volume for each system.

In the Class 1 study, the lifting body vehicle was determined to be substantially superior in performance to the wing/body types because of high slenderness ratio, elimination of second stage base drag through submergence, and attainment of stabilizing surface at low unit weight.

Subsequent analysis of the Class 1 lifting body vehicle in the Class 2 phase, indicated inadequate stability margin in the hypersonic, low angle of attack region, and a deficiency in effective control surface subsonically and hypersonically. Modifications to rectify these conditions were as follows:

1. The horizontal surface area was increased from 800 to 2612 sq ft.
2. The second stage was positioned forward on the first stage vehicle to provide a prestaging burnout center of gravity at 64 percent of the body length, with a consequent reduction in forebody slenderness ratio.
3. The vertical stabilizer and rudder areas were increased to augment the directional stability and control.

The lifting body configuration employed a modified conical fuselage where the forebody was a blunted cone with a depth-to-width ratio of 0.4 at any station. The maximum cross section of the fuselage was at 73 percent of the body length, as measured from the virtual nose (apex). The fuselage nose radius was 1 ft, and the planform area was 13,612 sq ft.

The horizontal stabilizer has a leading edge sweep of 65° and an area of 2612 sq ft. The airfoil section is double-wedged, with a 2-in. leading edge radius. The movable horizontal control surfaces comprise 2000 sq ft.

The horizontal control surface rotates against the vertical stabilizer with forward extending dorsal fins, to alleviate the thermal problem associated with the sharp edges of the control surface under high speed deflected conditions.

The twin vertical stabilizers have a total exposed area of 1200 sq ft and a leading edge radius of 2 in. No toe-in was provided for the verticals; rather, a concept of utilizing small outward rudder deflections to load the surfaces during hypersonic operation where the control surface lift curve slope was zero at zero deflection was proposed to maintain minimum vehicle drag.

All panel surfaces have a thickness ratio of 5 percent. Figures 290, 291, and 292 indicate that only minor modifications of the lifting body configuration in the area of the propulsion system package are required to adapt the three types of engines and in the second stages, to reflect a gross weight variation for the various systems. The major system differences are outlined below.

The engine complement selection for the Class 2 vehicles and the second stage gross weights are given in Section 8.6.2.3.

8.6.1.1.2 Very Advanced Rocket Vehicle

The Very Advanced Rocket system was presented in Figure 133 and described in Section 7.6.1.5. The system was reanalyzed in the Class 2 phase in further depth and, in addition to the horizontal gear takeoff case, it was also evaluated for horizontal externally powered sled takeoff operation and vertical takeoff operation.

The operational profile of the horizontal gear takeoff system is illustrated in Figure 293. System liftoff was at 400 fps (T/W = 1.5) in a distance of 1710 ft, with a 4930 ft runway requirement. The boost proceeds on a normal load factor ascent path (minimum propellant) to the staging point at 5500 fps, where the 291,354 lb second stage was deposited at 145,715 ft altitude at an attitude (γ) of 25.2° above the local horizontal.

For the HTO gear takeoff system, the wing loading was 180 lb/ft^2 and the ground run propellants were carried on board. The HTO sled system utilizes propellants from the ground accelerator during the takeoff to 650 fps; the wing loading was 235 lb/ft^2 and the staging velocity is 7500 fps. The vertical takeoff system has a wing loading of 350 lb/ft^2 and a staging velocity of 6500 fps.

8.6.1.1.3 Second Stage Vehicle

The second stage vehicle was previously described in Sections 7.6.1.1.6 and 7.6.1.5. No change in second stage external configuration was made for the Class 2 analysis. The vehicle was scaled as a function of gross weight shown in Figure 149. See the discussion in Section 8.6.1.6 for further details.

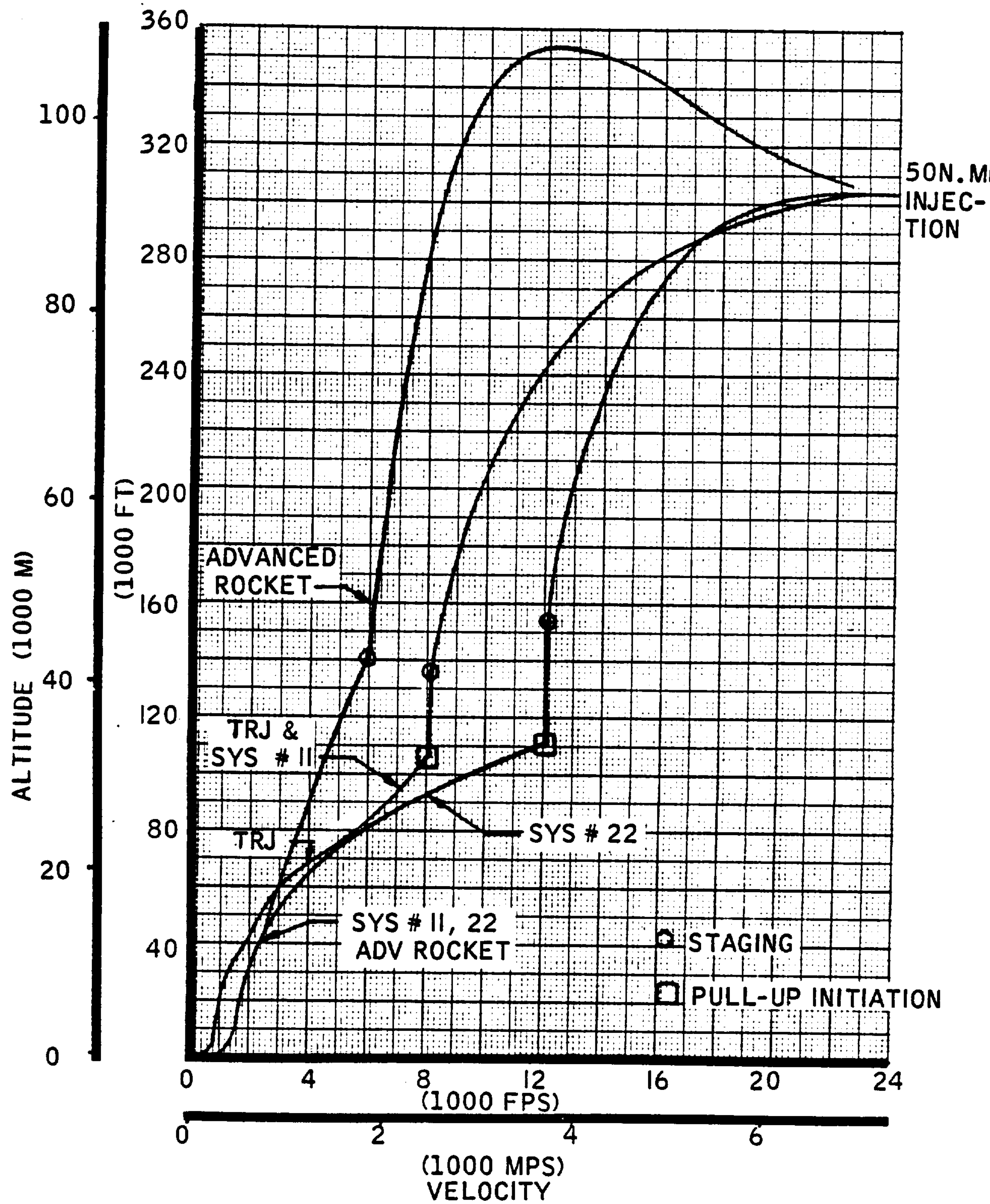

FIGURE 293. Ascent Profiles for Class 2 Systems

8.6.1.1.4 Operational Profiles

The flight profiles of all of the Class 2 systems are shown in Figure 293.

8.6.1.2 Aerodynamics

The aerodynamic analysis in the Class 1 study was limited to an assessment of the system lift and drag characteristics. The Class 2 analysis reevaluated the lifting body configuration lift and drag, and investigated the longitudinal stability and control characteristics.

8.6.1.2.1 Axial Force Coefficient

The technique for computing the zero-lift axial force coefficient is outlined in Section 7.6.1.2.1. The coefficients for the Class 2 lifting body were reevaluated and a breakdown of the component contribution is provided in Table L. The total coefficients are plotted in Figure 294.

The variation of the fuselage axial force with the angle of attack at subsonic speeds was estimated with the methods developed in Reference 37. At supersonic and hypersonic speeds, a modification of the tangent cone/Prandtl-Meyer method was used. From test data on conical configurations appearing in References 30, 34, 35, and 46, the ratio of the tested and computed axial force increment due to angle of attack was determined as a function of Mach number. The values of this correction factor were then applied to the axial force increments computed for the fuselage using the tangent cone/Prandtl-Meyer method to obtain the estimated values. The fuselage friction forces also were adjusted to account for the increased pressures acting over the fuselage.

The variation of the axial force on the horizontal tail with angle of attack at subsonic speeds was determined from the induced drag data of Reference 47. The axial force increments due to angle of attack at supersonic and hypersonic speeds were determined from data provided by Reference 46. (In Class 1, the total drag due to lift was calculated from $KC_L \tan \alpha$, with $K = 1$.)

8.6.1.2.2 Normal Force Coefficients

The lifting body normal force coefficients were computed utilizing the technique described in Section 7.6.1.2.2.

8.6.1.2.3 Lift-Drag Polars

The lift and drag coefficients of the vehicle were obtained from the resolution of the normal and axial force coefficients using the following equations:

TABLE L

SUMMARY OF ZERO LIFT DRAG COEFFICIENTS FOR THE CLASS 2 LIFTING BODY VEHICLE

Reference Area = Fuselage Planform Area

Mach Number	0.6	1.2	1.5	2	3	4	6	8	12
Fuselage									
Forebody pressure drag	0	- -	- -	0.00415	0.00346	0.00308	0.00268	0.00247	0.00226
Afterbody pressure drag	0	- -	- -	0.00640	0.00520	0.00440	0.00225	0.00126	0.00056
Friction drag	0.00411	0.00378	0.00349	0.00310	0.00292	0.00240	0.00187	0.00181	0.00179
Horizontal Tail									
Blunt leading edge drag	0	0	0	0.00016	0.00029	0.00035	0.00039	0.00040	0.00041
Wave drag	0	- -	- -	0.00151	0.00098	0.00073	0.00048	0.00038	0.00028
Friction drag	0.00077	0.00076	0.00067	0.00057	0.00051	0.00041	0.00025	0.00019	0.00018
Vertical Tail									
Blunt leading edge drag	0	0	0.00010	0.00017	0.00027	0.00031	0.00033	0.00034	0.00034
Wave drag	0	- -	- -	0.00064	0.00041	0.00030	0.00020	0.00015	0.00010
Friction drag	0.00037	0.00037	0.00032	0.00028	0.00025	0.00020	0.00012	0.00010	0.00009
Second Stage Vehicle									
Payload vehicle drag	0.00073	0.00101	0.00097	0.00094	0.00081	0.00073	0.00063	0.00058	0.00055
Vehicle drag									
Transonic wave drag	- -	0.01460	0.01380	- -	- -	- -	- -	- -	- -
TOTAL VEHICLE DRAG	0.00598	0.02052	0.01935	0.01792	0.01510	0.01291	0.00920	0.00768	0.00656

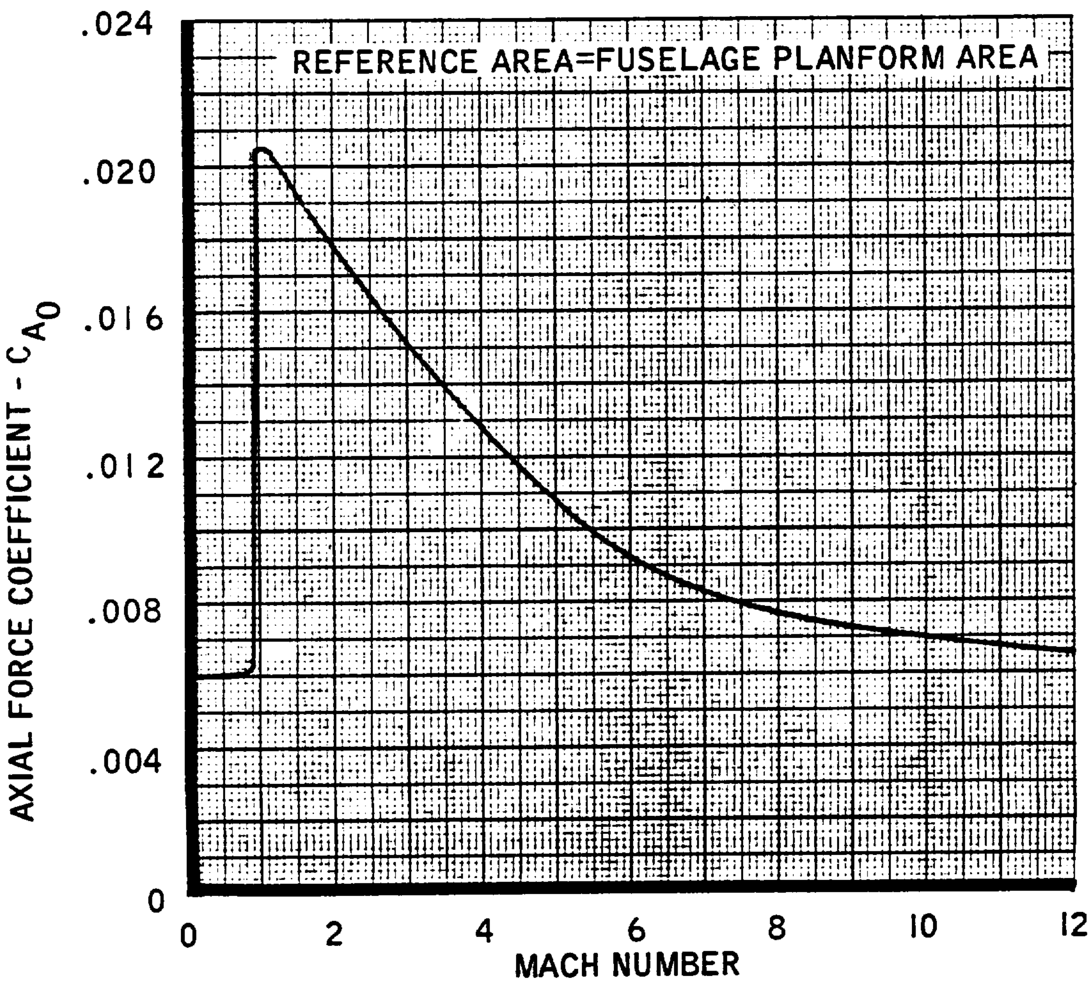

FIGURE 294. Variation of Zero-Lift Axial Force Coefficient for the Class 2 Lifting Body Vehicle with Mach Number

$$C_L = C_N \cos \alpha - C_A \sin \alpha$$

$$C_D = C_N \sin \alpha + C_A \cos \alpha$$

8.6.1.2.4 Vehicle Pitching Moment Coefficient

The fuselage pitching moment at subsonic speed was estimated using the methods of Reference 28. The moments were taken about a pitch axis located at 64 percent of the fuselage length behind the virtual nose (apex) of the fuselage. The fuselage pitching moment at supersonic and hypersonic speeds was determined by allowing the normal force contributions of the forebody and the afterbody to act at the centroid of the respective component planform areas. The pitching moment contribution of the fuselage afterbody decreased rapidly with increasing Mach numbers. Accordingly, the fuselage became unstable in the hypersonic speed regime.

The contribution of the horizontal tail to the vehicle pitching moment was determined for several control surface deflection angles. The methods of Reference 38 were used to determine the horizontal tail pitching moments in the subsonic, transonic, and supersonic flight modes. Shock expansion techniques were used to determine the horizontal tail contributions at hypersonic speeds.

8.6.1.3 Engine Installation Considerations

8.6.1.3.1 Ascent Profiles (Airbreathing Systems)

Acceleration flight trajectory characteristics and engine operating techniques for the Class 2 composite systems and the turboramjet system are described in this section. The All-Rocket System is covered in Section 8.6.1.6. Ascent through staging pull-up is covered individually for each engine below.

To complete the operational profile, all systems utilize a prestaging, airbreathing pull-up and a first stage, poststaging sequence similar to those of Class 1. Subsequent Sections 8.6.2.6 and 8.6.2.7 describe these operational modes in detail.

8.6.1.3.2 Supercharged Ejector Ramjet (Engine No. 11)

The Supercharged Ejector Ramjet system has a takeoff thrust-to-weight ratio of 1.075. Five 215,000 lb (SLS) engines comprise the propulsion complement (Figure 290). The system accelerates under full supercharged ejector mode operation to a liftoff velocity of 405 fps (1.1 $V_{L.O.}$). Liftoff is effected in a distance of 2420 ft (CAR runway length = 5900 ft for an aborted takeoff).

At Mach 0.4, the system initiates transition to the Fan Ramjet Mode, with primary rocket operation terminated. Fan ramjet operation continues to Mach 2.5, where fan operation ceases and the fan is stowed out of the stream into the top of the inlet diffuser. The remainder of the system airbreathing boost phase is on subsonic combustion ramjet operation.

The Supercharged Ejector Ramjet system ascends a relatively high dynamic pressure path (1750 psf maximum, so constrained because of structural implications) to maximize the air augmentation per pound of engine weight. The path is altered from the 1750 psf level at Mach 3 to become tangent to a 150 psia inlet diffuser pressure line which is maintained until the pull-up maneuver.

8.6.1.3.3 <u>ScramLACE (Engine No. 22)</u>

The ScramLACE system thrust loading of 1.038 provides for liftoff at 1.1 $V_{L.O.}$ = 419 fps in 2690 ft (CAR runway for aborted takeoff = 6090 ft). Six 173,000 lb (SLS) engines were selected (Figure 291).

The ScramLACE vehicle initially ascends the same path as the Supercharged Ejector Ramjet to Mach 4, and effects transition from the Liquid Air Cycle Ejector Mode to the Subsonic Combustion Ramjet Mode at Mach 2.5. From Mach 4 to 10 (maximum airbreathing Mach number), the vehicle flies a maximum performance angle of attack schedule (+ 1° to + 2.5°) corresponding to a dynamic pressure level of 1500 psf and a maximum inlet internal transition from subsonic to supersonic combustion.

8.6.1.3.4 <u>Turboramjet (Engine No. X)</u>

The airbreathing boost path of the Turboramjet (TRJ) system is significantly different than its Mach 8 system composite counterpart, the Supercharged Ejector Ramjet (SERJ). The TRJ system accelerates with a thrust loading of 0.528 to a liftoff velocity (1.1 $V_{L.O.}$) of 423 fps. Seven 75,000 lb (SLS) engines were used (Figure 292). Liftoff is initiated in 5470 ft, while provision for aborted takeoff requires an 11,250 ft runway (considerably greater than all of the composite propulsion systems due to the low thrust loading).

The Turboramjet vehicle ascends through a transonic dynamic pressure level of 600 psf while intersecting a 1000 psf path at Mach 2. At Mach 3.1, the path is altered to intersect the Supercharged Ejector Ramjet path at Mach 6, which subsequently maintains the 150 psia inlet pressure constraint. The higher flight path of the Turboramjet system during the Turbojet Mode results from the very high specific impulse characteristics ($\sim$5000 sec), tending to make the vehicle approach a flight attitude near L/D_{max}, to maximize the effective impulse.

8.6.1.3.5 Subsonic Combustion Mode Ramjet Inlet for the Supercharged Ejector Ramjet (Engine No. 11) and the Turboramjet (Engine No. X)

The inlet used in the Class 2 studies was the same as that described in Class 1 (Section 7.6.1.3.1) with the exception that further refinement of inlet-engine matching required a recalculation of the inlet drag and capture area ratio as indicated in Figure 295. The inlet contours for various Mach numbers are shown in Figure 296.

8.6.1.3.6 Supersonic Combustion Ramjet Mode Inlet for the ScramLACE (Engine No. 22)

The inlet used in the Class 2 studies was the same as that described in Class 1 (Section 7.6.1.3.2), with the exception that the ramp surface in front of the mixer entrance was hinged so that additional subsonic diffuser area was provided during the time that air liquefaction was required (Mach 0 to 2.4). The ramp also incorporates louvers which are used to close off the entrance to the heat exchangers when not in use (See Section 7.4.2.1 for details).

The inlet kinetic energy recovery in the supersonic combustion mode was decreased (as shown in Figure 297) from the value of 0.985 to a more realistic value of 0.975 in the Class 2 studies. The inlet capture area ratios and drag coefficients were also reevaluated and they are shown in Figure 298 for the primary mode and in Figure 299 for the subsonic combustion ramjet. Inlet contraction ratios of 3, 4, and 5 are presented.

The inlet contours are shown in Figure 296 and the design concept applicable to both subsonic and supersonic combustion systems is presented in Figure 300.

8.6.1.4 Vehicle Weight Analysis

The analysis of the selected Class 2 systems and the comparison turbomachine system utilized the same approach as was used in the Class 1 study, developed and presented in Section 7.6.1.4. Some of the unit weight factors were refined and modified during this phase. This was particularly true for those data sensitive to maximum airbreathing Mach number selection. These items are discussed in the following sections.

The first stage burnout weight was calculated using Equation (12) from Section 7.6.1.4.2. For the design baseline vehicles shown in Figures 290, 291, and 292, the stage fixed weights were computed using Equation (25) from Section 7.6.1.4.3. The weight fractions and unit weights are presented below. Variable weights are also summarized below.

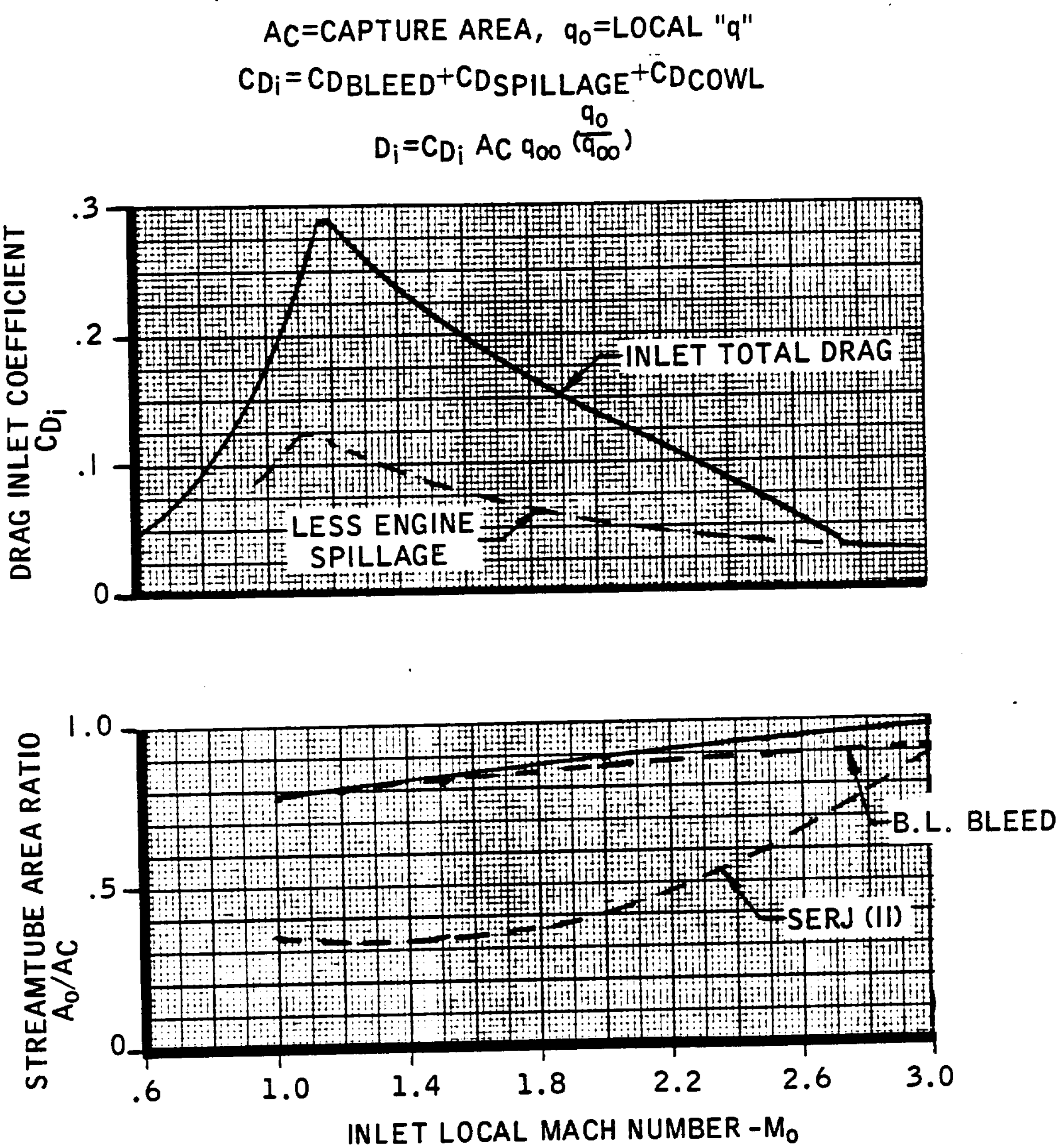

FIGURE 295. Inlet Characteristics of the Class 2 Subsonic Combustion System

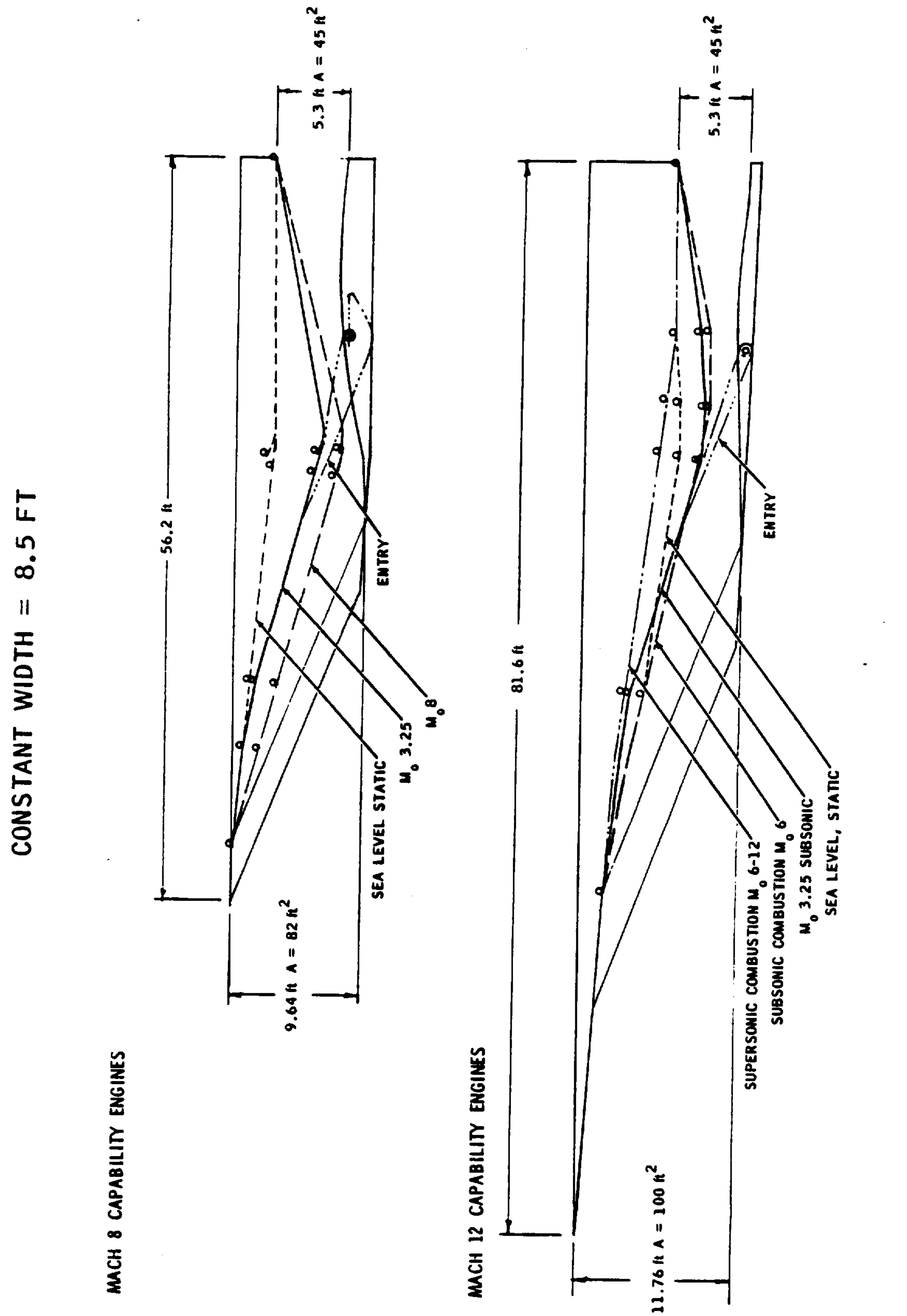

FIGURE 296. Class 2 Inlet Contours for Various Flight Space Conditions

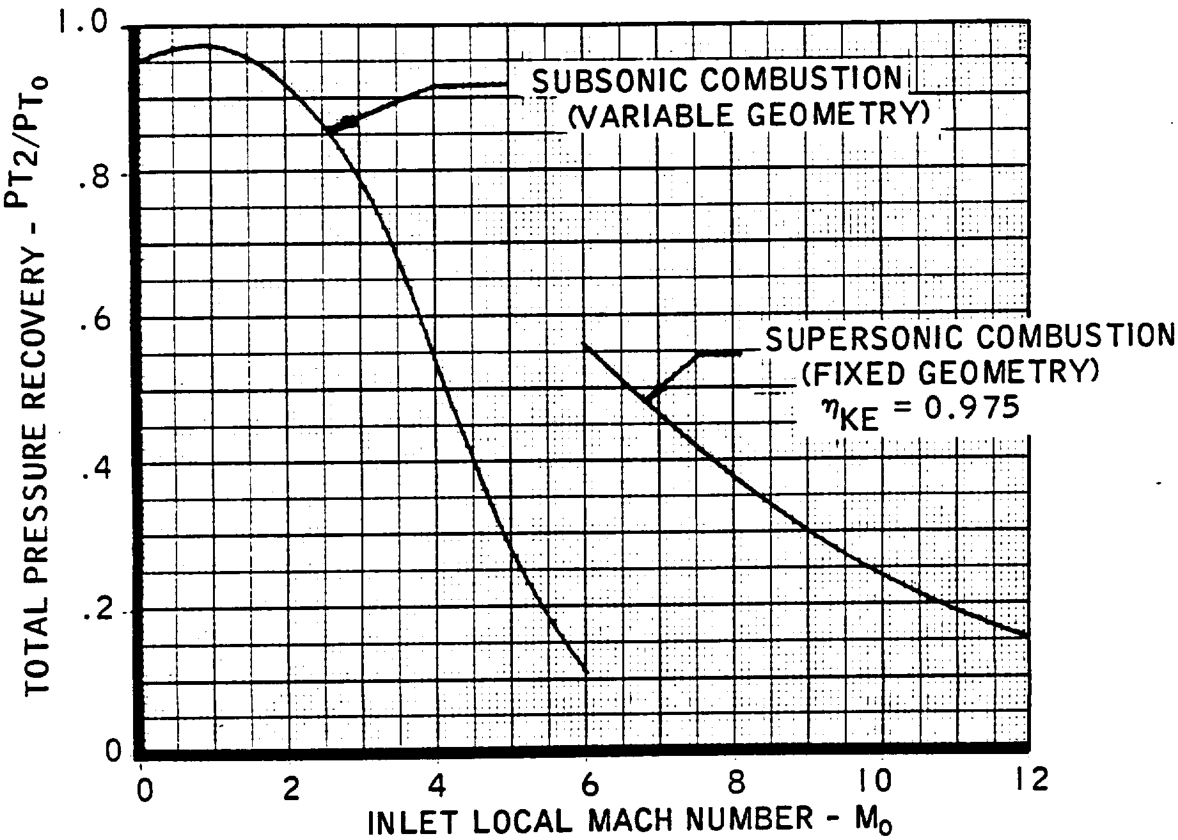

FIGURE 297. Inlet Pressure Recovery for the Class 2 ScramLACE (Engine No. 22)

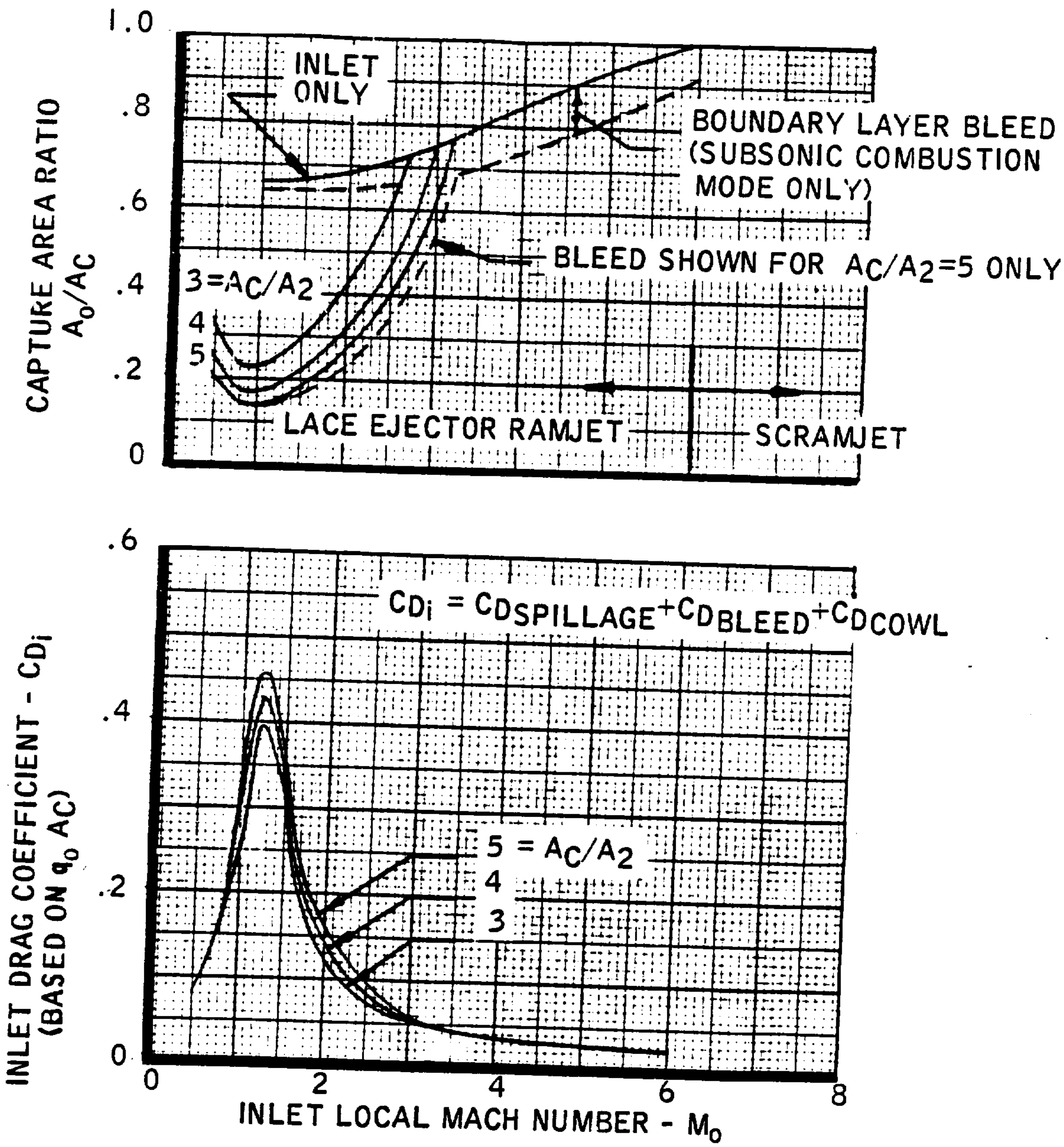

FIGURE 298. Primary Mode Inlet Characteristics for the Class 2 ScramLACE (Engine No. 22)

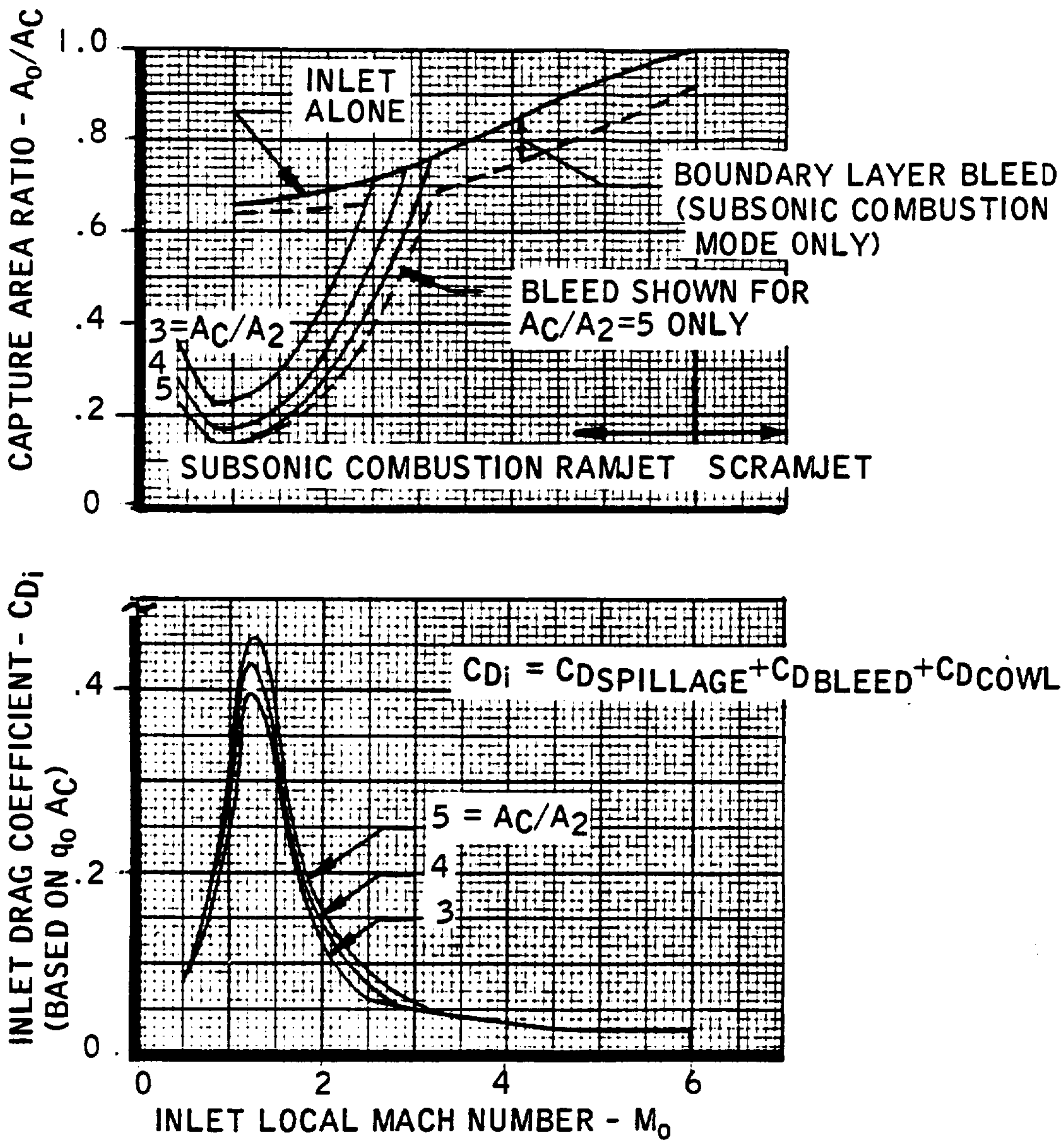

FIGURE 299. Subsonic Combustion Ramjet Mode Inlet Characteristics for the Class 2 ScramLACE (Engine No. 22)

(MACH 8 CAPABILITY ENGINES, TYPICAL)

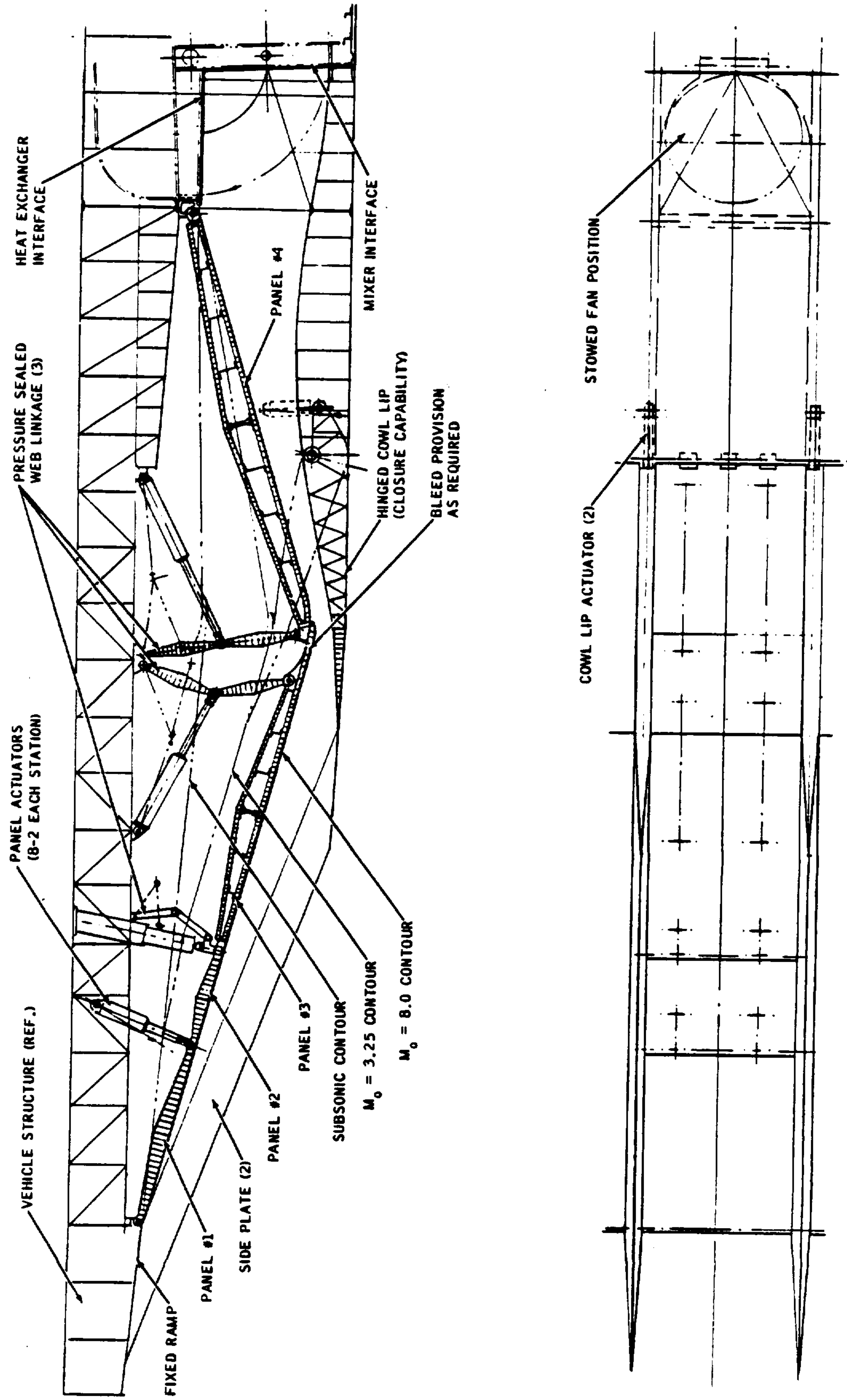

FIGURE 300. Mechanization of Two-Dimensional, Moving Panel Inlet

8.6.1.4.1 Weight Fractions and Unit Weights

The specific weights of the heat shield, insulation, aft structure, and fin were based on the structural concepts described in Section 7.6.1.4.4. The unit weights appearing in Table LI are for a maximum air-breathing Mach number of 8. The representative hypersonic vehicle boost trajectories and temperatures of Reference 41 were used as the basis for the surface materials and temperatures presented in Figure 301. The Mach 8 unit weights were then modified for other Mach numbers by use of Figures 302, 303, and 304.

The surface temperatures plotted in Figure 302 represent an average point on the vehicle. A local surface temperature of 1500°F or greater was selected as the point where the use of columbium heat shield material would be required. The resulting area requirements for each heat shield type are shown. The relative weights for these materials and the area coverage are shown in Figure 302.

To establish the relative insulation weight of Figure 303 for a boost vehicle, a linear variation of the external insulation thickness with surface temperature was assumed. An average value of the upper and lower surface temperature of Figure 302 was used.

Figure 304 presents the effect of Mach number on the fin unit weight. In computing this value, 40 percent of the total fin unit weight, (i.e., the surfaces) was assumed to be dependent on surface temperature. The temperature, in conjunction with the material strength-to-density ratio, allowed the relative fin weight to be determined.

To establish a basis for the inlet weights, an estimate was made for the Class 2 Supercharged Ejector Ramjet and Turboramjet inlet. The representative inlet (illustrated in Figure 305) has a capture area of 38 sq ft per engine and a maximum internal pressure of 120 psia. This sized inlet was slightly smaller than those finally selected for the Class 2 systems. However, the normalized weight/capture area ratio being determined was readily applicable to these systems. This is a two-dimensional, variable geometry inlet. The external ramp is radiation cooled and the internal ramps and diffuser sections are regeneratively cooled. The effect on the specific weight of varying maximum internal pressure is also presented. The supersonic combustion system utilizes the same inlet unit weight as that presented in Section 7.6.1.4.4.

The body/tank unit weight of 2.22 lb/ft^2 (from Section 7.6.1.4.4) was applied to the three vehicles (Figures 290, 291, and 292). The resulting tankage weight factors are presented in Figure 306 for the subsonic and supersonic combustion vehicles.

Due to the minor variation with hydrogen weight, the nominal values indicated on the figure were utilized in the analysis.

TABLE LI

SUMMARY OF CLASS 2 AVERAGE UNIT WEIGHTS
Airbreathing Mach Number = 8

Weight Fraction	Unit Weight (lbs/ft^2)
$\frac{W_{HS}}{S_{HS}}$	1.42
$\frac{W_{INS}}{S_{INS}}$	1.07
$\frac{W_{AS}}{S_{AS}}$	2.86
$\frac{W_E}{S_E}$	12.05
$\frac{W_{VF}}{S_{VF}}$	8.10

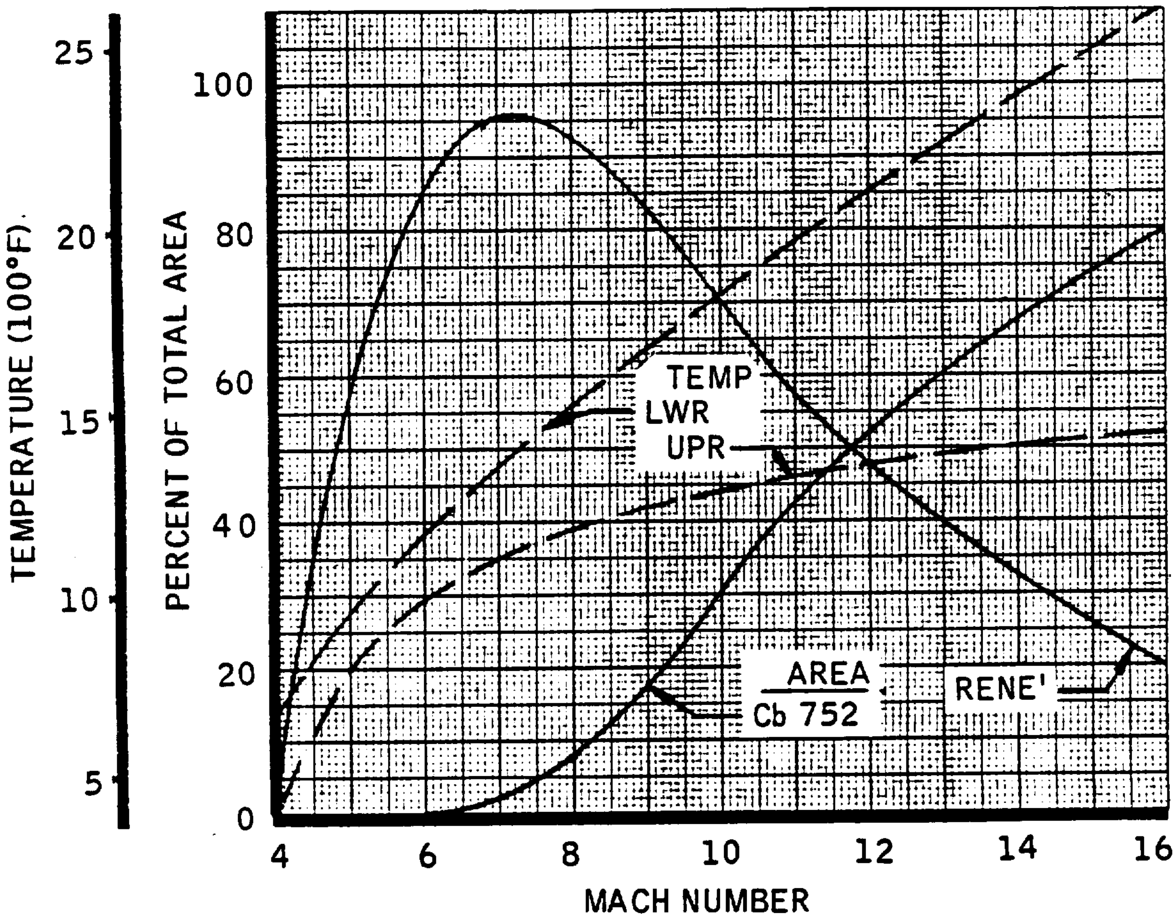

FIGURE 301. Surface Materials and Temperatures for the Class 2 Vehicle

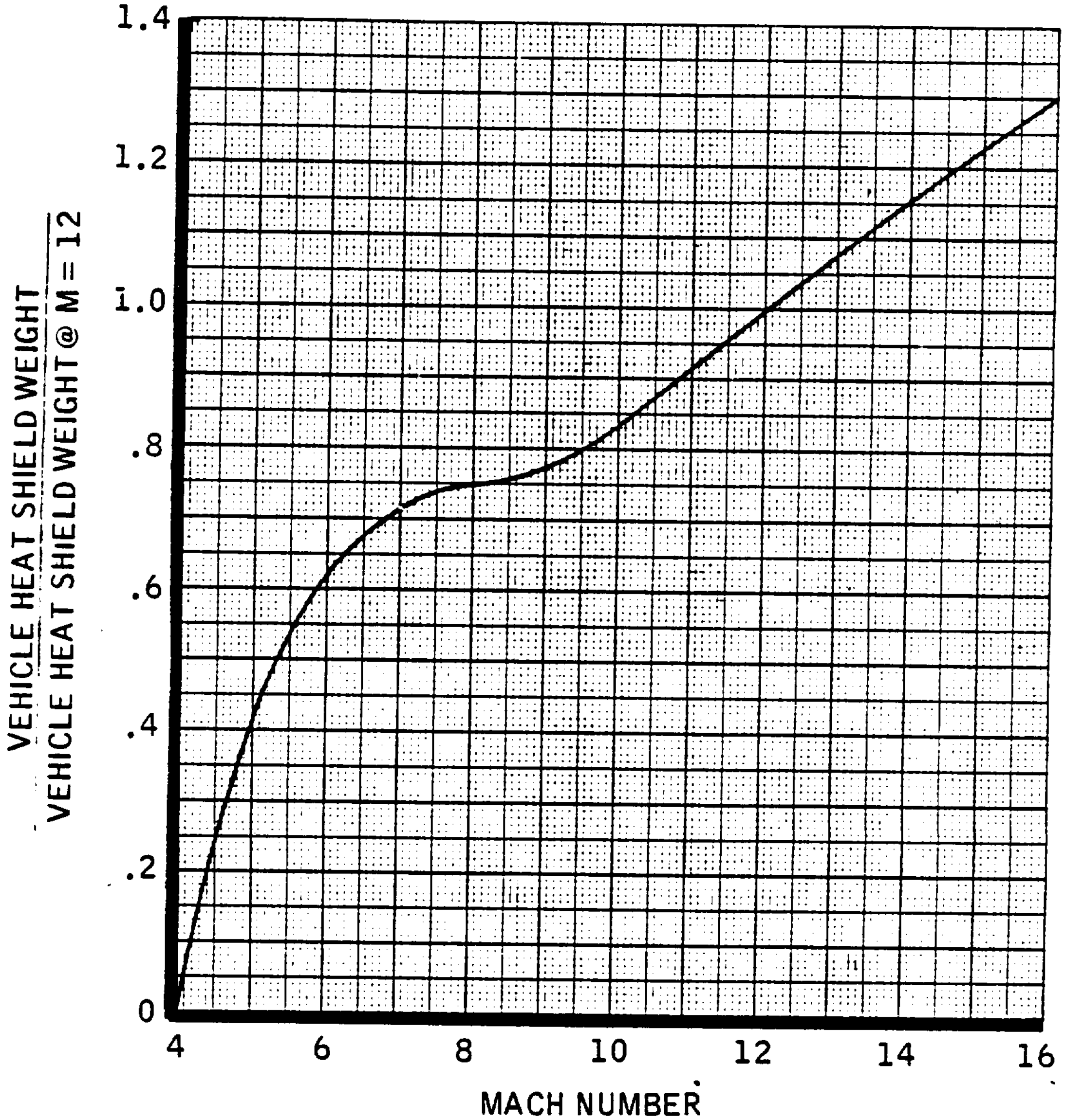

FIGURE 302. Heat Shield Weight for the Class 2 Vehicle

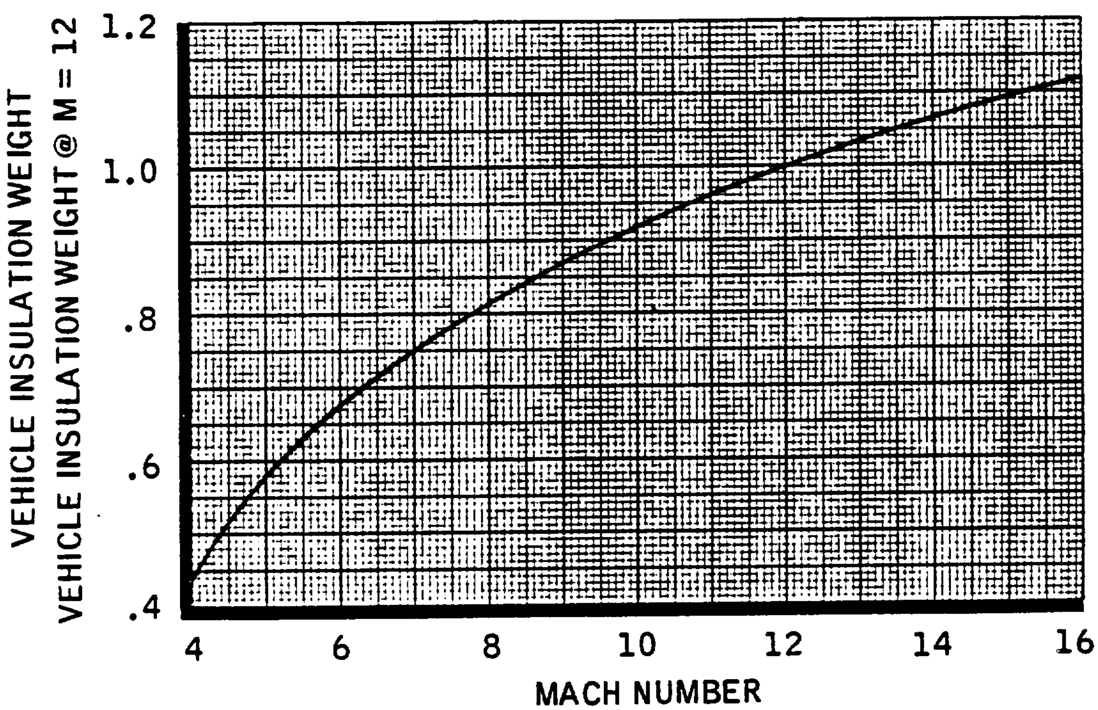

FIGURE 303. Boost Insulation for the Class 2 Vehicle

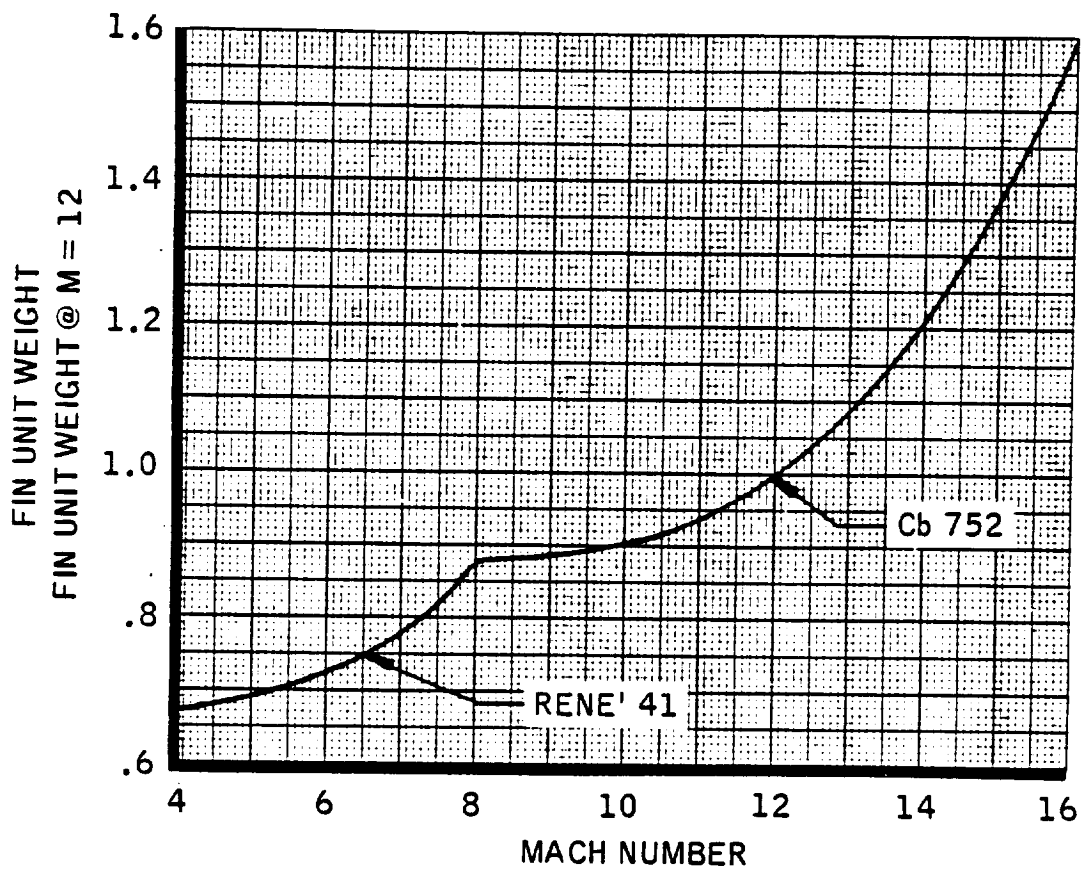

FIGURE 304. Fin Unit Weights for the Class 2 Vehicle

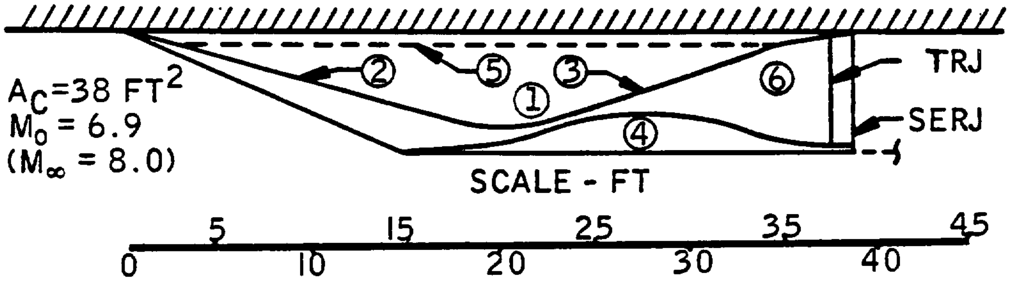

		AREA(FT^2)	WEIGHT (LBS)
1	INLET SIDE WALLS	179	1,432
2	RADIATION COOLED RAMP	100	600
3	REGENERATIVELY COOLED RAMP	131	1,048
4	COWL AND TRANSITION	127	508
5	PRESSURE SHELL	223	669
6	DUCT	39 & 55	156 & 220
	RAMP ACTUATION	-	247
	LH_2 MANIFOLDS	-	330
	BLEED SYSTEM & BYPASS DUCTS	-	380
	ACCESS & SERVICE PROVISIONS	-	179

TRJ = 146 LB/FT^2 OF A_C
SERJ = 148 LB/FT^2 OF A_C
@ P_{T2} = 120 PSIA

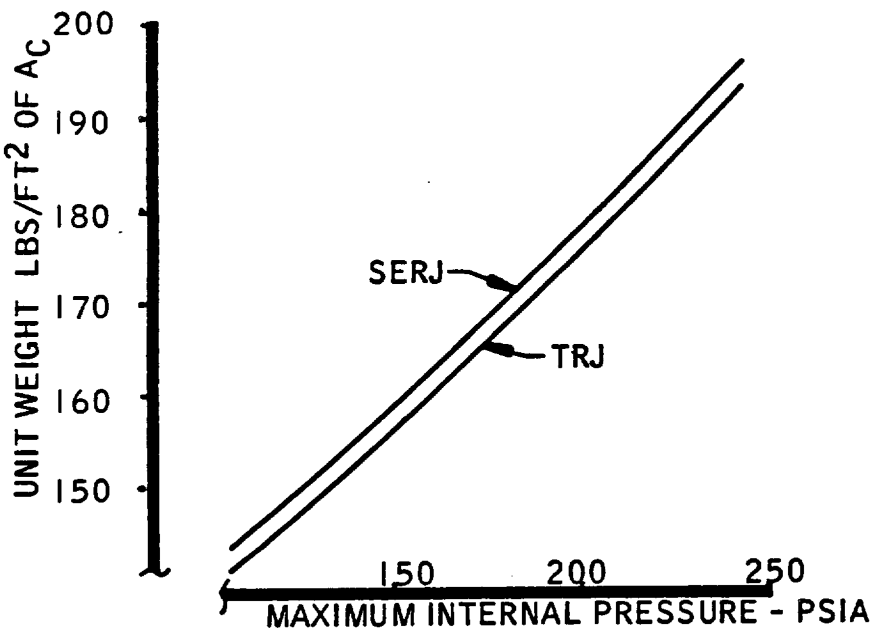

FIGURE 305. Inlet Weight Estimate for the Class 2 Vehicle

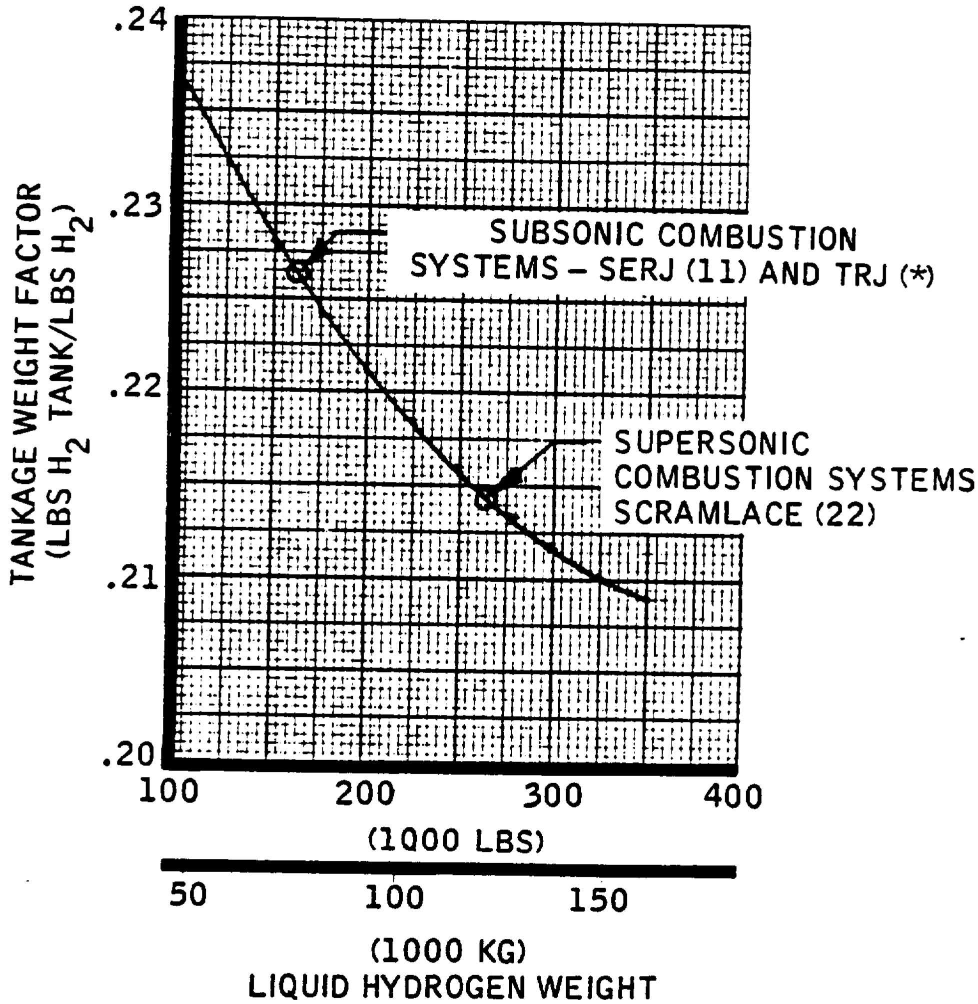

FIGURE 306. Hydrogen Tankage Weight Factor for the Class 2 Vehicles

The uninstalled engine thrust-to-weight ratios of Table LII were based on a unit engine having T_{SLS} = 250,000 lbs and $P_{T_{2_{max}}}$ = 100 psia for the Supercharged Ejector Ramjet and ScramLACE systems. They were modified for other maximum internal pressures according to Figure 307. The slopes of the curves in this figure were established from the engine data supplied by Marquardt during the Class 1 phase. The data for the Turboramjet engine were from Reference 26.

Table LIII presents the propellant and engine system weight/thrust factors. These data are essentially as discussed in Section 7.6.1.4.4.

The cruise and landing factors shown in Table LIV were based on performance criteria outlined in Section 7.6.1.6.3.

8.6.1.5 System Performance

System performance for the Class 2 candidate engines was evaluated by utilizing the data from Sections 8.6.1.1. through 8.6.1.4. For the Class 2 systems performance analysis, emphasis was directed toward the following:

1. Re-evaluation of the boost performance based upon updated propulsion and aerodynamic data

2. A study of the prestaging pull-up characteristics for payload maximization

3. Generation of a first stage postseparation sequence to minimize the return-to-base and landing propellant consumption

4. Integration of the first stage performance and weight elements to establish second stage gross weight (first stage payload)

The Class 2 systems were individually assessed with respect to the airbreathing boost Mach number corresponding to maximum payload yield. The sensitivities of the systems to aerodynamic drag, propulsion system specific impulse and installed thrust-to-weight ratio, and vehicle inert weight elements were evaluated. The potential alternate mission capability of the first stage was assessed and is reported in Appendix D.

8.6.1.5.1 Ascent Performance

The ascent performance of the Supercharged Ejector Ramjet (Engine No. 11) and the ScramLACE (Engine No. 22) systems was re-evaluated and a Turboramjet (Engine No. X) was analyzed to provide a turbomachine based airbreather reference. The Class 1 ascent profiles were retained except when alteration afforded increased performance.

TABLE LII

THRUST-TO-WEIGHT RATIOS FOR CLASS 2 ENGINES

System	Airbreathing Mach Number M_{AB}	Maximum Internal Pressure (psia)	$\left.\frac{T}{W}\right)_{uninst}$
Supercharged Ejector Ramjet	8	150	20.66
	5	110	21.65
	6	112	21.57
	7	125	21.20
	9	200	19.92
	10	227	19.64
ScramLACE	12	120	19.19
	8	120	19.19
	10	120	19.19
	14	120	19.19
	16	120	19.19
Turboramjet	8	150	
	5	110	
	6	112	Reference 48
	7	125	
	9	200	
	10	227	

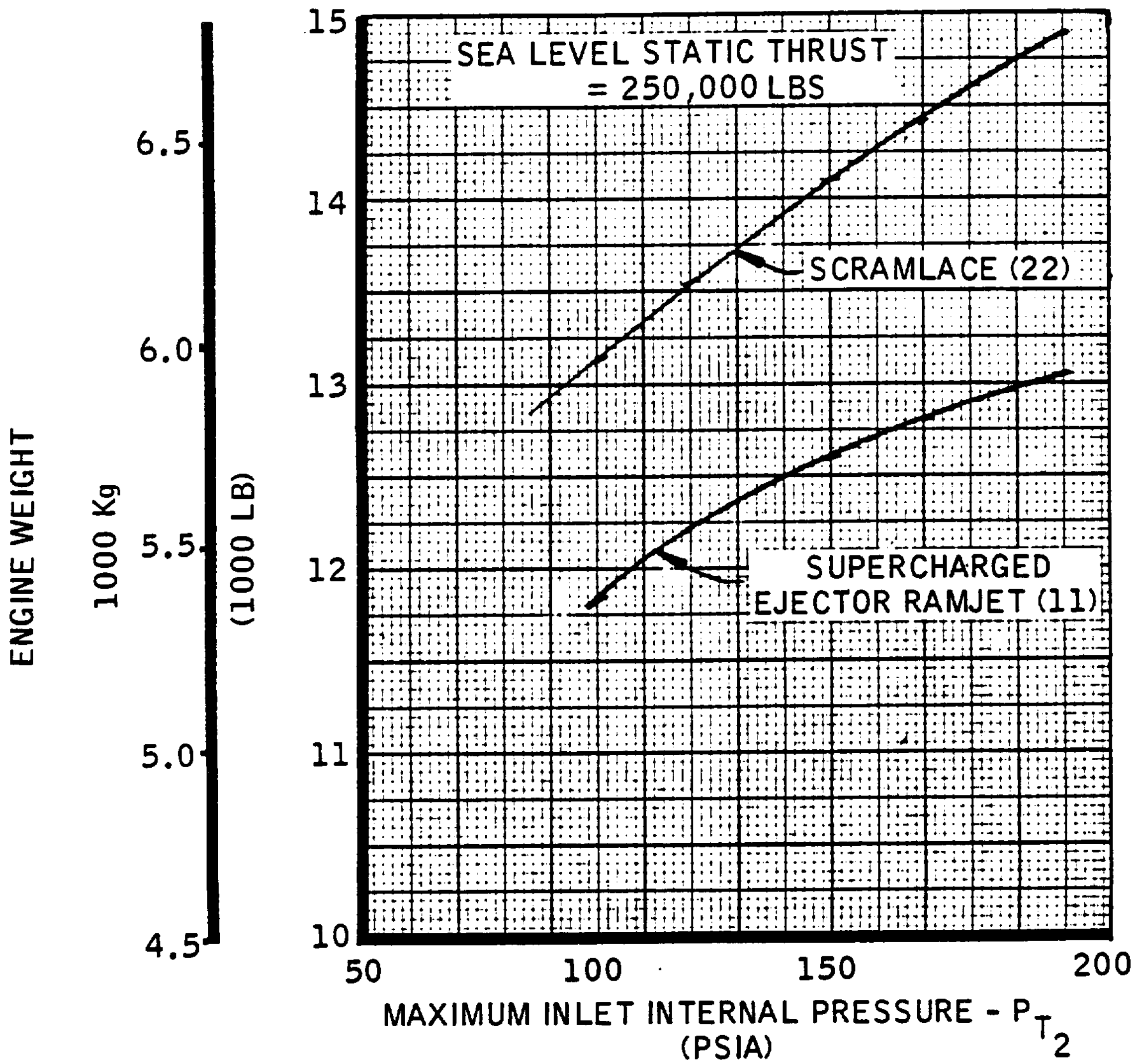

FIGURE 307. Variation of Engine Weight with Inlet Internal Pressure for Class 2 Systems

TABLE LIII

WEIGHT/THRUST RATIOS FOR CLASS 2 PROPELLANT AND ENGINE SYSTEMS

Component	$\frac{W}{T}$
Engine controls, engine compartment and tank cooling provisions, etc.	0.0012
Fuel distribution, vent, drain, control systems, etc.	0.0040
Oxidizer distribution, vent, drain, control systems, etc.	0.0030
Engine mounting structure, thrust load carrying structure, and engine fairings	0.0070
Provisions for cooling initial nozzle surface for subsonic combustion ramjets	0.00325

TABLE LIV

CRUISE AND LANDING PROPELLANT FACTORS FOR CLASS 2 ENGINES

System	Airbreathing Mach Number M_{AB}	$\frac{\Delta W_C}{W_{lbo}}$	$\frac{\Delta W_{LD}}{W_c}$
Supercharged Ejector Ramjet	8	0.0160	0.0032
	5	0.0182	0.0032
	6	0.0180	0.0032
	7	0.0173	0.0032
	9	0.0189	0.0032
	10	0.0231	0.0032
ScramLACE	12	0.0290	0.0152
	8	0.0160	0.0152
	10	0.0145	0.0152
	14	0.0330	0.0152
	16	0.0550	0.0152
Turboramjet	8	0.0265	0.0074
	5	0.0170	0.0074
	6	0.0178	0.0074
	7	0.0218	0.0074
	9	0.0302	0.0074
	10	0.0356	0.0074

8.6.1.5.2 First Stage, Poststaging Performance

Return of the first stage to the launch site involves a complex optimization, including consideration of executing a variable banked boost to minimize the displacement from base and to orient the system properly at staging.

For the Class 2 analysis, however, the operational approach utilized was as follows:

1. An unbanked ascent to staging

2. A first stage, poststaging banked descent, power-off, to minimize the down range displacement while miximizing the turn angle displacement

3. A power-on turn to complete the vehicle orientation with the launch base

4. A cruse at $(L/D)_{max}$

5. A power-off glide scheduled at α for $(L/D)_{max}$

6. A power-on subsonic loiter at L/D_{max} for 5 minutes at the launch site

7. A nominal power-on landing (Landing performance was evaluated for an emergency, power-off condition.)

This approach provided a basis for a realistic assessment of the Class 2 systems.

8.6.1.6 All-Rocket Vehicle Comparison System

An analysis to determine the payload capability of an advanced all-rocket two-stage rocket vehicle was also made under the study guidelines. The majority of the data used in the analysis was obtained from the Reusable Orbital Transport Study (Reference 19). The Class 2 effort broadened considerably the case for the comparison rocket system with respect to the Class 1 coverage.

The scope of the investigation included three basic operational configurations, namely, HTO - gear takeoff, HTO - sled launched, and VTO.

Maximum performance ascent paths for all rocket systems were utilized as described in Reference 19.

Table LV shows the pertinent system parameters and the excursions made with respect to first stage wing loading at liftoff $(W/S)_{L.O.}$ and effective aspect ratio $(AR)_E$. In all cases, the staging velocity was varied parametrically in the range between 4500 and 8500 fps, thus providing for maximum payload staging point selection.

TABLE LV

ADVANCED ROCKET SYSTEM CHARACTERISTICS

Configuration	$(T/W)_I$	$V_{L.O.}$ (fps)	$(L/D)_{\text{Return Cruise}}$	$(W/S)^*_{L.O.}$ (psf)	$(AR)_E$
HTO - gear takeoff	1.50	400	9 (First stage)	180 235	1.5
HTO - sled launched	1.27	650	8 (First stage)	180 235 300	1.5
VTO	1.50	0	7 (First stage)	180 235 300 350	1.5

* Based on projected wing area

The following assumptions were made:

1. The aerodynamic characteristics (C_D, C_L) were the same as those for the final Reusable Orbital Transport vehicle. Thus, velocity losses due to drag were assured to be the same for all systems investigated.

2. Only minimum fuel paths were used. Sonic overpressure restraints were not a consideration.

3. Combined first/second stage vehicle abort was not considered.

The following data were used in sizing the system stages and determining the payload capability:

1. Ideal Velocity

   The variation of ideal velocity with staging velocity is shown in Figure 308. In the case of the HTO-gear takeoff vehicle, the first stage ideal velocity included an increment for the ground run, takeoff velocity differentials, and associated losses. The second stage ideal velocities included a post-injection ΔV of 1523 fps and assumed an injection orbit of 50 n. miles following eastward launch.

2. Propulsion Data

   First stage impulse rocket engines
   $$\begin{cases} (I_{sp})_{VAC} = 460 \text{ sec} \\ (I_{sp})_{S.L.} = 390 \text{ sec} \\ (I_{sp})_{AVE} = 436 \text{ sec} \end{cases}$$

   Basic rocket engine $(T/W)^{R}_{EN}$ = 160

   Return to base A/Bs $(I_{sp})_{CRUISE}$ = 12,000 sec

   Installed $(T/W)^{AB}_{ENG}$ = 2.26

3. Structural Data

   Structural data are presented in Table LVI.

Performance results are presented in Section 8.6.2.8.

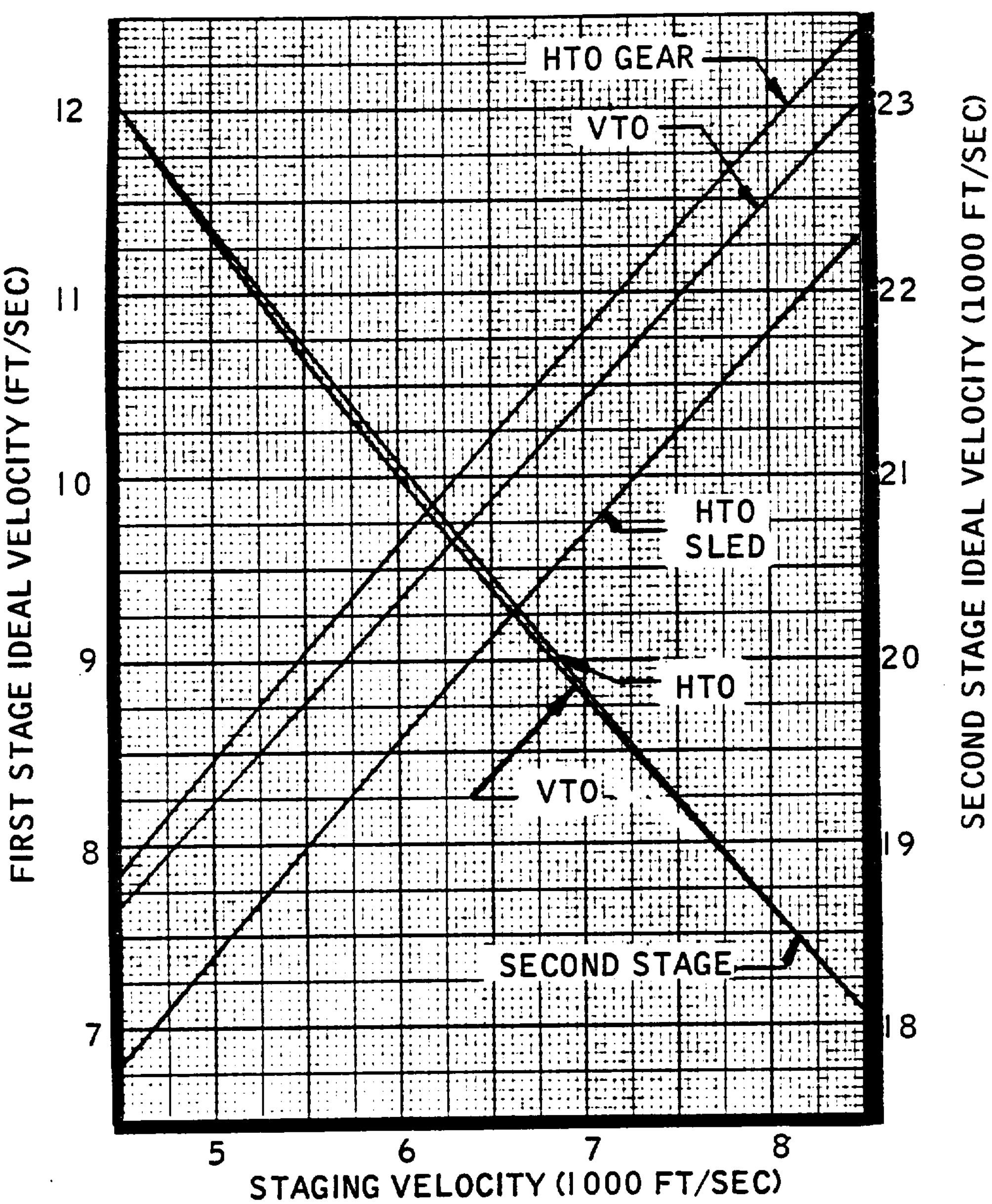

FIGURE 308. Ideal Characteristic Velocities for the Class 2 Advanced Rocket (Engine No. 0)

TABLE LVI

STRUCTURAL WEIGHT DATA FOR THE CLASS 2 ADVANCED ROCKET VEHICLE

Case: Mode	Case: V_{STAG}	Case: $(W/S)_I$	Case: RLG*	Fuselage Unit Weight $\frac{W_{PROP}}{W_{FUS}}$	Main Wing Unit Weight $\frac{W_W}{S_G}$	Mass Fraction $\frac{W_{PROP}}{W_{STAGE}}$
HTO-gear takeoff	4500	180	0.1258	11.20	7.82	0.6609
	5500			11.22		0.6731
	6500			11.22		0.6819
	7500			11.22		0.6884
	8500			11.28		0.6930
	4500	235	0.1258	11.20	8.27	0.6772
	5500			11.22		0.6885
	6500			11.22		0.6966
	7500			11.22		0.7025
	8500			11.28		0.7067
HTO-sled launched	4500	180	0.0600	11.20	8.66	0.6835
	5500			11.22		0.6987
	6500			11.22		0.7095
	7500			11.22		0.7173
	8500			11.28		0.7230
	4500	235	0.0600	11.20	9.15	0.7029
	5500			11.22		0.7168
	6500			11.22		0.7266
	7500			11.22		0.7337
	8500			11.28		0.7387
	4500	300	0.0600	11.20	9.64	0.7180
	5500			11.22		0.7308
	6500			11.22		0.7397
	7500			11.22		0.7462
	8500			11.28		0.7508
VTO	4500	180	0.0600	12.43	6.84	0.7027
	5500			12.49		0.7103
	6500			12.52		0.7152
	7500			12.60		0.7180
	8500			12.65		0.7183
	4500	350	0.0600	12.42	7.32	0.7415
	5500			12.46		0.7471
	6500			12.48		0.7505
	7500			12.52		0.7521
	8500			12.58		0.7517

*Landing gear coefficient

8.6.2 Results

8.6.2.1 Vehicle Aerodynamic Performance

Values of the lift coefficient as a function of angle of attack and Mach number are given in Figure 309. Drag polars (C_L versus C_D)are presented for various Mach numbers in Figures 310 and 311. The drag polars indicate that the vehicle has untrimmed maximum lift/drag ratios of 8 at subsonic speeds, 3.8 at Mach 6, and 3.3 at Mach 12.

The pitching moment characteristics of the vehicle are shown in Figures 312 through 316 as functions of angle of attack and control deflection angle for a range of Mach numbers.

Conclusions drawn from the Class 2 aerodynamic analysis are outlined below.

8.6.2.1.1 Drag

The zero-lift drag of the Class 2 lifting body relative to that of the Class 1 lifting body indicates decreased drag in the subsonic and transonic regions, with slightly increased drag hypersonically. The differences accrued to the increased afterbody and decreased forebody fineness ratios resulting from repositioning the second stage.

8.6.2.1.2 Lift

The fuselage aft body contribution to vehicle lift at low angle of attack, supersonically and hypersonically, was less than that estimated for the Class 1 vehicle.

8.6.2.1.3 Stability and Control

The longitudinal aerodynamic stability and control characteristics of the system indicate the following:

1. Takeoff speed will increase slightly due to trim lift loss. For a 16° liftoff angle of attack, the control surface deflection to trim is -24° with the 64 percent C.G. location. Proper distribution of propellants in forward and aft tanks can provide a C.G. close to 64 percent for takeoff to minimize control deflection and lift loss.

2. A substantial static stability (10 percent of body length, minimum) margin exists subsonically.

3. For the vehicle transonic (Mach 1.5) angle of attack range (1° to 2°), a very small trim penalty was indicated (less than 4° deflection) with adequate static margin (12 percent, minimum).

REFERENCE AREA = FUSELAGE PLANFORM AREA
= 13,612 SQ FT

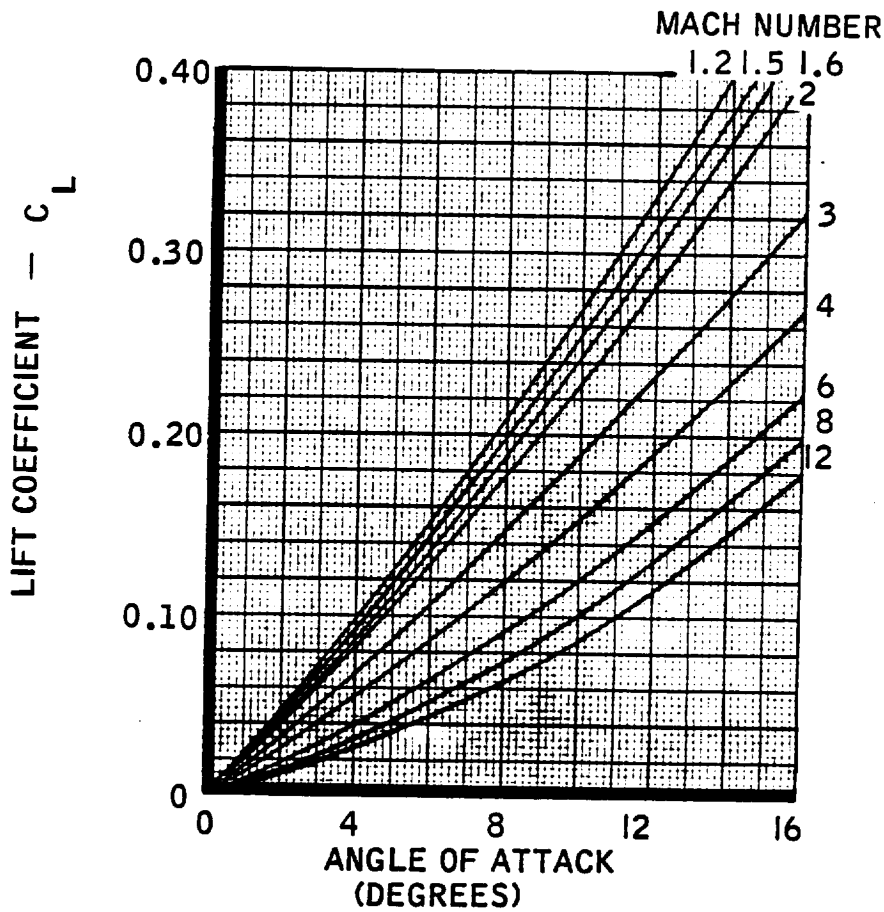

FIGURE 309. Variation of Lift Coefficient with Angle of Attack for Class 2 Vehicles

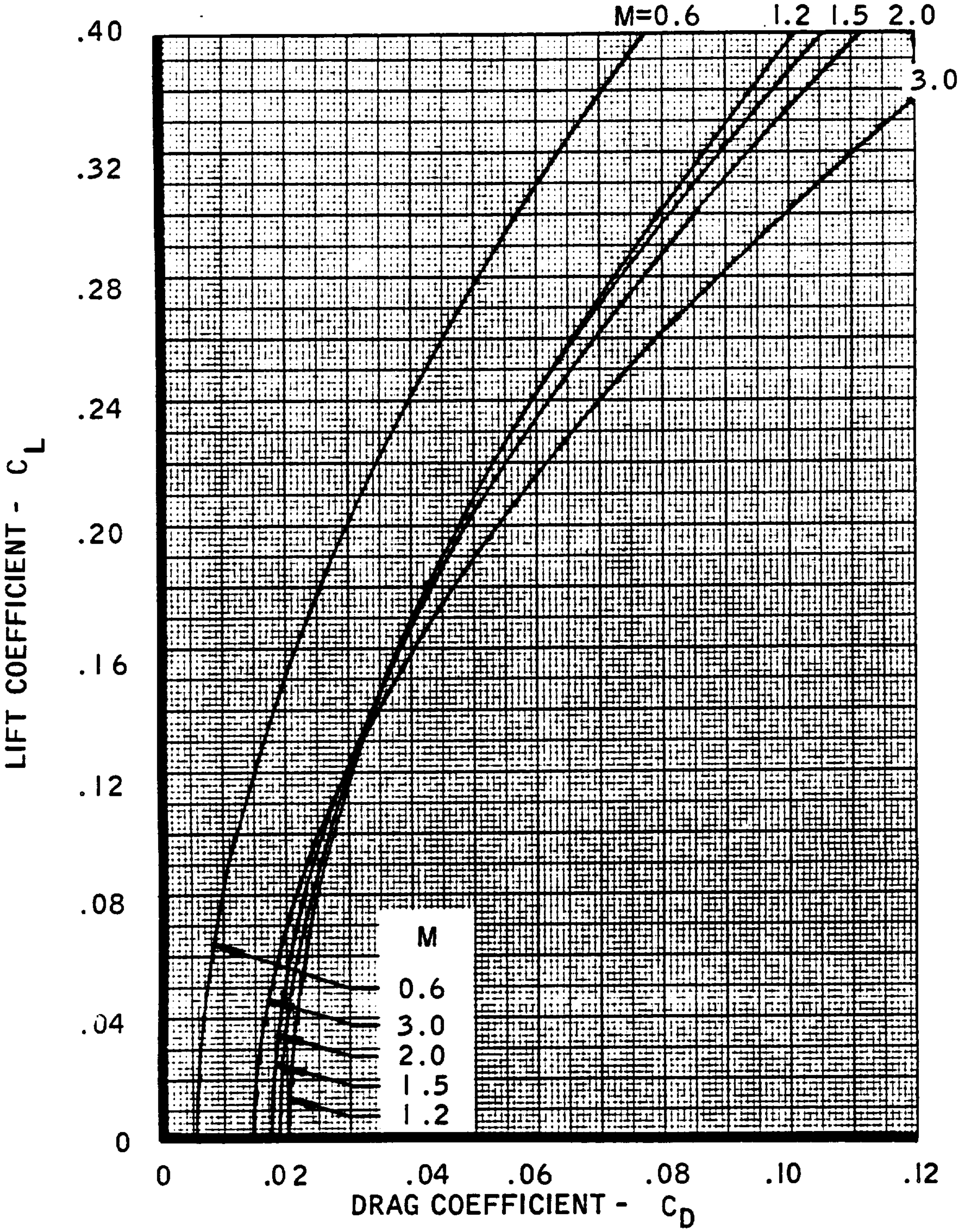

FIGURE 310. Lift-Drag Polars for the Class 2 Vehicle, Mach 0.6 to 3.0

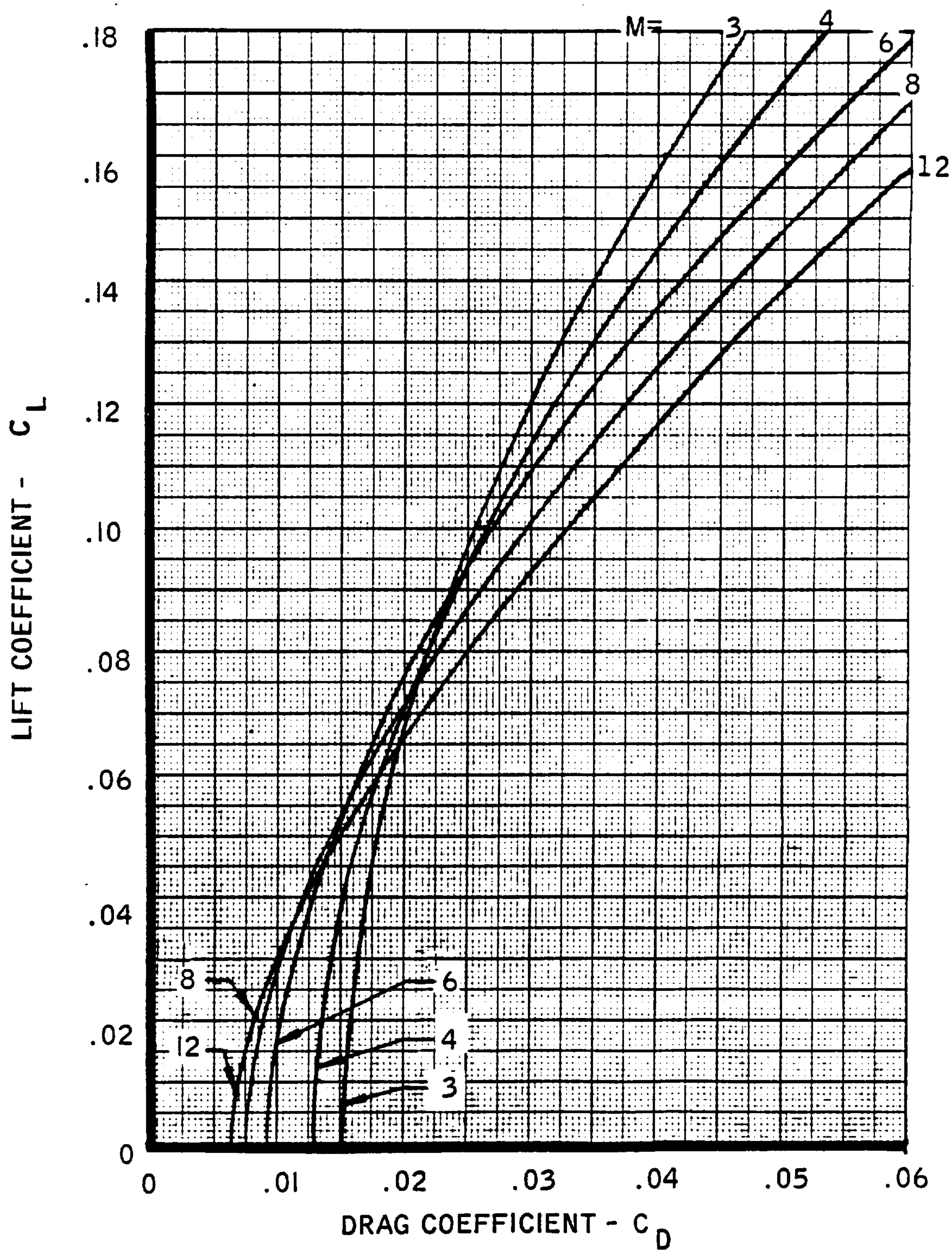

FIGURE 311. Lift-Drag Polars for the Class 2 Vehicle, Mach 3 to 12

REFERENCE AREA = FUSELAGE PLANFORM AREA
REFERENCE LENGTH = VIRTUAL FUSELAGE LENGTH
C.G. AT .64 L_{REF}

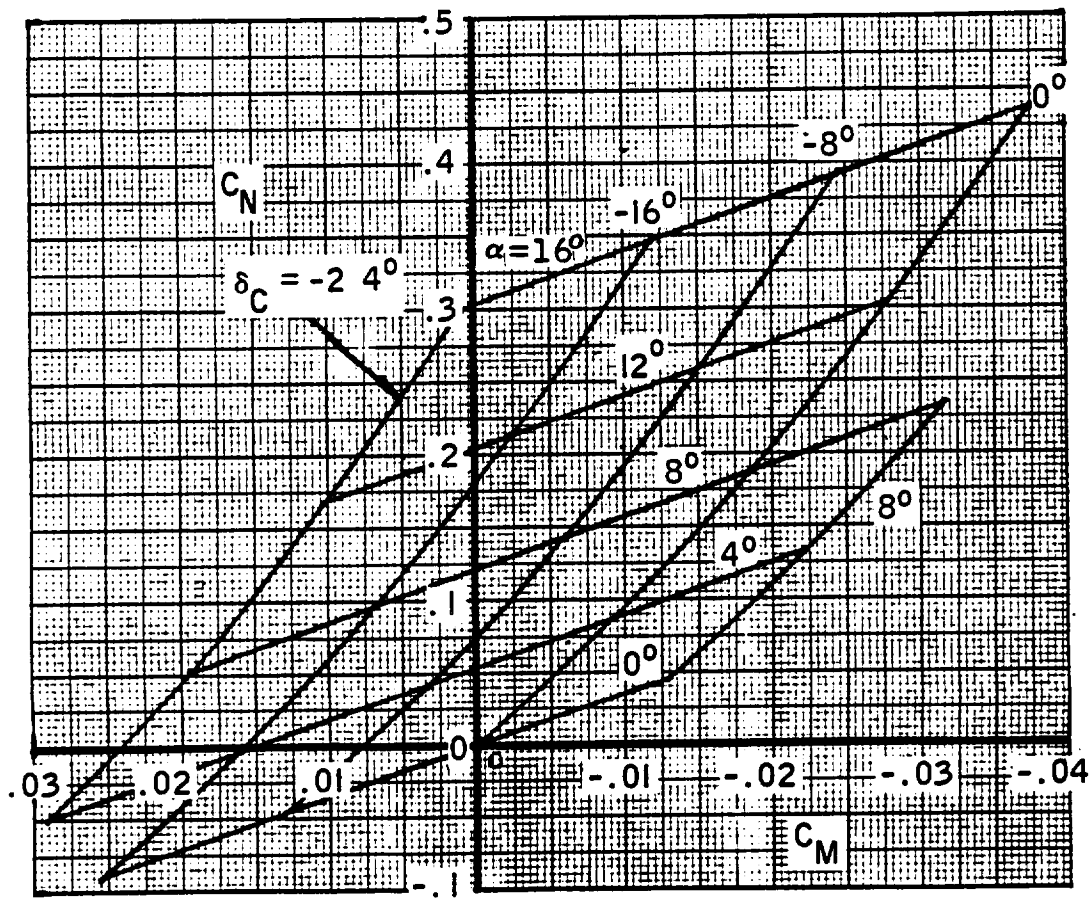

FIGURE 312. Pitching Moment Characteristics of the Class 2 Vehicle, Mach 0.6

REFERENCE AREA = FUSELAGE PLANFORM AREA
REFERENCE LENGTH = VIRTUAL FUSELAGE LENGTH
C.G. AT .64 L_{REF}

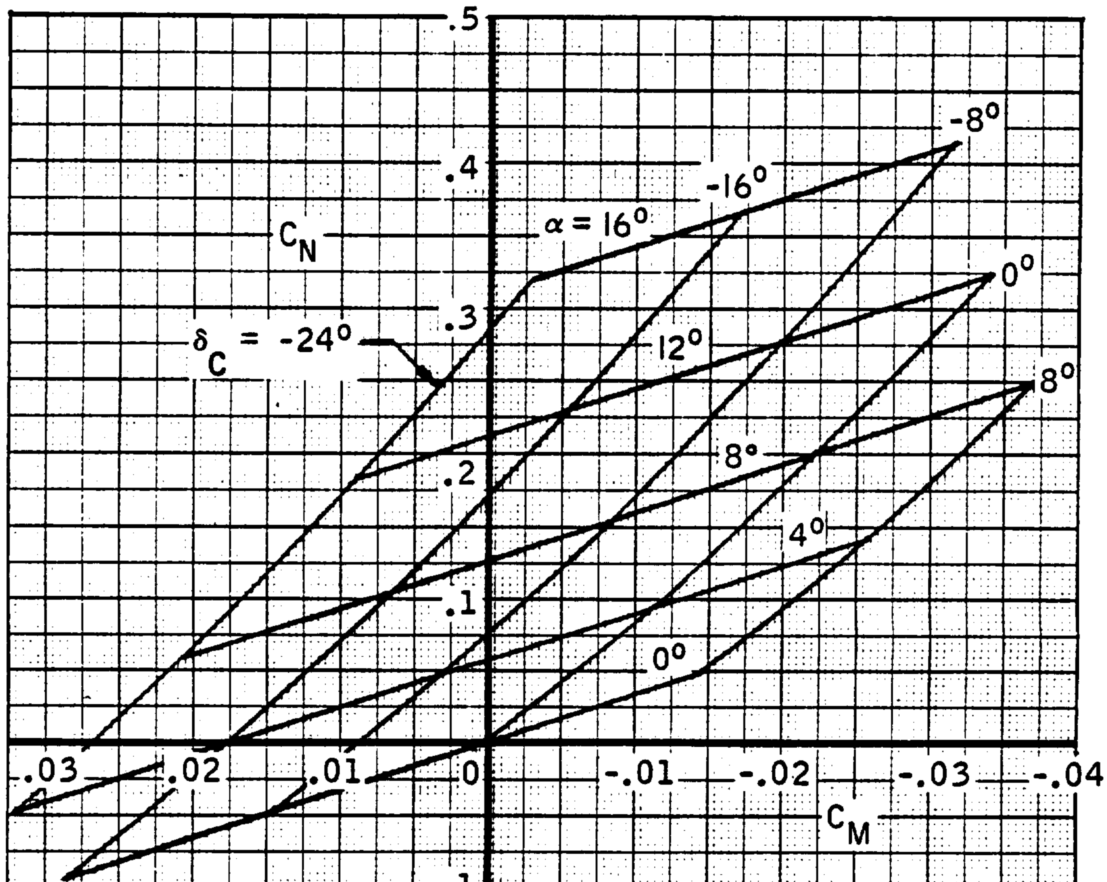

FIGURE 313. Pitching Moment Characteristics of the Class 2 Vehicle, Mach 1.5

REFERENCE AREA = FUSELAGE PLANFORM AREA
REFERENCE LENGTH = VIRTUAL FUSELAGE LENGTH
C.G. AT .64 L_{REF}

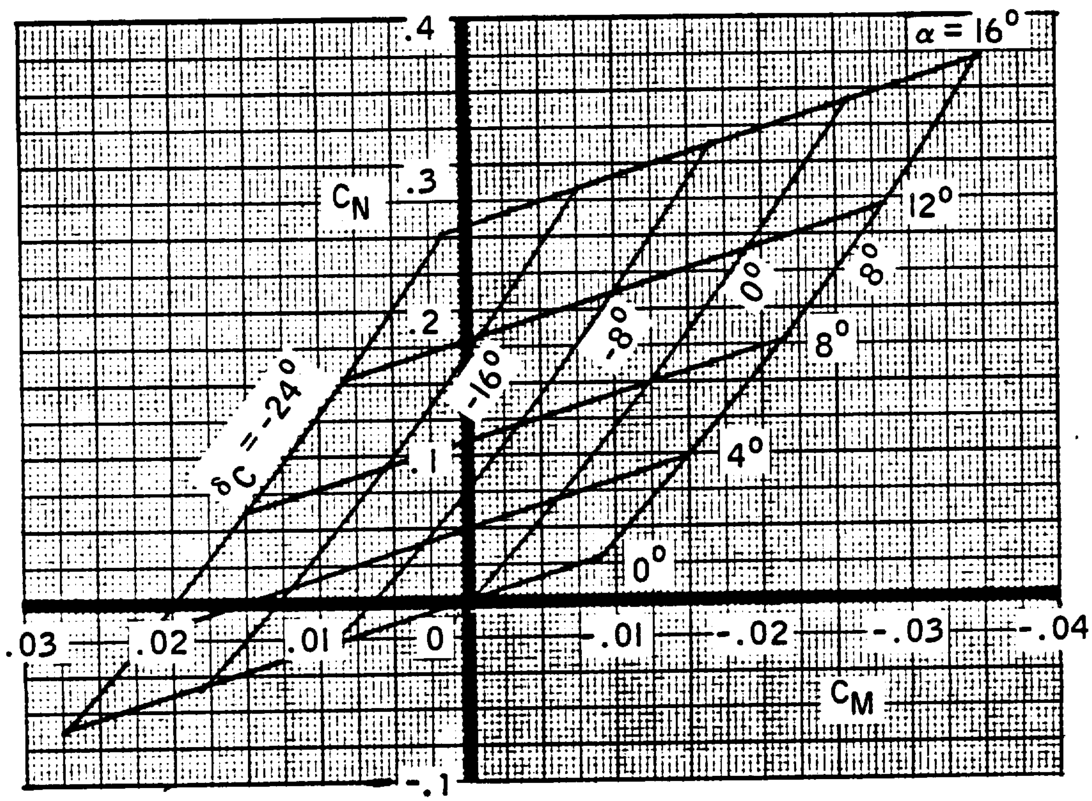

FIGURE 314. Pitching Moment Characteristics of the Class 2 Vehicle, Mach 3

REFERENCE AREA = FUSELAGE PLANFORM AREA
REFERENCE LENGTH = VIRTUAL FUSELAGE LENGTH
C.G. AT .64 L_{REF}

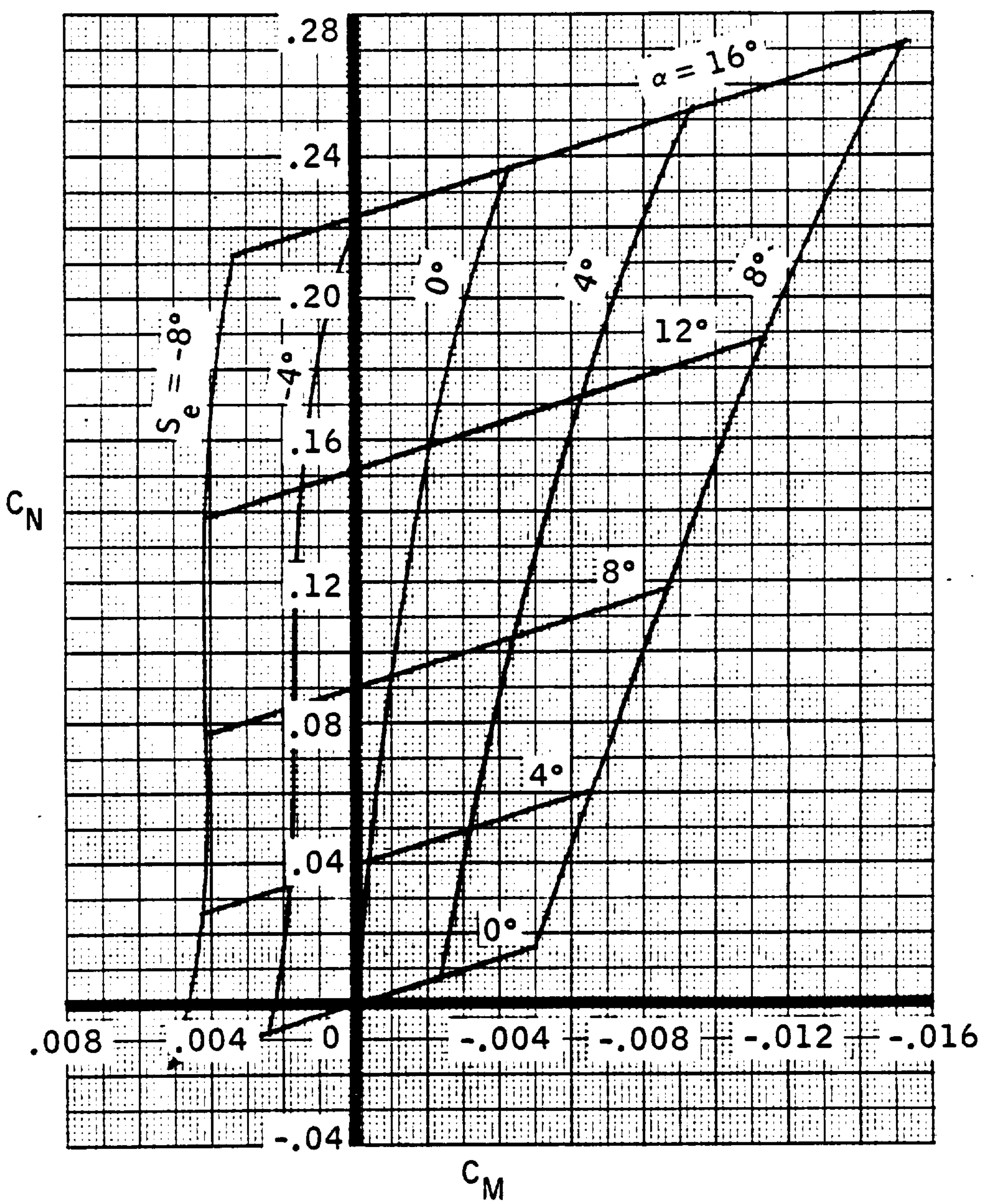

FIGURE 315. Pitching Moment Characteristics of the Class 2 Vehicle, Mach 6

REFERENCE AREA = FUSELAGE PLANFORM AREA
REFERENCE LENGTH = VIRTUAL FUSELAGE LENGTH
C.G. AT .64L_{REF}

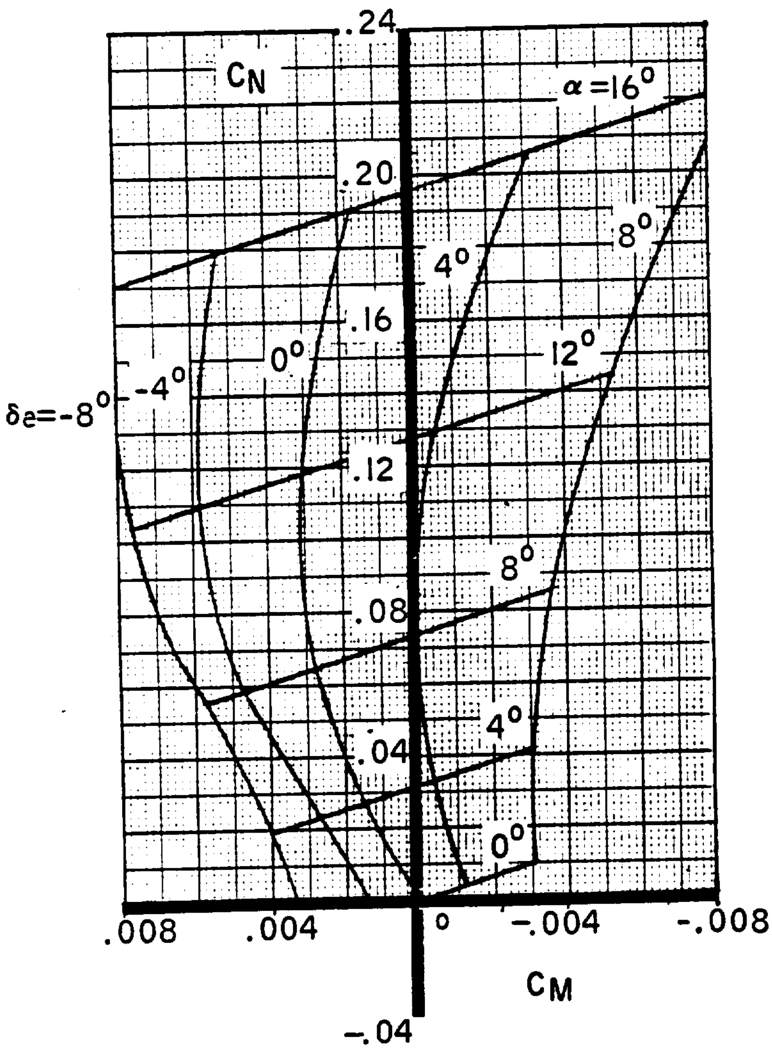

FIGURE 316. Pitching Moment Characteristics of the Class 2 Vehicle, Mach 12

4. At supersonic speeds, the 2° angle of attack schedule requires less than 3° trim deflection, with a static margin of about 10 percent.

5. For the subsonic combustion system (Mach 8, maximum) in the Mach 6 to 8 range where the angle of attack was in the 6° to 8° range, the trim requirement is less than 2° due to the decreased static stability margin (2 percent). The supersonic combustion system (Mach 12 maximum) operates at a 3° angle of attack in the Mach 6 to 8 region, and has virtually no trim penalty.

6. At Mach 12, the supersonic combustion system is slightly unstable, but controllable with augmentation, at the operational angle of attack of 2°. The control deflection required to trim is 2° indicating only a slight trim drag penalty from Mach 10 to 12.

In general, the vehicle has adequate stability and control, with minimum trim drag penalties, and it is adaptable to either the Mach 8 subsonic combustion or the Mach 12 supersonic combustion configuration.

8.6.2.2 Installed Propulsion Characteristics

8.6.2.2.1 Supercharged Ejector Ramjet (Engine No. 11)

A fundamental change in operational usage of Engine No. 11, in the Ejector and Fan Ramjet Modes (M_∞ = 0 to 3), compared with that in Class 1, was introduced in Class 2. The introduction of the supercharger (fan) to the basic Ejector Ramjet permits continued operation of the fan after the primary rockets are shut down, resulting in a supercharged, or Fan Ramjet Mode. Operation in this fashion is characterized by higher mass flows, thrust, and I_{sp} values compared with the pure Ramjet Mode, most evident in the subsonic low Mach region. The installed performance along the flight trajectory is shown in Figure 317 for both modes of operation. The installed performance includes the effects of reduced inlet spillage drag, compared to the pure Ramjet Mode. The thermal environment limits fan operation to about Mach 2.5.

The use of the vehicle base as an exhaust surface in the Subsonic Combustion Mode (M_∞ = 1 to 8) provides more nozzle expansion than in the Class 1 analysis. Further refinement of engine internal flow areas and inlet mass flow-drag characteristics results in the subsonic combustion ramjet net thrust coefficients and I_{sp} values shown in Figures 318 and 319.

The installed performance included the effects of inlet recovery and drag, engine mass flow limitations, and nozzle nonequilibrium losses along the selected trajectory.

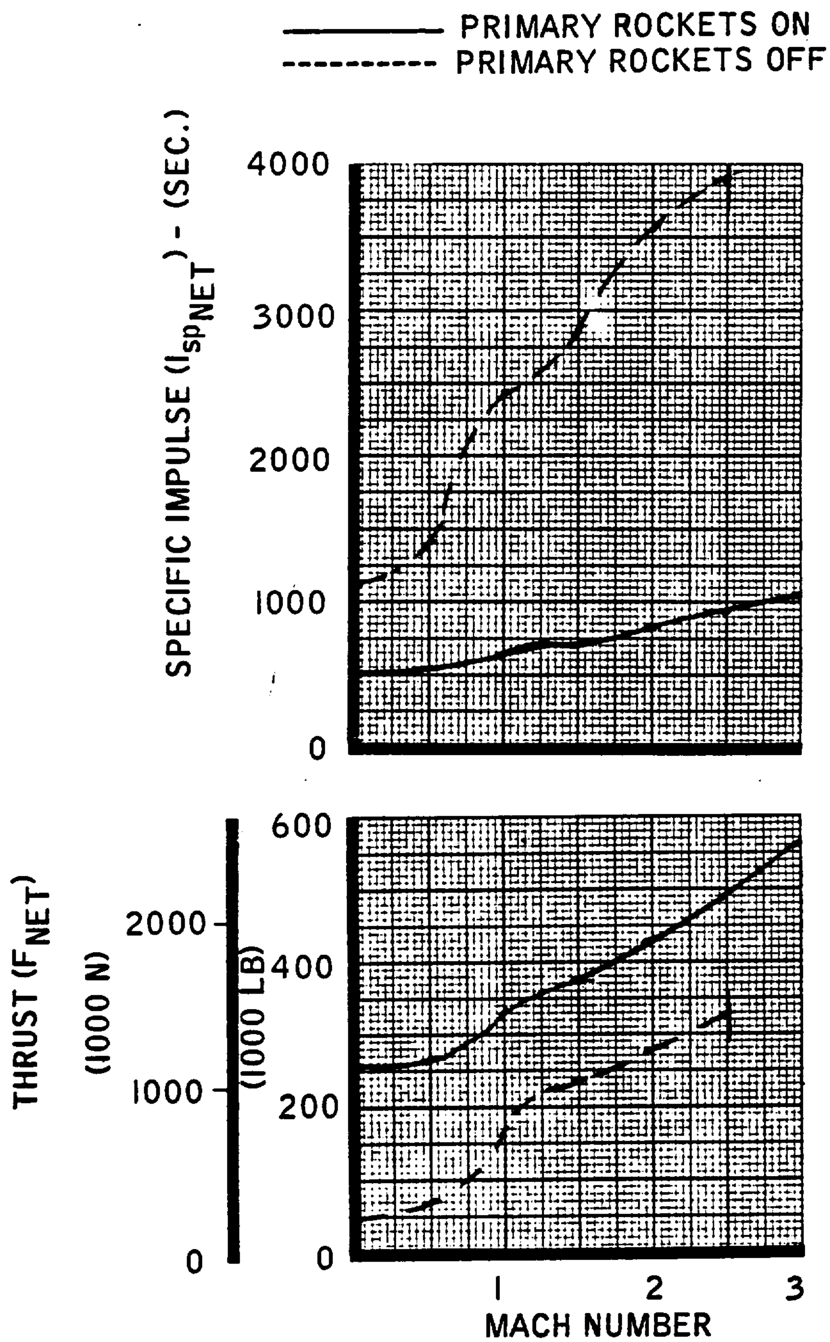

FIGURE 317. Installed Performance of the Class 2 Supercharged Ejector Ramjet (Engine No. 11), Mach 0 to 3

MACH 3.25 D.P. INLET
2-D PRESSURE FIELD
$\phi = 1.0$

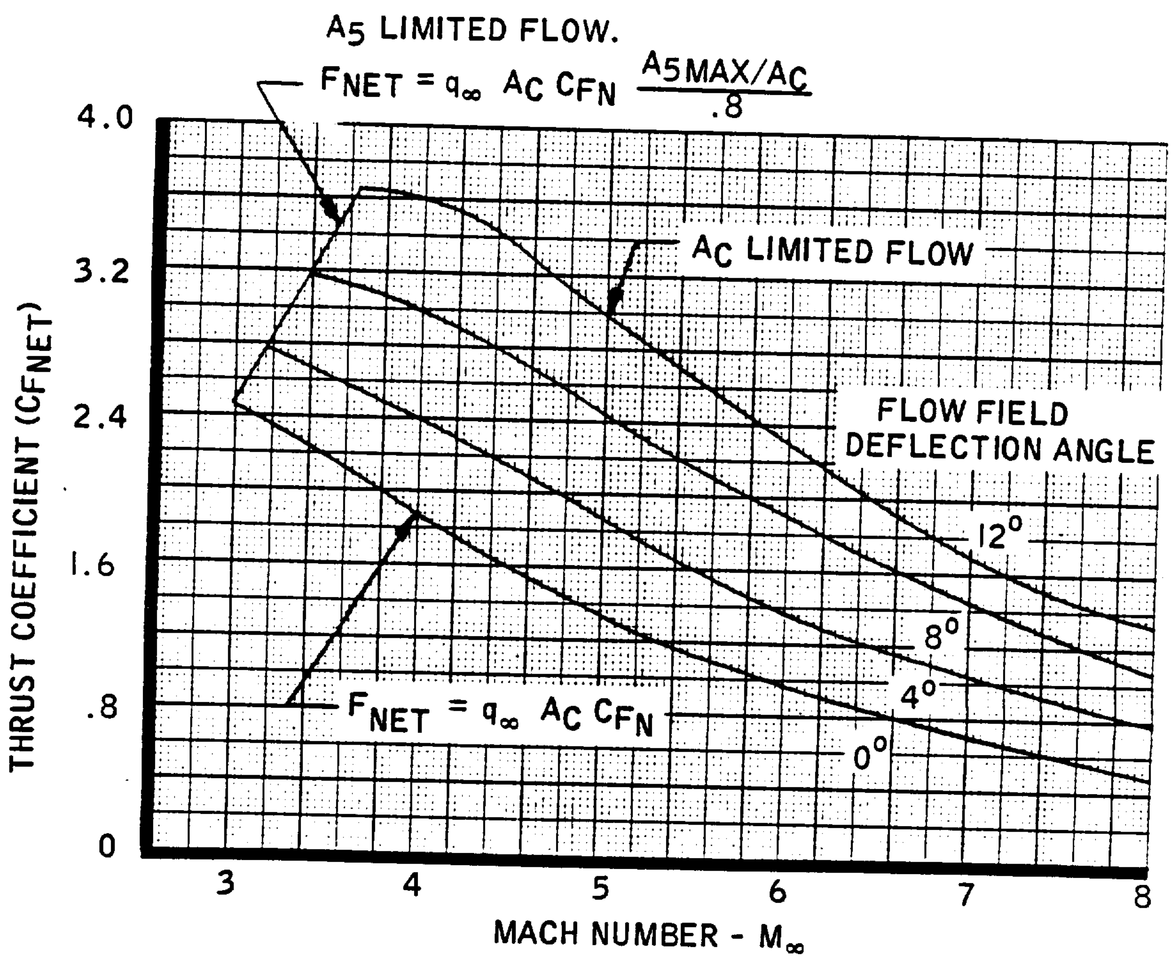

FIGURE 318. Ramjet Mode Net Thrust Coefficient of the Class 2 Supercharged Ejector Ramjet (Engine No. 11)

MACH 3.25 D.P. INLET
2-D PRESSURE FIELD
ϕ = 1.0

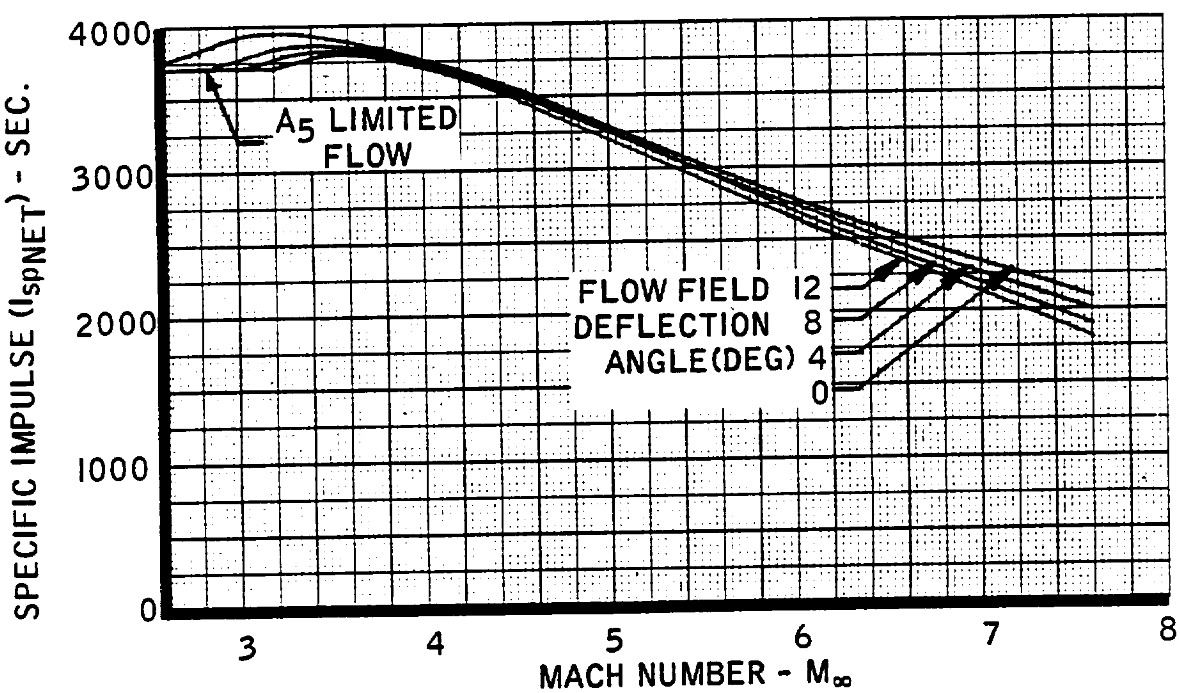

FIGURE 319. Ramjet Mode Specific Impulse of the Class 2 Supercharged Ejector Ramjet (Engine No. 11)

8.6.2.2.2 ScramLACE (Engine No. 22)

For the Class 1 study phase, the uninstalled Scramjet performance was taken from Reference 49 and is characterized as point calculated "goal type" data. Class 2 included recently published parametric data (Reference 20) which more realistically reflected the performance which can be expected for Scramjet operation.

Using the basic (uninstalled) performance supplied by Marquardt for an engine with a design mass flow ratio of 1.5:1, the installed performance was calculated and shown in Figure 320 for contraction ratios of 3, 4, and 5 along the trajectory. As in Class 1, the performance has been corrected for inlet drag. The degradation of thrust with increasing contraction ratio was due to the limiting of air flow by the engine flow areas available. The I_{sp} decrease was caused by the increase of inlet spillage drag associated with lower internal mass flows.

8.6.2.2.3 Subsonic Combustion Mode (M_∞ = 1 to 6)

The use of the vehicle base as an exhaust surface necessitated recalculation of the ramjet performance used in Class 1. Additional nozzle exit area provides higher nozzle gross thrust in the Mach 4 to 6 region. The installed thrust coefficient and I_{sp} is presented in Figure 321 as a function of the flow field deflection angle (δ) along the trajectory.

The performance presented includes the effects of decreased inlet recovery to maintain a reasonable maximum internal pressure, inlet mass flow and contraction ratio limitations, inlet drag, and nozzle nonequilibrium losses.

8.6.2.2.4 Supersonic Combustion Mode (M_∞ = 6 to 16)

The basic performance of the engine in the supersonic mode was supplied by Marquardt, and includes the sensitivity to such variables as altitude, inlet geometric versus effective contraction ratio, flow field deflection, equivalence ratio, inlet recovery, and nozzle expansion ratio.

The installed thrust coefficient and I_{sp} values are presented in Figures 322 through 329 for the conditions noted, and for geometric contraction ratios of 3, 4, 5, and 6 along 1000 and 1500 psf dynamic pressure trajectories. The performance includes the effects of inlet mass flow limitations and associated spillage drag below the inlet local design Mach number of 6.

8.6.2.3 Engine Complement Selection

In describing the number and thrust sizing of first stage engines, reference is made to the vehicle layout drawings for each of the four systems investigated in the Class 2 phase of the study.

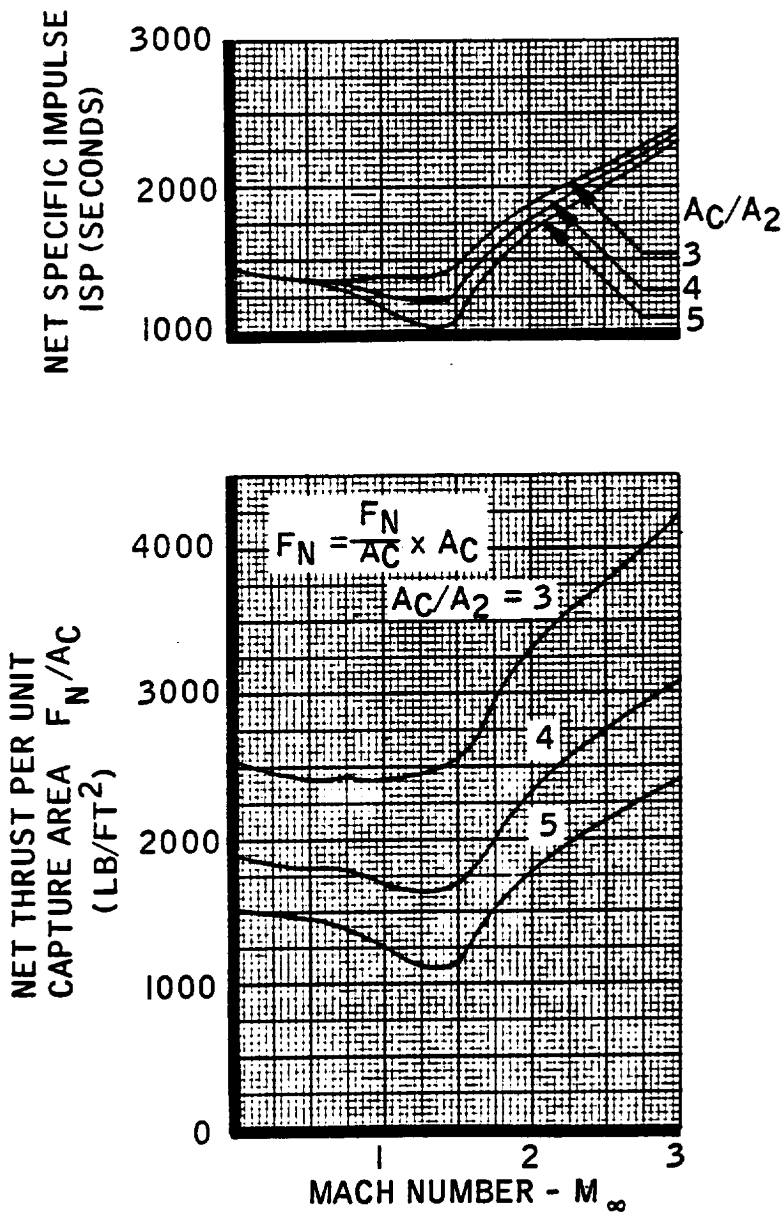

FIGURE 320. Primary Mode Performance of the Class 2 ScramLACE (Engine No. 22)

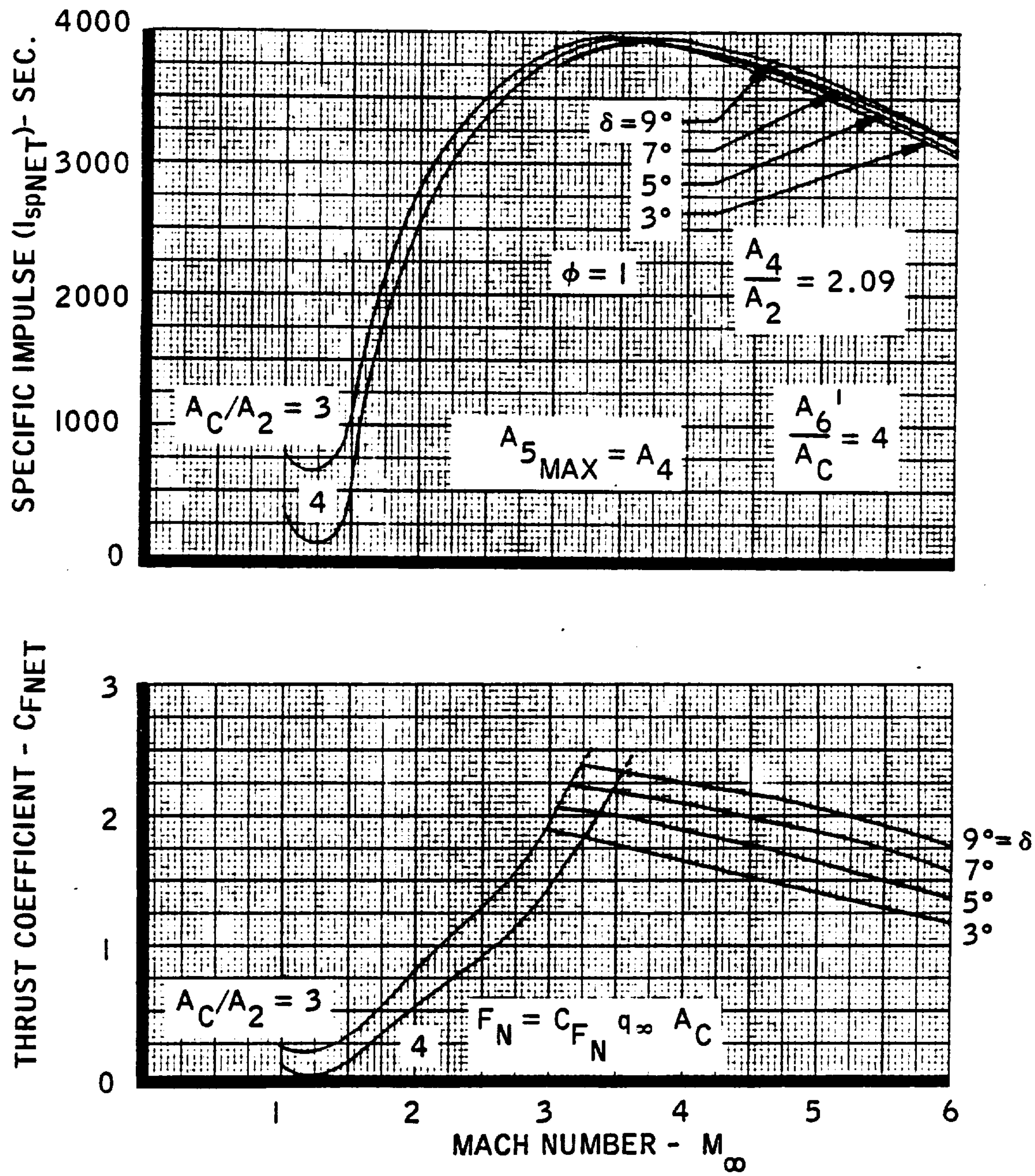

FIGURE 321. Subsonic Combustion Ramjet Performance of the Class 2 ScramLACE (Engine No. 22)

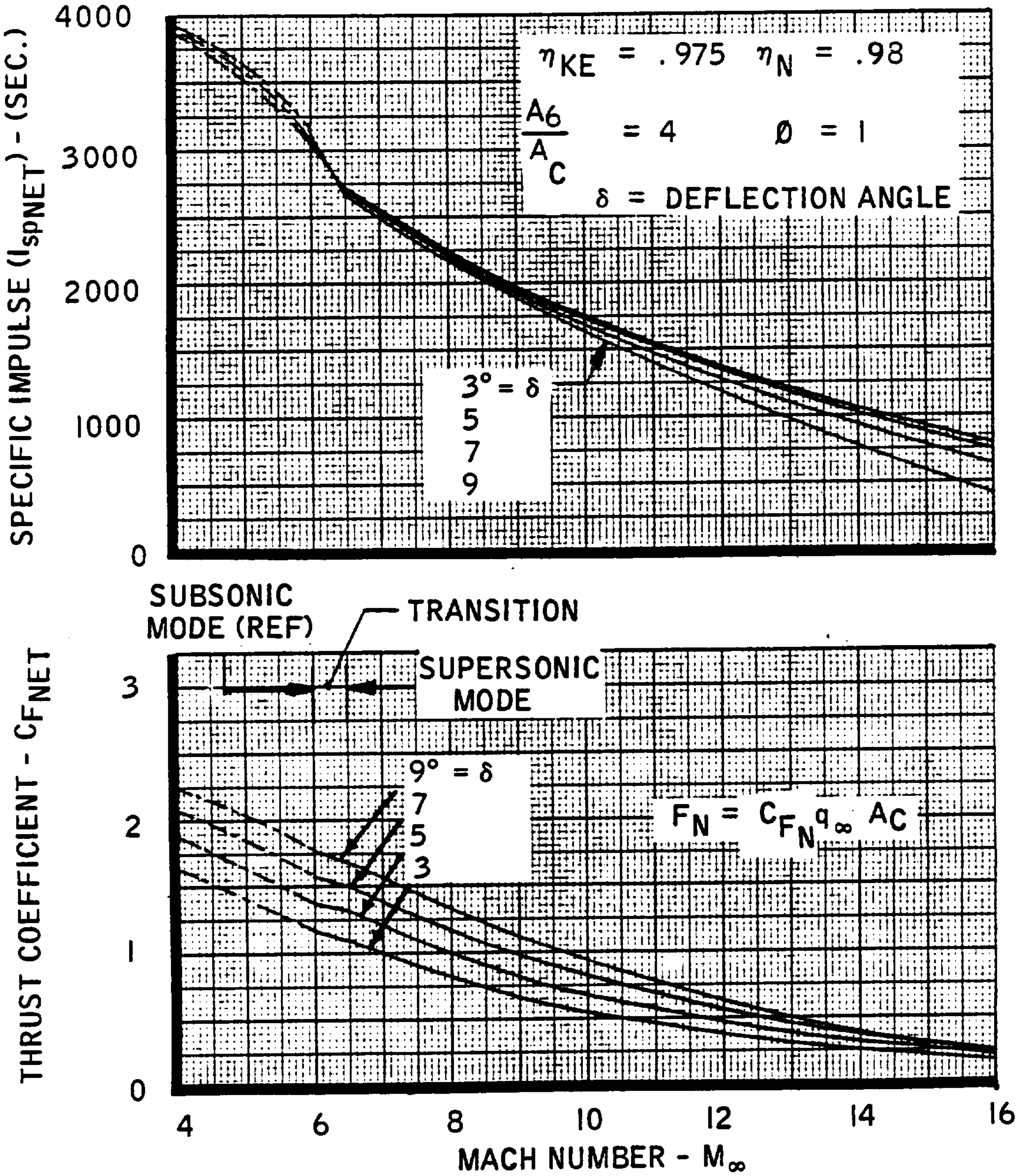

FIGURE 322. Supersonic Combustion Ramjet Performance of the Class 2 ScramLACE (Engine No. 22), $A_c/A_{2_{geom}}$ = 3, q = 1000 psf

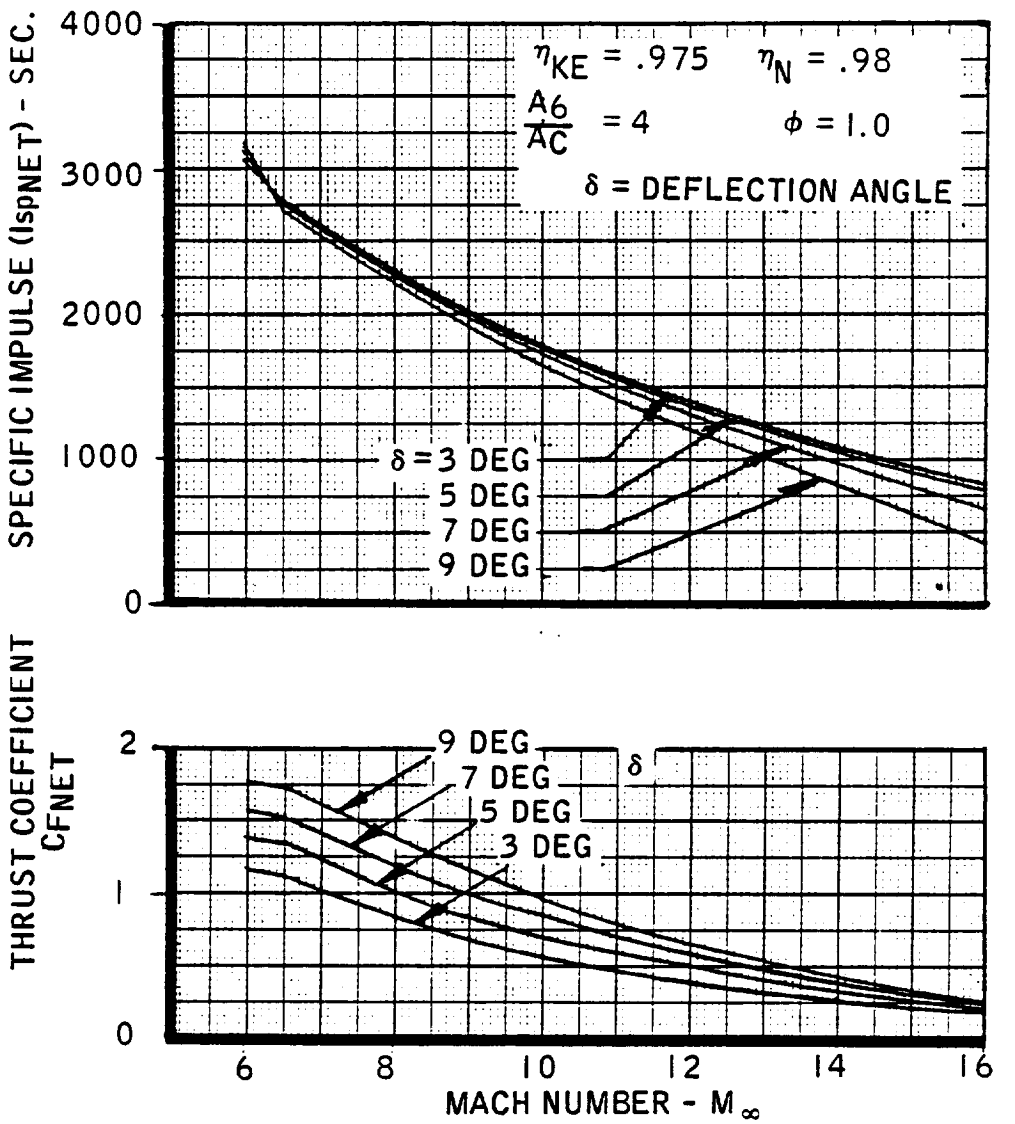

FIGURE 323. Supersonic Combustion Ramjet Performance of the Class 2 ScramLACE (Engine No. 22), $A_c/A_{2_{geom}}$ = 3, q = 1500 psf

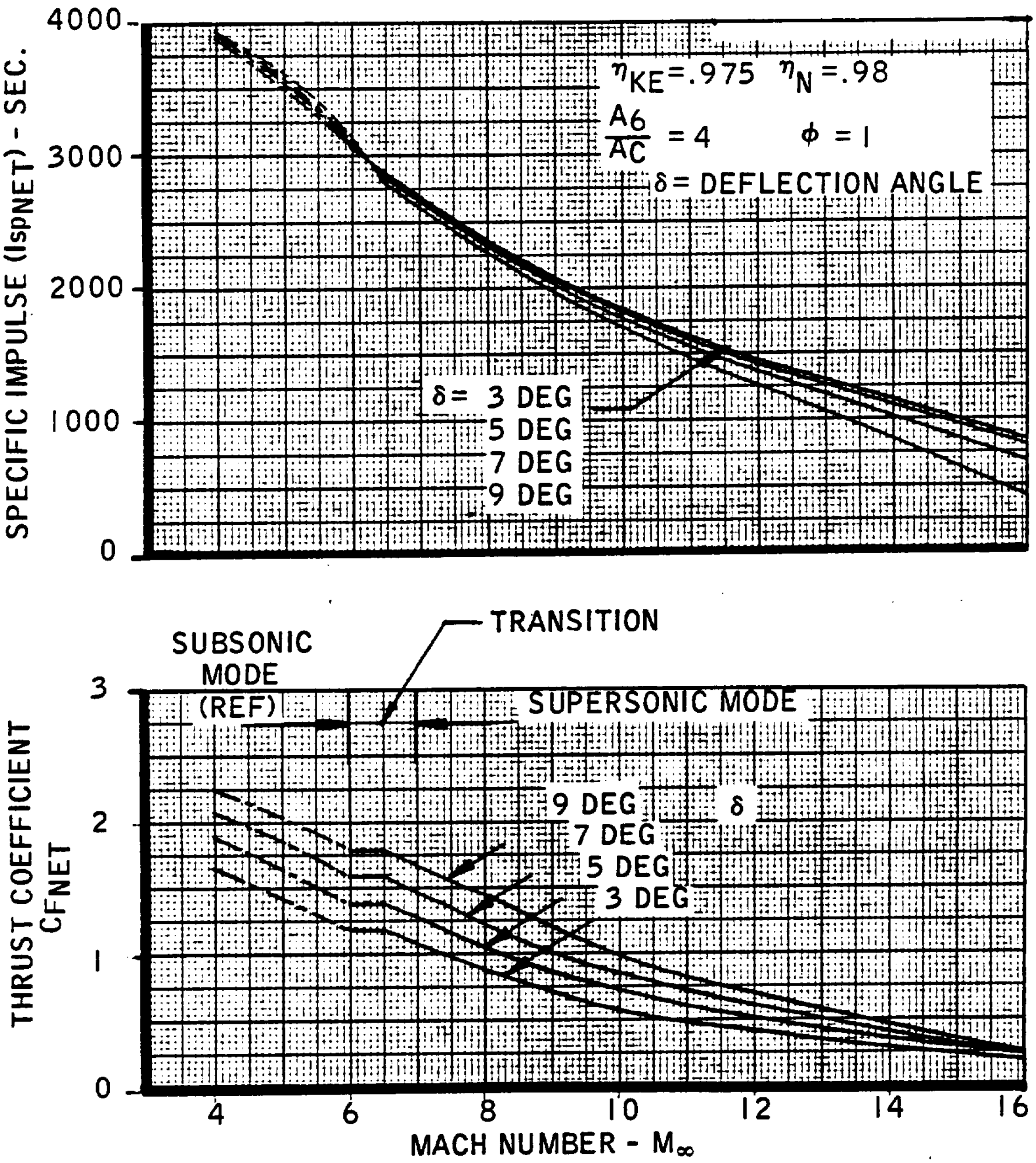

FIGURE 324. Supersonic Combustion Ramjet Performance of the Class 2 ScramLACE (Engine No. 22), $A_c/A_{2_{geom}}$ = 4, q = 1000 psf

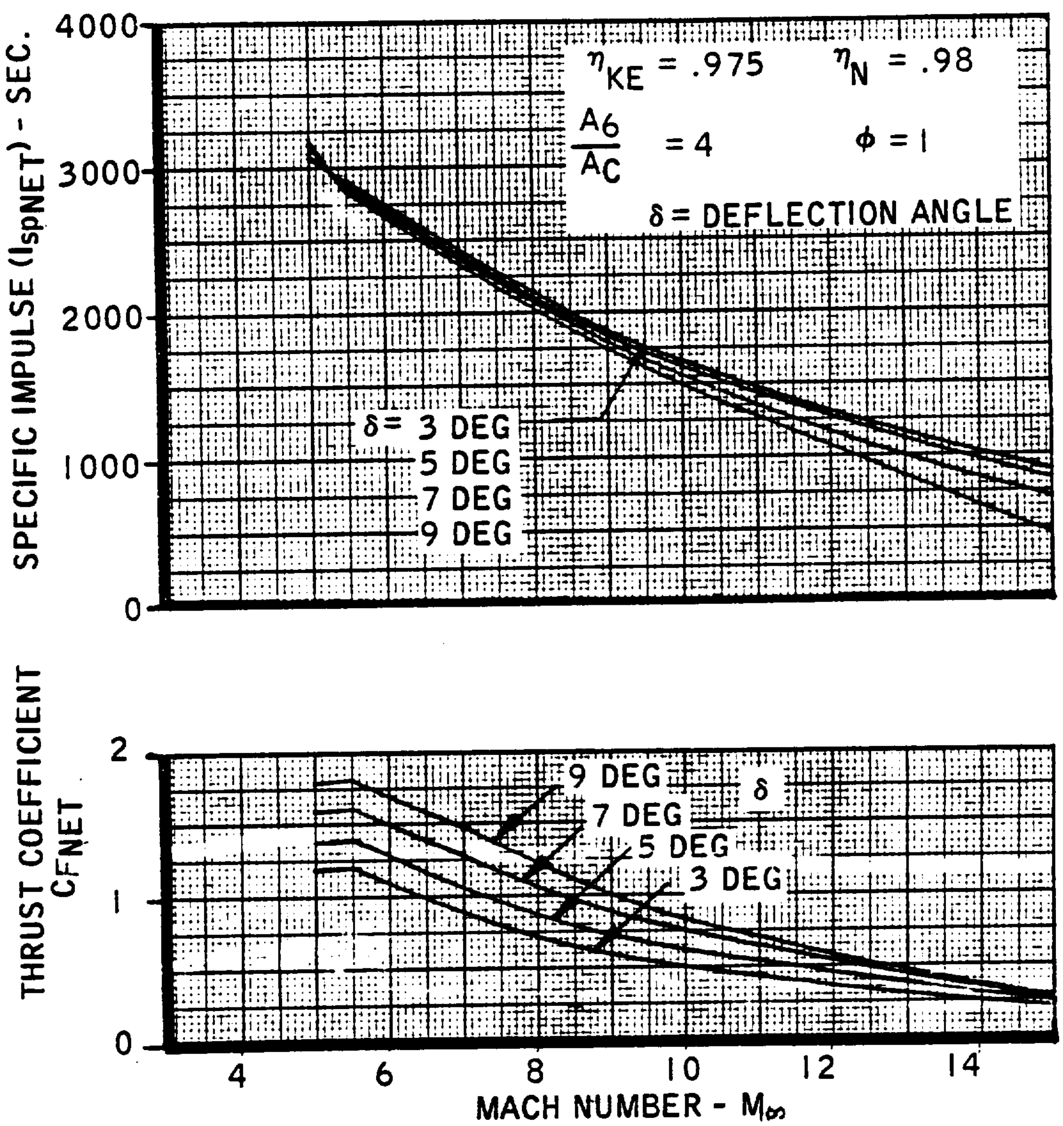

FIGURE 325. Supersonic Combustion Ramjet Performance of the Class 2 ScramLACE (Engine No. 22), $A_c/A_{2_{geom}}$ = 4, q = 1500 psf

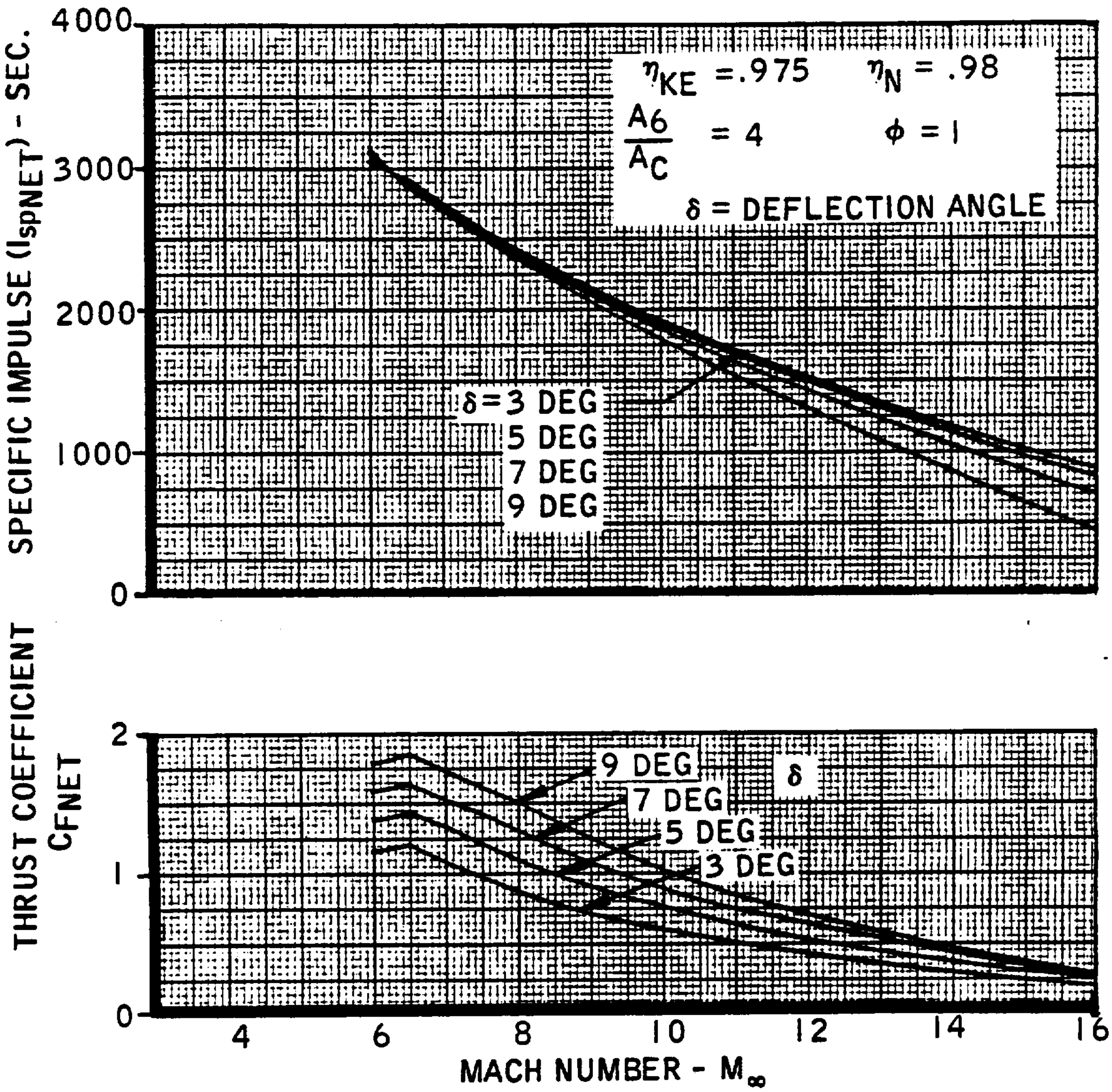

FIGURE 326. Supersonic Combustion Ramjet Performance of the Class 2 ScramLACE (Engine No. 22), $A_c/A_{2_{geom}}$ = 5, q = 1000 psf

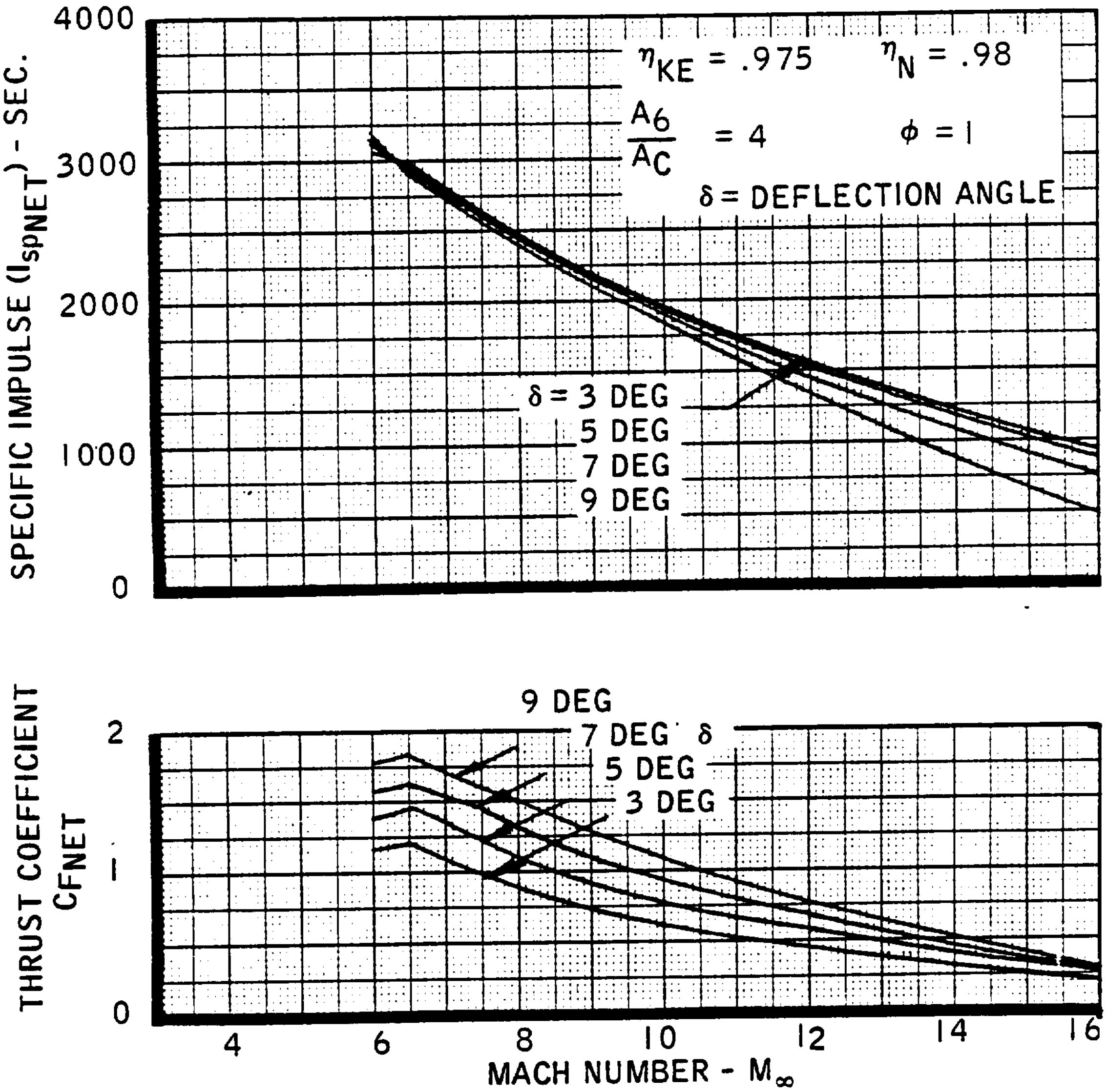

FIGURE 327. Supersonic Combustion Ramjet Performance of the Class 2 ScramLACE (Engine No. 22), $A_c/A_{2_{geom}}$ = 5, q = 1500 psf

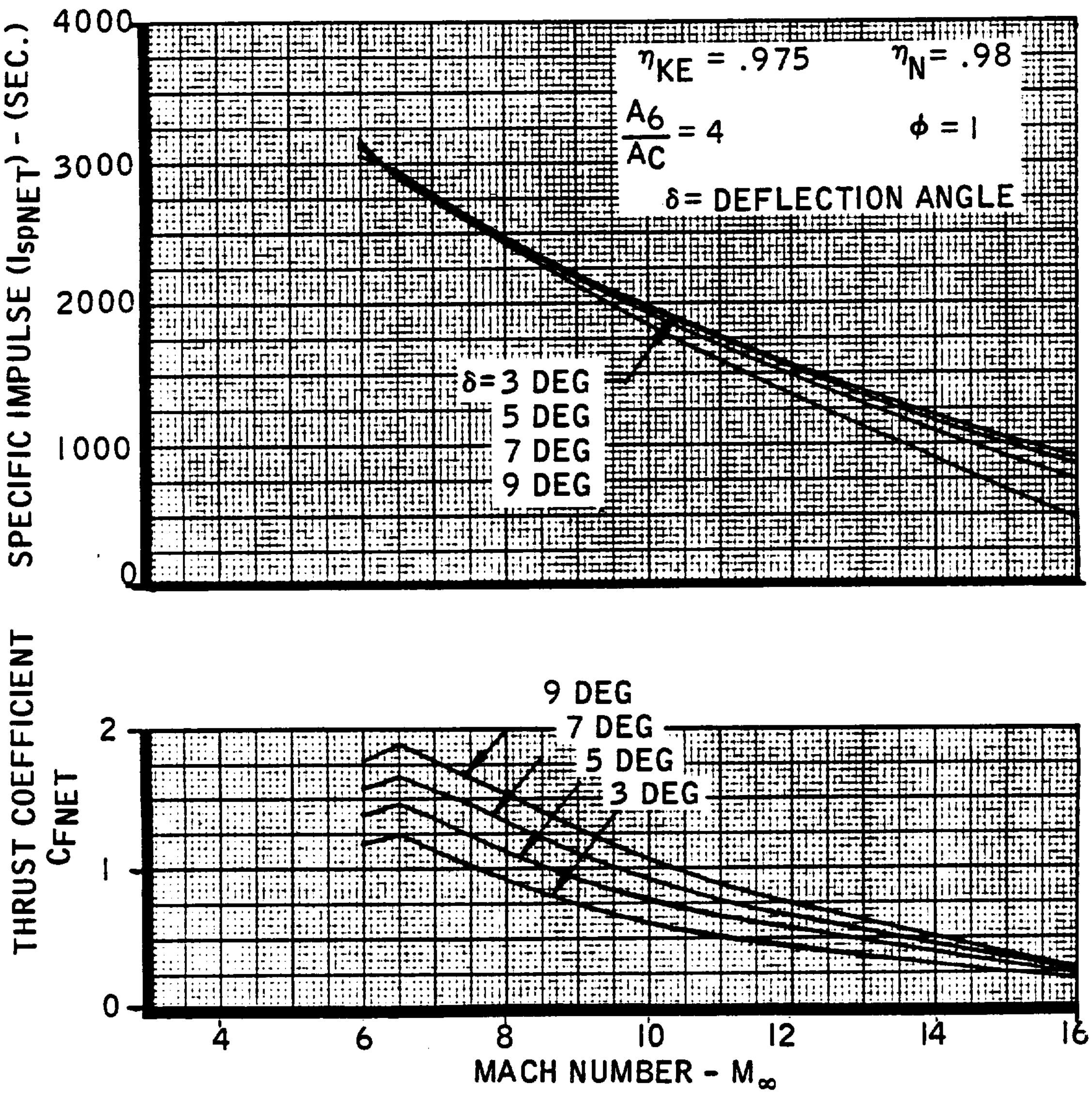

FIGURE 328. Supersonic Combustion Ramjet Performance of the Class 2 ScramLACE (Engine No. 22), $A_c/A_{2_{geom}}$ = 6, q = 1000 psf

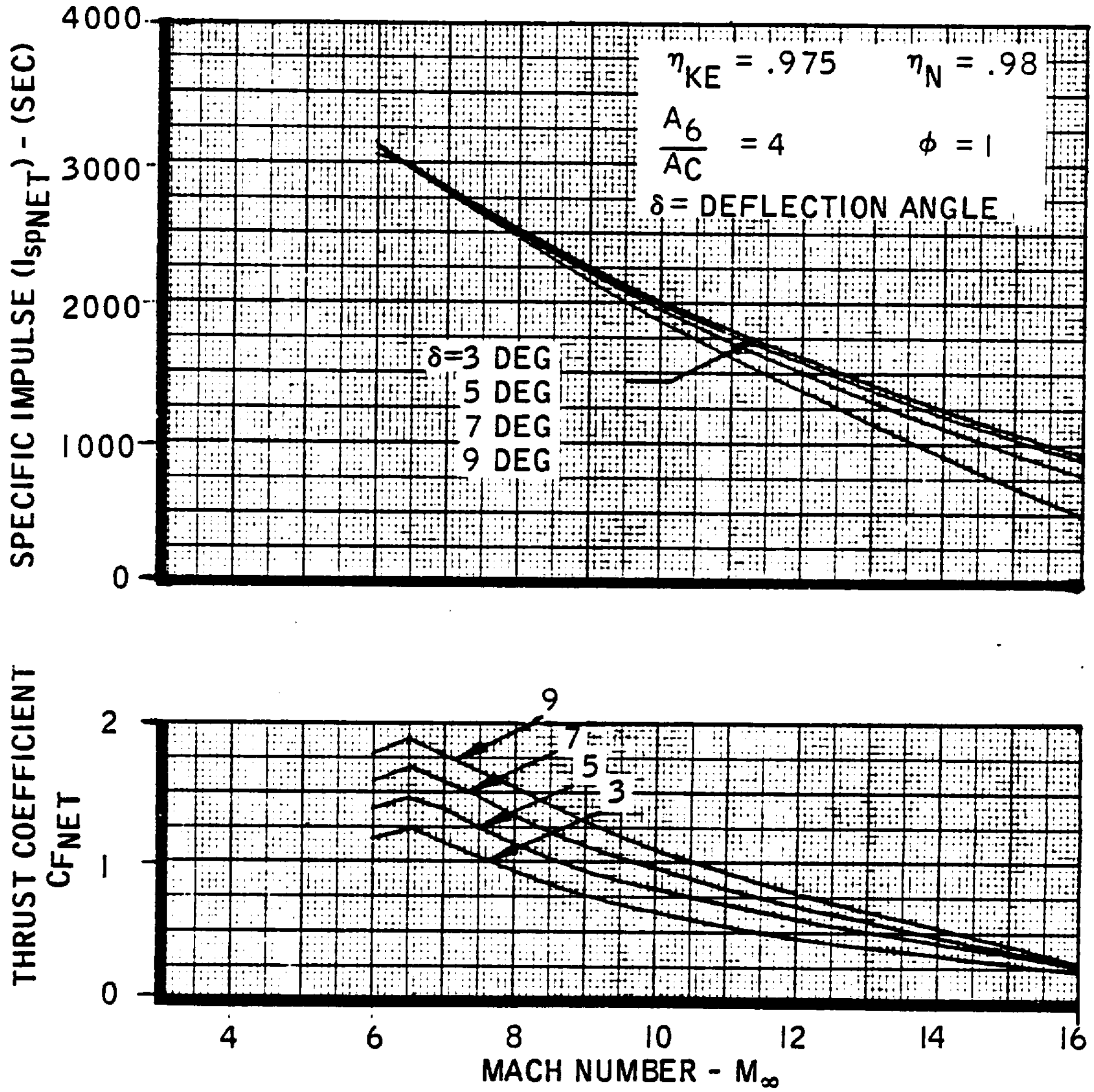

FIGURE 329. Supersonic Combustion Ramjet Performance of the Class 2 ScramLACE (Engine No. 22), $A_c/A_{2_{geom}}$ = 6, q = 1500 psf

8.6.2.3.1 Very Advanced Rocket (Engine No. 0) (Reference Figure 133)

The all-rocket systems varied in first thrust selection depending on the takeoff technique (See Section 8.6.1.6 for numerical data). A single rocket engine assembly -- varying in thrust from 1,270,000,000 to 1,500,000 lbs (sea level) depending on the takeoff mode -- is considered for the first stage system as revealed in the layout drawing.

8.6.2.3.2 Supercharged Ejector Ramjet (Engine No. 11) (Reference Figure 290)

The Supercharged Ejector Ramjet Mach 8 vehicle has a complement of five 215,000 lb sea level static thrust engines (T/W = 1.075) with a capture area of 352 sq ft integrated beneath the fuselage. The second stage gross weight is 445,054 lbs.

8.6.2.3.3 ScramLACE (Engine No. 22) (Reference Figure 291)

The ScramLACE vehicle incorporates an aft hydrogen tank due to increased hydrogen requirements and a propulsion package consisting of six engine modules of 173,000 lb thrust each (T/W = 1.038), with a 408 sq ft total capture area. A slight modification of the vehicle underside (nozzle contour) was effected for the ScramLACE vehicle to accommodate the supersonic combustion mode exhaust expansion to Mach 10. The system second stage gross weight is 397,573 lbs.

8.6.2.3.4 Turboramjet (Engine No. X) (Reference Figure 292)

A complement of seven 75,428 lb thrust engines (T/W = 0.528) is installed in the Turboramjet system (Engine No. X), with a capture area of 352 sq ft for Mach 8 operation. The first stage vehicle has no aft tank, and it carries a second stage gross weight of 474,845 lbs.

8.6.2.4 System Weight Estimates

A summary of the Class 2 system weights is presented in Table LVII.

The body/tank structure weights reflect hot aft structure surface areas of 16,431 to 4,910 sq ft (equal body wetted areas) for the subsonic and supersonic combustion systems, respectively. In the case of the ScramLACE systems, the aft body is liquid hydrogen tankage with insulation and heat shielding whereas the subsonic combustion system is empty hot structure. The body/tank structure, insulation, and heat shield weights must be summed for a comparison between subsonic and supersonic systems. The insulation and heat shield weights reflect the penalties of increased maximum airbreathing Mach number as described in Section 8.6.1.4. Note that for the ScramLACE (SL) system, both Mach 10 and Mach 12 maximum airbreathing point version weight statements are presented.

TABLE LVII

SUMMARY OF CLASS 2 FIRST STAGE SYSTEM WEIGHTS

System	M_{AB}	Engine	Inlet and Nozzle	Prop. Sys. & Thrust Structure	Equip. & Sys.	Landing Gear	Fins	Body/Tank Structure	Insulation and Heat Shield
Supercharged Ejector Ramjet	8	52,030	55,968	19,834	24,333	35,700	42,750	87,528	35,850
ScramLACE	12	57,749	63,148	13,296	28,561	35,700	48,600	80,352	83,000
ScramLACE	10	54,101	59,160	12,456	25,582	35,700	44,200	64,750	71,800
Turboramjet	8	61,040	55,264	8,052	23,708	35,700	42,750	86,780	35,850

System	W_{Dry}	W_{Prop} Cruise (Less Resid)	W_{Prop} Ldg (Less Resid)	W_{bo} (Incl Resid Cruise, Ldg)	W_{Prop} Boost	W_1
Supercharged Ejector Ramjet	353,993	5,861	1,153	366,290	188,656	554,946
ScramLACE	410,406	12,686	6,457	437,458	273,800	711,258
ScramLACE	367,749	5,587	5,771	385,277	217,150	602,427
Turboramjet	349,144	9,702	2,637	366,110	159,045	525,155

8.6.2.5 System Ascent Performance

This section presents the takeoff to staging pull-up ascent phase results for the three airbreathing mode systems (Engines Nos. 11, 22, and X). The rocket system (Engine No. 0) is separately described in Section 8.6.2.8.

8.6.2.5.1 Ascent Performance - Supercharged Ejector Ramjet (Engine No. 11)

Figure 330 shows the flight path and the corresponding dynamic pressure history for the Supercharged Ejector Ramjet system. Figure 331 indicates the finalized Supercharged Ejector Ramjet system weight, thrust, drag, and specific impulse characteristics during the airbreathing boost to Mach 8 and Figure 332 shows the accumulated time and the boost displacement distance.

The Class 2 Supercharged Ejector Ramjet differed considerably from its Class 1 counterpart due to the introduction of the Fan Ramjet mode (primary rockets inoperative, full fan and afterburner operation). Figure 333 presents effective specific impulse $[I_{sp}\ (1 - \text{Drag/Thrust})]$ as a function of Mach number for the three modes of operation: (1) Ejector mode (including fan supercharging), (2) Fan Ramjet, and (3) Ramjet, for various complements of the basic 250,000 lb thrust engine. Figure 333 indicates the dominance of the Fan Ramjet mode. While the effective impulse curves for the selected engine complement (4.3 engines) actually cross below Mach 0.4, the low thrusts available with the Fan Ramjet operation are marginal in accommodating the high drag at the instant of system liftoff (Mach = 0.363). The transition point from the Fan Ejector mode to the Fan Ramjet mode was established at Mach 0.4, subsequent to system liftoff and return to a moderate angle of attack. The effective impulse also indicated the desirability of extending the Fan Ramjet mode beyond Mach 2.5. However, the thermal problems associated with fan operation beyond this speed dictate transition to pure ramjet operation at this point, as defined by Marquardt. The system overall oxidizer-to-fuel ratio during the Mach 0 to 0.4 acceleration on Fan Ejector mode operation was 6.86:1.

On the basis of the described operational mode scheduling, the basic Supercharged Ejector Ramjet engine complement was sized by summing the propellant, engine, and tankage weight to Mach 3.0 (as discussed in Section 6.5.1.3.3). Figure 334 presents this parameter as a function of the complement of 250,000 lb thrust engines. As indicated, the parameter was a minimum at 4.3 engines, or a sea level static thrust loading of 1.075.

Sizing of the vehicle capture area was accomplished by assessing the total weight of fuel, inlet, and tankage from Mach 3 to 8. The minimum value of this parameter (indicated by Figure 335) occurs for an inlet performance capture area of 310 sq ft.

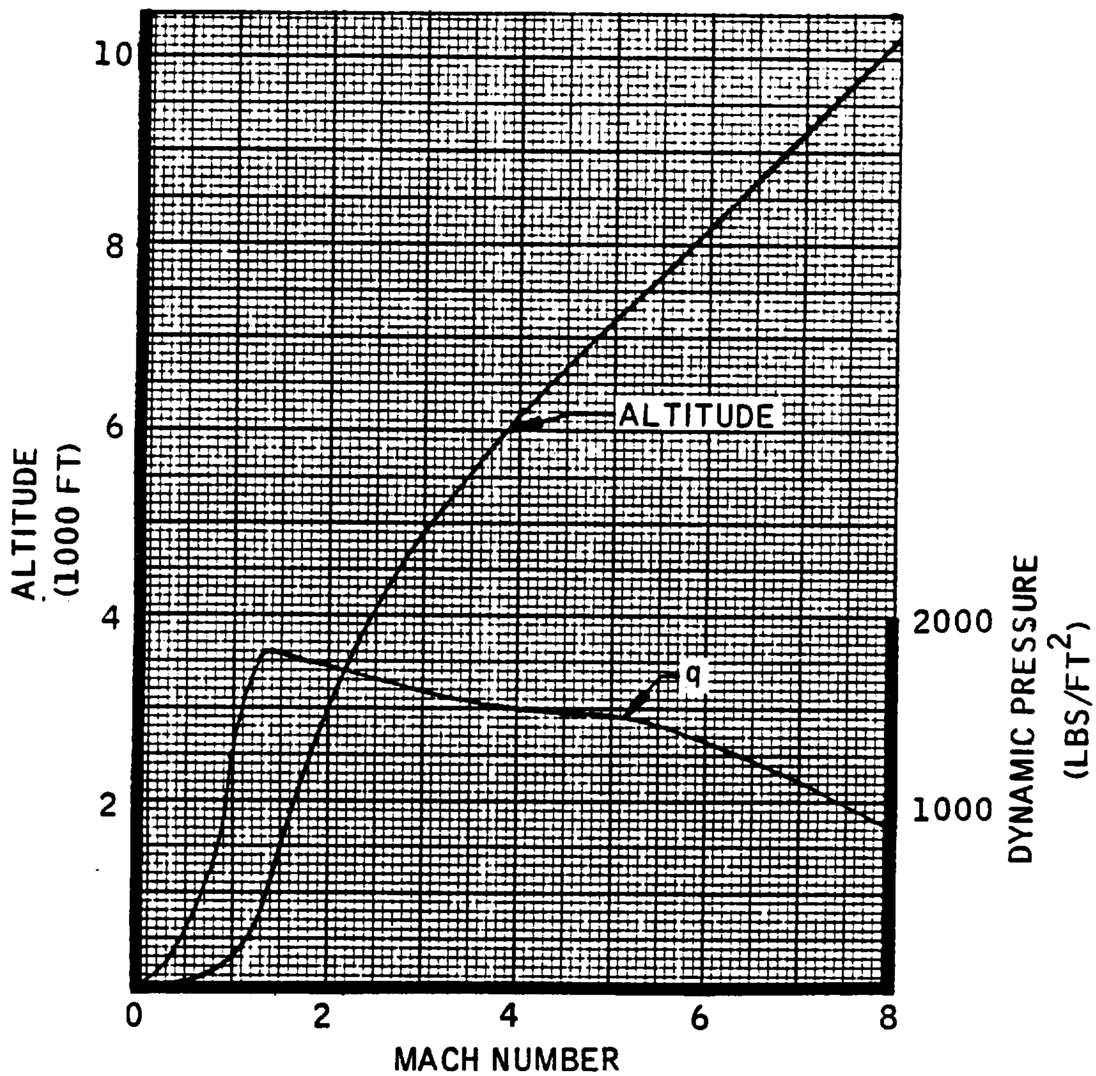

FIGURE 330. Ascent Path and Dynamic Pressure History for the Class 2 Supercharged Ejector Ramjet (Engine No. 11)

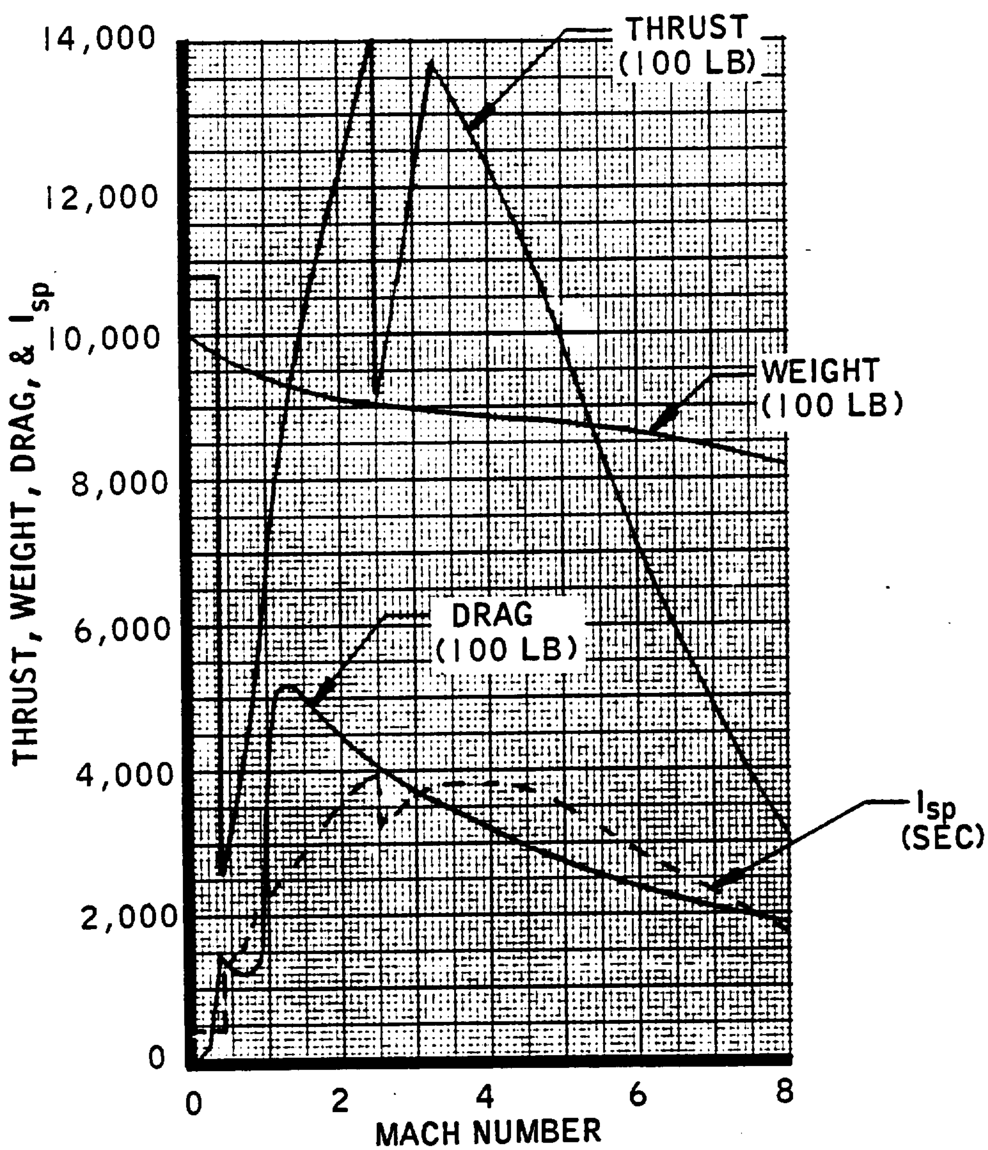

FIGURE 331. Ascent Performance Characteristics of the Class 2 Supercharged Ejector Ramjet (Engine No. 11)

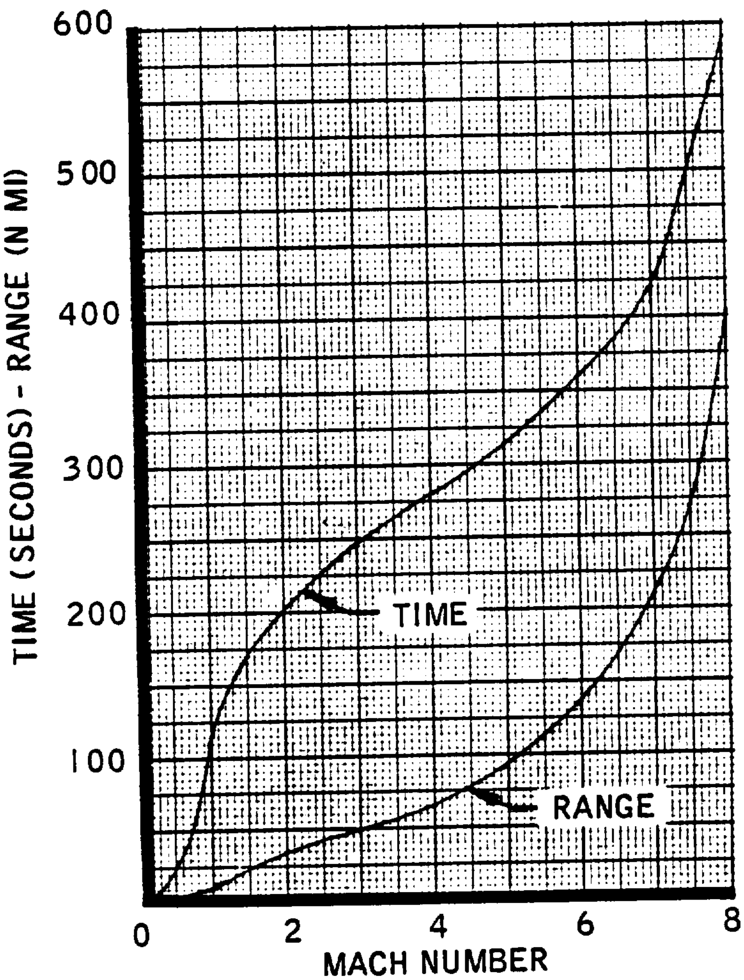

FIGURE 332. Ascent Time and Range Displacement for the Class 2 Supercharged Ejector Ramjet (Engine No. 11)

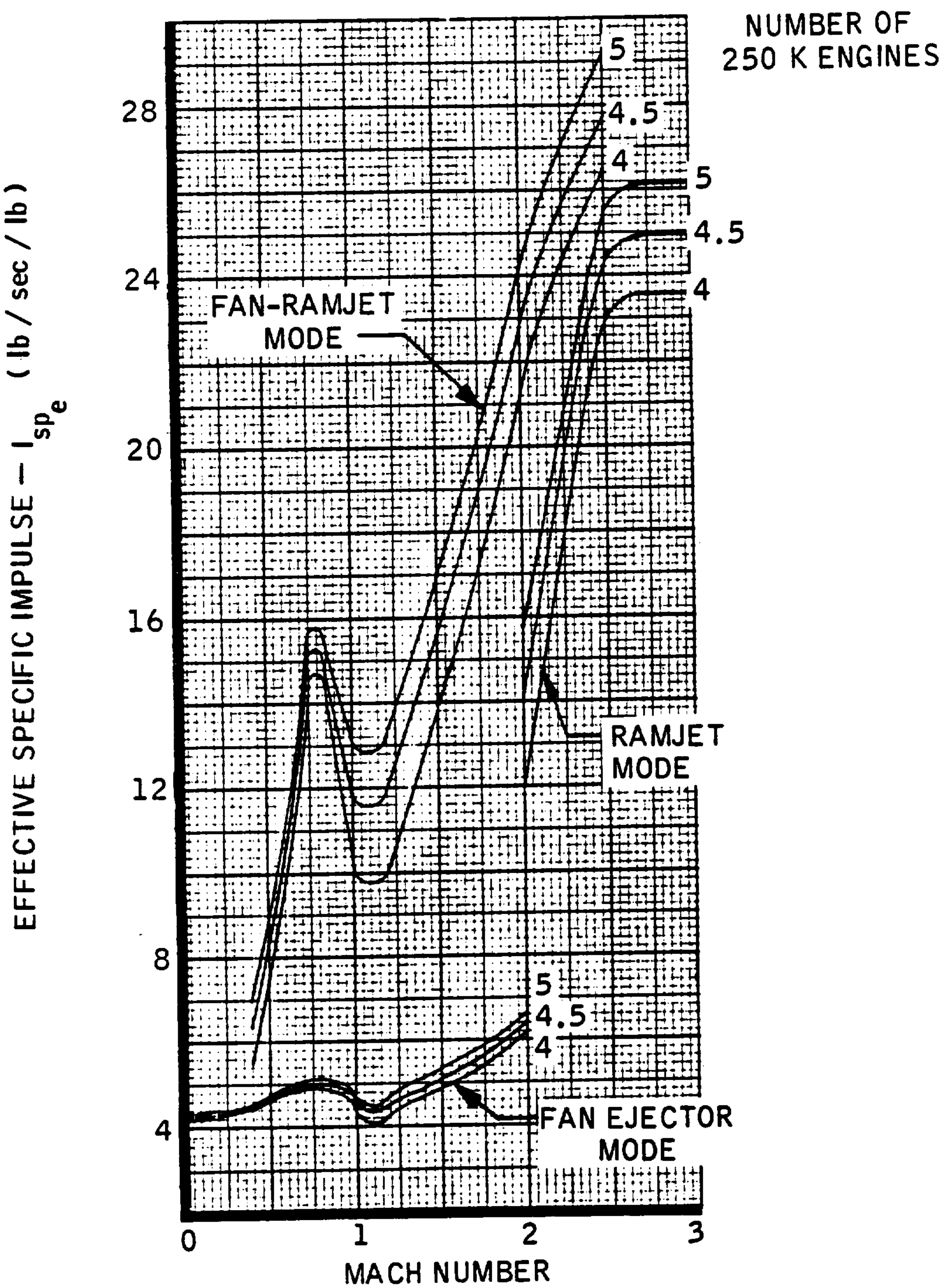

FIGURE 333. Variation of Effective Specific Impulse with Mach Number for the Class 2 Supercharged Ejector Ramjet (Engine No. 11)

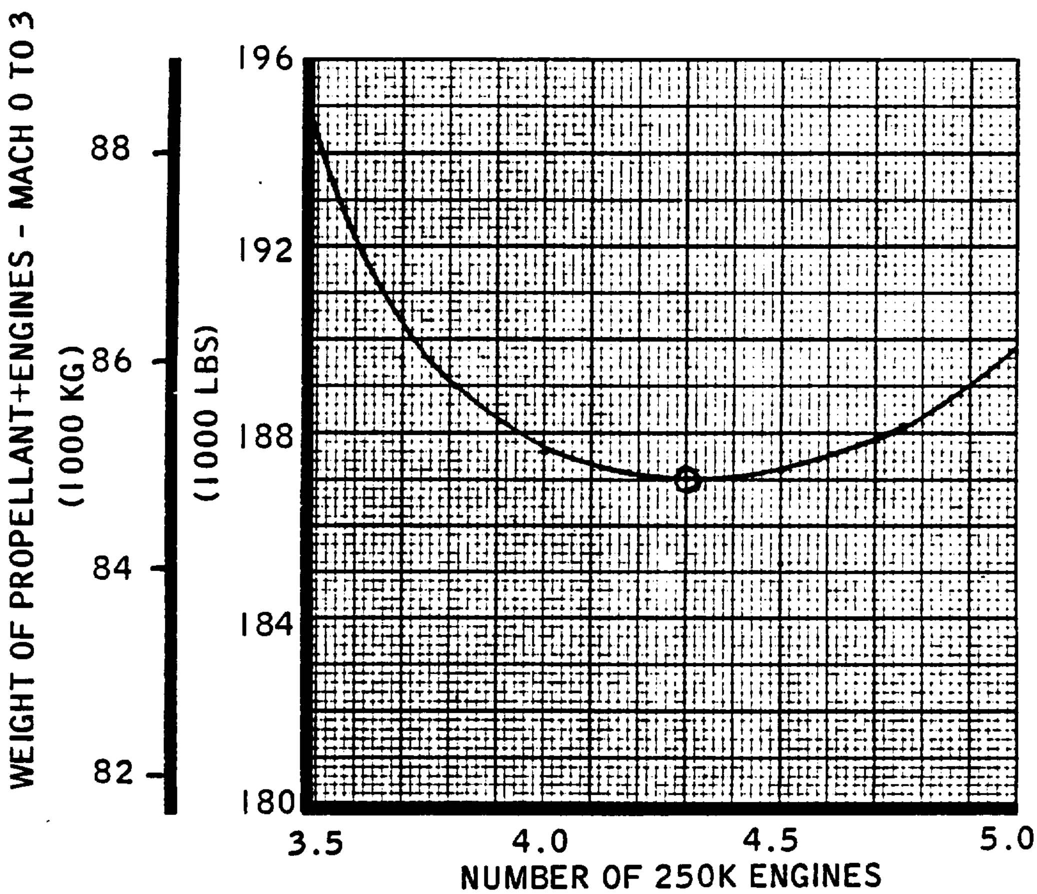

FIGURE 334. Engine Complement Sizing for the Class 2 Supercharged Ejector Ramjet (Engine No. 11)

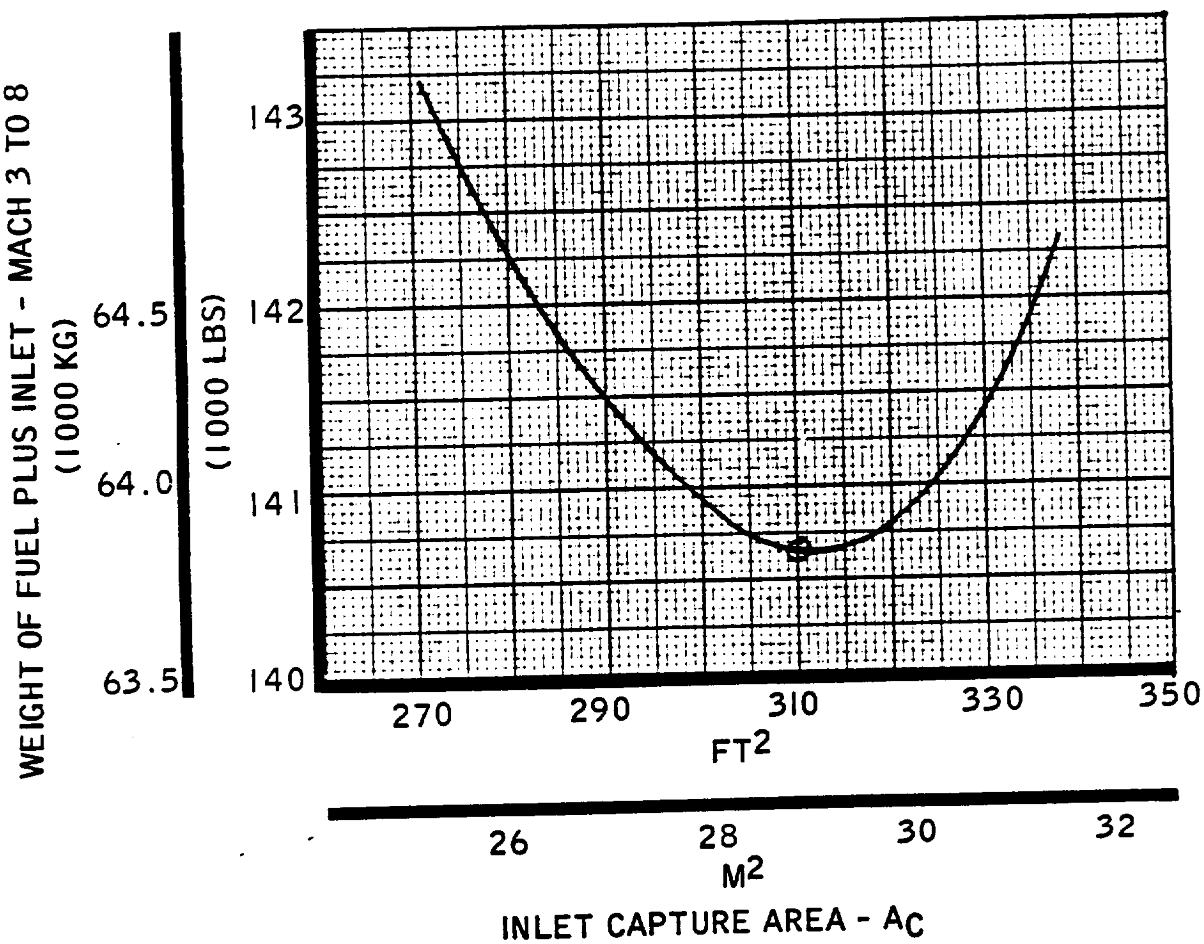

FIGURE 335. Inlet Capture Area Sizing for the Class 2 Supercharged Ejector Ramjet (Engine No. 11)

The Supercharged Ejector Ramjet system was evaluated with respect to maximum airbreathing boost Mach numbers from 5 to 10. No alteration of the selected thrust loading (1.075) was made, since only the vehicle capture area was affected by the terminal Mach number variation (Ramjet Mode). The flight paths were altered (Figure 336) so that a dynamic pressure level of 850 psf exists for all systems at the maximum airbreathing boost Mach number to insure equitable pull-up performance. The maximum inlet diffuser pressure encountered by each system governs the inlet weight per unit capture area.

The system drag, thrust coefficient, and specific impulse characteristics are presented in Figure 337 for the various maximum Mach number Supercharged Ejector Ramjet systems. Using the baseline Supercharged Ejector Ramjet system weight at Mach 4 as a base, the mass fractions of the various systems were determined as a function of inlet capture area. The weight of fuel plus inlet (based on maximum internal pressure) plus tankage then described the maximum performance capture area for each system. Figure 338 presents the system mass fractions and the inlet sizing parameter as a function of capture area. The circled points represent the selected capture areas for each system.

System weight as a function of the maximum airbreathing Mach number is presented in Figure 339 for the maximum performance capture area sizing.

8.6.2.5.2 Ascent Performance - ScramLACE (Engine No. 22)

The inlet contraction ratios considered for the Class 2 ScramLACE system were 3, 4, and 5. The contraction ratio of 5 was eliminated by its excessive combined engine weight and fuel consumption required to overcome the transonic drag rise.

The flight path and dynamic pressure for the ScramLACE system are presented in Figure 340. The transition Mach numbers from the primary mode to the subsonic combustion ramjet mode at equal equivalent impulse are shown in Figure 341 for the various cowl sizes and contraction ratios.

The 1000 psf dynamic pressure path ($M_\infty = 4$ to 12) of Class 1 was evaluated initially, but due to the decrease in lift coefficient with vehicle angle of attack (C_{L_α}), excessive fuel consumption results in the Scramjet mode. The 1500 q trajectory finally selected results in more reasonable angles of attack and, consequently, lower fuel consumption.

Computer runs were made for a wide range of cowl sizes for each of the contraction ratios to determine the propellant consumption to Mach numbers of 8, 10, 12, 14, and 16. The sum of propulsion, fuel, and tankage weights is shown in Figure 342 for the various cowl sizes and Mach numbers. The increasing influence of the lower contraction ratio on the Mach 0 to 3 performance is evident for Mach 8 and 10, with the superior Scramjet performance

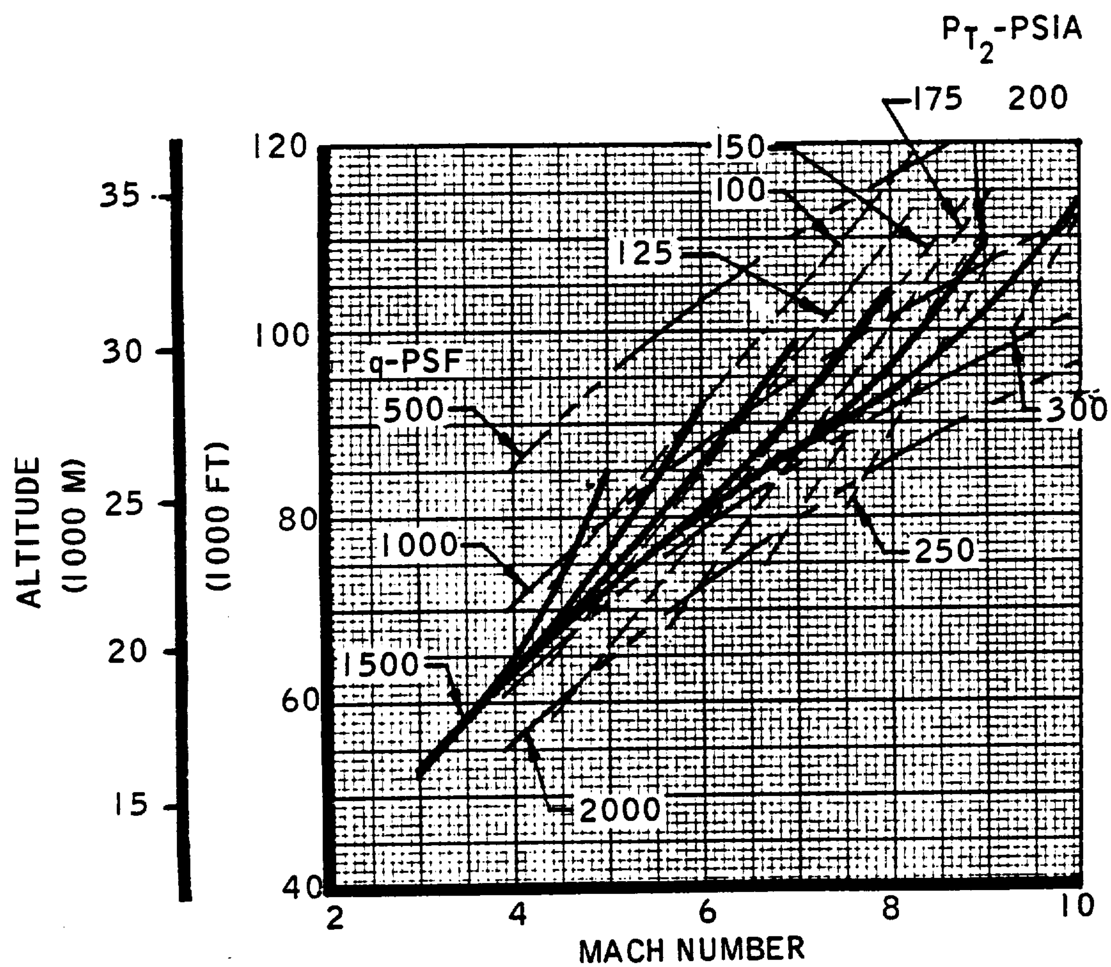

FIGURE 336. Ascent Paths for Various Airbreathing Boost Mach Number Systems for the Class 2 Supercharged Ejector Ramjet (Engine No. 11)

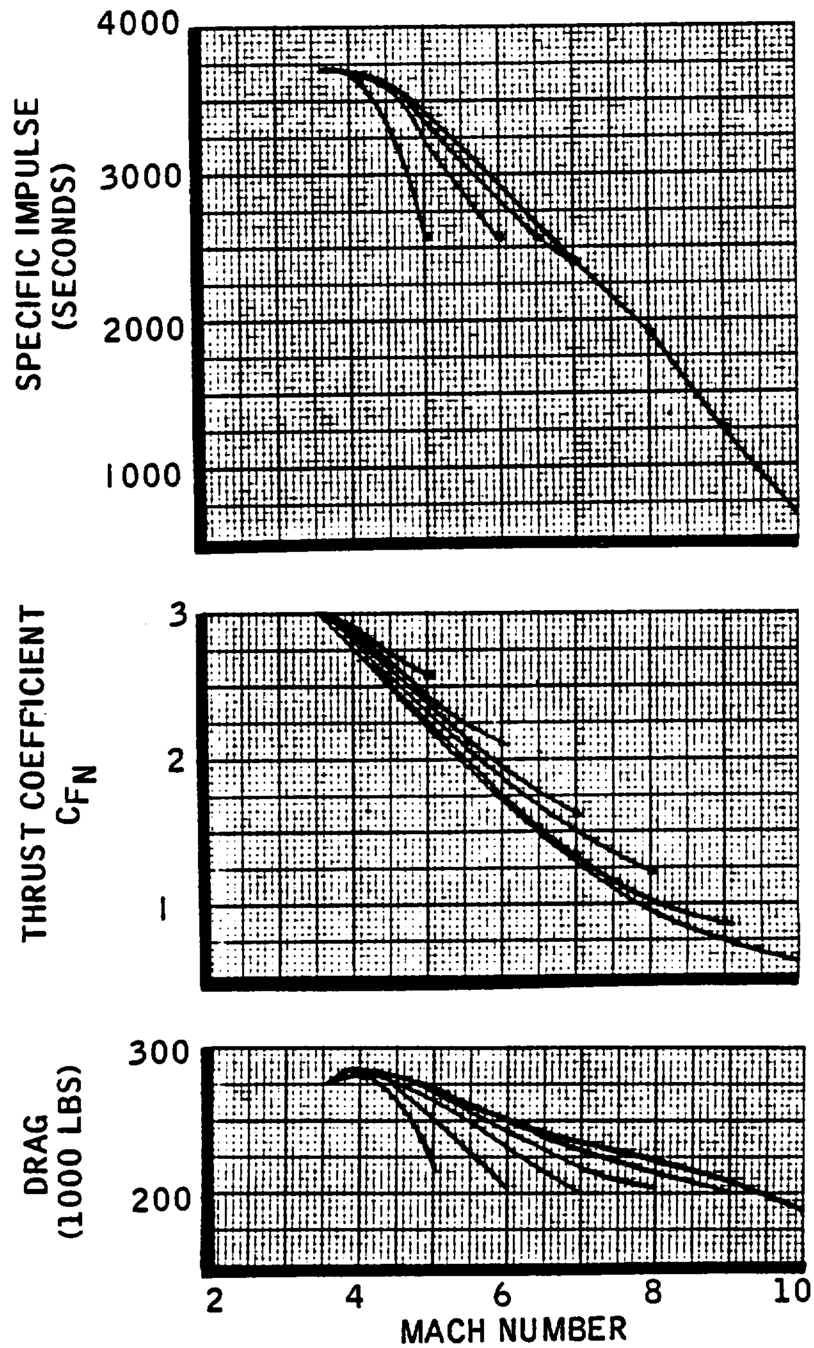

FIGURE 337. Performance Parameters for Various Airbreathing Boost Mach Numbers for the Class 2 Supercharged Ejector Ramjet (Engine No. 11)

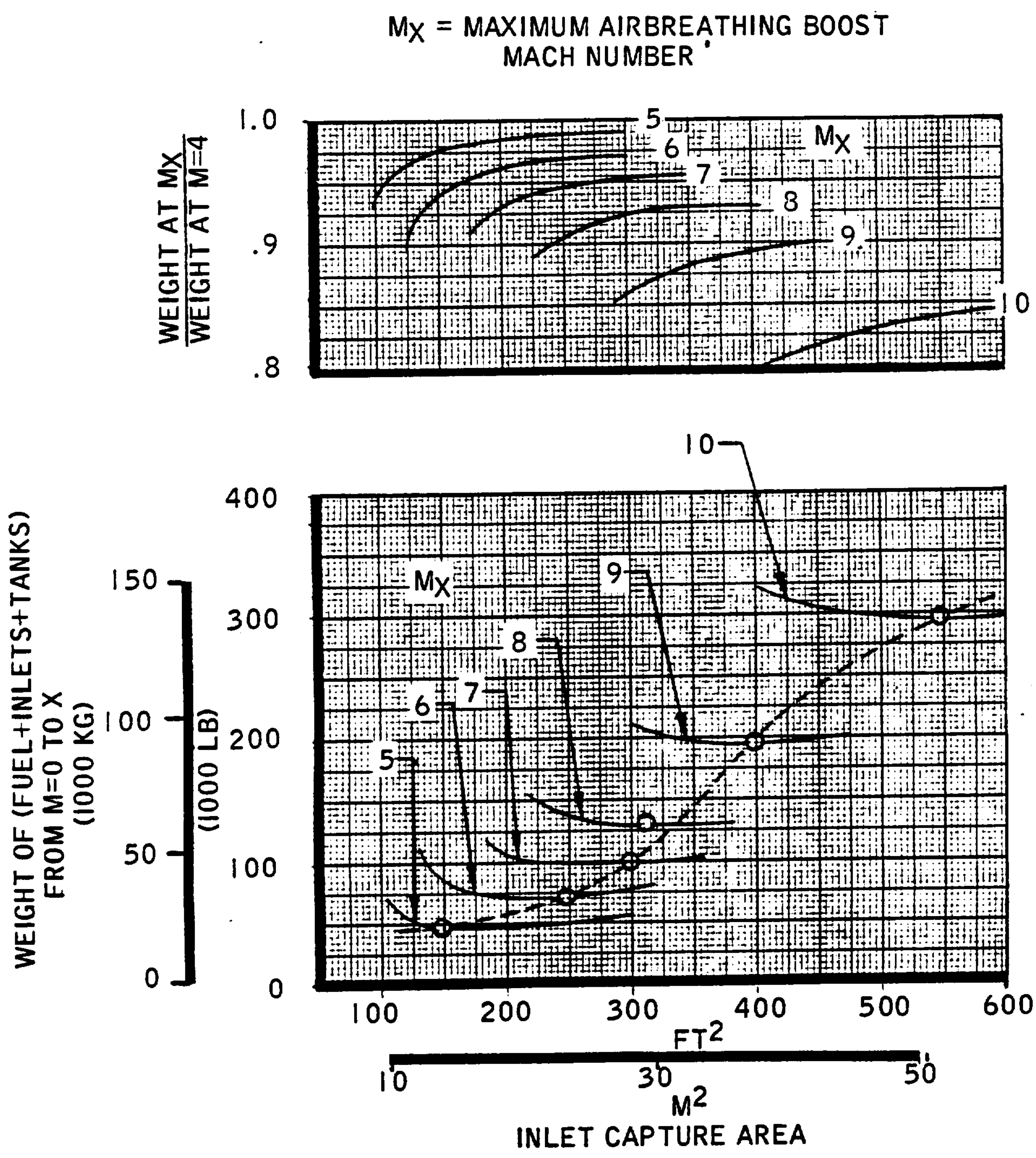

FIGURE 338. Ascent Performance and Inlet Capture Area Sizing for Various Airbreathing Boost Mach Numbers for the Class 2 Supercharged Ejector Ramjet (Engine No. 11)

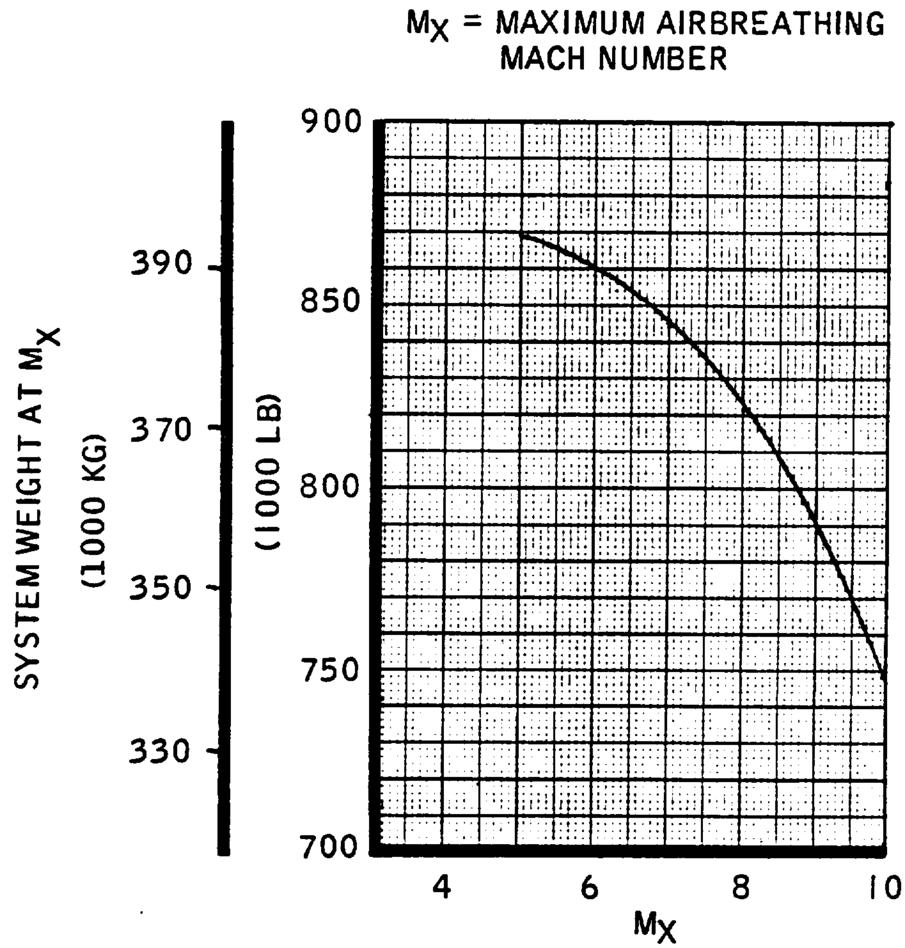

FIGURE 339. Terminal Weights of Various Airbreathing Boost Mach Number Systems for the Class 2 Supercharged Ejector Ramjet (Engine No. 11)

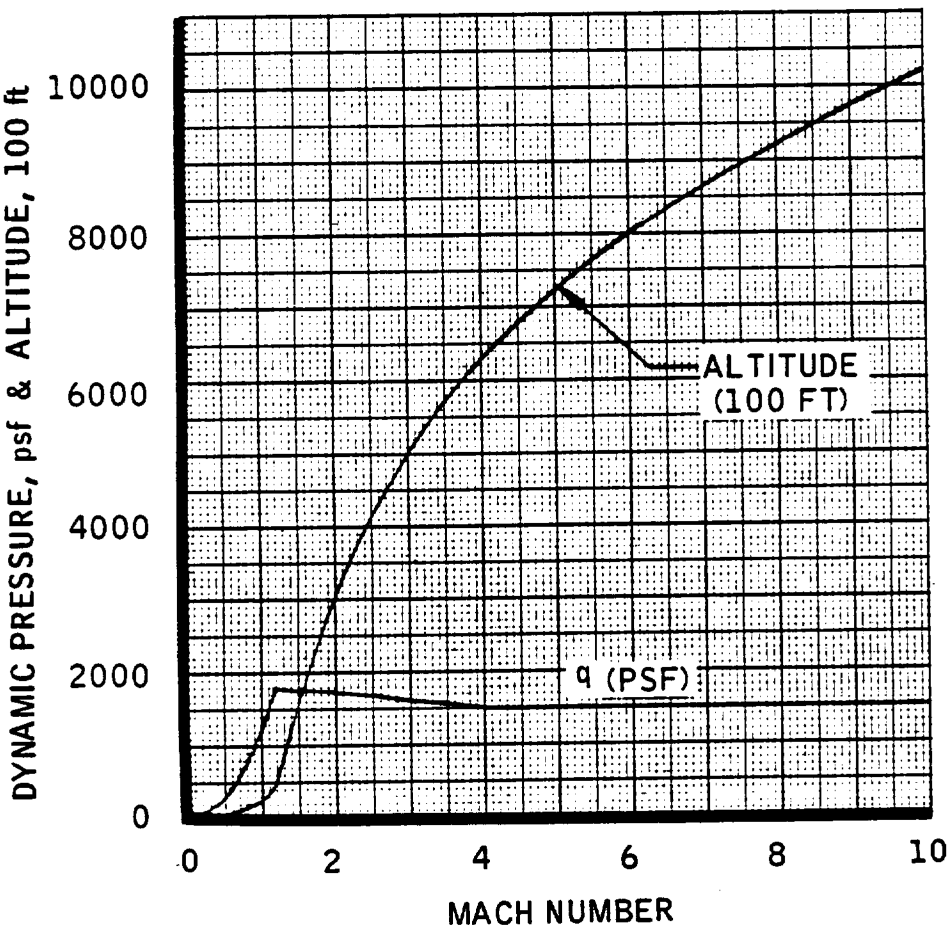

FIGURE 340. Ascent Path and Dynamic Pressure History for the Class 2 ScramLACE (Engine No. 22)

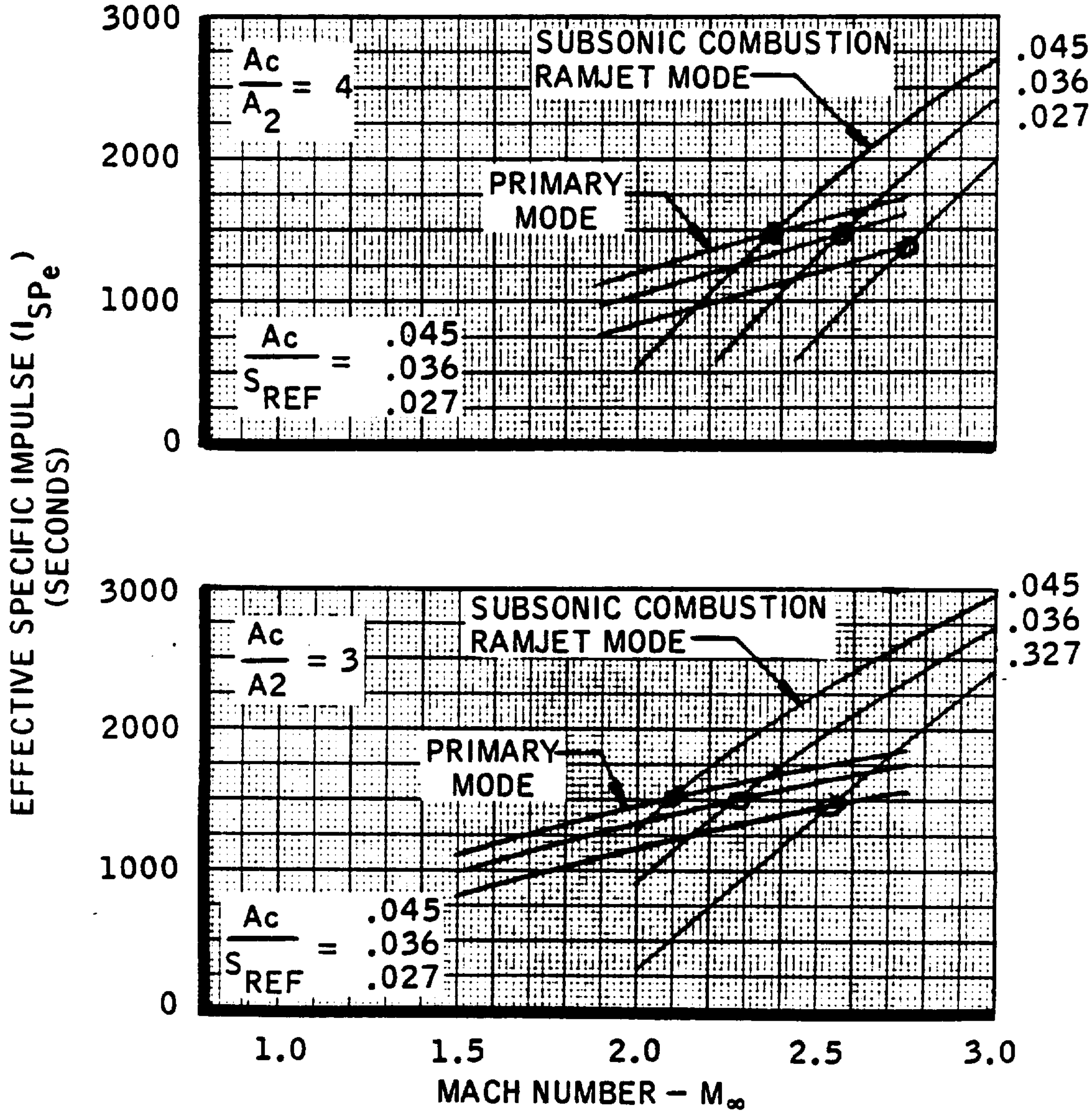

FIGURE 341. Transition Mach Numbers, Primary Mode to Subsonic Combustion Ramjet Mode, for the Class 2 ScramLACE (Engine No. 22)

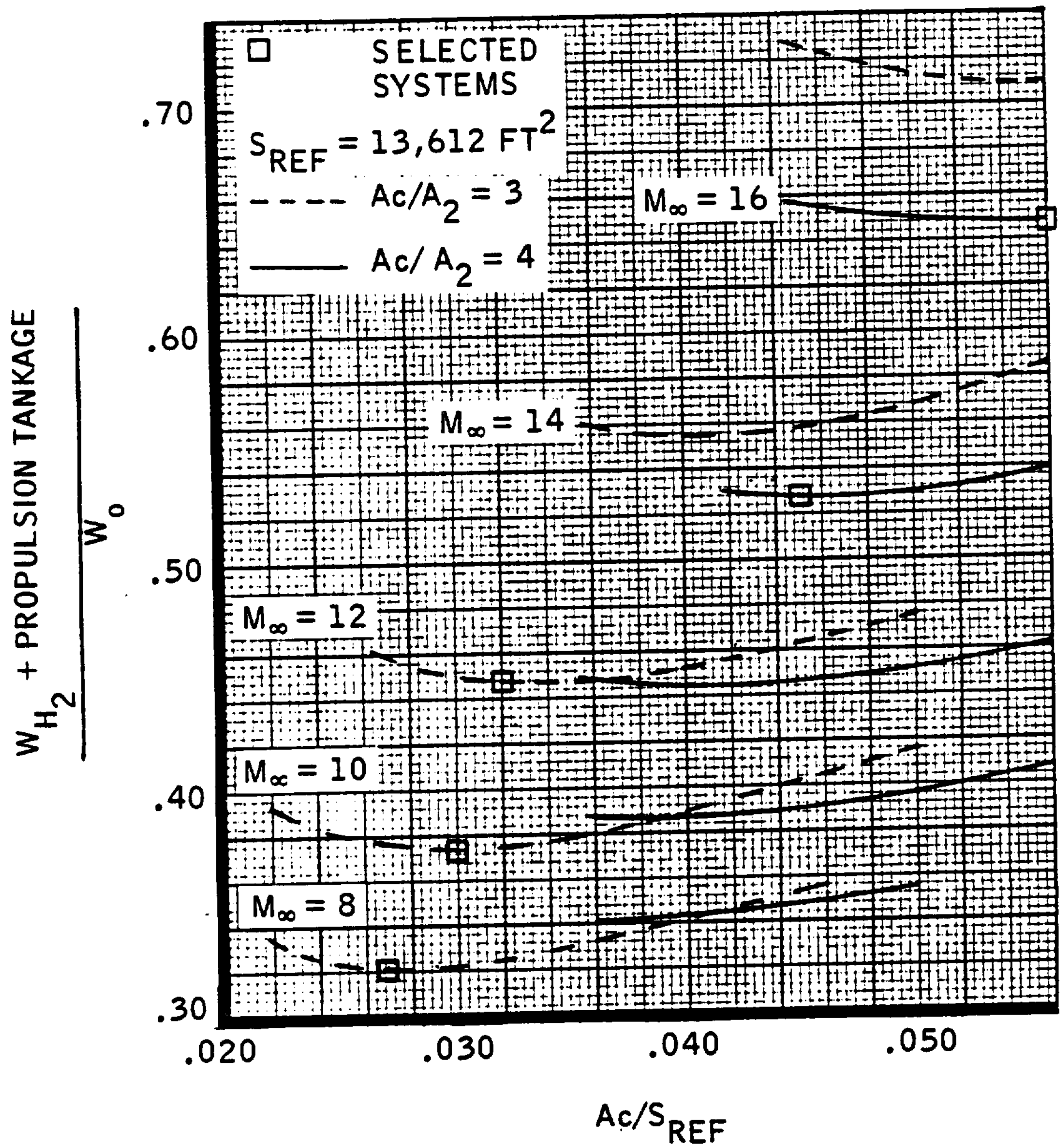

FIGURE 342. Inlet Capture Area Sizing at Various Airbreathing Boost Mach Numbers for the Class 2 ScramLACE (Engine No. 22)

of the 4:1 contraction ratio shown for Mach 14 and 16. Note that the Mach 12 case shows an almost equal trade-off, with the 3:1 contraction ratio selected because of the lower cowl area.

The vehicle drag, thrust, specific impulse and weight history of the Mach 10 system are shown in Figure 343. Figure 344 presents the boost and time displacements.

8.6.2.5.3 Ascent Performance - Turboramjet (Engine No. X)

The Turboramjet system flight path, dynamic pressure, and drag are presented in Figure 345 as a function of boost Mach number. The system weight history and range displacement are shown in Figure 346.

Propulsion system sizing was accomplished by the same technique applied to the Supercharged Ejector Ramjet system. The engine complement was sized by utilizing the installed engine performance and weight data presented in pp 90 to 100 of Reference 26. The system inlet capture area was sized by summing the fuel, inlet, and tankage weights from Mach 4 to 8. Figure 347 presents the inlet sizing parameter as a function of capture area and indicates essentially the same for the Turboramjet system as that determined for the Supercharged Ejector Ramjet system. The propulsion sizing resulted in a sea level static thrust loading of 0.528 for the Turboramjet system, with a performance capture area of 310 sq ft.

The mass fractions presented in Figure 333, as determined for the Supercharged Ejector Ramjet system, were applied to the Turboramjet system to study the effect of maximum airbreathing boost Mach number. The application of these mass fractions was acceptable, since the small weight difference in the systems during ramjet operation effects only a minor change in the performance parameters. The system weight at the various maximum airbreathing Mach numbers is presented in Figure 348 for the Turboramjet system.

8.6.2.6 Prestaging Pull-up Performance

The operational profile of the airbreathing system included a prestaging pull-up under airbreathing thrust from the maximum boost termination point to the staging point. This maneuver was accomplished by pulling a normal load factor and basically exchanging kinetic energy for potential energy. The maneuver provides for increased flight path angle for the system and a less hostile staging environment.

The pull-up performance characteristics were determined as a function of normal load factor for the Mach 8 and 12 systems and they are presented in Figures 349 and 350 as a function of dynamic pressure history during the pull-up.

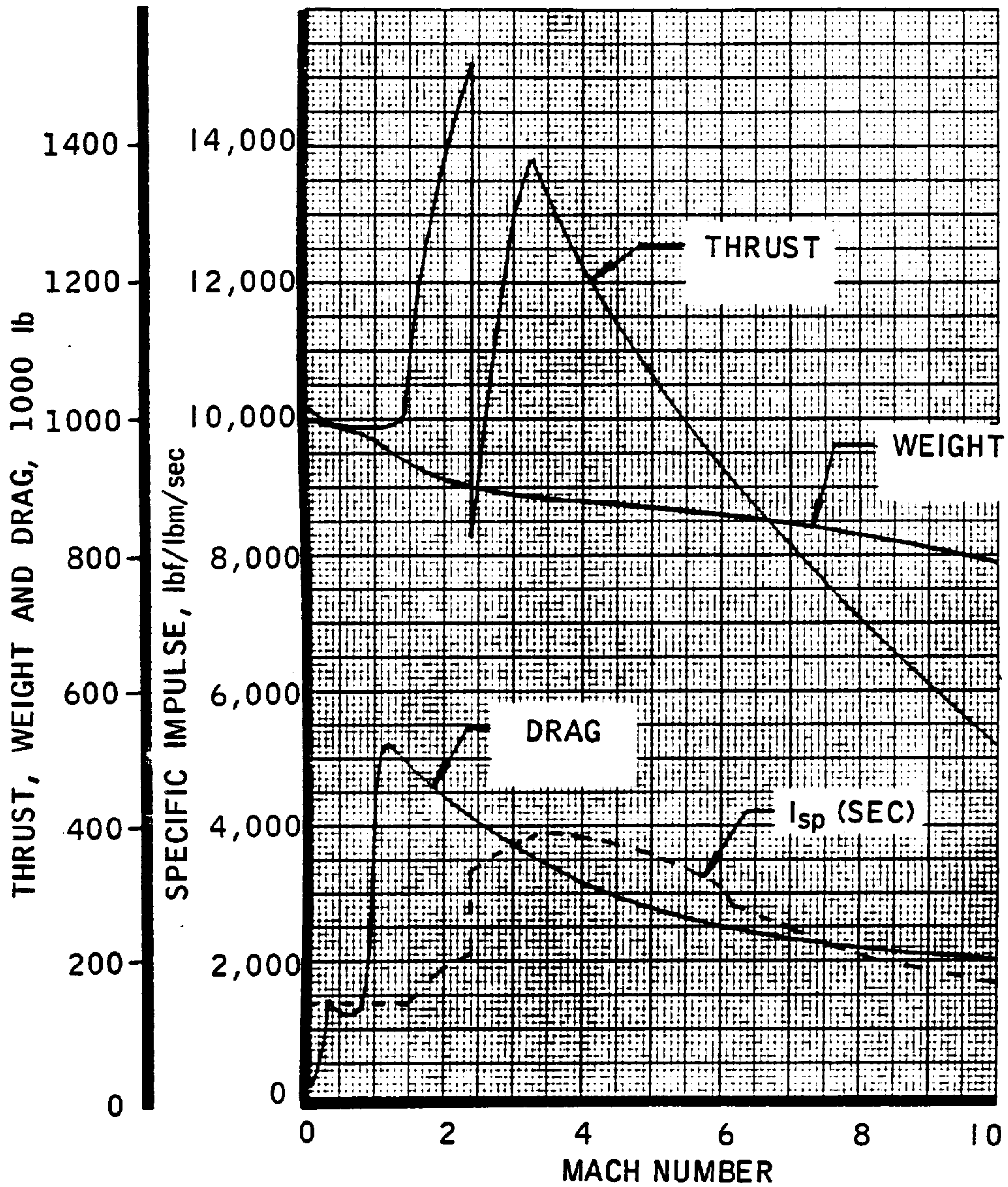

FIGURE 343. Ascent Performance Characteristics of the Class 2 ScramLACE (Engine No. 22)

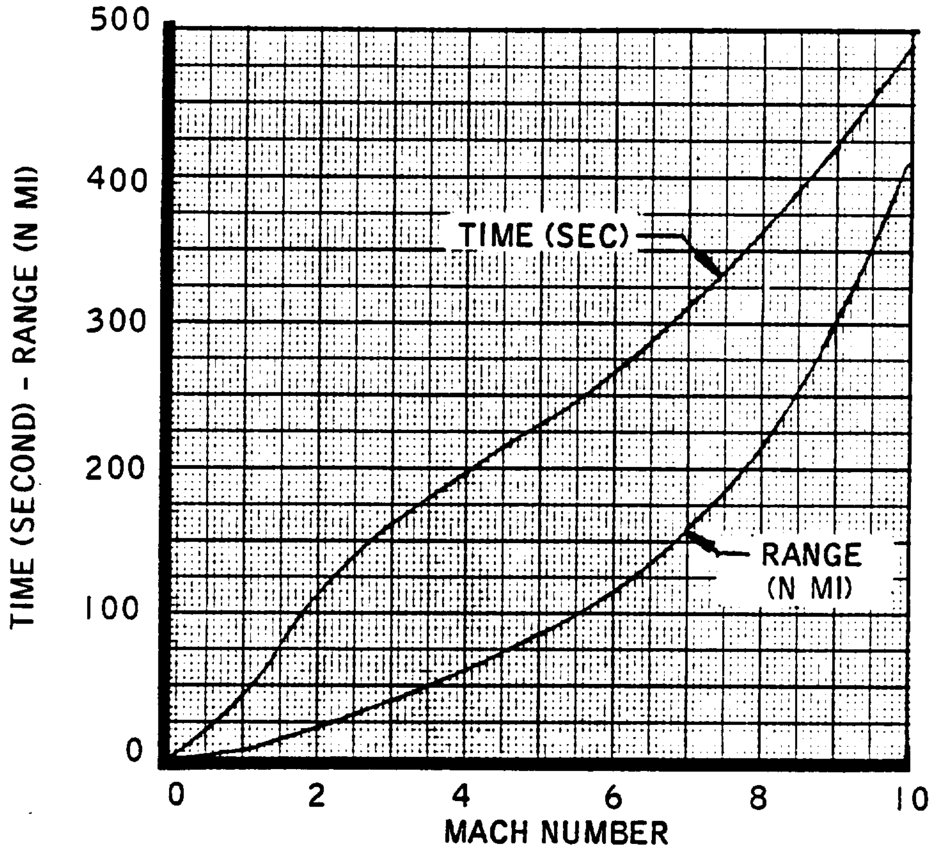

FIGURE 344. Ascent Time and Range Displacement for the Class 2 ScramLACE (Engine No. 22)

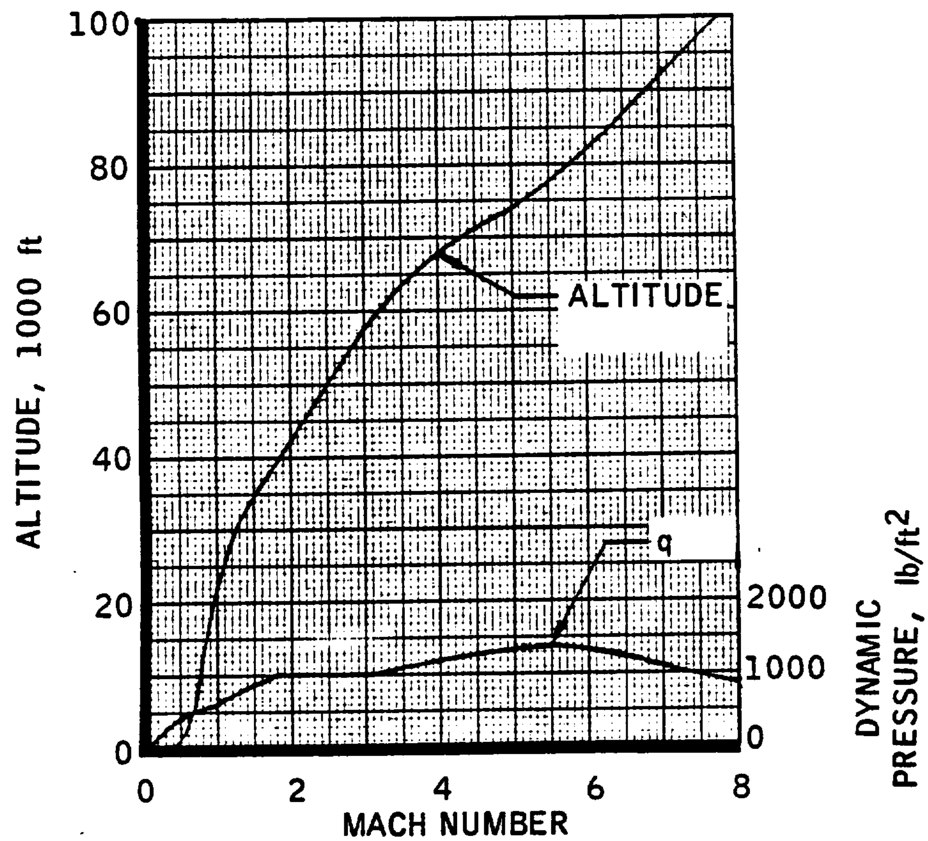

FIGURE 345. Ascent Path and Dynamic Pressure History of the Class 2 Turboramjet (Engine No. X)

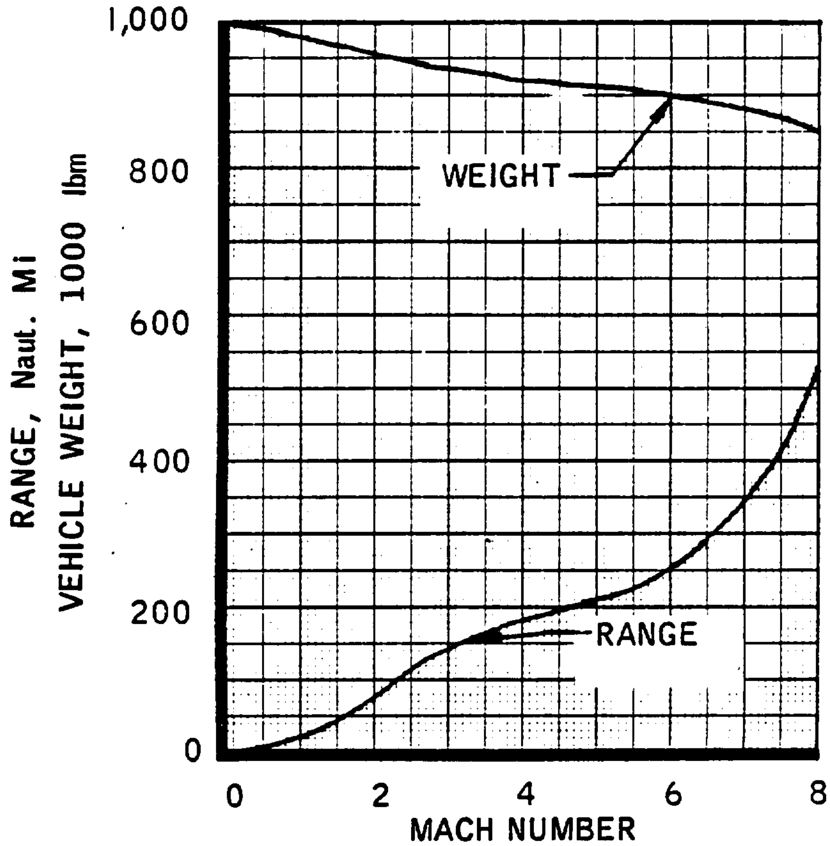

FIGURE 346. Ascent Range Displacement and Weight History of the Class 2 Turboramjet (Engine No. X)

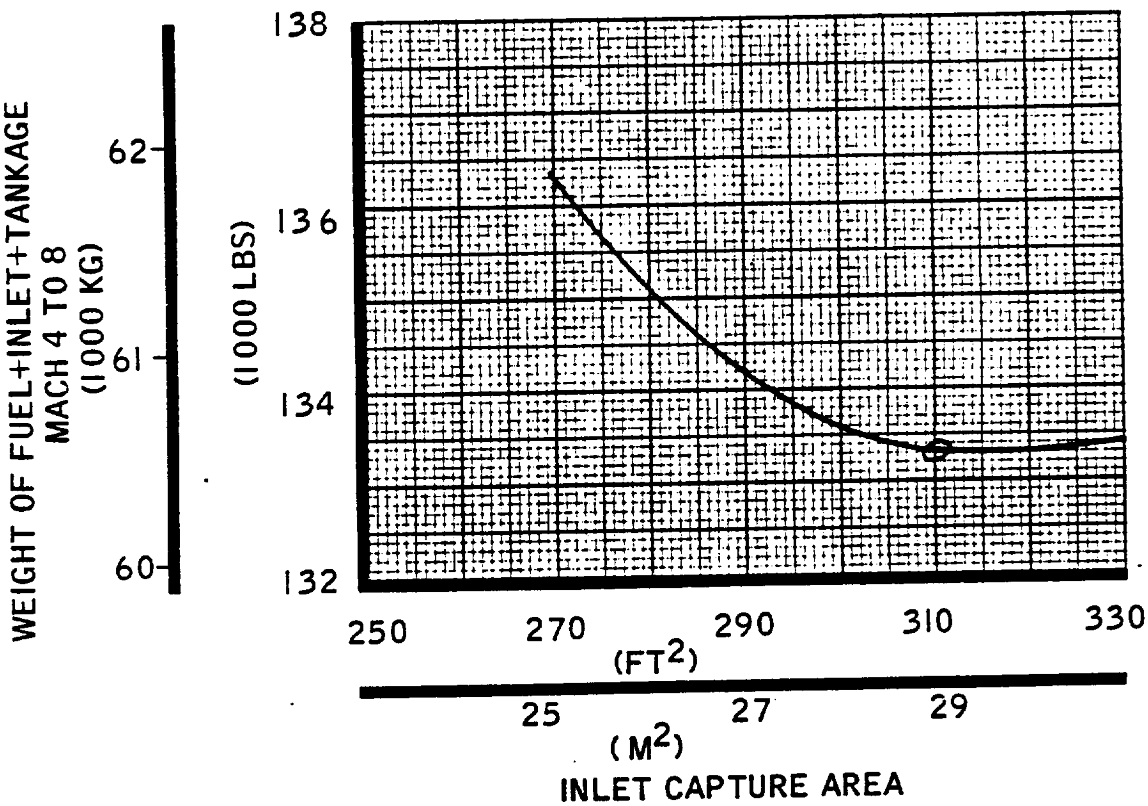

FIGURE 347. Inlet Capture Area Sizing for the Class 2 Turboramjet (Engine No. X)

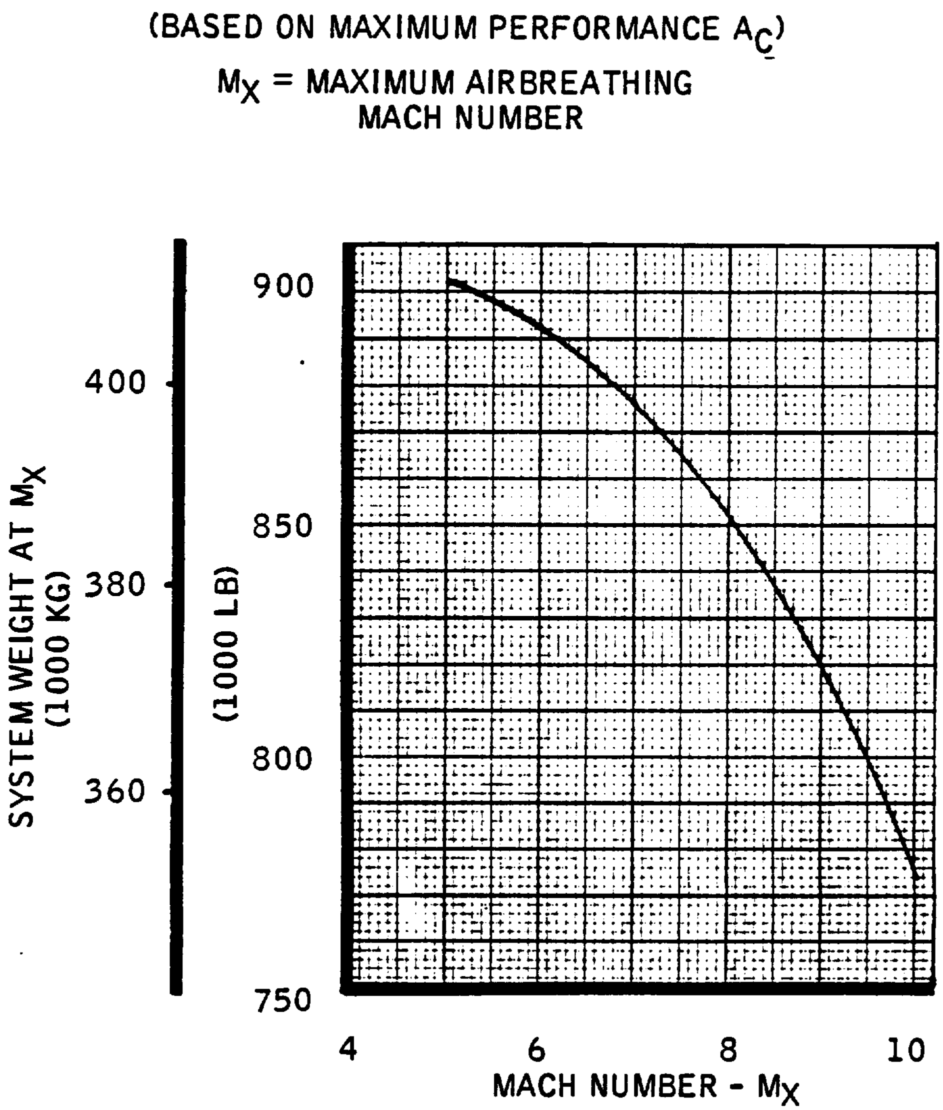

FIGURE 348. Terminal Weights of Various Airbreathing Boost Mach Number Systems for the Class 2 Turboramjet (Engine No. X)

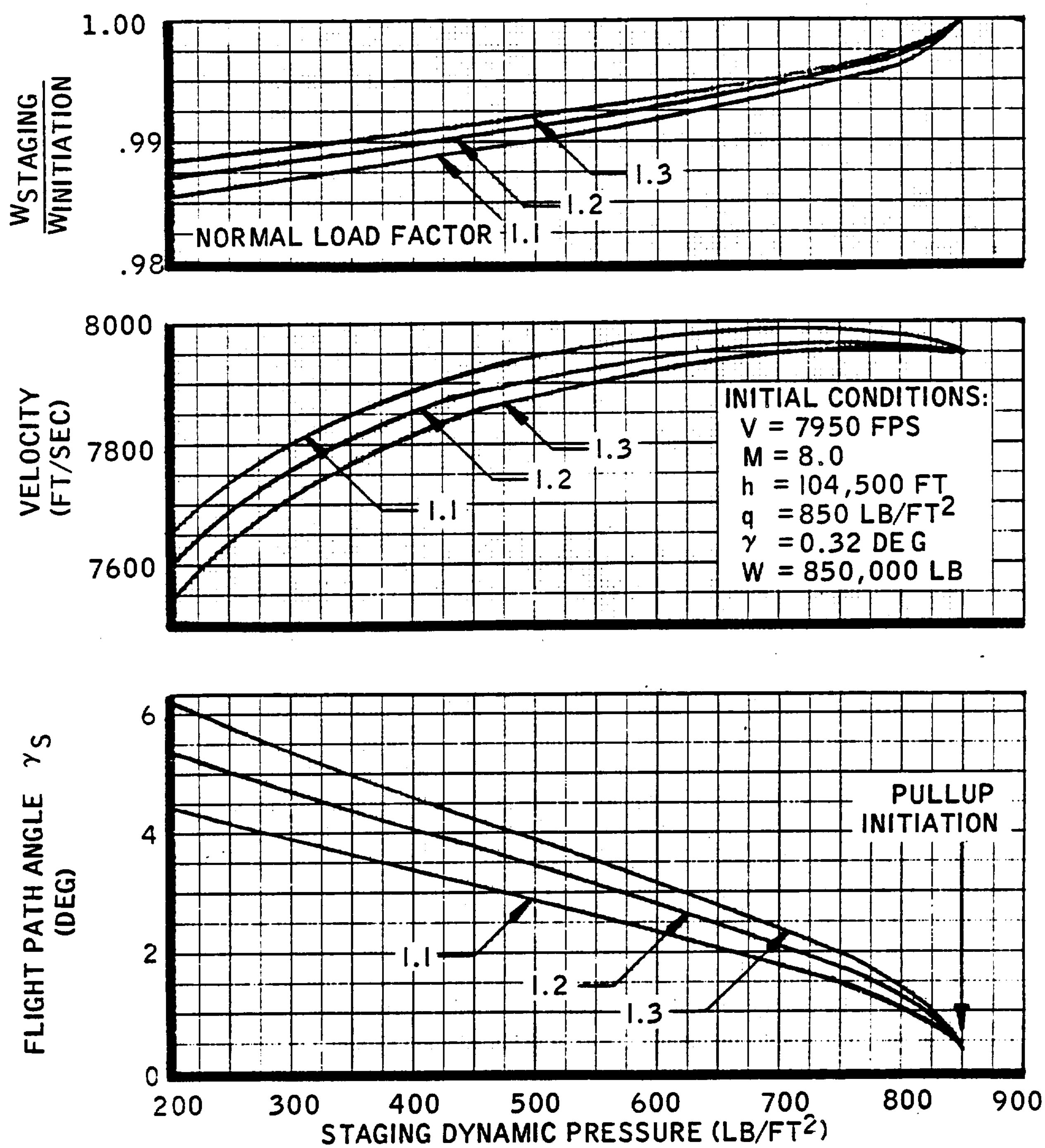

FIGURE 349. Prestaging Pull-up Performance of the Class 2 Subsonic Combustion System

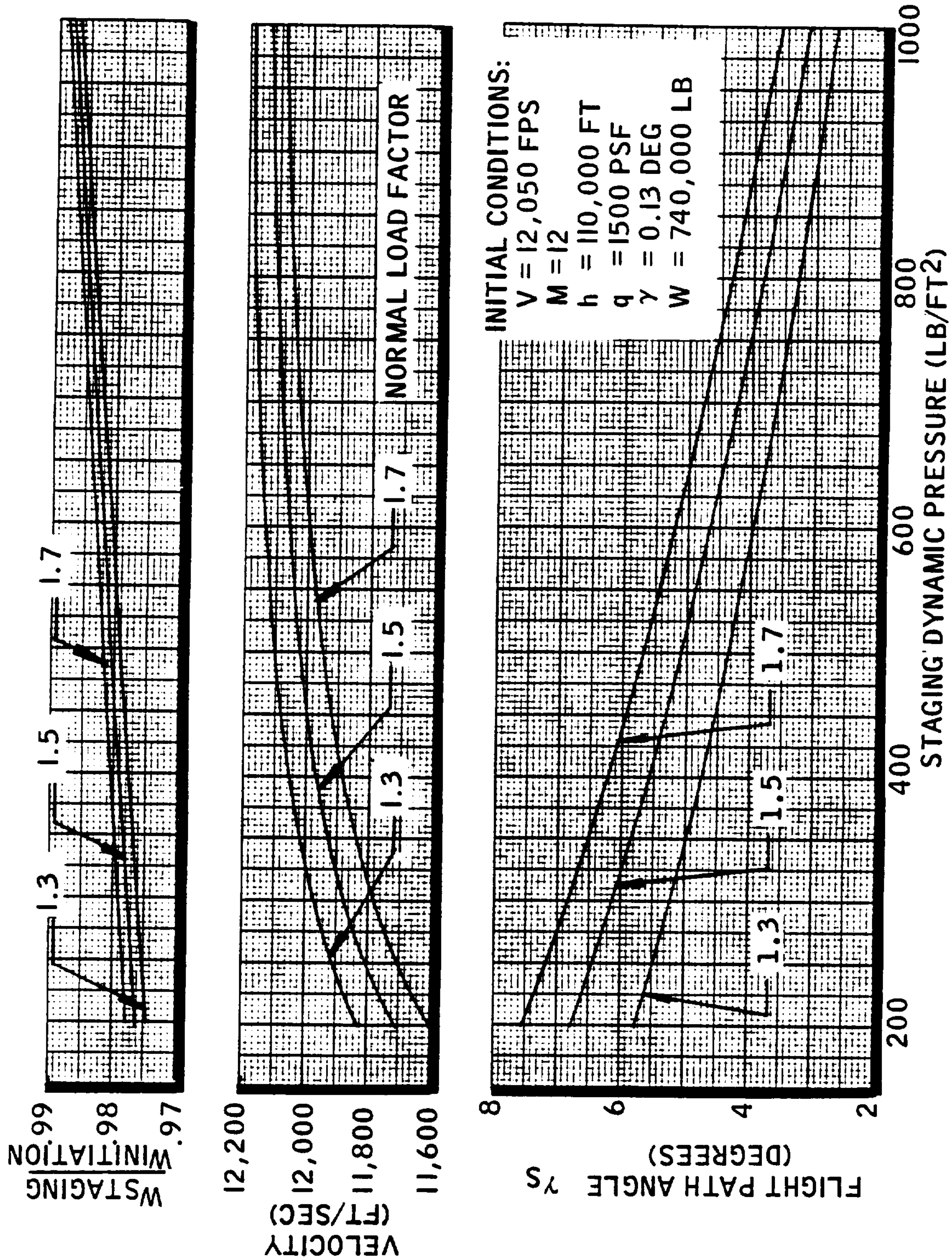

FIGURE 350. Prestaging Pull-up Performance of the Class 2 Supersonic Combustion System

Consideration of the system staging velocity (V_S), flight path angle (γ_S), and mass fraction (W_S/W_X = Ratio of weight at staging to weight at maximum airbreathing Mach number) at each dynamic pressure level during the pull-up alters the second stage gross weight and characteristic velocity requirement. This resulted in the effect on the system payload performance illustrated in Figure 351 which presents the ratio of payload to the "no pull-up" value as a function of the dynamic pressure level during the pull-up for various normal load factors.

As indicated in Figure 351, maximum payload occurred for no pull-up for the Mach 8 system and with a pull-up to 500 psf dynamic pressure for the Mach 12 system. The payload variation was small, however, and the cost of providing a 200 psf staging environment was modest. When the second stage structural and thermal implications were considered, the progressively reducing $q\alpha_{max}$ occurring during the pull-up may provide for substantially greater payloads by staging at the low dynamic pressure levels.

8.6.2.7 First Stage Poststaging Performance

8.6.2.7.1 Return to Base

Figure 352 presents the turn-cruise fuel weight in terms of first stage burnout weight as a function of the turn-cruise Mach number and load factor during the turn. The minimum fuel requirement occurs at Mach 5 with the maximum 3 g load factor during the turn. The result is typical for all Class 2 first stage vehicles.

The power-off, poststaging descent profile was determined by utilizing a three-dimensional steepest ascent program. With the initial conditions fixed by the system staging point, the terminal conditions were established at Mach 5 and an altitude required for engine restart (96,000 feet). The descent operation minimized the down range displacement while maximizing the turning angle within the 3 g study constraint (Section 3.1). The power-off descent trajectory characteristics are presented in Figure 353 for the Supercharged Ejector Ramjet system.

Figure 354 summarizes the return to base mass fractions as a function of terminal airbreathing boost Mach number for the three Class 2 airbreathing systems. The lower Mach number systems required no cruise-back, since the glide distance from Mach 5 (525 n. miles) was in excess of the total range displacement. The Supercharged Ejector Ramjet system has a shorter boost displacement, due to higher T/W ratio than the Turboramjet, and consequently it has less return to base penalty.

8.6.2.7.2 Loiter and Landing

A 5 minute loiter at sea level altitude was evaluated by utilizing the throttled specific impulse values and vehicle subsonic aerodynamic characteristics.

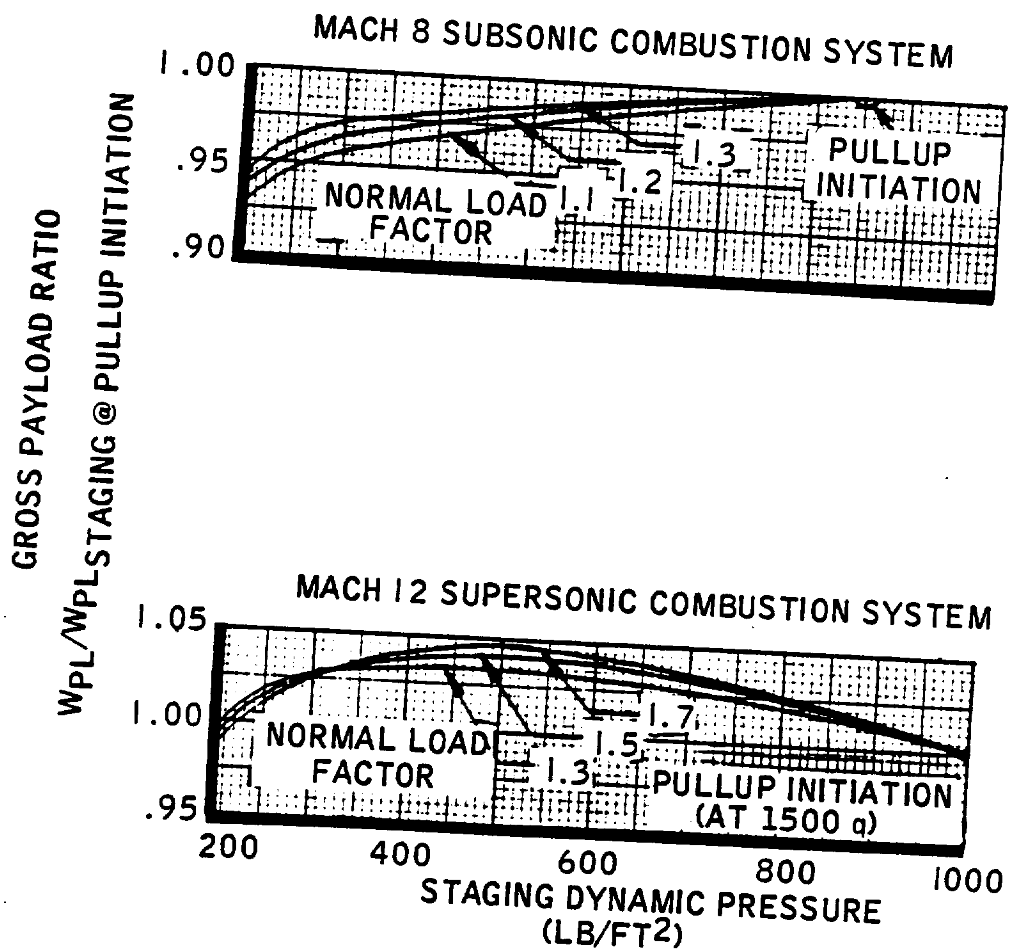

FIGURE 351. Effect of Staging Dynamic Pressure and Pull-up Load Factor on the Payload Performance of the Class 2 Mach 8 and 12 Systems

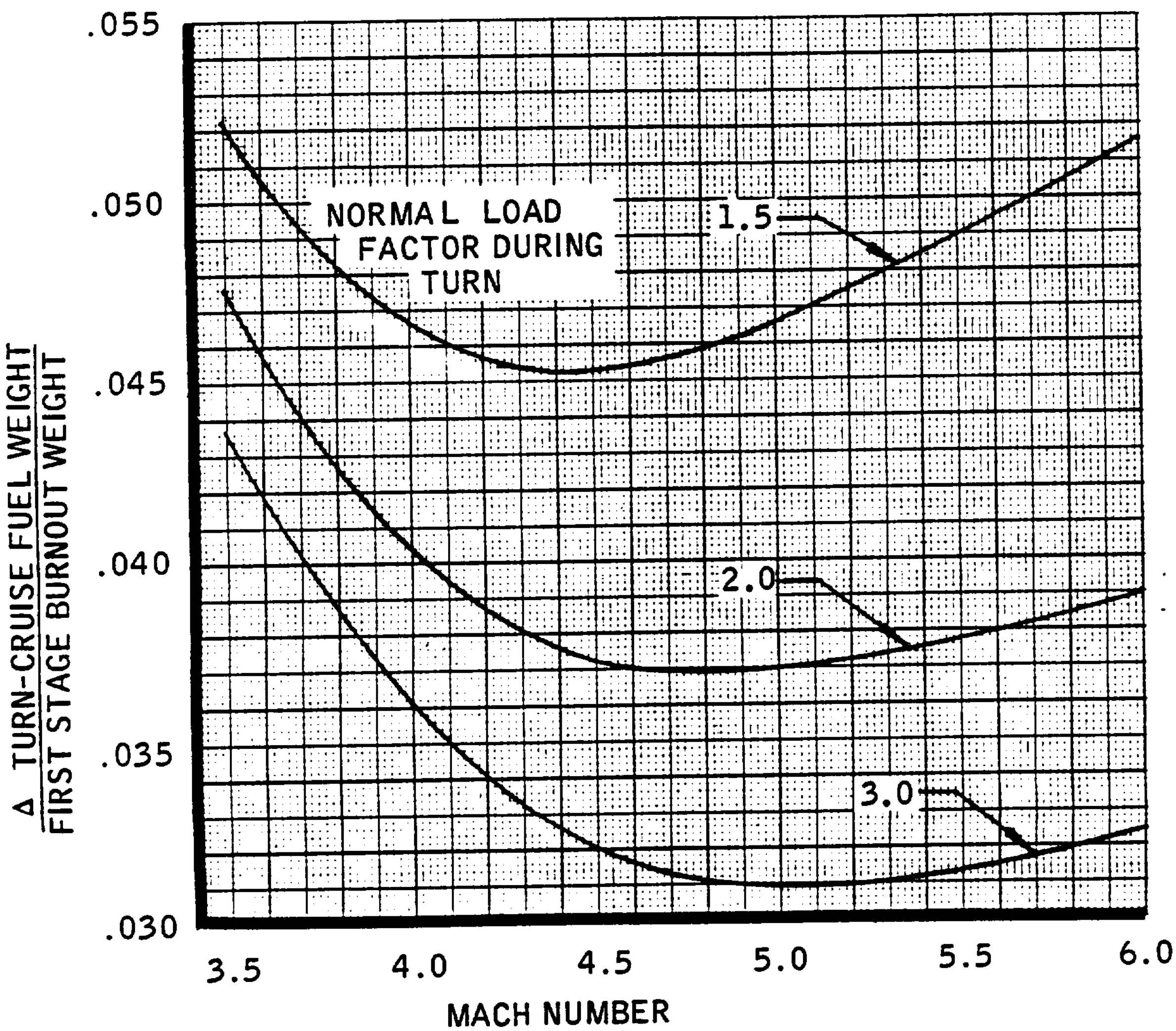

FIGURE 352. First Stage Return to Base Turn and Cruise Mach Number, Class 2 Vehicles

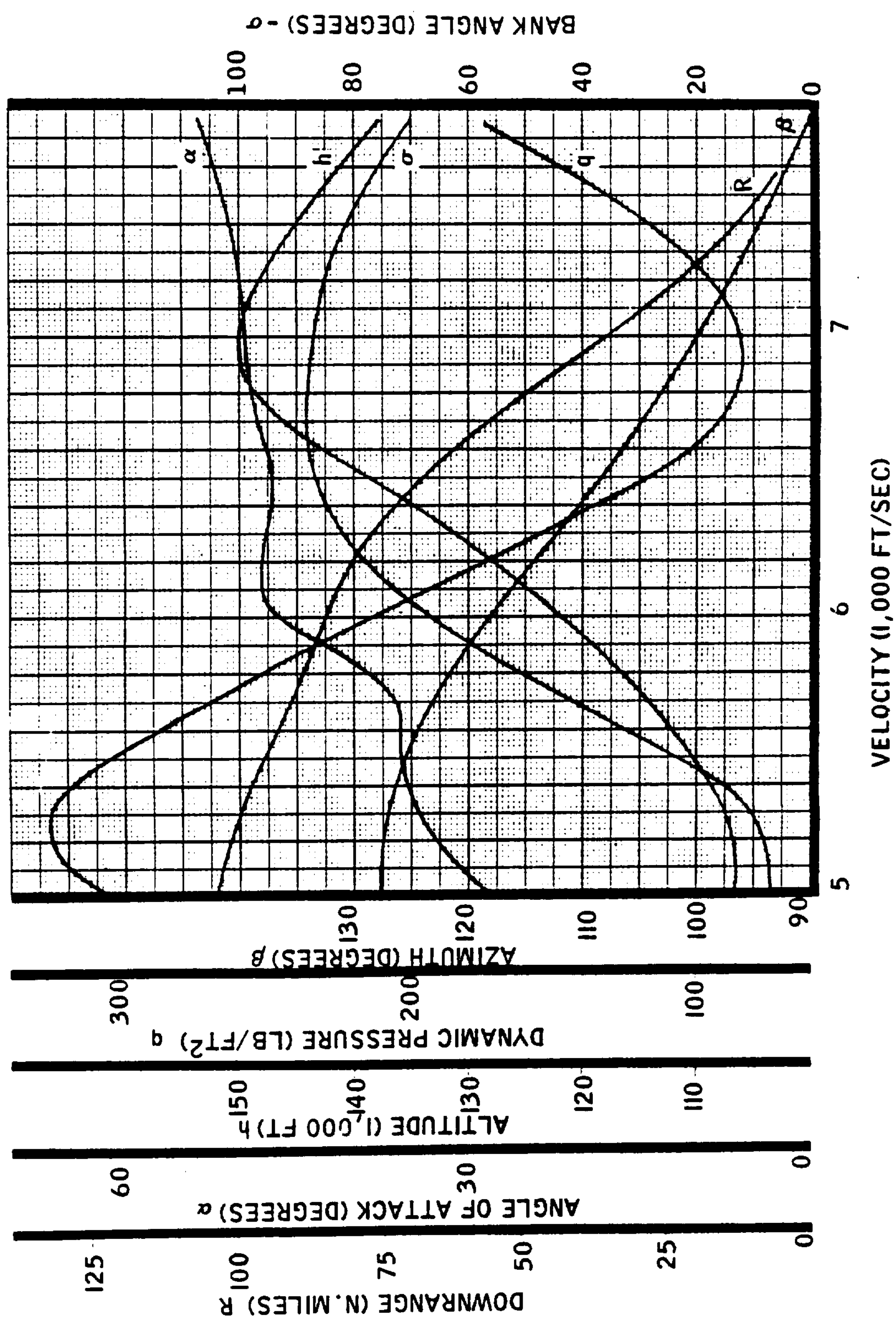

FIGURE 353. First Stage Descent Characteristics of the Subsonic Combustion System

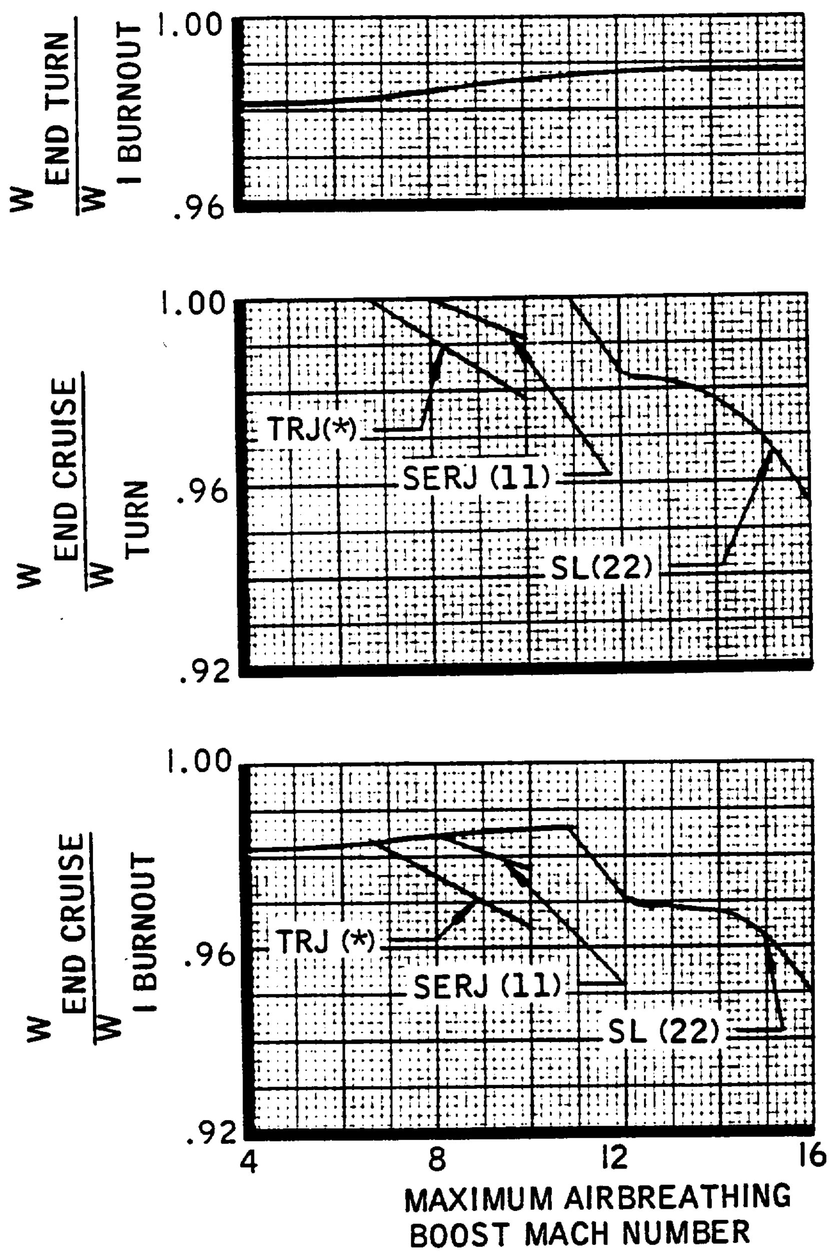

FIGURE 354. First Stage Return to Base Fuel Requirement as a Function of Airbreathing Boost Mach Number for the Class 2 Airbreathing Systems

In the case of the Supercharged Ejector Ramjet, fan-only operation was found to provide adequate thrust for loiter (primaries and afterburning inoperative). The loiter characteristics of the Supercharged Ejector Ramjet system are presented in Figure 355 which indicates the minimum fuel consumption resulting at a loiter Mach number of 0.35. The fuel penalty was 0.32 percent of the loiter initiation weight. For the ScramLACE and Turboramjet systems, the respective loiter penalties were 1.52 percent and 0.74 percent.

The system trimmed landing velocities for a power-off condition at $\alpha = 12°$ (with 10 percent margin) were as follows:

Supercharged Ejector Ramjet (No. 11)	296 fps
ScramLACE (No. 22)	320 fps
Turboramjet (No. X)	295 fps

The total return to base and loiter penalties in percentage of first stage burnout weight were 1.92, 4.42, and 3.39 percent, respectively.

8.6.2.8 <u>All-Rocket Vehicle Comparison Summary</u>

Reference is made to preceding Sections 8.6.1.1 and 8.6.1.6 for a description of the Very Advanced first stage rocket (Engine No. 0) system and analysis approach.

The results of the investigation are presented in Figures 356 through 358. The second stage sizing was based on a cabin volume for 10 passengers and 2 crewmen. The gross payload in Figure 356 is defined as follows:

$$W_{P.C.} = 4819.37 + (84.64 + 0.159032\ Cp)\ N + 45.114\ (W/S)_{RE} + (255.5 + Cp)\ N$$

Where

Cp = Cargo per man (Passengers + Crewmen)

N = Number of men

$(W/S)_{RE}$ = Wing loading at entry (Landing)

Gross payload was used as the study measure of system performance.

Net payload capability as defined by General Dynamics/Convair for the second stage vehicle is as follows:

$$W_{PL_{NET}} = (255.5 + Cp)\ N\ \text{lb (Reference: Table XXX, in Volume 2)}$$

$\phi_{AB} = 0$

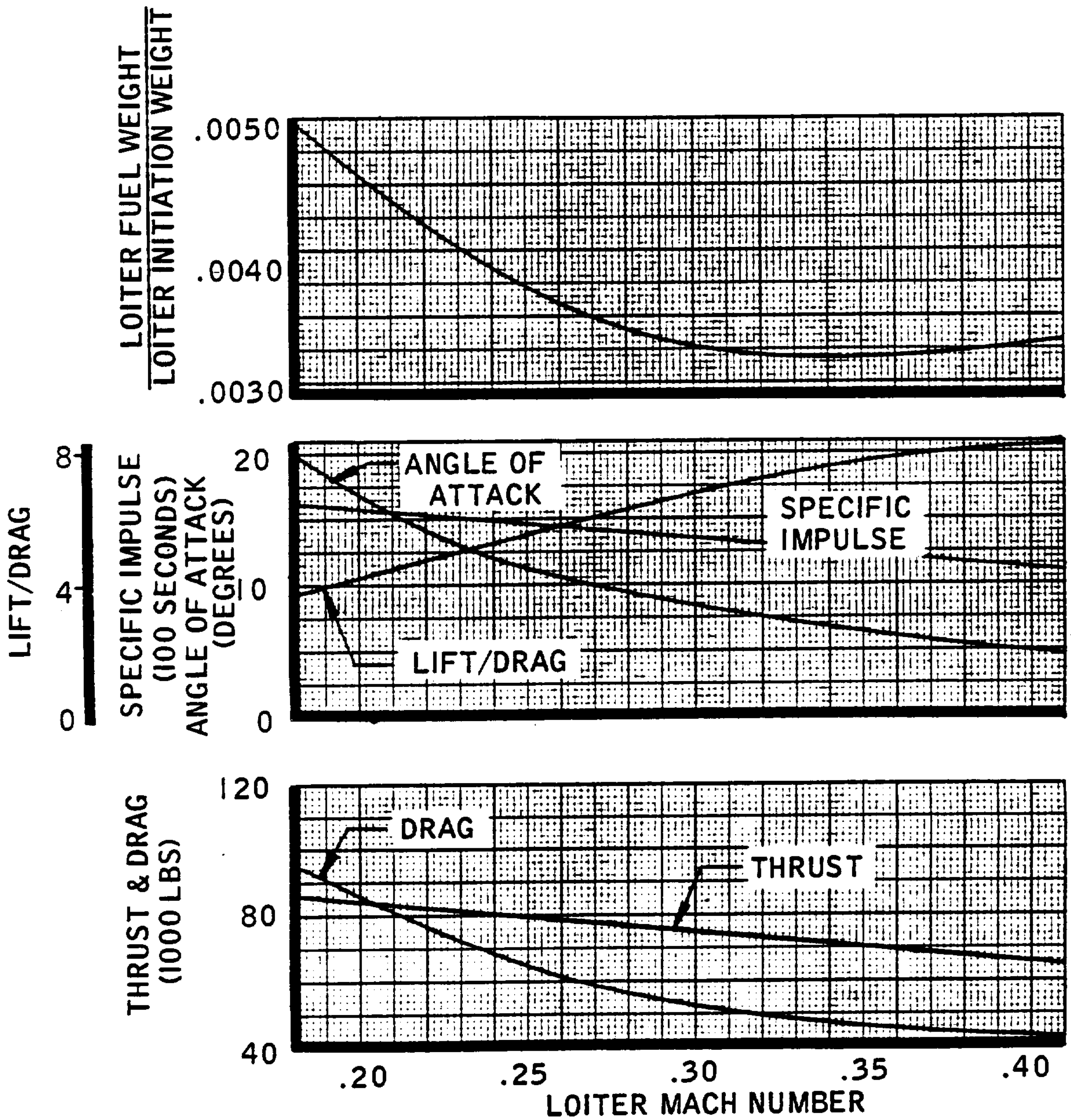

FIGURE 355. Loiter Performance of the Class 2 Supercharged Ejector Ramjet (Engine No. 11)

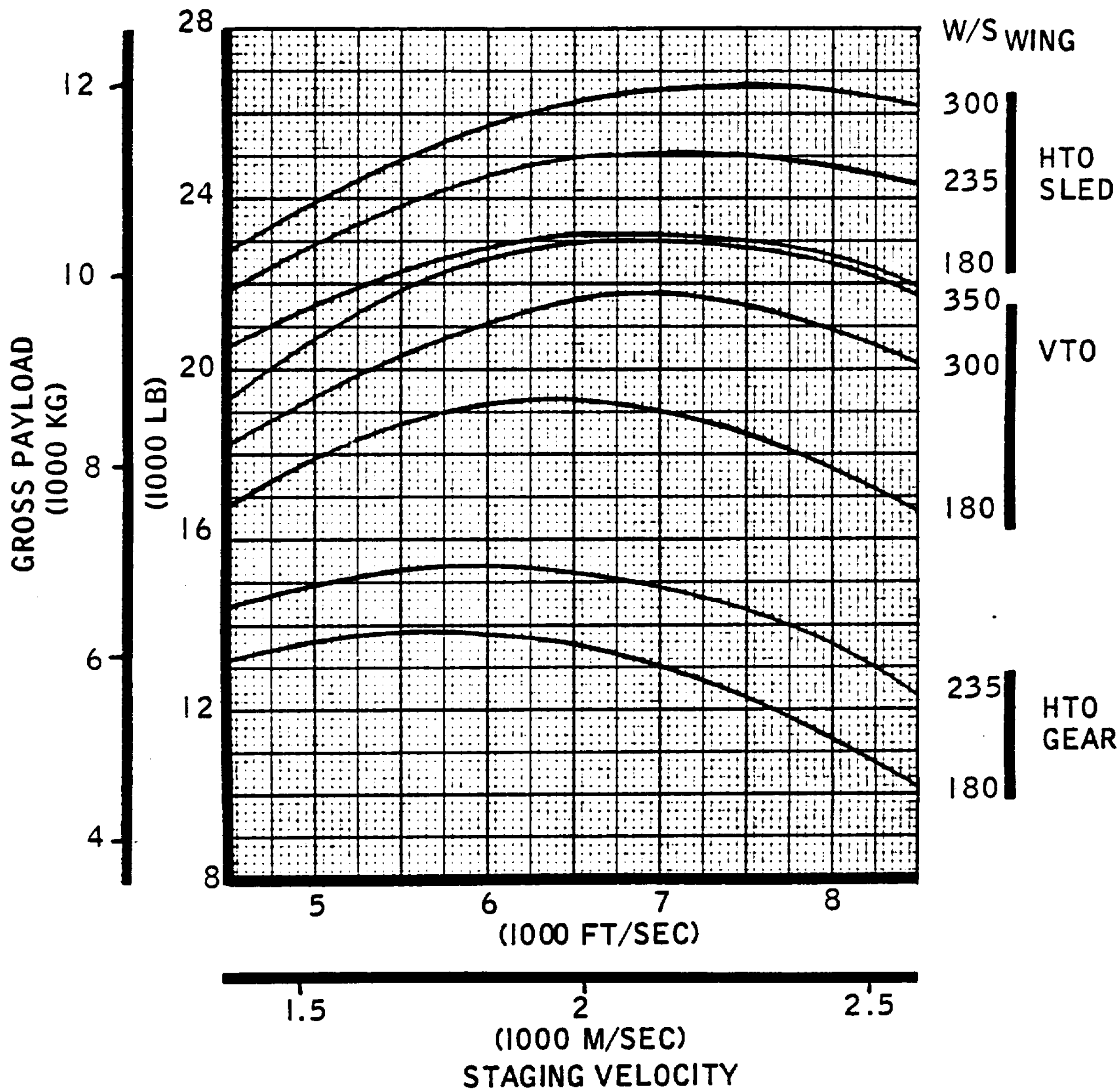

FIGURE 356. Payload as a Function of Staging Velocity for the Class 2 Advanced Rocket (Engine No. 0)

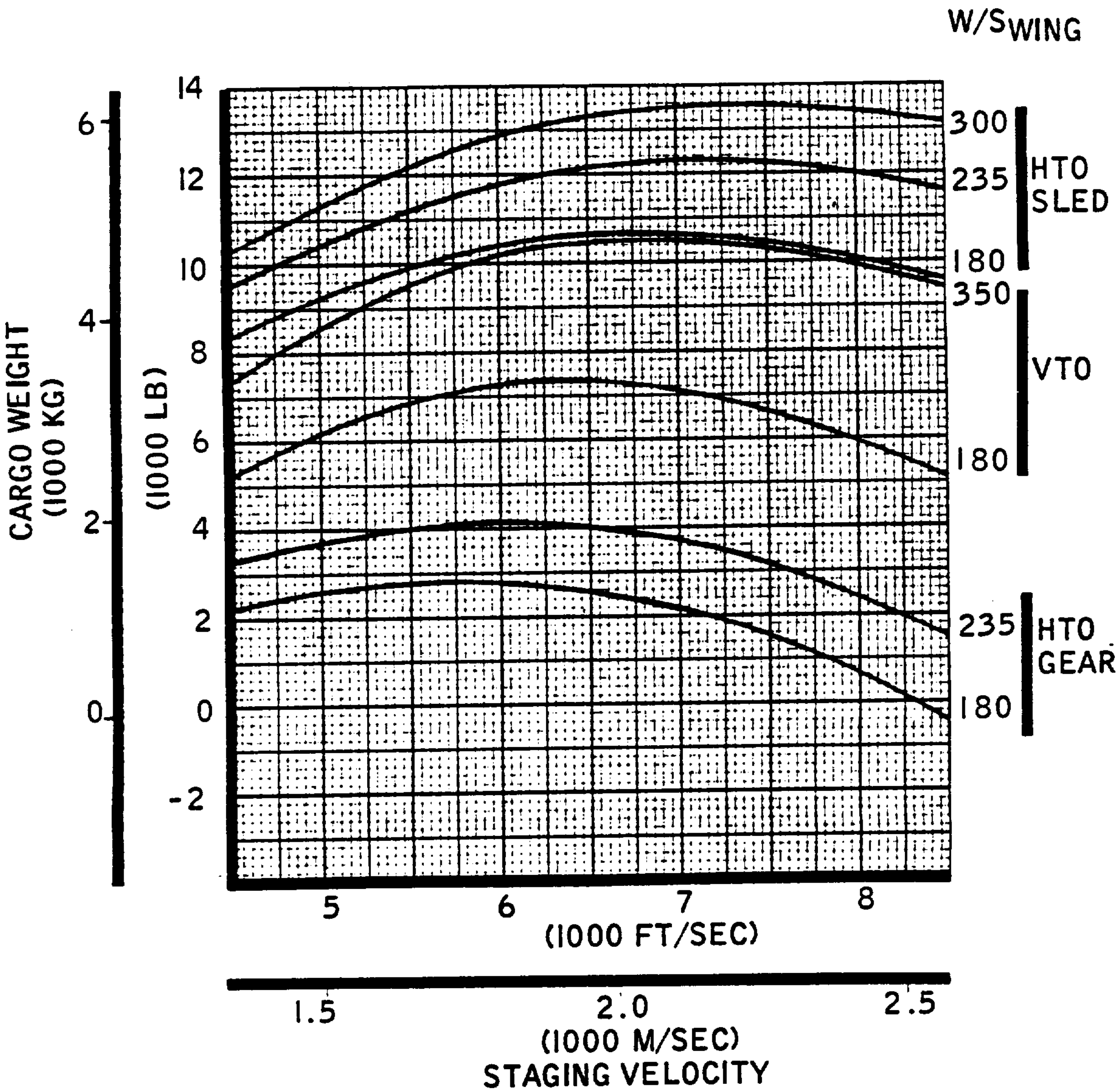

FIGURE 357. Cargo Weight versus Staging Velocity for a Personnel Complement of 12 for the Class 2 Advanced Rocket (Engine No. 0)

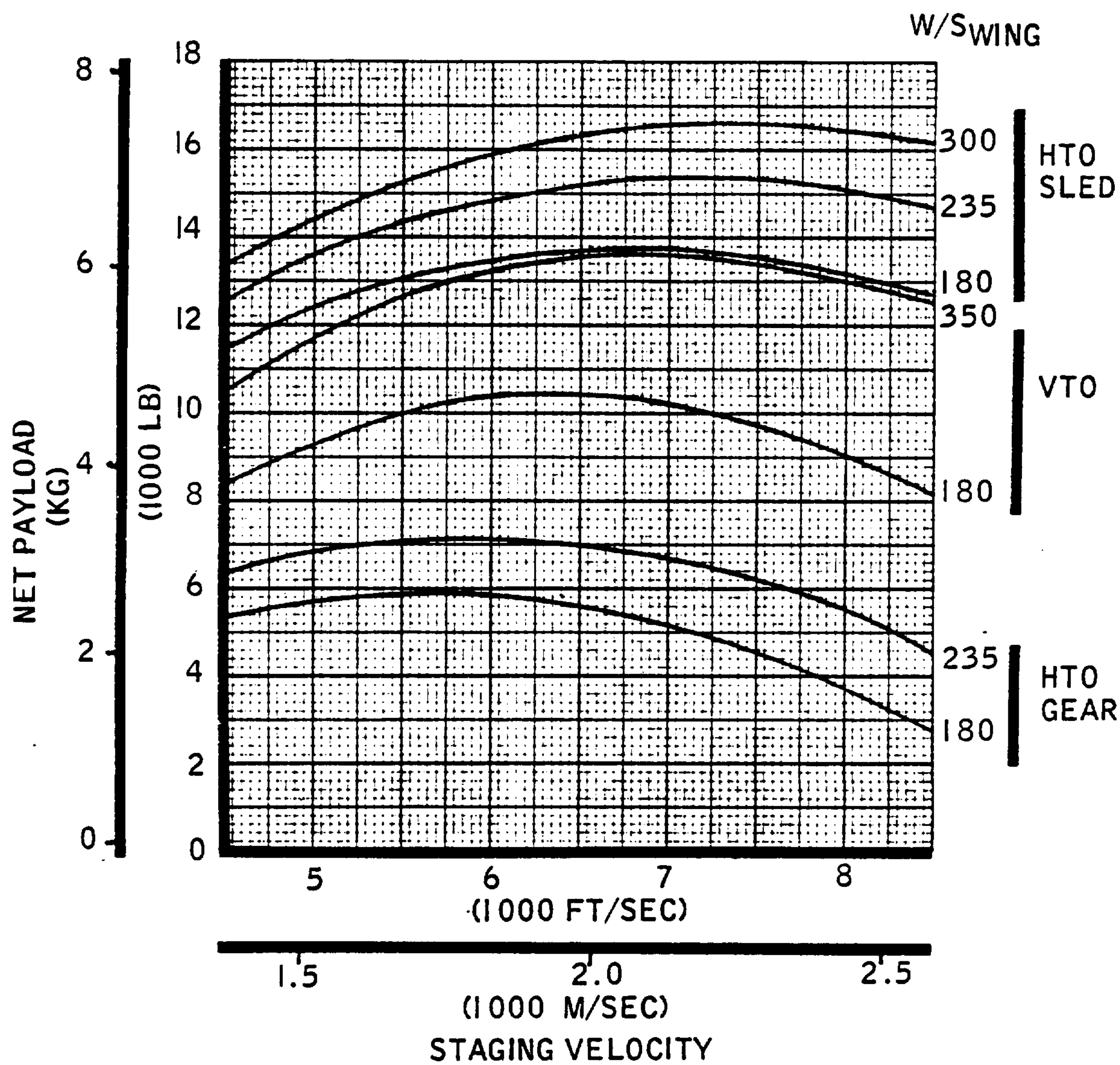

FIGURE 358. Net Payload versus Staging Velocity for the Class 2 Advanced Rocket (Engine No. 0)

The above equation was used to obtain the total cargo weight shown in Figure 357 (in addition to the 12 men). Total net payload is shown in Figure 358.

The conclusions resulting from the advanced rocket analysis are summarized as follows:

1. The optimum staging velocities are

   5800 to 6000 fps for the HTO -gear takeoff
   6800 to 7000 fps for the VTO
   6800 to 7500 fps for the HTO-sled launched vehicle

2. Wing loading selection must be based on the limiting lift capability conditions related to the most critical of the takeoff and landing situation for each system. The nominal $(W/S)_{L.O.}$ values tabulated below were based on a qualitative judgment assessment. For each case, gross payload, total net payload, and total cargo were shown for the optimum staging velocities.

Advanced Rocket System	$(W/S)_{L.O.}$	Gross Payload (lbs)	Total Net Payload (lbs)	Total Cargo* (lbs)
HTO-gear takeoff	180	13,800	5,900	2,800
VTO	350	22,900	13,566	10,500
HTO-sled launch	235	25,100	15,296	12,230

* In addition to 12 men

8.6.2.9 System Payload Performance Summary

Utilizing the ascent, pull-up, and first stage poststaging performance input data in conjunction with the vehicle weight data (Section 8.6.2.4), the second stage gross weight at the staging point was defined. The staging conditions then define the second stage characteristic velocity and payload. The subsequent sections describe the payload performance of the Class 2 systems and conclude with a summary presentation.

8.6.2.9.1 Supercharged Ejector Ramjet (Engine No. 11)

Figure 359 presents the second stage gross weight and the corresponding payload yield for the Supercharged Ejector Ramjet system as a function of the maximum airbreathing boost Mach number. The maximum performance system was indicated to be that corresponding to Mach 8.

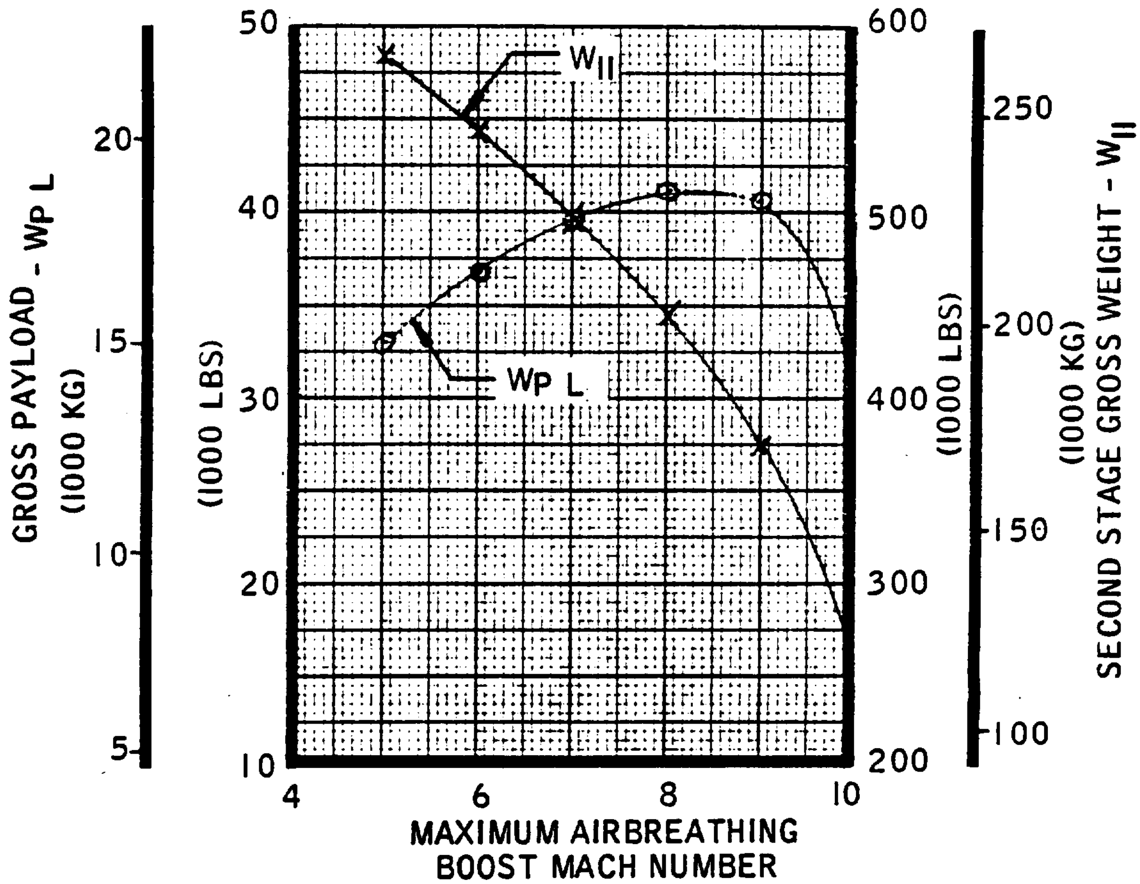

FIGURE 359. System Performance as a Function of Airbreathing Boost Mach Number for the Class 2 Supercharged Ejector Ramjet (Engine No. 11)

Superior boost performance due to the introduction of the Fan-Ramjet Mode to the Supercharged Ejector Ramjet cycle in Class 2 resulted in a substantially increased second stage weight for the Mach 8 system of 445,054 pounds, relative to the Class 1 value of 376,067 pounds. The comparative payloads were 41,200 and 34,600 pounds, respectively, for the Class 2 and Class 1 Supercharged Ejector Ramjet systems.

8.6.2.9.2 <u>ScramLACE (Engine No. 22)</u>

The variation of ScramLACE second stage gross weight and payload for the various airbreathing boost Mach numbers is presented in Figure 360. The Class 2 ScramLACE exhibits a maximum payload potential at Mach 10 of 56,000 pounds. A comparison of the Mach 12 system with the Class 1 counterpart (Mach 12) indicated a second stage gross weight decrease to 288,742 pounds from the Class 1 value of 358,113 pounds; the corresponding payloads were as follows:

Class 2 = 53,000 pounds
Class 1 = 68,000 pounds

The reduction in ScramLACE payload performance relative to Class 1 resulted from

1. Decreased supersonic and hypersonic vehicle lift
2. Revised (downward) Scramjet performance (See Section 8.6.2.2.2)
3. Increased tankage weight fractions

8.6.2.9.3 <u>Turboramjet (Engine No. X)</u>

Analysis of the Turboramjet for various maximum airbreathing boost Mach numbers resulted in a maximum performance payload yield of 45,000 pounds for the Mach 8 system, as indicated in Figure 361. The corresponding second stage gross weight was 474,845 pounds. (The Turboramjet system, analyzed on the basis of Class 1 input data, yields a 48,300 lb payload and a 482,920 lb second stage gross weight. The decreased payload was due to a Class 2 staging flight path angle of 5°, as compared to 7° for Class 1.)

8.6.2.9.4 <u>Performance Summary</u>

A comparison of the Class 2 system payload capabilities is presented in Figure 362 as a function of the maximum performance boost Mach number (or staging velocity, in the case of the advanced rocket systems).

A summary of the performance characteristics of the maximum performance systems is presented in Table LVIII. The Mach 12 ScramLACE system is also shown to provide a link for comparison with Class 1.

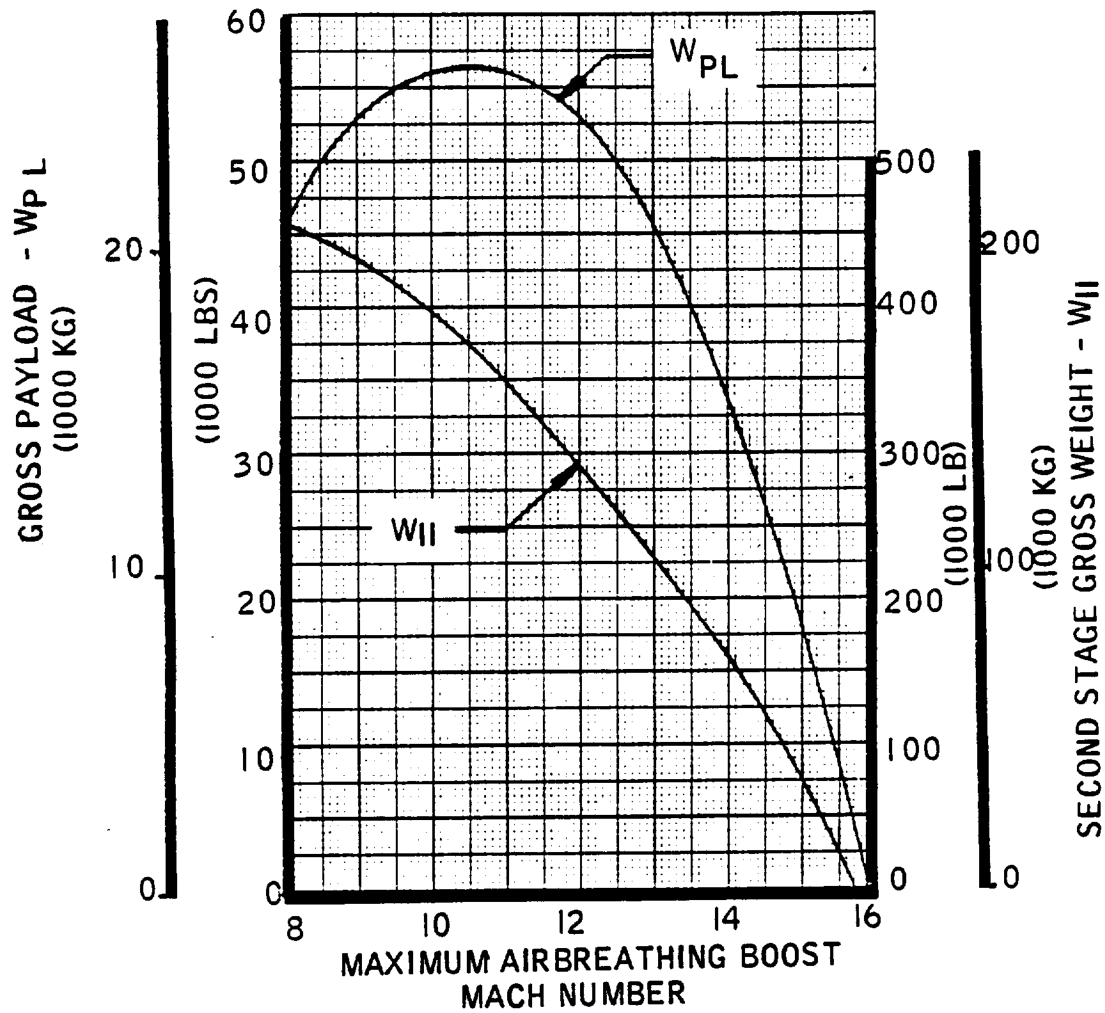

FIGURE 360. System Performance as a Function of Airbreathing Boost Mach Number for the Class 2 ScramLACE (Engine No. 22)

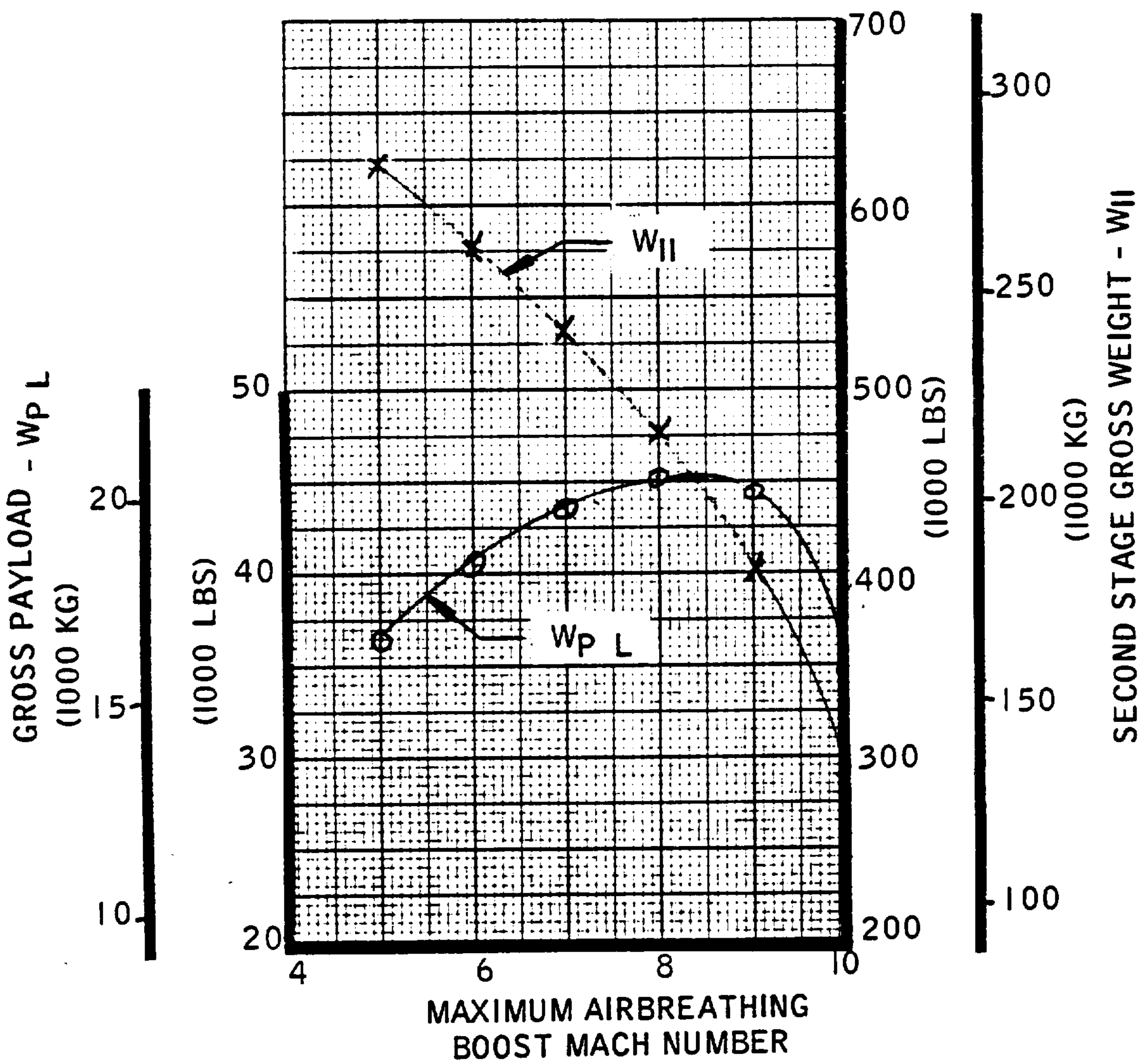

FIGURE 361. System Performance as a Function of Airbreathing Boost Mach Number for the Class 2 Turboramjet (Engine No. X)

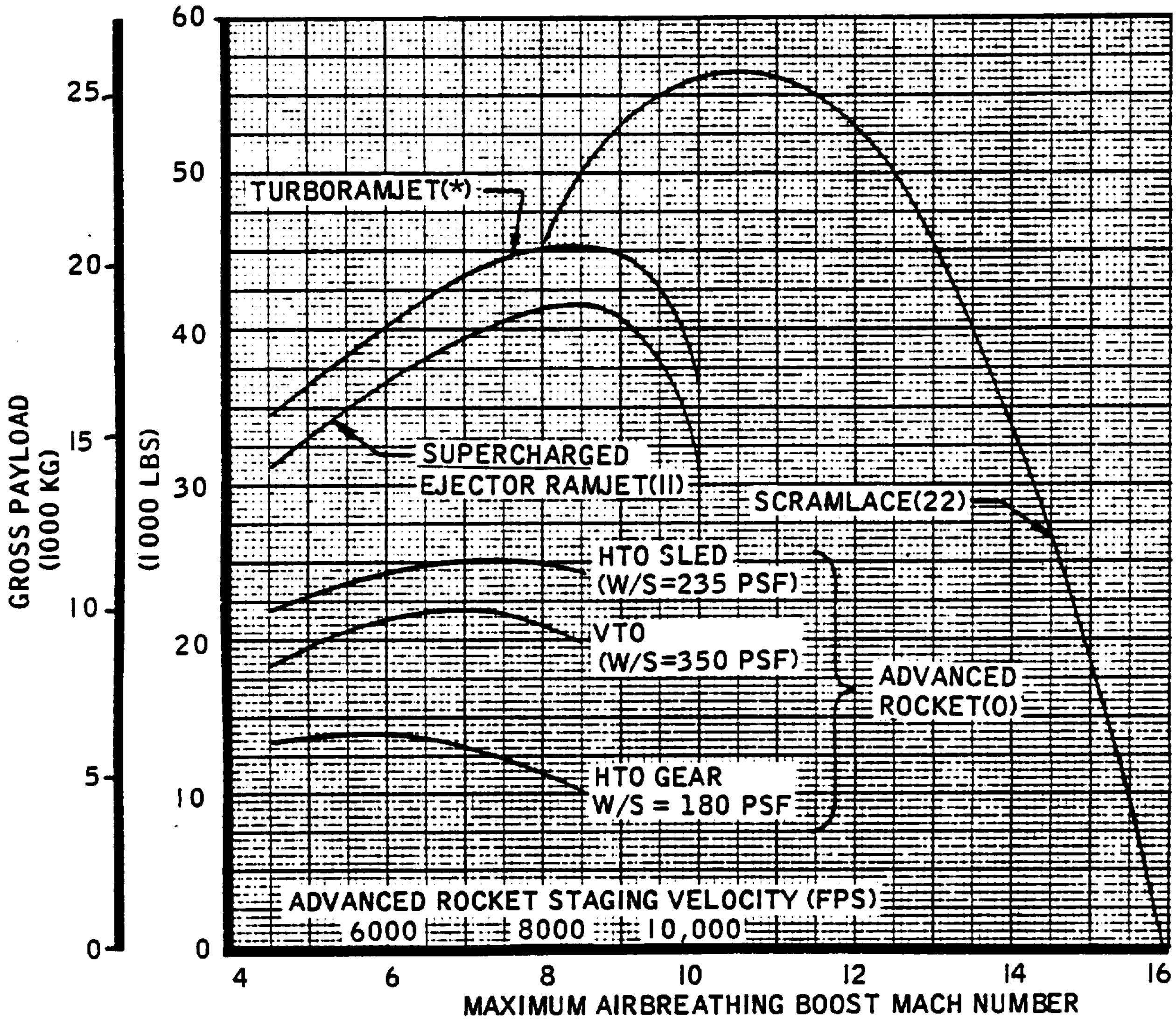

FIGURE 362. Payload Performance Comparison for Class 2 Systems

TABLE LVIII

CLASS 2 SYSTEM PERFORMANCE SUMMARY

(W_o = 1.0 million lbs)

System (Engine No.)	Advanced Rocket (0)			Supercharged Ejector Ramjet	ScramLACE (22)		Turboramjet
	HTO-Gear Takeoff	HTO-Sled Launched	VTO	SERJ (11)	Mach 10	Mach 12	TRJ (X)
SYSTEM							
W_I	708,646	707,355	674,984	554,946	602,427	711,258	525,155
W_{II}	291,354	292,645	325,016	445,054	397,573	288,742	474,845
$W_{Payload}$	13,800	25,100	22,900	41,200	56,000	53,000	45,000
$W_{AB\ max}$	--	--	--	820,202	793,000	740,000	850,136
$W_{STAGING}$	519,511	478,640	487,457	811,344	782,850	726,200	840,955
$M_{AB\ max}$	--	--	--	8	10	12	8
$q_{AB\ max}$ (psf)	--	--	--	850	1,500	1,500	850
$V_{STAGING}$ (fps)	5,500	7,500	6,500	7,751	9,802	11,925	7,751
$q_{STAGING}$ (psf)	75	25	50	200	200	200	200
W_o/S_{REF} (psf)	180	235	350	73.5	73.5	73.5	73.5
1.1 $V_{liftoff}$ (α = 16°) (fps)	400	650	0	405	419	392	423
Takeoff distance (ft)	1,680	4000	0	2,420	2,690	2,200	5,470
Boost Displacement (n. miles)	30	60	55	376	415	740	525
W_{II} Dry	48,498	49,996	53,555	67,334	64,358	52,581	70,799
W_{DRY} Total	245,151	208,604	185,095	421,327	432,107	462,987	419,943
$W_{DRY}/W_{Payload}$	17.76	8.31	8.08	10.23	7.72	8.74	9.33
FIRST STAGE							
$W_{STAGING}$	228,157	185,995	162,441	366,290	385,277	437,458	366,110
$W_{LANDING}$	222,402	177,565	147,659	359,276	373,919	418,315	353,771
W_{DRY}	196,653	158,608	131,540	353,993	367,749	410,406	349,144
$W_{PROPULSION}$	*38,328	*28,906	*31,299	127,832	125,717	134,193	124,356
$W_{HYDROGEN}$	69,034	75,969	80,865	176,571	234,678	300,852	176,011
W_{LOX}	442,959	472,778	462,579	24,382	--	--	--
Cruise range (n. miles)	236	385	307	0	0	215	102
1.1 $V_{LANDING}$ (α = 12°, power off) (fps)	345	354	405	296	302	320	295
PROPULSION							
T/W_o	1.50	1.27	1.50	1.075	1.038	1.108	0.528
T/W_{INSTL}	39.14	43.94	47.92	8.41	8.26	8.26	4.25
A_c (Geometric) (sq ft)	--	--	--	352	408	436	352
$P_{T_2\ max}$ (Inlet diffuser pressure) (psia)	--	--	--	150	120	120	150

*Rocket + Return to base A/B propulsion

The bar chart of Figure 363 presents a comparison of the payload and the hardware cost indicating parameter (system dry weight per pound of payload delivered) for the Class 2 systems.

8.6.2.10 System Sensitivity Study

The Class 2 systems were perturbed for variations in

1. Total aerodynamic drag

2. Propulsion system specific impulse and thrust-to-weight ratio

3. Inert weight elements

to determine the relative system payload performance sensitivities.

The approach to the sensitivity analysis was to perturb the integrated systems for gross percentage variations of the key parameters, rather than to consider each contributing parameter such as combustor efficiency, inlet unit weight, etc. Having established the gross sensitivity, the effects on system payload of individual performance perturbations may then be evaluated as desired

8.6.2.10.1 Ascent Performance Sensitivity

The boost mass fraction variations due to drag and specific impulse perturbations are presented in Figure 364 for the Supercharged Ejector Ramjet (Engine No. 11), ScramLACE (Engine No. 22), and Turboramjet (Engine No. X) systems.

The first stage weight summary presented in Table LIX was developed from the weight estimation procedures outlined in Section 8.6.1.4 and the performance of Figure 364. The stage weight changes due to varying drag and specific impulse mainly reflect the propellant and tankage weight changes. The total installed propulsion weight was varied to arrive at the thrust-to-weight ratio sensitivity.

8.6.2.10.2 Payload Sensitivity to Drag, I_{sp}, and T/W

The effects on second stage gross weight and payload weight due to the drag, specific impulse, and thrust-to-weight ratio perturbation are presented in Figure 365 for the Supercharged Ejector Ramjet (Engine No. 11) system, Figure 366 for the ScramLACE (Engine No. 22) system (Mach 10 and Mach 12 versions), and Figure 367 for the Turboramjet (Engine No. X) system.

8.6.2.10.3 Payload Sensitivity to Vehicle Inert Weight Elements

The effects of vehicle inert weight element perturbations on system payload were investigated on a statistical basis to provide the combined

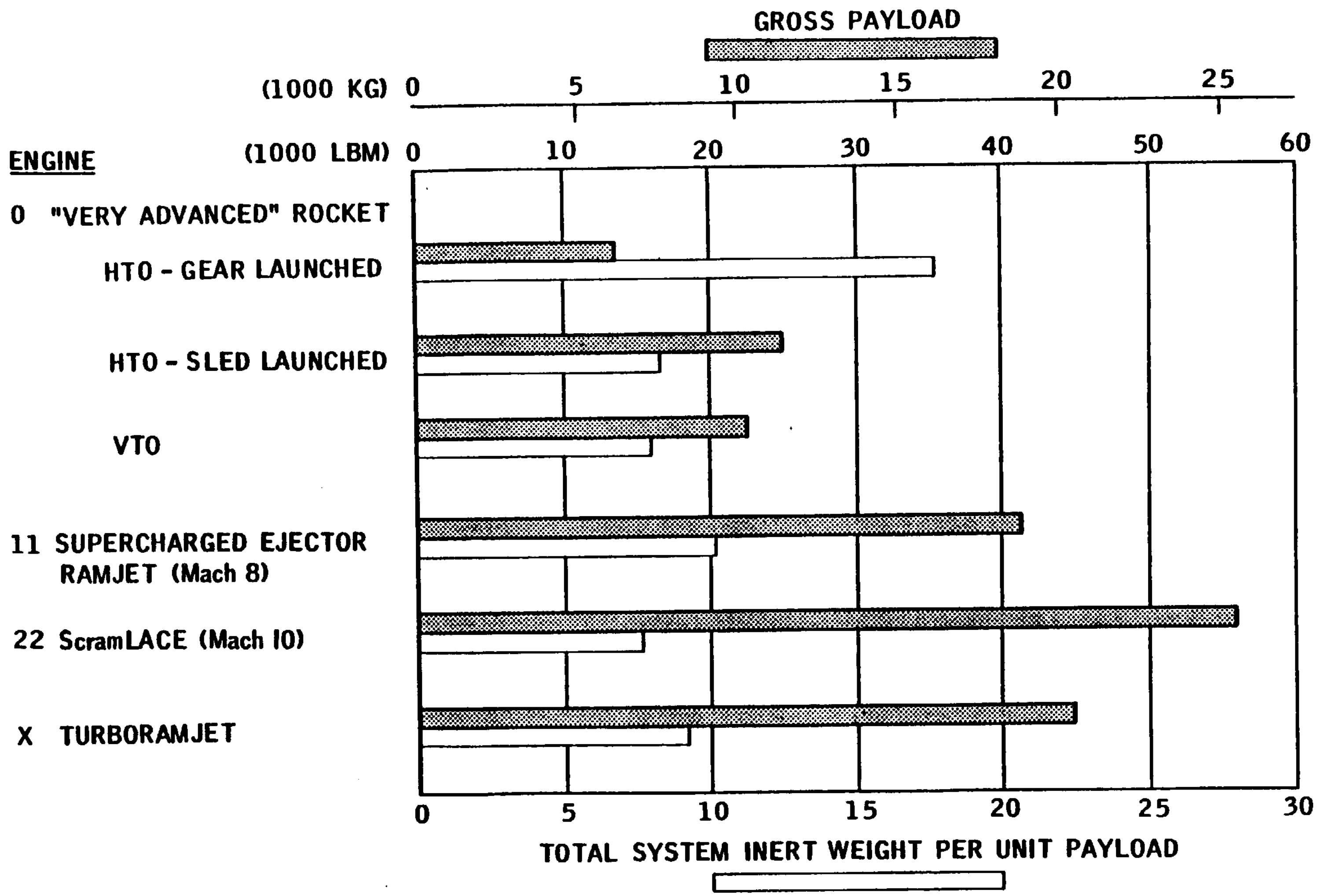

FIGURE 363. Summary of System Payload Performances for the Class 2 Systems

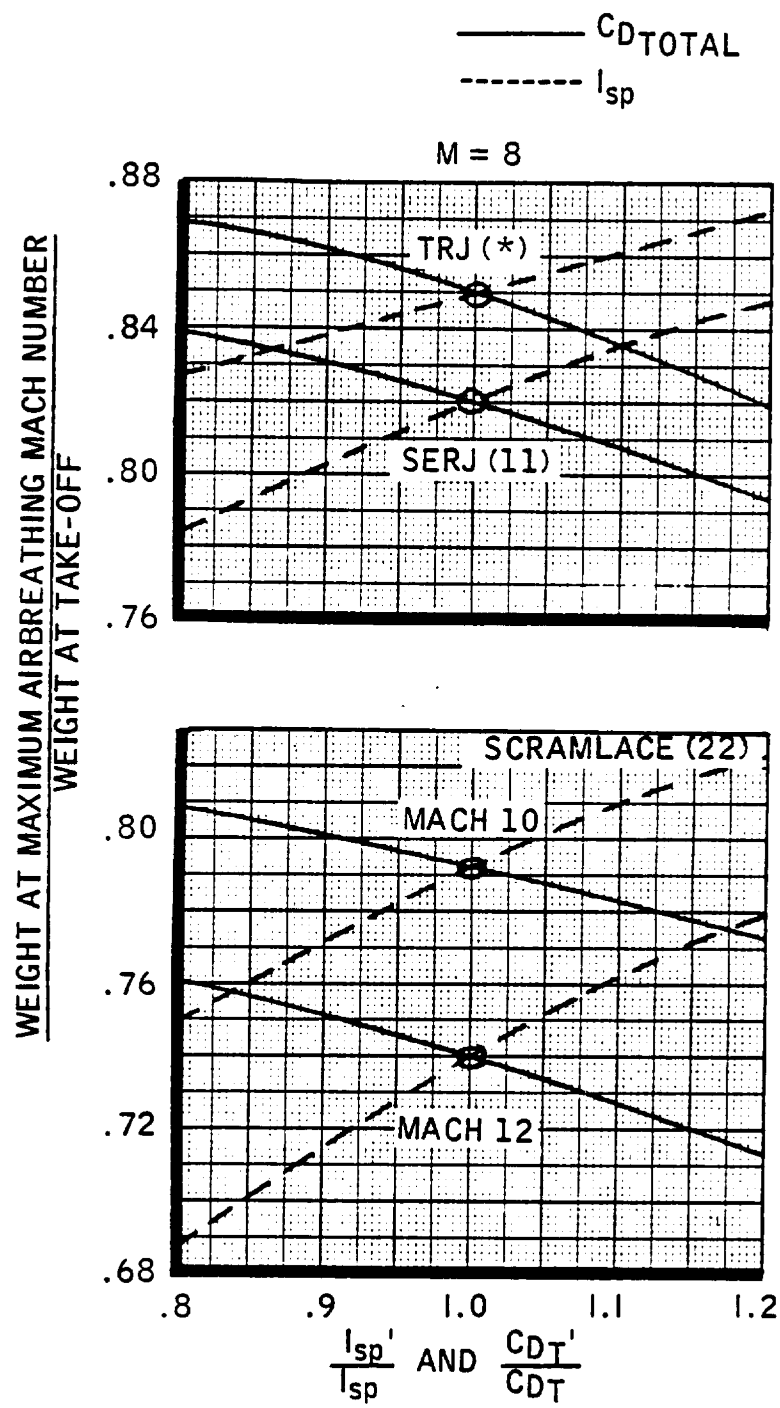

FIGURE 364. Ascent Performance Sensitivity for the Class 2 Supercharged Ejector Ramjet, ScramLACE, and Turboramjet Systems

TABLE LIX

FIRST STAGE WEIGHT SUMMARY FOR CLASS 2 SYSTEMS ASCENT PERFORMANCE SENSITIVITIES

System	M_{AB}	W_{DRY}	W_{LDG}	W_{CRUISE}	W_{bo}	W_I
Supercharged Ejector Ramjet - Basic	8	353,993	359,276	360,429	366,290	554,946
0.8 C_{DT}	8	349,190	353,979	355,115	360,889	531,327
1.2 C_{DT}	8	360,814	366,797	367,975	373,958	588,415
0.8 I_{SP}	8	362,436	368,714	369,898	375,913	601,226
1.2 I_{SP}	8	347,707	352,258	353,389	359,135	520,779
0.6 $T/W)_{INSTL}$	8	442,721	448,051	449,489	456,798	645,454
1.5 $T/W)_{INSTL}$	8	309,615	314,875	315,886	321,022	509,678
ScramLACE - Basic	10	367,749	373,919	379,690	385,277	602,427
0.8 C_{DT}	10	363,611	369,334	375,035	380,553	581,312
1.2 C_{DT}	10	372,964	379,696	385,556	391,229	629,027
0.8 I_{SP}	10	378,777	386,136	392,096	397,865	658,693
1.2 I_{SP}	10	360,031	365,368	371,007	376,466	563,041
0.6 $T/W)_{INSTL}$	10	445,240	461,482	468,605	475,500	692,650
1.5 $T/W)_{INSTL}$	10	323,991	330,125	335,220	340,152	557,302
ScramLACE - Basic	12	410,406	418,315	424,772	437,458	711,258
0.8 C_{DT}	12	405,064	412,397	418,762	431,269	684,002
1.2 C_{DT}	12	416,971	425,588	432,157	445,064	744,747
0.8 I_{SP}	12	423,761	433,110	439,795	452,930	779,385
1.2 I_{SP}	12	400,920	407,806	414,100	426,468	662,860
0.6 $T/W)_{INSTL}$	12	504,181	512,206	520,112	535,646	809,446
1.5 $T/W)_{INSTL}$	12	363,505	371,356	377,088	388,350	662,150
Turboramjet - Basic	8	349,144	353,771	356,408	366,110	525,155
0.8 C_{DT}	8	344,003	348,103	350,698	360,244	499,948
1.2 C_{DT}	8	357,301	362,776	365,470	375,419	565,158
0.8 I_{SP}	8	357,816	363,333	366,042	376,006	567,681
1.2 I_{SP}	8	343,331	347,362	349,952	359,478	496,658
0.6 $T/W)_{INSTL}$	8	435,831	440,540	443,824	455,905	614,950
1.5 $T/W)_{INSTL}$	8	305,786	310,373	312,687	321,199	480,244

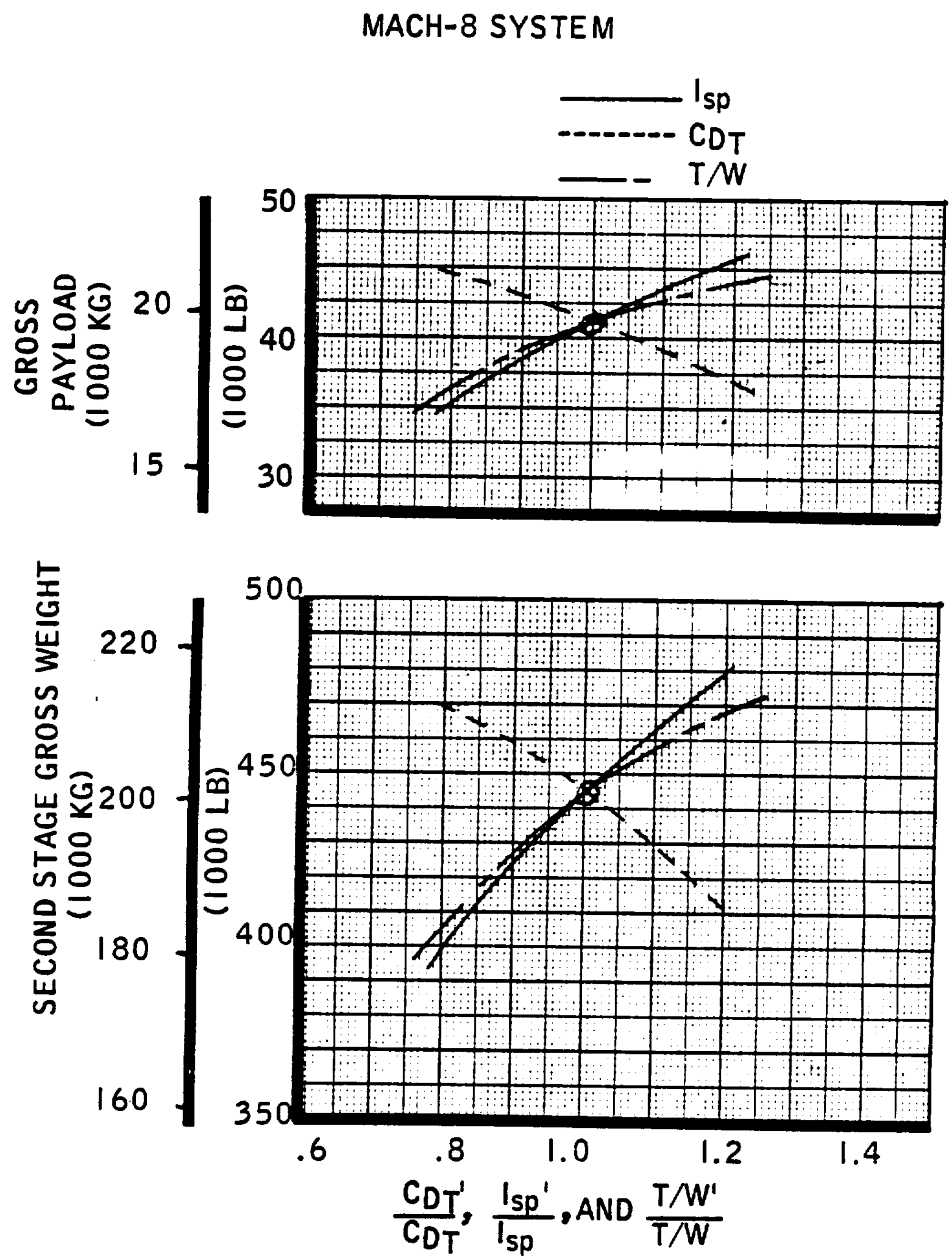

FIGURE 365. System Performance Sensitivity for the Class 2 Supercharged Ejector Ramjet (Engine No. 11)

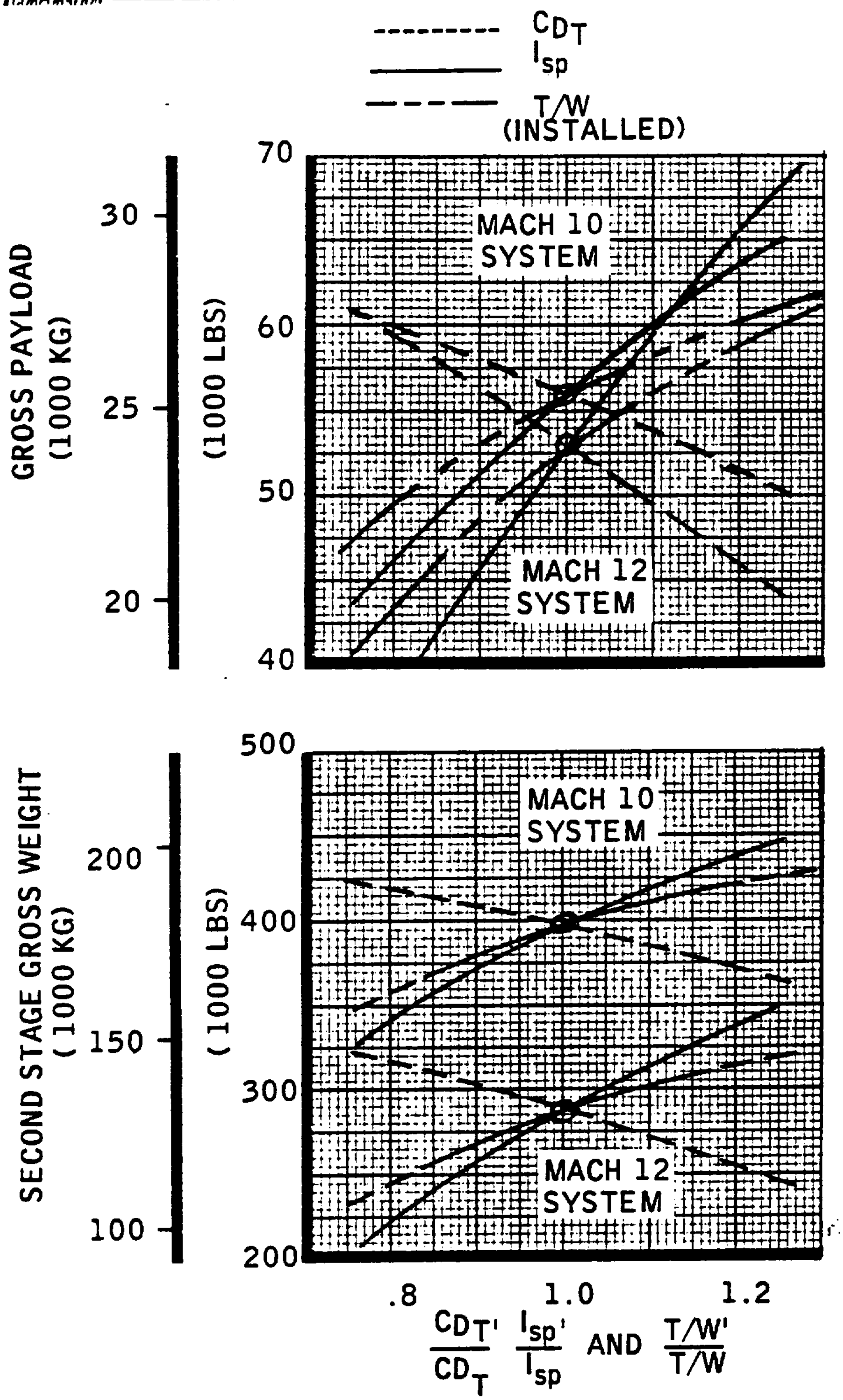

FIGURE 366. System Performance Sensitivity for the Class 2 ScramLACE (Engine No. 22)

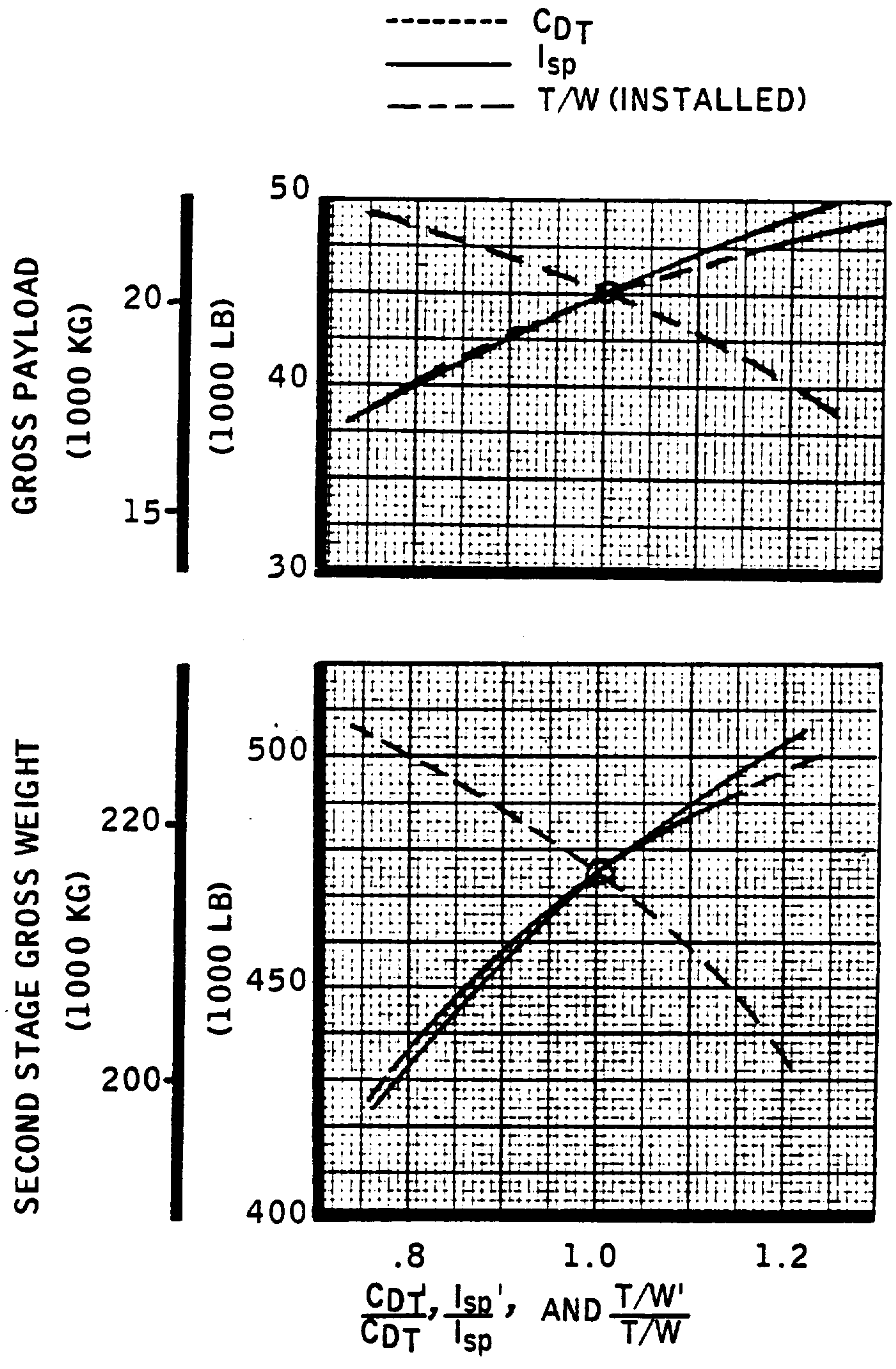

FIGURE 367. System Performance Sensitivity for the Class 2 Turboramjet (Engine No. X)

effect of possible deviations in all first stage vehicle elements. The results are presented in terms of first stage dry weight probability. This is defined as the probability that the first stage dry weight will be within a specific range of weights from the nominal value.

Estimates of the standard deviation (σ) for each of the major vehicle groups are presented in Tables LX through LXII. The weight deviations were derived from historical trends and from comparing flight vehicles with their preliminary design estimates. Assuming the vehicle groups were independent of one another, the standard deviation of the total vehicle is equal to the square root of the sum of the individual group variances. Thus,

$$\sigma_T = \sqrt{\sigma_1^2 + \sigma_2^2 + \ldots}$$

The first stage burnout weight may be expressed as follows:

$$W_{1_{bo}} = K\,W_{PB} + W_D + (1 + K)\,(\Delta W_C + \Delta W_{LD})$$

$$= K\,W_{PB} + W_D + (1 + K)\left[\left(\frac{\Delta W_C}{W_{1_{bo}}}\right) W_{1_{bo}} + \left(\frac{\Delta W_{LD}}{W_C}\right) W_C\right]$$

Substitute

$$W_C = W_{1_{bo}} - \Delta W_C$$

and rearranging

$$W_{1_{bo}} = \frac{K\,W_{PB} + W_D}{1 - (1 + K)\left[\left(\frac{\Delta W_C}{W_{1_{bo}}}\right) + \left(\frac{\Delta W_{LD}}{W_C}\right)\left(1 - \left(\frac{\Delta W_C}{W_{1_{bo}}}\right)\right)\right]}$$

TABLE IX

ESTIMATED WEIGHT VARIANCE FOR THE CLASS 2
SUPERCHARGED EJECTOR RAMJET VEHICLE

Vehicle Element	Weight (lbs)	Standard Deviation σ_n
Body		
Aft structure	55,300	9,954
Tank structure	29,840	3,581
Heat shield	18,600	3,348
Insulation	14,000	2,100
Fins	18,550	3,896
Landing gear	35,700	3,570
Equipment and systems	25,408	3,557
Propulsion		
Engines	47,270	9,454
Inlet	55,770	13,385
Support structure & systems	23,065	3,229
TOTAL VEHICLE DRY WEIGHT	323,503	--
$\sqrt{\sum \sigma_n^2} = \sigma_T$	--	21,100
$\sigma_T/W = 6.5$ percent		

TABLE LXI

ESTIMATED WEIGHT VARIANCE FOR THE CLASS 2 SCRAMLACE VEHICLE

Vehicle Element	Weight (lbs)	Standard Deviation σ_n
Body		
Aft structure	35,200	6,336
Tank structure	48,000	5,760
Heat shield	29,100	5,238
Insulation	25,227	3,784
Fins	24,800	5,208
Landing gear	35,700	3,570
Equipment and systems	26,360	3,690
Propulsion		
Engines	57,335	11,467
Inlet	46,440	11,146
Support structure and systems	11,545	1,616
TOTAL VEHICLE DRY WEIGHT	339,707	--
$\sqrt{\sum \sigma_n^2} = \sigma_T$	--	20,600
$\sigma_T/W = 6.1$ percent		

TABLE LXII

ESTIMATED WEIGHT VARIANCE FOR THE CLASS 2 TURBORAMJET VEHICLE

Vehicle Element	Weight (lbs)	Standard Deviation σ_n
Body		
Aft structure	55,300	9,954
Tank structure	32,800	3,936
Heat shield	23,600	4,248
Insulation	17,863	2,679
Fins	18,550	3,896
Landing gear	35,700	3,570
Equipment and systems	23,430	3,280
Propulsion		
Engines	53,700	10,740
Inlet	67,260	16,142
Support structure and systems	7,045	986
TOTAL VEHICLE DRY WEIGHT	335,248	--
$\sqrt{\sum \sigma_n^2} = \sigma_T$	--	23,600
$\sigma_T/W = 7.0$ percent		

Where

K = Residual and trapped propellant fraction

W_{PB} = Boost propellant

W_D = First stage dry weight

ΔW_C = Cruise propellant

W_C = Weight at end of cruise

ΔW_{LD} = Landing propellant

By using this equation, the effect of the dry weight standard deviation on the burnout weight was calculated. Correspondingly, the change in second stage weight and payload was determined at a fixed takeoff weight. The results of these computations, based on a normal distribution, are presented in Figure 368.

8.7 Conclusions

The Class 2 Systems Study Phase completed the specific propulsion and vehicle investigations of the program with a point design oriented technical penetration. The two representative composite engines, the Supercharged Ejector Ramjet and the ScramLACE, were carried into a detailed conceptual design depth with emphasis on determining subsystem requirements and interaction effects within the engine. The sensitivities to component operating point and process efficiency variations on overall engine performance were ascertained for nominal conditions.

Engine/vehicle integration was completed, both on a physical installation basis and in terms of flight path definition, e.g., maximum airbreathing velocity determination, dynamic pressure, and angle of attack schedules. The rocket and airbreathing comparison engine cases were also refined to the same technical level. Finally, the alternate mission (cruise) capabilities for the two Class 2 composite engines were determined. Supercharged Ejector Ramjet performance (range, endurance) was contrasted with that of the Turboramjet comparison system.

Specific conclusions which were reached during the Class 2 study phase are listed below:

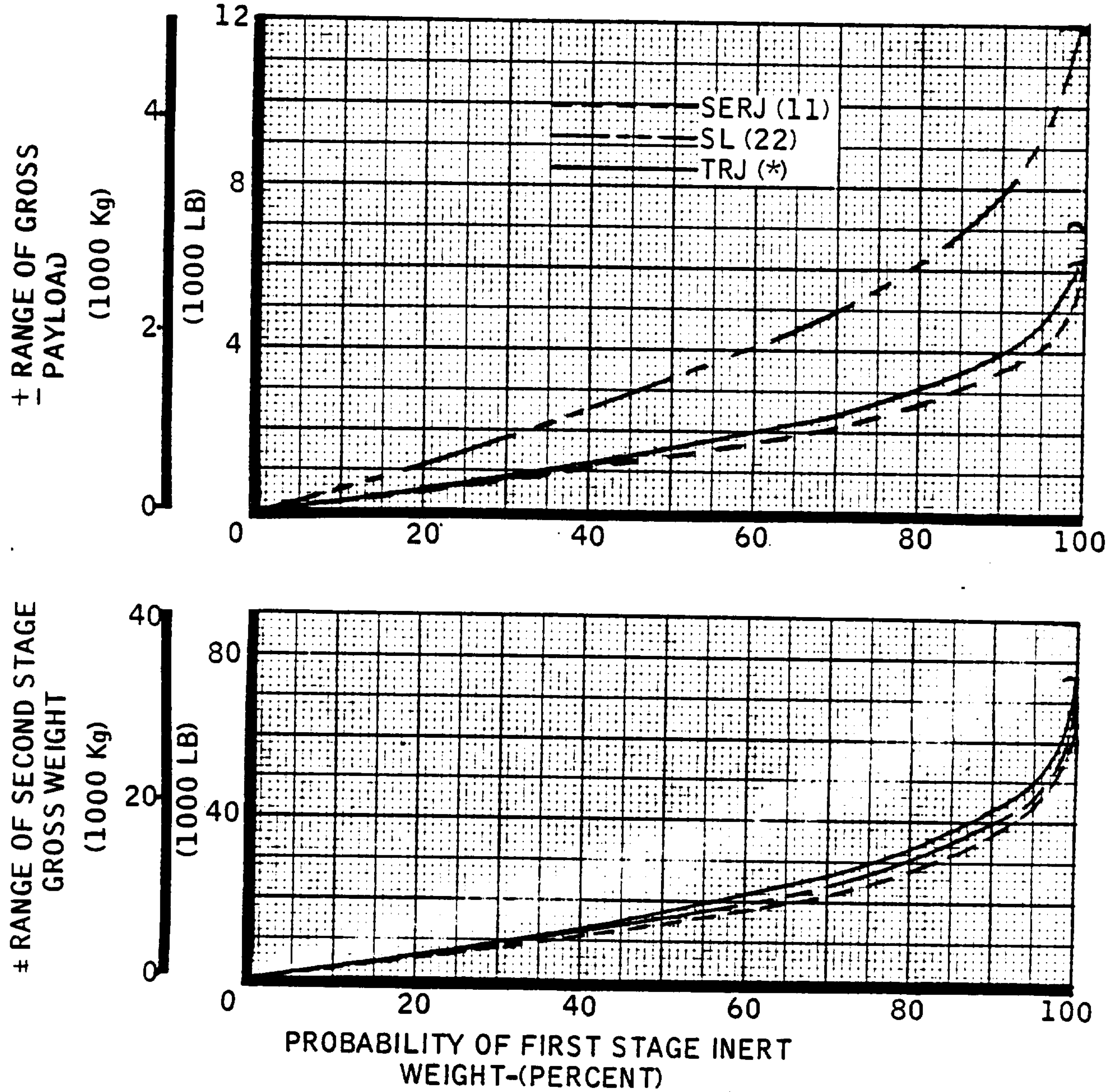

FIGURE 368. Class 2 Systems Sensitivity to First Stage Inert Weight Element Deviations

8.7.1 Engine Related Conclusions

1. The Supercharged Ejector Ramjet (non-Scramjet) engine is most advantageously installed in an axisymmetric arrangement, both for maximum structural efficiency and for geometric compatability with the retractible fan subsystem. On the other hand, the ScramLACE system is very strongly influenced by Scramjet mode requirements resulting, ultimately, in the choice of a two-dimensional arrangement.

2. Engine performance sensitivity to engine component operating efficiencies, e.g., nozzle efficiency (η_N), generally reveals modest trends over the operating limits explored. Significantly stronger effects are revealed for basic engine specifying variables, particularly fan pressure ratio (Engine No. 11) and heat exchanger equivalence ratio (Engine No. 22).

3. Two fan-drive means for the Supercharged Ejector Ramjet are feasible, to the depth of the investigation: (1) airbreathing gas generator (Turbojet) and (2) bipropellant gas generator (akin to conventional rocket turbopump drives). Overall performance considerations during the associated fan operating modes favor the airbreathing gas generator approach as follows: (1) Fan only mode (loiter, landing) - very significant advantage, (2) Fan Ramjet mode - some advantage, and (3) Supercharged Ejector mode - an almost insignificant advantage. Although system weight considerations would seem to favor the bipropellant approach, the method of actually mechanizing the fan drive is unclear (perhaps a gearbox/shaft drive is necessary). On the other hand, the airbreathing approach, viz., tip-turbine aerodynamic coupling is an already demonstrated approach (See later Section 9.2.2 for development status). The weight of the accessory turbojet for driving the fan is modest, being of the same order as the primary rocket turbopump assembly. Were it a thrust producer itself, it would be rated at roughly 5 percent of full engine takeoff thrust.

4. Mechanization of the supersonic combustion ramjet mode in the ScramLACE system (true of Ejector Scramjet based engines also) is conceptually feasible. The chosen approach was (1) phasing the fuel injection and combustion into the (minimum area) mixer section, from the afterburner, to effect a maximum fixed geometry inlet contraction ratio (A_c/A_3), (2) utilizing the external structure of the primary rocket chambers (cooled) for fuel injection, and (3) actuating the variable exit throat to a full-open, minimum blockage position. Further potential for increased contraction ratio would be achieved by partially closing the variable geometry inlet, and injecting fuel at or near the inlet throat. This approach was not, however, incorporated in the design of the engine.

5. Primary rocket problems appear to center about the cooling difficulty posed by moderately high combustion chamber pressure (1500 psia) in hydrogen/oxygen, annular chambers (in Engine No. 11). Limitations posed to the overall powerplant are in terms of (1) ultimate chamber pressure to be chosen, and

(2) length of the mixer, since single annular configurations only, as opposed to a more desirable dual concentric ring, may be in order from throat gap/heat transfer restrictions. The dual concentric approach, or its multiple "Linear Rocket" equivalent (as shown in the ScramLACE design) appears practical for further mixer length reduction in the air liquefaction engines, where the primary cooling problem is far less severe.

6. Stoichiometric hydrogen-oxygen operation (O/F = 8.0) appears to offer no more of a cooling problem than normal rocket mixture ratio (O/F = 5.0 to 6.5) settings, for the same configuration and combustion pressure. The possibility of a slightly more severe tube wall oxidation situation is associated with stoichiometric operation, but no conclusion is tendered, for this program. Also, some indications are found to the point that high combustion efficiency may be more difficult to attain at stoichiometric conditions, as opposed to normal fuel rich conditions. Again no conclusions are made.

8.7.2 Vehicle/Mission Related Conclusions

1. The ScramLACE system yields a greater payload (56,000 pounds) than the subsonic combustion, Supercharged Ejector Ramjet and Turboramjet systems (with payloads of 41,200 pounds and 45,000 pounds, respectively. The Advanced Rocket payloads range from 13,800 to 24,900 pounds, depending on the launch mode.

2. The maximum payload occurs for maximum airbreathing boost Mach numbers of 8 and 10, respectively, for the subsonic and supersonic combustion systems. For the subsonic combustion systems (Supercharged Ejector Ramjet and Turboramjet), decreasing the boost Mach number from 8 to 6 decreases payload by only 11 percent, or approximately 5000 pounds, but allows for utilization of radiation structure on the first stage devoid of advanced and relatively undeveloped materials (coated columbium, etc.).

3. The hardware cost indicator (system dry weight per pound of payload delivered) indicates only a minor variational range from 8 to 10 lb/lb for all systems, with the exception of the HTO gear Advanced Rocket. This type of launch mode excessively penalizes the rocket system (and somewhat penalizes the Supercharged Ejector Ramjet system).

4. The sensitivity studies indicate only a 10 percent reduction (5000 pounds) in payload for a 20 percent degradation in drag, specific impulse, or T/W. A 20 percent increase in ScramLACE I_{sp} increases the maximum performance Mach number from 10 to 12. The vehicle inert weight sensitivity study indicates a 90 percent probability that the payload will be within ± 4000 pounds for the subsonic combustion systems and ± 6000 pounds for the ScramLACE system.

This page intentionally left blank.

9.0 TECHNOLOGY ASSESSMENT PHASE

9.1 General Considerations

The objective of this section is to provide a logical engineering assessment of the state of the technology for possible future development of composite engine propelled launch vehicles. It is not the intention to comment on the national space program as a whole, nor to argue or comment on the relative merits of composite engine powered launch vehicles as compared to more conventional propulsion and launch vehicle approaches. Attention will be focused upon composite engine oriented systems with primary attention given to those items of technology which are unique to composite engines. It is the intention to identify those items of technology which are critical to the development of composite engines and, in particular, technology which is associated with advanced airbreathing and rocket engines in general, including that being developed under programs currently being funded.

In this regard, plans for developing composite engine propelled launch vehicles will be given only in a gross sense, with attention focused upon near-term planning in the next few years for those items of technology identified as being critical with respect to the need to reestablish the feasibility and practicability of the approach. It will be obvious from the large amount of documentation presented on cycle performance, operating characteristics, and vehicle application studies, that the majority of the funds of the current program were devoted to that kind of activity, with a lesser portion devoted to the technology assessment effort. Thus, the depth of these survey and planning studies was inherently limited by the design of the program. Furthermore, these studies were in some aspects limited due to the lack of full access to state of the art component investigations, development status, and cost data from other companies. On this basis, the survey studies were, to some extent, limited. Further, emphasis was placed on near-term activities.

To properly orient this section, it is of interest to review a preliminary system component weight and cost estimation made by Lockheed in a prior launch vehicle system study (References 19 and 26). In that study, the influences of several components were assessed for a reusable orbital transport with a Mach 8 airbreathing engine propelled first stage. The analysis was with respect to the relative systems contribution to:

1. Total system gross weight

2. First stage vehicle cost

3. Total system RDT&E cost (several billions of dollars)

4. Percentage of individual component RDT&E times the estimated development span

The results are presented in Table LXIII.

TABLE LXIII

RELATIVE COMPONENT INFLUENCE FOR A REUSABLE ORBITAL TRANSPORT

Vehicle Component	System Gross Weight (percent)	First Stage Vehicle Cost (percent)	System RDT&E Cost ($3x10^9$) (percent)	System Development, $/Year (percent)
First Stage				
Equipment	5.9	23.6	14.9	10.1
Takeoff gear	3.6	7.7	1.0	0.3
Fixed & variable	2.3	15.9	13.9	9.8
Fuselage	8.8	18.6	9.0	5.4
Basic shell	3.5	6.1	1.5	0.5
Hydrogen tank	3.7	7.7	7.0	4.6
Shielding	1.6	4.8	0.5	0.3
Wings and fins.	8.2	17.5	4.5	2.6
Basic structure	5.2	10.1	2.0	1.0
L. E. caps	1.0	2.8	2.0	1.3
Shielding	2.0	4.6	0.5	0.3
Propulsion system	15.5	40.3	28.3	24.8
Powerplant	9.0	27.0	18.3	19.9
Inlet	6.5	13.3	10.0	4.9
Propellant (H_2)	18.0			
Second Stage	43.6		43.3	57.1

It should be noted that the largest contribution to the total dollar/year development cost (57 percent) and system gross weight (44 percent) is made by the second stage. However, in accordance with the emphasis given to composite engines here, the technology implications of utilizing composite engines in a two-stage orbital vehicle are reflected almost exclusively in the first stage. Therefore, the technology assessment will be made on the first stage basis. The airbreathing propulsion system contribution to the first stage vehicle cost is 40 percent, and 25 percent to the total development dollar/years. For this reason, and because the total launch vehicle concept is dependent upon the nature of the propulsion system, it would appear that the primary emphasis on first stage development should be placed on the propulsion system.

This study has indicated favorable characteristics for the application of composite rocket-airbreathing engines to launch vehicles in the 1.0 million pound takeoff weight class. To a large degree, these types of engines represent a relatively new technology. While there is a limited design and component research background related to the Ejector Ramjet and Liquid Air Cycle Engines, the conceptual studies of this composite engine program have shown a clear need for greater breadth and depth in the design and vehicle integration of propulsion systems for these advanced applications. Many of the components which are required for composite engines are based upon technologies which are currently being developed for other propulsion system types (rocket, ramjet, Scramjet, etc.). While this background has been valuable for the current study, it is pertinent to review the broad and specific technology implications relating to the engines which this study has indicated to have the greatest promise.

It will be recalled that 36 engine types were considered in the Class 0 study. The number of engines evaluated was reduced to 12 in the Class 1 study, and further reduced to two types for the Class 2 study. It was the objective to progressively eliminate the less promising engine types to permit increased depth of penetration as the study progressed. In a real sense, the Class 1 engines represent broadly the more attractive composite engines, and they should therefore be examined for technology implications. However, the degree of penetration aspect favors emphasis on the Class 2 engines for this purpose. Moreover, it is not necessary to make a firm distinction in terms of overall technology requirements, since the two Class 2 engines include essentially all of the critical components which are required for one or another of the 12 Class 1 engines (the exception is recycled hydrogen operation).

The morphological chart shown in Figure 369 illustrates this component technological commonality between the two Class 2 engines and the other ten engines involved in Class 1. Except for the fan and air liquefaction, there is a general across-the-board technological similarity for all systems. For the two remaining technologies, the fan is covered in the Supercharged Ejector Ramjet, and air liquefaction is covered by the ScramLACE engine. Thus, it is possible to concentrate the greater effort on the two specific (but widely

CLASS 2 ENGINES

Technology	Engine Number	9	10	11	12	21	22	23	24	29	30	31	32
	Engine Symbol	ERJ	ESJ	SERJ	SESJ	RL	SL	RRL	RSL	SRL	SSL	RSRL	RSSL
DESIGN STUDIES		X	X	X	X	X	X	X	X	X	X	X	X
INLET		X	X	X	X	X	X	X	X	X	X	X	X
FAN				X	X					X	X	X	X
AIR LIQUEFACTION						X	X	X R	X R	X	X	X R	X R
PRIMARY ROCKET		X	X	X	X	X	X	X	X	X	X	X	X
AIR AUGMENTATION		X	X	X	X	X	X	X	X	X	X	X	X
COMBUSTION RJ/SJ		X	X	X	X	X	X	X	X	X	X	X	X
EXIT NOZZLE		X	X	X	X	X	X	X	X	X	X	X	X
STRUCTURES, COOLING MATERIALS		X	X	X	X	X	X	X	X	X	X	X	X
CONTROLS, AUXILIARY POWER		X	X	X	X	X	X	X	X	X	X	X	X
CRYOGENIC PROPELLANT TECHNOLOGY		X	X	X	X	X	X	X SH	X SH	X	X	X SH	X SH

LEGEND:

X = Required
R = Recycle
SH = Slush hydrogen

FIGURE 369. Commonalities of Class 1 and Class 2 Engine Component Technologies

different) Class 2 engine types to analyze the essential technological base for the broader spectrum of engine types. It is upon this premise that the technology assessment which follows is made.

Figure 370 graphically illustrates the specific areas to be covered in the following text. In addition to the individual component technologies, two systems oriented activities will be discussed. They are (1) vehicles and application, and (2) engine activities. While a considerable part of the current study was fundamentally concerned with these two areas, these efforts were directed toward the broader aspects of the problem. In the future, it will be essential to conduct more detailed engine design work to take advantage of the latest developments in all areas, and it will be equally important to evaluate the significance of the various supporting activities in terms of application to the vehicle system.

It is the objective of this section to critically review (1) the propulsion system and component technology requirements, (2) the status of available data in each pertinent area, and (3) the status of programs known to be in progress. From this base, a projection will be made to delineate those areas requiring additional study and research, where possible, in terms of the degree of technical criticality. The results of this analysis, then, can be used for general planning purposes for future programs.

The degree of criticality will differ for various engine concepts, particularly with respect to time. In the case of each area covered, an assessment will be made relative to the state of the art and, where pertinent, the relative dollar value of research and development which is being conducted in other programs. Each area or subarea will be identified in one of the following terms of decreasing emphasis: (1) critical, (2) first order, and (3) second order. Following the individual technological assessments, an integrated programmatic evaluation will be presented from the perspective of overall planning implications, both near-term and future. The individual technology area assessments follow.

9.2 Technology Areas

9.2.1 Inlet Technology

9.2.1.1 Significance

Composite engines intrinsically operate as a group in conventional airbreathing (e.g., ramjet) or "air using" (e.g. Air Augmented Rocket) modes at one point or another in the launch mission profile. Hence, an air induction subsystem is invariably required for the installed composite powerplant. The wide range of flight speeds over which the composite engine is required to operate (Mach 0 to Mach 8 or higher) imposes challenging inlet requirements with respect to capture area and geometry. Since inlet weight

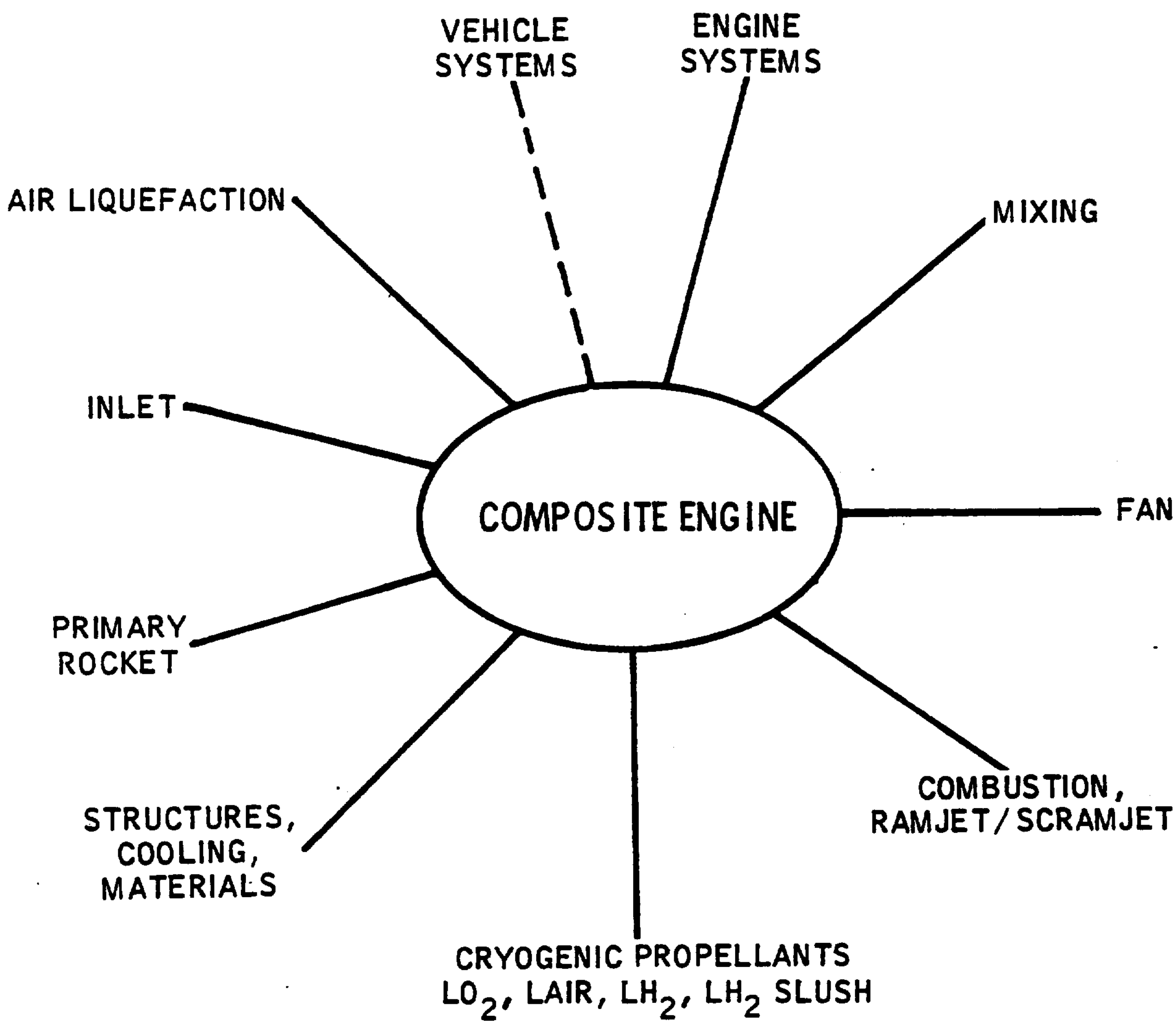

FIGURE 370. Related Technology Areas for Composite Engines

and complexity can be a major factor, it is of high order of importance to generate the simplest, lightest, and most effective concept when considering all of the factors of the propulsion-vehicle system and the mission.

9.2.1.2 Technology Status

The more attractive composite engine concepts have been determined to require a reasonably efficient air induction system throughout the speed range from sea level static conditions to the staging point at Mach 6.0 (minimum) or Mach 12. In appraising present day inlet technology, nowhere is there to be found an all-round satisfactory inlet concept capable of meeting this requirement.

A recent survey of the state of the art of inlet technology as recorded in extant references was performed by the Lockheed Missiles and Space Company under a NASA Marshall Space Flight Center Contract (Reference 50). A general conclusion given in this reference is that there are two major problem areas in supersonic and hypersonic inlet designs: (1) inlet boundary layer and (2) real gas effects. A very recent popular summary of high speed inlet status is that of Reference 51.

Quoting from the introduction of a recent United Aircraft Corporation Research Laboratory paper (Reference 52):

> "Airbreathing Propulsion Systems which operate over a wide Mach number range require high inlet performance over the entire speed range for efficient operation. Present day inlet technology enables good design point performance to be obtained at supersonic or hypersonic speeds; however, inlets designed for hypersonic Mach numbers have exhibited poor performance off-design, especially in the low supersonic speed range. There is a paucity of data in the existing literature relative to inlet configurations having a wide range of efficient off-design performance."

The experimental work reported in the above paper centered about the dual mode subsonic-supersonic combustion ramjet application in which the initial accelerating engine was of a turbojet type. The composite engine inlet problems are similar to those encountered by a turboramjet system, although the requirement for processing less air in the transonic region may result in a simpler inlet for the composite system. Also, yet to be validated, composite systems may be significantly less sensitive to inlet diffuser flow distortion. There is implied by this point a possibility of using shorter, lower weight inlet diffusers as compared to typical turbomachine required systems. On the other hand, there exists a probable need to effect closure of the inlet following airbreathing termination in order to withstand entry conditions, and to preclude cooling of the engine during non-propulsive phases of the mission. The single approach reflected in the study, and one which has

a demonstrated capability for responding to the diverse requirements is the two-dimensional, moving ramp, mixed compression type variable geometry inlet. This approach was used in the vehicle integrated engine designs given in this report.

A general status report on inlet technology which addresses certain composite engine requirements by way of specific designs (conventional and unconventional) is presented in Reference 53. Only the Hyperjet (Engine No. 1) and the basic Liquid Air Cycle Engine (Engine No. 3) inlets are directly discussed in the above report. Considerable emphasis is given also to the implementation of subsonic combustion ramjet inlets. However, supersonic combustion ramjet requirements are not reflected.

9.2.1.3 Critical Area Assessment

For advanced composite engine installations, particulary those which involve the supersonic combustion ramjet mode, there is a compelling requirement for physical integration of the vehicle, engine, and inlet. Vehicle forebody precompression ahead of the inlet cowl is mandatory for practical applications of this type. Therefore, inlet designs will remain a prime concern of both propulsion and vehicle contractors, with both recognizing the need for an integrated attack on the problem.

There is much room for mechanical ingenuity in terms of inlet designs to achieve both wide range efficient operation and low weight. This point is suggested in the inlet concept for the Marquardt axisymmetric VTOL single stage to orbit concept shown in Appendix E. Here a somewhat specific (though largely problematic) approach for mechanizing the composite engine's wide range inlet requirements is projected, attempting to take full advantage of vehicle flow field compression ahead of the individual module cowls. The concept is perhaps exemplary of a need for considerable mechanical ingenuity to accomplish lightweight, acceptably simple physical concepts.

The integrated, or two-dimensional type inlet has been shown in this study to be generally superior to the separate or pod mounted axisymmetric inlet approach (See Section 7.6.2.3.3). However, it is not without its problems: advanced materials and manufacturing techniques required for low weight designs, internal and external boundary layer control and removal, cooling circuits, reliability of actuation, and control of contour with adequate dynamic response, etc.

9.2.1.4 Future Program Implications

It is apparent that significant work should be done relative to basic inlet design concepts and performance together with investigations of means of mechanization of the more attractive approaches. This work can, by and large, stem from continuing research in the inlet area, but some effort

should be apportioned to obtaining a satisfactory solution to both the general problem associated with composite engines (namely, very wide range operation) and the special problem of a particular vehicle design and mission profile which might entail composite propulsion, such as the possible need for inlet closure during the staging pull-up and entry.

9.2.2 Fan Technology

9.2.2.1 Significance

Inclusion of low pressure ratio, lift/cruise type fans in the composite engine provides two distinct advantages. These are (1) provision of an optimum propulsion mode for low speed loiter and landing and (2) increased initial acceleration performance. This capability is achieved without compromising the high speed ramjet mode potential via retraction of the fan into the adjacent structure. The acceleration mode advantage breaks down into two basic contributory aspects: (1) addition of a second stage of compression ahead of the jet compressor (Air Augmented Rocket section) which yields increased specific impulse during the Supercharged Ejector mode, and (2) provision of an intermediate Fan Ramjet mode which permits transition from the high propellant consumption ejector mode at an earlier point in the flight profile than is possible without the fan (ramjet takeover point).

9.2.2.2 Technology Status

The candidate fan concepts considered in the composite engine program were derived from the technology and development currently being performed on lift/cruise fans for aircraft application. The most advanced application of the fan subsystem actually demonstrated to date is the propulsion system for the Army's XV-5A research aircraft. This Ryan aircraft is powered by two J85/LF1 convertible lift fan systems provided by the General Electric Company and it has completed its initial exploratory flight tests. The XV-5A utilizes three thin profile, single stage, low pressure ratio (1.1 to 1.15) fans for vertical takeoff and landing operation. Two larger fans are located in the wings of the aircraft and a smaller third fan is located in the nose section to provide a balancing control moment for stability purposes as well as for lift. The entire system is driven by two small turbojet gas generators (J85) mounted remotely from the fan systems. Connecting ducting is capable of being valved off to provide the J85 as a straight turbojet propulsive device once the aircraft reaches transition speed. The fans are tip-turbine driven, low hub-to-tip ratio devices.

The cruise fan technology derives from the lift fan. In this instance, the fan is used for normal forward propulsion for subsonic flying vehicles and is fixed in nacelle type installations. These high bypass lift/cruise fans feature overall bypass ratios (fan air/gas generator air flow) of 8 to 12. Current work, particularly for cruise fan applications, is concentrated on

pressure ratios of 1.3. The newer configurations accordingly have a somewhat higher hub-to-tip ratio (0.5) as compared to 0.4 for the lower pressure ratio lift fans. A comprehensive summary of lift/cruise fan state of the art is presented in Reference 54. Results of installed cruise fan testing conducted in the Ames low speed wind tunnel are reported in Reference 55. Informative surveys of the lift fan technology are provided in References 22 and 56.

A level of cruise fan technology which will correspond to that considered for the composite engine designs should be achieved as a result of current efforts by the General Electric Company. Sponsored by the United States Air Force, exploratory development of an 80 inch tip diameter cruise fan is under way which will provide a pressure ratio in excess of 1.3. (Reference 54)* An advanced J79 gas generator will be utilized to power the fan which will produce 27,000 pounds sea level static thrust. A follow-on flight test demonstration is also under consideration. Further technology developments beyond that program have also been considered. These, in the main, concentrate on decreasing the weight and increasing the performance of the fan subsystem with particular emphasis on the improvement of the airbreathing gas generator. For example, the General Electric Company has considered its GE-1 turbojet, an advanced concept engine, for use in a modified form for driving a large cruise fan.

9.2.2.3 Critical Area Assessment

A salient area to be investigated in lift fan technology in order to make it adaptable to the composite engine application is in higher Mach 2.5 to 3.0 air temperature operation. The fan, of course, being behind the inlet diffuser processes only subsonic air. However, the air becomes increasingly hot due to the stagnation temperature increase with Mach number. An assessment of the increased temperature requirement effect on the fan design and weight should be made.

Techniques for moving the fan by way of retracting it from the main flow stream of a composite engine have already been treated conceptually for certain VTOL applications. Reference 56 reflects an aircraft concept in which fuselage mounted fans are rotated about the trunnion joints (which duct the airbreathing gas generator to the tip turbine) to stow these fans flush into the fuselage for high speed operation. As will be noted, it is this basic approach which is being considered here for the composite engine. The fan retraction concept itself is credited to the Air Force Aero Propulsion Laboratory at Wright-Patterson Air Force Base. Mechanizing removal and closure or protection of the fan from the high flight speed flow passage of the engines appears feasible but requires further design studies and practical demonstration.

- - - - - - - - - - - -

* It is interesting to note that the 80 inch diameter and 1.3 pressure ratio are exactly those utilized in the Class 2 Supercharged Ejector Ramjet engine design shown in Figure 274.

An area of technological interest may result from the interaction between the fan discharge air and the rocket exhaust in the basic jet compressor. It is expected that the operating fan ahead of the primary rockets will act, or can be caused to act, as a "dynamic turbulator" which may accelerate air-rocket gas mixing, providing an opportunity for shortening the mixer. Another interaction which must be considered in the design of supercharged composite engines is the effect of the gas generator turbine exhaust being released into the mixing section of the engine. Engine designs evolved in this program reflect an annular exhaust at the external plane of the fan subsystem from which the turbine gas is exhausted axially back along the mixer walls, possibly adding a minor ejector effect in itself (See Figure 274). In connection with this, it will be noted that employing an airbreathing gas generator drive means that the turbine exhaust gases are lean and, therefore, no excess fuel is injected into the mixer to cause degradation of cycle performance (See discussion in Section 7.2.2.1 and Figure 57). If bipropellant gas generators are considered (those which operate fuel rich) it is likely that the turbine gas should be ducted elsewhere, either to the afterburner or to an overboard dump in order not to "spoil" the afterburning cycle augmentation process. If, on the other hand, the simultaneous mixing and combustion cycle is utilized, there may be no problem with this fuel addition at the rocket station.

In technical circles, the achievement of the required cruise fan development (except for high temperature capability) is associated with a 1968 time period. It is this 1968 technology level that was used as a basis for supercharged composite engine designs of the present study. One additional development would be required before the fan technology area is satisfied with respect to the study assumptions, namely, a hydrogen conversion of the gas generator, currently running on hydrocarbon fuel. Based on the significant experimental development history of hydrogen fueled turbomachines, such a hydrogen conversion does not appear to offer any serious technology uncertainties. See Reference 57 for discussion of such a conversion of an existing turbojet engine circa 1956.

9.2.2.4 Future Program Implications

The following lift/cruise type fan technology achievements are indicated to be of first order significance in achieving a composite engine preliminary engineering basis:

1. Feasibility determination of high temperature fan operation associated with flight speeds up to about Mach 2.5

2. Evaluation of possible fan induced rocket/air mixing benefits (viz., shortened mixer), and assessment of other interaction effects, if any, such as turbine exhaust effects on the mixer

3. Determination, to a significantly higher degree of authority, of fan drive approaches including both airbreathing and bipropellant gas

generators. Unconventional approaches should also be included, e.g., "pinwheel" drive.

4. Development of criteria for the selection and detailed design of fan stowage mechanization approaches. Also, ramifications of fan freewheeling in place should be examined. Alternate approaches should be sought and evaluated, e.g., blade folding or retraction.

9.2.3 Air Liquefaction Technology

9.2.3.1 Significance

The ejector type engine which uses a liquefied air-hydrogen rocket has been shown to have an increased vehicle payload in orbit potential with respect to non-liquefaction systems. The Class 1 payload comparison of Figure 212 clearly delineates this trend. The effectiveness of the RamLACE/ScramLACE engine family depends upon the development of lightweight, high performance heat exchangers, effective anti-icing, and advances in the hydrogen para-ortho catalyst technology.

Capitalization on the air liquefaction process as a means of achieving a high performance, lightweight engine is essentially unique to the composite engine domain, although exceptions exist, e.g., the Liquid Air Turborocket.

9.2.3.2 Technology Status

Intrinsic in the RamLACE/ScramLACE type cycles investigated in the current program is the air liquefaction heat exchanger subsystem. This unit operates from takeoff through the initial acceleration mode of the engine up to flight speeds of Mach 2 to 3. Thereafter, the heat exchanger subsystem is deactivated and remains inactive until, in some instances, the vehicle enters the return flight and loiter phase of the mission profile. This discussion does not include other air liquefaction applications, for example, air collection and enrichment systems which are beyond the scope of the program (Section 3.1.2).

9.2.3.2.1 Design

A significant analytical, design, and experimental background exists for air liquefaction heat exchangers for propulsion system applications. Reference 14 presents systematic analytical and experimental evaluations of various heat exchanger precooler and condenser unit tube matrices. The referenced report presents tabulations of the heat transfer coefficients which permit the design of heat exchanger systems applicable to any required air flow rate. There is, to the extent of documentation such as Reference 14, a sound extant engineering basis for the design and fabrication of experimental lightweight air liquefaction units.

The initial work with air liquefaction heat exchangers was directed toward the fundamental Liquid Air Cycle Engine (LACE) which was Engine No. 3 in the Class O study. A number of experiments were conducted by The Marquardt Corporation, the culmination of which was the 1961 demonstration of a 16 sq in. face area (4 in. by 4 in.) precooler and condenser assembly which was connected to a small hydrogen-air combustor for demonstration firings. A representative LACE engine design is described in Reference 58. The heat exchangers for this engine were placed in a cruciform arrangement to form a minimum diameter cylindrical engine which could be mounted externally in a pod installation.

More recent design studies have determined that improvements in the weight characteristics of the heat exchangers packaging is possible. A number of these were explored in Reference 17. A specific design of a flat face heat exchanger was made to determine the minimum heat exchanger weight possible with no restirctions on diameter. This condition might correspond to the engines treated in the current study in which an internal vehicle installation is considered, as shown in Figure 163. The design was created for the Nuclear Liquid Air Cycle Engine studied and reported in Reference 15. A low speed design utilized precooler installations with beryllium finned, 6061 aluminum tubes and a bare tube aluminum condenser. The precooler shell was titanium, with the remainder of the structure being aluminum. A significant advancement in heat exchanger installed weight was reflected in Reference 15.

Other structural approaches have been analyzed and experimental fabrication work has been accomplished on three basic configurations: (1) bare tube, (2) finned tube, and (3) plate foil. The bulk of the work accomplished to date has been performed with bare tubes and finned tubed units. The potential of the three fabrication approaches has been compared on the following basis: weight and volume, price per pound, (for both experimental, low production, and high production operations) and the reliability potential of the units, (susceptibility to mechanical shock, thermal distortion, and vibration).

9.2.3.2.2 Fouling and Icing

Following the initial basic LACE oriented investigation of heat exchangers, the more complex, higher performance potential of air collection and air separation systems came into focus under the general Aerospaceplane technology activity circa 1962-1964. During this period, the susceptibility of the heat exchangers to atmospheric ingredient fouling was found to be of major concern. The fouling occurs in two different flight condition regimes: (1) low flight speed-low altitude takeoff and initial acceleration has icing problems due to the atmospheric water vapor content at low altitudes even with total flight time in this regime, and (2) long term, high speed, high altitude air collection has a carbon dioxide accumulation problem as the concentration of carbon dioxide does not decrease significantly with altitude as does the

water vapor content. The momentary icing regime, at the initial takeoff condition and extending to roughly 20,000 feet altitude, appears to be capable of practical solution within a system connotation. The problem of capturing and momentarily carrying ice in the system appears to be a minor one with respect to any payload penalty. However, the potential of malfunctioning or degrading the heat exchanger subsystem by virtue of ice pickup remains unanswered. A number of approaches other than ice collection are available for alleviating heat exchanger fouling, most of which were tested to some extent during the air collection system experimental investigations reported in References 59 and 60. Representative water and carbon dioxide icing alleviation methods which were evaluated included spray deicing, cyclic deicing, coated surfaces, and ultrasonic vibration of the precooling and ice condensing surfaces. The first two methods appeared the most promising. However, cyclic deicing presents an increased heat exchanger requirement or a periodic reduction or cessation of liquefied air.

9.2.3.2.3 Para-Ortho Catalyst

The consideration of catalysts in the air liquefaction unit stems from the very fundamental advantage of utilizing the highly endothermic para-to-equilibrium conversion of hydrogen (in effect a para-ortho conversion since equilibrium hydrogen comprises both forms at the temperature considered) which may be catalytically effected during the warmup of the hydrogen in the heat exchanger circuits. The energy absorbed in this conversion decreases the hydrogen flow rate required to liquefy a given amount of air. In other words, the heat exchanger equivalence ratio can be significantly lowered. The use of a catalyst can, for example, lower the heat exchanger equivalence ratio from about 12 down to 8 (See discussion in Section 6.2.2.2.1). Clearly, this catalytic conversion is very desirable for improved engine performance.

The development of an effective para-ortho hydrogen conversion catalyst has been pursued (but not intensively) since the phasing out of investigations of the Aerospaceplane type powerplants. A notable catalyst development of this period is that entitled "Apachi" which was developed by Air Products Incorporated (Reference 14). One recent development yielding a superior catalyst candidate is the work performed by Englehard Industries for the Air Force Aero Propulsion Laboratory (Reference 18). A very promising catalyst has been identified as 30% ruthenium or a granular S_iO_2 - AL_2O_3 carrier, and it has an activity index of 4.5 pounds of catalyst per pound of hydrogen per second for 70 percent conversion. This new ruthenium catalyst offers a weight saving of almost a factor of five over the earlier "Apachi" catalyst.

9.2.3.3 Critical Area Assessment

Four heat exchanger areas are considered to be critical. Each is discussed below.

9.2.3.3.1 Design

Currently viewed, the "practical problem" areas of the heat exchanger relate to its mechanical aspects. Improvements in overall design approaches are necessary to decrease the weight of the heat exchanger system and to improve its reliability and cost. There is a need for new and novel approaches for arranging and assembling these units. Also, the most advanced materials and structural concepts have not yet been brought to bear on heat exchanger casing fabrication technology. For example, the use of composite structures such as a filament-wound epoxy structure for the pressure vessel of the heat exchanger would appear possibly attractive on two counts: (1) high strength-to-weight ratio in the modest temperature environment and (2) a natural insulating characteristic as compared to all-metal or sheet construction pressure vessels. In the heat exchanger core itself, the demonstration of the applicability of the light metals such as magnesium alloys and beryllium also remains to be done. New bonding tecnhiques such as electron beam welding have not been brought to bear on the problem of cryogenic heat exchanger design.

9.2.3.3.2 Fouling and Icing

All of the antifouling techniques described above have been tested and have shown generally promising, but not wholly conclusive, results. Relative to the composite engine as treated here, the water icing potential is the primary problem. To handle this, there are basically two approaches which appear to be potentially applicable.

The first of these approaches is strictly a passive one. In this system "sacrificial" ice collecting tubes carrying cold hydrogen would be installed ahead of the precooling section of the heat exchanger. This bank of ice collecting tubes would presumably agglomerate ice as the vehicle passed through the icing area of the flight profile and in so doing, would thereby preclude ice or water vapor from being passed into the heat exchanger proper. When the air liquefaction heat exchanger is shut down at Mach 2 to 3 flight speed, the ice would melt and pass into the air stream processed through the engine. This conceptual approach offers the obvious advantages of requiring no active controls or elements, and assesses only a minor weight penalty for the additional ice collecting tube banks.

The second approach, which is backed up by some experimental work, is the use of an active deicer which would be sprayed in liquid form into the air stream ahead of the heat exchanger. The active deicer fluid (a candidate is ethylene glycol) would absorb the water and carry it into the precooling section where it would be separated and collected in a sump. If a separator system were provided, the deicer could be recirculated through the heat exchanger for the operating time required. A secondary benefit of note is the fact that the deicing fluid acts to promote a two-phase air-side heat transfer

on the tube surfaces in the precooler. Experiments have indicated that the heat transfer coefficients may be increased as much as an order of magnitude relative to pure air precooling (Reference 61). There is, then, an implication that the active deicer two-phase heat transfer situation might well permit a significant reduction in the weight and size of the precooler hardware. It may even be surmised that this saving in weight and size would more than pay for the additional weight and complexity of the active deicer approach.

9.2.3.3.3 Para-Ortho Catalyst

The rapid gains in para-ortho catalyst technology over the past five to ten years is suggestive that greater weight efficiency is still to be derived from yet undiscovered catalytic agents. This is an important point, since the catalyst weight in a typical heat exchanger application currently is of the same order of magnitude as the heat exchanger core weight itself. Further catalyst developments will significantly lighten the air liquefaction unit.

An attendant problem which must be investigated is the mechanical incorporation of the catalyst in the heat exchanger. Apparently, a preferred approach is to distribute the catalyst in the multipass header sections of the heat exchanger. Such an approach is described in Reference 62. This approach provides a distributed catalytic action permitting, in concept, a gradual conversion of the hydrogen as the air is condensed. This approach has not been experimentally demonstrated to date.

9.2.3.3.4 Pumps

Very little work has been done to date on liquid air pumps for composite engines. Since air liquefaction must initially take place at low pressures (usually subatmospheric) to provide a positive pressure drop through the heat exchanger assembly, the pumping out problem may be significant. Normally, it would be preferable that a liquid air pump would have at least a slightly pressurized supply system to meet the net positive suction head requirement of the pump. The sump of an air liquefaction heat exchanger is necessarily at a low pressure at the initial low flight speed conditions and, therefore, pump problems are introduced.

One solution to this problem is the application of an in-sump boost pump such as the units being used on the Centaur upper stage vehicle (Reference 63). This approach is reflected in the conceptual design of the Class 2 ScramLACE (Figure 276). In general, the high pressure pump would be placed in such an orientation with respect to the air liquefaction sump as to maximize the acceleration/gravity head. Another approach is to subcool the air below boiling to alleviate the pump inlet requirement (See Section 8.3.2.5). However, this may have a significantly negative effect on the overall heat exchanger equivalence ratio.

9.2.3.4 Future Program Implications

The following air liquefaction technology achievements are indicated to be of first order significance in establishing a preliminary engineering basis for air liquefaction dependent composite engines:

1. Demonstration of practical and economical approaches for the design, fabrication, and installation as a subsystem, of air liquefaction heat exchangers, including the para-ortho hydrogen catalyst material
2. Evaluation of the potential icing problem for the specific composite engine application (as opposed to air collection system schemes). If the problem is significant, determination of recommended passive and/or active deicing approaches, and assessment of their engineering implications.
3. Furtherance of investigations to date of practical, lightweight hydrogen (para-ortho stage) catalysts and determination of methods of their physical incorporation into heat exchangers

Of lesser criticality, but a technology area requiring significant further technology oriented effort, is that of liquid air pumps and the coupling of these pumps to the heat exchanger subsystem.

9.2.4 Primary Rocket Technology

9.2.4.1 Significance

The primary rocket is a critical component in the composite engine and, while much significance can be drawn from the many current and projected advanced rocket programs which are being conducted, there are several specialized requirements which necessitate new research. These areas include stoichiometric rocket operation, the need for high interfacial shear area between rocket gases and the air, and internal cooling of the rocket during primary operation coupled with external cooling during the high recovery temperature ramjet/Scramjet modes, when the rocket is inoperative.

9.2.4.2 Technology Status

The analysis of the rocket technology requirements made during the study have pointed out a singular conclusion of importance: The technology requirements for primary rocket subsystems broadly parallel and overlap those of certain advanced rocket configurations currently being actively pursued. For example, the performance and sizing payoffs attendant to higher pressure combustion and annular nozzle configurations are shared by the pure rocket and the composite engine. The concomitant problems are adequate cooling means and development of structural materials which will withstand the high heat

fluxes which occur at this operating condition. The technology needs which are associated with materials and cooling concepts to withstand the conditions of advanced high performance rockets are essentially identical with those defined for the composite engine requirement. This mutual technology interrelationship will greatly benefit ultimate composite engine engineering development.

A significant number of efforts currently are underway in the advanced rocket area which are expected to yield results directly applicable to the composite engine primary rocket subsystem requirement. Examples of these are moderate to high pressure annular combustor technology; advanced turbopumps of reduced weight, higher efficiency, and reliability; improved propellant inlet condition requirements (lower NPSH requirement); and generally improved system operational flexibility, such as the multiple restart capability.

A significant background or rocket engine technology is applicable to the rocket used in the composite engine. Two of these activities are discussed below.

Major advanced development programs were initiated by the Air Force on 1 March 1965 with Rocketdyne (Contract AF04 611-11399) and Pratt and Whitney Aircraft (Contract AF04 611-11401). NASA also is participating in these efforts. For demonstration of advanced rocket engine concepts, these programs have as objectives the demonstration of two specific, but diverse approaches for mechanizing a 250,000 lbf thrust liquid hydrogen-oxygen rocket engine concept. The Phase 1 efforts are funded at approximately $5 million and they are scheduled for completion in September 1967.

Of the two programs cited above, it is the Rocketdyne contract which is especially applicable, in terms of its technology content, to the needs of the composite engine. This is because the Rocketdyne advanced engine is the annular combustor concept which, in slightly modified form, is an attractive approach for composite engine primary rocket configurations. This information and that given below is applicable to the Rocketdyne Phase 1 effort and was received by Marquardt on a visit to the Air Force Rocket Propulsion Laboratory at Edwards, California on 3 March 1966 (Reference 64).

The purpose of the Rocketdyne Phase 1 advanced development program entitled "High Performance Cryogenic Liquid Rocket Technology (H_2/O_2)" is to demonstrate major elements of a 250,000 lbf thrust rocket engine concept meeting the following general requirements (This information is classified Confidential):

1. Toroidal aerospike concept

2. Multiple restart capability

3. Nominal chamber pressure = 1500 psia

4. Specific impulse goal (vacuum) = 450 sec

5. 100-inch diameter static envelope

6. Throttling ratio, continuous = 5 to 1

7. Life at full thrust = 10 hours (Not to be demonstrated in total system but, rather, in subsystem component rigs)

8. Very low NPSH: hydrogen = 60 ft; oxygen = 16 ft

9. Oxidizer-to-fuel ratio overall = 5.0 to 7.0; nominal of 6.5

10. Aero tapoff turbopump drive concept

11. Overall maximum expansion area ratio = 80 to 1

The Pratt and Whitney technical concept involves very high combustion pressure, a staged combustion turbopump drive cycle and a conventional bell nozzle configuration for the 250,000 lbf thrust engine. This concept incorporates an extendable two-position nozzle and is described in Reference 65. In this form, the engine appears to be significantly less amenable for use as a primary rocket subsystem in the composite engine under consideration. It is not untenable, however, to consider modifications of the Pratt and Whitney concept which would provide a more acceptable air/rocket mixing configuration. However, the transpiration cooling feature could pose significant cycle problems (See Section 7.2.2.1).

The NASA participation in this area is at a somewhat lower funding level and is concentrating on specific technical areas, such as the dynamics of start-up and shutdown. The Air Force is considering a Phase 2 for this program.

The USAF Aero Propulsion Laboratory has funded hydrogen-air and hydrogen-oxygen rocket work as part of research and feasibility demonstration programs related to the Ejector Ramjet (References 8, 11, and 12). These rockets are relatively small scale research units (100 to 200 pound thrust per rocket), they are operated at moderate chamber pressures (500 psia maximum), and they are water cooled. They are used in clusters of eight, and they operate at the stoichiometric mixture ratio. These research devices will provide much useful composite engine and component performance data. However, they serve, in essence, as gas generator units to obtain mixing and engine performance data, and they will not necessarily provide information which is directly applicable to the design of primary rocket subsystems, per se.

Another indicated technology area concerns the protection of the rocket during high speed nonoperating periods, during which it will exist in an environment of very high temperature air. Although it seems unlikely that retraction of the rocket thrust chambers from the high flight speed air stream will be necessary or desirable (a concept for retraction is displayed in Section 7.3.2.1), passive and/or active cooling techniques are required for protecting the hardware.

The extensive heat transfer and cooling work which is being conducted under Marquardt hypersonic ramjet programs (Reference 44) and Scramjet programs (References 44, 45, and 49) can, to a large degree, be considered as applicable to cooling the external surfaces of the rocket while the composite engine operates in the pure ramjet or Scramjet mode. This results from a direct similarity between the heat flux and the environmental conditions.,

The design of the rocket for an operational life of 10 hours presents an area of uncertainty. However, much of the advanced rocket work which is being conducted is directed toward goals of a similar magnitude, and it does not appear that any separate effort directed specifically toward the composite engine is warranted.

9.2.4.3 Critical Area Assessment

Since the composite engine primary rocket technology requirements parallel, to a large extent, those of advanced pure rockets, attention should be directed toward those requirements which are peculiar to the composite engine. The more important of these are discussed below.

9.2.4.3.1 Combustion

The stoichiometric operating condition stipulated for the primary rockets in the afterburning cycle engines (all of the Class 1 and Class 2 systems) introduce some unknowns in terms of combustion performance (primarily in H_2/LAIR operation) and materials considerations. One of these is the possibility of oxidation at the stoichiometric condition (primarily H_2/LO_2 operation. Another unknown arises from some very scattered and preliminary evidence that good combustion performance may be more difficult to obtain at the stoichiometric condition than at the normal fuel-rich ratio.

The introduction of hydrogen-liquid air rocket operation presents an area of relatively little applicable technical experience. Hydrogen-air rockets have been operated by Marquardt and others (Reference 66). However, the experimental work is not abundant. This is particularly true for the higher combustion pressure (1000 psi) and stoichoimetric conditions reflected in the engine designs of the current program. Theoretical performance with this propellant combination is apparently amply provided in a number of references. An example is Reference 67.

The combustion performance of the liquid air-hydrogen rocket primary is a major uncertainty. The mixture ratio (34.3:1) of this engine is far greater than that normally encountered in rocket engines. The injector design must be specially tailored to provide proper droplet formation and distribution. In addition to the injector design problems, the combustion chamber itself may require significant design and development effort to assure sufficient dwell time for high combustion efficiency.

9.2.4.3.2 Mechanical Design of Primary Rocket

The lightweight honeycomb material used as backup structure for the rocket primary has serious brazing problems. The honeycomb has been successfully brazed for a flat interface configuration but significant success has yet to be achieved with curved contours.

The exterior surface cooling problems of the rocket primary structure during high speed ramjet mode operation have not been fully evaluated, although two approaches are available. The "integrated coolant control tube" concept used for leading edge cooling is one possible design approach for protection of the high heat flux stagnation point region; another is a solid leading edge section of a high temperature refractory material, such as hafnium-tantalum alloy.

The use of part of the rocket primary structure for fuel injection purposes during Scramjet operation is a unique design feature of the ScramLACE engine. The desired design characteristics of a supersonic combustion fuel injector remain uncertain (See discussion of Scramjet combustion, Section 9.2.6). With reference to Figure 242, the transpiration cooling provided by the "Rigimesh" leading edge structure is an attempt to incorporate cooling and some fuel injection in a simple design configuration.

9.2.4.3.3 Cooling and Materials

The high heat flux associated with the LO_2/H_2 rocket results in small regenerative coolant tubes and high coolant stagnation pressures (to prevent choking). To achieve reasonable tube sizes with stainless steel tubes, a multipass arrangement must be used. The use of refractory tube materials will alleviate this situation. However, such materials are generally subject to oxidation and hydrogen embrittlement damage. It is likely that suitable coatings will have to be developed to protect the base material. The $LAIR/H_2$ rocket primary also uses a multipass regenerative cooling circuit. Refractory tube materials may allow a single pass arrangement. Regenerative tube external oxidation problems due to stoichiometric engine operation (as opposed to normal fuel-rich operation) have not been evaluated.

9.2.4.3.4 Mixing (See also Section 9.2.5)

Relative to the rocket chamber configurations which are applicable to the composite engines, a need is clearly expressed for high rocket gas/air shear areas. The need is supported by experimental efforts such as those reported in References 12, 68, 69, and 70. The goal is to accelerate the mixing process toward yielding a short physical mixing length with the objective of reducing engine weight and size. Generally, the two approaches which have been considered in air augmentation schemes to date are either a multiple cluster of conventional bell type nozzle rockets, or a single or multiple annular rocket device, such as that reflected in the present study. Fortunately, the annular type combustor is receiving a significant amount of interest for the advanced rocket application and this technology is definitely being carried forward in advanced development programs, as discussed above.

The annular rocket could probably be further improved from the mixing standpoint by adapting many small nozzles to the ring type chamber. The improvement in shear area is obtained at the expense of an increased cooling problem and, perhaps, some detrimental effect on performance. Further investigation of the mixing characteristics of (1) the annular rocket, (2) the annular chamber with multiple nozzles, and (3) multiple individual nozzles is warranted, with and without mixing aids such as static vortex generators.

In composite engines employing a supersonic combustion ramjet mode, the use of the primary rocket external structure as a fuel injector station was discussed in the design of the Class 2 ScramLACE system (Section 8.4.2.2). This unique approach is potentially of interest. However, analysis and experimental verification are lacking.

9.2.4.3.5 Turbomachinery

The bearing DN and seal speed limits used in this study represent performances that should be achieved by a continuous advancement in component technology. The life and reliability factors assigned to these components will be severe requirements to meet. Hydrostatic bearings and seals ideally should have long life capability, since no contact or rubbing occurs. Designing the turbopump components to operate in propellants which are very poor lubricants is a particularly difficult problem, but limited feasibility has been demonstrated. The impeller and turbine tip speeds used are higher than those normally used today. The preinducer and retractable bearings are conceptual designs which have not been reduced to practice. These problems will be solved during the normal course of the research and development programs currently in progress and scheduled for the future in the USAF and NASA high performance hydrogen-oxygen rocket activities, and it does not appear that additional programs over and above these currently are warranted.

9.2.4.4 Future Program Implications

The following primary rocket technology requirements are indicated to be of first order significance to achieving a preliminary engineering basis for the composite engine:

1. Determination of operating characteristics, performance, and cooling aspects of stoichiometric liquid hydrogen/liquid air primary rocket operation including development of design criteria for injector and chamber designs

2. Exploration of detailed design approaches toward implementing lightweight, long life primary rocket chamber designs for both liquid oxygen and liquid air operation including environmental protection and other utilization aspects of the nonoperating primary unit

3. Turbopump (primary and secondary) technology appropriate for long life composite engine applications should be developed. Determination of those areas not otherwise being advanced in rocket programs should be determined and these areas evaluated, e.g., liquid air turbopump bearing lubrication.

4. Other novel two-dimensional rocket and/or nozzle design concepts which might have advantages over the annular concept (in terms of structural integrity, weight, cooling, mixing area, blockage, load transfer, etc.)

9.2.5 Mixing and Air Augmentation Technology

9.2.5.1 Significance

Mixing (air augmentation) comprises a basic jet compression process involving the mixing and, in some instances, further processing of the mixed primary rocket exhaust gases and induced air. The more attractive composite engine concepts (afterburning cycles) use postmixing heat addition to achieve maximum augmentation for the initial acceleration mode. The scope of the following discussion is concerned with the more immediate aspects of primary/air mixing (and, often, combustion) as opposed to overall cycle performance and control. These latter areas are viewed as engine system areas, to be discussed subsequently (Section 9.2.9). However, some discussion of performance is used for comparison purposes in the following technology status section.

9.2.5.2 Technology Status

The concept of increasing the thrust and specific impulse of a rocket by means of the air augmentation process is, of course, not a new one. Augmentation of rockets has been examined over a number of years under various

titles: Air Augmented Rocket, Ducted Rocket, Shrouded Rocket, Ram-Rocket, Rocket Engine Nozzle Ejector, and Ejector Ramjet. In recent years, however, the concept of the Air Augmented Rocket has had basically two forms: (1) a conventional rocket or rockets surrounded by a simple geometric shroud for air entrainment and mixing (References 68, 70, and 71), and (2) a non fuel-rich rocket or rockets in a specially contoured duct in which the air mixing process is followed by discrete afterburning of secondary fuel (References 12 and 72). The former will be referred to as the basic air augmented rocket in the discussion to follow. Reference 48 reported a broad across-the-cycle analysis of air augmentation, which was somewhat limited by restraints relating to the overall objective of the study. (The study focused on the definition of a research device.)

The basic air augmented rocket has in recent times been prominently investigated by the Martin Company under Air Force sponsorship, and by the Applied Physics Laboratory of Johns Hopkins University under Naval sponsorship. Martin's concept of the simple or basic air augmented rocket has been termed "RENE" which stands for Rocket Engine Nozzle Ejector. Nominally, the RENE cycle is based on diffused subsonic air being mixed with a supersonic rocket exhaust in a simple diverging shroud to produce a net supersonic flux of mixed exhaust gases. This cycle, termed the sub-super cycle by some investigators (Reference 48), offers the potential of high performance and simple lightweight hardware implementation. The Applied Physics Laboratory under Navy sponsorship has also accomplished significant theoretical and experimental results (Reference 70) on air augmented rockets of the basic cycle variety. However, an adequate experimental confirmation of the cycle precept has yet to be achieved.

Specifically, for launch vehicle applications, the basic air augmented concept (that is, Engine No. 5 in the candidate systems addressed in the Class 0 phase) has been studied only to a limited extent. The NASA sponsored "Investigation of Vehicle Integration Rocket Powerplants with Air Augmentation" study performed by the Boeing Company in 1963-1964 is perhaps the most recent study to address this cycle in a launch vehicle application (Reference 3). Boeing's neutral-to-negative prognosis relative to the payload potential of air augmentation in this form was basically corroborated by the Class 0 systems analysis of the present study (Section 7.6.2 and Volumes 4 and 5). A general conclusion was that simple air augmentation (with no capability of or transition to the ramjet mode) does not offer a promise of significant payload improvement over a comparison rocket. Other vehicle/mission application studies of note touching on basic augmentation were concerned with very large launch vehicle applications (Reference 5) such as the NOVA and other post-Saturn vehicle concepts.

The second form for the air augmented rocket noted above, namely the afterburning cycle engine, did not receive significant attention until recent years. Under Air Force Aero Propulsion Laboratory support, The Marquardt Corporation has over the past four years (References 12, 73, and 74) evolved the afterburning cycle concept from a level of theoretical considerations and simple

pipe hardware testing to a technology demonstration hardware level in an 18-inch diameter apparatus (Reference 12). It has been determined in this work that the thermodynamic cycle advantage of this approach, with respect to the basic air augmented rocket, offers practical system advantages including, for instance, a designed-in ability to convert readily to ramjet mode operation.

The present study compares the two versions of the augmented rocket and has indicated that definite performance and practical advantages of the after-burning cycle as reflected in the substantiated selection of the Class 1 and Class 2 engines concepts, all of which are afterburning cycle devices (See discussion in Section 6.5.2.2.8). The final of the last cited references reports results achieved with sea level static and simulated flight condition testing of a boilerplate eight-rocket cluster afterburning cycle device. Programs at Marquardt, continuing under Air Force sponsorship, are directed toward the Ejector Ramjet concept for aircraft applications, as opposed to launch systems. The current composite engine study was the first to investigate the applicability of the afterburning cycle family of engines specifically for advanced launch vehicle applications.

9.2.5.3 Critical Area Assessment

As indicated, the only reported experimental work concerning this cycle is that conducted in the past and that currently underway under Air Force sponsorship at The Marquardt Corporation. This work, although consistently funded and supported since its initiation in 1962, has been accomplished at a relatively modest level of effort to date. The experimental work in particular has been accomplished at a level of effort of the order of 200,000 to 300,000 dollars over the past several years. The investigations to date have been limited to the Ejector Ramjet cycle, and have not included significant derivative items such as fan supercharging. Also, the RamLACE cycle (air liquefaction based afterburning cycle) has not been experimentally investigated. Only limited theoretical and design activity has transpired. It therefore appears in view of the net attractiveness of the afterburning cycle air augmented rocket demonstrated in this study, that significant technological activity focusing on this cycle is now appropriate. Programs aligned with Ejector Scramjet and the RamLACE/ScramLACE concepts were initiated in 1966.

Further analytical studies are required to describe the mixing process and provide guidance for mixing optimization and component matching tests, including the definition of parameter groupings for test data correlation. The joining of a theoretical effort with overall experimental programs would provide the parametric information needed in defining both the design and internal performance characteristics of the jet compressor section of the composite engines.

The key independent parameters of the jet compression problem are as follows:

1. Primary rocket pressure and mass flow
2. Secondary air pressure and mass flow
3. O/F ratio of primary stream
4. Primary and secondary stream interfacial area
5. Mixing duct shape
6. Impingement angle
7. Innerbody size (when applicable)
8. Secondary combustion effects

Other flow parameters are either implied by the appropriate thermodynamic and gas dynamic relations, or specified by system or hardware considerations.

9.2.5.4 Future Program Implications (See also Section 9.2.9)

For both oxygen and air primary rocket operation, the following air augmentation technology achievements are indicated to be of first order significance to achieving a preliminary engineering basis for the composite engine:

1. Evaluation of the sensitivity of the afterburning cycle to off-design conditions, particularly those involving precombustion of primary-issued free hydrogen with the induced air. The free hydrogen may stem from (1) fuel-rich mixture ratio deviation from stoichiometric, (2) nonhomogeneous exhaust pattern (e.g., "fuel curtain" surrounding the exhaust jet), and (3) fuel introduced by mass transfer chamber cooling schemes (film, transpiration).

2. Determination of broad mixer/diffuser/afterburner geometrical and thermodynamic criteria with the measure of merit being the overall system performance.

3. Assessment of the fan in a role of "dynamic turbulator" with respect to possible mixer length reductions. Also, assessment of other deliberately designed mixing aids for the same purpose.

4. Comparison of single and dual concentric annular primary configurations in terms of mixing length, and single and multiple conventional (bell) configurations. Consideration of unconventional primary configurations, (e.g., "linear" primary). Also, evaluation of unconventional primary rocket divergent nozzle shapes, in order to provide better mixing and/or less secondary air flow blockage by the primary rocket combustors.

It will be noted that the above strongly suggests an engine system level orientation (for example, consideration of overall performance, thrust, and specific impulse) as a measure of merit for judging mixing efficacy.

9.2.6 Combustion Technology

9.2.6.1 Significance

All attractive composite engine concepts involve a subsonic combustion ramjet mode. A number of these also phase over to a supersonic combustion mode at the higher flight speeds. Combustion, as a subject here, is taken to cover ramjet/Scramjet fuel injection and mixing, burning, and exhaust gas expansion (exit nozzle). Not included are primary rocket combustion and secondary burning in the augmented rocket mode.

9.2.6.2 Technology Status

9.2.6.2.1 Subsonic Combustion Ramjet Technology

Over the past several years, along with in-depth theoretical and application studies (Reference 75), The Marquardt Corporation has successfully evaluated experimental hydrogen fueled, cooled ramjet combustor and nozzle assemblies. For hypersonic application, this work has been extensively performed in the 18-inch diameter size class. Under simulated ground run conditions (storage heater plus vitiation), Mach numbers as high as 8 have been simulated and combustion pressures as high as 265 psia have been achieved with regenerative cooling. Both ambient temperature and heated coolant (hydrogen) have been utilized. The heated hydrogen simulates the condition in which the cryogenic hydrogen fuel is required to heat adjacent sections of the engine or vehicle prior to being injected into the ramjet combustor cooling jacket. A cooling jacket inlet temperature of 1400°R was used for this situation. Hot wall (Hastelloy X) temperatures were sustained at temperatures as high as 2300°R in these tests. A total run time in excess of 40 minutes was achieved with a set of hardware. This combustion and cooling experience is reported in Reference 44.

One of the important results of this test program was the determination of the combustor length requirement for hydrogen fuel. The experiments demonstrated that very short combustion lengths would suffice for complete (subsonic) combustion of the hydrogen fuel. This was accomplished by a progressive shortening of the fuel injector to throat condition dimension in the experimental hardware. The program also demonstrated the durability of super-alloy structures (Hastelloy X was utilized for regenerative tubes) and also developed practical advanced instrumentation techniques for flightweight structures. Heat transfer rates for subsonic combustion ramjet conditions were evaluated, and the conventional correlations were found to be validated except in the throat region of the ramjet. Here new correlations have been postulated based on the experiments indicating that the cooling problem is not as severe as would otherwise be predicted, e.g., the Bartz equation. Another aspect of this program is that the effects of vitiated air testing on performance was investigated.

In addition to the success achieved to date, continuation and intensification of technology investigations of the 18-inch subsonic combustion ramjet are planned. Under consideration is a program in conjunction with the Air Force which would lead to a flightweight demonstration ramjet engine incorporating all of the advancements which have been noted to date in this general activity.

9.2.6.2.2 Scramjet Technology

The context of composite engine usage of the supersonic combustion ramjet mode is considered to be a potentially attractive operating mode permitting the composite powerplant to penetrate into the hypersonic airbreathing region further than is possible with the subsonic combustion ramjet mode alone. Beginning with small scale demonstrations of feasibility in the 1957-1958 time period with simulated flight velocities in the Mach 4 to 8 region, supersonic combustion technology has advanced considerably, particularly in the last several years.

Past performance and mission studies of Scramjet engines at Marquardt (References 45 and 49) have been recently amplified in the area of parametric performance computations (Reference 20). This technology work has been performed by Marquardt and others to an estimated funding level of the order of $10 million to date. The technology programs have been supported predominantly by the Air Force, with NASA recently becoming involved.

Currently, programs are underway at General Electric, Pratt and Whitney, Garrett, and Marquardt. Those at The Marquardt Corporation in the area of Scramjet technology are four in number, namely:

1. The NASA Hypersonic Ramjet Experiment. The program has as its objectives: (1) definition of the best possible hypersonic (up to Mach 8) research engine to be applied to the X-15 research airplane (Phase 1, completed), (2) the design development and delivery of an engine designed in the program, and (3) actual flight tests with the engine. Phase 1 was recently completed by three contractors (Marquardt, General Electric, and Garrett) at a funding level of approximately $500,000 each. The Phase 2 activity was initiated by the NASA Langley Center with the Garrett Corporation.

2. A Scramjet Flight Test Program is being undertaken by Marquardt in conjunction with the Lockheed-California Company under Contract AF 33(615)-2815. The technical objectives of this program are to be met by a ballistically launched, zero-lift, aerodynamically stabilized Scramjet powered stage which will be boosted to operating speed by a Castor solid propellant rocket. The objectives are: (1) operation of a Scramjet engine at flight velocities in excess of 6000 ft per second, (2) acceleration by Scramjet power over a ΔV of at least 1000 ft per second, and (3) a Scramjet operating time of greater than 5 seconds.

This program, which has proceeded through its design phase, is preparing for a first cold flow or dummy vehicle flight within the next few months. Concurrently, ground testing of engine modules (4) and a complete ground test engine will be conducted. This will be followed by a flight readiness test of a Scramjet unit with flight testing commencing in calendar year 1967.

3. A Dual Mode Ramjet Program is being conducted by Marquardt under Contract AF33(615)-2834. The objective of this ground test engine program is to determine the feasibility and to evaluate the performance obtainable from a fixed geometry propulsion system capable of both subsonic combustion and supersonic combustion. Inlet and combustor tests have taken place at the Ordnance Aerophysics Laboratory free jet test facility, using a three-dimensional engine with a capture area of approximately 100 square inches. Complete engine tests are scheduled for late 1966. The current work concerns itself with the Mach 3 to 5 region and concentrating on an evaluation of the speed range at which the combustion modes would be shifted from supersonic to subsonic. A potential program extension would evaluate the high speed Mach 8 to 12 performance of the test hardware. These program results will be of interest to the composite powerplant, since it is indicated that the Scramjet mode is in fact to be preceded by a subsonic combustion mode. Examination of the dynamics and performance aspects of the transition modes will take place in the dual mode test program, currently funded at the $1.0 million level.

4. Hypersonic Heat Transfer and Cooling Program. An integrated heat transfer and cooling program is being conducted by Marquardt under Air Force Contract AF 33(615)-1467. This program is experimental in nature and it will include both the subsonic and supersonic combustion conditions for which heat flux data will be gathered with regenerative and transpiration cooling. It is a continuation of the work reported in Reference 44 in some areas. Major experiments will be conducted using an 18-inch hypersonic ramjet model as a test bed. Instrumentation of this superalloy, regeneratively cooled, contoured chamber will include hot wall temperature and coolant temperature rise instrumentation. An advanced two-dimensional test article has also been constructed by Marquardt, employing superalloy cooling tubes and leading edges constructed of advanced hafnium-tantalum alloys which are capable of operation at 5000°R. This 15 month program is funded at approximately $2 million.

9.2.6.3 Critical Area Assessment

The characteristics of the hydrogen fueled subsonic combustion ramjet as noted in this subscale experimental program are applicable to a larger composite engine involving the subsonic combustion ramjet mode. It is estimated

that the high performance achieved in the small scale experiments can be equaled and probably exceeded in a larger engine and that the cooling problem will be significantly alleviated in going to larger hardware. This remains to be demonstrated for both subsonic and supersonic combustion ramjets. Although no particular problems are foreseen, such aspects as combustion stability remain unexplored.

9.2.6.4 Future Program Implications

The following combustion technology achievements are indicated to be of first order significance to achieving a preliminary engine firing basis for the composite engine:

1. Analytical and design evaluation of large (8 to 10 ft diameter) hydrogen fueled subsonic combustion ramjets capable of operation to Mach 8. The relevancy of subscale design and testing to the ultimate combustion and cooling problems will be determined at full scale.

2. Extension of the present Scramjet component and subscale engine experimentation to higher speeds (up to at least Mach 12) using steady state facilities with adequate free flight simulation

9.2.7 Structures, Cooling, and Materials Technology

9.2.7.1 Significance

The basic advantage of the composite engine concept is based to a large degree upon the inherent simplicity of the engine and the high thrust-to-weight ratios which result therefrom. The conceptual design studies that have been completed as part of the current program were based upon a combination of current state of the art and advanced structures, cooling, and materials technologies which are currently projected for rockets and ramjet/Scramjet engines of the future.

9.2.7.2 Technology Status

All of the composite engines which were considered in the study profit from the application of the latest advances in structures, cooling, and materials and -- as the operating flight Mach number increases -- the need becomes increasingly more severe. The engine components involved include the following:

1. Inlet
2. Fans
3. Heat exchangers
4. Rocket
5. Mixer
6. Combustor
7. Exit nozzle

It will be noted that the technology status of these components has been discussed in preceding sections including to some degree, the significant structures, cooling, and materials areas.

9.2.7.3 Critical Area Assessment

9.2.7.3.1 Inlet

The inlet is in a generally favorable environment, having the advantages of (1) being subjected only to ram temperatures and (2) being partially exposed so that at least part of the thermal load can be dissipated through radiation. Vehicle studies indicate that conventional superalloys can be used up to approximately Mach 6. Above this flight speed, refractory materials such as coated columbium are indicated. The same philosophy should apply generally to inlets.

The conceptual inlet structural designs which have been made are based on more detailed previous studies conducted by Lockheed and Marquardt. Where variable geometry is required, the structures and mechanisms are heavier than would be desired, but they are generally suitable for the present. If fixed geometry inlets can be adapted to the composite engine, the structure problem would be reduced, but the materials and cooling problems would be of the same order.

There is considerable related work in progress on advanced inlets at Marquardt, General Applied Science Laboratories, General Electric, and Pratt and Whitney (References 50 through 53), and it appears that the results of work on inlets for high flight Mach number ramjets, Scramjets, and turbomachines are generaly applicable. Current programs appear to be adequate for the moment.

9.2.7.3.2 Fans

Since there is little advantage in operating the fan above Mach 2.5, it can be concluded that the current programs (References 22, 14, 55, and 56) provide a satisfactory base for the present. The effect of elevated air temperatures on the fan blading requires examination, however. No active cooling is required for the fan components except for the closure plate or device that seals off the fan unit from the high speed-high temperature environment. Studies should be conducted, however, to consider the application of advanced materials and structural concepts to the fan components in the context of the composite engine operating regime. Advances in either area could lead to lower component weights and possible fan use at higher flight speeds.

9.2.7.3.3 Heat Exchangers

The available materials and cooling technologies are probably satisfactory for the present; however, processing, fabrication, and structures

problems exist (References 13 through 17). The need for uniformity and quality control of tubes and headers and the development of high quality fabrication techniques remains. The work which was previously done at Marquardt and AiResearch provides a very encouraging background, but more work is required relative to design, fabrication, and demonstration. This is considered to be a first order problem.

9.2.7.3.4 Rocket

The structures, cooling, and materials problems of the rocket are, to say the least, challenging. In addition to the internal problems associated with high pressure hydrogen-oxygen rockets of the annular type, composite engines generally subject these units to a high external temperature environment during operation at high flight Mach numbers.

If the rockets remain permanently in the air stream, some means of protecting the structure from the environmental temperature is essential. During ramjet operation, it will very likely be necessary to cool the external surfaces with fuel which will be subsequently injected into the combustor. During Scramjet operation, it may be practical to inject the rocket cooling fuel at the station, either externally or internally through the rocket injectors.

The structure, cooling, and material problems in the rocket are interrelated and, although much work is currently in progress in the rocket, ramjet, and Scramjet areas (References 2, 4, 44, and 45), it remains a critical problem area which requires a carefully considered research program. High temperature corrosion resistant materials are essential, and very sophisticated structures are required to achieve the low weight which is essential for this engine. Full advantage must also be taken of the advanced work in regenerative, film, and transpiration cooling to achieve the lowest possible weight which is consistent with the operational design requirements.

9.2.7.3.5 Mixer

The environmental problems in the mixer are similar to, but less severe than those in high Mach number, subsonic combustion ramjet combustors. The mixer is exposed to high aerodynamic turbulence (and, therefore, relatively high heat transfer coefficients) as the hot, high velocity rocket exhaust mixes with the secondary air. However, the mixed stream temperatures are typically less than the Mach 8 inlet total temperatures, the mixer pressures are relatively low, and there is no throat or constricted area. At the higher flight speeds where the engine operates in the ramjet or Scramjet modes, the mixer surface area does present an additional cooling problem in terms of coolant heat sink capacity. Hence, in broad terms, the mixer problems are similar to those of the combustor (excluding the exit nozzle) of the Hypersonic Ramjet and Scramjet and, since significant basic work is in progress for these engines (References 44 and 45), it does not appear that additional composite engine oriented programs in this area are warranted at the present time.

9.2.7.3.6 Combustor

Structures, cooling, and materials problems in the combustor during ejector mode or primary rocket operation are similar to those described above for the mixer, but are more severe due to the generally higher temperature level. One compensating factor is that the combustor length for hydrogen fueled engines is relatively short; hence, the exposed surface area is minimized. At low flight speeds during the ejector mode operation, the environmental conditions in the combustor or afterburner are still no more severe than Mach 8 ramjet conditions. Hence, the structures, cooling, and materials research and development work which is being done for the Hypersonic Ramjet and Scramjet engines (See References 44 and 45) appear to be adequate at the present time.

9.2.7.3.7 Exit Nozzle

The exit throat area variation requirements for composite engines are specified almost entirely by the subsonic combustion ramjet mode operation. For acceleration applications only, compromises in ramjet performance (low inlet pressure recovery) and in maximum ramjet flight speed (maximum Mach number < 6) can possibly eliminate the variable geometry exit requirement. However, for best overall engine performance, a variable exit is required and the structure, cooling, and materials problem of the exit nozzle are considered to be critical. The problem of properly designing cooled variable geometry exits is common to all high flight speed propulsion systems. Several research and development programs are in progress in this area (References 44 and 45) and the engines studied in this report have operating requirements which are generally less rigorous. Effort is needed, however, to define more compact, lightweight variable exits. In the field of axisymmetrical designs, the Marquardt translating ring nozzle concept (Figure 274) warrants structure, materials, and cooling research beyond the aerodynamic tests now under Air Force contract. In the field of two-dimensional designs, the aerodynamic problems are less difficult, but the resulting structure problem is more severe than the corresponding axisymmetrical design. And, since it is difficult to separate cooling and materials studies from structures, it follows that critical component design work is also required to more definitively localize specific problems.

9.2.7.4 Future Program Implications

1. Detailed design studies of each of the above engine components are required to provide specific quantitative data on the structural and thermal loads so that the materials and the cooling requirements can be more clearly identified. While it is desirable to include all major components of the engine, it is essential that a concerted effort be directed toward the rocket external cooling problem and the exit nozzle problem.

2. Design studies of the application of composite fiber technology to critical high temperature components should be conducted. Among others, silicon carbide and graphite fibers should be evaluated.

3. Current research work in high temperature protective and insulating coatings for metals like columbium and molybdenum should be adapted to the design of the overall engine, with specific attention to the exit nozzle.

4. Current research work on transpiration cooling should be adapted to the mixer, combustor, and exit nozzle of the engine.

9.2.8 Cryogenic Propellants Technology

9.2.8.1 Significance

Propellant requirements for composite engines for launch systems will likely involve cryogenic fluids. Hydrogen is unquestionably the leading fuel contender. This point was reflected in the guidelines which limited the scope of the study to hydrogen. Hydrogen not only provides a maximum specific impulse potential while being a superior coolant, but makes possible the attractive air liquefaction based systems, e.g., ScramLACE. Hydrogen plays an important operational role in current launch vehicles and its characteristics are well known (See, for example, Reference 76). Therefore, liquid hydrogen, in its conventional form, will not be further discussed here.

The subcooled, slush (solid/liquid) form of hydrogen plays a vital role in those liquefaction cycles which seek (ejector mode) specific impulse performance improvement via recycle mode operation (See Sections 7.2.2.3 and 7.6.2.5 for a discussion of recycle operation and its performance potential).

Liquid air (also a cryogenic fluid) was used directly as the oxidizer for ejector mode primary rocket operation in the liquefaction cycles. Once taken aboard, it may also be stored and processed subsequently in the flight profile. It is again noted that the collection was not within the scope of this program. It was, however, touched upon at two points, relative to the "Refill Rocket" concept (Appendix A) and relative to a ScramLACE payload augmentation potential (Appendix F).

The remaining propellant encompassed is liquid oxygen, the oxidizer for the non-liquefaction cycles and a prospective "service oxidizer" for driving ramjet mode pumps, etc. This propellant has a great deal of in-service experience behind it dating back over 30 years, and it will not be further discussed.

This section, rather, concentrates on those special aspects of the cryogenic propellants which are peculiar to the composite engine. These are

essentially two: (1) liquid air as associated with air liquefaction within the engine (RamLACE/ScramLACE family of powerplants), (2) liquid-solid hydrogen mixtures, or slush hydrogen.

9.2.8.2 Technology Status

By virtue of the ground rules of the composite engine study (Section 3.1) the propellant combinations of hydrogen and oxygen and hydrogen and liquid air were the only combinations examined. With the hydrogen/oxygen propellant combination now entering service on the Centaur and Saturn launch vehicles upper stages, it is evident that the technology base for the manufacturing and field handling of these propellants is well in hand. Therefore, it is properly assumed that the design, fabrication, and material considerations for propulsion systems and launch vehicles capable of utilizing this propellant combination is also a well entered upon technological area. Hence, the emphasis here on cryogenic technology peculiar to composite systems.

9.2.8.2.1 Slush Hydrogen

The subcooling of liquid hydrogen from its normal boiling condition (36°R at standard atmospheric pressure) carries with it some strong, though perhaps long range, implications to propulsion. A pertinent application of slush hydrogen in the composite engine area is in the recycled versions of the air liquefaction based composite cycles. Recycle operation, it will be recalled, consists of recycling to the tank some of the warmed up hydrogen utilized in the condenser for liquefying air. The purpose of this is to reduce the overall fuel richness of the cycle, intrinsic in the heat exchanger operation, thereby increasing the specific impulse of the powerplant during air liquefaction operation. In order to accomplish this, it is necessary to provide a heat sink within the hydrogen tank itself. This takes the form of the subcooled fluid, generally taken to be in the form of slush (solid/liquid mixture). The current study considered for example a 50% solid/liquid slush composition at 25°R.

There is a significantly broad base of pilot model and laboratory experimentation in the production, processing, and logistics of the characteristics of slush hydrogen. The work has been accomplished at the National Bureau of Standards and also by several contractors working in the cryogenic field. Recent work at NBS has, for example, concentrated on production methods applicable to a large quantity slush hydrogen manufacturer. Vacuum pumping has been used for this work to form a crust of solid hydrogen on the surface of the liquid. Thereafter, under a careful pressure modulation, the solid porous mass breaks loose, breaks into fine particles and sinks to the bottom of the container. This process is repeated until the proper ratio of solid to liquid hydrogen has been accomplished. The Linde Division of the Union Carbide Corporation has also been active in slush hydrogen production and recently reported (Reference 77) research on production techniques for obtaining over 50% solid

slush hydrogen. Although this work was performed on a laboratory scale, the approaches under consideration are clearly applicable to production operations. NASA Marshall is sponsoring studies of the general utility aspects of slush hydrogen, with emphasis on the increased storability and density of slush hydrogen (Reference 78). Further comments are made below.

9.2.8.2.2 <u>Liquid Air</u>

Many engineering aspects of liquid air are relatively well documented. The technology base here stems largely from the Aerospaceplane propulsion activity of the late 1950's and early 1960's. As noted in Section 9.2.3 of this technology assessment discussion, air liquefaction hardware tests have been conducted with no particular technological problems evidenced in the liquid air circuits as such.

A more recent consideration given to liquid air stems from a situation associated with liquid hydrogen tankage for launch vehicle applications. Improper or inadequate insulation techniques provide an opportunity for atmospheric air liquefaction against the side of the the filled vehicle hydrogen tank. The compatibility of the liquid air with various engineering materials is therefore of interest.

A recent project at the NASA Marshall Space Flight Center was conducted to determine the effect of liquid nitrogen dilution on liquid oxygen impact sensitivity (Reference 79). In this experimental project, about a dozen materials were surveyed for impact sensitivity over various percentages of nitrogen in the liquid oxygen up to that of liquid air (80% LN_2). Tested were adhesives, sealants, insulation, metallic alloys, and other engineering materials currently in use for launch vehicle applications. Conclusions from this work include those listed in the following paragraph.

The sensitivity of most materials to impact with LO_2 was found to be decreased by dilution of the LO_2 with LN_2. The extent of dilution necessary to effect an appreciable decrease in activity is large. Although all materials were insensitive to liquid air (20% LO_2), several were sensitive at 30% LO_2 and the sensitivity of some materials at 50% LO_2 approached that of pure liquid oxygen.

9.2.8.3 <u>Critical Area Assessment</u>

Although the mission implications of slush hydrogen (recycle mode) in terms of payload improvement as reported here (Section 7.6.2) appear to be more or less nominal, the full implication has perhaps not been fully uncovered. If, after further analysis in which more detail cycle considerations are brought into play, the use of the recycle mode is of definite interest, then slush hydrogen technology may deserve a prominent place in any composite engine oriented technology inquiry.

As noted above, there is general interest in slush hydrogen for other than the composite cycle engines recycle application as examined in the present report. These stem basically from two other aspects of slush hydrogen: (1) its increased propensity for long term storage, and (2) its nominal increased density over the boiling liquid (the order of 15%). Long term storage of liquid hydrogen in an orbital tanker has been considered where the additional heat sink or refrigerative capability of slush hydrogen provides marked operational benefits, in terms of reduced boiloff losses and/or decreased insulation requirements. Primarily to appraise this potential, a recent request for proposal was issued from the NASA Marshall Space Flight Center (Reference 78).

The point which can be made in summary is that the application of slush hydrogen to aerospace requirements may, in fact, come about irrespective of any interest for composite engine cycle reasons. If it does, a significant composite engine potential growth capability may, in a general sense, be in the offing in the form of recycle operation for air liquefaction based composite engines. However, at the present time, there is a lack of technology achievements and experience concerning the engineering mechanization and operation of typical recycling fuel systems using slush hydrogen.

From the existing base of liquid air technology, there appear to be no particular difficulties or technology uncertainties which would warrant further investigations of a technological nature in this specific area. Comments relative to liquid air utilization in primary rocket combustors and turbopumps have already been given in Section 9.2.4.

9.2.8.4 Future Program Implications

The following cryogenic propellant technology achievements are indicated to be of first order significance to achieving a composite engine preliminary engineering basis:

1. Development of broad engineering guidelines for liquid air systems, including instrumentation, materials compatibility specifications, field handling and servicing procedures, and general hazard appraisement. The objective would be to bring the general liquid air technological state of the art up to that existing for liquid oxygen.

2. If recycle hydrogen operation, after further system analysis, appears attractive (perhaps as a growth potential area), then studies covering the production, transportation, vehicle servicing, and vehicle design aspects of slush hydrogen should be started or intensified. Simultaneous engineering approaches for actually mechanizing the propulsion system recycle loop should be devised -- control, tank return technique, etc.

9.2.9 Engine Systems Technology

9.2.9.1 Significance

The design studies of the many engines which have been considered in this program can be classified as "conceptual" and, to a large degree, as has been stated, they are based on previous Ejector Ramjet preliminary design and experimental studies. The excursions from this base are significant in concept as well as in scale, and they are of such a nature that more definitive conceptual design studies are required on those particular engines which have the most promising characteristics.

9.2.9.2 Technology Status

Prior to the present program, the larger part of the design studies relating to composite engines have been directed toward high performance aircraft (cruise) type applications. The essence of this work has been that sponsored by the Air Force with The Marquardt Corporation over approximately the past four years, and the additional work summarized in this report as funded by NASA. References 11, 12, 73, and 74 represent this activity. Of the twelve Class 1 systems which have been taken as representing the "attractive composite engines," only two, the Ejector Ramjet and the Ejector Scramjet (particularly the former), have received significant attention. There has been some attention given to RamLACE (Marquardt MA175-XAA) and significantly less to the Supercharged Ejector Ramjet (Marquardt MA176-XAA-A hydrocarbon engine design). A very limited preliminary design study of the Ejector Ramjet for a launch vehicle application is described in Reference 72.

The RamLACE/ScramLACE design and analysis area will be advanced with limited funding under the current (1966) Air Force "Advanced Ramjet Concepts" Program (Contract AF33(615)-3734); also some experimental work will be performed on the Ejector Scramjet under the same program. With regard to the two engines chosen for the Class 2 phase, the Supercharged Ejector Ramjet and the ScramLACE, design study work, other than the conceptual work conducted in this program, has not been performed.

As far as engine experimental evaluation status is concerned, the 18-inch test apparatus reported in Reference 12 represents the only system oriented work. This effort is being extended by the Air Force/Marquardt currently with an improved free jet test engine of the same size and it is scheduled for testing approximately at the time the present report is distributed.

9.2.9.3 Critical Area Assessment

Preliminary design work is indicated for both the Supercharged Ejector Ramjet and the ScramLACE engines to more clearly define the structures, weights, and envelopes for the engines. The critical areas to be considered

involve the design details of all components, and include heat transfer analysis, stress analysis, tentative choice of materials, preliminary analysis of fabrication methods, variable geometry mechanisms, engine cooling systems, etc. Specific critical components which warrant special attention are discussed in the following sections:

9.2.9.3.1 Fan (Supercharged Ejector Ramjet)

Design studies of various fan and fan drive subsystems are required to clearly define the better methods of incorporating this important component. The means for removing the fan from the air stream during high flight Mach number operation has been demonstrated in principle in connection with the tip driven lift-cruise fan configuration, but the full application of this device to composite engines involves problems of a considerably higher magnitude, such as fan/mixer dynamic interactions (Section 9.2.5).

9.2.9.3.2 Cryogenic Heat Exchanger (ScramLACE)

While there is a base for the cryogenic heat exchangers in past Liquid Air Cycle engine programs, design work in relation to the large composite engine is very much needed. An example is the mechanization of tube banks to condense and freeze out the water in the air or various antifreeze systems, as suggested in Section 9.2.3. Materials, fabrication methods, and controls are candidates for review, since the ScramLACE engine criteria are significantly different than those for the earlier Liquid Air Cycle engines. (In some cases less critical.)

9.2.9.3.3 Rockets

The present study shows the advanced annular primary rocket approach almost exclusively. The current programs sponsored by NASA and the USAF-RPL are largely adequate in terms of evolving basic technology, but the various methods of designing alternating nozzle sections warrants study. Also, it is in order to conduct design studies of arrangements of conventional "bell" type rockets as an alternate to the annular approach. A definitive design comparison in this area may lead to modular concepts which could significantly reduce development time and cost.

9.2.9.3.4 Variable Area Exit Nozzle

The operative requirements of the composite engine leads to the need for advanced exit nozzles which are capable of large variations in throat and expansion area ratio. One type which shows promise includes a stationary plug and a sliding ring and, while a limited off-design characteristics analysis has been completed and small scale aerodynamic tests are scheduled in 1966 under USAF-APL sponsorship, the mechanical design problems as they relate to composite engines have not been solved. They are very much needed.

The above four items have been cited for special attention. However, it is important to place almost equivalent emphasis on the overall system integration problem. Greater penetration is required to properly relate the several interrelated components of the engines with a balanced emphasis on the many previously mentioned factors that must be considered in any design activity which proceeds beyond the initial conceptual stage.

9.2.9.3.5 Effort Required

The composite engines, identified and characterized in terms of the analytical and design effort contained in this program, have no substantial experimental basis. As noted, the only effort which has provided basic confirmatory information on such items as Ejector Ramjet positive sea level augmentation (a feature of the afterburning cycle) is the 1963 - 1964 Air Force/Marquardt "Advanced Ramjet Concepts" program. The supercharged and air liquefaction cycles included in the listing of favorable cycles are without an experimental basis.

A systems approach, although providing abundant opportunities for component oriented research, would concern itself with the determination of overall thrust and specific impulse characteristics as a function of the engine operating condition. For example mixing length results would not be stated as "percent mixing", but as a (continuous) characteristic: I_s vs. mixer length.

The first order subsystems of composite engines -- primary rocket, air liquefaction heat exchanger, etc. -- can be carried forward somewhat separately, as discrete items. Performance ratings of these subsystems as determined by, say, separate rig experiments, would be used to establish a simulation basis for concurrent systems tests. An example is provided by the air liquefaction heat exchanger whose performance is represented by its equivalence ratio. While work is proceeding with a heat exchanger apparatus, the RamLACE ejector mode might be tested with a simulated heat exchanger, the simulation tie-point being equivalence ratio, represented by the overall fuel-air ratio supplied to the system test apparatus. Figure 371 reflects this general approach.

It can be seen that component/process research can be effectively conducted in a systems apparatus simultaneously with systems measurements of thrust, propellant flow, etc. Mixer primary plume/air profiles can, for example, be evaluated by rake measurements in the apparatus while thrust is being taken from a load cell.

Internal flow parameters are of considerable concern in achieving system performance. It has been determined from computational manipulation that the end-of-mixer Mach number (M_3) is a highly significant parameter in that it, in effect, specifies mixer inlet Mach number (M_2). This, in turn, rather strongly affects overall specific impulse.

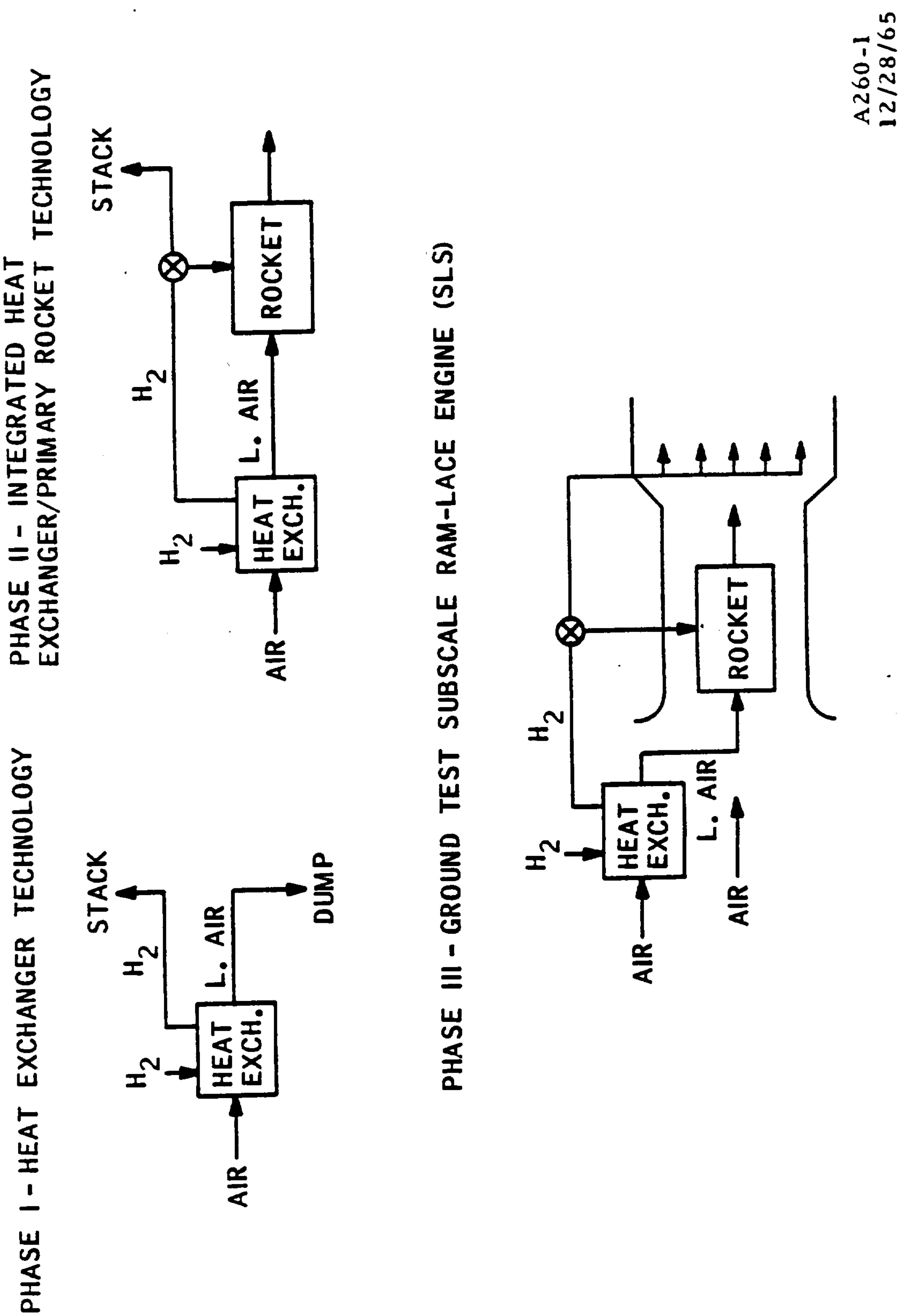

FIGURE 371. Progressive Technology Steps for the RamLACE Cycle

Experimental checking of this and related effects are therefore indicated. Establishing the degree to which the sonic flow mixer exit can be approached under real run conditions might be a typical test objective.

9.2.9.4 Future Program Implications

At this point in time, the design need can be broadly classed as conceptual or predesign rather than preliminary design. The conceptual studies to date must be reviewed and modified based on more detailed study of the many critical factors which are involved. For both Class 2 engines, preliminary thermal and stress analyses are required for the entire engine, with particular emphasis on the use of advanced fabrication techniques, materials, and methods of cooling. Further sensitivity design studies are also required to investigate thrust-to-weight ratio effects and engine off-design operation including component efficiency variations over the flight regime.

For the Supercharged Ejector Ramjet engine in particular, supplementary detailed design studies are required to evaluate alternative fan retraction methods and drive systems. The problem of swinging the fan upward appears practical and there are some earlier bases for following this approach, but the environmental conditions for these launch vehicle engines are possibly much more severe. In particular, the bearing and actuator systems require close inspection. The present studies show an airbreathing gas generator and a tip driven fan. While this arrangement is desirable from many standpoints, a preliminary investigation of geared drives and of rocket type gas generators should also be considered.

For the ScramLACE engine, supplementary detailed design studies are required of the air liquefying heat exchanger to achieve a compact arrangement with the lowest practical weight. Designs for various types of deicing systems require design study as a critical item in the process of selecting the most favorable approach.

Relative to experimental technology tasks, the following engine systems technology approach is typical of the work now required:

1. Experimental validation of design point composite engine specific impulse and thrust values for a large number of the attractive composite engine initial acceleration modes (i.e., ejector mode) of which there are six in the Class 1 grouping. This work would be followed by simulated flight speed and off-design point conditions. (As pointed out above, simultaneous component level research can and should be conducted to establish insight into system improvement.) For this work, air liquefaction operation can be simulated by using high pressure ambient temperature air in the primary rocket and a stipulated afterburner rich equivalence ratio. Thus, "hot cycle" aspects only would be tested, and the equipment requirements would be greatly eased.

2. For selected engine cycles (e.g., Supercharged Ejector Ramjet, RamLACE), a progressive component to system experimental approach

would be such as that illustrated in Figure 371. This appears to be a logical means of achieving engine systems level testing, while developing critical component technical expertness.

In a large sense, the immediate need is for continued exploratory design, adding more depth to the conceptual studies that have already been completed. It is anticipated that this activity should be continued for approximately one year, after which preliminary design and the fabrication and test of critical structural elements should be considered. As noted, engine systems oriented experiments on a subscale basis are the next indicated steps.

9.2.10 Vehicle Systems Technology

9.2.10.1 Significance

The goals of the current program were directed toward the formulation of composite propulsion system design concepts for the reusable vehicle requirement. A serious judgment of the feasibility and desirability of reusable launch vehicles per se is clearly outside the scope of this program. The relation of the launch vehicle to the propulsion system is, however, critical and has been emphasized in the performance of the program because of the implicit need to utilize a vehicle frame of reference in order to judge the merit of the propulsion systems.

Although this report is primarily concerned with composite propulsion concepts, it has been shown to be essential that supporting vehicle design, engine/vehicle integration, and mission studies be conducted in order to most effectively take advantage of the particular characteristics of this new class of engines. It will be equally important to continue such studies in future engine oriented programs to provide a sound evaluation basis to ensure that the various propulsion subsystems be integrated into the most effective propulsion package for the particular application.

9.2.10.2 Technology Status

Reusable Space Launch Vehicles for missions such as orbital ferry operations have been studied. A broad and representative spread of concepts, reflecting the level of study activities was presented about three years ago in Reference 80. Under both NASA and Air Force sponsorship, as well as under Marquardt sponsored activities, a large number of vehicle concepts and mission modes have been evaluated, primarily for the orbital launch mission. Both all-rocket concepts and first stage airbreathing concepts have been examined, with the rocket receiving more prominent attention. As a note, one paper which was presented about the time the present composite engines study was initiated, cited the composite engine potential (Reference 81).

A critical review of the principal issues governing the feasibility and desirability of reusable launch vehicle systems was presented in Reference 81.

A feature of this paper is that it included in its preview the implications of the supersonic combustion ramjet, previously not assessed by vehicle/mission studies in the open literature. Reusable vehicles, the paper concludes, are always significantly less expensive than expendable systems if the research and development costs are excluded. Also, the aerodynamic heating and materials problems were stated to be apparently less critical than had been suggested in previous studies.

In the overview, it is concluded that the vehicle and mission analysis work which has been conducted to date has been valuable in establishing an effective systems base for recoverable launch vehicles. It has approximately defined the vehicle and mission performance characteristics and the critical technology areas, and it has provided an index of relative cost of the various systems. For the greater part, these studies were directed toward rockets, turbomachines, ramjets, and Scramjets singly, or as combination propulsion devices. The current study is the first exploration of the composite engine approach and, while this work has been clearly illuminating, it has not been conducted to the ultimate depth that would be desired prior to a vehicle/engine commitment for the reusable launch vehicle mission.

9.2.10.3 <u>Critical Area Assessment</u>

The critical areas pertinent to the composite engine powered first stage vehicle are as follows:

1. Air breathing mode propulsion system performance and installation
2. Hydrogen stowage and feed system
3. Thermal protection systems (Active and passive)
4. Vehicle flight characteristics

9.2.10.3.1 <u>Propulsion System</u>

The following items are considered to be of major importance in the definition of the installed propulsion system development:

1. Propulsion system performance and weight assessment
2. Technology of lightweight, radiative, and regenerative cooling of airframe and inlets
3. Inlet designs and controls capable of operation over the entire vehicle flight spectrum
4. Integration of inlet and exit nozzle geometry with the airframe for effecting minimization of vehicle inert weight and maximization of installed propulsion performance
5. Performance of large expansion ratio nozzles at design and off-design conditions such as those which occur in the critical transonic region

9.2.10.3.2 Hydrogen Stowage and Feed System

The hydrogen tank is a significant contributing element to the system cost and development. As indicated in Table LXIII, the contribution of the hydrogen tank to vehicle unit cost is 8 percent, and the contribution to the total system development dollars-years is 5 percent. Continued development is required in the following areas:

1. Selection of insulation material with consideration of complete inspectability after each flight

2. Applicable purge systems compatible with the reusable system concept

3. Alternate methods of support for the heat shields

4. Experimental evaluation of rigidized Fiberfrax blocks and reinforced polyurethane foam at elevated temperature and when subjected to the applicable acoustic environment

9.2.10.3.3 Thermal Protection Systems

The present study utilized an advanced structural concept consisting of near state of the art materials and processes. The importance of minimum weight structure for a two-stage vehicle system and its crucial significance for single stage concepts (Appendix E) warrants further research and development of potential weight saving concepts. Critical technology items include the following:

1. Development of high strength, high temperature, oxidation resistant material systems

2. Development and/or improvement of insulation materials (hot or cold) for thermal protection systems applicable to a reusable system

3. Development of uncooled, reusable, lightweight, composite material systems for application to leading edges and nose caps

4. Development and advances in high temperature mechanism design including bearings, seals, and lubricants

9.2.10.3.4 Vehicle Flight Characteristics

The aerodynamic design of the first stage vehicle was directed toward achieving the maximum attainable aerodynamic efficiency per unit weight, while maintaining adequate stability and control and airport performance characteristics. Major areas requiring further analysis and experimental confirmation are identified as follows:

1. Combined and first-stage-alone lift and drag characteristics as a function of Mach number and vehicle attitude

2. Static and dynamic stability and control characteristics of combined and individual stages throughout the operational spectrum with emphasis on stage separation

3. Aeroelastic effects

4. Aerothermodynamic characteristics; in particular, the determination of shock impingement magnification factor and area definition for leading edge design

5. Evaluation of propulsion system-vehicle interactions such as the effects of asymmetric thrust on vehicle stability

6. Evaluation of staging techniques and development of criteria

9.2.10.4 Future Program Implications

Although all technologies are important, only those areas relative to the installed propulsion system and vehicle flight characteristics will be considered to be immediately applicable to future composite engine activities, since it is assumed that propellant and aircraft thermal protection systems will be covered under current or anticipated vehicle oriented programs. For the immediate future, the prime need for airframe oriented activities relate to the following two areas:

9.2.10.4.1 Installation

The designs of engines, in terms of length, configuration (axisymmetric versus two-dimensional), thrust rating, etc. are affected to a large degree by the airframe. Close liaison with a qualified vehicle design organization is required, but the effort can almost be of a nominal consulting nature rather than a scheduled activity.

9.2.10.4.2 Engine-Vehicle Performance

Approximately one year later, it will be necessary to evaluate significant changes in design and performance parameters in terms of their effect on the vehicle, the desired trajectory, and the payload. Only a moderate activity will be required to evaluate significant perturbations and to keep in step with vehicle development. It is estimated that this scope of activity will be required for perhaps one year while the engine definition program is in progress.

Once the engines are defined in greater detail with respect to configuration, performance, weight, and operating modes, it will be desirable to expand the vehicle oriented activities to evaluate one or more specific engine types from the overall systems standpoint. It is anticipated that this and subsequent vehicle oriented programs will be conducted within the framework

of studies relating to recoverable launch vehicle programs that have been sponsored by NASA and, it is presumed, will be sponsored by NASA in the future.

9.3 Summary and Critical Technology Program Implications

Each of the basically related technology areas for composite propulsion systems as presented (Figures 369 and 370), has been briefly discussed to the end of summing up the current status and critical technology requirements. Future program implications have been generally singled out on the basis of unique requirements of the composite engine.

At this point, it is pertinent to take the larger view of the sum total of the technology needs of the composite engine with an orientation toward program recommendations. The overall objective, again, is to provide a balanced substantial preliminary engineering basis for the initiation of study and research leading to a possible composite engine development program.

Figure 372 reflects the introduction of this element of perspective into the straight listing of technology areas given earlier. Each technology area is associated with one or more of the following situations: (1) a significant pertinent background exists, (2) it is an area under current investigation, (3) both of these, or (4) neither of these. Such an illustrative device necessarily oversimplifies the situation, but it is, however, useful for the development of an overview.

Figure 372 indicates that for all of the areas (excepting the "engine systems" category) a significant background exists, or current programs are in progress to provide this background, or both. However, it is to be observed that specific technology items which demand further attention fall into each of the cited categories, even where significant background already exists. This was indicated by the "Future Program Implication" items noted at the end of each preceding section.

Again, in the larger view, a vehicle systems level of involvement is indicated. However, in keeping with the propulsion orientation of the study, attention is directed specifically to the engine system, and its subsystem areas. In Figure 372, the engine system technology area is indicated to be a major area of concern. Neither an adequate background exists nor are current programs underway to broadly explore those composite systems which have been shown to be the leading contenders, viz., the Class 1 systems.

Highlighting the engine systems area as the critical technological area carries with it the following proviso: Many of the component/subsystem areas have not been adequately developed to the point where they can fully support a full scale composite engine systems preliminary design activity. For instance, primary rocket technology must be moved significantly ahead before serious engineering thought can be given to development of an actual engine.

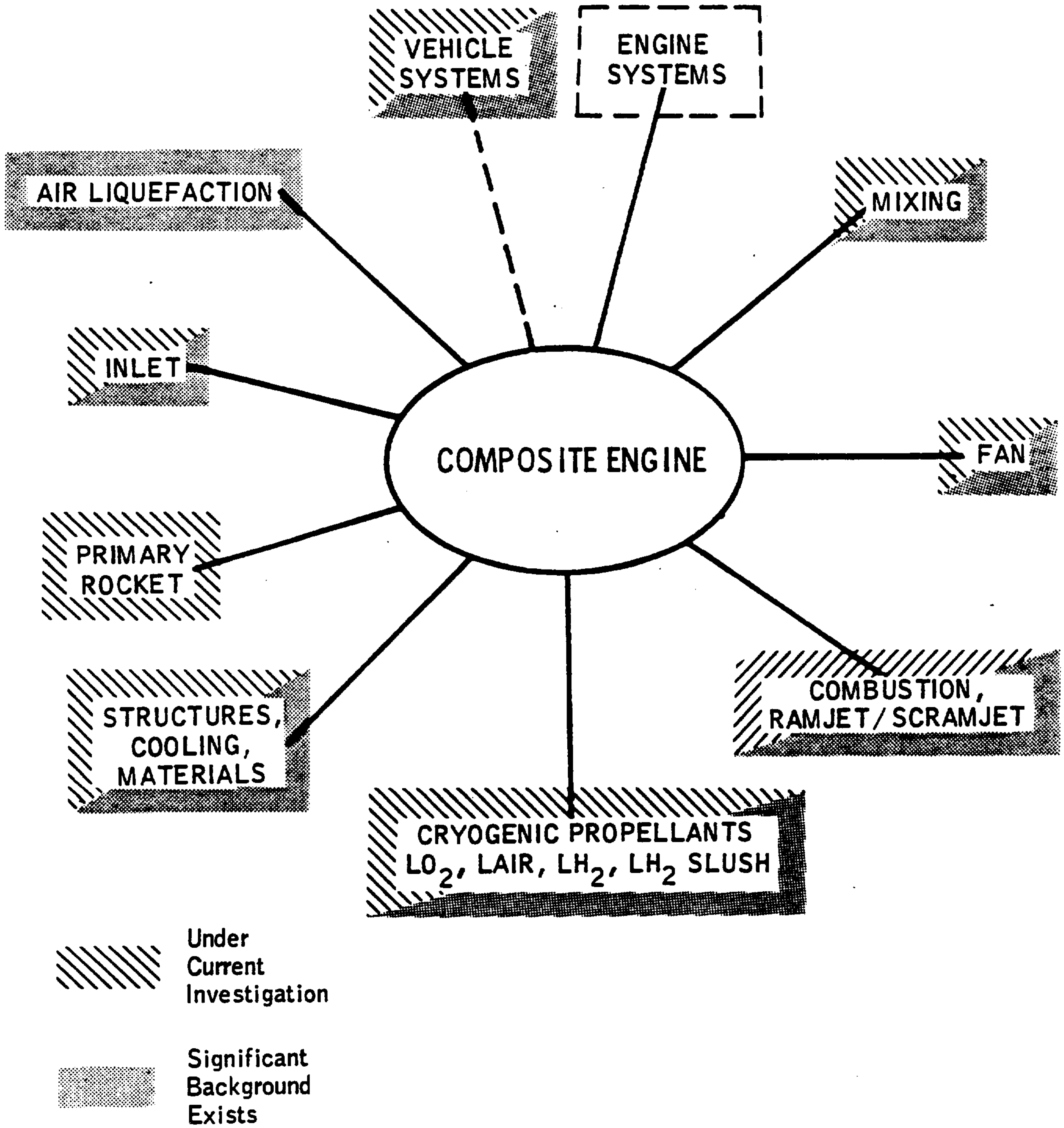

FIGURE 372. General Status of Related Technology Areas for Composite Engines

Also, a systems oriented technology program implicitly contains a componentry base. This base must be brought along, technologically speaking, with the overall system to achieve a sound net advancement. Figure 371 and its associated commentary proposes just this.

Therefore, in providing for the composite engine systems technology (Figure 372), where it is absent or poorly developed, the subsystem areas (mixing, combustion, etc.) can and should be treated somewhat independently. This is (1) to accomplish the systems level work, and (2) to provide the ultimate subsystem base for actual composite engine engineering efforts.

This page intentionally left blank.

10.0 RESULTS

10.1 Summary of Results

The objectives of the study (See Section 2.0) appear to have been unconditionally satisfied in the performance of the program conducted under Contract NAS 7-377. This section briefly reviews the objectives in the light of the findings of the study. Stated differently, the primary results of the study are summarized with respect to the three basic objectives of the study.

10.1.1 Objective No. 1 - Appraisal of the Significance of Composite Engines to Advanced Launch Vehicles

All identifiable composite propulsion systems (See Section 3.0 for definitions and restrictions) applicable, in concept, to advanced reusable launch vehicles were examined within a common vehicle/mission model. Thirty-six concepts were explored in the Class 0 phase. Using orbital payload performance as a primary measure of merit, the identified candidate composite systems were ranked. Tempering the ranking with secondary criteria (technical risk, operational feasibility, and a system cost indication), a grouping of the twelve more attractive engine concepts was selected for further evaluation in the Class 1 phase.

The Class 0 phase of the study achieved the following with respect to Objective No. 1:

1. The overall payload performance potential of composite propulsion systems were determined.

2. The effects of the degree of vehicle reusability, from "minimum" (parachute/ocean recovery) to "full" (both stages horizontal landing at base), on payload performance were shown for a representative composite engine as compared with a very advanced rocket.

3. The criteria for specifying maximum payload performance of composite propulsion systems were established.

4. Relatively unattractive composite system types (for reusable vehicle applications) were identified and documented.

The twelve Class 1 engines were examined in significantly further depth (parametric performance analysis, conceptual design studies, vehicle/engine integration) to achieve a refined payload ranking. Based on a technology consideration, two engine concepts were selected for further technical penetration in the final stage of the study (Class 2).

The Class 1 phase of the study accomplished the following with respect to Objective No. 1:

1. The relative payload potential of the select composite propulsion system was determined and referenced to that of the comparison systems, namely, the very advanced rocket and the representative advanced turbomachine-based airbreather.

2. The contributive performance potentials offered by each -- (1) Scramjet (2) air liquefaction (but not collection), with and without recycled (slush) hydrogen operation, and (3) fan subsystem -- were determined, within the composite engine context.

3. The total system potential hardware cost potentialities were monitored via the parameter payload/total system dry weight ratio for both composite and comparison systems.

4. Vehicle configurations (two-stage) reflecting marked superiority over competing types for first stage composite engine propulsion were conceived and evaluated.

5. Single stage to orbit vehicle concepts employing composite engines were considered (two discrete approaches), but only preliminary conclusions were reached (Appendix D). Problem areas, as well as potentials, were highlighted, however.

The Class 2 composite engines were carried into detailed conceptual designs wherein subsystems were characterized and component interactions were addressed. An important aspect of this phase was the determination of engine performance sensitivity to component/process efficiency and operating point variations. Also, comparison cases (vehicle/mission oriented) based on a very advanced rocket and on an advanced turboaccelerator type airbreather were prepared and documented.

The Class 2 effort achieved the following results with respect to Objective No. 1:

1. Based on a significantly refined reusable vehicle/mission basis, comparative payload performance results for the selected composite engine systems, a very advanced rocket, and a representative advanced turboramjet engine were developed and documented.

2. The payload implications of relaxing the peak airbreathing flight speeds (e.g., from Mach 8 to 6) were determined in the interest of appraising vehicle/engine potential based on incorporating state of the art materials and structural approaches.

3. The effects on payload of off-design engine specific impulse and thrust/weight ratio (as well as vehicle drag) were determined and presented in statistical terms over ranges estimated (on a historical basis) to encompass any anticipated deviation which might occur in the development process.

4. Engine/vehicle (physical) integration problems were evaluated and tentative solutions were described in the documentation. Also, detailed primary rocket/engine integration techniques were determined and documented.

5. The alternate mission capability of the Class 2 composite engine first stages (with and without auxiliary fuel tanks) was determined, as was that for the comparison airbreather. Two cruise-type missions were evaluated and documented (Appendix D) as follows:

   (a). Zero-payload range at Mach 5 (Mach 8 for Scramjet) cruise conditions

   (b). Endurance (time on station) for various station radii and payload values

The basic incentive to explore the composite engines, because of their intermediate characteristics between pure rockets and airbreathers, appears to be justified from the results presented in the previous sections of this report. For example, it is now possible, using the study results, to make a quantitative reconstruction of the specific impulse versus engine thrust/weight ratio chart often used to compare competing powerplant types such as turbomachine type airbreathers and rockets (See Sketch A in Section 1.2). Figure 68 presents a log plot of I* (equivalent effective specific impulse as defined on the figure) and uninstalled engine thrust/weight ratio. Note that the data points are those Class 0 concepts nominally staging at 8000 ft/sec (no Scramjet mode engines). Note the position of the very advanced rocket.

As expected, there is a general and well-known performance/weight ratio trend to be observed here: specific impulse and thrust/weight vary inversely in a first approximation. The mission performance significance of this "natural" performance/weight ratio coupling was, in many respects, the essence of the overall study.

10.1.2 Objective No. 2 - Assessment of the Critical Technology Requirements of Composite Engines

Technology areas which have a bearing upon the leading composite propulsion systems were defined, and the significance and status of each were enumerated. Delineation of critical items was emphasized. Where feasible,

the program direction of current and/or programmed efforts was noted. Within the technology frame of reference thus established, the implications to a broad technology program were evolved and described in Section 9.0.

The engine bases utilized for satisfaction of the critical technology assessment objective were as follows:

1. The Class 1 (intermediate selection) composite propulsion systems were taken to be leading representatives of the composite engine as a type.

2. Their component and system technology requirements, viewed together, form a basis for assessment.

3. The design penetration down to the subsystem/component level in the Class 2 phase provided general insight for viewing this larger Class 1 system collection in further detail than would otherwise be possible.

Specifically, the technology assessment phase of the study accomplished the following with respect to Objective No. 2:

1. Leading composite propulsion systems were characterized in terms of technology-area dependence.

2. These technology dependence areas were reviewed for status and, where feasible, for program direction.

3. In view of on-going applicable technology efforts, as well as that base already existing, a composite engine oriented technology program was broadly formulated, without considerations of scheduling and cost.

4. An example near-term program targeting on critical composite engine technology areas which are identifiable was subsequently outlined.

10.1.3 Objective No. 3 - Generation of Systematic Composite Engine Documentation

Consistent documentation was developed for the composite engine concepts surveyed in each of the three phases (Classes 0, 1, and 2). The depth of this documentation for each engine naturally increased as a result of the progression from many, to a few concepts (See Figure 6). Thus, the Class 0 documentation is characterized by a large number of brief Fact Sheets, whereas the published Class 2 information approaches complete engine technical information report format.

All of these engine oriented data are cast into a user handbook format, and included as volumes (Volumes 4 to 7) of the final report of the study (See Figure 6). The main technical report (Volumes 2 and 3) contains technical considerations relating to engine sizing, internal parametric analysis, and component/subsystem design considerations. Also, the very considerable vehicle/mission effort (conducted to satisfy Objective No. 1) is also reported in the main technical report. The Summary Report (Volume 1) is a condensed description of the overall study effort, specially oriented for management level personnel.

Documentation for the program provides the following, by way of satisfying Objective No. 3:

1. Fact Sheet documentation of a large number (in intent, all) of diverse composite production system candidates (Volumes 4 and 5)

2. Parametric information on selected composite engines which fully reflects the characteristics of the more attractive system (Volume 6)

3. Point design information in some depth, along with expanded parametric data, on a representative few of the leading composite concepts, with considerable emphasis on the engine effects of component/subsystem operating point and process efficiency variations (Volume 7).

4. Engine sizing and trade-off information utilized in the engine studies of Items 1 to 3 above (Volumes 2 and 3)

5. Primary rocket subsystem detailed preliminary design and analysis results (Volumes 2 and 3)

6. Vehicle and mission design and performance analysis results, including substantial vehicle/engine integration results (Volumes 2 and 3)

10.2 Qualification of Results

In summarizing the study results, it is appropriate to indicate the principal qualifications which were influential, perhaps even decisive, in arriving at the results which are reported. A number of these qualifications are implicit in the study guidelines given in Section 3.1, and in the definitions, for the purposes of the study, of "Composite Propulsion Systems" and "Advanced Launch Vehicles" (Sections 3.2 and 3.3, respectively). Additional qualifications cited below are more of the nature of definition of the depth of the study in local areas.

Finally, the relative stress given to alternative approaches and guiding philosophies, which were chosen or emphasized as the study proceeded, was in itself influenced by those general trends and projections which the project team

could surmise as being valid at the time. An example is the progressive emphasis of the study on fully reusable launch vehicle operations.

10.2.1 Study Not Cost Oriented

Considerations of cost comprised a secondary, qualitative criterion in the ranking and selection of concepts. Only system procurement, or hardware cost was included in an attempt to monitoring of the relative expensiveness. The parameter used was the system inert/payload ratio. Development and operating cost potentialities remain basically unaddressed.

10.2.2 Combination Propulsion Schemes Not Evaluated

Figure 1 (Section 1.2) contrasts composite propulsion systems with combination schemes. Combination systems are those which utilize functionally separate engine systems (e.g., rocket engine plus ramjet engine) to provide vehicle propulsion across the mission profile. The study was distinctly limited to composite systems, with the exception of the rocket (and to a considerably less degree) the turbomachine-based airbreathing comparison cases. Therefore, no conclusion is made with respect to composite versus combination propulsion systems. It might be noted that such a comparison has been accomplished for hypersonic cruise systems, with favorable findings for the composite approach (Reference 8). However, this comparison was not accomplished in the present launch vehicle study program.

10.2.3 Variable Depth of Design Penetration

As fewer candidate composite propulsion systems were examined in the Class 0, 1, and 2 progression, the design penetration accomplished by the study team members did increase commensurately as suggested by Figure 6. However, the allocation of manhour resources was such as to accomplish a marked decrease in technical penetration gradient as one views successively: (1) the primary rocket subsystem (Rocketdyne), (2) the composite engine system (Marquardt), and (3) the vehicle and its mission aspect (Lockheed). Illustrating the point, the report presents highly conceptual vehicle outline drawings and, at the same time, an advanced hydrogen turbopump layout, which entailed bearing and rubbing seal criteria for long life operation. This apparent disparity in penetration is characteristic of what one would expect in a vehicle-oriented propulsion system study, stressing the rocket engine and its technological assessment. The "penetration gradient" here should, however, be comprehended by the reader, and it is therefore noted here.

10.2.4 Second Stage Concept Borrowed

The basis for determining orbital payload, starting at a staging point and second stage light-off weight (achieved by the composite engine powered first stage) was the upper stage vehicle defined by General Dynamics/Convair under the Reusable Orbital Transport Study (Contract NAS8-11463, Reference 1) as

noted in Section 7.6.1.5. This vehicle is a point design of 326,711 lbm gross weight with a total mission velocity of 21,687 ft/sec. The gross payload is 18,380 lbm, based on the same definition as used in the current study (See description under General Evaluation Criteria above). Scaling equations from Reference 1 were processed by Lockheed to provide the link between orbital payload and second stage weight/staging velocity and staging conditions. As has been shown (e.g., Table XLII), both the second stage weights and the staging velocities varied widely with the effectiveness and operating speed characteristics of the various composite engines. There is, therefore, a considerable increase in numerical uncertainty associated with the required extrapolations undertaken from the second stage design point basis. Since the overall performances of the second stages strongly influence the payload magnitude (high payload sensitivity), the numbers themselves must be used cautiously. The relative ranking of system potential was accomplished on a more solid basis. Second stage weight delivered to a staging condition, by itself, will prove a much more accurate measure of the effectivity of the composite engines and the rocket and turbomachine-based airbreather comparison engines.

10.2.5 Staging Mechanization Not Explored

As discussed in the vehicle model description (Section 3.3), the second stage is mounted in a buried, parallel installation included in the first stage. This approach, as was substantially illustrated in the Class 1 vehicle discussion, provides definite aerodynamic and weight advantages. Also posed with this design, and as a matter of fact, with all related designs, are potential problems of physical stage separation. Outside of holding the staging dynamic pressure consistently at 200 psf, no attention was given to the staging mechanism itself, in the study. There is however a weight assessment for separation subsystem items, e.g., separation rockets (See Table XXVII).

10.2.6 Sonic Boom Not Assessed

Generation of ground overpressure transients (sonic booms) is characteristic of airbreathing mode vehicle propulsion systems once supersonic flight is attained. (The HTO rocket vehicle can cause strong, but highly localized, overpressure conditions.) Composite propulsion systems have been noted to be significantly more flexible than turbomachine-type airbreathers in reducing and even avoiding the acceleration sonic boom intensity but, however, not without a reduction in payload performance (Reference 8). The sonic overpressure situation for large hydrogen fueled launch vehicles is highly complex and associated with many unknowns. These are being addressed to a certain extent by General Dynamics-Convair in the concurrent study of hydrogen fueled hypersonic transport systems under Contract NAS 2-3180. The sonic boom implications of the engine/vehicle systems included in the present study were not addressed.

10.2.7 Post Liftoff Abort Situation Not Included

The capability for safe mission abort can have a very significant effect on vehicle design and operating profile selection. Although the study team was aware of the possible significance of abort capability, it was not exercised as a restraint.

10.2.8 Less Than Full Recovery Approach De-emphasized

In keeping with inferences drawn from the time of application guideline of the study (viz., 1975 to 1985), emphasis was progressively given to full recovery of all vehicle stages as the study proceeded. By this is meant controlled, horizontal landing at a designated base of operations for both vehicle stages. In the mission model used, this equated to first stage postentry flyback to the launch point including a 5 minute power-on subsonic loiter/landing, and a typical power-off second stage horizontal landing. It is known that lower order recovery techniques can significantly ameliorate the payload penalty implicit in this full recovery modus operandi. An example is the parachute/touch-down rocket approach associated with ocean recovery of large rocket stages (Reference 82). This mode appears especially beneficial to typical all-rocket nonlifting vehicle concepts, but it requires associated naval support operations and poses other operational problems. The full spectrum of recoverability was cursorily examined in the initial phase (Class 0) of the program. The results are shown in Figure 69. Thereafter, full recoverability alone was considered.

10.2.9 Single Stage To Orbit Cases Remained Undeveloped

As stipulated by the guidelines, single stage to orbit vehicles using composite propulsion systems were examined in the study in all phases but the final phase (Class 2). Two separate engine/vehicle approaches were briefly examined in the Class 1 Phase: one a lifting body HTOHL concept (Lockheed), the other an axisymmetric VTOVL concept (Marquardt). The results are presented in Appendix E. High payload sensitivity to vehicle and engine structural weight was evidenced as expected. It is clear that much greater penetration into the specific and unique problems of the single stage is necessary to establish a definitive conclusion on feasibility. Commensurately, it was prudent that full resources of the study be concentrated on the two-stage vehicle concept. Thus, the composite engine powered single stage remains essentially as an undeveloped, not to say unpromising, concept requiring significant further attention.

10.2.10 Gross Weight of Comparison All-Rocket Systems Substantially Off Payload-Optimum Values

This study was based on a fixed launch weight of 1.0 million lbs (Section 3.1.1) which for typical reusable rocket systems (Reference 19) results in a substantially off-optimum payload ratio, and a pessimistic total system inert weight/payload ratio. For example, on the basis of a fixed payload weight of 35,000 lbs, the all-rocket system would indicate payload

maximization at a significantly higher gross vehicle weight (2.0 million lb class), while a competing airbreathing system would remain in the 1.0 million lb gross weight class. This point should be taken note of when comparing the rocket and airbreathing (composite and turboaccelerator systems) first stage payload results presented.

In this study, the complete examination of the Very Advanced Rocket in a fully recovered vehicle frame of reference is provided in the Class 2 results and, specifically, in Section 8.6.2. The Class 1 results should be considered preparatory to these final findings in that all takeoff modes were not considered.

10.3 Study Critique

At the conclusion of the study, it was evident that there were a number of technical areas which require further investigation to provide an increased confidence level in the overall program results. These areas centered about engine design and analysis, particularly for the two Class 2 engines which were selected, the Supercharged Ejector Ramjet and the ScramLACE, for which some detailed conceptual design work had been accomplished. These technical aspects were identified as a direct result of the increased design penetration in the final study phases.

An example is the assumption (based on significant previous and concurrent study at Marquardt) that the high speed supersonic combustion mode of the ScramLACE powerplant would demand hydrogen cooling flows not exceeding those associated with stoichiometric burning. The most severe condition would be the Mach 10 airbreathing termination point, which Lockheed found to be the maximum payload staging velocity for engines with supersonic combustion modes (Section 8.6.2.9).

What is now required is a significantly deeper penetration into associated design details, such as the heat transfer and structural design areas. In response to the potential Scramjet mode cooling problem cited above, the Mach 10 flight condition should now be analytically imposed on the regeneratively cooled sections of both the engine and the inlet and a comparison made between the total heat flux and the available hydrogen heat sink. Should significantly higher than stoichiometric hydrogen requirements be indicated, then the payload capability of ScramLACE system would be correspondingly degraded. Another potential cooling problem which was not appraised was that of engine aftercooling subsequent to engine shutdown in flight. Should excessive hydrogen be required for this aftercooling, it is obvious that the overall vehicle performance will be affected.

The particular variable geometry exit nozzle concepts reflected in the Class 2 engine designs represent nominal attempts to satisfy the area ratio requirements of both the ejector and subsonic combustion ramjet modes. Alternative nozzle designs may prove to be significantly superior. Moreover, a completely fixed geometry approach would provide an attractive potential for

reduction of weight and complexity. The performance penalty associated with a fixed exit has yet to be determined, however.

In general, propulsion system performance was calculated for the various engine operating modes assuming that all components were operating at on-design conditions, albeit at realistic efficiencies. In the Class 2 phase sensitivity analysis, the individual engine component efficiencies and operating conditions were sequentially varied about a nominal value in accordance with an assumed schedule. By this means, the effects of component efficiencies on overall specific impulse and thrust were documented for isolated component efficiency excursions for all feasible engine modes and flight conditions. What remains to be performed is a basic off-design analysis wherein nonideal performance component matching is addressed. Such an effort would assess the realistic situation of definite upstream and downstream component interaction.

Another area wherein additional efforts are likely to be fruitful is in a broadened and deepened subsystem inquiry for selected components. This should include such items as air liquefaction units operating in the recycle mode with tanked slush hydrogen (as a heat sink). The basic performance virtues of recycled air liquefaction operation were demonstrated in the study. However, in investigating specific mechanization approaches, considerations of the physical characteristics of slush hydrogen, for example, were not accomplished. Inquiry here may uncover technical problems which could reflect less or more favor on this particular operating cycle with respect to its position relative to the lower performance nonrecycle operation. The performance of this and other tasks, similar in nature, should do much to add authority and increased confidence to the findings of the basic study.

Over and above the technical areas mentioned above, there are a number of propulsion technology issues which the study illuminated as being fundamental to composite engine feasibility, such as induced mixing of rocket exhaust and air with and without combustion, fan interaction with the mixing process, liquid air-hydrogen rocket primary components (combustors, pumps), fan performance and retraction techniques for composite engines, and the general thermodynamic and control feasibility of multimode operation -- the key to composite engine flexibility and wide range capabilities.

These and other technology areas will require further study and experimentation. Indeed, they provide a potential program basis, both analytical and experimental, for advancing the status of composite engines to a point of demonstrated feasibility over the next several years.

11.0 CONCLUSIONS

Based upon this initial and exploratory study of composite propulsion systems and their application to advanced reusable launch vehicles, the following specific conclusions appear to be supportable:*

1. Composite propulsion systems provide for increased payload capability relative to very advanced rocket powered vehicles for fully recoverable, orbital launch systems (A factor of 2 to 3 for the model used.) However, the composite systems presently appear to offer no significant reduction in system dry weight per pound of payload. Composite systems do offer significantly increased operational flexibility by virtue of their capability to cruise effectively.

2. Composite propulsion systems, as applied to launch vehicles, are directly competitive with advanced turboaccelerator airbreathing systems from the standpoint of payload performance, operational flexibility, technical risk, and system dry weight per pound of payload. In addition, based on a brief analysis of the cruising mission performance potential, composite systems appear to be also competitive with turboaccelerators.

3. Viewed broadly, composite engines provide a spectrum of increasing performance capability with increasing component and/or operational complication. The higher performance systems will require considerable advances in the state of the art (e.g., the Scramjet and air liquefaction systems), whereas few technological unknowns are associated with the modest performance systems.

4. The more attractive composite propulsion systems are characterized as ejector or air augmented rocket systems which are capable of ramjet operation following the initial acceleration phase. Particularly important among candidate systems are those characterized by a low pressure ratio fan followed by an ejector unit capable of afterburning operation.

5. Normally, composite engines utilize airbreather-typical paths to maximize the delivered payload. These paths are characterized as high dynamic pressure paths limited by structural and aerodynamic constraints. The wide range of thrust scheduling possibilities characteristic of composite engines appears to afford operational flexibility not generally available with turboaccelerators.

6. No extraordinary technology requirements accompany composite propulsion systems although considerable further systems and component level analytical and experimental efforts are needed to (1) provide increased confidence in the "best estimate" results obtained to date and (2) establish design criteria and define technical approaches for composite propulsion systems.

- - - - - - - - - - - -

*Specific reference sections supporting each of the conclusions presented here are listed at the end of this section.

Substantiation of the thesis that composite propulsion systems can be a third, full contender -- along with the all-rocket and the turbomachine based airbreathing systems -- for the powerplant role in advanced launch vehicles is, perhaps, the principal finding of this study. Ramifications of this finding will develop ultimately as a function of the degree and pace of composite engine study activities and exploratory research and development efforts, which are now in order.

LISTING OF SUPPORTING REFERENCE SECTIONS

Conclusion No.	Supporting Section Nos.
1, 2	8.6.2.9, Appendix D
3	6.5.2.1, 7.6.2.5, 8.6.2.9, Appendix F
4	6.5.2.1, 6.5.2.2.8, 7.6.2.5, 8.6.2.9
5	6.5, 7.6.2, 8.6.2
6	9.0

REFERENCES

1. General Dynamics/Convair, Reusable Orbital Transport Second Stage Detailed Technical Report, Parametric and Analytical Studies and Vehicle Subsystems (U), GD/C-DCB-65-018, Volume III, Contract NAS8-11463, April 1965. [redacted].

2. R-6226, Interim Report - Toroidal Systems Analysis Study, Rocketdyne, Canoga Park, 30 June 1965. [redacted].

3. Investigation of Vehicle-Integrated Rocket Powerplants with Air Augmentation, Final Report on Contract NAS8-11017, The Boeing Company Document D2-23217-1, June 1964. [redacted]. Title - Unclassified.

4. R-5905, J-2T Aerodynamic Spike Thrust Chamber, Phase Zero Final Report, Rocketdyne, Canoga Park, 15 May 1965. [redacted].

5. "Part III - Launch Vehicle Study Final Report (NAS 8-11123), Vol. II," Martin, Baltimore Division, Baltimore, Maryland, November 196[redacted].

6. Fey, Wayne A., and Builder, Carl H., A Comparative Parametric Performance Analysis of VTO and HTO Launch Modes for Aerospace Vehicles, SSD-TDR-63-347, The Aerospace Corporation, 20 December 1963. [redacted]

7. Jackson, Charlie M., Jr., Flight Performance Estimation with Closed Form Approximations to the Equations of Motion, Proposed technical report, NASA, Langley Research Center, April 1965. [redacted]

8. Frank, H., 1964 Advanced Ramjet Concepts Program - Propulsion System Effectiveness Investigation, Technical Report AFAPL-TR-65-32, Volume II, The Marquardt Corporation, May 1965. [redacted] - Unclassified.

9. Kalvinskas, L. A., "Literature Search No. 269 - Composite Rocket/Air-breathing Propulsion Systems," Rocketdyne, A Division of North American Aviation, Inc., Canoga Park, California, June 1965. [redacted]

10. Langley Research Center, Bibliography 63-4 (Volumes 1 and 2), Air Augmented Rockets a Selected Anotated Bibliography.

11. Final Summary Technical Report on the Calendar Year 1963, Ramjet Technology Program, Volume 2 of 12, Jet Compressor Research -- Ejector Ramjet Investigation, The Marquardt Corporation Report No. 25,116, April 1964. [redacted]

REFERENCES (Continued)

12. Flornes, B. J., and Stroup, K. E., Advanced Jet Compression - (Volume 1 (of 6)), Final Report - 1964 Advanced Ramjet Concepts, Technical Report AFAPL-TR-65-32, Volume 1, Marquardt Report 25,155, Contract AF 33(615)-1581, May 1965. [redacted]d.

13. Advanced Heat Exchanger Structural Design Concepts and the Reduced Weight and Volume Potential using Small Diameter Tubes, Marquardt Report 5947, 21 December 1962, Contract AF 33(657)-8626, Project 274.

14. Ryan, J. D. and Rosevear, J. E., Heat Exchanger Component Evaluation, Volume III (of 7), Annual Report under Contract AF 33(616)-7046, Marquardt Report 5880. [redacted] - Unclassified.

15. Nuclear Liquid Air Cycle Engine Studies - Phase I Summary Technical Report of the CY1962 Air Force-Marquardt Contributing Engineering Program, Volume 4, Report No. 25065, 8 March 1963, [redacted].

16. Flornes, Bruce J., The Nuclear Liquid Air Cycle Engine, a paper for the AIAA-ASME Hypersonic Ramjet Conference, Naval Ordnance Laboratory, White Oak, Maryland, April 23-25, 1963, Marquardt Report MR 20245, [redacted]

17. Program Summaries Electromagnetic Ramjet Research and Advanced Liquid Air Cycle Concepts -- Phase I, Summary Technical Report of the CY1962 Air Force-Marquardt Contributing Engineering Program, Marquardt Report No. 25065, 1 March 1963. [redacted].

18. Harry, A. J. and Hindin, S. G., Investigation of the Para-Ortho Conversion of Hydrogen, Englehard Industries, Inc., Technical Report AFAPL-TR-65-59, July 1965, Contract AF 33(657)-11125. UNCLASSIFIED.

19. Lockheed-California Company, Design Studies of a Reusable Orbital Transport, First Stage - Final Detailed Technical Report LR 18791, 21 May 1965, Contract NAS8-11319. [redacted].

20. Brewster, F. E., Parametric One Dimensional Scramjet Performance Using Hydrogen Fuel, Marquardt Preliminary Design Study 155-2006, 29 November 1965. [redacted]TIAL. Title - Unclassified.

21. Dipprey, D. F. and Sabersky, R. H.", "Heat and Momentum Transfer in Smooth and Rough Tubes at Various Prandtl Number," Int. J. Heat and Mass Transfer 6, 1963. pp 329-353.

22. Goldsmith, R. H., Lift-Fan Technology, Astronautics and Aeronautics, September 1965. UNCLASSIFIED.

REFERENCES (Continued)

23. Malvestuto, F. S., and others, Study to Determine Aerodynamic Characteristics on Hypersonic Re-Entry Configurations, Part II - Analytical Phase, WADD TR 61-56, May 1961.

24. Peterson, J. B., A Comparison of Experimental and Theoretical Results for the Compressible Turbulent-Boundary-Layer Skin Friction with Zero Pressure Gradients, NASA TN D-1795, March 1963.

25. Schmidt, J. F., Turbulent Skin-Friction and Heat-Transfer Coefficients for an Inclined Flat Plate at High Hypersonic Speeds in Terms of Free-Stream Flow Properties, NASA RN D-869, May 1961.

26. Lockheed-California Company, Advanced Airbreathing Vehicles, Supporting Report R.O.T. 1-4, LR 19015, Contract NAS8-11319, Burbank, California, 8 June 1965. [redacted]

27. Saltzman, E. J., Base Pressure Coefficients Obtained from the X-15 Airplane for Mach Numbers up to 6, NASA TN D-2420, August 1964.

28. Seager, D. B. and Meyer, J. E., An Investigation of the Subsonic Aerodynamic Characteristics and the Landing Flare Maneuver for Hypersonic Re-Entry, ASD-TDR-62-271, April 1962. [redacted]

29. Jorgensen, L. H., Elliptic Cones Alone and with Wings at Supersonic Speeds, NACA Report 1376, 1958.

30. McDevitt, J. B., and Rakich, J. V., The Aerodynamic Characteristics of Several Thick Delta Wings at Mach Numbers to 6 and Angles of Attack to 50°, NASA TM X-162, March 1960. [redacted]

31. Spencer, B., Jr., Phillips, W. P. and Fournier, R. H., Supersonic Aerodynamic Characteristics of a Series of Bodies Having Variations in Fineness Ratio and Cross-Section Ellipticity, NASA TN D-2389, August 1964.

32. Spencer, B., Jr., and Phillips, W. P., Transonic Aerodynamic Characteristics of a Series of Bodies Having Variations in Fineness Ratio and Cross-Sectional Ellipticity, NASA TN D-2622.

33. Stivers, L. S. Jr., and Levy, L. L., Jr., Longitudinal Force and Moment Data at Mach Numbers from 0.6 to 1.40 for a Family of Elliptic Cones with Various Semi-apex Angles, NASA TN D-1149, December 1961.

34. Wiggins, L. E. and Kaatari, G. E., Supersonic Aerodynamic Characteristics of Triangular Plan-Form Models at Angles of Attack to 90 Degrees, NASA TM X-568, July 1961. [redacted]

REFERENCES (Continued)

35. Dennis, D. H., and Cunningham, B. E., Forces and Moments on Pointed and Blunt-Nosed Bodies of Revolution at Mach Numbers from 2.75 to 5.00, NACA RM A52E22, August 1952.

36. Penland, J. A., Aerodynamic Force Characteristics of a Series of Lifting Cone and Cone-Cylinder Configurations at a Mach Number of 6.83 and Angles of Attack up to 130°, NASA TND-840, June 1961.

37. United States Air Force, Stability and Control Datcom, 1960.

38. Pitts, W. C., Nielsen, J. N., and Kaatari, G. E., Lift and Center of Pressure of Wing-Body-Tail Combinations at Subsonic, Transonic, and Supersonic Speeds, NACA Report 1307, 1959.

39. Bassett, M. T., Structural Design Considerations and Analysis of a Manned Hypersonic Cruise Vehicle, Lockheed Technical Memo LTM 50861, 1 June 1965.

40. Mijares, R. D., Parametric Weight Synthesis of a Lifting-Body Hypersonic Cruise Vehicle, Lockheed Technical Memo LTM 50855, 28 May 1965.

41. Mastroly, F. R., Jr., Forsythe, C. G., and McGlothlin, C. E., Thermal Analysis of Two Mach 12 MHCV-Airbreathing Propulsion Vehicles: Systems H and L, Lockheed Technical Memo LTM 50864, June 1965.

42. General Dynamics/Astronautics, Weight Analysis of Hypersonic Airbreathing Aircraft, Final Technical Report, GD/A-DCB-64-073, Volume II, Contract NAS2-1870, October 1964. [redacted]AL.

43. Weirich, R. L., Analytical Determination of the Take-off Performance of Some Representative Supersonic Transport Configurations, NASA TN D-2308, June 1964.

44. Status Report. Hypersonic Ramjet Heat Transfer and Cooling Program Marquardt Report MP 1412. [redacted]ed.

45. Burnette, T. D., Pearlman, E. J., and Thomson, R. W., The Performance and Structural Design of the Marquardt MA114-XAA Supersonic Combustion Ramjet, Contract AF 33(657)-8491, Marquardt Report MR 20,222, February 1963[redacted].

46. V. G. Rockhold, C. M. Onspaugh, W. L. Marcy, Study to Determine Aerodynamic Characteristics on Hypersonic Re-Entry Configurations, Part I - Experimental Phase, WADD TR 61-56, March 1961. C[redacted]

47. D. B. Seager and others, A Fundamental Study of the Problems Associated with the Approach and Landing of Advanced Flight Vehicles, LR 14534, June 1960. [redacted]

REFERENCES (Continued)

48. Escher, W. J. D., Flornes, B.J., Goldstein, A.E., and Odegaard, E.A., Air Augmented Rocket Propulsion System Study, Final Report on Contract NAS 4-661, The Marquardt Corporation Report 25,148 November 1964. [redacted]. Title - [redacted]

49. Brown, M. L., Woodgrift, K. E., and Ozawa, R. I., Applied Research and Advanced Technology for the Supersonic Combustion Ramjet for 1964, Part I, Technical Report AFAPL-TR-65-15, The Marquardt Corporation, April 1963. [redacted]d.

50. Bradie, P. R., Supersonic and Hypersonic Inlet State of the Art Survey, Lockheed Missiles and Space Company, Huntsville Research and Engineering Center, Technical Memorandum TM 54/20-47, Contract NAS8-20082, July 1965.

51. Yaffee, M. L., Inlet Progress Key to Development of Advanced Aircraft, Aviation Week, April 4, 1966.

52. Karanian, A. J. and Kepler, C. E., Experimental Hypersonic Inlet Investigation with Application to Dual-Mode SCRAMJET, AIAA Paper Nu 65-588, United Aircraft Corporation Research Laboratories. UNCLASSIFIED.

53. Inlet Development Status Report, Report MP 1175, The Marquardt Corporation, August 1963, [redacted]. Title - Unclassified.

54. Fashing, W. A., and Asmus, F. J., High Bypass Lift/Cruise Fan The State of The Art. SAE Paper 650202, April 1965. UNCLASSIFIED.

55. Giulianetti, Demo J., Biggers, James C., and Corsigua, Victor R., Wind Tunnel Test of a Full-Scale, 1.1 Pressure Ratio, Ducted Lift-Cruise Fan, NASA TND-2498, November 1964.

56. Yaffee, M. L., Lift Fans Gain Favor for VTOL Aircraft, Aviation Week, August 9, 1965.

57. Fleming, W. A., Kaufman, H. R., Harp, J. L. Jr., Chelko, L. J., Turbojet Performance and Operation at High Altitudes with Hydrogen and JP-4 Fuels, NACA RM E56E14, 1956.

58. Builder, C. H., and Kroll, R. W., Preliminary Model Specification MA70-XAA Liquid Air Cycle Engine, Marquardt Report No. MR 20,100, June 1960. [redacted]ied.

59. Rosevear, J. E., Ryan, J. D., and Benz, O. E., (U) Contamination Alleviation Techniques to Prevent Heat Exchanger Fouling, (APL-TDR-64-14), (Marquardt Report 6057), 31 October 1963. [redacted]

60. Schroeder, T. T. and Sedgwick, T. A., (U) Contamination Alleviation System Design, APL-TDR-64-30,(Marquardt Report 6060), 27 January 1964. [redacted]

REFERENCES (Continued)

61. Acrivos, A., Ahern, J. E., Nagy, A. R. Jr., Research Investigations of Two-Component Heat Transfer, Aerospace Research Laboratories Report ARL 64-116, July 1964.

62. Ahern, J. E., Apparatus and Method of Utilizing the Conversion of Parahydrogen to Orthohydrogen to Obtain a Refrigeration Effect, U. S. Patent No. 3,043,110, 10 July 1962.

63. Rose, D. B., Progress Report on Cryogenic Engineering at Pesco Products Division for Aerospace Applications, Engineering Report No. 3238, April 25, 1961. UNCLASSIFIED.

64. Discussion with Mr. G. Sayles, AF Rocket Propulsion Laboratory, Edwards Air Force Base, 3 March 1966.

65. Alexander, George, P&W Designs Extendable Skirt for RL20 Rocket Engine, Aviation Week, 19 September 1966, pp 60-65.

66. Simulated Liquid Air Combustion with Liquid Hydrogen in a Two-Dimensional Thrust Chamber, RTD-TOR-63-1041. May 1963. CONF[redacted] Title [redacted]

67. Peterson, Glen N., Theoretical Performance of Liquid Hydrogen with Liquid Oxygen and Nitrogen Over a Wide Range of Mixture Ratios, Boeing Company D3-20940, 1963.

68. Harper, R. E. and Zimmerman, J. H., An Investigation of Rocket Engine Thrust Augmentation with a Nozzle-Ejector System, AEDC TDR-62-42, March 1962. [redacted]ied.

69. Simonson, A. J. and Schmeer, J. W., Static Thrust Augmentation of a Rocket Ejector System with Heated Supersonic Primary Jet, NASA TN D-1261, May 1962. UNCLASSIFIED.

70. Walker, R. E., Deklau, B., and Dugger, G. L., Results of Recent Tests on Rocket Thrust Augmentation, Paper delivered at AIAA Aerospace Propulsion Conferences, Cleveland, Ohio and 31st Bumblebee Propulsion Panel Meeting, Applied Physics Laboratory, Howard County, Maryland, May 1964. [redacted]d.

71. Mossman, E. A., Rozycki, R. C., and Holle, G. F., RENE - A Concept for Thrust Augmentation of Rocket Engines, Martin-Denver Research Report R-63-16, October 1963. [redacted] Title - Unclassified.

72. Escher, W. J. D., et al, MA 158 Launch Vehicle Engine, Preliminary Information, Marquardt Report MR 20,316, March 1965. [redacted]nclassified.

REFERENCES (Continued)

73. Cox, P. B., Phase I Summary Technical Report of the CY 1962 Air Force-Marquardt Contributing Engineering Program, (Volume 2 of 8), Jet Compressor Research, Marquardt Report No. 25,065, March 1963. [redacted]

74. Cox, P. B., Phase I Summary Technical Report of the CY 1962 Air Force-Marquardt Contributing Engineering Program, Volume 3 of 8, Advanced Engine Concepts and Advanced Logistics Systems Studies, Marquardt Report No. 25,065, March 1963. [redacted]ssified.

75. Mahoney, J. J., and Panek, G. J., Hypersonic Ramjet Program for the Period 1 March to 31 December 1964, Volume 2, Ramjet Engines for Hypersonic Cruise and Boost Applications, Technical Report No. AFAPL-TR-65-36, May 1965. [redacted]

76. Liquid Hydrogen Technology, Report No. AE62-0774, General Dynamics Astronautics, September 1962.

77. Niendorg, L. R. and Noichl, O. J., Research of Production Techniques for Obtaining Over 50% Solid in Slush Hydrogen, Technical Report AFAPL-TR-64-151, Linde Division, Union Carbide Corporation, February 1965.

78. Request for Quotation DCN 1-6-52-01080, Hydrogen Slush and/or Hydrogen Gel Utilization, NASA-Marshall Space Flight, 17 December 1965.

79. Key, C. F. and Gayle, J. B., Effect of Liquid Nitrogen Dilution on LOX Impact Sensitivity, NASA TMX-53208, NASA-MSFC, February 15, 1965.

80. Astronautics and Aeronautics, January 1964.

81. Woodcock, G. R. and Thompson, D. D., Application of Airbreathing Propulsion to Reusable Launch Vehicles, a paper presented at the Propulsion Specialist Meeting AIAA, Colorado Springs, July 1965, NASA Space Flight Center.

82. The Liquid Propellant Hyperjet, Marquardt Report S-122, January, 1959 [redacted] Unclassified.

This page intentionally left blank

APPENDIX A

EVALUATION OF ROCKET ORIENTED COMPOSITE PROPULSION SYSTEMS

By:

H. A. Singer and M. E. Pucker

Rocketdyne Division,
North American Aviation, Inc.

This page intentionally left blank

APPENDIX A

EVALUATION OF ROCKET ORIENTED COMPOSITE PROPULSION SYSTEMS

A-1. Introduction

Approaching the problem of air augmentation from the starting point of a conventional all-rocket engine/vehicle concept, the Rocketdyne Division evaluated two special types of composite propulsion systems. These were, (1) air augmentation of rocket engine turbine exhaust (alone) and, (2) the Augmenter LACE concept (Engine No. 33) and derivatives of this system employing air collection. Mission analyses were based on nonlifting trajectories with variable initial pitch-over (kick) angles, which was the vehicle mission for the Augmenter LACE systems. The results of the air collection version, the Refill Rocket concept, are reported here. Augmentation of turbine exhaust was examined on an engine performance analysis basis only and will be discussed first. The standard Class 0 reference trajectories and conditions were used for this analysis.

A-2. Air Augmentation of Turbopump Exhaust Gases

With respect to rocket type, nonwinged, vertically launched vehicles, the prospects of air augmentation have been analyzed in various guises. The general approach has been to place an air induction system (as well as a mixing and combustion shroud) around the normally fuel rich rocket, thereby achieving the augmentation benefits of mixing induced air with the rocket gas. This cycle is usually referred to as the simultaneous mixing and combustion cycle, or basic augmentation (Reference A-1). However, the acceptance of air augmentation in this guise as a practical propulsion scheme has been withheld, perhaps primarily because of the extraordinarily large size and weight of the associated hardware, when compared with the compact, lightweight basic rocket. Studies have actually indicated negative payload advantages for such a scheme (Reference A-2).

In view of this, a smaller scale prospect for air augmentation which has been investigated by Rocketdyne is the use of atmospheric air to augment the performance of the base region of aerodynamic spike type rocket engines. Here the air is introduced into the base region of the vehicle along with the fuel rich turbine exhaust gases to provide a higher base pressure, and thereby provide thrust augmentation. The base pressure, upon examination, is influenced by the change in the thermodynamic properties of the secondary flow as well as by the increased secondary flow rate. The extent of mixing and reaction between the air and turbine exhaust gases has not been rigorously determined, but some bounds on the upper limit of performance augmentation have been defined. These results stem from consideration of mixing and reaction which results in the highest possible mixer C*. (A simple hydrogen oxygen chemical reaction was taken to be the only reaction occurring and it was considered to be instantaneous and completed when either the fuel or the oxygen component was consumed.)

A basic cycle schematic is given in Figure A-1-A. The engine performance of this scheme was determined over the three referenced trajectories shown in Figure 25 (in Volume 2). No vehicle oriented studies were performed as such.

In deriving the performance of this system, the momentum of the inlet air was subtracted from the base thrust increase to get the net thrust increase. This net thrust was then used in the determination of the specific impulse augmentation. The referenced rocket was taken to have an exit area ratio of 80, an aerotapoff cycle, a 15 percent nozzle length (referenced to a 15° conical nozzle), a chamber pressure of 2,000 psia, and a mixture ratio of 6.5. The engine produced 1.5 million lbs of thrust at sea level conditions. The mixture ratio of the turbine exhausts was assumed to be 1.376. The performance results are given in Figures A-1-B and A-1-C for two values of air flow-to-turbine exhaust flow ratio (R*).

As noted in these curves, there is a requirement for an "air compressor" below a certain velocity condition. This stems from the fact that the base pressure of the vehicle/engine combination is greater than the ambient stagnation pressure at the low flight velocities and altitudes. At a lower speed, the air cannot be induced into the inlet by ram pressure alone. The implication here is that additional compression means (probably a mechanical compressor) will be required to make this cycle operate in the area where it is providing its best theoretical benefit, namely at the lower flight velocities. Further the base pressure increases with the secondary flow rate in general, so the higher the flow rate, the more compression is required at any one velocity. The result of this is that the velocity at which the air compressor is no longer required is extended to a higher and higher value. The crossovers in Figure A-1-C are due to the inlet momentum penalty increasing faster with air flow rate than the base thrust. The implication here is that it is desirable under certain conditions to limit the amount of air captured for this cycle.

The conclusions of this cycle analysis are: (1) for a fixed capture area inlet, it is desirable to operate on as low a trajectory as possible, (2) the maximum gain occurs in the low velocity regions, (3) to operate in this maximum gain area, a mechanical air compressor (or its equivalent) may be required.

A-3. Augmenter LACE and an Air Collection Derivative

A-3.1 Augmenter LACE

The Augmenter LACE concept, which is Engine No. 33 in the Class O listing, is the product of merging an advanced all-rocket engine with the basic Liquid Air Cycle Engine (LACE) concept. In this scheme (Figure A-2), all of the hydrogen going to the two-sectioned engine is utilized for liquefying air, which is fed to the liquid air cycle combustor. The rocket engine otherwise operates normally on hydrogen-oxygen propellants at a normal O/F ratio. The Augmenter LACE concept provides an overall propulsion system with the potential of modest gains over the parent rocket, at a relatively low expense in terms of installed weight.

The characteristics of this cycle (Engine No. 33) and of a recycle version (Engine No. 34) are provided in the Class O Fact Sheets presented in Volume 5.

The purpose of this section is to describe the Refill Rocket, which is a derivative concept based on the Augmenter LACE concept.

A-3.2 Refill Rocket

Air liquefaction is one of the many promising techniques for utilizing the oxygen in the air as the primary or supplementary oxidizer for chemical propulsion rocket vehicles. Once air has been liquefied in an air liquefaction system, there are basically two courses of action, namely, to use it immediately or to store it for later use. The intermediate choice of using some and storing some is also a possibility but this is merely a weighted combination of the two primary alternatives.

A schematic of a propulsion system that stores the liquefied air is shown in Figure A-3. This cycle is referred to as the Refill Rocket concept, since the liquid air is stored in a depleted oxidizer tank and this refills the tank. The Refill Rocket concept presumes that the air is kept separate from the pure oxygen by some sort of a separation device. If the air and remaining oxygen are allowed to mix, the "dilution" rocket results, which is not analyzed here. The liquid air thus collected throughout the boost portion of the flight is stoichiometrically burned with hydrogen in a later portion of the trajectory.

Single stage to orbit trajectory simulations were made for two Refill Rocket vehicles - one with a design inlet capture area of 178 sq. ft. Both vehicles traversed zero-lift rocket type trajectories. The basic premise was that, while the rocket was traveling through the lower atmosphere, it would be collecting, liquefying, and storing the air which would then be used at the end of the mission to provide an increased velocity increment. The primary rocket engine (oxygen/hydrogen aerodynamic spike engine; in effect, Engine No. 0) would, conceptually, thus be used for a shorter time with a consequent saving in propellant and tankage weights. This thesis, which leads to improved payload potential, is tested in the analysis which follows.

A separate engine was used for the liquid air/hydrogen combustion, since the mixture ratio of 34.3:1 was much different from the usual oxygen/hydrogen mixture ratios.

The amount of air collected during the mission is a function of the vehicle trajectory and the amount of air liquefaction equipment carried. Previous studies of air liquefaction systems had indicated the desirability of capturing as much air as possible, so the initial effort was to lower the oxygen/hydrogn engine mixture ratio to 5.5:1 from the otherwise preferred 6.5:1 This gave a higher H_2 flow rate, thus effecting a greater amount of liquid air production. The 5.5:1 mixture ratio allowed the use of air liquefaction equipment having a design inlet capture area of 178 sq. ft.

When it became apparent that a maximization of air capture was, in fact, not beneficial for this particular air liquefaction concept, the mixture ratio of the oxygen/hydrogen engine was reverted to 6.5:1 and the design capture area of the air liquefaction equipment carried was reduced to 90 sq. ft. This capture area processes less than the maximum amount of air that the hydrogen flow rate associated with the 6.5:1 mixture ratio would liquefy.

The maneuver sequence used for this mission analysis was as follows: (1) vertical rise until a velocity of 300 ft/sec was reached, (2) instantaneous rotation to the assigned angle, followed by zero angle of attack flight until the potential altitude was attained, (3) transfer to the potential altitude, and (4) orbital circularization. A variable pitch correction program was used to maintain constant altitude if a zero degree flight path angle was encountered in the trajectory. When the liquid air/hydrogen engine was ignited, a constant pitch angle maneuver was used as necessary.

The weight of air collected during the mission is shown in Figure A-4 as a function of vehicle kick angle for both inlet capture area cases. Air collection was terminated at Mach 5.0. The low kick angles indicated for the larger capture area case were due to the fact that the rocket cannot satisfactorily perform the mission with a greater weight of collected air. A higher kick angle allowed the system to capture more air, however, the vehicles would then require the addition of aerodynamic lift with its weight implications in order to achieve orbit. This effect was indicated for the smaller capture area case also. In comparison, the baseline all-rocket vehicles described earlier had a kick angle of about 11° indicating that the Refill Rocket tends toward the low kick angles solely due to the collected air weight effect.

Several trajectories for the Refill Rocket are shown in Figure A-5. The superimposed lines reflect constant air total pressure after the inlet losses. The higher velocity part of the larger capture area (the 3.5° kick angle curve) closely followed an 8 psia total pressure line. This implies a larger heat exchanger for a given air flow rate, since the heat exchanger tubes must be made larger to reduce the pressure drop. The 6° kick angle, smaller capture area trajectory, indicates how significant the weight of the collected air is on the vehicle behavior. This trajectory manipulation, as an aside, required delicate maneuvering of the vehicle to attain orbit.

A-4. Results

Table A-1 indicates the comparison between the Refill Rocket and the rocket alone. The anticipated saving in propellant and tank weights did not materialize since a substantial weight of air was carried as essentially "dead" weight until ignition was so poor (I_s = 238.7 lbf-sec/lbm) compared to the oxygen/hydrogen engine that only a relatively small velocity increment

could be obtained from it. The increase in propellant and tank weights, coupled with an increased engine weight (including all the air liquefaction equipment), resulted in a negative payload for the vehicle.

The major conclusion to be drawn from the Refill Rocket mission analysis study was that the Refill Rocket is not an attractive propulsion concept at least for rocket type vehicles. It can be further surmised that the best approach for a composite engine system utilizing an air liquefaction cycle (but not including separation) would be one which immediately used the air as it was liquefied. In retrospect, it is seen that once the air is stored on the vehicle, it is somewhat equivalent to an in-flight propellant loading operation. In this case, however, the high energy oxygen/hydrogen propellant combination is being replaced by the low energy air/hydrogen combination. The high mixture ratio of the air/H_2 engine (34.3:1) means that a large weight of air must be collected, thus impeding the rocket during the latter portion of its acceleration phase.

REFERENCES

A-1. Escher, W.J.D., Flornes, B. J., Goldstein, A. E., and Odegaard, E. A., Air Augmented Rocket Propulsion System Study, Final Report on Contract NAS 4-661, The Marquardt Corporation Report 25,148 , November 1964. [redacted]

A-2. Investigation of Vehicle-Integrated Rocket Powerplants with Air Augmentation, Final Report on Contract NAS 8-11017, The Boeing Company Document D2-23217-1, June 1964. [redacted]

TABLE A-I

COMPARISON OF REFILL ROCKET WITH BASE ROCKET

Parameter	Rocket Base	Refill Rocket	
		A_c = 90 sq ft	A_c = 178 sq ft
Gross weight, lbf	1,000,000	1,000,000	1,000,000
Propellant weight*, lbf	867,194	910,500	912,400
Chamber pressure**, psia	2,000	1,500	1,500
Mixture ratio**	6.5:1	6.5:1	5.5:1
Liquid air weight collected, lbf	--	122,754	223,744
Burnout weight, lbf	132,806	89,500	87,600
Engine weight, lbf	8,378	17,183	25,815
Tank weight, lbf	44,227	46,797	50,560
Thrust structure weight, lbf	7,500	7,500	7,500
Miscellaneous weight, lbf	36,100	36,100	36,100
Payload weight, lbf	36,600	-18,080	-32,375

* Includes hydrogen needed for liquid air combustion but not the weight of the air itself

** LO_2/H_2 engine

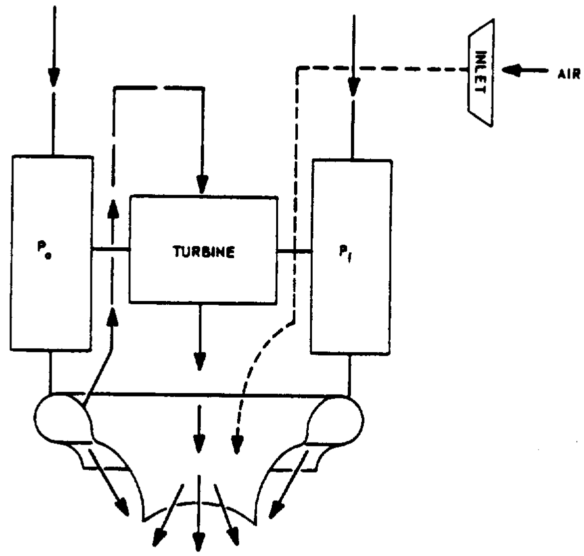

A. Basic Schematic of Aerotapoff Cycle
Plus Secondary Air Augmentation

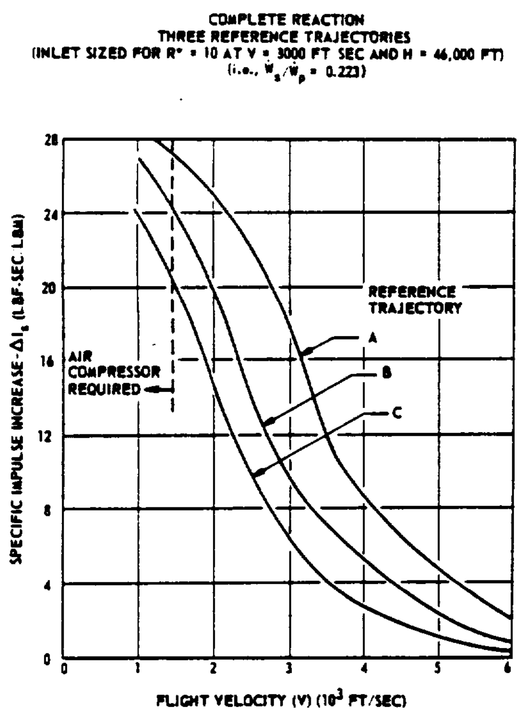

B. Specific Impulse Increase, R* = 10

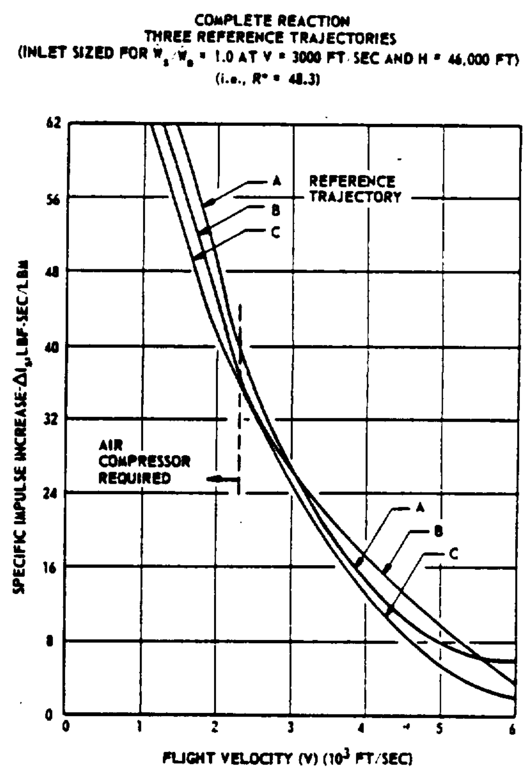

C. Specific Impulse Increase, R* = 48.3

FIGURE A-1. Air Augmentation of Turbine Exhaust Gases

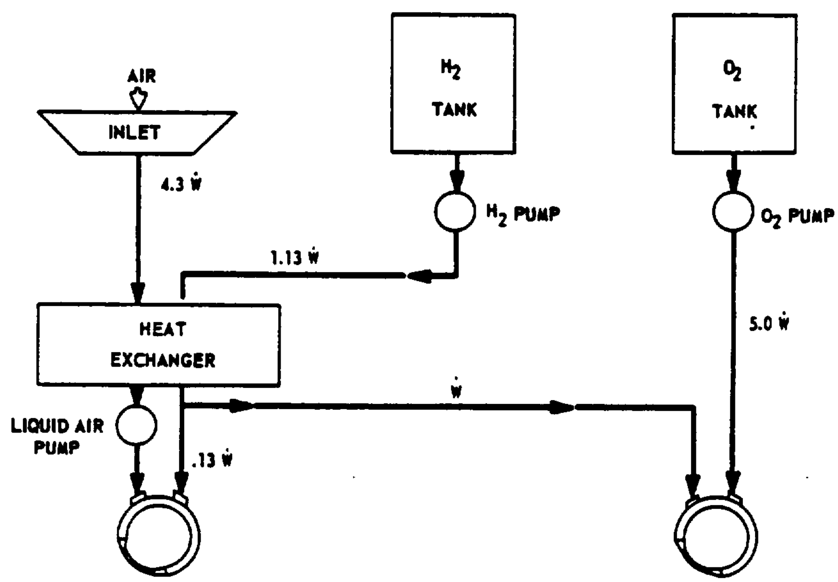

FIGURE A-2. Schematic of Augmenter LACE Engine (No. 33)

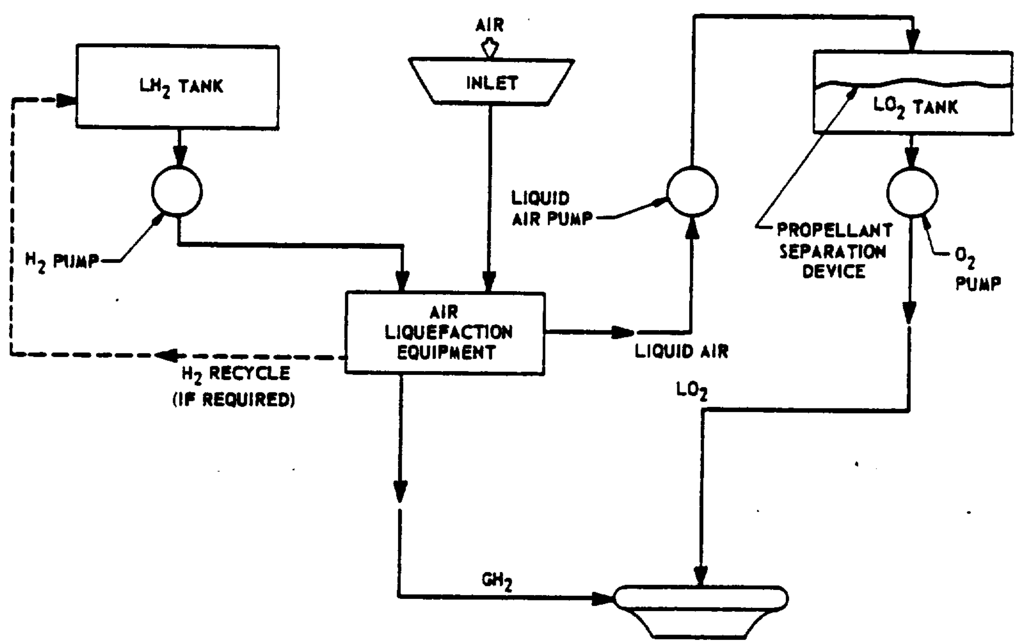

FIGURE A-3. Schematic of Refill Rocket Concept

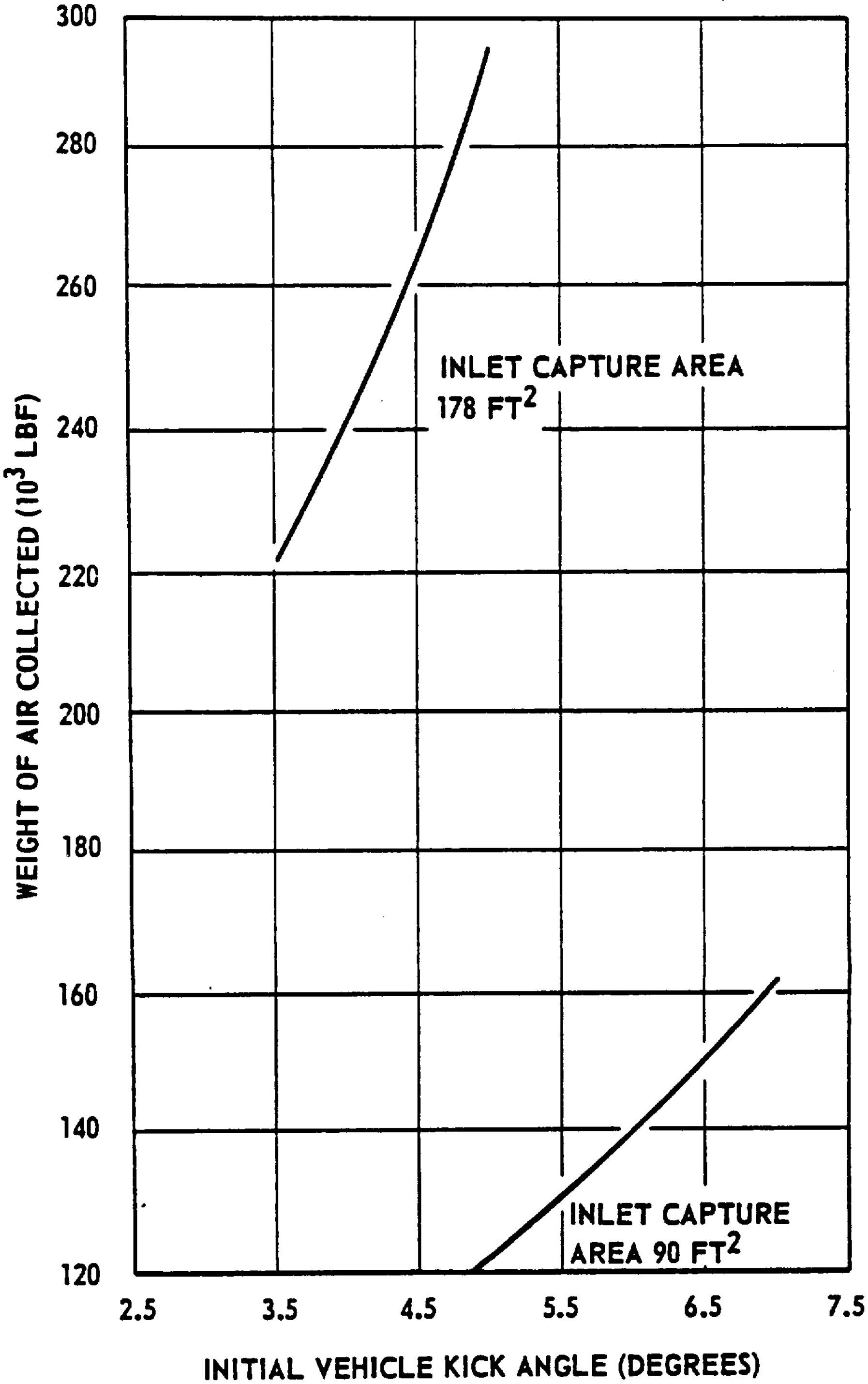

FIGURE A-4. Weight of Air Collected vs. Initial Kick Angle for the Refill Rocket

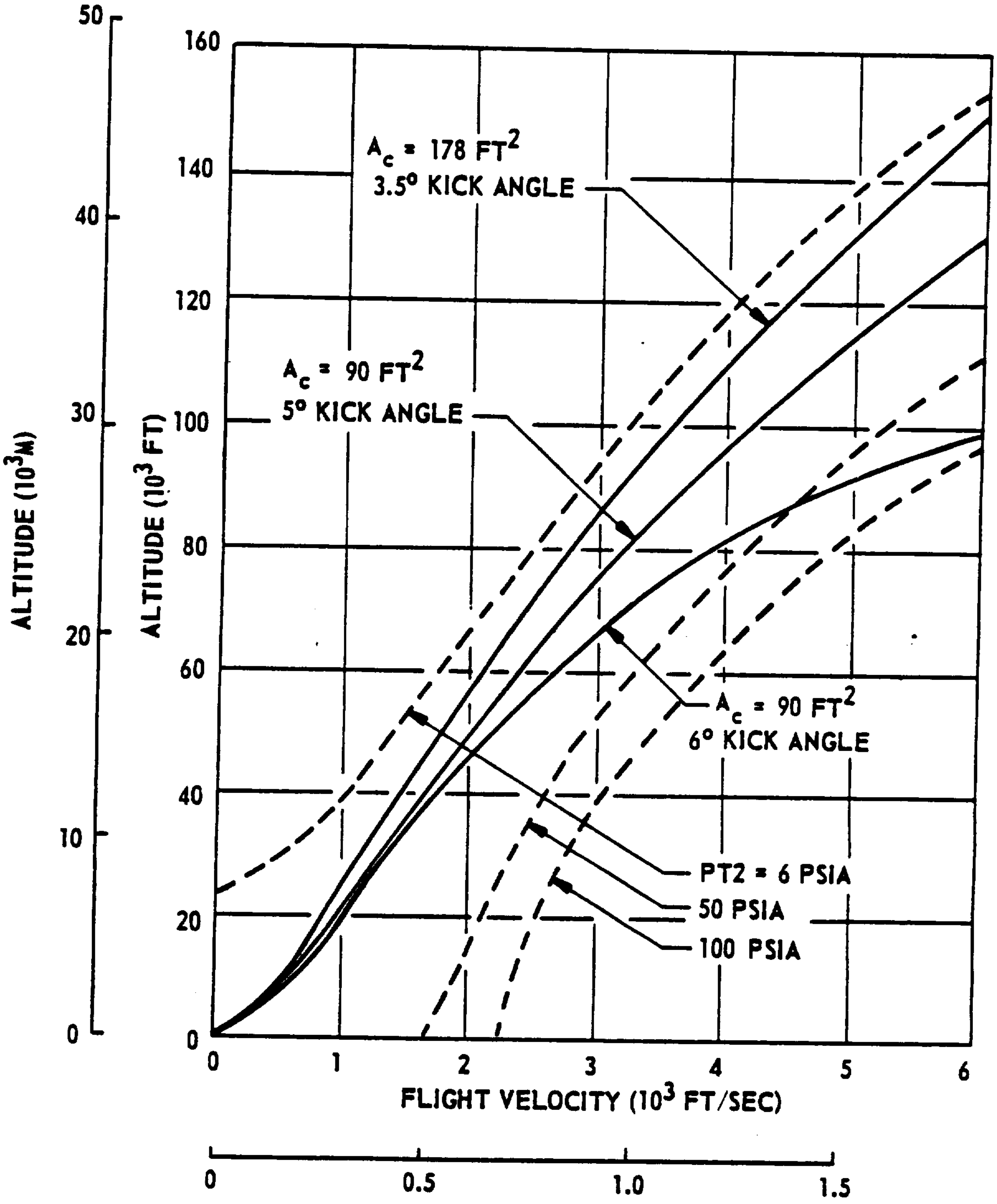

FIGURE A-5. Refill Rocket Trajectories

This page intentionally left blank

APPENDIX B

EJECTOR MODE

PERFORMANCE ANALYSIS METHOD

By:

B. J. Flornes

The Marquardt Corporation

This page intentionally left blank

APPENDIX B

EJECTOR MODE PERFORMANCE ANALYSIS METHOD

B-1. Introduction

The basic analysis methods used for cycle investigations and the engine performance for all of the air augmented or ducted propulsion systems included in this study are based on a one-dimensional treatment of flow. The analysis approach is modeled after the "simplified analysis" methods developed in References B-1 and B-2 for the prediction of ramjet engine performance characteristics. Realistic performance is obtained with the one-dimensional analytical approach by incorporating appropriate component and process efficiencies and thermodynamic property variation correlations in the analysis. The cycle analysis methods and engine performance computer programs were developed under Air Force sponsored studies of the Ejector Ramjet and RamLACE engine cycles. Mixing, cycle, and engine tests have been conducted and the experimental results have checked and verified the analytical predictions and methods.

A general engine schematic and station nomenclature sketch is presented in Figure B-1. The schematic illustrates the diffusion and afterburning cycle (DAB). For simultaneous mixing and combustion cycles (SMC), the basic change is elimination of the diffusion from Stations 3 to 3' ($A_3 = A_{3'} = A_4$) and elimination of the secondary fuel injector assembly or relocation of the injectors to the exit plane of the primary rocket chamber. Inasmuch as the DAB cycles involve more discrete processes, the general cycle analysis method will be outlined for this type of cycle. SMC cycles eliminate or combine some of the processes.

B-2. Basic Analysis Method

The general analysis method considers the major engine sections or components individually. Calculation of engine performance is based upon matching flow rates and state conditions between components, and upon maintaining one-dimensional continuity of mass and conversion of energy and momentum for each flow process. The basic cycle input data require specification of engine geometry or secondary-to-primary mass flow ratio, flight conditions (Mach number and altitude), propellant properties, and individual component efficiencies. The major engine section or component breakdown is as follows:

1. Inlet
2. Primary rocket
3. Mixer
4. Afterburner or combustor
5. Exit nozzle

The analysis method for each section plus a brief outline of the final performance computations are described below:

B-2.1 Inlet

The inlet calculation determines the secondary (air) flow rate through the engine as a function of the flight speed and altitude. The option of either a fixed or variable geometry inlet design is achieved from the specification of inlet capture area schedule or mixer-inlet Mach number, assuming adiabatic flow, respectively. The inlet pressure recovery (P_{t_2}/P_{t_o}) is determined from the inlet kinetic energy efficiency when operating with a variable inlet design; or from a specified schedule when operating with a particular inlet design. Values of static pressure, velocity, Mach number, enthalpy, and flow rate are determined for the secondary air flow entering the mixer section.

The inlet kinetic energy efficiency (η_{KE}) is defined by

$$\eta_{KE} = \frac{{V'_o}^2}{{V_o}^2}$$

where V'_o is the velocity resulting from the isentropic reexpansion of the flow from the static pressure at the exit of the inlet (P_2) to the free stream static pressure (P_o). The inlet total pressure recovery (P_{t_2}/P_{t_o}) is related to the kinetic energy efficiency by

$$\frac{P_{t_2}}{P_{t_o}} = \left[1 + \frac{\gamma - 1}{2} M_o^2 \left(1 - \eta_{KE}\right)\right]^{-\frac{\gamma}{\gamma-1}}$$

Specifications of the inlet kinetic energy efficiency and the inlet exit Mach number (M_2) are sufficient to establish the performance characteristics of a variable geometry inlet.

B-2.2 Primary Rocket

The primary flow rate (W_p) is determined by the rocket geometry, chamber pressure, and propellant properties, and it is generally considered to be fixed in this study. The total enthalpy of the primary stream (H_{tp}) is determined from the primary oxidizer-to-fuel ratio $(O/F)_p$ and the initial enthalpy of the propellants, as given below:

$$H_{tp} = \frac{(O/F)_p H_{ox} + H_f + \epsilon \eta_{c_1} H_{c_1}}{1 + (O/F)_p}$$

where H_{ox} and H_f are the sensible enthalpies of the oxidizer and fuel entering the combustion chamber, H_{c_1} is the lower heating value of the fuel, η_{c_1} is the combustion efficiency, and ϵ is a step function limiting the heat released in combustion to the stoichiometric value. The parameter ϵ has the following forms depending upon the relationship of $(O/F)_p$ to the stoichiometric oxidizer-to-fuel ratio $(O/F)_{st}$:

$$\epsilon = 1 \text{ for } \phi_p \leq 1$$

$$\epsilon = \frac{1}{\phi_p} \text{ for } \phi_p > 1$$

where $\phi_p = \dfrac{(O/F)_{st}}{(O/F)_p}$

The flow through the primary rocket nozzle is derated from the ideal (isentropic flow) by means of a nozzle kinetic energy efficiency term defined by

$$\eta_n = \frac{V_p^{\,2}}{V_{p_i}^{\,2}} \;, \quad \left(\eta_{n\text{ stream thrust}} = \sqrt{\eta_{n\text{ kinetic energy}}} \right)$$

where V_{p_i} is the nozzle exit velocity corresponding to an isentropic expansion from the primary combustion chamber pressure (P_c) to the local exit pressure (assumed to be equal to P_2). Over and underexpansion losses due to fixing the rocket nozzle area ratio were neglected. Through the use of the above definition of nozzle kinetic energy efficiency and the usual isentropic flow relationships, the exhaust velocity of the primary jet can be expressed as

$$V_p = \sqrt{2g\, J\, \eta_n\, H_{t_p} \left[1 - (P_2/P_c)^{\frac{\gamma_p - 1}{\gamma_p}} \right]}$$

The static enthalpy of the high energy fluid issuing from the primary nozzle can be obtained from

$$h_p = H_{t_p} - \frac{V_p^{\,2}}{2gJ}$$

B-2.3 Mixer

The mixer computations involve the simultaneous solution of the equations of state, continuity, conservation of momentum, and conservation of energy to obtain the final conditions of the mixed stream. The final expression for the mixer exit velocity results in a quadratic equation in the form

$$V_3 = \frac{\psi^2 \pm \sqrt{\psi^2 - K H_{t_3}}}{C}$$

where ψ represents the initial specific momentum of the primary and secondary streams, and C, K are constants which are functions of gas properties and mixer geometry. These terms are defined as follows:

$$\psi = \frac{g}{W_3}\left(\frac{W_p V_p}{g} + P_p A_p + \frac{W_s V_2}{g} + P_2 A_2\right)$$

$$K = gJ\left[2\left(\frac{\gamma - 1}{\gamma}\right)\left(1 + \frac{1}{D}\right) - 1/2\left(\frac{\gamma - 1}{\gamma}\right)^2\left(1 + \frac{1}{D}\right)^2\right]$$

$$C = 2 - \left(\frac{\gamma - 1}{2\gamma}\right)\left(1 + \frac{1}{D}\right)$$

where D represents the mixer divergence area ratio ($\frac{A_3}{A_2 + A_p}$). Two roots to the quadratic equation for V_3 are possible. The negative sign preceding the radical provides the subsonic mixing solution, whereas the positive root results in a supersonic mixed velocity.

An experimentally determined correlation for static pressure mixing efficiency (η_M) is used to derate the mixer exit pressure from the ideal value associated with complete mixing as given by the momentum equation. This mixing efficiency is defined as

$$\eta_M = \frac{P_3 - P_2}{P_{3i} - P_2}$$

where P_{3i} is the mixer exit pressure given by ideal one-dimensional mixing analysis.

B-2.4 Afterburner or Combustor

When secondary fuel is burned in the mixed stream (supplied either from excess fuel from rich primary operation or from direct secondary fuel injection), the enthalpy rise due to this combustion is determined from the secondary fuel-air equivalence ratio (ϕ_s) and the heat of combustion for the secondary fuel (H_{c_2}). The physical model used treats the secondary heat addition effect as if combustion occurred instantaneously at the end of the afterburner (DAB) or mixer-combustor (SMC). The final total enthalpy after combustion is given by

$$H_{t_4} = \frac{W_3}{W_4} H_{t_3} + \eta_{c_2} H_{c_2} \epsilon 2 \left(\frac{f}{a}\right)_{st} \frac{W_s}{W_4}$$

where the total enthalpy of the mixed stream is defined by energy conservation as

$$H_{t_3} = \frac{W_p}{W_3} H_{t_p} + \frac{W_s}{W_3} H_{t_o}$$

and

$$W_4 = W_3 + W_{f_2} = W_p + W_s + W_s \phi_s \left(\frac{f}{a}\right)_{st}$$

where

$$\phi_s = \frac{(f/a)}{(f/a)_{st}}$$

$$\epsilon_2 = \phi_s \text{ for } \phi_s \leq 1.0$$

$$\epsilon_2 = 1.0 \text{ for } \phi_s > 1.0$$

The conservation of momentum relationship is again established for the geometry and flow conditions through the combustor section. Combustion was assumed to take place in a constant area duct. Solution of the momentum equation to obtain combustor exit properties thus accounts for heat addition pressure losses.

B-2.5 Exit Nozzle and Performance

The exhaust flow through the engine exit nozzle is also derated from the ideal (isentropic flow) by the kinetic energy efficiency defined for the exit nozzle as

$$\eta_n = \frac{V_6^{\,2}}{V_{6i}^{\,2}}$$

where V_{6i} is the nozzle exit velocity for isentropic expansion from the afterburner or combustor chamber pressure (P_{t_4}) to ambient static pressure (P_o). The exit nozzle efficiency on a stream thrust basis is again related to the kinetic energy efficiency by

$$\eta_{n_{\text{stream thrust}}} = \sqrt{\eta_{n_{\text{kinetic energy}}}}$$

Using the kinetic energy efficiency and isentropic flow relationships, the engine exhaust velocity is

$$V_6 = \sqrt{2gJ\,\eta_n\,H_{t_4}\left[1 - \left(P_6/P_{t_4}\right)^{\frac{\gamma_4 - 1}{\gamma_4}}\right]}$$

where γ_4 is the effective isentropic exponent for the exhaust expansion process.

The net jet or internal engine thrust is then determined from the change in momentum of the flow through the engine plus the unbalanced hydrostatic forces due to area change from the inlet to the exit station by

$$T_{NJ} = \frac{W_4\,V_6}{g} - \frac{W_s\,V_o}{g} + (P_6 - P_o)\,A_6$$

Net jet specific impulse is obtained by

$$I_{sp_{NJ}} = \frac{T_{NJ}}{W_{ft}}$$

where W_{ft} is the total stored propellant flow to the engine.

B-3. Computer Programs

Two basic computer programs based on the above general analysis methods were employed for cycle investigation and engine performance: one a parametric program and one a fixed geometry program.

The parametric analysis program was designed to investigate the performance effects of various cycle variables and to specify, as outputs, the engine geometric area ratios. Engine performance outputs such as propellant specific impulse and thrust coefficient at any input flight condition (Mach number, altitude) are also obtained. The geometric area ratios for a selected set of engine cycle variables are converted to a specific engine design by selecting a desired engine thrust level at a flight condition.

The discrete cycle or component variables that can be specified and otherwise investigated are as follows:

1. Secondary/primary mass flow ratio
2. Inlet kinetic energy efficiency, or inlet pressure recovery
3. Primary chamber pressure
4. Primary equivalence ratio
5. Primary combustion efficiency
6. Primary rocket nozzle efficiency
7. Mixer inlet Mach number, related to mixer exit Mach number
8. Mixer static pressure rise efficiency
9. Variable mixer geometry (converging, diverging, constant area, and constant pressure)
10. Diffusion ratio (combustor inlet/mixer exit area ratio), specified by means of combustor inlet Mach number
11. Afterburner equivalence ratio
12. Afterburner combustion efficiency
13. Afterburner geometry, constant area or constant pressure
14. Engine exit nozzle efficiency

A separate version of the same parametric program is also available for the RamLACE cycle.

The fixed geometry program computes engine performance for specific engine designs, initially determined from the parametric program data. The same basic analysis techniques are used, the differences being primarily in the program inputs and outputs. Output geometric area ratios of the parametric program provide engine area inputs to the fixed geometry program. The complete range of cycle or component variables listed for the parametric program can also be investigated with the fixed geometry program, providing off-design performance as affected by the particular variable or combination of variables. The fixed geometry program provides design and off-design performance at various flight conditions for a given (fixed) mixer configuration. The fixed geometry mixer can be combined with inlet and exit geometry variations as follows:

1. Variable and fixed inlet capture area
2. Variable and fixed exit nozzle throat area
3. Variable and fixed exit expansion ratio

The geometry variations possible provide eight combinations of inlet, exit throat, and expansion ratio in conjunction with a particular fixed mixer. The fixed inlet and/or fixed exit throat engine performance is obtained by allowing selected cycle or component variables, such as mixer inlet Mach number and inlet kinetic energy efficiency, to adjust appropriately for the particular flight condition and fixed areas. The fixed geometry program is also capable of computing engine performance with throttled primary flow. Primary flow can be varied by chamber pressure or by shutdown of primary chambers. Fully throttled (zero primary flow) or ramjet operation performance can also be obtained with the fixed geometry program.

Both the parametric and fixed geometry programs are capable of computing simultaneous mixing and combustion engine performance by running a zero diffusion ratio case. Another feature of the fixed geometry program allows evaluation of low primary chamber combustion efficiencies and subsequent combustion of the unburned fuel in the mixer. This also provides the capability of analyzing various degrees of simultaneous mixing and combustion, followed by diffusion and afterburning.

The parametric and fixed geometry programs, as initially available to the study, were programmed for an IBM 1620 computer. The fixed geometry program was not at the onset of the program completely updated for RamLACE cycle computations. Therefore, two new 1620 programs were written for RamLACE -- one for diffusion and afterburning and one for simultaneous mixing and combustion -- to provide maximum flexibility and minimum 1620 machine time (typewriter output). The output formats of these programs incorporated a long and short output option to provide maximum information for initial investigations, while allowing minimum output time for more routine calculations. The short output data items were those tabulated for Class 0 engines in the Class 0 Fact Sheets (Volumes 4 and 5).

The IBM 1620 computer programs were used for the Class 0 performance computations. At the end of the Class 0 study phase, the IBM 1620 computer use was terminated; the work continuing with the IBM 7040, which provided increased data generation capability. Both the parametric and fixed performance programs were consequently converted for the IBM 7040 computer. All of the above listed features were retained and both programs were modified to be capable of computing performance for all composite cycles including RamLACE. These two programs were then used to size and compute engine performance for the Class 1 and Class 2 engines. Minor modifications and updating of techniques were made throughout these two phases to facilitate computations.

Where symbols are not specifically defined, the general nomenclature section located at the end of this volume should be consulted.

REFERENCES

B-1. Mager, Arthur, "Simplified Analysis of Hypersonic Ramjet Performance", Marquardt Report No. MR 20,054, July 1959. UNCLASSIFIED.

B-2. Lindley, C. A., "Simplification of Cycle Analysis", Marquardt Report No. MR 20,097, June 1960. [redacted] Unclassified).

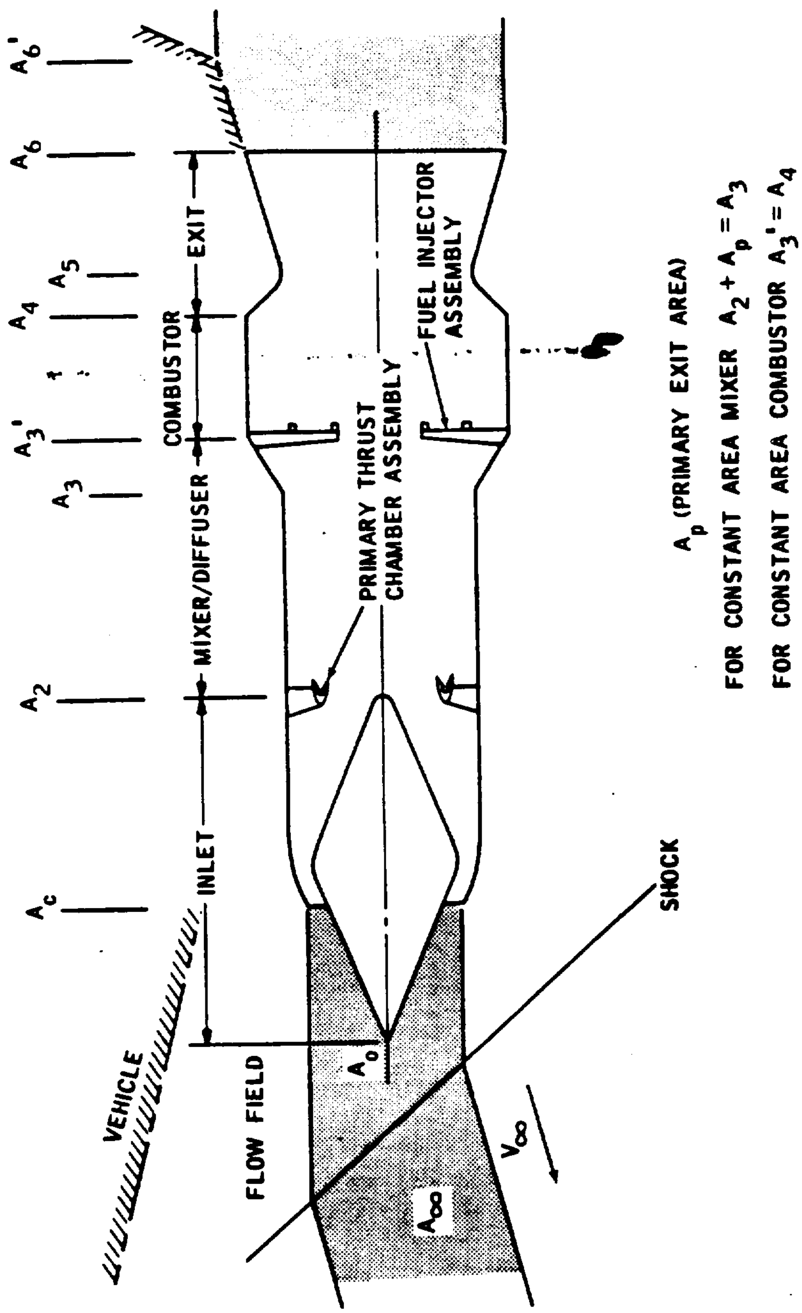

FIGURE B-1. Installed Engine Station Nomenclature

APPENDIX C

DESCRIPTION OF PATH FOLLOWER COMPUTER PROGRAM

By:

H. Frank

The Marquardt Corporation

This page intentionally left blank

APPENDIX C

DESCRIPTION OF PATH FOLLOWER COMPUTER PROGRAM

The following discussion describes a method for calculating the performance of a lifting flight vehicle on a specified path. This method uses certain simplifications to reduce the problem to one not requiring the direct solution of the differential equations of motion. These simplifications realize a considerable saving in computer time without greatly sacrificing computational accuracy.

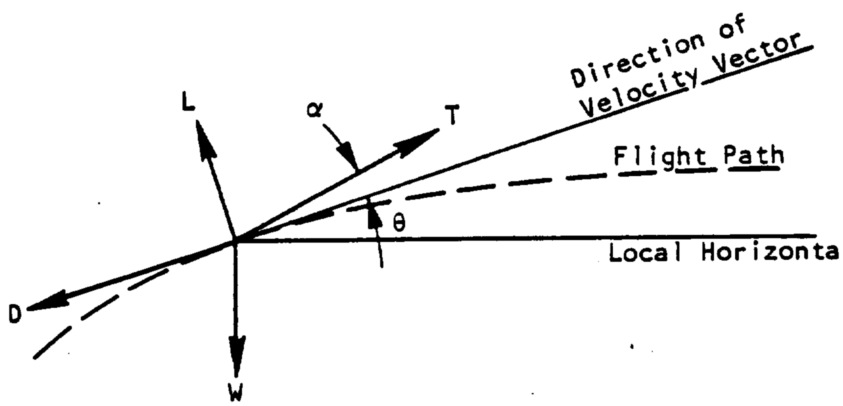

The equations of motion of a point in a place are

$$\frac{W}{g_o} \frac{dV}{dt} = T \cos \alpha - D - W \left(\frac{R_o}{R_o + h}\right)^2 \sin \theta \qquad (C\text{-}1)$$

$$\frac{W}{g_o} V \frac{d\theta}{dt} = T \sin \alpha + L + \frac{W V^2 \cos \theta}{g_o \left(R_o + h\right)} - W \left(\frac{R_o}{R_o + h}\right)^2 \cos \theta \qquad (C\text{-}2)$$

The kinematic relationships are

$$\frac{dh}{dt} = V \sin \theta \qquad (C\text{-}3)$$

$$\frac{dr}{dt} = \left(\frac{R_o}{R_o + h}\right) V \cos \theta \qquad (C\text{-}4)$$

The propulsion system characteristics relate the rate of mass depletion, thus

$$\frac{dm}{dt} = -\frac{T}{I_s} = \frac{dW}{dt} \qquad \text{(C-5)}$$

The five differential equations stated above define the flight performance of the vehicle.

In order to facilitate the solution of the above equations, the following assumptions were made :

1. $\sin \alpha = \alpha_r$

2. $\cos \alpha = 1$

For reasonable values of angle of attack, $\alpha < 10°$, these are quite accurate approximations.

It is desired to solve for the aircraft performance on a specified trajectory in the h-V plane

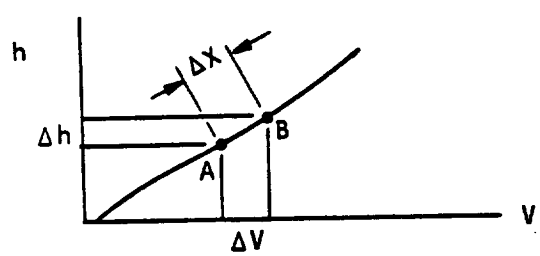

A simple solution may be obtained if the trajectory is divided into small intervals of ΔX and the following parameters are assumed to be constant over this interval :

1. T
2. I_s
3. L
4. D
5. V
6. W
7. $R_o + h$
8. α
9. θ
10. $\frac{d\theta}{dt} = 0$

Equations (C-1) through (C-5) reduce to the following:

$$\frac{W}{g_o} \frac{dV}{dt} = T - C_D \; q \; S - W \left(\frac{R_o}{R_o + h} \right)^2 \sin \theta \qquad (C\text{-}6)$$

$$0 = T \alpha_r + C_L \; q \; S + \left[\frac{W}{g_o} \left(\frac{V^2}{R_o + h} \right) - W \left(\frac{R_o}{R_o + h} \right)^2 \right] \cos \theta \qquad (C\text{-}7)$$

$$\frac{dh}{dt} = V \sin \theta \qquad (C\text{-}8)$$

$$\frac{dr}{dt} = \left(\frac{R_o}{R_o + h} \right) V \cos \theta \qquad (C\text{-}9)$$

$$\frac{dW}{dt} = - \frac{T}{I_s} \qquad (C\text{-}10)$$

The aerodynamic coefficients (for both subsonic and supersonic flight) were specified as follows:

$$C_L = C_{L_0} + \frac{dC_L}{d\alpha} \alpha + \frac{dC_L}{d\alpha^2} \alpha^2$$

$$C_D = C_{D_{0_T}} + C_L \tan \alpha$$

where $C_{D_{0_t}} = C_{D_0} + C_{D_{E_1}} \left(\frac{A_{c_1}}{S} \right) + C_{D_{E_2}} \left(\frac{A_{c_2}}{S} \right) + C_{D_B} \left(\frac{A_B}{S} \right)$

Introducing these aerodynamic coefficient expressions into Equation (C-7)

$$\frac{T \alpha}{57.296} + q \; S \left(C_{L_0} + \frac{dC_L}{d\alpha} \alpha + \frac{dC_L}{d\alpha^2} \alpha^2 \right)$$

$$+ \left[\frac{W}{g_o} \left(\frac{V^2}{R_o + h} \right) - W \left(\frac{R_o}{R_o + h} \right)^2 \right] \cos \theta = 0$$

$$\overbrace{\left[q\ S \frac{dC_L}{d\alpha^2} \right]}^{A} \alpha^2 + \overbrace{\left[\frac{T}{57.296} + q\ S \frac{dC_L}{d\alpha} \right]}^{B} \alpha + q\ S\ C_{L_0}$$

$$+ \underbrace{\left[\frac{W}{g_o} \left(\frac{V^2}{R_o + h} \right) - W \left(\frac{R_o}{R_o + h} \right)^2 \right]}_{C} \cos \theta = 0$$

$$\alpha = \frac{- B + \sqrt{B^2 - 4AC}}{2A} \qquad \text{(C-11)}$$

Combining Equations (C-6) and (C-8) with the aerodynamic coefficient expression results in the following,

$$\left[\frac{W}{g_o} \frac{\Delta V}{\Delta h} V + W \left(\frac{R_o}{R_o + h} \right)^2 \right] \sin \theta = T - \left[C_{D_{O_T}} + \left(C_{L_0} + \frac{dC_L}{d\alpha} \alpha + \frac{dC_L}{d\alpha^2} \alpha^2 \right) \tan \alpha \right] q\ S \qquad \text{(C-12)}$$

An iteration of this equation results in the solution for θ.

Note also that the differentials dV and dh have been replaced by the discrete intervals ΔV and Δh.

The solution at any point is now completely specified:

α - Equation (C-11)

θ - Equation (C-12) iteration required

$$\Delta t = \frac{\Delta h}{V \sin \theta}$$

$$\Delta W = \frac{T}{I_s} \Delta t$$

$$\Delta R = \left(\frac{R_o}{R_o + h}\right) \frac{V \cos \theta \, \Delta t}{6080}$$

$$\Delta V_{ideal} = g_c \, I_s \, \ln\left(\frac{W}{W + \Delta W}\right)$$

$$I_{eff} = I_s \frac{\Delta V}{\Delta V_{ideal}}$$

During the takeoff ground run, a part of the trajectory problem is reduced to a simpler form by making the assumption that, prior to a specified takeoff velocity,

1. $\alpha = 0$
2. $\theta = 0$

A nomenclature listing follows.

NOMENCLATURE
(For Appendix C)

Symbol	Description
A_B	Vehicle base drag reference area, sq ft
A_C	Engine drag reference area, sq ft
C_D	Drag coefficient
C_{D_B}	Vehicle base drag coefficient
C_{D_E}	Engine drag coefficient
$C_{D_{O_T}}$	Total zero lift drag coefficient
C_L	Lift coefficient
D	Drag, lbf
$dC_L/d\alpha$	Lift curve slope, per degree
$dC_L/d\alpha^2$	Slope of C_L vs. α^2 curve, per degree
g_o	Acceleration due to gravity at sea level, ft/sec^2
h	Altitude, ft
I_s	Net jet specific impulse, lbf sec/lbm
I_{eff}	Effective impulse, lbf sec/lbm
L	Lift, lbf
M	Mach number
m	Mass, lbm
q	Dynamic pressure, lbf/ft^2
R	Ground range, nautical miles
R_o	Radius of the earth = 20.926×10^6 ft

NOMENCLATURE (Continued)

Symbol	Description
r	Ground range, ft
S	Aerodynamic reference area, sq ft
T	Thrust, lbf
t	Time, sec
V	Velocity, ft/sec
W	Weight at sea level, lbf
X	Trajectory arc length (in h-V plane)
α	Angle of attack, degrees
α_r	Angle of attack, radians
θ	Vehicle angle of climb, degrees to local horizontal
Subscripts	
1	Engine system No. 1
2	Engine system No. 2

This page intentionally left blank

APPENDIX D

ANALYSIS OF

ALTERNATE MISSION FOR

FIRST STAGE VEHICLE (CLASS 2)

By:

N. B. Williams

Lockheed-California Co.

This page intentionally left blank

APPENDIX D

ANALYSIS OF ALTERNATE MISSION FOR FIRST STAGE VEHICLE (CLASS 2)

D-1. First Stage Alternate Performance

The three Class 2 first stage vehicles having airbreathing capability were cursorily analyzed with respect to payload/range, acceleration, and endurance characteristics. The purpose of this effort was to illuminate the operational flexibility (Section 4.2.3) of the first engine/vehicle combinations in the sense of alternate mission capability.

The analytical approach was as follows:

1. To evaluate the baseline first stage vehicle "as is", with no second stage on board
2. To add hydrogen tankage in the second stage cavity and fuselage aft body to exploit the maximum performance and the full 1.0 million lb design gross weight capability of the first stage vehicle

The configuration presented in Figure D-1 illustrates the auxiliary tankage as applied to the baseline first stage vehicle. A comparative weight breakdown is presented in Table D-I for the baseline first stage vehicle and the auxiliary tankage configuration.

D-2. Subsonic Combustion Ramjet Capability Vehicles, Supercharged Ejector Ramjet (No. 11) and Turboramjet (No. X)

This section presents the alternate performance characteristics of the Supercharged Ejector Ramjet and the Turboramjet first stage vehicles. Figure D-2 presents the first stage acceleration performance in terms of mass fraction, range displacement, and time to terminal boost Mach number, as a function of first stage takeoff weight. The cruise and glide range parameter characteristics are presented in Figure D-3 as a function of Mach number.

The maximum cruise performance Mach number was determined by utilizing these data. Figure D-4 illustrates the variation in total displacement range (acceleration, cruise, and glide) as a function of cruise Mach number for the baseline first stage. (Increasing first stage gross weight did not alter the variation.) Figure D-4 indicates that maximum range occurs for Mach 5 cruise. However, the variation from Mach 3 to 6 was small. The payload quantity indicated included payload, boil-off hydrogen, and reserve fuel.

The payload-range characteristics of the vehicles are presented in Figure D-5 for Mach 5 cruise for gross weights corresponding to the following:

1. Baseline vehicle, i.e., second stage removed, no other changes

2. Volume-limited vehicle with maximum auxiliary fuel added in the second stage cavity and aft body

3. Maximum design gross weight vehicle, with full auxiliary fuel plus payload added to yield a 1.0 million lb takeoff weight

Figure D-5 indicates maximum zero payload ranges of 8320 and 8640 n. miles for the Supercharged Ejector Ramjet and Turboramjet systems, respectively.

The endurance (or time on station at subsonic conditions) performance of the two vehicles was analyzed under the following ground rules:

1. The volume-limited vehicle with full auxiliary fuel was utilized (832,368-lb Supercharged Ejector Ramjet and 827,645-lb Turboramjet).

2. Station radius was achieved by an acceleration-glide sequence, with no cruise.

3. Loiter endurance was at subsonic speed at zero altitude.

4. Return to base was provided for by the acceleration-glide technique.

5. Payload includes real payload, boil-off hydrogen, and contingent fuel.

(The typical boil-off rate at subsonic speeds was 2000 lbs/hr)

The results of the endurance analysis are presented in Figure D-6 which presents time to station and time on station as a function of station radius and payload. The superior endurance potential of the Supercharged Ejector Ramjet was due to the fan-only mode specific impulse. However, the assumption was made for the Supercharged Ejector Ramjet that the fan-only mode (no afterburning) provided sufficient thrust for the on-station loiter. A check was subsequently made which indicated that the thrust requirements for the heavy initial loiter situation would, in fact, require some plenum burning. Hence, the results for endurance of the Supercharged Ejector Ramjet may be considerably optimistic. Nevertheless, its superiority to the Turboramjet was still indicated on a "worst case" analysis check.

D-3. Supersonic Combustion Vehicle, ScramLACE (Engine No. 22)

The alternate capability of the selected ScramLACE Mach 10 vehicle was evaluated in terms of the payload-range characteristics at various cruise Mach numbers.

The ability of the vehicle to cruise at the angle of attack for maximum L/D, and with Thrust = Drag, was limited by the engine cooling-cowl size relation. In order to determine the cruise I_{sp} and L/D, the cooling equivalence ratio of Figure D-7 was assumed. In cases where the cooling limitation required excess thrust at L/D_{max}, the angle of attack was increased (L/D decreased) until thrust and drag were equal. The resulting Breguet range parameter versus Mach number is shown in Figure D-8. The boost displacement and glide range (at maximum L/D) of the vehicle are shown in Figure D-9. To select the correct cruise Mach number, the vehicle was assumed to have an auxiliary tank in the second stage cavity and also in the aft portion of the fuselage. The resulting range versus Mach number for the conditions noted is shown in Figure D-10, from which the Mach 8 cruise point was selected.

The payload-range characteristics of the Mach 8 vehicle are presented in Figure D-11 for two cases. The upper curve (W_o = 1.0 million lbs) assumed that as fuel plus tankage was removed, payload was added to maintain the takeoff weight at 1.0 million lbs. The lower curve shows the payload performance of the unaltered vehicle, i.e., with no extra tankage. The intersection of the two curves represents the point at which no extra tankage is possible - all the extra tankage plus fuel had been replaced by payload. The indicated payload includes reserves and boil-off fuel.

It should be noted that despite the greater Breguet range factor at Mach 8 of the ScramLACE system (No. 22) as compared to the (Supercharged Ejector Ramjet (No. 11), the maximum range was less, due to the higher dry weight and reduced fuel loading.

TABLE D-I

FIRST STAGE WEIGHTS

Vehicle	W_{DRY} (lbs)	W_{RESID} (lbs)	W_{EMPTY} Wet (lbs)	W_{FUEL} (lbs)	$W_{T.O.}$ (lbs)
Supercharged Ejector Ramjet					
Baseline (Mach 8)	353,993	5,283	359,276	195,670	554,946
Maximum Range Configuration	417,967	11,067	429,034	403,334	832,368
Turboramjet					
Baseline (Mach 8)	349,144	4,627	353,771	171,384	525,155
Maximum Range Configuration	413,244	11,067	424,311	403,334	827,645
ScramLACE					
Baseline (Mach 10)	367,749	6,170	373,919	228,508	602,427
Maximum Range Configuration	419,977	11,067	431,044	403,334	834,378

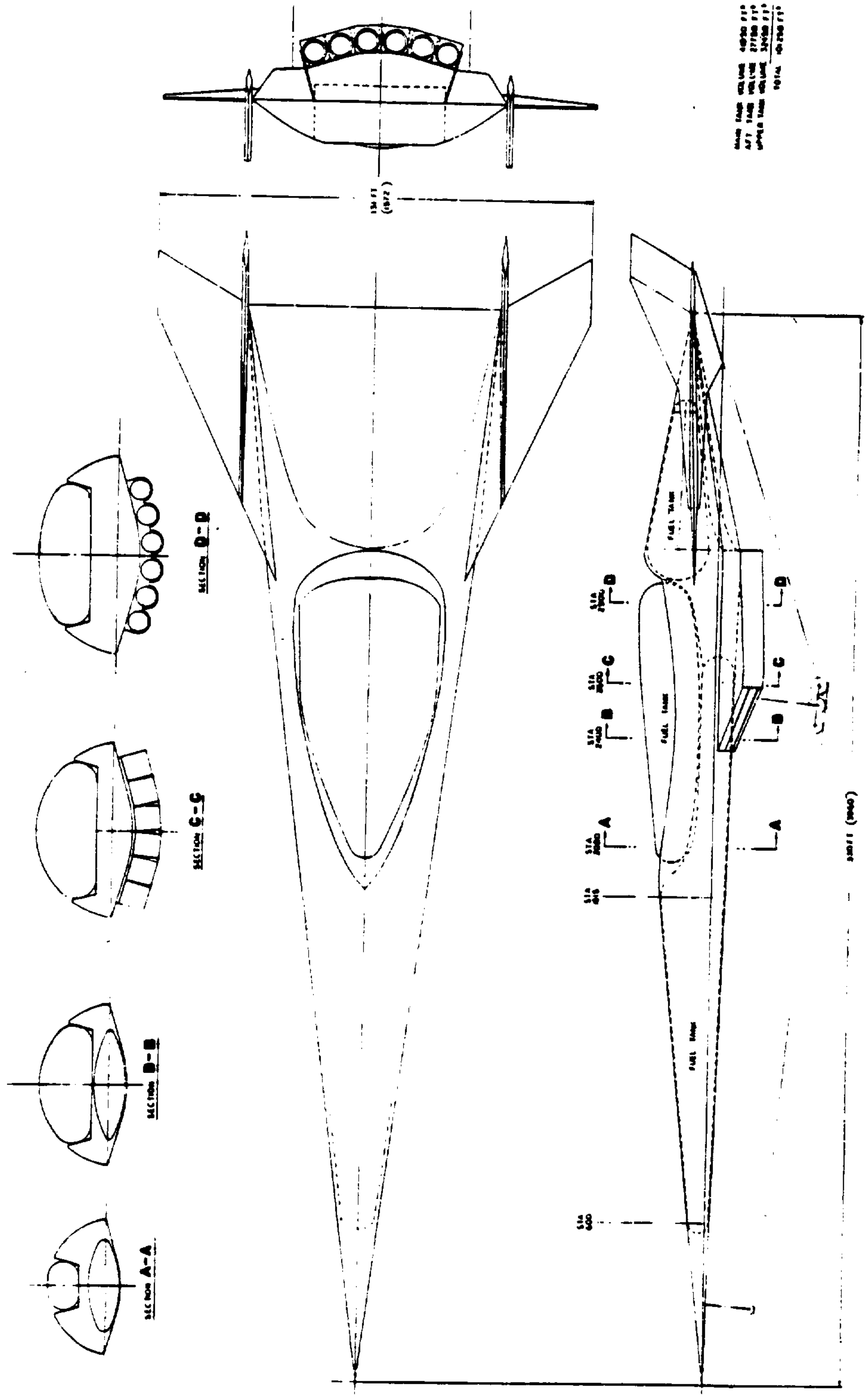

FIGURE D-1. Layout of Lifting Body Vehicle Installation for the Baseline First Stage Engine

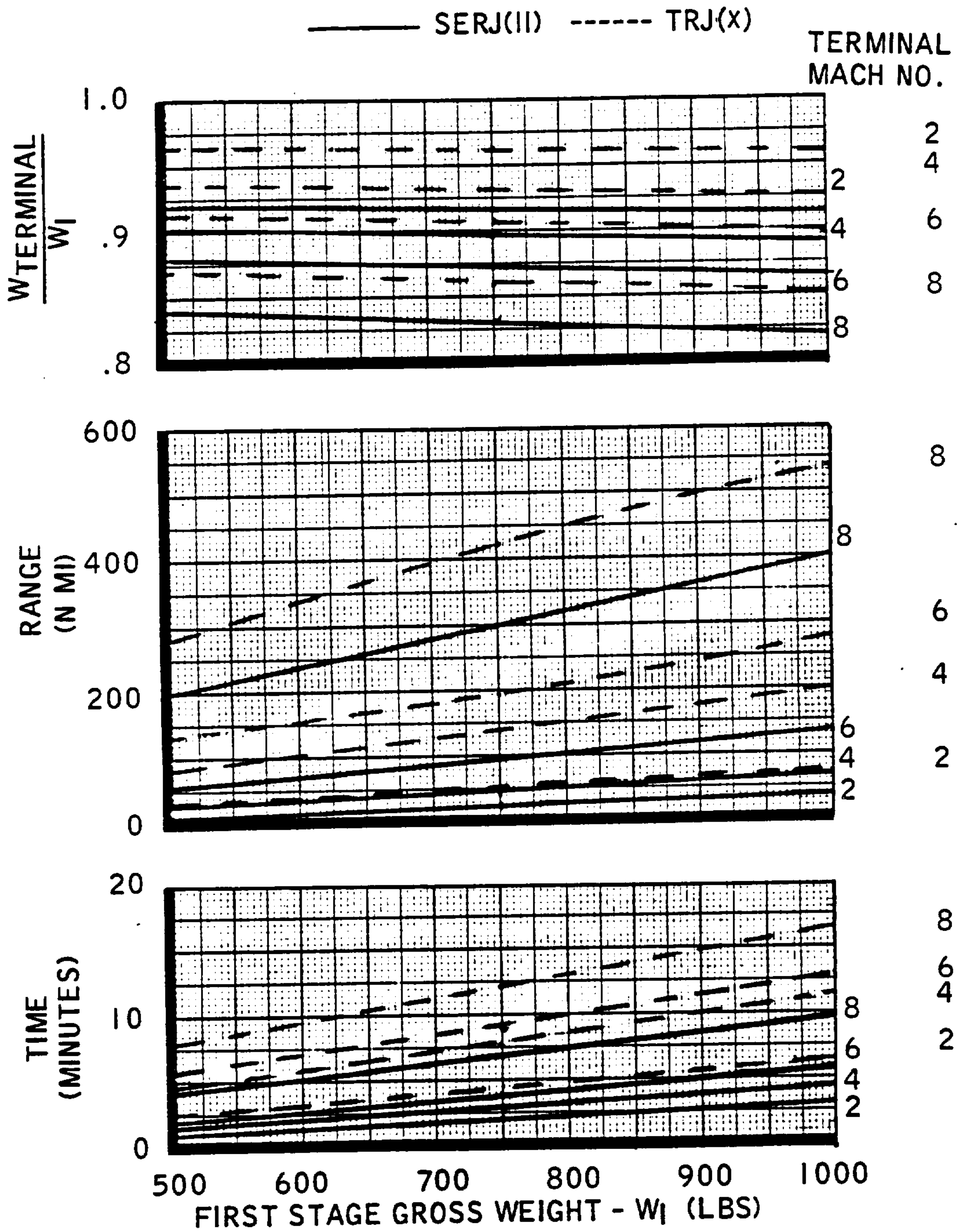

FIGURE D-2. Alternate Performance, Acceleration Characteristics for the First Stage Subsonic Combustion Vehicles

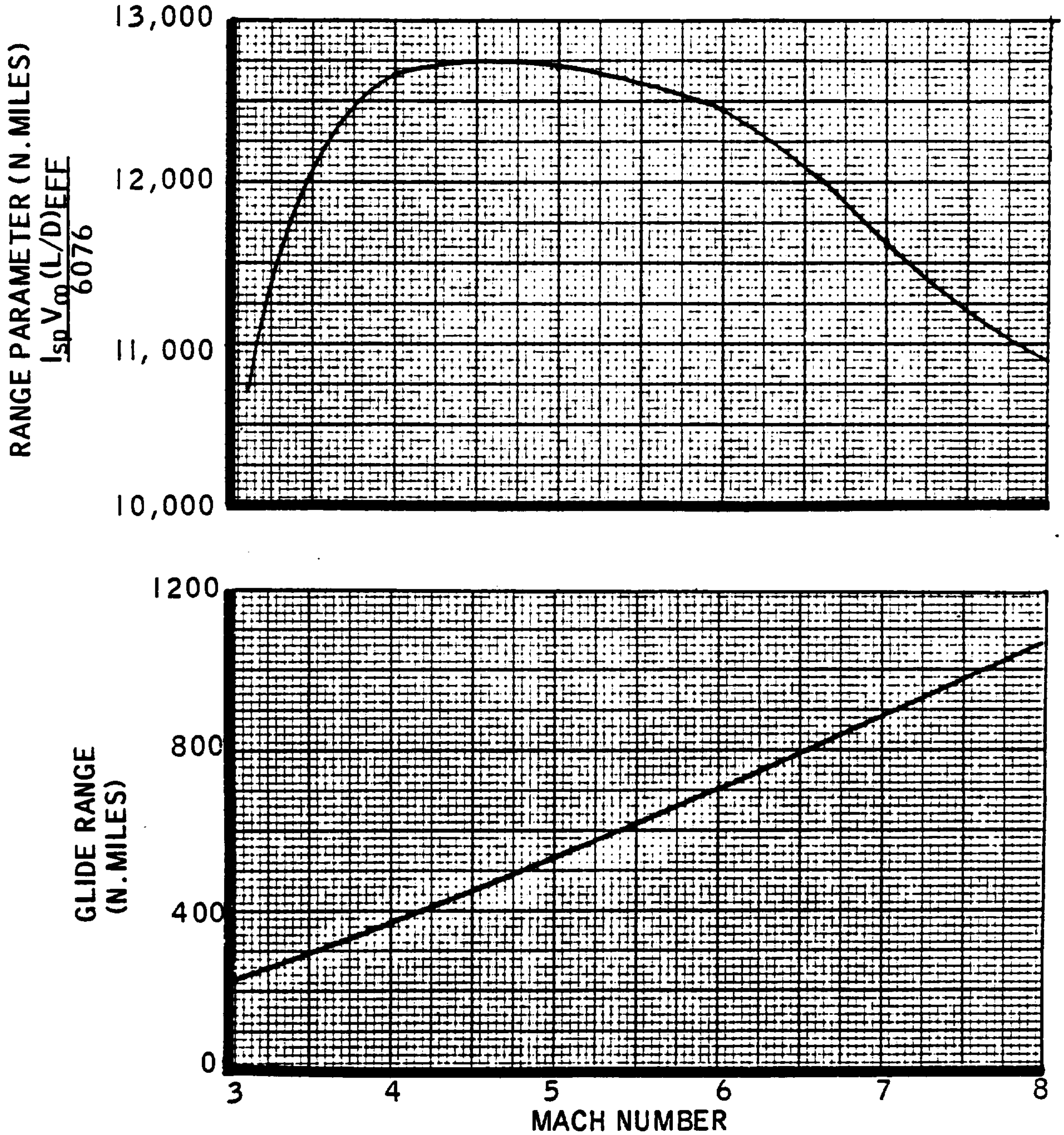

FIGURE D-3. Alternate Performance, Range Parameter and Glide Range as a Function of Cruise Mach Number for the First Stage Subsonic Combustion Vehicles

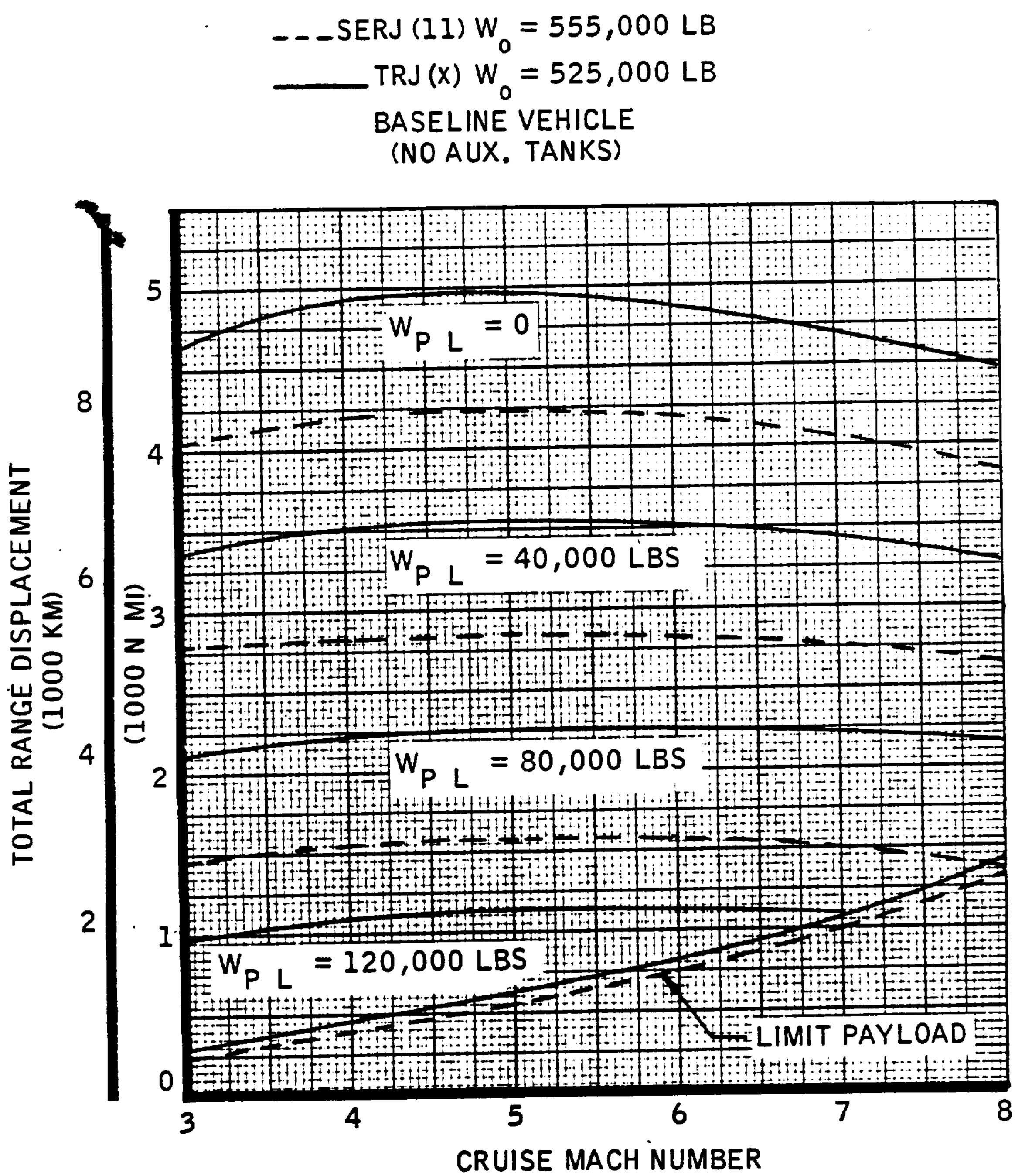

FIGURE D-4. Alternate Performance, Total Range Displacement as a Function of Cruise Mach Number for the First Stage Subsonic Combustion Vehicles

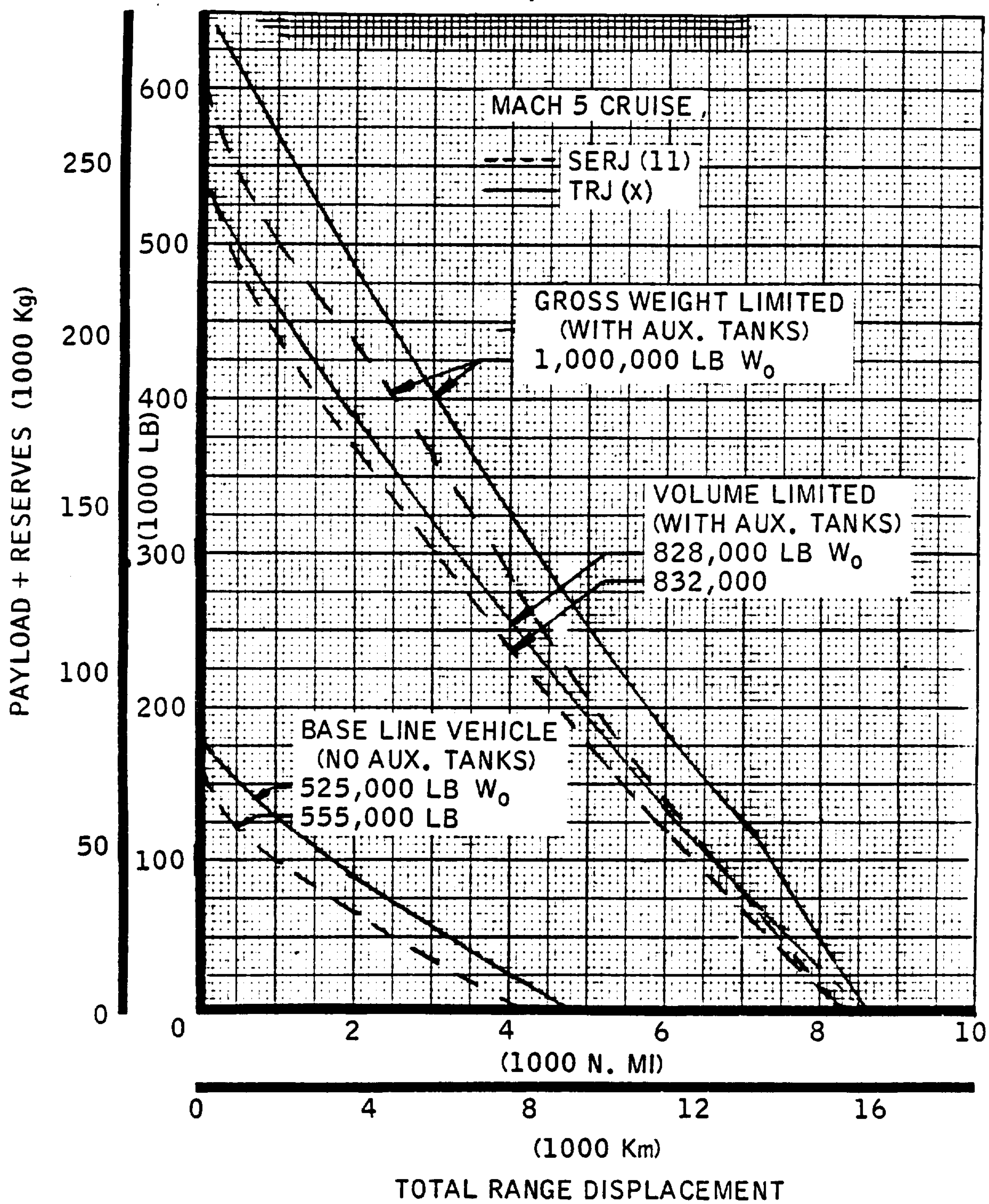

FIGURE D-5. Alternate Performance, Payload-Range Capability for the First Stage Subsonic Combustion Vehicles

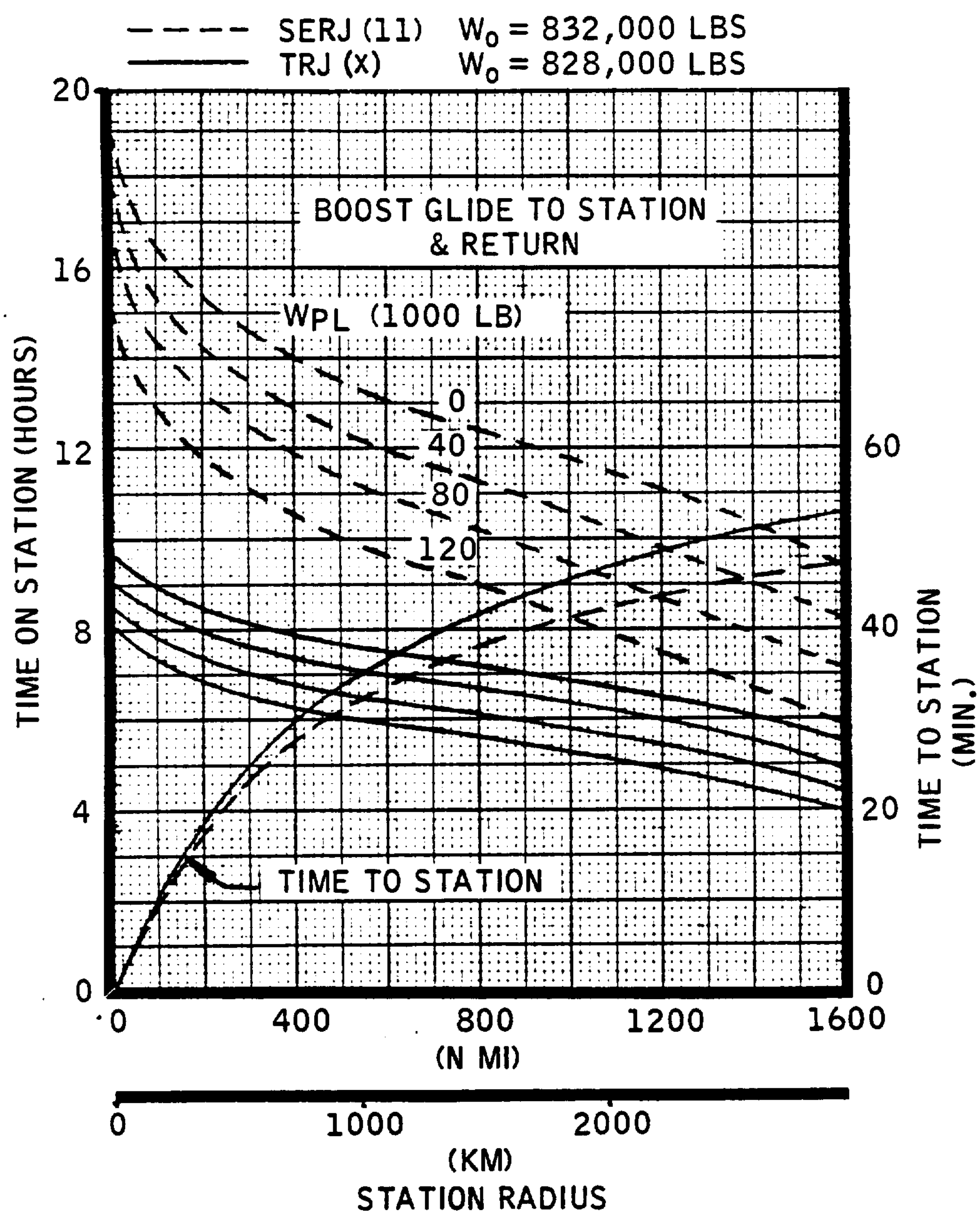

FIGURE D-6. Alternate Performance, Endurance Capability for the First Stage Subsonic Combustion Vehicles

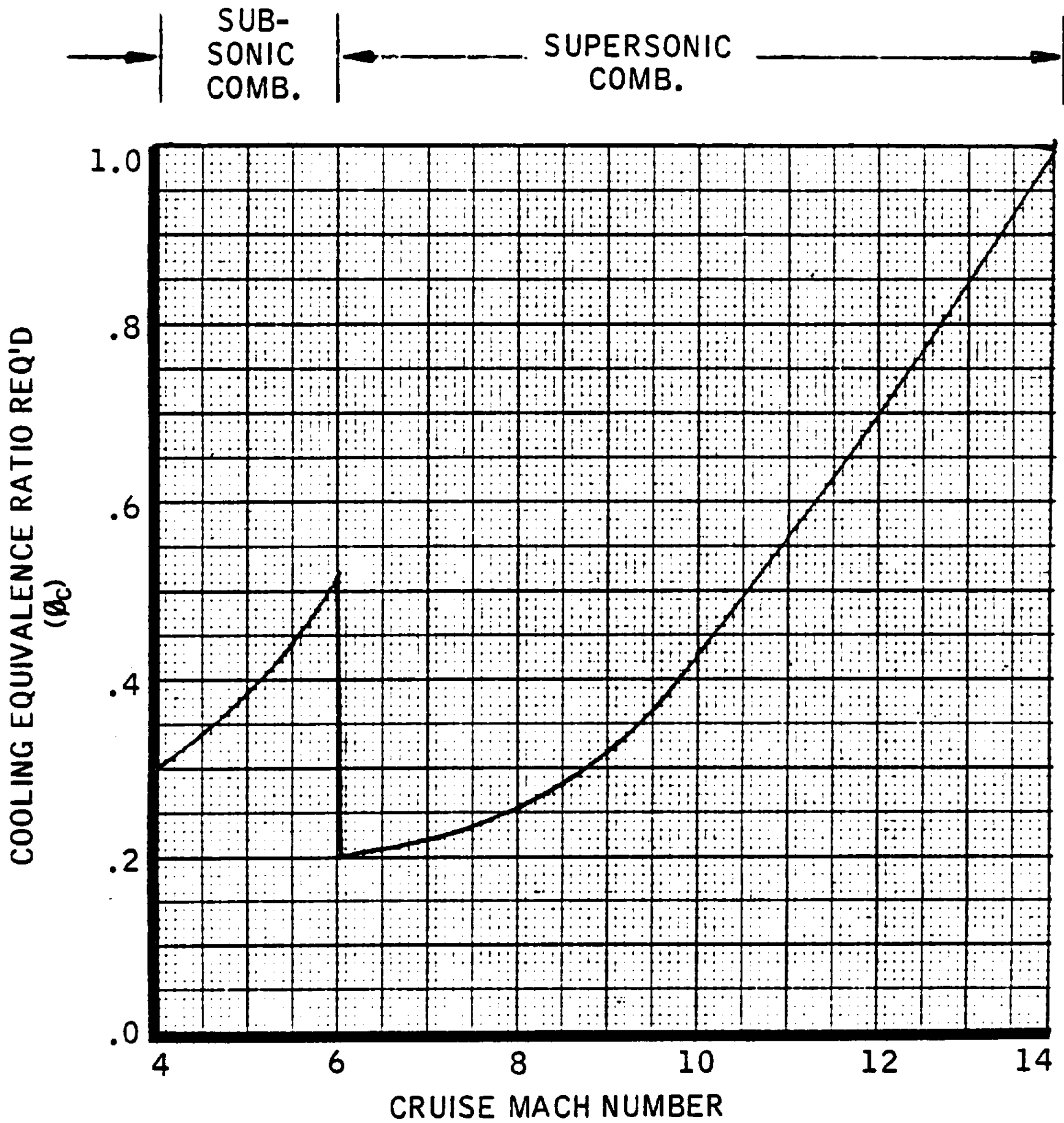

FIGURE D-7. Alternate Performance, Cooling Equivalence Ratio as a Function of Cruise Mach Number for the First Stage ScramLACE Vehicle

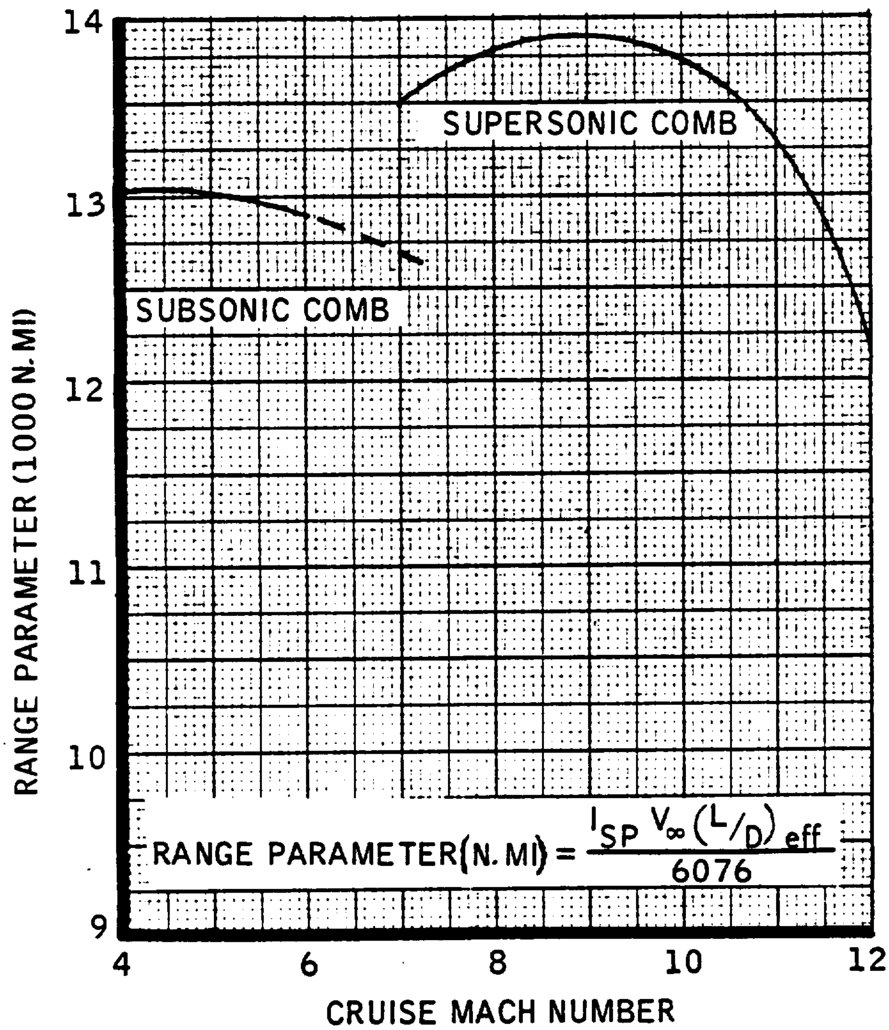

FIGURE D-8. Alternate Performance, Range Parameter as a Function of Cruise Mach Number for the First Stage ScramLACE Vehicle

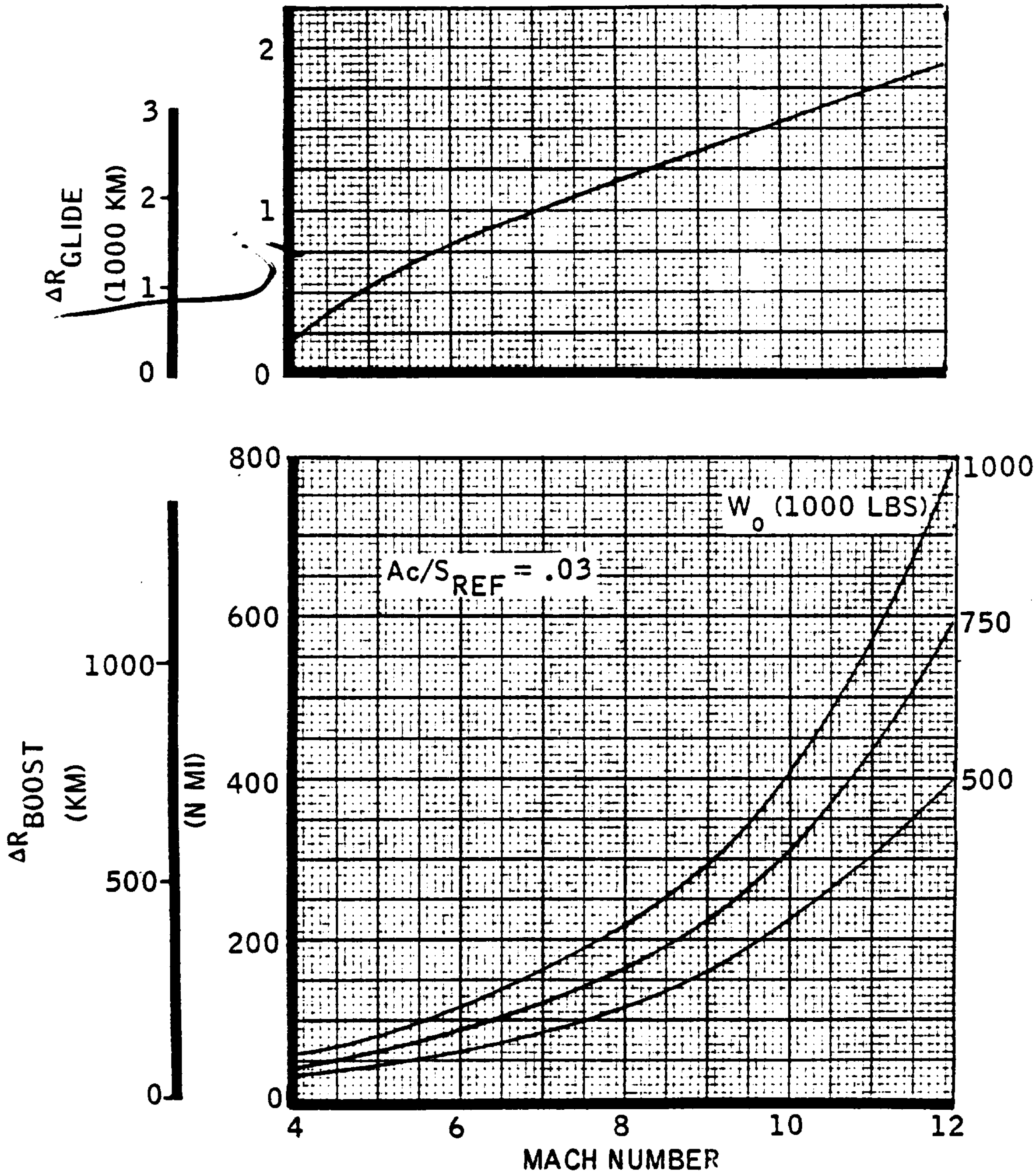

FIGURE D-9. Alternate Performance, Boost and Glide Ranges for the First Stage ScramLACE Vehicle

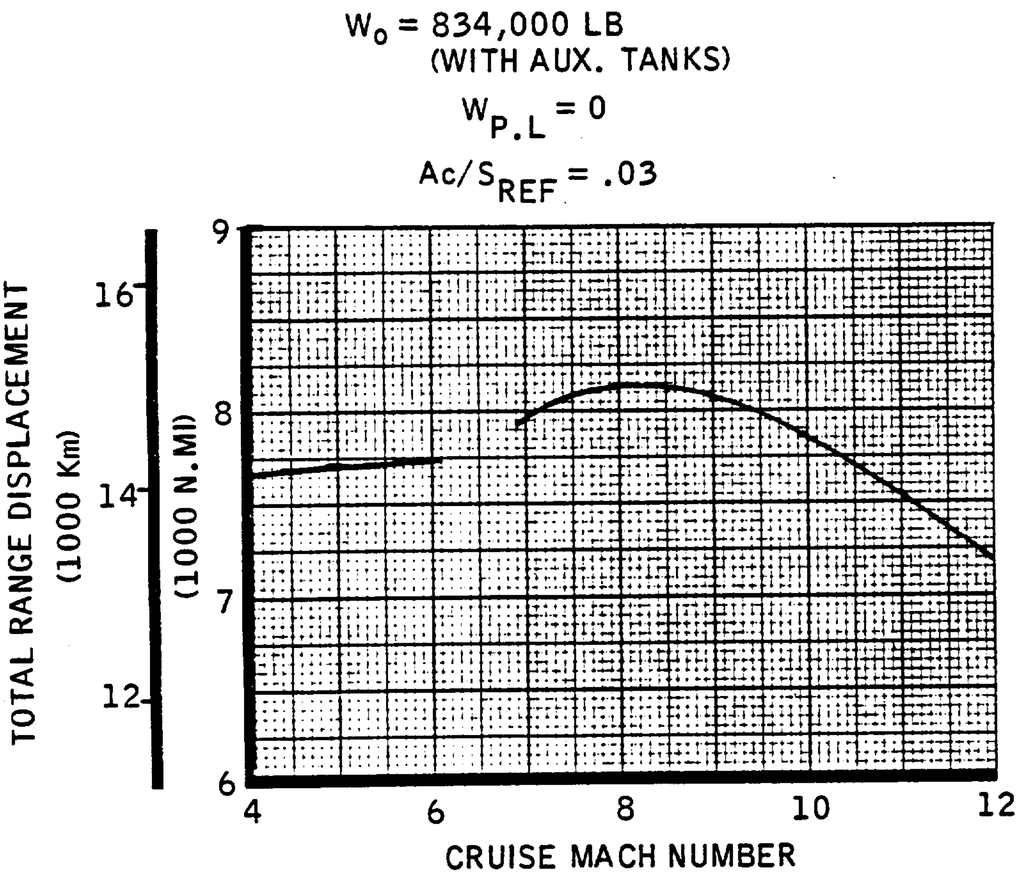

FIGURE D-10. Alternate Performance, Total Range Displacement as a Function of Cruise Mach Number for the First Stage ScramLACE Vehicle

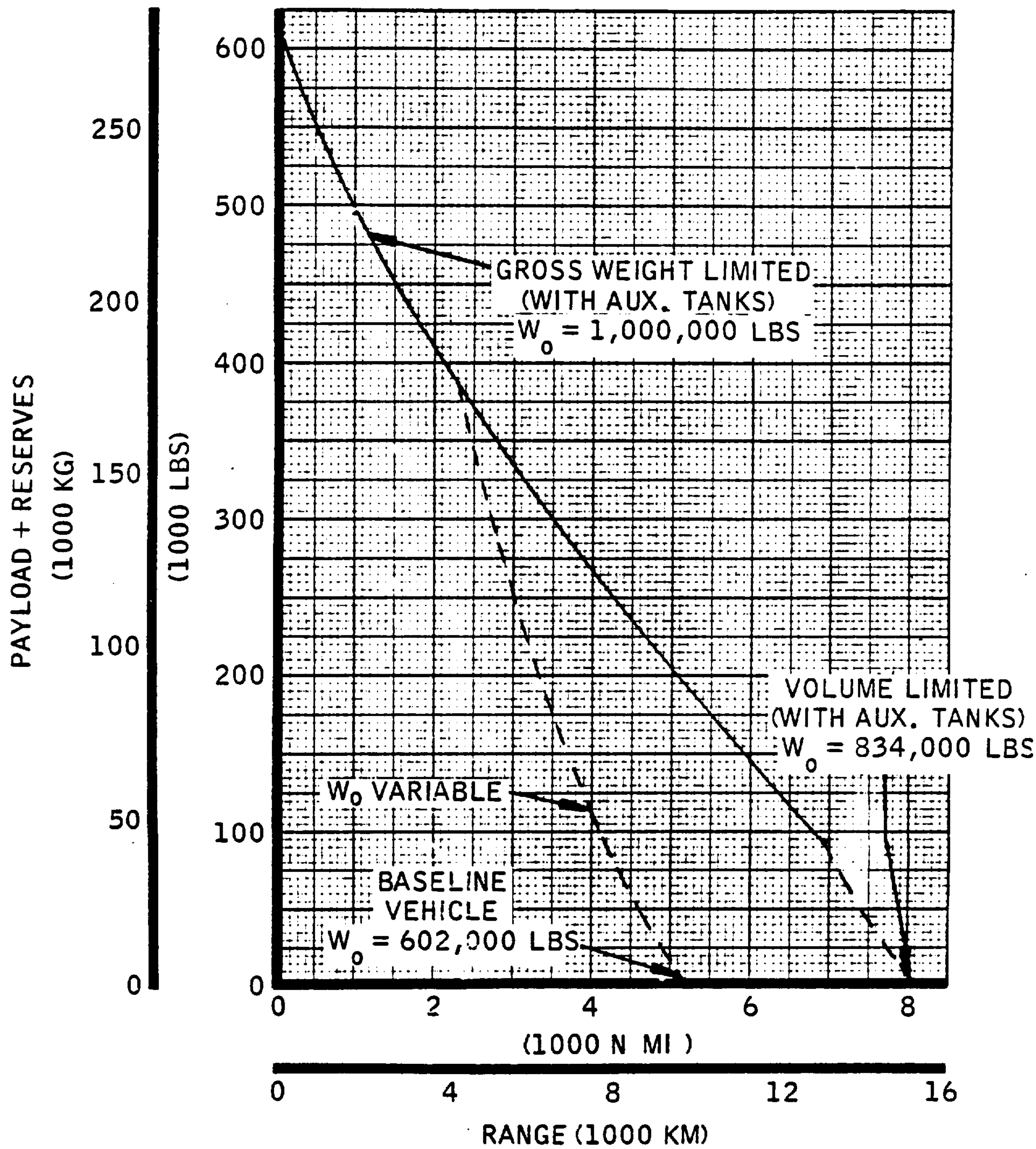

FIGURE D-11. Alternate Performance, Payload-Range Capability of the First Stage Mach 10 ScramLACE Vehicle (Mach 8 Cruise)

This page intentionally left blank

APPENDIX E

ANALYSIS OF

SINGLE STAGE TO ORBIT

VEHICLE/MISSION (CLASS 1)

Part I: Lifting Body Vehicle (HTOHL) Approach

By:

N. B. Williams and R. E. Morris
Lockheed - California Co.

Part II: Axisymmetric Vehicle (VTOVL) Approach

By:

H. Frank and W. J. D. Escher
The Marquardt Corporation

This page intentionally left blank.

APPENDIX E

ANALYSIS OF SINGLE STAGE TO ORBIT VEHICLE/MISSION (CLASS 1)

E-1. Introduction

A feature of the study guidelines (Section 3.1) was the examination of the single stage approach for achieving the reusable orbital transport cycle, as well as two-stage operation. The latter has, of course, been significantly demonstrated in the main body of the report (e.g., Sections 6.5, 7.6, and 8.6).

It became increasingly clear as the study proceeded that dependence on the two-stage vehicle models gave considerably higher confidence results in establishing comparative propulsion system results. The particular single stage model examined in the Class 1 phase by Lockheed, in fact, demonstrated a lack of positive payload capability. Very high sensitivity to the vehicle inert weight fraction, as expected, was evidenced here. It was there decided to relegate the single stage work to a secondary role in the succeeding work, and this approach was omitted altogether from the Class 2 phase effort. Nevertheless, the limited work accomplished is believed to have significance and is therefore presented in this appendix to the Main Technical Report.

Two rather widely varying vehicular concepts for the single stage mission are presented below. The first examines a lifting body horizontal takeoff and landing capability vehicle, a direct extrapolation in essence of the Class 1 phase first stage vehicle types. This assessment was performed to a significant level of aerodynamic and weight detail by Lockheed, commensurate with the technical penetration characteristic of the Class 1 phase.

The second concept was evolved and evaluated for single stage mission capability by Marquardt with somewhat lower technical penetration, being based by and large on an existing reference as noted. The configuration examined was an axisymmetric vehicle launched and landed in a vertical mode.

E-2. PART I. Lifting Body Vehicle (HTOHL) Approach

E-2.1 Description of Concept

A typical lifting body single stage to orbit system is presented in Figure E-1. In order to evaluate the potential of composite engine powered

vehicles to achieve single stage to orbit, an investigation was conducted in which the following ground rules were applied:

1. The basic propulsion system was the ScramLACE (Engine No. 22) with an inlet contraction ratio (A_c/A_2) of 3.0.

2. A lifting body configuration with aerodynamic characteristics as described in Sections 7.6.1.2 and 8.6.1.2 was assumed.

3. Weight at takeoff = 1.0 million lbs.

4. Zero payload (1523 fps post-injection ΔV) and 5000 lbs landing fuel are provided.

5. Final transfer from air breathing termination to orbit by liquid oxygen-hydrogen rocket with a vacuum I_{sp} of 460 seconds. It was further assumed that the primary rockets could be used (inlet closed) so that no weight penalty was incurred for separate rockets. This approach is reflected as the "Fourth Mode" for the ScramLACE Power plant. (Volume 7, Page 110).

6. No additional thermal protection penalty was assessed beyond that required for the Mach 12 vehicle by following a constant equilibrium lower skin-temperature path. (See Sections 8.6.1.4, and 8.6.2.4.)

7. A fuel equivalence ratio, as dictated by engine cooling considerations, can be maintained at 1.0.

E-2.2 Performance

The installed propulsion performance from takeoff to Mach 12 is described in Section 8.6.2.5. The extended performance assumed to Mach 26 is shown in Figure E-2. Although such performance was optimistic, in view of the contraction ratio chosen for the low speed regime (Mach 0 to 4), it was assumed to be achievable by the combination of flow field contraction, engine variable geometry, or increased blockage of the inlet by the primary rocket sections.

The choice of the trajectory shown in Figure E-3 was dictated by the requirement of minimum fuel consumption, as influenced by the relation between thrust-drag and vehicle angle of attack. A gross vector deflection angle of 6° from the vehicle axis was assumed to provide jet lift, in order to avoid high

values of dynamic pressure and aero heating. The value of the parameter $\frac{W}{q_\infty S_{Ref}}$ necessary to maintain the desired low angle of attack is shown in Figures E-4 and E-5 and the effective impulse (I_{sp_e}) is shown in Figure E-6.

E-2.3 Weights

The minimum sum of propulsion, hydrogen, oxygen, and tankage weight fractions required to achieve orbit for the selected air breathing termination velocities (V_{AB}) of 14,000, 18,000, and 24,600 fps is shown in Figure E-7 as a function of the ratio of capture area to reference area.

As a measure of the feasibility of the single stage to orbit vehicle described, the dry weight required to achieve orbit injection was determined from the overall mass ratio for each of the three air breathing terminal velocities which were considered. This weight was then compared to the values generated by the weight analysis described in Section 8.6.1.4. The resulting comparison is tabulated below in terms of absolute weight, and as the percentage reduction in dry weight required to make single stage to orbit capability possible.

Parameter	V_{AB}, ft per sec		
	14,000	18,000	24,600
Reference planform area, sq ft	10,820	13,300	15,800
Capture area, sq ft	390	479	853
W_{dry} (Required), lbs	280,500	313,000	400,800
W_{dry} (Weight analysis), lbs	349,090	400,920	521,490
Reduction required to accomplish mission, %	19.6	21.9	23.2

E-2.4 Discussion

Although in this limited study of the single stage to orbit vehicle was marginal at best, it may be possible that other configurations (such as an axisymmetric vehicle) might favor the large capture areas required with the potential of lower vehicle drag and reduced inert weight. This alternative approach was, in fact, cursorily examined (by Marquardt) and the results are presented in the next section. In any event, those benefits which may accrue could also be applied to the two-stage vehicle with decreased sensitivity and increased payload capability.

E-3. PART II. Axisymmetric Vehicle (VTOVL) Approach

E-3.1 Background

As noted, two approaches were taken in reviewing the potentials and the problems of the single stage to orbit concept. The first of these was generated by Lockheed and it is discussed in the preceding section. Figure E-8 reflects the essentials of an alternate vehicle concept which might be applicable to direct orbit cycles. Being based on a prior Marquardt assessment of Scramjet to orbit operation (Reference E-1), the vehicle concept is, pictorially at least, an all-inlet, all-exit concept, the vehicle body containing the propellants and payload being, in this way, utilized for basic propulsion operation. For this model, twelve Recycled Supercharged ScramLACE engines (No. 32) were employed by way of instilling a maximum performance potential composite propulsion system. As noted in Figure 212 (in Volume 2), this engine concept reflects a superior payload in the two-stage system model. Also, fan propulsion plays an important role in the loiter/landing phase, as will be described.

E-3.2 Description of Concept

The 1.0 million lbm vertically launched vehicle has twelve 105,000 lbf powerplants providing an initial thrust/weight ratio of 1.25. The maximum capture area (full frontal profile stream tube) is 2040 sq ft. The overall vehicle concept, and specific propulsion performance for the above Mach 8 flight conditions were taken from the previously mentioned Marquardt study of Scramjet to orbit system, the MA114 system (Reference E-1).

Since it was desired to use fan mode propulsion (Engine No. 32), an axisymmetric, or "square" uninstalled engine shape was indicated, rather than the complete annular arrangement of the MA114. Consequently, as shown in Figure E-8, a multiple, integrated nacelle configuration was selected. This configurational switch implied the loss of the sought-for full capture characteristic of the MA114 (full vehicle stream processed through the engines at the on-design condition). This was because vehicle-forebody precompressed

air would, in large share, pass between the nacelles.

To correct this, a major innovation was introduced, namely, the split, flexible aerodynamic fence concept. This is shown in Figure E-8 in the between-engine areas mounted on the forebody in radial centerline planes.

Details of the concept are not related here, but the concept also plays a part in the following additional problem areas:

1. Engine thrust rebalancing while flying at angles of attack via differential engine air flow control

2. Lift production, particularly for low speed operation

The installed engine thrust/weight ratio was taken as 13:1, allowing for some minor inlet-associated weight. (Recall that the vehicle forebody provides basic compression, or diffusion.)

E-3.3 Mission Profile

The full mission profile from lift-off to landing is outlined in Figure E-9.

The vehicle is accelerated into orbit through multimode operation including a rocket vacuum mode at the high speed end. The performance in terms of payload was assessed for various airbreathing termination velocities, i.e., points where conversion to rocket mode was made in the orbital ascent path. (The results are given in Figure E-10.) The mission profile continued with a return leg which consisted of retro from orbit, entry, deceleration to approximately Mach 4.5 and flyback on ramjet mode at a cruise point of Mach 4.5 for 300 n. miles to the landing point. Deceleration to subsonic velocity then followed and operating on high specific impulse ducted fan power, a 20-minute loiter in the vicinity of the landing point was assessed. Landing consisted of rotation to a vertical attitude and a tail first let down on fan power with plenum burning. This final maneuver was considered to take approximately one minute.

This vehicle-mission profile concept, though obviously a somewhat problematic one, is - in the first order - consistent with the number of design approaches reflected from previous studies involving the high speed Scramjet-to-orbit approach (Reference E-1).

E-3.4 Trajectory and Aerodynamics

The trajectory, following vertical takeoff and kickover, was a $q = 1500\ lb/ft^2$ path to Mach 8. Thereafter the dynamic pressure was diminished

to q = 650 lb/ft^2 at Mach 25 (altitude = 163,000 ft). The nominal angle of attack variations (decreasing) were from $\alpha = 11°$ at Mach 1, to $\alpha = 8°$ at Mach 8, to $\alpha = 2.2°$ at Mach 25.

The aerodynamic characteristics were based on the following assumptions:

1. Normal force coefficient, $C_N \approx C_L$ based on a 7.5° cone from NACA Report 1135
2. Induced drag coefficient, $C_{D_i} = C_L \cdot \tan \alpha$
3. Zero lift drag coefficient (C_{D_o}) based on that of Reference E-1

The drag is reflected in Figure E-11.

E-3.5 Performance

Figure E-11 presents thrust, specific impulse, and drag as a function of flight speed for the single stage concept. The engine operating modes and performance references are tabulated below:

Flight Velocity	Operating Mode	Performance Reference
0 to 2000 ft/sec	Recycled Supercharged Ejector Mode	Volume 6, Engine No. 32
2000 to 8000 ft/sec	Subsonic Combustion Ramjet	Volume 6, Engine No. 32 (With increased capture limit)
8000 to 14,000/20,000/25,177 ft/sec	Supersonic Combustion Ramjet (Fuel rich past Mach 14) for various termination points	Reference E-1
14,000/20,000 Orbital	Rocket Vacuum Mode, I_s = 460 sec	Volume 7, Engine 22 Operating mode schematic, page 110

E-3.6 Payload Performance

Gross payload to orbit is shown as a function of propellant mass fraction of the single stage vehicle (Conventional λ term for rocket type systems), as a function of Scramjet mode termination and conversion to rocket mode velocity in Figure E-10. For reference purposes, a comparable advanced single stage all-rocket (very advanced baseline engine) version is shown in the lower left hand corner (Section 5.2.3.2.1, Volume 2). Although a very significant payload magnification potential occurs in the composite cycle system, the high sensitivity to vehicle mass fraction actually obtainable is still clearly evident.

For the particular vehicle concept reflected above, it was not feasible, within the bounds of the study to estimate the mass fraction that might be obtained, the structure concept being particularly unconventional. Therefore, no conclusion can be offered as to absolute payload performance. Instead the observation can be made that although striking potential is presented, a high sensitivity to structure remains, as is the case with the all-rocket single stage.

If direct non-staged ground to orbit transportation continues to be of interest, it is clear that much further analytical and design work is required to establish a structural efficiency associated with the vehicle concept. The need to carefully integrate the propulsion systems with the vehicle is also clearly apparent.

REFERENCES

E-1. Burnette, T. D., Pearlman, E. J., and Thomson, R. W., "The Performance and Structural Design of the Marquardt MA114-XAA Supersonic Combustion Ramjet", Contract AF 33(657)-8491, Marquardt Report MR 20,222, February 1963. [redacted].

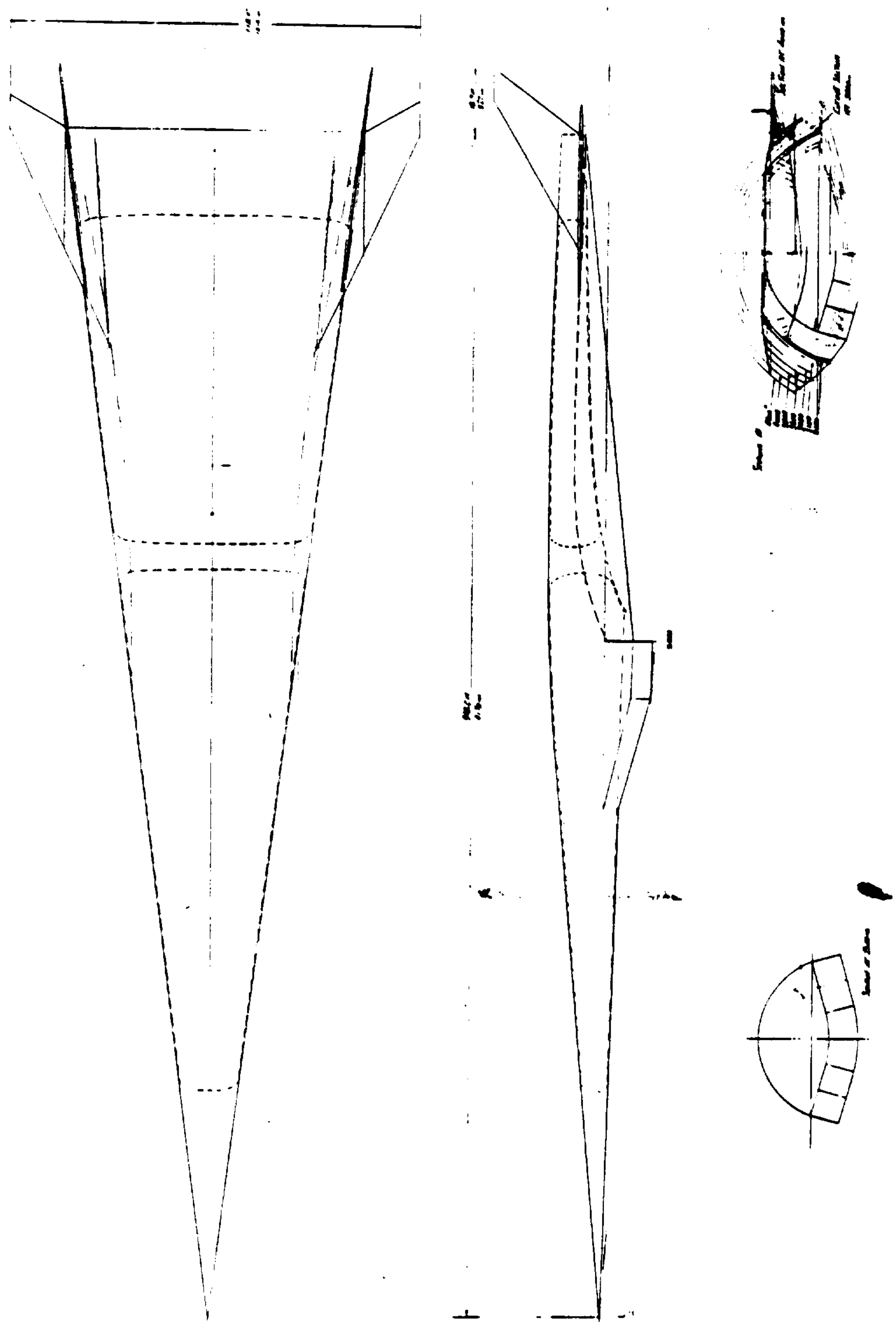

FIGURE E-1. Layout of Lifting Body Single Stage to Orbit Vehicle Installation for the ScramLACE System

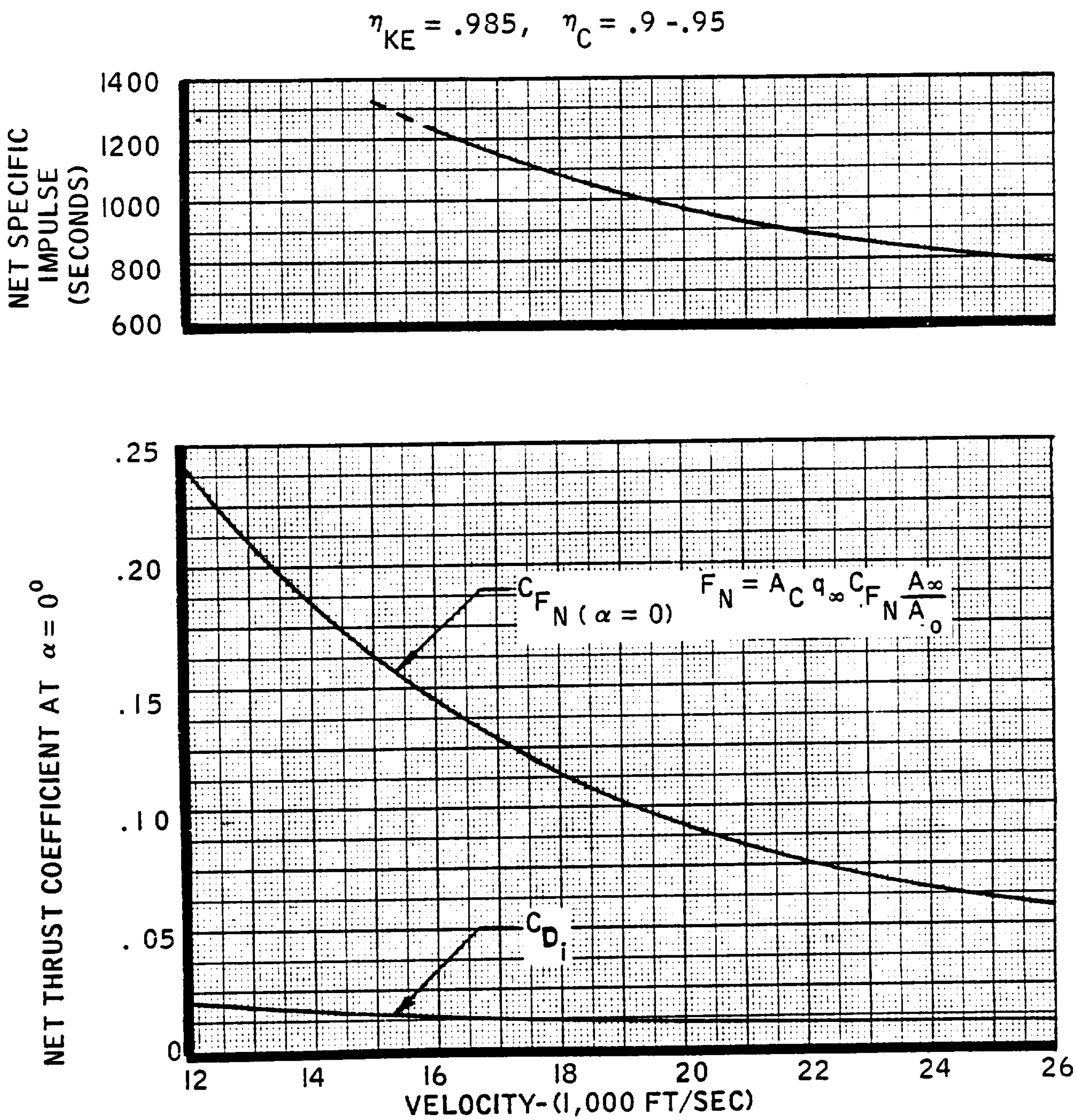

FIGURE E-2. Installed Propulsion Performance of the Single Stage to Orbit System (Mach 12 to 26)

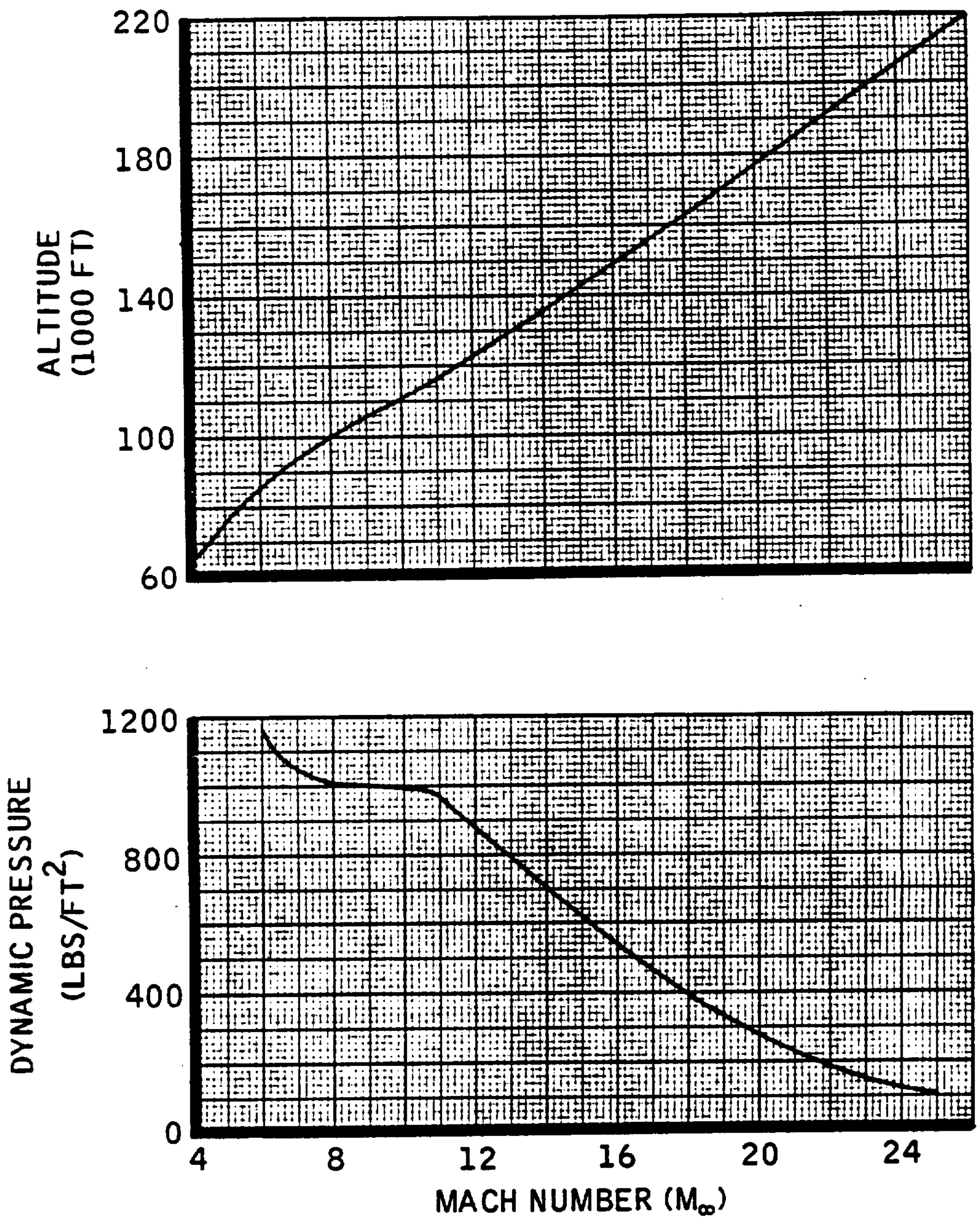

FIGURE E-3. Ascent Trajectory and Dynamic Pressure History of the Single Stage to Orbit System

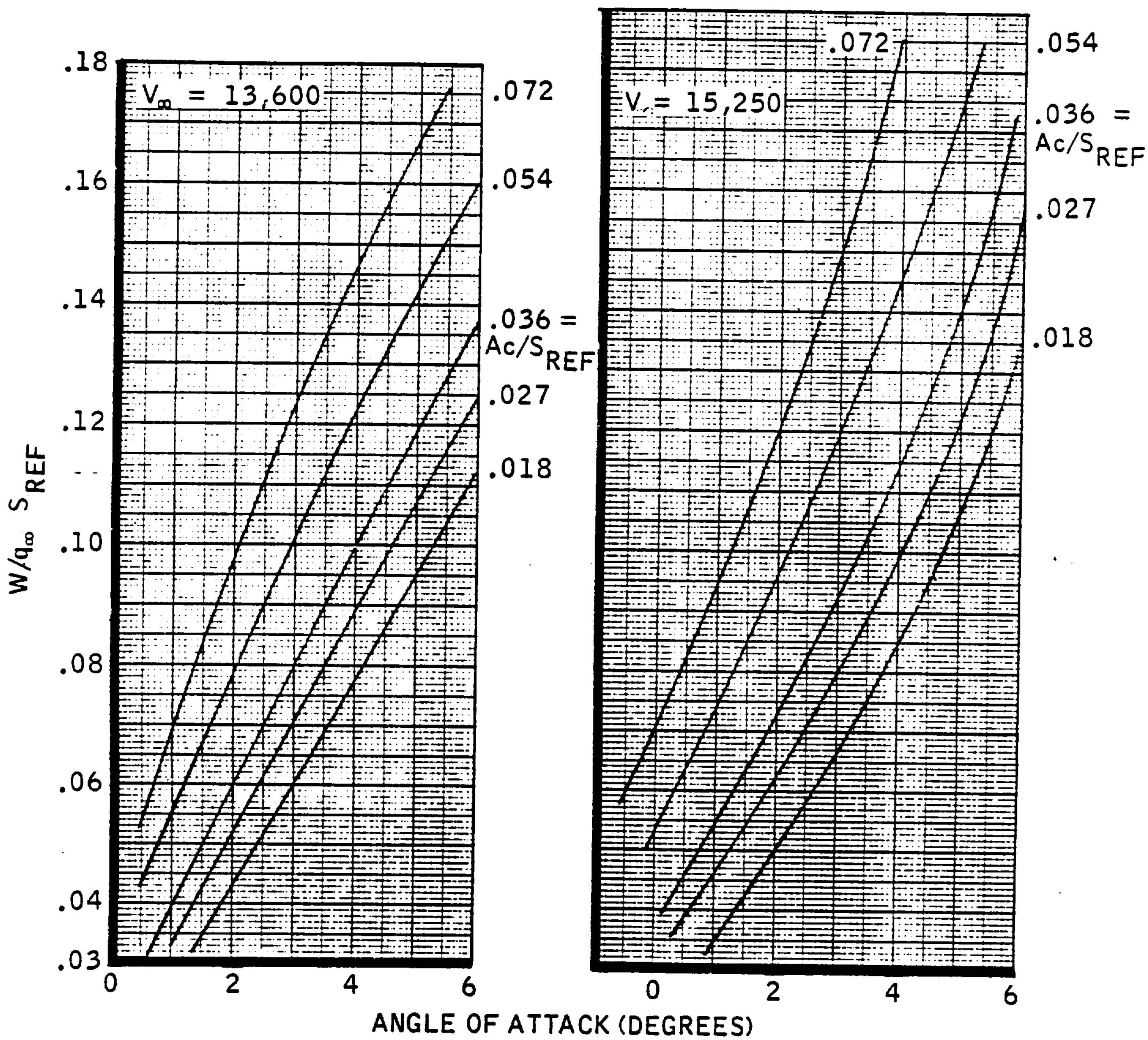

FIGURE E-4. Flight Characteristics of the Single Stage to Orbit System at 13,600 and 15,250 fps

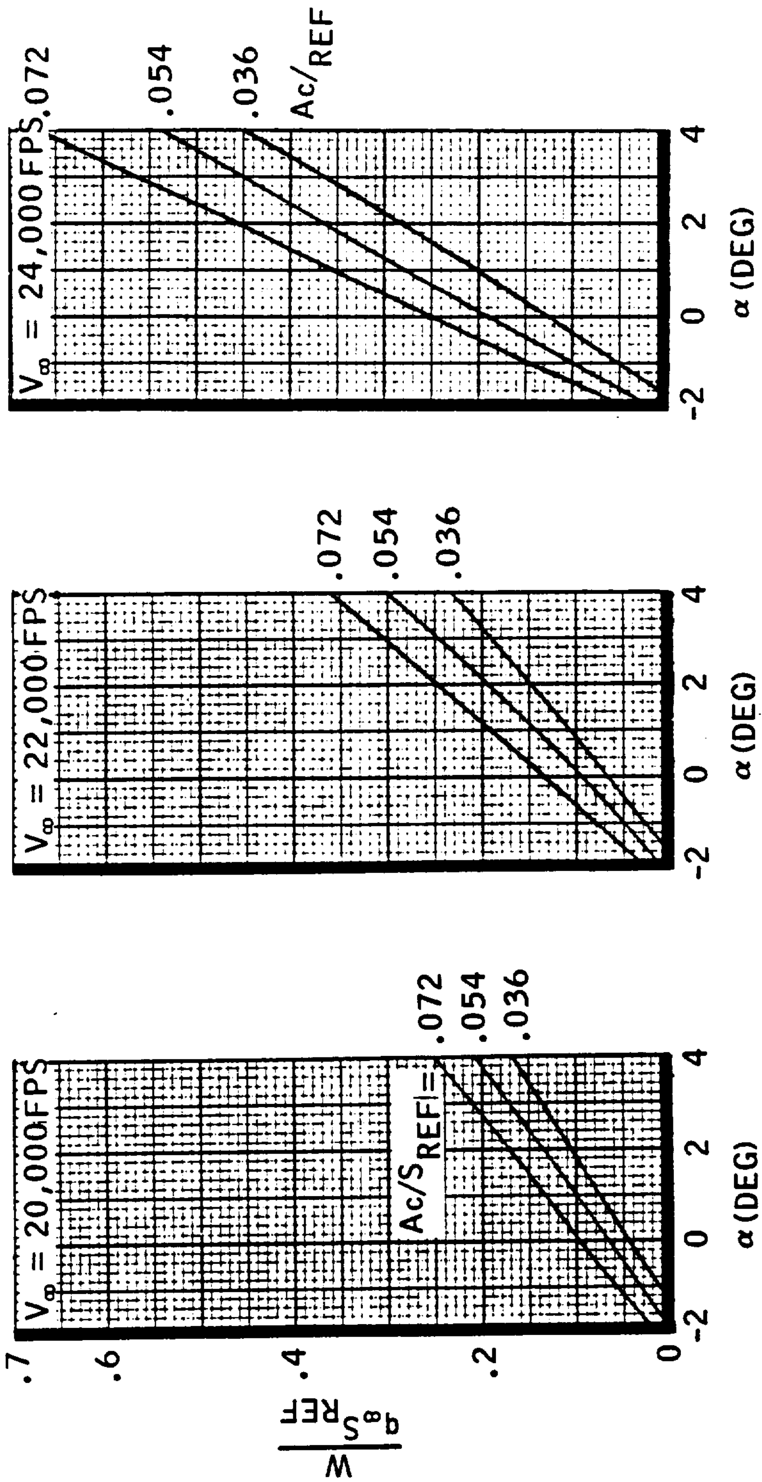

FIGURE E-5. Flight Characteristics of the Single Stage to Orbit System at 20,000 to 24,000 fps

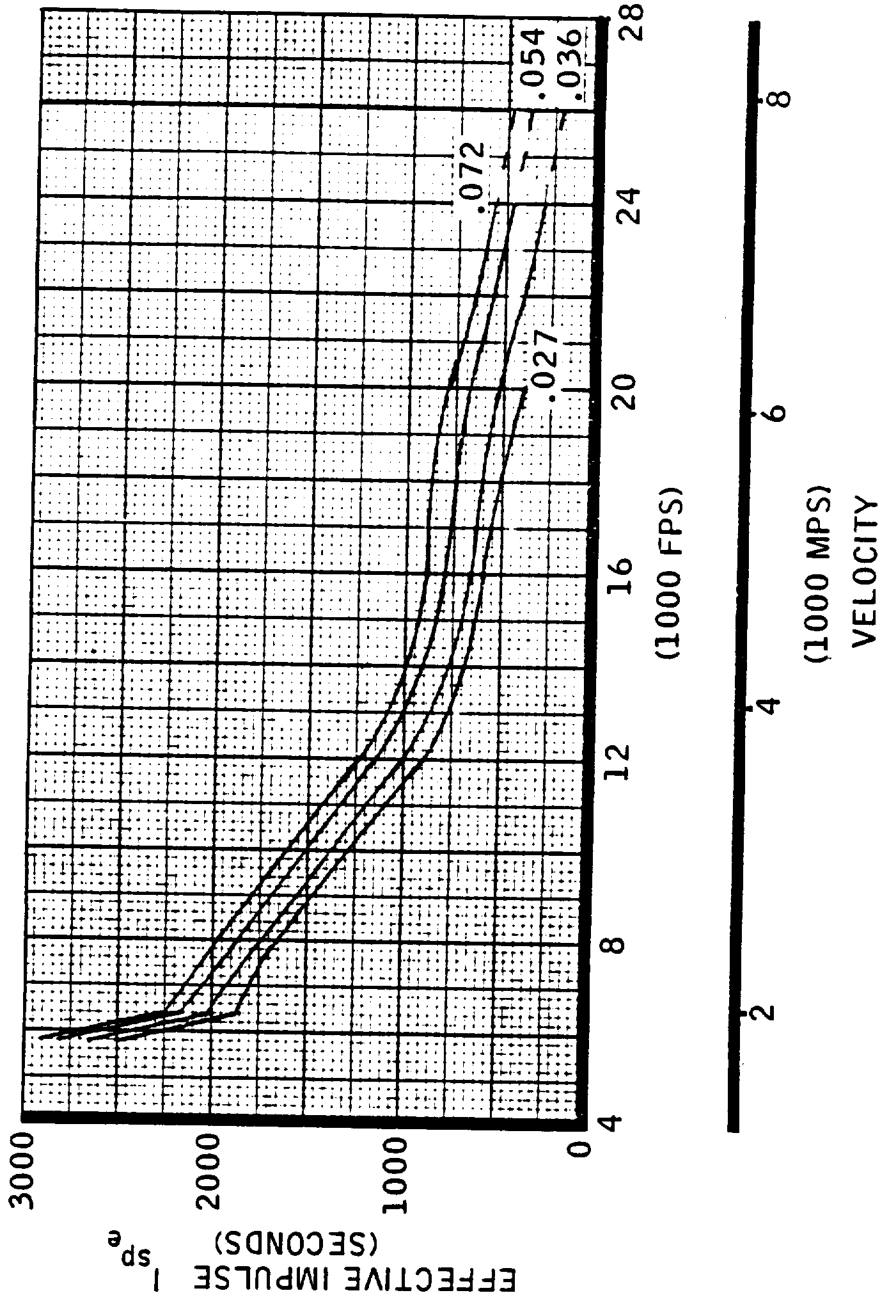

FIGURE E-6. Supersonic Combustion Mode Effective Impulse of the Single Stage to Orbit System

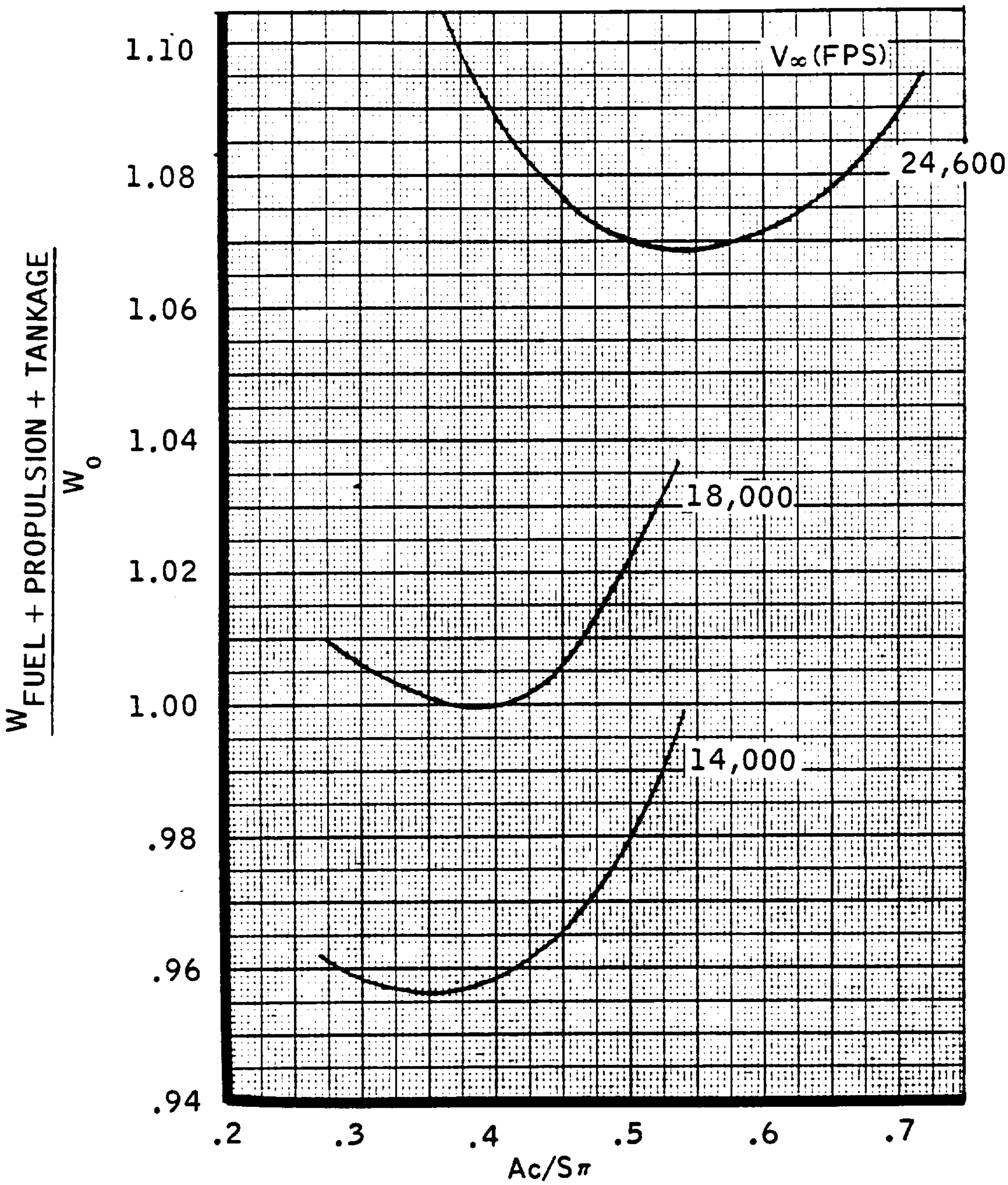

FIGURE E-7. Capture Area Sizing for the Single Stage to Orbit System

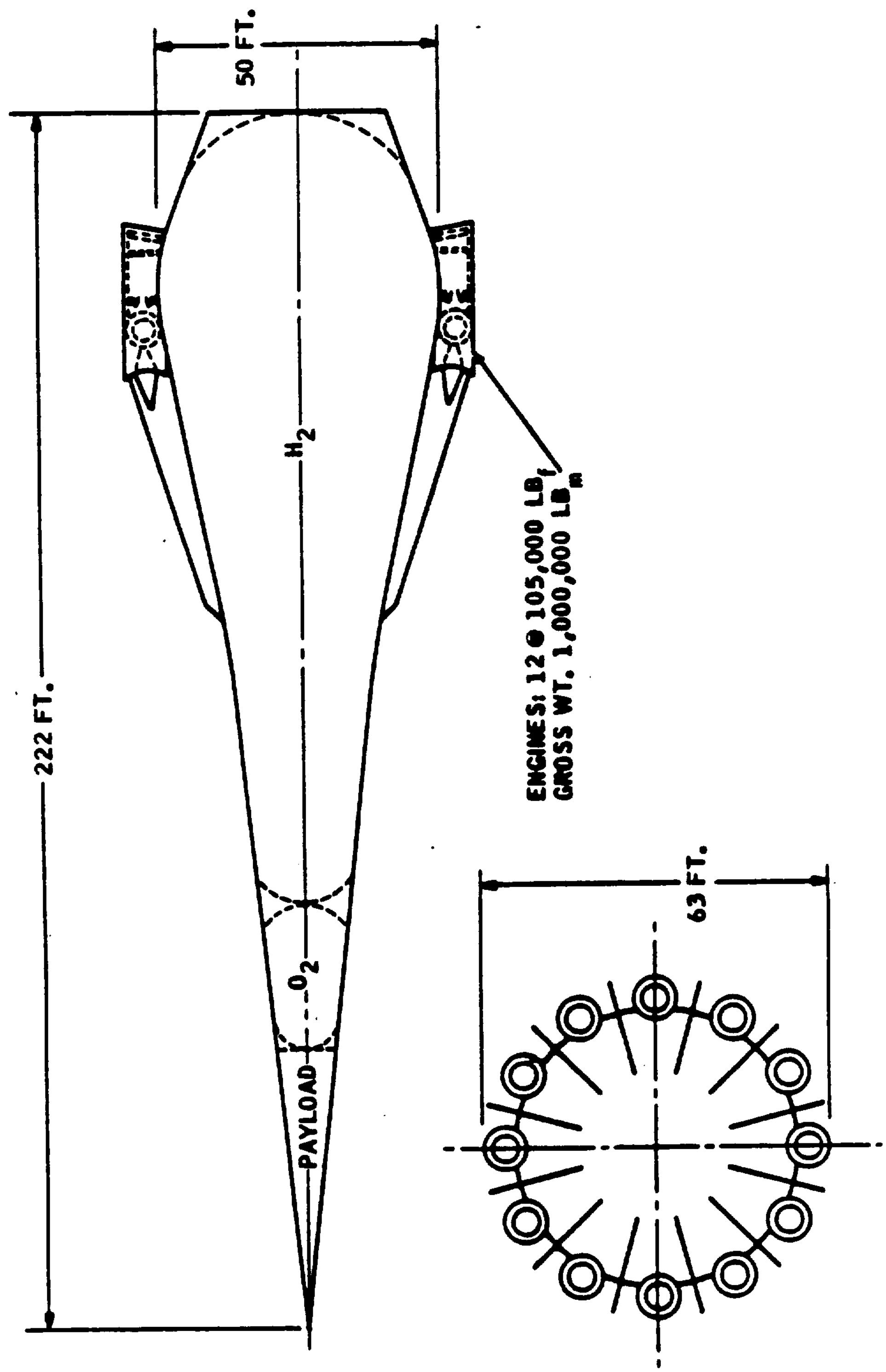

FIGURE E-8. Layout of VTOVL Single Stage to Orbit Concept, Supercharged Recycled ScramLACE Engine (No. 32)

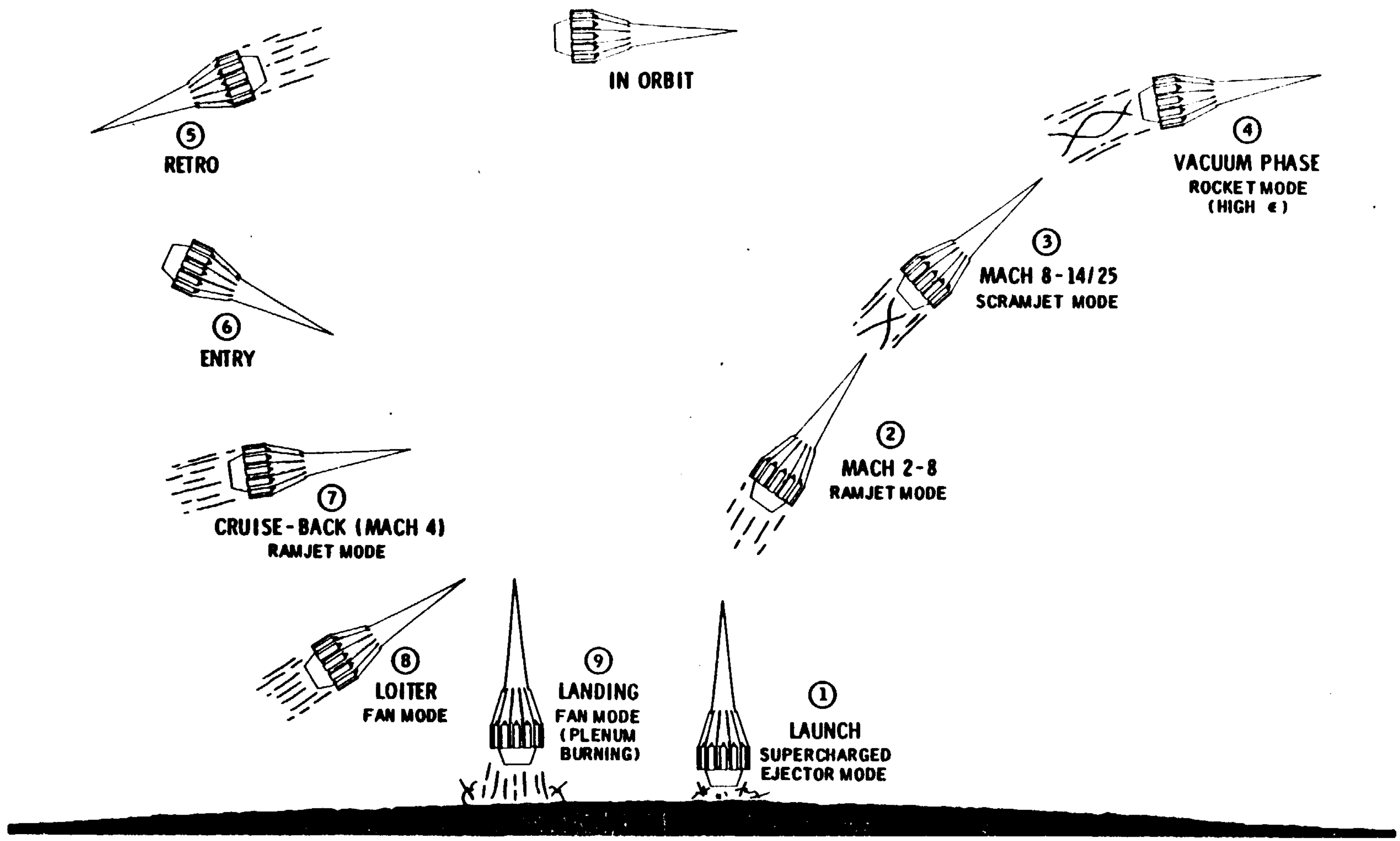

A276-1

FIGURE E-9. Mission Profile for the Single Stage to Orbit Concept, Supercharged Recycled ScramLACE Engine (No. 32)

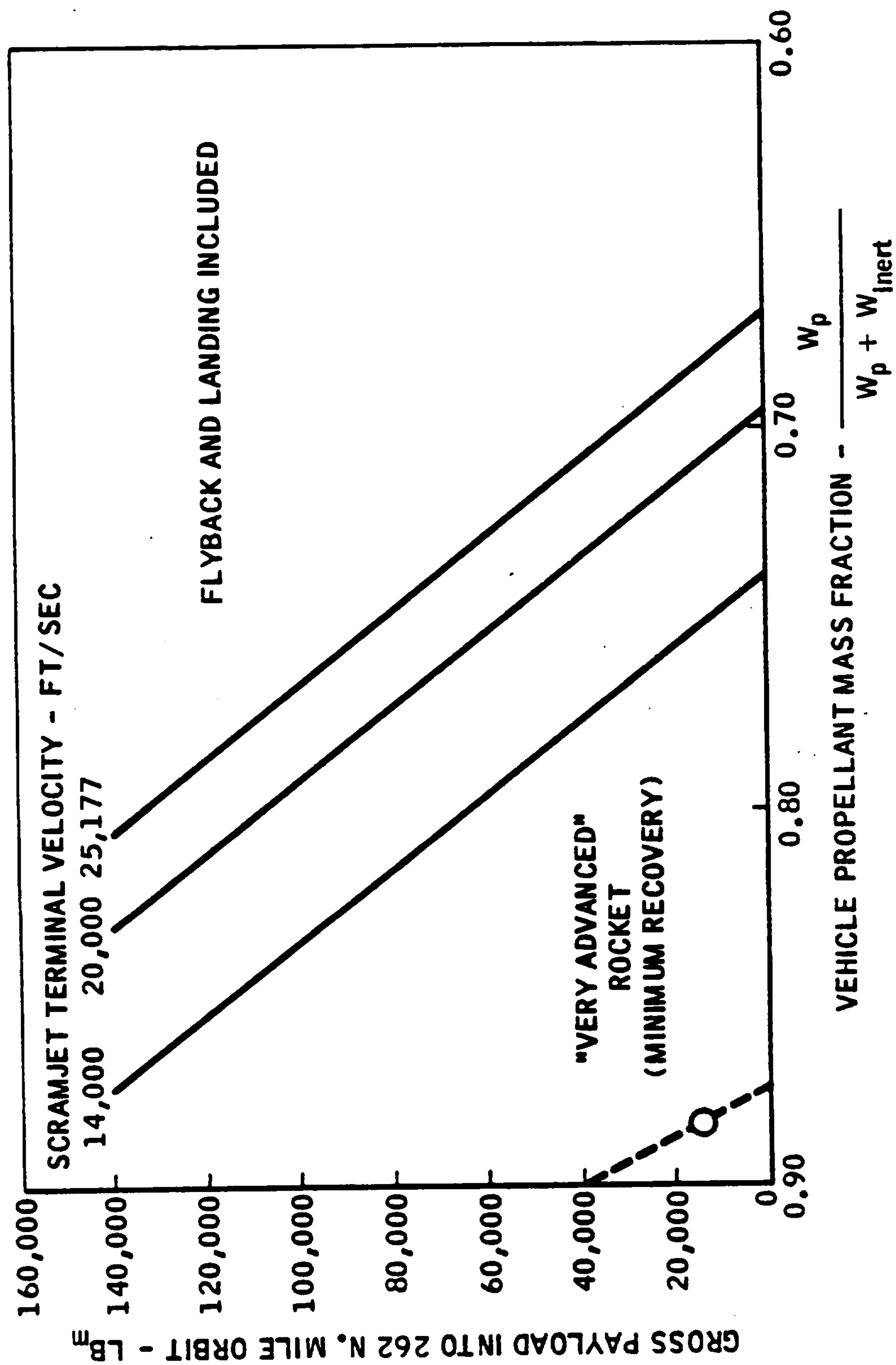

FIGURE E-10. Payload Performance of the Single Stage to Orbit Concept, Supercharged Recycled ScramLACE Engine (No. 32)

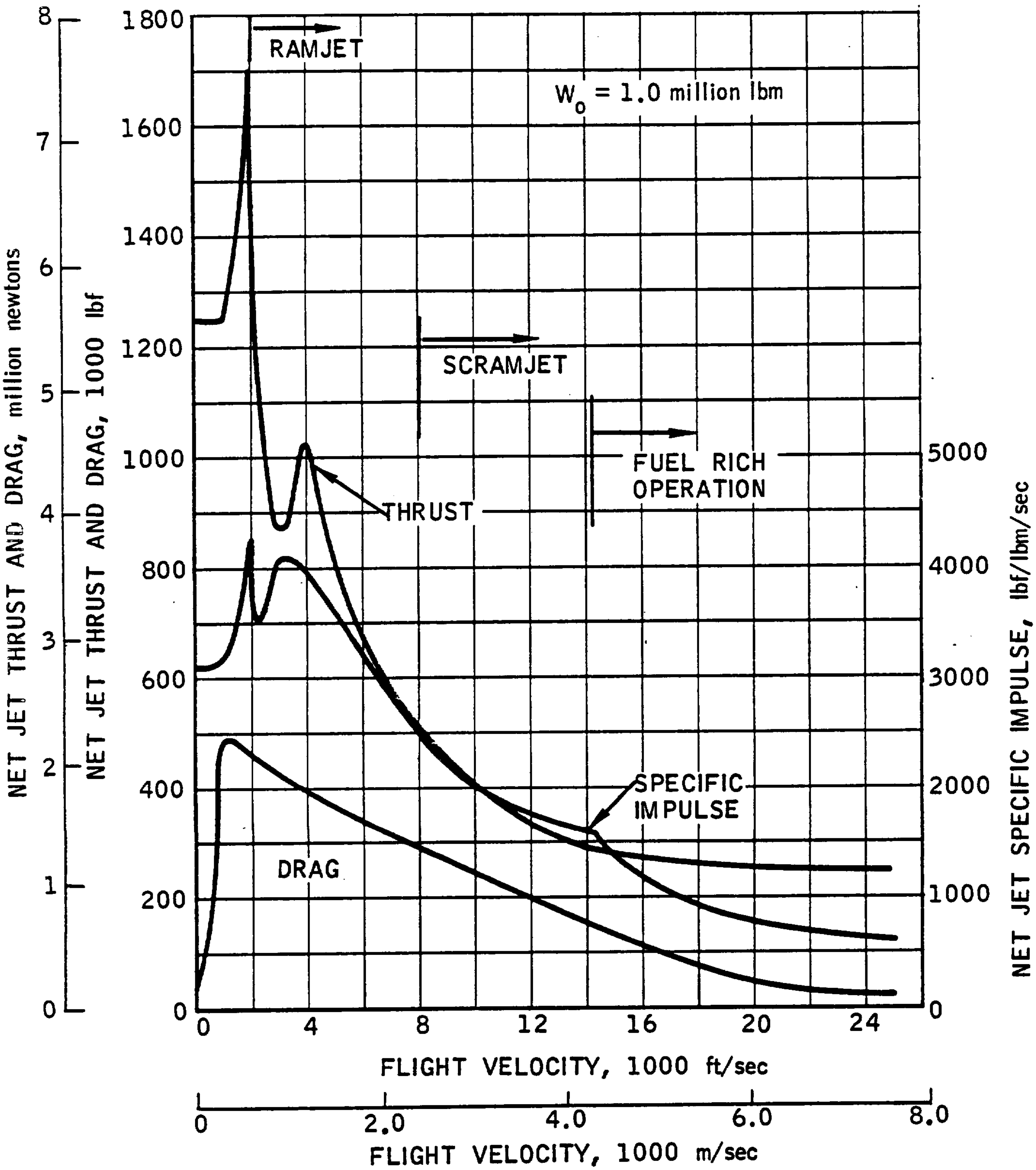

FIGURE E-11. Aerodynamic Performance of the Single Stage to Orbit Concept, Supercharged Recycled ScramLACE Engine (No. 32)

APPENDIX F

A METHOD OF AUGMENTING PAYLOAD IN CERTAIN AIR LIQUEFACTION BASED COMPOSITE PROPULSION SYSTEMS

By:

R. E. Morris

Lockheed-California Co.

This page intentionally left blank

APPENDIX F

A METHOD OF AUGMENTING PAYLOAD IN CERTAIN AIR LIQUEFACTION BASED COMPOSITE PROPULSION SYSTEMS

F-1. Description of Systems

In an effort to fully utilize the performance potential inherent in air liquefaction capability systems, alternate modes of operation were investigated. Specifically, the air collection "Quasi-Mode" suggested in Section 5.4.1 was explored for the ScramLACE system. The most severe compromise in the operation of this basic system is the low inlet/mixer contraction ratio required for low speed (ejector mode) operation and the higher ratio desired for the supersonic combustion mode. An increase in contraction ratio from the Class 2 value of 3:1 selected for the basic system would result in lower propulsion weight and decreased fuel consumption in the Mach 6 to 10 region, if adequate thrust were available in the transonic region. The inherent ability of the system to generate oxidizer in the form of liquid air suggests the use of the heat exchangers to store liquid air at times of high thrust/drag ratio, to be used when the thrust-drag margin is low, for example, at transonic and airbreathing termination. Oxidizer tankage, supply system, and rescheduling of the basic modes must be provided.

The effect on payload performance of these changes was investigated, based on the Mach 10 point design vehicle with a nominal payload of 56,000 pounds, a capture area of 408 ft^2, and a contraction ratio of 3. No attempt was made to resize the cowl or heat exchangers, but only to examine the change in payload due to modification of operating modes, installed propulsion weight, and staging velocity.

The operation of the system was as follows:

1. Mach 0 to 1.0: Part of the available air capacity of the basic heat exchangers is stored in the auxiliary tank.

2. Mach 1.0 to 1.8: The stored air is utilized in addition to that liquified by the full capacity of the heat exchangers and injected into the primary rockets to augment the transonic thrust.

3. Mach 1.8 to 2.3: Normal operation at maximum heat exchanger capacity.

4. Mach 2.3 to 3.2: Subsonic combustion ramjet plus heat exchangers and primary rockets with an overall equivalence ratio of 1.0.

5. Mach 3.2 to 4: Subsonic combustion ramjet.

6. Mach 4 to 6.5: Subsonic combustion ramjet. Collect and store air for post-airbreathing ascent to staging.

7. Mach 6.5 to airbreathing termination: Supersonic combustion ramjet.

8. Airbreathing termination to staging: Stored air and hydrogen are used in primary rockets (inlet closed) during pull-up to staging.

F-2. Propulsion Performance

The initial estimate of vehicle system performance using air storage was based on an inlet contraction ratio (A_c/A_3) of 4:1 compared to the baseline value of 3:1, with no storage.

F-2.1 Mach 0 to 1.0

In order to evaluate performance under varying ratios of secondary to primary flow (W_s/W_p), Marquardt performance for no secondary flow (LACE - Engine No. 3), W_s/W_p = 1.5 (Engine No. 22-1), and W_s/W_p = 3 (Engine No. 22-2) were plotted as shown in Figure F-1. From this curve, the approximate relative increase in thrust (referred to basic LACE) can be determined as less liquid air is injected and more is diverted to storage. Although the total thrust is reduced, compared to no storage, the I_{sp} is not reduced to the same extent due to increased augmentation (W_s/W_p increases), the increase in gross thrust due to fuel-rich operation, and the external heating of fuel by the stored air. The installed total thrust and drag are shown in Figure F-2 and I_{sp} and weight history are shown in Figure F-3. The thrust and I_{sp} include the effect of inlet drag, drag of collected air, and the total fuel flow required for air liquefaction.

F-2.2 Mach 1.0 to 1.8

During this phase, the system is operated at full heat exchanger capacity (normal operation) plus the addition of stored air such that the total primary chamber flow is 4000 lb/sec. The relative thrust change due to varying W_s/W_p was evaluated from Figure F-1 with the fuel flow (and I_{sp}) determined by the heat exchanger capacity. The total primary flow dictates the weight penalty required for the supply system, turbopumps, and primary rockets. The installed performance is shown in Figures F-2 and F-3.

F-2.3 Mach 1.8 to 2.3

Upon exhaustion of the stored air, the system reverts to the basic or normal operation (full heat exchanger capacity, ϕ_{HX} = 8). Figures F-2 and F-3 show the installed thrust and I_{sp} performance, respectively.

F-2.4 Mach 2.3 to 3.2

During this phase, subsonic combustion ramjet operation is used, with the heat exchangers supplying liquid air to the primary rockets at reduced capacity such that the overall equivalence ratio is 1.0.

F-2.5 Mach 3.2 to 4

Subsonic combustion ramjet operation is used in this phase. The performance is shown in Figures F-2 and F-3.

F-2.6 Mach 4 to 6.5

Subsonic combustion ramjet operation plus air stored by the heat exchangers is used in this phase. The assumed ratio of air stored to fuel flow is shown in Figure F-4. The curve in the Mach 5 to 6.5 region reflects the limitation in air flow dictated by engine cooling requirements. A slight increase in specific gross thrust during this mode is caused by the external heating of the fuel by the liquid air. The performance is again shown in Figures F-2 and F-3, and it includes the effects of inlet drag and the drag of the collected air. The vehicle drag reflects the increasing weight of the vehicle.

F-2.7 Mach 6.5 to Airbreathing Termination

Supersonic combustion ramjet ($A_c/A_3 = 4$) ($q = 1500$) operation is used in this phase.

F-2.8 Airbreathing Termination to Staging

At Mach 10, the pull-up is initiated with a normal load factor of 1.5. The Scramjet mode is terminated (inlet closed), and the primary rocket mode is initiated when the propellant consumption is equal. The pull-up is shown in Figure F-5 to the terminal staging velocity (in this case, 11,100 fps with a flight path angle γ of 9.2°).

F-3. Vehicle Weight and Payload

The vehicle weight breakdown is presented in Table F-I for three staging velocities. The weights shown include the effect of liquid air tankage and supply, hydrogen and tankage, and propulsion and thermal protection systems. The resulting payloads indicate a maximum of 69,000 lbs for a staging velocity of 10,150 fps. This is comparable to the 56,000 lb payload of the basic Mach 10 ScramLACE system.

The 9800 fps staging velocity shown in Table F-I represents a system in which air is collected in the Mach 0 to 1 range only, e.g., no air is collected from Mach 4 to 6.5. No post-airbreathing rocket pull-up is made, and the terminal conditions at staging are identical to the basic Mach 10 system. ($V_s = 9800$ fps, $\gamma_s = 7°$). The resulting payload is 61,400 lbs.

TABLE F-I

SYSTEM PERFORMANCE SUMMARY-AIR STORAGE OPERATION

Parameter	System		
	Subsonic Collect Only	Subsonic & Supersonic Collect	
W_I, lbs	574,262	567,382	620,046
W_{II}, lbs	425,738	432,618	379,954
$W_{Payload}$, lbs	61,400	69,000	67,000
$W_{Staging}$, lbs	795,700	809,000	780,400
$M_{AB\ Max}$	10	9	10
$V_{Staging}$, fps	9,800	10,150	11,100
$q_{Staging}$, psf	200	200	200
W_{II} Dry, lbs	67,485	68,544	61,136
W_{Dry}Total, lbs	419,067	423,656	432,927
$W_{Dry}/W_{Payload}$	6.83	6.14	6.46
First Stage			
$W_{Staging}$, lbs	370,614	376,491	400,555
$W_{Landing}$, lbs	359,688	365,392	383,027
W_{Dry}, lbs	351,582	355,102	371,791
$W_{AB\ Propulsion}$, lbs	110,549	111,748	111,748
$W_{Hydrogen}$, lbs	222,680	212,280	248,255
W_{Lox} (Liquid air), lbs	85,651	179,109	179,109
Propulsion			
T/W_o	*0.983	*0.983	*0.983
$T/W_{instl.}$	8.89	8.80	8.80
A_c (Geometric), sq ft	408	408	408
P_{T_2} Max. (Inlet diffuser pressure), psia	120	120	120

* Average thrust value

F-4. Conclusions

Within the limited depth of the study, the payload potential of this mode of operation would appear to warrant further consideration. Its advantage lies in the thrust flexibility of the system utilizing components already required for those composite systems using air liquefaction (e.g., RamLACE, ScramLACE).

It also appears from past investigations, that systems not already employing heat exchangers (Ejector Ramjet, Turboramjet, etc.) would exhibit similar payload increases by the use of such auxiliary equipment.

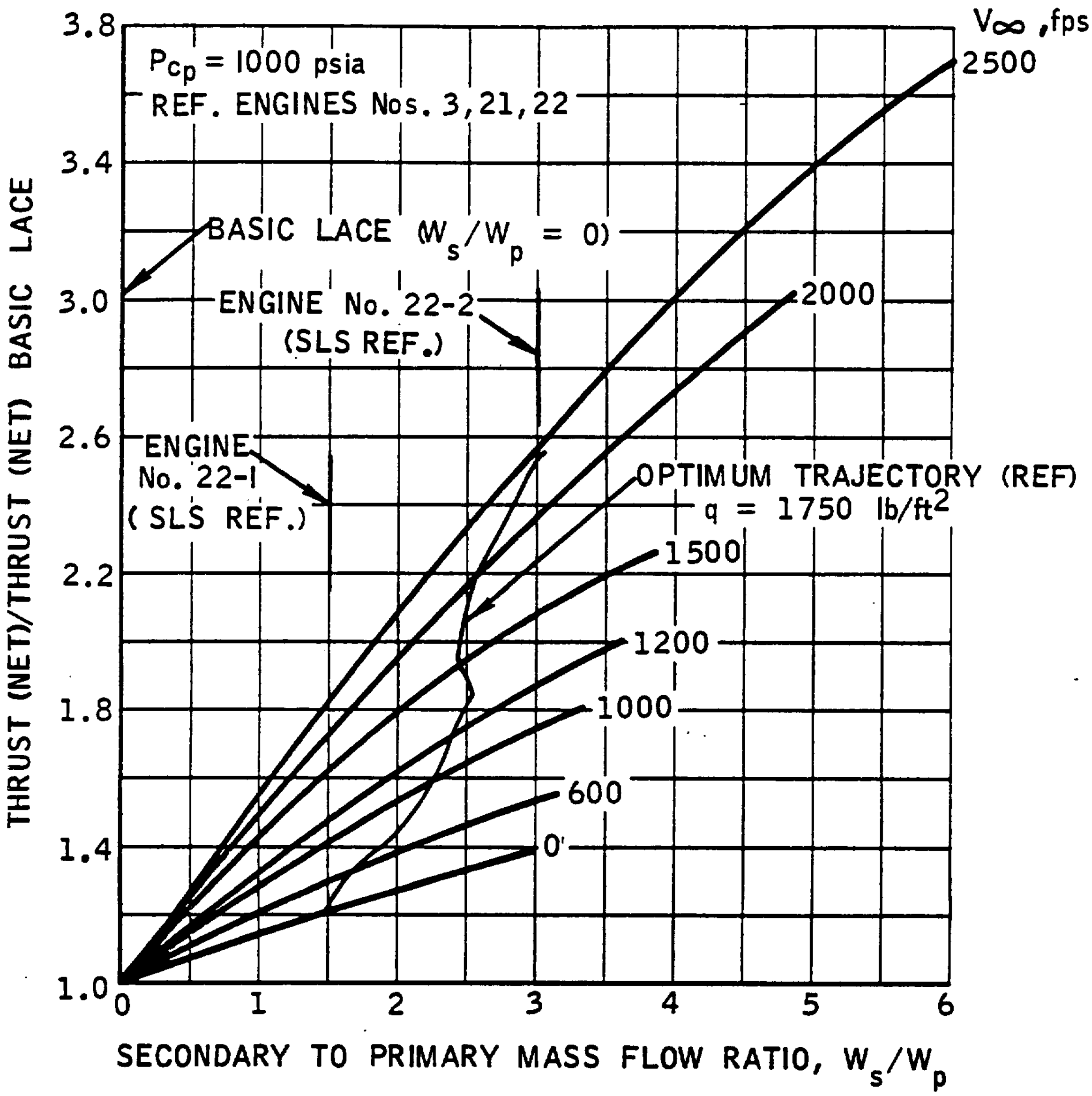

FIGURE F-1. Augmentation Ratios (Referenced to Basic LACE) vs. Mass Flow Ratio for Air Collection Quasi-Mode Operation

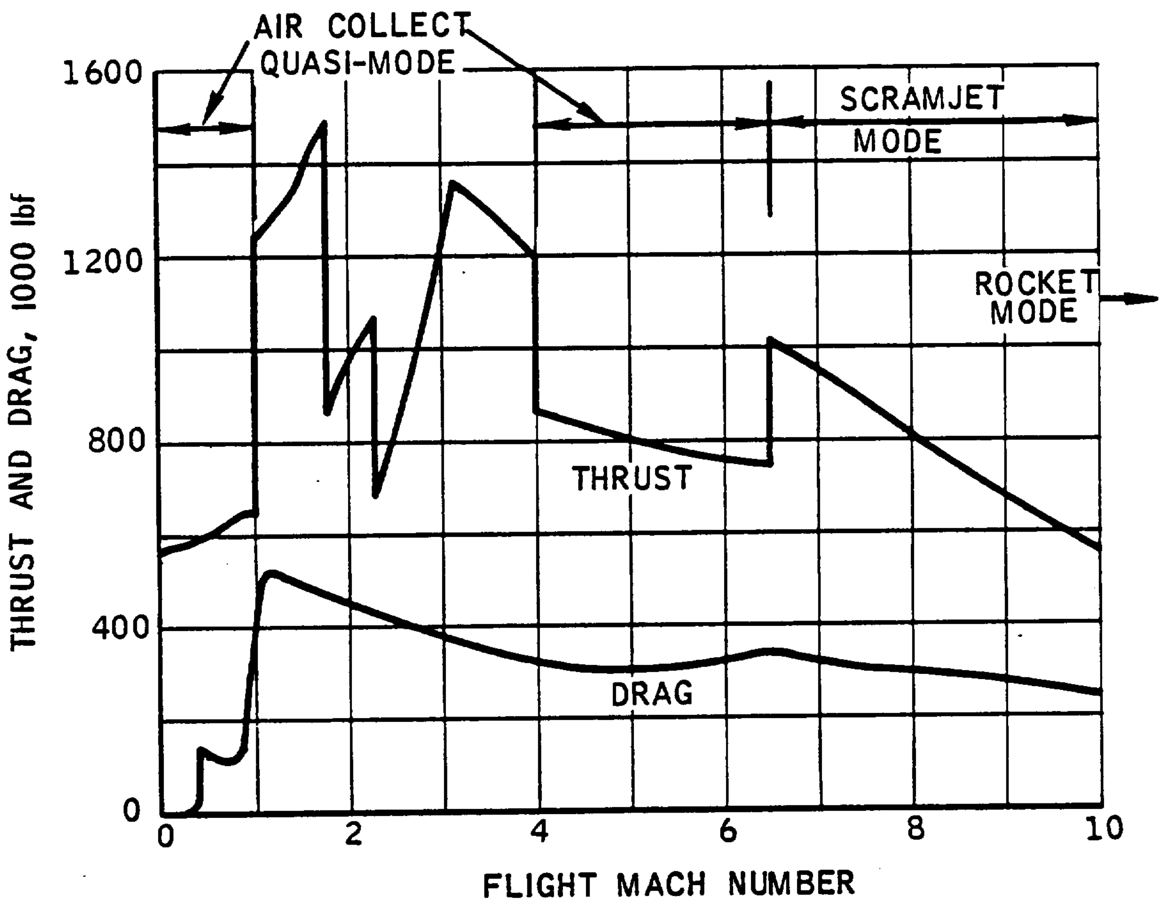

FIGURE F-2. Thrust and Drag History for Air Collection Quasi-Mode Operation

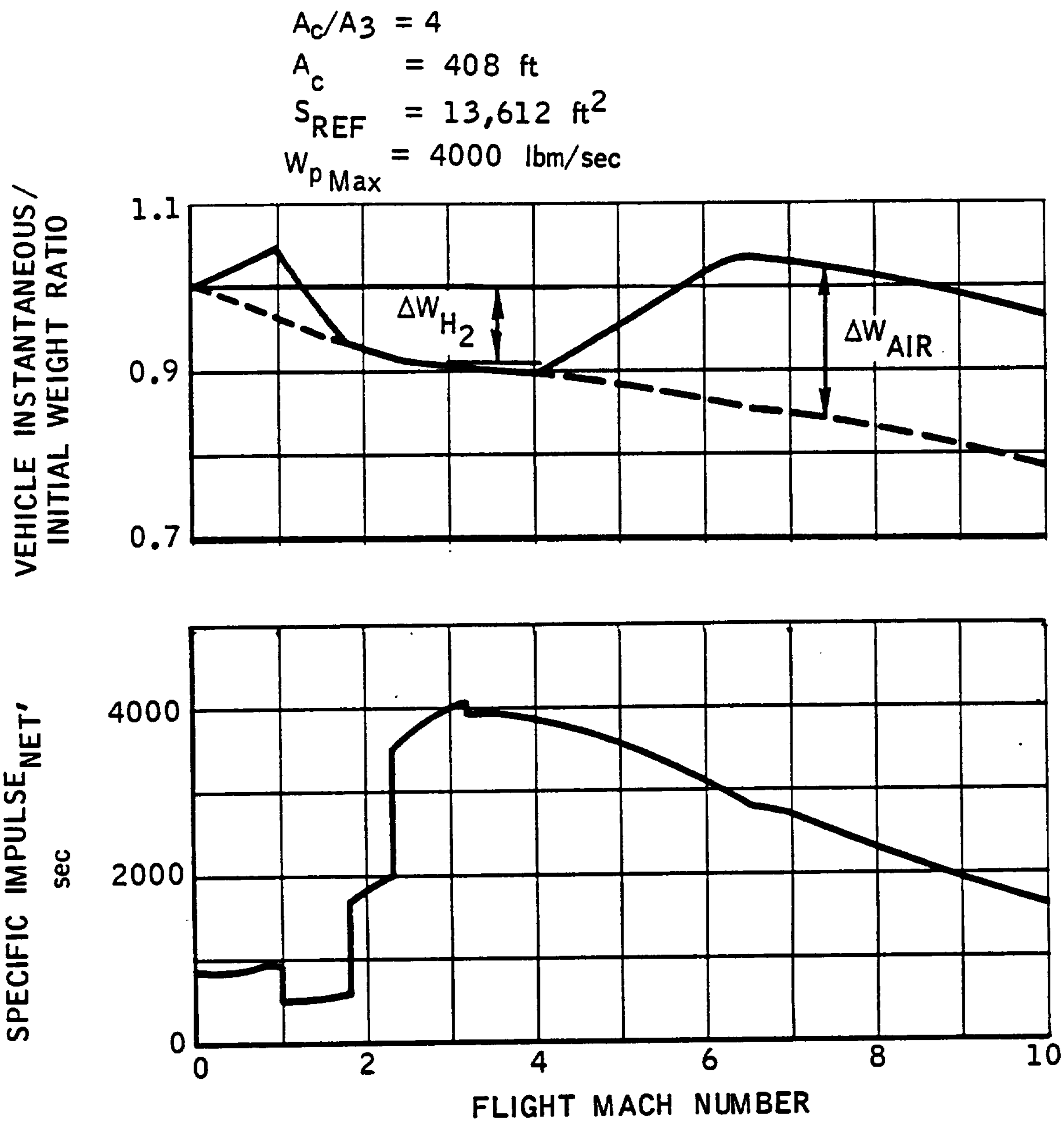

FIGURE F-3. Installed Performance and Instantaneous Vehicle Mass History for Air Collection, Quasi-Mode Operation

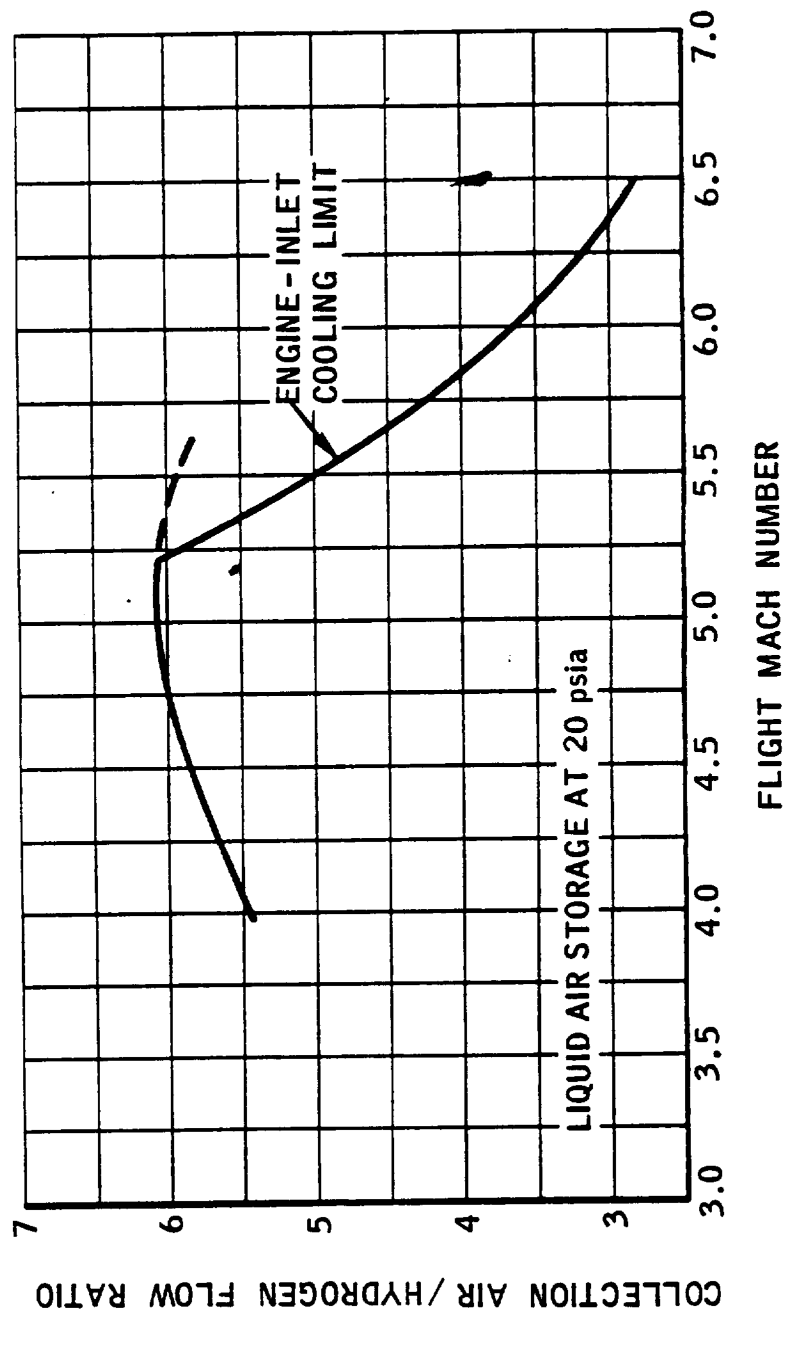

FIGURE F-4. Air Collection Schedule for Quasi-Mode Operation

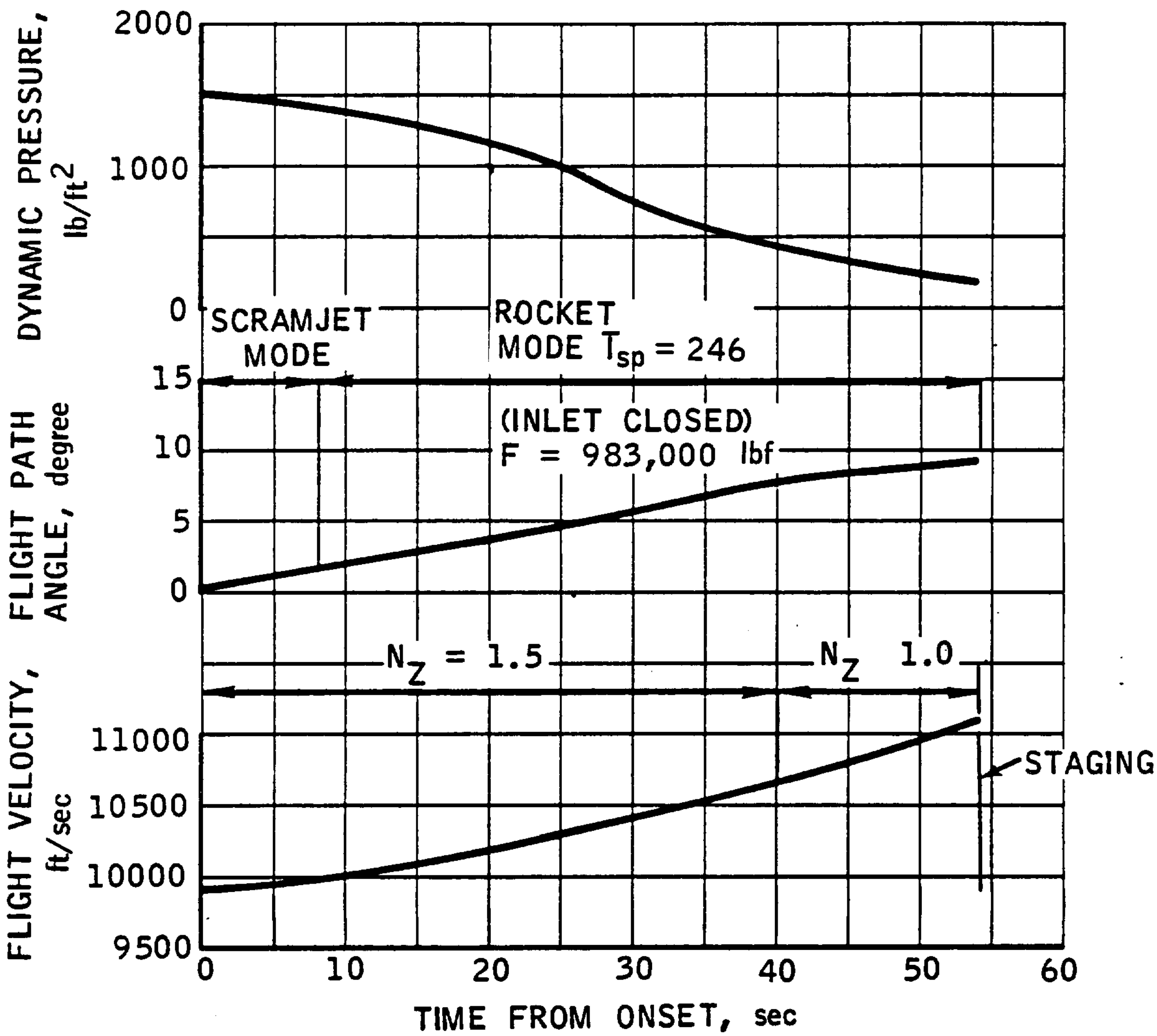

FIGURE F-5. Pull-up Time History for Air Collection Quasi-Mode Operation

APPENDIX G

EXCHANGE FACTORS FOR A TWO-STAGE ADVANCED ROCKET

By:

H. A. Singer

Rocketdyne Division
North American Aviation, Inc.

This page intentionally left blank.

APPENDIX G

EXCHANGE FACTORS FOR A TWO-STAGE ADVANCED ROCKET

Stage Point

$$\frac{\Delta P}{(\Delta W_2)^2} = -1.83 \times 10^{-6} \text{ lbf}^{-1} \text{ (Parabolic fit)}$$

Upper Stage Impulse

$$\frac{\partial P}{\partial \bar{I}_2} = 332 \text{ lbm/sec}$$

Upper Stage Area Ratio

$$\frac{\partial P}{\partial \epsilon_2} = 9 \text{ lbf/point}$$

Lower Stage Area Ratio

$$\frac{\partial P}{\partial \epsilon_1} = 27.5 \text{ lbf/point}$$

Kick Angle

$$\left|\frac{\partial P}{\partial \Gamma}\right| = -1500 \text{ lbf/degree}$$

Upper Stage Thrust

$$\frac{\partial P}{\partial F_2} = 0.0047$$

Upper Stage Mixture Ratio (Nonlinear)

$$\frac{\partial P}{\partial_{\mu 2}} = \begin{matrix} 400 \text{ lbf/point at 0.5 point below design} \\ 0 \text{ lbf/point at design} \\ -500 \text{ lbf/point at 0.2 point below design} \end{matrix}$$

Lower Stage Diameter

$$\frac{\partial P}{\partial D_1} \approx \begin{matrix} 0 \text{ lbf/ft, } \epsilon_1 \text{ varying with } D_1 \\ -217 \text{ lbf/ft, } \epsilon_1 \text{ held constant} \end{matrix}$$

This page intentionally left blank.

SUMMARY OF NOMENCLATURE

Symbol	Description
A	Area, ft^2; or rocket fuel turbopump designation
A_c	Cowl area, ft^2
A_1	Minimum area station in inlet (Inlet throat), ft^2
A_2	Inlet diffuser exit area (Air stream only), ft^2
A_3	Mixer exit area, ft^2
A_3'	Aft diffuser exit area, ft^2
A_4	Afterburner exit area, ft^2
A_4/A_3	Afterburner/Mixer diffusion ratio
A_5	Engine nozzle throat area, ft^2
A_6, A_6'	Nozzle exit area, ft^2
A_6/A_5	Exit nozzle expansion area ratio
A_6/A_c	Exit-to-capture area ratio (Scramjet)
A_o	Inlet capture area, ft^2
AB	Afterburner
B	Rocket oxidizer turbopump designation
BL	Baseline
C	Constant; or ramjet AB turbopump designation
C°	Ramjet afterburner turbopump designation
C_A	Axial force coefficient
C^*	Characteristic velocity, ft/sec
C_D	Vehicle drag coefficient
C_f	Friction coefficient

SUMMARY OF NOMENCLATURE (Continued)

Symbol	Description
C_F	Theoretical vacuum thrust coefficient
C_F, CF	Thrust coefficient based on inlet capture area
C_L	Lift coefficient
C_M	Pitching moment coefficient
C_N	Normal force coefficient
C_{N_α}	Normal force coefficient curve slope at zero angle of attack, dC_N/d_α - per degree
C_p	Specific heat at constant pressure, Btu/lbm-°F
C_v	Specific heat at constant volume, Btu/lbm-°F
D	Drag, lbf; or diameter, in.
DAB	Diffusion and afterburning cycle
DN	Bearing diameter-speed factor
f	Friction factor
f/a	Fuel-air ratio
F	Thrust, lbf
F_N	Net thrust
F_{NJ}	Net jet thrust
F/W	Vehicle thrust-to-weight ratio
g	Gravitational constant
G	Mass velocity, lbm/in.^{2}-sec
H	Altitude, ft
I_s	Specific impulse, lbf-sec/lbm

SUMMARY OF NOMENCLATURE (Continued)

Symbol	Description
I_{sp}	Specific impulse, lbf/lbm/sec
I_{sp_e}	Effective impulse [I_{sp} (1-Drag/Thrust)]
k	Thermal conductivity, Btu/in.-sec°F
K	Thousand; Constant (Function of gas properties and mixer geometry)
K_B	Ratio of induced lift on the fuselage to the lift of the tail alone for variable angle of attack
K_T	Ratio of the lift on the tail in the presence of the fuselage to the lift of the tail alone
L	Length, in.
%L	Nozzle percent length (Refers to 15° conical nozzle)
M, M_∞	Flight Mach number
M^*_D	Local velocity/Sonic velocity at throat
M_o	Local Mach number
MR	Mixture ratio (O/F)
N	Speed, rpm
N_s	Turbopump specific speed
NS	Normal shock inlet
NPSH	Net positive suction head, ft
Nu	Nusselt number
O/F	Oxidizer-to-fuel mixture ratio
P	Pressure, psia
P_o	Ambient static pressure, psia
P_c	Primary chamber pressure, psia

SUMMARY OF NOMENCLATURE (Continued)

Symbol	Description
Pr	Prandtl number
PR_f	Fan pressure ratio
$\bar{P}_s$	Average static pressure on a surface, lb/ft^2
P_{T_o}	Inlet total pressure, psia
P_{T_2}	Inlet recovered total pressure, psia
P_{T_2}/P_{T_o}	Inlet total pressure recovery ratio
P_{T_4}	Combustion chamber pressure, psia
P_∞	Free stream static pressure, lb/ft^2
q	Dynamic pressure, lb/ft^2
Q	Heat flux, Btu/sec
R	Gas constant
R*	Air turbine exhaust flow rate ratio
Re	Reynolds number
Ref	Reference
RPM, rpm	Revolutions per minute
R_t	Throat radius of equivalent bell nozzle, in.
SLS	Sea level static
SMC	Simultaneous mixing and combustion cycle
SFC, SPC	Specific fuel or propellant consumption, lbm/hr-lbf
S_{REF}	Vehicle reference area, ft^2
St	Stanton number
t	Regenerative tube wall thickness, in.
T	Temperature, °R

SUMMARY OF NOMENCLATURE (Continued)

Symbol	Description
T	Thrust, lbf
T_{NJ}	Net jet thrust, lbf
V	Velocity, ft/sec
V_o	Local velocity, ft/sec
ΔV	Ideal velocity increment, ft/sec
W	Weight, lbm
$\dot{W}$	Flow rate, lbm/sec
W_p	Primary flow rate, lbm/sec
W_S/W_P	Secondary/primary flow ratio
W_s	Secondary air flow, lbm/sec
x	Tank weight factor
X	Nozzle axial coordinate, in.
Y	Nozzle radial coordinate, in.

Greek Letters

α	Vehicle angle of attack, deg
γ	Ratio of specific heats (C_p/C_v); Ratio of specific heats of primaries; Path angle referenced to horizontal
Γ	Vehicle kick angle, deg
δ	Two-dimensional wedge half angle, deg; Flow field deflection angle, deg
Δ	Increment
ϵ	Nozzle area ratio or tube roughness height, in.

SUMMARY OF NOMENCLATURE (Continued)

Symbol	Description
ϵ^*	Nondimensionalized tube roughness height
η_{AB}	Efficiency to correct for nozzle afterburning
η_c	Combustion efficiency based on enthalpy rise
η_{c^*}	Characteristic velocity efficiency based on velocity, or thrust
η_{C_F}	Nozzle efficiency, rocket
η_{DRAG}	Efficiency to correct for viscous drag losses
η_{GEOM}	Efficiency to correct for geometric nozzle losses
η_{KE}	Inlet kinetic energy process efficiency
η_M	Mixing efficiency based on static pressure rise
η_N	Nozzle efficiency based on velocity, or thrust
θ	Momentum thickness of boundary layer
θ_m	Flow angle in nozzle
λ_p	Propellant weight fraction
μ	Mixture ratio (O/F)
ρ	Radius, in.; or density, lbm/ft^3
τ	Turbine exhaust/Thrust chamber flow rate ratio
ϕ	Equivalence ratio or curvature enhancement factor
ϕ_{AB}	Combustor equivalence ratio
ϕ_{cond}	Condenser equivalence ratio
ϕ_{HX}	Heat exchanger equivalence ratio
ϕ_P	Primary rocket equivalence ratio
ϕ_{prec}	Precooler equivalence ratio
ϕ_s, ϕ_{sec}	Secondary equivalence ratio

Subscripts

∞	Free stream
0	Vehicle shock field
1	First stage

SUMMARY OF NOMENCLATURE (Continued)

Symbol	Description
2	Second stage
2	Diffuser exit or engine face
3	Mixer exit
4	Combustor
5	Nozzle throat
6, 6'	Nozzle exit
a	Ambient conditions
aw	Adiabatic wall
b	Bulk or base region
c	Chamber, condenser, or capture
CURV	Curvature
D	Diameter
e	Exit conditions
ENG	Engine
f	Fuel
i	Inlet
o	Oxidizer or initial conditions
p	Primary conditions or precooler
s	Secondary or base conditions
sl, SL	Sea level
t	Throat conditions
T	Total
TC	Thrust chamber
TE	Turbine exhaust
VAC	Vacuum
w	Wall
WG	Hot gas side wall
WC	Coolant side wall

This page intentionally left blank

OUTLINE OF REPORT

OUTLINE OF REPORT (Continued)

OUTLINE OF REPORT (Continued)

OUTLINE OF REPORT (Continued)

OUTLINE OF REPORT (Continued)

OUTLINE OF REPORT (Continued)

Section | Page

OUTLINE OF REPORT (Continued)

OUTLINE OF REPORT (Continued)

Section | Page

OUTLINE OF REPORT (Continued)

Section | Page

OUTLINE OF REPORT (Continued)

OUTLINE OF REPORT (Continued)

Section | Page

OUTLINE OF REPORT (Continued)

OUTLINE OF REPORT (Continued)

OUTLINE OF REPORT (Continued)

OUTLINE OF REPORT (Continued)

Section Page

OUTLINE OF REPORT (Continued)

OUTLINE OF REPORT (Continued)

Section | Page

OUTLINE OF REPORT (Continued)

OUTLINE OF REPORT (Continued)

OUTLINE OF REPORT (Continued)

DISTRIBUTION

Copy No.	Transmitted to
1.	NASA Office of Resident Representative Jet Propulsion Laboratory 4800 Oak Grove Drive Pasadena, California 91103 Attn.: Office of Technical Information
2.	NASA Office of Resident Representative Jet Propulsion Laboratory 4800 Oak Grove Drive Pasadena, California 91103 Attn.: Contracts Management Division
3.	NASA Office of Resident Representative Jet Propulsion Laboratory 4800 Oak Grove Drive Pasadena, California 91103 Attn.: General Counsel for Patent Matters
4 to 7.	NASA Headquarters Washington, D. C. 20546 Attn.: Chief, Liquid Propulsion Technology, RPL Office of Advanced Research and Technology
8 to 32.	NASA Scientific and Technical Information Facility P. O. Box 33 College Park, Maryland 20740
33.	NASA Headquarters Washington, D. C. 20546 Attn.: Mr. Vincent L. Johnson Director, Launch Vehicles and Propulsion, SV Office of Space Science and Applications
34.	NASA Headquarters Washington, D. C. 20546 Attn.: Mr. Edward L. Gray Director, Advanced Manned Missions, MT Office of Manned Space Flight
35.	NASA Ames Research Center Moffett Field, California 24035 Attn.: Mr. Clarence A. Syvertson Mission Analysis Division

DISTRIBUTION (Continued)

Copy No.	Transmitted to
36.	Marshall Space Flight Center Huntsville, Alabama 35812 Attn.: Technical Monitor Mr. Donald Thompson
37.	Langley Research Center Langley Station Hampton, Virginia 23365 Attn.: Mr. Kenneth Pierpont
38.	NASA Ames Research Center Moffett Field, California 94035 Attn.: Mr. Thomas Gregory Mission Analysis Division
39, 40.	NASA Ames Research Center Moffett Field, California 94035 Attn.: Harvey J. Allen Director
41, 42.	NASA Goddard Space Flight Center Greenbelt, Maryland 20771 Attn.: Merland L. Moseson Code 620
43, 44.	NASA Jet Propulsion Laboratory California Institute of Technology 4800 Oak Grove Drive Pasadena, California 91103 Attn.: Henry Burlage, Jr. Propulsion Div., 38
45, 46.	NASA Langley Research Center Langley Station Hampton, Virginia 23365 Attn.: Dr. Floyd L. Thompson Director
47, 48.	NASA Lewis Research Center 21000 Brookpark Road Cleveland, Ohio 44135 Attn.: Dr. Abe Silverstein Director

DISTRIBUTION (Continued)

Copy No.	Transmitted to
49, 50.	NASA Marshall Space Flight Center Huntsville, Alabama 35812 Attn.: Hans G. Paul Code R-P&VED
51, 52.	NASA Manned Spacecraft Center Houston, Texas 77001 Attn.: Dr. Robert R. Gilruth Director
53, 54.	NASA Office of Resident Representative Jet Propulsion Laboratory 4800 Oak Grove Drive Pasadena, California 91103 Attn.: Robert W. Kamm Director
55, 56.	NASA John F. Kennedy Space Center Cocoa Beach, Florida 32931 Attn.: Dr. Kurt H. Debus
57.	Aeronautical Systems Division Air Force Systems Command Wright-Patterson Air Force Base Dayton, Ohio 45433 Attn.: D. L. Schmidt Code ASRCNC-2
58.	Air Force Missile Development Center Holloman Air Force Base, New Mexico Attn.: Maj. R. E. Bracken Code MDGRT
59.	Air Force Missile Test Center Patrick Air Force Base, Florida Attn.: L. J. Ullian
60.	Air Force Systems Division Air Force Unit Post Office Los Angeles 45, California Attn.: Col. Clark Technical Data Center

DISTRIBUTION (Continued)

Copy No.	Transmitted to
61.	Arnold Engineering Development Center Arnold Air Force Station Tullahoma, Tennessee Attn.: Dr. H. K. Doetsch
62.	Bureau of Naval Weapons Department of the Navy Washington 25, D. C. Attn.: J. Kay RTMS-41
63.	Defense Documentation Center Headquarters Cameron Station, Building 5 5010 Duke Street Alexandria, Virginia 22314 Attn.: TISIA
64.	Headquarters, U. S. Air Force Washington 25, D. C. Attn.: Col. C. K. Stambaugh AFRST
65.	Picatinny Arsenal Dover, New Jersey 07801 Attn.: I. Forsten, Chief Liquid Propulsion Laboratory SMUPA-DL
66.	Air Force Rocket Propulsion Laboratory Research and Technology Division Air Force Systems Command Edwards, California 93523 Attn.: H. Main, RPRR
67.	Research and Technology Division Air Force Aero Propulsion Laboratory Wright-Patterson Air Force Base, Ohio 45433 Attn.: H. C. Long, APRP
68.	U. S. Atomic Energy Commission Technical Information Services Box 62 Oak Ridge, Tennessee Attn.: A. P. Huber Oak Ridge Gaseous Diffusion Plant (ORGDP) P. O. Box P

DISTRIBUTION (Continued)

Copy No.	Transmitted to
69.	U. S. Army Missile Command Redstone Arsenal Alabama 35809 Attn.: Dr. Walter Wharton
70.	U. S. Naval Ordnance Test Station China Lake, California 93557 Attn.: Chief, Missile Propulsion Division Code 4562
71.	Air Force Systems Command Space Systems Division Inglewood, California 90045 Attn.: Lt. Col. Kenneth Mc Aaron
72.	Chemical Propulsion Information Agency Applied Physics Laboratory 8621 Georgia Avenue Silver Spring, Maryland 20910 Attn.: Neil Safeer
73.	Aerojet-General Corporation P. O. Box 296 Azusa, California 91703 Attn.: L. F. Kohrs
74.	Aerojet-General Corporation P. O. Box 1947 Sacramento, California 95809 Attn.: R. Stiff Technical Library, Bldg. 2015, Dept. 2410
75.	Aeronutronic Philco Corporation Ford Road Newport Beach, California 92663 Attn.: D. A. Carrison
76.	Aerospace Corporation 2400 East El Segundo Boulevard P. O. Box 95085 Los Angeles, California 90045 Attn.: John G. Wilder Propulsion Dept. MS-2293

DISTRIBUTION (Continued)

Copy No.	Transmitted to
77.	Arthur D. Little, Inc. 20 Acorn Park Cambridge, Massachusetts 02140 Attn.: E. Karl Bastress
78.	Astropower Laboratory Douglas Aircraft Company 2121 Paularino Newport Beach, California 92663 Attn.: Dr. George Moc Director, Research
79.	Astrosystems International, Inc. 1275 Bloomfield Avenue Fairfield, New Jersey 07007 Attn.: A. Mendenhall
80.	Atlantic Research Corporation Edsall Road and Shirley Highway Alexandria, Virginia 22314 Attn.: A. Scurlock
81.	Beech Aircraft Corporation Boulder Division Box 631 Boulder, Colorado Attn.: J. H. Rodgers
82.	Bell Aerosystems Company P. O. Box 1 Buffalo, New York 14240 Attn.: W. M. Smith
83.	Bendix Systems Division Bendix Corporation 3300 Plymouth Road Ann Arbor, Michigan Attn.: John M. Brueger
84.	Boeing Company P. O. Box 3707 Seattle, Washington 98124 Attn.: J. D. Alexander

DISTRIBUTION (Continued)

Copy No.	Transmitted to
85.	Missile Division Chrysler Corporation P. O. Box 2628 Detroit, Michigan 48231 Attn.: John Gates
86.	Wright Aeronautical Division Curtiss-Wright Corporation Wood-Ridge, New Jersey 07075 Attn.: G. Kelley
87.	Missile and Space Systems Division Douglas Aircraft Company, Inc. 3000 Ocean Park Boulevard Santa Monica, California 90406 Attn.: R. W. Hallet Chief Engineer, Advanced Space Tech.
88.	Aircraft Missiles Division Fairchild Hiller Corporation Hagerstown, Maryland 10 Attn.: J. S. Kerr
89.	General Dynamics/Astronautics P. O. Box 1128 San Diego, California 92112 Attn.: Frank Dore Library & Information Services (128-00)
90.	Re-Entry Systems Department General Electric Company 3198 Chestnut Street Philadelphia, Pennsylvania 19101 Attn.: F. E. Schultz
91.	Advanced Engine & Technology Dept. General Electric Company Cincinnati, Ohio 45215 Attn.: D. Suichu
92.	Grumman Aircraft Engineering Corp. Bethpage, Long Island New York Attn.: Joseph Gavin

DISTRIBUTION (Continued)

Copy No.	Transmitted to
93.	Ling-Temco-Vought Corporation Astronautics P. O. Box 5907 Dallas, Texas 75222 Attn.: Warren C. Trent
94.	Lockheed-California Company 2555 North Hollywood Way Burbank, California 91503 Attn.: G. D. Brewer
95.	Lockheed Missiles and Space Company P. O. Box 504 Sunnyvale, California 94088 Attn.: Y. C. Lee Technical Information Center
96.	Lockheed Propulsion Company P. O. Box 111 Redlands, California 92374 Attn.: H. L. Thackwell
97.	Baltimore Division Martin-Marietta Corporation Baltimore, Maryland 21203 Attn.: John Calathes (3214)
98.	Denver Division Martin-Marietta Corporation P. O. Box 179 Denver, Colorado 80201 Attn.: J. D. Goodlette (A-241)
99.	McDonnell Aircraft Corporation P. O. Box 516 Municipal Airport St. Louis, Missouri 63166 Attn.: R. A. Herzmark
100.	Space & Information Systems Division North American Aviation, Inc. 12214 Lakewood Boulevard Downey, California 90241 Attn.: H. Storms

DISTRIBUTION (Continued)

Copy No.	Transmitted to
101.	Rocketdyne North American Aviation, Inc. 6633 Canoga Avenue Canoga Park, California 91304 Attn.: E. B. Monteath Library, 586-306
102.	Northrop Space Laboratories 3401 West Broadway Hawthorne, California Attn.: Dr. William Howard
103.	Astro-Electronics Division Radio Corporation of America Princeton, New Jersey 08540 Attn.: S. Fairweather
104.	Reaction Motors Division Thiokol Chemical Corporation Denville, New Jersey 07832 Attn.: Arthur Sherman
105.	Republic Aviation Corporation Farmingdale Long Island, New York Attn.: Dr. William O'Donnell
106.	Space-General Corporation 9200 East Flair Avenue El Monte, California 91734 Attn.: C. E. Roth
107.	Stanford Research Institute 333 Ravenswood Avenue Menlo Park, California 94025 Attn.: Lionel Dickinson
108.	Space Technology Laboratories TRW Incorporated One Space Park Redondo Beach, California 90278 Attn.: G. W. Elverum

DISTRIBUTION (Continued)

Copy No.	Transmitted to
109.	TAPCO Division TRW, Incorporated 23555 Euclid Avenue Cleveland, Ohio 44117 Attn.: P. T. Angell
110.	Thiokol Chemical Corporation Huntsville Division Huntsville, Alabama Attn.: John Goodloe
111.	Research Laboratories United Aircraft Corporation 400 Main Street East Hartford, Connecticut 06108 Attn.: Erle Martin
112.	United Aircraft Corporation Pratt and Whitney Aircraft Division East Hartford, Connecticut 06108 Attn.: W. Sens
113.	United Aircraft Corporation Pratt and Whitney Aircraft Division Florida Research and Development Center West Palm Beach, Florida 33401 Attn.: R. Coar